

Synthesis, Structural Characterization and Reactivity of 13- and 14-vertex Carboranes

ZHANG, Jian

A Thesis Submitted in Partial Fulfillment
of the Requirements for the Degree of
Doctor of Philosophy
in
Chemistry

The Chinese University of Hong Kong

April 2011

UMI Number: 3492041

All rights reserved

INFORMATION TO ALL USERS

The quality of this reproduction is dependent on the quality of the copy submitted.

In the unlikely event that the author did not send a complete manuscript and there are missing pages, these will be noted. Also, if material had to be removed, a note will indicate the deletion.



UMI 3492041

Copyright 2011 by ProQuest LLC.

All rights reserved. This edition of the work is protected against unauthorized copying under Title 17, United States Code.



ProQuest LLC.
789 East Eisenhower Parkway
P.O. Box 1346
Ann Arbor, MI 48106 - 1346

Thesis/Assessment Committee

Professor Kin Shing Chan (Chair)

Professor Zuowei Xie (Research Supervisor)

Professor Hung Kay Lee (Committee Member)

Professor Zhenyang Lin (External Examiner)

Acknowledgement

I would like to express my sincere thanks to my supervisor, Professor Zuowei Xie, for his guidance, encouragement, and help during my study in the past five years. He is responsible for involving me in the fascinating research of carborane chemistry and helping me complete writing of this dissertation as well as the challenging research that lies behind it.

I would like to thank Ms. Hoi-Shan Chan for the determination of single-crystal X-ray structures, and Mr. Chi-Chung Lee and Miss. Hau-Yan Ng for mass spectra measurement.

I am also grateful to my group mates, Dr. Meihua Xie, Dr. Liang Deng, Dr. Yi Sun, Dr. Mak-Shuen Cheung, Dr. Hao Shen, Dr. Mei-Mei Sit, Ms. Dongmei Liu, Dr. Shikuo Ren, Dr. Zaozao Qiu, Mr. Xiaodu Fu, Ms. Jingying Yang, Mr. Fengrui Zheng, Mr. Rixin Wang, Mr. Xiao He, Mr. Yang Wang for their helpful discussion.

I also thank my friends and officers of the Department of Chemistry and Graduate School for their help and supports during the course of my study.

I am greatly indebted to The Chinese University of Hong Kong for the award of a Postgraduate Studentship and to the Hong Kong Research Grants Council for the financial support.

Abstract

This thesis describes the synthesis, structural characterization and reactivities of a series of 13- and 14-vertex carboranes, as well as the corresponding 14- and 15-vertex metallocarboranes. Several 13-vertex CAd (Carbon-Atoms-Adjacent) carboranes bearing different C,C'-linkages were synthesized via [12+1] polyhedral expansion protocol. These 13-vertex carboranes have unique structural and spectroscopic features such as the short cage C-C bonds and the downfield chemical shifts of the cage carbons. The corresponding CAp (Carbon-Atoms-Apart) 13-vertex carboranes 1,2-Me₂-1,2-C₂B₁₁H₁₁ and 1,12-Me₂-1,12-C₂B₁₁H₁₁ were prepared via the desilylation of μ -1,2-Me₂Si(CH₂)₂-1,2-C₂B₁₁H₁₁ upon column chromatography on silica gel. 1,2-Isomer can be converted into the 1,12-isomer upon heating. This result suggests that the C,C'-linkage does not have any obvious effects on the stability of 13-vertex carboranes. Several 14-vertex CAd 2,3- and 2,8- carboranes were prepared via a [13+1] protocol from the reaction of 13-vertex *nido*-carborane dianions and HBr₂, or a [12+2] protocol from the reaction of CAd 12-vertex *arachno*-carborane tetraanions with HBr₂. In a similar manner, 2,4-, 2,8- and 2,9-Me₂C₂B₁₂H₁₂ were also prepared and structurally characterized. A class of CAd and CAp 14-vertex ruthenacarboranes and a 15-vertex ruthenacarborane were synthesized from the reaction of corresponding *nido*-carborane salts with [(*p*-cymene)RuCl₂]₂.

The 13-vertex CAd carborane $1,2-(\text{CH}_2)_3-1,2-\text{C}_2\text{B}_{11}\text{H}_{11}$ underwent cage carbon-extrusion reaction with several nucleophiles to form 2-substituted monocarbadodecaborate anions $1,2-(\text{CH}_2)_3\text{CH}(\text{Nu})-1-\text{CB}_{11}\text{H}_{10}^-$, $1,2-(\text{CH}_2)_2\text{CH}(\text{Nu})\text{CH}_2-1-\text{CB}_{11}\text{H}_{10}^-$ and $1,2-(\text{CH}_2)_2\text{CH}=\text{CH}-1-\text{CB}_{11}\text{H}_{10}^-$. They also underwent cage boron extrusion reactions. $1,2-(\text{CH}_2)_n-1,2-\text{C}_2\text{B}_{11}\text{H}_{11}$ ($n = 3, 4$) reacted with MeOH in the presence of inorganic or organic base to afford $[\mu-7,8-(\text{CH}_2)_n\text{CHB}(\text{OMe})_2-7-\text{CB}_{10}\text{H}_{11}]^-$ anions, which were oxidized to $[\mu-7,8-(\text{CH}_2)_n\text{CHOH}-7-\text{CB}_{10}\text{H}_{11}]^-$ or hydrolyzed to $[\mu-7,8-(\text{CH}_2)_n\text{CHB}(\text{OH})_2-7-\text{CB}_{10}\text{H}_{11}]^-$. $1,2-(\text{CH}_2)_3-1,2-\text{C}_2\text{B}_{11}\text{H}_{11}$ reacted with pyridines, bipy or phen to give $\mu-2,4-(\text{CH}_2)_3\text{CHBH}(\text{RC}_5\text{H}_4\text{N})_2-2-\text{CB}_{10}\text{H}_9$, 4-(bipy)B-1,2-(CH_2) $_n$ -1,2- $\text{C}_2\text{B}_{10}\text{H}_9$ or 4-(H₂phen)B-1,2-(CH_2) $_n$ -1,2- $\text{C}_2\text{B}_{10}\text{H}_9$, respectively. Reaction of 13-vertex CAp carborane $1,12-\text{Me}_2-1,12-\text{C}_2\text{B}_{11}\text{H}_{11}$ with MeOH gave 2-substituted CB_{11}^- anions while 7-substituted CB_{11}^- anion was obtained by treatment with NaH or NaBH₄ in THF. On the other hand, treatment of 14-vertex *closo*-carboranes 2,3- and 2,8-(CH_2)₃- $\text{C}_2\text{B}_{12}\text{H}_{12}$ in MeOH at 70 °C gave the CB_{11}^- anions. In the presence of Me₃N, the same reaction afforded $[\mu-8,9-(\text{CH}_2)_3-\mu-11,12-(\text{MeO})\text{BH}-8,9-\text{C}_2\text{B}_{11}\text{H}_{11}]^-$, which was converted to the 2,3-isomer of 14-vertex carborane in the presence of acid such as HCl, or underwent further deboration to give $[\mu-8,9-(\text{CH}_2)_3-8,9-\text{C}_2\text{B}_{11}\text{H}_{12}]^-$.

摘要

本論文描述了 13 和 14 頂點碳硼烷以及相應的 14 和 15 頂點金屬碳硼烷的合成，結構鑒定以及反應性。一些具有籠碳碳原子橋鏈取代基的籠碳碳原子相鄰的 13 頂點碳硼烷通過[12+1]的多面體擴籠反應來合成。這些 13 頂點碳硼烷有獨特的結構和波譜性質，比如較短的籠碳碳鍵長以及位於低場的籠碳原子化學位移。1,2-Me₂-1,2-C₂B₁₁H₁₁ 以及相應的籠碳碳原子不相鄰的 13 頂點碳硼烷 1,12-Me₂-1,12-C₂B₁₁H₁₁ 由 μ -1,2-Me₂Si(CH₂)₂-1,2-C₂B₁₁H₁₁ 通過矽膠柱色譜脫矽得到。其中 1,2-異構體可以在加熱下轉化成 1,12-異構體。這個結果表明籠碳碳橋鏈取代基對 13 頂點碳硼烷的穩定性沒有明顯影響。一些 14 頂點籠碳碳相鄰的 2,3-和 2,8-碳硼烷通過[13+1]的反應由 13 頂點鳥巢型碳硼烷二價陰離子和二溴硼烷來合成。這些化合物也可以通過[14+2]的反應途徑由 12 頂點蛛網型碳硼烷四價陰離子和二溴硼烷反應得到。用類似的方法，2,4-、2,8-以及 2,9-Me₂C₂B₁₂H₁₂ 也合成出來並得到結構鑒定。一些籠碳碳原子相鄰和不相鄰的 14 頂點鈦雜碳硼烷以及 15 頂點鈦雜碳硼烷由相應的鳥巢型碳硼烷陰離子鹽和 [(*p*-cymene)RuCl₂]₂ 反應得到。

13 頂點籠碳碳原子相鄰的碳硼烷 1,2-(CH₂)₃-1,2-C₂B₁₁H₁₁ 和親核試劑反應得到籠碳原子擠出的產物—2-取代的含一個碳原子的 12 頂點碳硼烷陰離子 1,2-(CH₂)₃CH(Nu)-1-CB₁₁H₁₀⁻、1,2-(CH₂)₂CH(Nu)CH₂-1-CB₁₁H₁₀⁻ 和 1,2-(CH₂)₂CH=CH-1-CB₁₁H₁₀⁻。13 頂點籠碳碳原子相鄰的碳硼烷也可以發生籠硼原

子擠出的反應。1,2-(CH₂)_n-1,2-C₂B₁₁H₁₁ (*n* = 3, 4)在無機或有機物的存在下和甲醇反應得到[μ-7,8-(CH₂)_nCHB(OMe)₂-7-CB₁₀H₁₁]陰離子，並進一步氧化得到[μ-7,8-(CH₂)_nCHOH-7-CB₁₀H₁₁]或水解得到[μ-7,8-(CH₂)_nCHB(OH)₂-7-CB₁₀H₁₁]。

1,2-(CH₂)₃-1,2-C₂B₁₁H₁₁ 和吡啶、聯吡啶或菲咯啉反應得到相應的 μ-2,4-(CH₂)₃CHBH(RC₅H₄N)₂-2-CB₁₀H₉、4-(bipy)B-1,2-(CH₂)_n-1,2-C₂B₁₀H₉ 或者 4-(H₂phen)B-1,2-(CH₂)_n-1,2-C₂B₁₀H₉。13 頂點籠碳碳原子相鄰的碳硼烷 1,12-Me₂-1,12-C₂B₁₁H₁₁ 和甲醇反應得到 2-取代的 CB₁₁ 陰離子，但和氫化鈉或者硼氫化鈉在四氫呋喃中反應得到 7-取代的 CB₁₁ 陰離子。14 頂點封閉型碳硼烷 2,3-和 2,8-(CH₂)₃-C₂B₁₂H₁₂ 和甲醇在 70°C 反應得到 CB₁₁ 陰離子。但在三甲胺的存在下，同樣的反應得到[8,9-(CH₂)₃-μ-11,12-(MeO)BH-8,9-C₂B₁₁H₁₁]。該離子在鹽酸的作用下得到 2,3-位的十四頂點碳硼烷，或者進一步脫硼得到 [8,9-(CH₂)₃-8,9-C₂B₁₁H₁₂]。

Abbreviation

Ac	Acetyl
bipy	2,2'-bipyridine
br	Broad
Bu	Butyl
CAd	Carbon-atoms-adjacent
CAP	Carbon-atoms-apart
COSY	Correlation spectroscopy (NMR)
Cp	Cyclopentadienyl
d	Doublet (NMR)
DEPT	Distortionless enhancement by polarization transfer (NMR)
DME	Dimethoxyethane
dppe	$\text{Ph}_2\text{PCH}_2\text{CH}_2\text{PPh}_2$
dppen	$\text{Ph}_2\text{PCH}=\text{CHPPh}_2$
DSD	Diamond-square-diamond
η	Shows hapticity in π -bonding ligands
EPR	Electron paramagnetic resonance
Et	Ethyl
Fe	Ferrocene
HMBC	Heteronuclear multiple bond correlation (NMR)
HRMS	High resolution mass spectrometry
HSQC	Heteronuclear single quantum coherence (NMR)
L	Generalized ligand, in particular a 2e ligand
Ln	Lanthanide element
μ	Descriptor for bridging

m	Multiplet (NMR)
<i>m</i> -	Meta
M	Generalized metal or metal fragment
Me	Methyl
MO	Molecular Orbital
NHC	<i>N</i> -heterocyclic carbene
NMR	Nuclear magnetic resonance
Nu, Nu ⁻	Generalized nucleophile
<i>o</i> -	Ortho
<i>p</i> -	Para
Ph	Phenyl
PPN	Bis(triphenylphosphine)iminium cation
phen	1,10-Phenanthroline
PS	Proton Sponge [®]
py	Pyridine
q	Quartet (NMR)
R	Substitution group, normally an alkyl or aryl group
RTF	Rotation of triangular faces
s	Singlet (NMR)
t	Triplet (NMR)
TBAF	Tetrabutyl ammonium fluoride
TBDMS	<i>t</i> -Butyldimethylsilyl
Tf	Trifluoromethanesulfonyl
THF	Tetrahydrofuran
TMS	Trimethylsilyl
X	Generally halogen element

List of Compounds

Compd. No.	Compd. Formula	Page No.
4	<i>closo</i> - μ -1,2-MeCH(CH ₂) ₂ -1,2-C ₂ B ₁₀ H ₁₀	28
5a	<i>closo</i> -3-Ph- μ -1,2-(CH ₂ CH=CHCH ₂)-1,2-C ₂ B ₁₁ H ₁₀	29
5b	<i>closo</i> -3-Ph- μ -1,2-(CH=CHCH ₂ CH ₂)-1,2-C ₂ B ₁₁ H ₁₀	29
6'	<i>closo</i> -3-Me- μ -1,2-(CH ₂) ₃ -1,2-C ₂ B ₁₁ H ₁₀	33
7	<i>closo</i> - μ -1,2-(CH ₂) ₄ -1,2-C ₂ B ₁₁ H ₁₁	31
7'	<i>closo</i> -3-Me- μ -1,2-(CH ₂) ₄ -1,2-C ₂ B ₁₁ H ₁₀	33
8	<i>closo</i> - μ -1,2-MeCH(CH ₂) ₂ -1,2-C ₂ B ₁₁ H ₁₁	31
[12a][Na ₄ - (THF) ₁₂]	<i>nido</i> -[7,7'-(CH ₂ CH ₂)-9,9'-Me ₂ -7,7',9,9'- (C ₂ B ₁₀ H ₁₀) ₂][Na ₄ (THF) ₁₂]	43
[12b][Na ₂ (18- crown-6)]	<i>nido</i> -[μ -7,8-O(CH ₂) ₂ -7,8'-C ₂ B ₉ H ₉]- [Na ₂ (18-crown-6)]	43
[14][Na ₂ - (THF) ₄]	<i>nido</i> -[μ -7,10-O(Me ₂ Si) ₂ -7,10-C ₂ B ₁₀ H ₁₀]- [Na ₂ (THF) ₄]	45
15	<i>closo</i> -1-TMSCH ₂ -2-Me-1,2-C ₂ B ₁₀ H ₁₀	47
16	<i>closo</i> - μ -1,2-Me ₂ Si(CH ₂) ₂ -1,2-C ₂ B ₁₁ H ₁₁	47
17a	<i>closo</i> -1,2-Me ₂ -1,2-C ₂ B ₁₁ H ₁₁	49
17b	<i>closo</i> -1,12-Me ₂ -1,12-C ₂ B ₁₁ H ₁₁	49
18b	<i>closo</i> -1-HOSiMe ₂ CH ₂ -12-Me-1,12-C ₂ B ₁₁ H ₁₁	51
18b'	<i>closo</i> -1,1'-O(Me ₂ SiCH ₂) ₂ -12,12'-Me ₂ - (1,12-C ₂ B ₁₁ H ₁₁) ₂	51
18b''	<i>closo</i> -1-TfOMe ₂ SiCH ₂ -12-Me-1,12-C ₂ B ₁₁ H ₁₁	51
19	<i>closo</i> -4-(<i>p</i> -cymene)- μ -1,2-(CH ₂) ₃ -4,1,2-RuC ₂ B ₁₀ H ₁₀	52
20	<i>closo</i> -1-TMSCH ₂ -12-Me-1,12-C ₂ B ₁₁ H ₁₁	57

21a	<i>closo</i> -4-(<i>p</i> -cymene)-1-TMSCH ₂ -2-Me- 4,1,2-RuC ₂ B ₁₀ H ₁₀	61
21b	<i>closo</i> -4-(<i>p</i> -cymene)-1-TMSCH ₂ -6-Me- 4,1,6-RuC ₂ B ₁₀ H ₁₀	61
[23][Na ₂ - (THF) ₄]	<i>nido</i> -[μ -1,2-Me ₂ Si(CH ₂) ₂ -1,2-C ₂ B ₁₁ H ₁₁]- [Na ₂ (THF) ₄]	66
[24][Na ₂ - (THF) ₄]	<i>nido</i> -[μ -1,2-(CH ₂) ₄ -1,2-C ₂ B ₁₁ H ₁₁][Na ₂ (THF) ₄]	66
[25][Na ₂ - (THF) ₄]	<i>nido</i> -[μ -1,2-MeCH(CH ₂) ₂ -1,2-C ₂ B ₁₁ H ₁₁]- [Na ₂ (THF) ₄]	66
[26a][Na ₂ - (THF) ₄]	<i>nido</i> -[1,2-Me ₂ -1,2-C ₂ B ₁₁ H ₁₁][Na ₂ (THF) ₄]	66
[26b][Na ₂ - (THF) ₄]	<i>nido</i> -[1,3-Me ₂ -1,3-C ₂ B ₁₁ H ₁₁][Na ₂ (THF) ₄]	66
28a	<i>closo</i> - μ -2,3-Me ₂ Si(CH ₂) ₂ -2,3-C ₂ B ₁₂ H ₁₂	73
28b	<i>closo</i> - μ -2,8-Me ₂ Si(CH ₂) ₂ -2,8-C ₂ B ₁₂ H ₁₂	73
29a	<i>closo</i> - μ -2,3-(CH ₂) ₄ -2,3-C ₂ B ₁₂ H ₁₂	73
29b	<i>closo</i> - μ -2,8-(CH ₂) ₄ -2,8-C ₂ B ₁₂ H ₁₂	73
30a	<i>closo</i> -2,3-Me ₂ -2,3-C ₂ B ₁₂ H ₁₂	74
30b	<i>closo</i> -2,8-Me ₂ -2,8-C ₂ B ₁₂ H ₁₂	74
30c	<i>closo</i> -2,4-Me ₂ -2,4-C ₂ B ₁₂ H ₁₂	75
30d	<i>closo</i> -2,9-Me ₂ -2,9-C ₂ B ₁₂ H ₁₂	76
31	<i>closo</i> -4-O(CH ₂) ₄ Br-1,12-Me ₂ -1,12-C ₂ B ₁₁ H ₁₀	75
32a	<i>closo</i> -1-(<i>p</i> -cymene)- μ -2,3-Me ₂ Si(CH ₂) ₂ - 1,2,3-RuC ₂ B ₁₁ H ₁₁	81
32b	<i>closo</i> -1-(<i>p</i> -cymene)- μ -2,8-Me ₂ Si(CH ₂) ₂ - 1,2,8-RuC ₂ B ₁₁ H ₁₁	81
33	<i>closo</i> -1-(<i>p</i> -cymene)-2,9-Me ₂ -1,2,9-RuC ₂ B ₁₁ H ₁₁	82

[34a][Na ₂ - (THF) ₄]	<i>nido</i> -[μ -2,3-Me ₂ Si(CH ₂) ₂ -2,3-C ₂ B ₁₂ H ₁₂]- [Na ₂ (THF) ₄]	85
34b][Na ₂ - (THF) ₄]	<i>nido</i> -[μ -1,2-Me ₂ Si(CH ₂) ₂ -1,2-C ₂ B ₁₂ H ₁₂]- [Na ₂ (THF) ₄]	85
35	<i>closo</i> -7-(<i>p</i> -cymene)- μ -1,4-Me ₂ Si(CH ₂) ₂ - 7,1,4-RuC ₂ B ₁₂ H ₁₂	85
[36a][Me ₃ NH]	<i>closo</i> -[μ -1,2-(CH ₂) ₃ CH(OMe)-1-CB ₁₁ H ₁₀][Me ₃ NH]	89
[36b][Me ₃ NH]	<i>closo</i> -[μ -1,2-(CH ₂) ₂ CH(OMe)CH ₂ -1-CB ₁₁ H ₁₀]- [Me ₃ NH]	89
[36i']][PSH]	<i>nido</i> -[μ - η : η : η -7,8,10-(CH ₂) ₃ CHB(OMe)- 7-CB ₁₀ H ₁₀][PSH]	114
[37][Me ₃ NH]	<i>closo</i> -[μ -1,2-(CH ₂) ₂ CH=CH-1-CB ₁₁ H ₁₀][Me ₃ NH]	90
[37][PSH]	<i>closo</i> -[μ -1,2-(CH ₂) ₂ CH=CH-1-CB ₁₁ H ₁₀][PSH]	107
[38a][Me ₃ NH]	<i>closo</i> -[μ -1,2-(CH ₂) ₃ CH(OEt)-1-CB ₁₁ H ₁₀][Me ₃ NH]	92
[38b][Me ₃ NH]	<i>closo</i> -[μ -1,2-(CH ₂) ₂ CH(OEt)CH ₂ -1-CB ₁₁ H ₁₀]- [Me ₃ NH]	92
39	<i>closo</i> - μ -1,2-(CH ₂) ₃ CH(N ^t BuH ₂)-1-CB ₁₁ H ₁₀	98
40a	<i>closo</i> - μ -1,2-(CH ₂) ₃ CH(NEt ₂ H)-1-CB ₁₁ H ₁₀	98
40b	<i>closo</i> - μ -1,2-(CH ₂) ₂ CH(NEt ₂ H)CH ₂ -1-CB ₁₁ H ₁₀	128
40i	<i>nido</i> -[μ - η : η : η -7,8,10-(CH ₂) ₃ CHB(NEt ₂)- 7-CB ₁₀ H ₁₀][H(NEt ₂ H)]	114
[40i']][PPN]	<i>nido</i> -[μ - η : η : η -7,8,10-(CH ₂) ₃ CHB(NEt ₂)- 7-CB ₁₀ H ₁₀][PPN]	115
41	<i>closo</i> - μ -1,2-(CH ₂) ₃ CH(PPh ₃)-1-CB ₁₁ H ₁₀	98
[42][PPN]	<i>closo</i> -[μ -1,2-(CH ₂) ₃ CHS(4-MeC ₆ H ₄)-1-CB ₁₁ H ₁₀]- [PPN]	100
[43][NMe ₄]	<i>closo</i> -[μ -1,2-(CH ₂) ₄ -1-CB ₁₁ H ₁₀][NMe ₄]	101
[43][Na(18- crown-6)(THF) ₂]	<i>closo</i> -[μ -1,2-(CH ₂) ₄ -1-CB ₁₁ H ₁₀]- [Na(18-crown-6)(THF) ₂]	101

[44][PPN]	<i>closo</i> -[μ -1,2-CH(CH ₂) ₂ -1,2-C ₂ B ₁₁ H ₁₁][PPN]	102
[45][PPN]	<i>closo</i> -[μ -1,2-CH(CH ₂) ₃ -1,2-C ₂ B ₁₁ H ₁₁][PPN]	102
46a	<i>closo</i> - μ -1,2-(CH ₂) ₃ CH(NEt ₃)-1-CB ₁₁ H ₁₀	105
46b	<i>closo</i> - μ -1,2-(CH ₂) ₂ CH(NEt ₃)CH ₂ -1-CB ₁₁ H ₁₀	105
47b	<i>closo</i> -1,2-(CH ₂) ₂ CH(4',5'-H(Me ₂ N) ₂ -C ₁₀ H ₅)CH ₂ -1-CB ₁₁ H ₁₀	107
[48][PSH]	<i>nido</i> -[<i>endo</i> - μ -7,8-(CH ₂) ₃ CHB(OMe) ₂ -7-CB ₁₀ H ₁₁]-[PSH]	132
[48'] [PSH]·THF	<i>nido</i> -[<i>endo</i> - μ -7,8-(CH ₂) ₃ CHB(OH) ₂ -7-CB ₁₀ H ₁₁]-[PSH]·THF	142
[49][Et ₃ NH]	<i>nido</i> -[3-OMe- μ -1,2-(CH ₂) ₄ -1,2-C ₂ B ₁₁ H ₁₁][Et ₃ NH]	136
[49][PSH]	<i>nido</i> -[3-OMe- μ -1,2-(CH ₂) ₄ -1,2-C ₂ B ₁₁ H ₁₁][PSH]	137
[50][PSH]	<i>nido</i> -[<i>endo</i> - μ -7,8-(CH ₂) ₄ CHB(OMe) ₂ -7-CB ₁₀ H ₁₁]-[PSH]	137
[50'] [PSH]	<i>nido</i> -[<i>endo</i> - μ -7,8-(CH ₂) ₄ CHB(OH) ₂ -7-CB ₁₀ H ₁₁]-[PSH]	142
[51][PSH]	<i>nido</i> -[<i>endo</i> - μ -7,8-(CH ₂) ₃ CHOH-7-CB ₁₀ H ₁₁][PSH]	140
[52][PSH]	<i>nido</i> -[<i>endo</i> - μ -7,8-(CH ₂) ₄ CHOH-7-CB ₁₀ H ₁₁][PSH]	140
53a	<i>closo</i> - μ -1,2-(CH ₂) ₃ CH(NC ₅ H ₅)-1-CB ₁₁ H ₁₀	144
53b	<i>closo</i> - μ -1,2-(CH ₂) ₂ CH(NC ₅ H ₅)CH ₂ -1-CB ₁₁ H ₁₀	144
54	<i>closo</i> - μ -2,4-(CH ₂) ₃ CHBH(C ₅ H ₅ N) ₂ -2-CB ₁₀ H ₉	145
55	<i>closo</i> - μ -2,4-(CH ₂) ₃ CHBH(MeC ₅ H ₄ N) ₂ -2-CB ₁₀ H ₉	145
56	<i>closo</i> - μ -2,4-(CH ₂) ₃ CHBH(^t BuC ₅ H ₄ N) ₂ -2-CB ₁₀ H ₉	145
57a	<i>closo</i> - μ -1,2-(CH ₂) ₃ CH(MeC ₅ H ₄ N)-1-CB ₁₁ H ₁₀	149
57b	<i>closo</i> - μ -1,2-(CH ₂) ₂ CH(MeC ₅ H ₄ N)CH ₂ -1-CB ₁₁ H ₁₀	150
58a	<i>closo</i> - μ -1,2-(CH ₂) ₃ CH(^t BuC ₅ H ₄ N)-1-CB ₁₁ H ₁₀	149
58b	<i>closo</i> - μ -1,2-(CH ₂) ₂ CH(^t BuC ₅ H ₄ N)CH ₂ -1-CB ₁₁ H ₁₀	150
59	<i>closo</i> -4-(2,2'-C ₁₀ H ₈ N ₂ B)- μ -1,2-(CH ₂) ₃ -1,2-C ₂ B ₁₀ H ₉	152

60	<i>closo</i> -4-(2,2'-C ₁₀ H ₈ N ₂ B)- μ -1,2-(CH ₂) ₄ -1,2-C ₂ B ₁₀ H ₉	152
61	<i>closo</i> -4-(4',7'-2 <i>H</i> -1',10'-C ₁₀ H ₈ N ₂ B)- μ -1,2-(CH ₂) ₃ -1,2-C ₂ B ₁₀ H ₉	155
62	<i>closo</i> -4-(4',7'-2 <i>H</i> -1',10'-C ₁₀ H ₈ N ₂ B)- μ -1,2-(CH ₂) ₄ -1,2-C ₂ B ₁₀ H ₉	155
[64][PSH]	<i>closo</i> -[μ -1,2-(CH ₂) ₃ CH(CH ₂ OMe)-1-CB ₁₁ H ₁₀]-[PSH]	164
[65][PSH]	<i>closo</i> -[μ -1,2-(CH ₂) ₅ -1-CB ₁₁ H ₁₀][PSH]	164
[67][PPN]	<i>closo</i> -[μ -1,2-(CH ₂) ₄ CHS(4-MeC ₆ H ₄)-1-CB ₁₁ H ₁₀]-[PPN]	168
68	<i>nido</i> -3-NEt ₂ H- μ -1,7-(CH ₂) ₄ -1,7-C ₂ B ₁₁ H ₁₁	170
[69][PPN]	<i>nido</i> -[9-NMe ₂ - μ -7,8,10-(CH ₂) ₄ CCH-B ₁₁ H ₁₀][PPN]	172
[70][PPN]	<i>nido</i> -[9-NEt ₂ - μ -7,8,10-(CH ₂) ₄ CCH-B ₁₁ H ₁₀][PPN]	172
[71a][Me ₃ NH]	<i>closo</i> -[1-Me-2-MeCH(OMe)-1-CB ₁₁ H ₁₀][Me ₃ NH]	176
[72][Me ₃ NH]	<i>closo</i> -[1-Me-2-CH ₂ =CH-1-CB ₁₁ H ₁₀][Me ₃ NH]	176
2-D-73	<i>closo</i> -1-Me-2-D-1,2-C ₂ B ₁₀ H ₁₀	179
[74][PPN]	<i>nido</i> -[7-Me-7,8-C ₂ B ₉ H ₁₁][PPN]	180
[75][PPN]	<i>closo</i> -[1-Me-2-HBMeS(4-MeC ₆ H ₄)-1,2-C ₂ B ₁₀ H ₁₀]-[PPN]	182
76	<i>closo</i> -1-Me-2-HBMe-1,2-C ₂ B ₁₀ H ₁₀	182
[77][Na(18-crown-6)(H ₂ O)]	<i>closo</i> -[1-Me-7-Et-1-CB ₁₁ H ₁₀]-[Na(18-crown-6)(H ₂ O)]	184
[78][PPN]	<i>arachno</i> -[C,C',N,N'-Me ₄ -NC ₂ B ₁₁ H ₁₁][PPN]	187
79	<i>closo</i> -8-BH ₃ PPh ₂ -1,2-Me ₂ -1,2-C ₂ B ₁₀ H ₉	190
[80][Me ₃ NH]	<i>nido</i> -[11,12-BH(OMe)-8,9-(CH ₂) ₃ -8,9-C ₂ B ₁₁ H ₁₁]-[Me ₃ NH]	193
[81][(Me ₃ NH) ₂ Cl]	<i>nido</i> -[8,9-(CH ₂) ₃ -8,9-C ₂ B ₁₁ H ₁₂][(Me ₃ NH) ₂ Cl]	196

List of Figures

Fig. No.	Compd. No.	Content	Page No.
2.1	4	Molecular structure of μ -1,2-MeCH(CH ₂) ₂ -1,2-C ₂ B ₁₀ H ₁₀ .	29
2.2	5a 5b	Molecular structures of 3-Ph- μ -1,2-(CH ₂ CH=CHCH ₂)-1,2-C ₂ B ₁₁ H ₁₀ (left) and 3-Ph- μ -1,2-(CH=CHCH ₂ CH ₂)-1,2-C ₂ B ₁₁ H ₁₀ (right).	30
2.3	6	Molecular structure of μ -1,2-(CH ₂) ₄ -1,2-C ₂ B ₁₁ H ₁₁ .	32
2.4	7	Molecular structure of μ -1,2-(CH ₂) ₄ -1,2-C ₂ B ₁₁ H ₁₁ .	32
2.6	7'	Molecular structure of 3-Me- μ -1,2-(CH ₂) ₄ -1,2-C ₂ B ₁₁ H ₁₀ .	34
2.7		Molecular structure of [Me ₃ S]Br.	34
2.11	[12a][Na ₄ (THF) ₁₂]	Molecular structure of [7,7'-(CH ₂ CH ₂)-9,9'-Me ₂ -7,7',9,9'-(C ₂ B ₁₀ H ₁₀) ₂][Na ₄ (THF) ₁₂]. The THF molecules are omitted.	44
2.12	[12b][Na ₂ (18-crown-6)]	Two-dimensional polymeric structure of [μ -7,8-O(CH ₂) ₂ -7,8-C ₂ B ₉ H ₉][Na ₂ (18-crown-6)].	44
2.13	[14] ²⁻	Structure of [μ -7,10-O(Me ₂ Si) ₂ -7,10-C ₂ B ₁₀ H ₁₀] ²⁻ , in [14][Na ₂ (THF) ₄].	46
2.14	16	Molecular structure of μ -1,2-Me ₂ Si(CH ₂) ₂ -1,2-C ₂ B ₁₁ H ₁₁ .	48
2.15	17a	Molecular structure of 1,2-Me ₂ -1,2-C ₂ B ₁₁ H ₁₁ .	50
2.16	19	Molecular structure of 4-(<i>p</i> -cymene)- μ -1,2-Me ₂ Si(CH ₂) ₂ -4,1,2-RuC ₂ B ₁₀ H ₁₀ .	53
2.17	11	Molecular structure of μ -1,2-Me ₂ Si(CH ₂) ₂ -1,2-C ₂ B ₁₀ H ₁₀ .	55
2.20	20	Molecular structure of 1-TMSCH ₂ -12-Me-1,12-C ₂ B ₁₁ H ₁₁ .	59
2.21	21a	Molecular structure of 4-(<i>p</i> -cymene)-1-TMSCH ₂ -2-Me-4,1,2-RuC ₂ B ₁₀ H ₁₀ .	62

2.22	21b	Molecular structure of 4-(<i>p</i> -cymene)-1-TMSCH ₂ -6-Me-4,1,6-RuC ₂ B ₁₀ H ₁₀ .	63
3.2	[23] ²⁻	Structure of [μ -1,2-Me ₂ Si(CH ₂) ₂ -1,2-C ₂ B ₁₁ H ₁₁] ²⁻ , in [23][Na ₂ (THF) ₄].	68
3.3	[26a] ²⁻ [26b] ²⁻	Structure of [1,2-Me ₂ -1,2-C ₂ B ₁₁ H ₁₁] ²⁻ in [26a][Na ₂ - (THF) ₄] (left) and [1,3-Me ₂ -1,3-C ₂ B ₁₁ H ₁₁] ²⁻ in [26b][Na ₂ (THF) ₄] (right).	69
3.4	[26a] ²⁻ [26b] ²⁻	Na ⁺ ···H-B interactions in the one dimensional poly- meric chains of [1,2-Me ₂ -1,2-C ₂ B ₁₁ H ₁₁][Na ₂ (THF) ₄] (top) and [1,3-Me ₂ -1,3-C ₂ B ₁₁ H ₁₁][Na ₂ (THF) ₄] (bot- tom). The THF molecules are omitted.	70
3.6	27a	Molecular structure of μ -2,3-(CH ₂) ₃ -2,3-C ₂ B ₁₂ H ₁₂ , in 27a·C ₁₀ H ₈ .	77
3.7	28a	Molecular structure of μ -2,3-Me ₂ Si(CH ₂) ₂ -2,3-C ₂ B ₁₂ H ₁₂ .	78
3.8	28b	Molecular structure of μ -2,8-Me ₂ Si(CH ₂) ₂ -2,8-C ₂ B ₁₂ H ₁₂ .	78
3.9	29b	Molecular structure of μ -2,8-(CH ₂) ₄ -2,8-C ₂ B ₁₂ H ₁₂ .	78
3.10	30d	Molecular structure of 2,9-Me ₂ -2,9-C ₂ B ₁₂ H ₁₂ .	79
3.11	32a	Molecular structure of 1-(<i>p</i> -cymene)- μ -2,3-Me ₂ Si(CH ₂) ₂ -1,2,3-RuC ₂ B ₁₁ H ₁₁ .	83
3.12	33	Molecular structure of 1-(<i>p</i> -cymene)-2,9-Me ₂ -1,2,9-RuC ₂ B ₁₁ H ₁₁ .	83
3.14	35	Molecular structure of 7-(<i>p</i> -cymene)- 1,4-Me ₂ Si(CH ₂) ₂ -7,1,4-RuC ₂ B ₁₂ H ₁₂ , in 35·CH ₂ Cl ₂ .	87
4.1	[36a] ⁻	Structure of [μ -1,2-(CH ₂) ₃ CH(OMe)-1-CB ₁₁ H ₁₀] ⁻ , in [36a][Me ₃ NH].	91
4.2	[36b] ⁻	Structure of [μ -1,2-(CH ₂) ₂ CH(OMe)CH ₂ -1-CB ₁₁ H ₁₀] ⁻ , in [36b][Me ₃ NH].	91
4.3	[38a] ⁻	Structure of [μ -1,2-(CH ₂) ₃ CH(OEt)-1-CB ₁₁ H ₁₀] ⁻ , in [38a][Me ₃ NH].	96
4.4	[37] ⁻	Structure of [μ -1,2-(CH ₂) ₂ CH=CH-1-CB ₁₁ H ₁₀] ⁻ , in [37][Me ₃ NH].	96
4.5	39	Molecular structure of μ -1,2-(CH ₂) ₃ CH(N ^t BuH ₂)-1-CB ₁₁ H ₁₀ .	99

4.6	40a	Molecular structure of μ -1,2-(CH ₂) ₃ CH(NEt ₂ H)-1-CB ₁₁ H ₁₀ .	99
4.7	41	Molecular structure of μ -1,2-(CH ₂) ₃ CH(PPh ₃)-1-CB ₁₁ H ₁₀ , in 41·CH ₂ Cl ₂ .	100
4.8	[43] ⁻	Structure of [μ -1,2-(CH ₂) ₄ -1-CB ₁₁ H ₁₀] ⁻ , in [43][Me ₄ N].	100
4.9	[44] ⁻	Structure of [μ -1,2-(CH ₂) ₂ CH-1,2-C ₂ B ₁₁ H ₁₁] ⁻ , in [44][PPN].	103
4.10	[45] ⁻	Structure of [μ -1,2-(CH ₂) ₂ CH-1,2-C ₂ B ₁₁ H ₁₁] ⁻ , in [45][PPN].	104
4.12	46a	Molecular structure of μ -1,2-(CH ₂) ₃ CH(NEt ₃)-1-CB ₁₁ H ₁₀ .	106
4.13	46b	Molecular structure of μ -1,2-(CH ₂) ₂ CH(NEt ₃)CH ₂ -1-CB ₁₁ H ₁₀ .	107
4.14	47b	Molecular structure of μ -1,2-(CH ₂) ₂ CH(4'-C ₁₀ H ₅ -1',8'-(NMe ₂) ₂ H)CH ₂ -1-CB ₁₁ H ₁₀ .	108
4.15	[37][PSH]	Molecular structure of [μ -1,2-(CH ₂) ₂ CH=CH-1-CB ₁₁ H ₁₀][PSH].	109
4.18	[36i' ⁻	Structure of [μ - η : η : η -7,8,10-(CH ₂) ₃ CHB(OMe)-7-CB ₁₀ H ₁₀] ⁻ , in [36i' ⁻][PSH].	116
4.19	[40i' ⁻	Structure of [μ - η : η : η -7,8,10-(CH ₂) ₃ CHB(NEt ₂)-7-CB ₁₀ H ₁₀] ⁻ , in [40i' ⁻][PPN], showing one of the two crystallographic independent molecules.	116
5.1	[48] ⁻	Structure of [<i>endo</i> - μ -7,8-(CH ₂) ₃ CHB(OMe) ₂ -7- <i>nido</i> -CB ₁₀ H ₁₁] ⁻ , in [48][PSH].	133
5.2	[49] ⁻	Structure of [3-OMe- μ -1,2-(CH ₂) ₄ -1,2-C ₂ B ₁₁ H ₁₁] ⁻ , in [49][PSH].	138
5.3	[50] ⁻	Structure of [<i>endo</i> - μ -7,8-(CH ₂) ₄ CHB(OMe) ₂ -7-CB ₁₀ H ₁₁] ⁻ , in [50][PSH].	139
5.5	[51] ⁻	Structure of [<i>endo</i> - μ -7,8-(CH ₂) ₃ CHOH-7-CB ₁₀ H ₁₁] ⁻ , in [51][PSH].	141
5.6	[52] ⁻	Structure of [<i>endo</i> - μ -7,8-(CH ₂) ₄ CHOH-7-CB ₁₀ H ₁₁] ⁻ , in [52][PSH].	142

5.7	[48']	Dimeric structure of [$\{endo-\mu-7,8-(CH_2)_3CHB(OH)_2-7-CB_{10}H_{11} \cdot THF\}_2\}^{2-}$ (left) and monomeric unit of [48'] (right), in [48'] [PSH] \cdot THF.	143
5.9	54	Molecular structure of $\mu-2,4-(CH_2)_3CHBH(C_5H_5N)_2-2-CB_{10}H_9$.	146
5.10	55	Molecular structure of $\mu-2,4-(CH_2)_3CHBH(CH_3C_5H_4N)_2-2-CB_{10}H_9$.	147
5.11	56	Molecular structure of $\mu-2,4-(CH_2)_3CHBH(tBuC_5H_4N)_2-2-CB_{10}H_9$, showing one of two crystallographically independent molecules.	148
5.12	53a	Molecular structure of $\mu-1,2-(CH_2)_3CH(NC_5H_5)-1-CB_{11}H_{10}$.	149
5.14	57a	Molecular structure of $\mu-1,2-(CH_2)_3CH(MeC_5H_4N)-1-CB_{11}H_{10}$, in 57a \cdot CH ₂ Cl ₂ .	150
5.16	59	Molecular structure of 4-(2,2'-C ₁₀ H ₈ N ₂ B)- $\mu-1,2-(CH_2)_3-1,2-C_2B_{10}H_9$, showing one of the crystallographically independent molecules.	154
5.17	60	Molecular structure of 4-(2,2'-C ₁₀ H ₈ N ₂ B)- $\mu-1,2-(CH_2)_4-1,2-C_2B_{10}H_9$.	156
5.19	61	Molecular structure of 4-(4',7'-2H-1',10'-C ₁₀ H ₈ N ₂ B)- $\mu-1,2-(CH_2)_3-1,2-C_2B_{10}H_9$, showing one of the crystallographically independent molecules.	158
5.20	62	Molecular structure of 4-(4',7'-2H-1',10'-C ₁₀ H ₈ N ₂ B)- $\mu-1,2-(CH_2)_4-1,2-C_2B_{10}H_9$, showing one of the crystallographically independent molecules.	159
6.3	[65]	Structure of [$\mu-1,2-(CH_2)_5-1-CB_{11}H_{10}$], in [65] [PSH], showing one of the two crystallographic independent molecules.	166
6.4	[67]	Structure of [$\mu-1,2-(CH_2)_4CHS(4-MeC_6H_4)-1-CB_{11}H_{10}$], in [67] [PPN] \cdot THF.	169
6.5	68	Molecular structure of 3-NEt ₂ H- $\mu-1,7-(CH_2)_4-1,7-C_2B_{11}H_{11}$ (68).	171
6.7	[69]	Structure of [9-NMe ₂ - $\mu-7,8,10-(CH_2)_4CCH-B_{11}H_{10}$], in [69] [PPN].	173
6.8	[70]	Structure of [9-NEt ₂ - $\mu-7,8,10-(CH_2)_4CCH-B_{11}H_{10}$], in [70] [PPN].	174

6.10	[71a] ⁻	Structure of [1-Me-2-CH(OMe)Me-1-CB ₁₁ H ₁₀] ⁻ , in [71a][Me ₃ NH].	178
6.11	[72] ⁻	Structure of [1-Me-2-CH ₂ =CH-1-CB ₁₁ H ₁₀] ⁻ , in [72][Me ₃ NH].	178
6.13	[74] ⁻	Structure of [7-Me-7,8-C ₂ B ₉ H ₁₁] ⁻ , in [74][PPN].	181
6.16	[77] ⁻	Structure of [1-Me-7-Et-1-CB ₁₁ H ₁₀] ⁻ , in [77][Na(18-crown-6)(H ₂ O)], showing one of the two crystallographically independent molecules.	185
6.17	[78] ⁻	Structure of [C,C',N,N'-Me ₄ -NC ₂ B ₁₁ H ₁₁] ⁻ , in [78][PPN].	188
6.20	79	Molecular structure of 8-BH ₃ PPh ₂ -1,2-Me ₂ -1,2-C ₂ B ₁₀ H ₉ (79).	191
6.21	[80] ⁻	Structure of [μ-8,9-(CH ₂) ₃ -μ-11,12-BH(OMe)-8,9-C ₂ B ₁₁ H ₁₁] ⁻ , in [80][Me ₃ NH], showing one of the two crystallographically independent molecules.	195
6.22	[81] ⁻	Structure of [μ-8,9-(CH ₂) ₃ -8,9-C ₂ B ₁₁ H ₁₂] ⁻ , in [81][(Me ₃ NH) ₂ Cl], showing one of the two crystallographically independent molecules.	196

Contents

Acknowledgement	I
Abstract (in English)	II
Abstract (in Chinese)	IV
Abbreviation	VI
List of Compounds	VIII
List of Figures	XIII
Contents	XVIII
Chapter 1. Introduction	1
1.1. Carboranes	1
1.1.1. Synthesis	2
1.1.2. C-Derivatization	4
1.1.3. B-Derivatization	6
1.1.4. Degradation	6
1.1.5. Reduction	8
1.2. Metallocarboranes Based on Icosahedral Carboranes	9
1.2.1. MC_2B_{10}	10
1.2.2. MC_2B_{10} bearing <i>arachno</i> - C_2B_{10} unit	12
1.2.3. $M_2C_2B_{10}$	13
1.3. Supercarboranes and Supermetallocarboranes	13
1.3.1. Synthesis of CAd 13-Vertex Carboranes	15
1.3.2. Electrophilic Substitution Reaction of CAd 13-Vertex Carborane	16
1.3.3. Redox Reaction of CAd 13-Vertex Carboranes	17
1.3.4. Synthesis of 14-Vertex Metallocarboranes	21
1.3.5. Synthesis of 14-Vertex Carboranes	22

1.3.6. Reduction of 14-Vertex Carboranes and Synthesis of 15-Vertex Metallocarboranes	25
1.4. Objectives	27
Chapter 2. Synthesis and Structure of 13-Vertex <i>closo</i>-Carboranes	28
2.1. Synthesis and Structure of CAd 13-Vertex <i>closo</i> -Carboranes	28
2.1.1. Synthesis of CAd 13-Vertex <i>closo</i> -Carboranes	28
2.1.2. Structural and NMR Feature of CAd 13-Vertex <i>closo</i> -Carboranes	34
2.2. Synthesis and Structure of CAp 13-Vertex <i>closo</i> -Carboranes and <i>closo</i> -Metallocarboranes	41
2.2.1. Screening the Ligand	41
2.2.2. Synthesis of μ -1,2-Me ₂ Si(CH ₂) ₂ -1,2-C ₂ B ₁₁ H ₁₁ and Unprecedented C-Si Bond Cleavage	47
2.2.3. Direct Synthesis of 13-Vertex CAp Carboranes and Structural Characterization	56
2.3. Summary	63
Chapter 3. Synthesis and Structure of <i>closo</i>-Carboranes and <i>closo</i>-Metallocarboranes with More than 13 Vertices	65
3.1. Synthesis and Characterization of 13-Vertex <i>nido</i> -Carborane Dianions	65
3.1.1. Synthesis	65
3.1.2. Characterization	68
3.2. Synthesis and Structure of 14-Vertex Carboranes	73
3.2.1 Synthesis	73
3.2.2. Characterization	77
3.3. Synthesis and Structure of 14-Vertex Ruthenacarboranes	81
3.4. Reduction of 14-Vertex Carboranes and Synthesis of a 15-Vertex Ruthenacarborane	85
3.5. Summary	87
Chapter 4. Cage Carbon Extrusion Reaction of CAd 13-Vertex Carborane μ-1,2-(CH₂)₃-1,2-C₂B₁₁H₁₁	89

4.1. Reaction of μ -1,2-(CH ₂) ₃ -1,2-C ₂ B ₁₁ H ₁₁ with Alcohols	89
4.2. Reaction of μ -1,2-(CH ₂) ₃ -1,2-C ₂ B ₁₁ H ₁₁ with ^t BuNH ₂ , Et ₂ NH, PPh ₃ , (4-MeC ₆ H ₄)SNa and NaBH ₄	98
4.3. Reaction of μ -1,2-(CH ₂) ₃ -1,2-C ₂ B ₁₁ H ₁₁ with NaH—Unprecedented Deprotonation of α -CH	101
4.4. Unusual Reaction of μ -1,2-(CH ₂) ₃ -1,2-C ₂ B ₁₁ H ₁₁ with Tertiary Amines	105
4.5. Mechanistic Study of Carbon-Extrusion Reaction	111
4.5.1. Reaction Intermediates	112
4.5.2. Formation of the Intermediates	118
4.5.3. Formation of the α -isomer	121
4.5.4. Formation of the β -isomer and alkenyl CB ₁₁ ⁻ anions	127
4.5. Summary	129
Chapter 5. Cage Boron Extrusion Reaction of CAd 13-Vertex Carboranes μ-1,2-(CH₂)_n-1,2-C₂B₁₁H₁₁ ($n = 3, 4$)	131
5.1. Reaction of 13-Vertex Carborane μ -1,2-(CH ₂) _n -1,2-C ₂ B ₁₁ H ₁₁ ($n = 3, 4$) with Basic MeOH	131
5.2. Reaction of 13-Vertex Carborane μ -1,2-(CH ₂) ₃ -1,2-C ₂ B ₁₁ H ₁₁ with Pyridine	143
5.3. Reaction of 13-Vertex Carboranes μ -1,2-(CH ₂) _n -1,2-C ₂ B ₁₁ H ₁₁ ($n = 3, 4$) with Bipyridines	152
5.4. Summary	162
Chapter 6. Nucleophilic Reaction of Other 13- and 14-Vertex Carboranes	163
6.1. Nucleophilic Reaction of 13-Vertex Carborane μ -1,2-(CH ₂) ₄ -1,2-C ₂ B ₁₁ H ₁₁	163
6.1.1. Reaction with Group 16 Nucleophiles	163
6.1.2. Reactions with Nitrogen Nucleophiles	169
6.2. Nucleophilic Reactions of CAp 13-Vertex Carborane 1,12-Me ₂ -1,12-C ₂ B ₁₁ H ₁₁	176
6.2.1. Reaction with Group 16 Nucleophiles	176

6.2.2. Reaction with NaBH ₄ or NaI	184
6.2.3. Reaction with Me ₂ NLi	187
6.2.4. Reaction with Ph ₂ PK	190
6.3. Nucleophilic Reaction of 14-Vertex Carborane μ -(CH ₂) ₃ -C ₂ B ₁₂ H ₁₂	191
6.4. Summary	199
Chapter 7. Conclusion	201
Chapter 8. Experimental Section	205
References	263
Appendix	282
I. Publications Based on the Research Findings	282
II. Crystal Data and Summary of Data Collection and Refinement	283
III. X-ray crystallographic data in CIF (electronic form)	

Chapter 1. Introduction

1.1. Carboranes

Carboranes are boron clusters with at least one carbon atom as part of the polyhedral cage. As the borane analogues, carboranes can be classified as *closo*-, *nido*-, *arachno*- and *hypho*- species, depending on the vertices and electron counting of the cluster. Generally, the *closo*- species adopt closed polyhedral structures with all faces triangulated. The structures of the latter three types can be viewed as sequential removal of one, two, or three vertices from the *closo*- one (Figure 1.1).¹ Of all known carboranes, the neutral *closo*- family with formula $C_2B_nH_{n+2}$ ($n = 3$ to 10) are extensively studied.^{2,3}

More specifically, carboranes refer to the icosahedral ones with formula $C_2B_{10}H_{12}$, or their derivatives. Three isomers exist as the cage carbons take up different positions on the cluster, which are named as *ortho*- (*o*-), *meta*- (*m*-), and *para*- (*p*-) according to the relative positions, or 1,2-, 1,7- and 1,12-, respectively (Figure 1.2). The chemistry of *o*-carboranes has been the most extensively studied,^{2,3a,3c,3e} owing to its commercial availability.

It is noted that in the following figures and schemes, an open circle in the polyhedrons represents a B(H) vertex, a grey circle stands for a boron atom, a black dot is for a carbon atom and a small circle with a centered dot is for a bridging hydrogen. If a vertex contains an atom other than B and C, the heteroatom is shown explicitly.

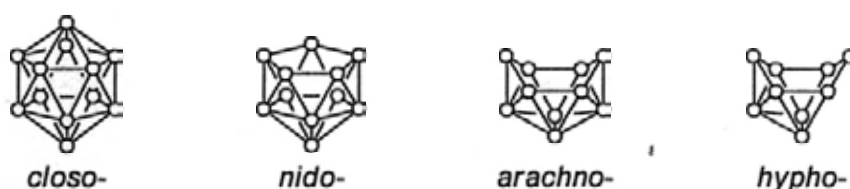


Figure 1.1. Polyhedral framework derived from a 12-vertex icosahedron.

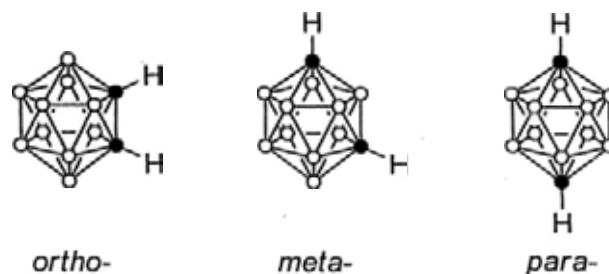
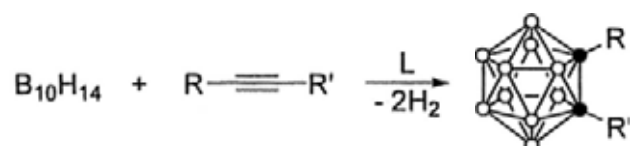


Figure 1.2. Three isomers of $C_2B_{10}H_{12}$.

1.1.1. Synthesis

o-Carboranes have been conveniently synthesized through reaction of alkynes with $6,9-B_{10}H_{12} \cdot L_2$ ($L = R_2S, MeCN$), or a mixture of decaborane (*nido*- $B_{10}H_{14}$) and Lewis base (L), which can in situ generate the $6,9-B_{10}H_{12} \cdot L_2$ (Scheme 1.1).⁴ While terminal alkynes give moderate to good results for this purpose, internal alkynes usually give low yields or even do not work. A recent development was reported by Sneddon to use biphasic toluene/ionic liquids as solvents, showing a remarkable improvement in the isolated yields and reaction time.⁵

Scheme 1.1. Synthesis of *o*-Carboranes from Reaction of *nido*- $B_{10}H_{14}$ with Alkynes.



The *m*- or *p*-carboranes are generally prepared from thermal rearrangement of the *o*-isomers. *o*- $C_2B_{10}H_{12}$ rearranges quantitatively to the *m*-isomer at 465 °C to 500 °C in an inert atmosphere (Scheme 1.2).⁶ The latter compound decomposes above 600 °C with the formation of *p*-carborane as a minor product.⁷ Diamond-square-diamond (*DSD*) process, which is developed by Lipscomb, is the most famous and widely used to account for the isomerization processes of polyhedral boron clusters.⁸ And for that of the icosahedral carboranes, a cuboctahedral intermediate is proposed to be involved (Figure 1.3).⁸ However, it cannot simply explain the *m*- to *p*- trans-

formation, and several other theories have been advanced, such as mutual rotation of pentagonal pyramidal halves of the icosahedral cage,^{6,9} rotation of triangular faces in the icosahedral ground state (*RTF*),¹⁰ a “modified *DSD*” involving rotations of triangles in the cuboctahedral intermediates,¹¹ and a “*DSD* involving *nido*-intermediate”.¹² Earlier experimental or theoretical evidences support an “extended *RTF*” pathway.¹³ A recent theoretical calculation indicates that from *o*- to *m*-C₂B₁₀H₁₂, the lowest free energy pathway is via the “extended *RTF*” mechanism, while from *m*- to *p*-C₂B₁₀H₁₂, the “*DSD* involving *nido*-intermediate” is preferred.¹⁴

Scheme 1.2. Thermal Rearrangement of *o*-Carborane.

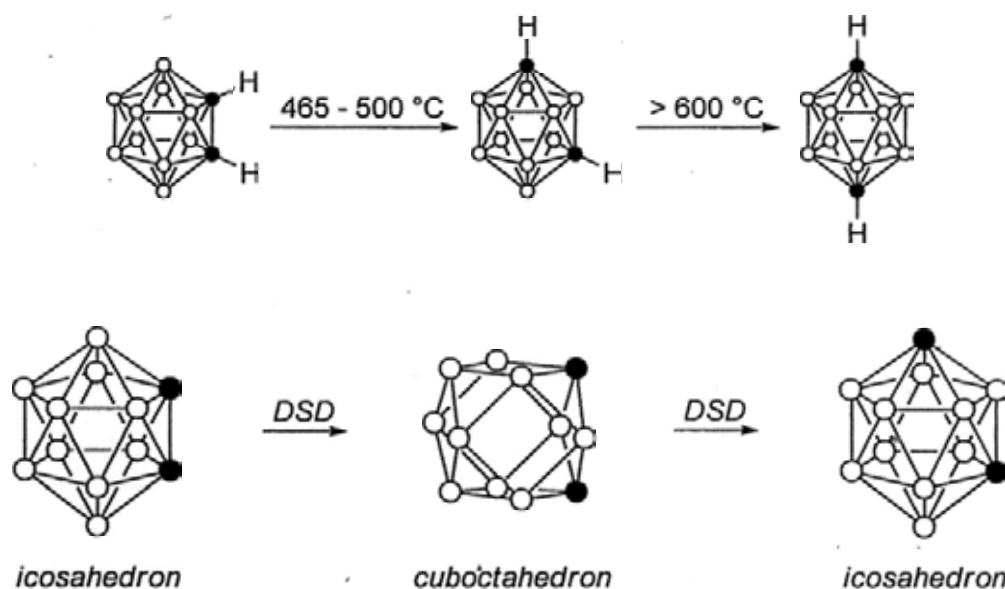
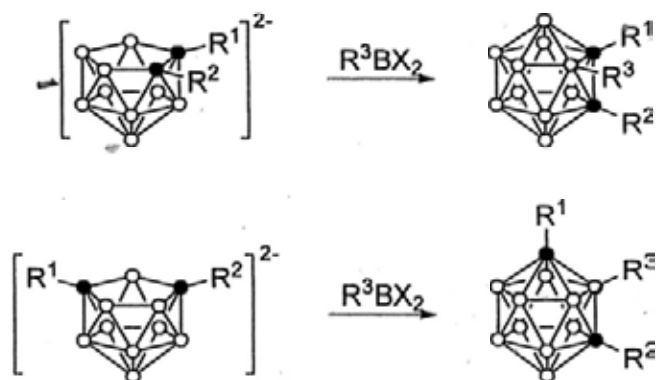


Figure 1.3. *DSD* rearrangement from *o*- to *m*-carborane.

The icosahedral framework of carboranes can also be reconstructed from boron insertion reaction of 11-vertex *nido*-carborane dianions and dihaloborane reagents. This method was first developed by Hawthorne in 1965 and 3-Ph-1,2-C₂B₁₀H₁₁ was synthesized from [7,8-C₂B₉H₁₁]²⁻ with PhBCl₂.¹⁵ It is very useful in the synthesis of 3-substituted *o*-carboranes from 7,8-C₂B₉²⁻, or 2-substituted *m*-carboranes from 7,9-C₂B₉²⁻, which can bear *exo*- B-C (with alkyl or aryl group), B-X (X = F, Br, I), B-O or B-N bonds (Scheme 1.3).¹⁶

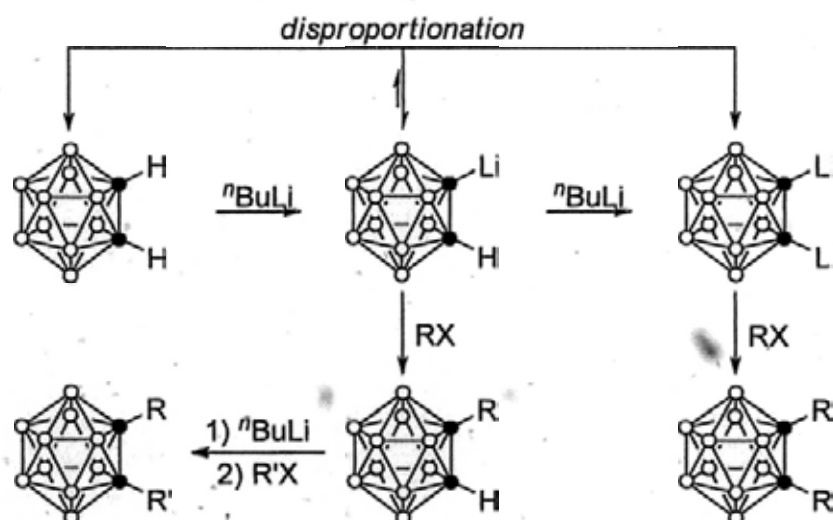
Scheme 1.3. Synthesis of *o*- or *m*-Carboranes via Boron Insertion Reaction.



1.1.2. C-Derivatization

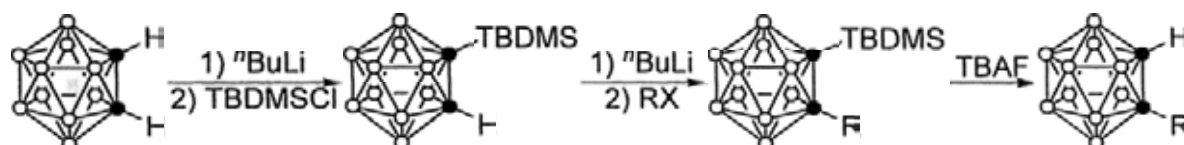
Replacement of hydrogen(s) on the cage carbon(s) of the carborane by other functionalized groups, especially alkyl or aryl substituents, is most conveniently achieved via deprotonation and subsequent nucleophilic substitution. The mildly acidic property of *o*-carborane C-H protons makes the metallation very easy using $n\text{BuLi}$ or PhLi .¹⁷ However, in solutions the mono-lithio species is in equilibrium with the dilithium salt and neutral *o*-carborane. Thus monosubstitution of the *o*-carborane via this route is problematic, as disubstituted carboranes are often generated as side products (Scheme 1.4).¹⁸

Scheme 1.4. Metallation and Functionalization of *o*-Carborane.



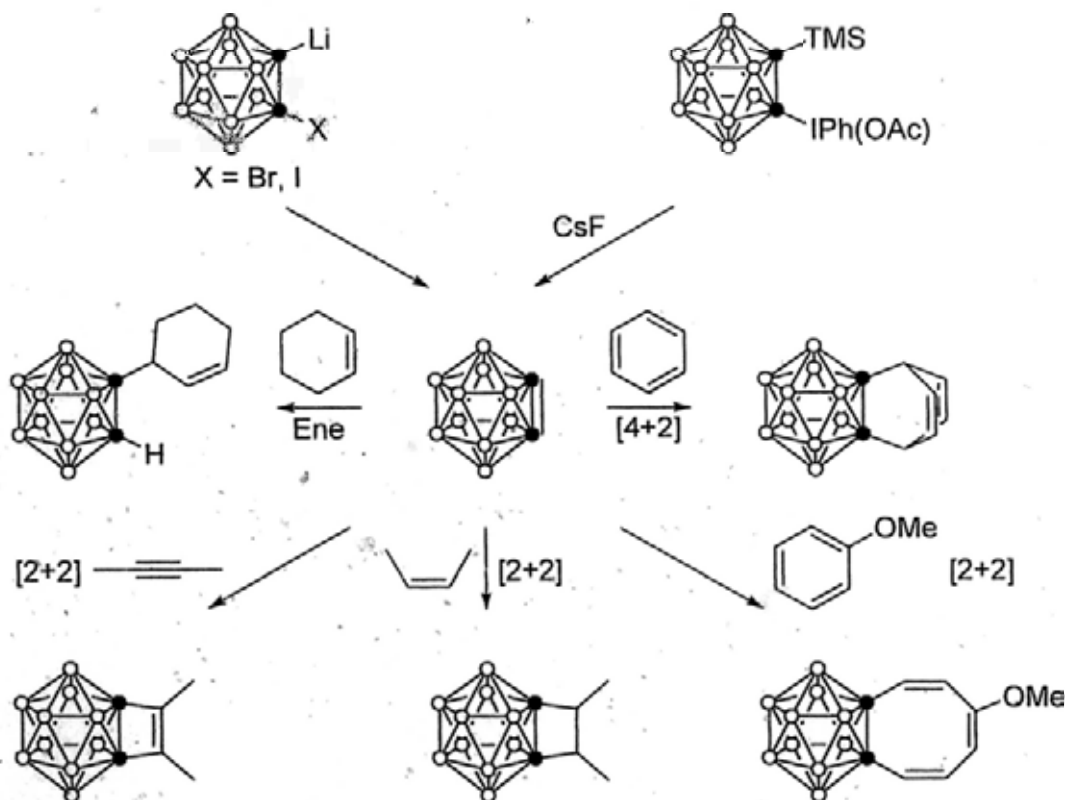
Improvements were reported to prepare monosubstituted carboranes and DME was a better solvent in some cases.¹⁹ Another route for the C-monofunctionalization of *o*-carborane involves the use of a bulky ^tBuMe₂Si (TBDMS) silyl group as a protecting group, which is easily removed with TBAF (Scheme 1.5).²⁰

Scheme 1.5. Synthesis of Monosubstituted Carboranes via Protection.



C-derivatives of *o*-carborane can also be synthesized from carboryne (1,2-dehydro-*o*-carborane). This intermediate is not isolable but can be generated by several methods and captured by unsaturated molecules via [4+2], [2+2] and ene type reactions (Scheme 1.6).²¹ Recently, metal-carboryne complexes have also been developed to synthesize C-substituted *o*-carboranes.^{22,23}

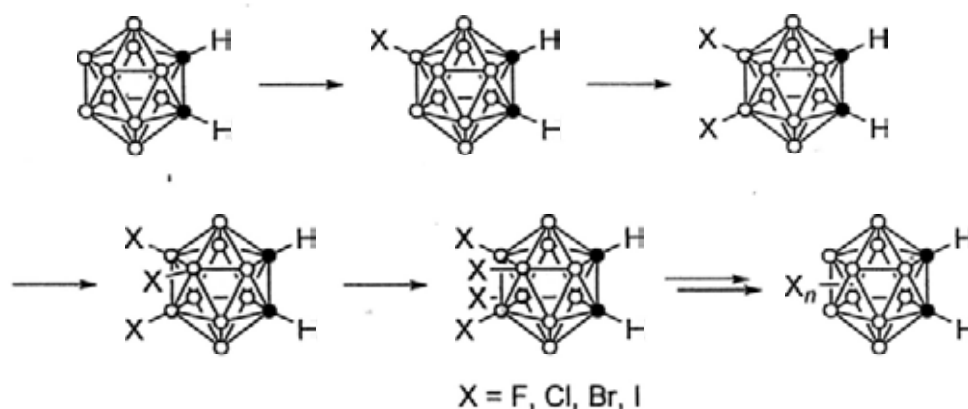
Scheme 1.6. Carboryne Mediated *o*-Carborane Functionalization.



1.1.3. B-Derivatization

Electrophilic substitution is one of the earliest and detailed studied fields in the chemistry of carboranes. In the Lewis acid catalyzed reactions of *o*-carborane, substitution occurs first at the 9,12-positions, which are the furthest to the cage carbons, and then on borons-8,10.^{16f,16k,24} Thus selective synthesis of 9-X-1,2-C₂B₁₀H₁₁, 9,12-X₂-1,2-C₂B₁₀H₁₀, 8,9,12-X₃-1,2-C₂B₁₀H₉, and 8,9,10,12-X₄-1,2-C₂B₁₀H₈ (X = F, Cl, Br, I) can be achieved under proper reaction conditions (Scheme 1.7).

Scheme 1.7. Sequential Halogenation of *o*-Carborane.



Carboranes with iodine atom attached to cage borons can undergo facile B-I bond activation by Pd⁰ complexes, which offers a good methodology for the synthesis of carborane derivatives containing *exo*- B-C bond. Several cross-coupling reactions, such as Kumada,^{16f,16i,24n,25} Suzuki-Miyaura,²⁶ Negishi,^{25m,25p,q,27} Sonogashira,^{25k,25p,q,28} or Heck type,²⁹ can be applied to this system. In recent years, B-I to B-P,³⁰ B-N,³¹ or B-O³² bond transformations are also developed (Scheme 1.8).

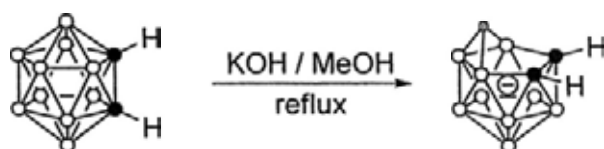
Scheme 1.8. Carborane B-I Bond Activation by Pd⁰.



1.1.4. Degradation

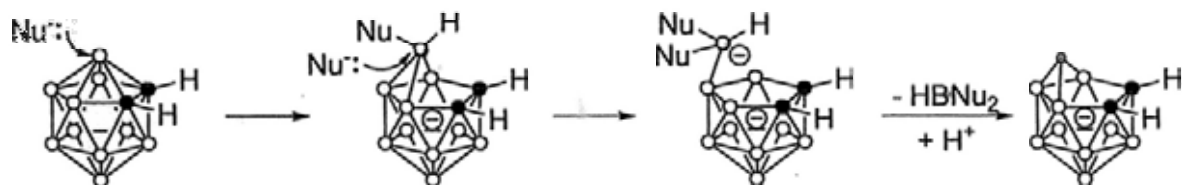
Although the carborane cages are thermally stable and resistant to several oxidants like KMnO_4 or reductants such as LiAlH_4 ,^{17b,33} it can be selectively degraded by strong bases such as KOH/MeOH to remove one boron atom from the cage, forming the $7,8\text{-C}_2\text{B}_9^-$ anion (Scheme 1.9), which is described as deboration or deboration.³⁴ In a similar manner, *m*-carborane can be deborated to the $7,9\text{-C}_2\text{B}_9^-$ anion.^{34b,35} This kind of deboration reaction can also be achieved by other nucleophiles such as piperidine³⁶ or fluorides.³⁷ The *p*-carborane, however, is resistant to cage degradation under these mild conditions,^{16d,37b,38} but in certain cases, especially under protective atmosphere, $2,9\text{-C}_2\text{B}_9^-$ anion can be synthesized.^{36k,39}

Scheme 1.9. Deboration of *o*-Carborane.



The deboration process of *o*-carborane is regarded to proceed via sequential addition of one and two nucleophiles to the B3 (B6) atom, which is adjacent to the two cage carbons, followed by elimination of this vertex to afford the final product (Scheme 1.10). The key intermediates are structurally characterized. $(\text{Me}_2\text{N})_3\text{P}=\text{NH}$ reacts with $o\text{-C}_2\text{B}_{10}\text{H}_{12}$ to form a 1:1 adduct $\mu\text{-}9,10,11\text{-BH}(\text{NH}=\text{P}(\text{NMe}_2)_3)\text{-}7,8\text{-C}_2\text{B}_9\text{H}_{11}$.^{38,40} The 2:1 adducts are also reported.⁴¹ Pyridine interacts with 1-Br-1,2- $\text{C}_2\text{B}_{10}\text{H}_{11}$ to give a 2:1 adduct $10\text{-BH}(\text{py})_2\text{-}7\text{-Br-}7,8\text{-C}_2\text{B}_9\text{H}_{10}$,^{41a} and NHCs can also react with *o*-carborane to afford similar products.^{41b}

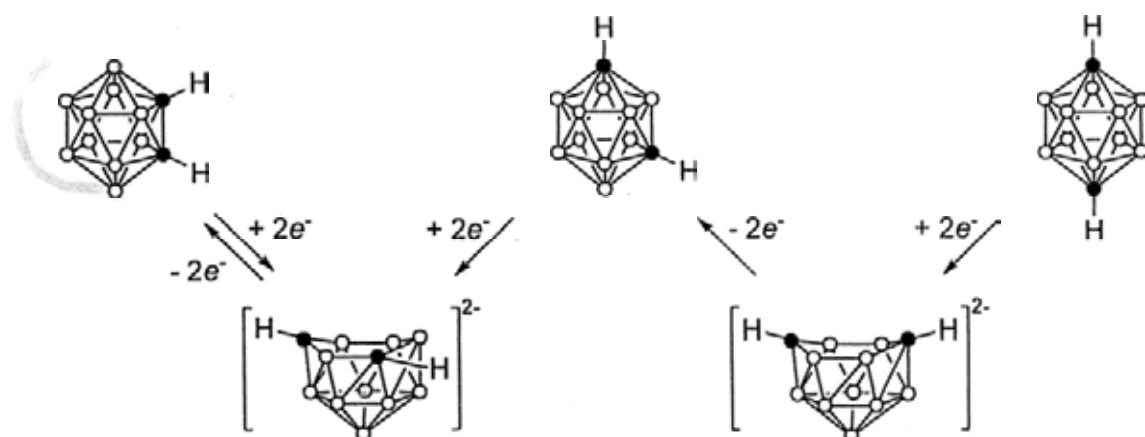
Scheme 1.10. Proposed Mechanism of *o*-Carborane Deboration.



1.1.5. Reduction

Icosahedral carboranes can be reduced by group 1 metals to the corresponding 12-vertex *nido*- dianions, which have been thoroughly studied since as early as 1963.^{4b,6} Formation of the product is highly dependent upon the positions of the cage carbons and whether the cage carbons are linked. Generally, if there is no bridging group to link the two cage carbons of *o*-carborane, reduction would afford the *nido*-7,9- $C_2B_{10}^{2-}$ species, in which the two cage carbons are separated by one boron atom in a 6-membered open face after taking up two electrons and breaking the cage C-C bond.⁴² Under the same conditions; the 1,7- isomer gives exactly the same product,^{42,43} whilst the 1,12- isomer gives a *nido*-7,10- $C_2B_{10}^{2-}$ dianion,⁴² which is not stable and would slowly rearrange to the 7,9- complex. Oxidation of the *nido*-7,9- $C_2B_{10}^{2-}$ dianion recovers the *o*-carborane; and for *nido*-7,10- $C_2B_{10}^{2-}$, *m*-carborane is obtained (Scheme 1.11).⁴²⁻⁴⁴

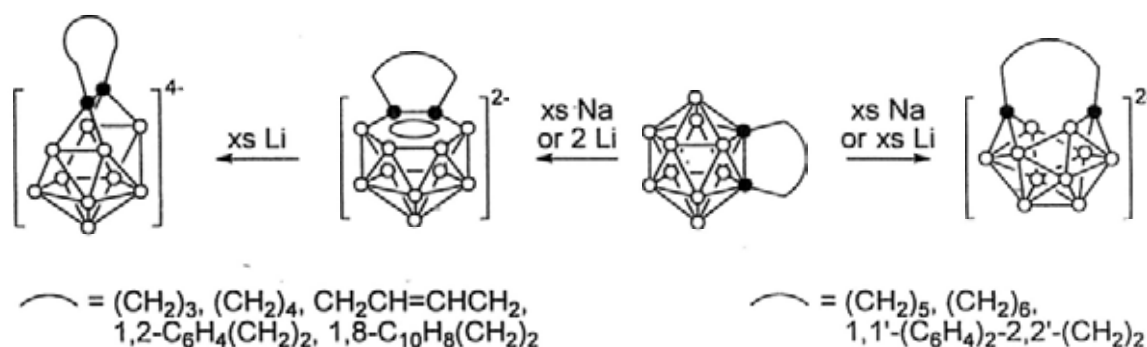
Scheme 1.11. Reduction of Icosahedral Carboranes without Linkage.



When the two cage carbons of *o*-carborane are linked by an *exo*- group, different kinds of *nido*- products would be obtained upon reduction, depending on the length of the linkage.⁴⁵ When an excess amount of Na metal or 2 equiv of Li metal was used, *o*-carborane with a short linkage usually gives the 12-vertex CAd (Carbon-Atoms-

Adjacent) *nido*-carborane anion $7,8\text{-C}_2\text{B}_{10}^{2-}$, with a geometry similar to that of the $7,9\text{-C}_2\text{B}_{10}^{2-}$ mentioned above, but bearing a trapezoidal open face that is composed by two adjacent cage carbons on the 6-membered open face and two boron atoms on the lower belt. In the case of a longer linkage, $7,10\text{-C}_2\text{B}_{10}^{2-}$ would be afforded, but it has a basket-like geometry which is different from that without linkage. The *CAD nido*-carborane anions $7,8\text{-C}_2\text{B}_{10}^{2-}$ can be further reduced by excess Li metal to the corresponding *arachno*-carborane tetraanions (Scheme 1.12).

Scheme 1.12. Reduction of Icosahedral Carboranes with Linkage.



1.2. Metallocarboranes Based on Icosahedral Carboranes

Metallocarboranes are carboranes incorporating one or more metal atoms in the cage structures. The dicarbollide ion, $[\text{C}_2\text{B}_9\text{H}_{11}]^{2-}$, which is isolobal to the Cp^- ligand, can bond to metals using $6e^-$ in the delocalized π -type orbitals. Accordingly, the first metallocarborane was prepared in as early as 1965.⁴⁶ Following this motif, a number of metallocarboranes, especially the late transition metal complexes, have been synthesized and characterized.^{47,48}

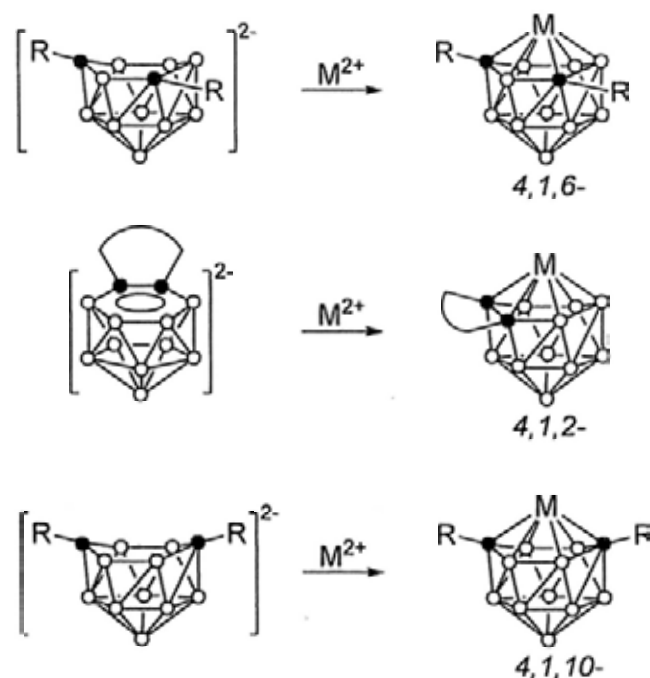
“Polyhedral expansion”, originally developed by Hawthorne, is a general method for the synthesis of metallocarborane.^{48c,49} It involves an n -vertex cage-opening reduction and insertion of a metal fragment as a new vertex into the open-face to construct an $(n+1)$ -vertex *closo*- polyhedron. Other methods involve polyhedron subrogation and thermal isomerization.^{48c}

Metallacarboranes derived from icosahedral carboranes are normally classified as 13-vertex MC_2B_{10} and 14-vertex $M_2C_2B_{10}$ which have *closo*- geometries, and 13-vertex metallacarborane bearing *arachno*- $C_2B_{10}^{4-}$ ligand. Other types of 13- and 14-vertex metallacarboranes are not discussed in this chapter.

1.2.1. MC_2B_{10}

In this system, 4,1,6- MC_2B_{10} is the most thoroughly studied. The first 13-vertex metallacarborane 4-Cp-4,1,6- $CoC_2B_{10}H_{12}$ was synthesized from $[7,9-C_2B_{10}H_{12}]^{2-}$ and a formal $CpCo^{2+}$ fragment in 1971 and then structurally characterized.⁵⁰ In view of the availability of 12-vertex *CAp nido*-carborane dianions $7,9-C_2B_{10}^{2-}$, a large amount of complexes of this type have been prepared, using the same “polyhedral expansion” methodology (Scheme 1.13).

Scheme 1.13. General Synthesis of 4,1,6-, 4,1,2-, and 4,1,10- MC_2B_{10} .



A few examples of insertion of a metal fragment into a 12-vertex *closo*-carborane to form the 4,1,6- MC_2B_{10} were also reported. Reactions of SmI_2 with 2 equiv of $[(C_5H_4)Me_2A(C_2B_{10}H_{11})]^-$ ($A = Si, C$) or $[(C_9H_6)Me_2Si(C_2B_{10}H_{11})]^-$ give trivalent

samarium complexes $[\eta^5:\eta^6-(C_5H_4)Me_2A(C_2B_{10}H_{11})]Sm(THF)_2$ or $[\eta^5:\eta^6-(C_9H_6)-Me_2Si(C_2B_{10}H_{11})]Sm(THF)_2$.⁵¹ Another example is that treatment of $[\eta^5:\sigma-(C_9H_6)-Me_2Si(C_2B_{10}H_{10})]ZrCl(NMe_2)$ with 1 equiv of *n*-BuLi in THF/pyridine gives $[\eta^5:\eta^6:\sigma-(C_9H_6)Me_2Si(C_2B_{10}H_{10}CH_2NMe)]Zr(NC_5H_5)$.⁵²

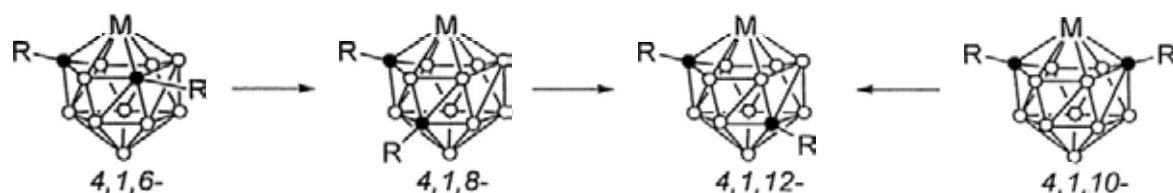
The first 4,1,2-MC₂B₁₀ compound was prepared several years ago via a similar insertion reaction. Co(PET₃)₄ reacts with *closo*-1-Me-1,2-C₂B₁₀H₁₁ in which the highly nucleophilic Co⁰ fragment inserts into the cage to give 4-Co(PET₃)₃-1-Me-4,1,2-CoC₂B₁₀H₁₁ as suggested.⁵³ Later, insertion of a metal fragment from CoCl₂ into a 12-vertex *arachno*-[(NC)C₂B₁₀H₁₄]K followed by air oxidation to give another 4,1,2-type of compound 4-Cp-1-CN-4,1,2-CoC₂B₁₀H₁₁ was achieved.⁵⁴

Like that of 4,1,6-MC₂B₁₀, a number of metallocarboranes of 4,1,2-MC₂B₁₀ type have been synthesized by "polyhedral expansion" in recent years, depending on the controlled synthesis of 12-vertex CAd *nido*-carborane dianions developed by our group (Scheme 1.13). The metal fragment may contain *f*-block,⁵⁵ early transition,⁵⁶ late transition,⁵⁷ and *p*-block elements.⁵⁸

In a similar manner, 4,1,10-MC₂B₁₀ metallocarboranes have recently been synthesized, using 7,10-C₂B₁₀²⁻, which can be formed by reduction of *p*-carborane (Scheme 1.13).^{57b,59}

Most of the other known isomers of the MC₂B₁₀ type are generally formed from thermal rearrangement, and two pathways have been established. The earlier one is from the 4,1,6- to 4,1,8- to 4,1,12-MC₂B₁₀ transformation.^{57b,60} In this case, the Co species are usually easier to isomerize at a lower temperature than the Ru analogues. Another pathway is from the 4,1,10- to 4,1,12- rearrangement (Scheme 1.14).^{57b,59a,59d,61} Only one example of 4,1,11-type has been reported, which is regarded from the capitation of a Ru²⁺ fragment to the 1,7-C₂B₁₀²⁻.⁶¹

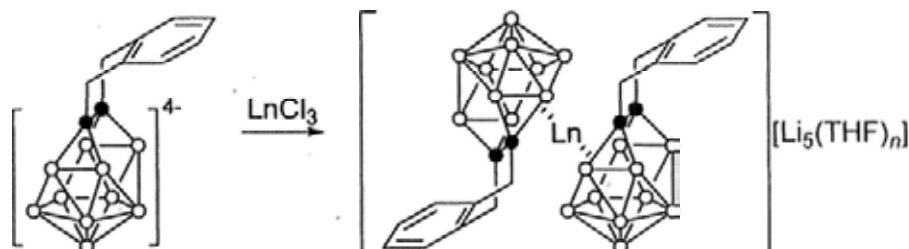
Scheme 1.14. Thermal Rearrangement in a MC_2B_{10} System.



1.2.2. MC_2B_{10} bearing *arachno*- C_2B_{10} unit

The 13-vertex lanthanacarboranes bearing CAD *arachno*- C_2B_{10} units can be readily prepared from CAD 12-vertex *arachno*- $C_2B_{10}^{4-}$ anions. Treatment of $[\mu-1,2-o-C_6H_4(CH_2)_2-1,2-C_2B_{10}H_{10}][Li_4(THF)_6]$ with $LnCl_3$ gives the corresponding $[\{\eta^6-\mu-1,2-o-C_6H_4(CH_2)_2-1,2-C_2B_{10}H_{10}\}_2Ln][Li_5(THF)_n]$, in which two *arachno*-carborane ligands are bonded to the Ln^{3+} in an η^6 fashion (Scheme 1.15).⁵⁵

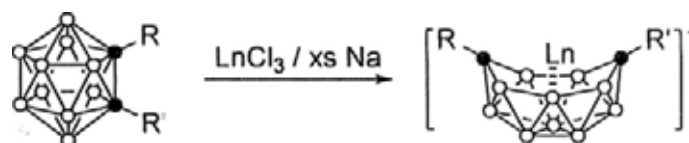
Scheme 1.15. Synthesis of Lanthanacarboranes Bearing CAD *arachno*- C_2B_{10} Units.



On the other hand, the ones bearing CAP *arachno*- C_2B_{10} units cannot be directly synthesized from simple salt metathesis reactions as the “free ligands” do not exist. However, reduction of *o*-carborane derivative $1,2-R,R'-1,2-C_2B_{10}H_{10}$ with group 1 metals in the presence of $LnCl_3$ gives novel 13-vertex metallocarborane in which the carborane units is reduced to *arachno*- tetraanion and bonds to the Ln^{3+} in an η^7 -fashion (Scheme 1.16).⁶² Recently, complexes that have similar structural features have been prepared via electron transfer process. CAP *nido*-carborane dianions bearing heteroatom-containing side arms can react with $ZrCl_4$ or SmI_2 to give the 13-vertex metallocarboranes $[\eta^1:\eta^1:\eta^7-(Me_2NCH_2CH_2)(RCH_2CH_2)C_2B_{10}H_{10}]Zr(\mu-Cl)Na$

(THF)₃ (R = MeO, Me₂N), or [$\{\eta^1:\eta^7\text{-}[(\text{Me}_2\text{NCH}_2\text{CH}_2)_2\text{C}_2\text{B}_{10}\text{H}_{11}]\text{Sm}(\text{THF})_4\text{Sm}\}$]-[Na(THF)₄], respectively.⁶³

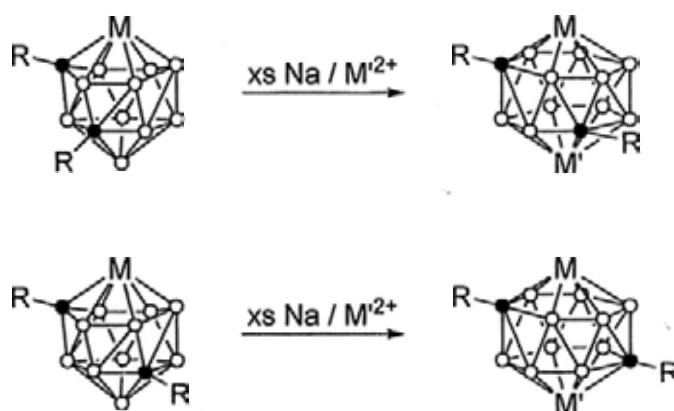
Scheme 1.16. General Synthesis of Lanthanacarboranes Bearing a CAP *arachno*-C₂B₁₀ Unit.



1.2.3. M₂C₂B₁₀

The first 14-vertex bimetalacarboranes were reported in 1974 using “polyhedral expansion”. Reduction of 13-vertex cobaltacarborane 4-Cp-4,1,12-CoC₂B₁₀H₁₂ or 4-Cp-4,1,8-CoC₂B₁₀H₁₂ with Na metal in the presence of naphthalene, followed by treatment with CoCl₂/NaCp and air oxidation, give 1,14-Cp₂-1,14,2,10-Co₂C₂B₁₀H₁₂ or 1,14-Cp₂-1,14,2,9-Co₂C₂B₁₀H₁₂, respectively (Scheme 1.17).⁶⁴ They were assigned to have bicapped hexagonal antiprismatic structures. Their 1,14,2,10-M₂C₂B₁₀ analogues 1,14-(*p*-cymene)₂-1,14,2,10-Ru₂C₂B₁₀H₁₂, and 1-(*p*-cymene)-14-(dppe)-1,14,2,10-RuNiC₂B₁₀H₁₂, which were structurally characterized, were synthesized via the same method in 2005.⁶⁵

Scheme 1.17. General Synthesis of 14-Vertex Bimetalacarboranes M₂C₂B₁₀.



1.3. Supercarboranes and Supermetallacarboranes

Supercarboranes, or supraicosahedral carboranes, as the name implies, are carboranes having more than 12 vertices. Compared to that of icosahedral carboranes, the knowledge regarding supercarboranes had been limited merely to the possible cage geometries predicted by theoretical work before 2003.⁶⁶ Theoretical calculations on the boranes *closo*-[B_nH_n]²⁻ show that the overall stability of these clusters increases as *n* gets larger, with the exception of *n* = 12 which is much more stable than the others.^{66d} Such an “icosahedral barrier” is often used to account for the failure in the synthesis of supercarboranes.^{67,68}

On the other hand, a series of 13-vertex metallocarboranes and a few 14-vertex metallocarboranes have been prepared, using “polyhedral expansion” methodology, which also works well in the reconstruction of *o*- or *m*-carboranes from the reactions of *nido*-C₂B₉²⁻ with RBX₂ (X = Cl, Br, I), as mentioned above.^{15,16} However, attempted insertions of [BR]²⁺ (R = alkyl, H, halide) into CAP *nido*-[7,9-C₂B₁₀H₁₂]²⁻ had never produced the desired 13-vertex carboranes.^{67,69} This is often attributed to the extraordinary stability of the B₁₂ icosahedron. The dramatic differences between CAd *nido*-[7,8-C₂B₉H₁₁]²⁻ and CAP *nido*-[7,9-C₂B₁₀H₁₂]²⁻ ions in reducing power are usually overlooked. It has been well documented that CAP *nido*-[7,9-C₂B₁₀H₁₂]²⁻ ions are very strong reducing agents that can reduce M⁴⁺ (Group 4 metal atom),^{56,70} and Ln³⁺ (Ln = Sm, Eu, Yb) to the corresponding divalent species.^{51b,71} The redox reactions between CAP *nido*-[7,9-C₂B₁₀H₁₂]²⁻ and R'BX₂ may be superior to the capitulation reactions, leading to the formation of *closo*-R₂C₂B₁₀H₁₀. Thus we thought that lowering the reducing power of *nido*-[R₂C₂B₁₀H₁₀]²⁻ ions can promote the capitulation reaction, resulting in the synthesis of desired supercarboranes. Our group have developed a method to synthesize three regioisomers of *nido*-[R₂C₂B₁₀H₁₀]²⁻ in a controlled manner in which the two cage carbons are in 7,8-, 7,9- and 7,10- positions,

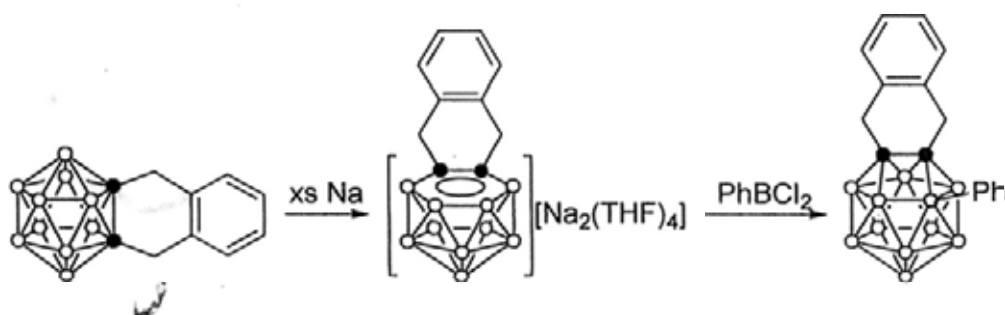
respectively.⁴⁵ The results show that the CAd *nido*-[7,8-R₂C₂B₁₀H₁₀]²⁻ isomers are weaker reducing agents than the CAP isomers, which offers a very valuable entry point to the synthesis of supercarboranes.^{48y,z}

1.3.1. Synthesis of CAd 13-Vertex Carboranes

The "polyhedral expansion" method works well when CAd *nido*-[7,8-R₂C₂B₁₀H₁₀]²⁻ anions are employed as starting materials. Such a [12+1] protocol is used as a general methodology for the synthesis of 13-vertex carboranes. Reduction of μ -1,2-*o*-C₆H₄(CH₂)₂-1,2-C₂B₁₀H₁₀⁷² with excess Na metal in THF gives a CAd *nido*-[μ -7,8-*o*-C₆H₄(CH₂)₂-7,8-C₂B₁₀H₁₀][Na₂(THF)₄],^{45b,c} which is treated with PhBCl₂ in petroleum ether to afford a CAd 13-vertex carborane 5-Ph- μ -1,2-*o*-C₆H₄(CH₂)₂-1,2-C₂B₁₁H₁₀ in 6% yield (Scheme 1.18).⁶⁹ The yield could be improved if a small C,C'-linkage (CH₂)₃ is used. Reaction of μ -1,2-(CH₂)₃-1,2-C₂B₁₀H₁₀⁷³ with excess Na metal generates the CAd *nido*-[μ -7,8-(CH₂)₃-7,8-C₂B₁₀H₁₀][Na₂(THF)_x]. Treatment of this salt with different dihaloborane reagents RBX₂ produces a series of CAd 13-vertex carboranes 3-R- μ -1,2-(CH₂)₃-1,2-C₂B₁₁H₁₀ (R = H, Ph, Z-EtCH=C(Et), E'-tBuCH=CH) in 20%-37% isolated yields (Scheme 1.19).⁷⁴ These results suggest that the C,C'-linkages and the nature of borane reagents have some effects on the capitation process. The electron-rich borane reagents and less-sterically demanding (CH₂)₃ C,C'-linkage led to higher yields than the *o*-C₆H₄(CH₂)₂ unit. Solvents also play an important role. Donor solvents, such as THF, DME, and Et₂O that may react with RBX₂ resulted in much lower yields.

All structurally characterized CAd 13-vertex carboranes have a common henicosahedral geometry bearing one or two trapezoidal open faces constructed by the two cage carbons and boron atoms of the B₅ belt (Figure 1.4). The more electronegative carbon atoms are less coordinated than the boron atoms.

Scheme 1.18. Synthesis of CAD 13-Vertex Carborane 5-Ph- μ -1,2-*o*-C₆H₄(CH₂)₂-1,2-C₂B₁₁H₁₀.



Scheme 1.19. Synthesis of CAD 13-Vertex Carboranes 3-R- μ -1,2-(CH₂)₃-1,2-C₂B₁₁H₁₀.

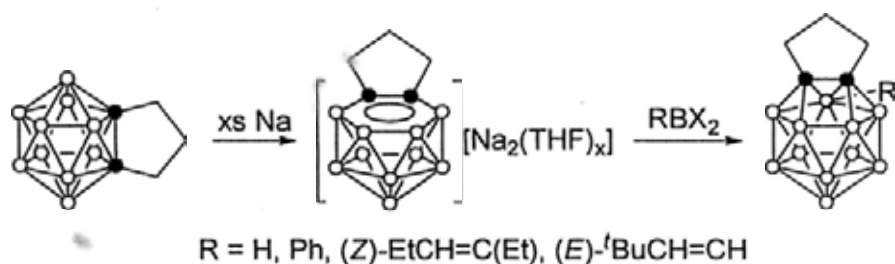


Figure 1.4. Trapezoidal open faces in the CAD 13-vertex carboranes.

1.3.2. Electrophilic Substitution Reaction of CAD 13-Vertex Carborane

Like 12-vertex carboranes, 13-vertex *closo*-carboranes can undergo electrophilic substitution reactions. Treatment of CAD μ -1,2-(CH₂)₃-1,2-C₂B₁₁H₁₁ with an excess amount of MeI, Br₂ or I₂ in the presence of a catalytic amount of AlCl₃ in CH₂Cl₂ at room temperature gives hexasubstituted CAD 13-vertex *closo*-carboranes 8,9,10,11,12,13-X₆- μ -1,2-(CH₂)₃-1,2-C₂B₁₁H₅ (X = Me, Br or I) (Scheme 1.20).⁷⁴ The results indicate that the BH vertices which are the farthest to the cage carbons are the most electron rich and the easiest to be attacked by electrophiles. On the other hand, interaction of CAD μ -1,2-(CH₂)₃-1,2-C₂B₁₁H₁₁ with H₂O₂ leads to a complete

degradation of the cage, resulting in the formation of $B(OH)_3$, which differs significantly from its icosahedral cousins.⁷⁵ These substitution reactions can be closely monitored by ^{11}B NMR spectroscopy as the resultant hexasubstituted CAd 13-vertex carboranes have distinct ^{11}B chemical shifts. As shown in Figure 1.5, the electronic effects of substituents on the ^{11}B chemical shifts are significant. A similar phenomenon is also observed in a $[7,8,9,10,11,12-X_6-1-CB_{11}H_6]^-$ system.⁷⁶ The cage geometry is very similar to that of its parent 13-vertex *closo*-carborane.

Scheme 1.20. Electrophilic Substitution Reaction of CAd 13-Vertex Carborane.

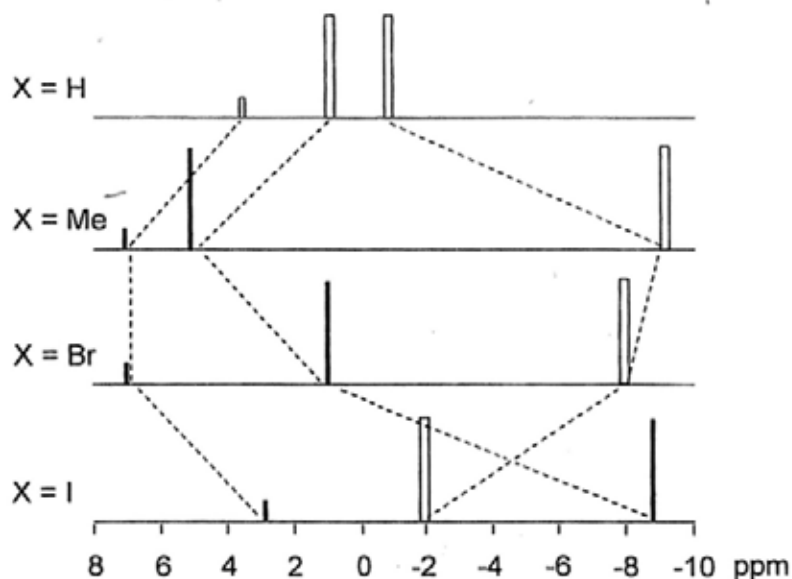
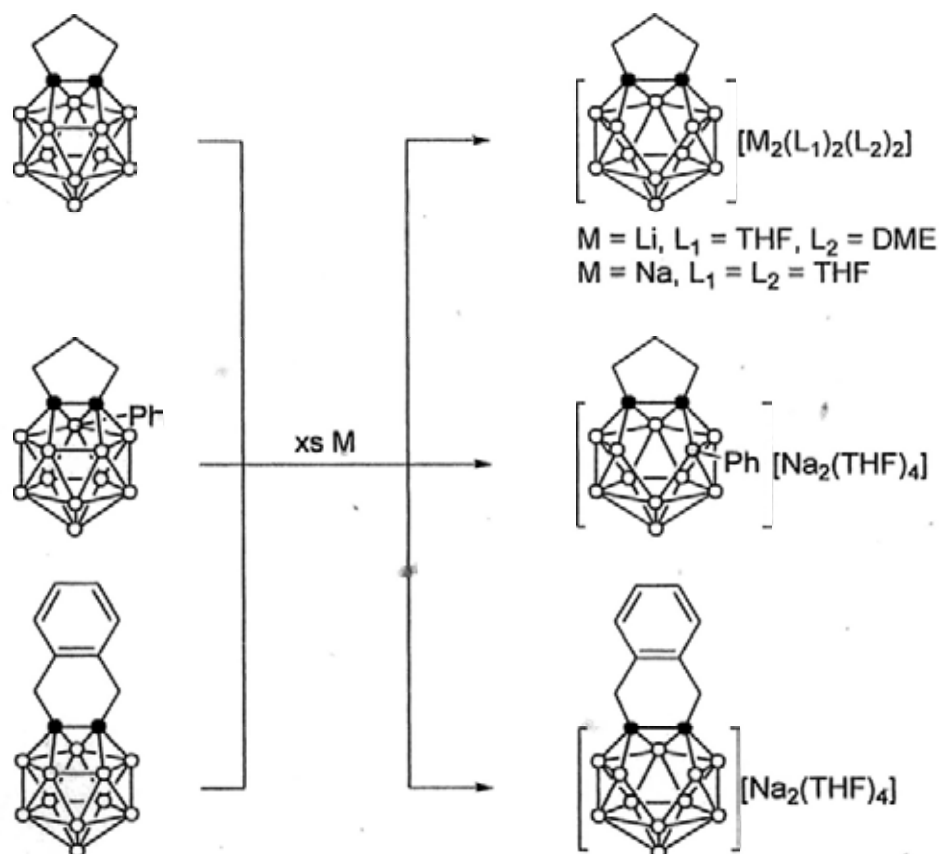


Figure 1.5. Stick representation of the chemical shifts and relative intensities in the $^{11}B\{^1H\}$ spectra of 8,9,10,11,12,13- $X_6-\mu-1,2-(CH_3)_2-1,2-C_2B_{11}H_5$. The hollow and solid sticks represent the BH and BX vertices, respectively.

1.3.3. Redox Reaction of CAd 13-Vertex Carboranes

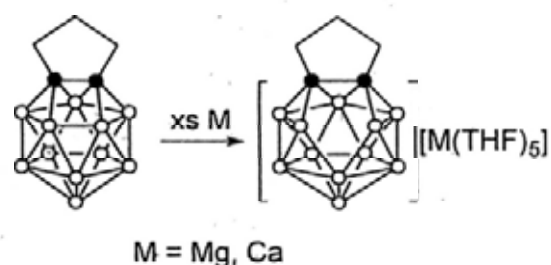
13-Vertex *closo*-carboranes are much easier to be reduced than their 12-vertex analogues, presumably due to the presence of the trapezoidal faces. Treatment of CAd μ -1,2-(CH₂)₃-1,2-C₂B₁₁H₁₁, 3-Ph- μ -1,2-(CH₂)₃-1,2-C₂B₁₁H₁₀ or μ -1,2-*o*-C₆H₄-(CH₂)₂-1,2-C₂B₁₁H₁₁ with an excess amount of finely cut Na metal in THF at room temperature give the corresponding CAd 13-vertex *nido*-carborane salts $[\mu$ -1,2-(CH₂)₃-1,2-C₂B₁₁H₁₁][Na₂(THF)₄], $[3\text{-Ph-}\mu$ -1,2-(CH₂)₃-1,2-C₂B₁₁H₁₀][Na₂(THF)₄], and $[\mu$ -1,2-*o*-C₆H₄(CH₂)₂-1,2-C₂B₁₁H₁₁][Na₂(THF)₄], respectively. These reactions proceeds very fast even in the absence of naphthalene. It is noteworthy that reduction of CAd μ -1,2-(CH₂)₃-1,2-C₂B₁₁H₁₁ with excess Li metal in THF affords only the CAd 13-vertex *nido*-carborane salt $[\mu$ -1,2-(CH₂)₃-1,2-C₂B₁₁H₁₁][Li₂(THF)₂(DME)₂], after recrystallization from DME, which cannot be further reduced to the *arachno*-species (Scheme 1.21).⁷⁴ This indicates that the 13-vertex *nido*-carboranes are stronger reductants than the 12-vertex *nido*-carboranes.

Scheme 1.21. Reduction of CAd 13-Vertex Carboranes by Group 1 Metals.



The CAd 13-vertex *closo*-carboranes can also be readily reduced by alkaline earth metals. Reaction of CAd μ -1,2-(CH₂)₃-1,2-C₂B₁₁H₁₁ with excess activated Mg or Ca metal in THF generate the alkaline earth metal complexes of *nido*-carborane dianions [μ -1,2-(CH₂)₃-1,2-C₂B₁₁H₁₁][M(THF)₅] (M = Mg, Ca) (Scheme 1.22).⁷⁴

Scheme 1.22. Reduction of CAd 13-Vertex Carborane by Group 2 Metals.



All CAd 13-vertex *nido*-carborane dianions have a similar bent pentagonal open face with the out-of-plane displacement of the B atom ranging from 0.68 to 0.72 Å and with the B...B separation being about 2.64 Å. Formally, such an open face can be viewed as the result of breaking one B-B bond in the trapezoidal face of the 13-vertex *closo*-carboranes after two-electron uptake from reductant. The cations in these complexes are not incorporated into the cage, rather bind with the peripheral terminal BH moieties via M...H-B bonding interactions, giving *exo-nido* species.

Dark-brown solution formation is observed during the reduction of μ -1,2-(CH₂)₃-1,2-C₂B₁₁H₁₁ with an excess amount of Na metal in THF, which slowly turns to a pale-yellow solution within 12 h and finally gives the CAd 13-vertex *nido*-carborane salt [μ -1,2-(CH₂)₃-1,2-C₂B₁₁H₁₁][Na₂(THF)₄] as colorless crystals. The dark-brown intermediate is isolated and characterized as the sodium salt of a carborane radical anion [$\{\mu$ -1,2-(CH₂)₃-1,2-C₂B₁₁H₁₁}]^{•-}[Na(18-crown-6)(THF)₂] after treatment of μ -1,2-(CH₂)₃-1,2-C₂B₁₁H₁₁ with 1 equiv of Na metal in THF at room temperature, followed by recrystallization from a mixed THF/*n*-hexane solution of 18-crown-6 (Scheme 1.23).⁷⁷ Cyclic voltammetry of μ -1,2-(CH₂)₃-1,2-C₂B₁₁H₁₁ shows one re-

versible and one quasi-reversible peaks corresponding to two one-electron reduction processes (Figure 1.6).

Scheme 1.23. Single-Electron Reduction of CAD 13-Vertex Carborane μ -1,2-(CH₂)₃-1,2-C₂B₁₁H₁₁.

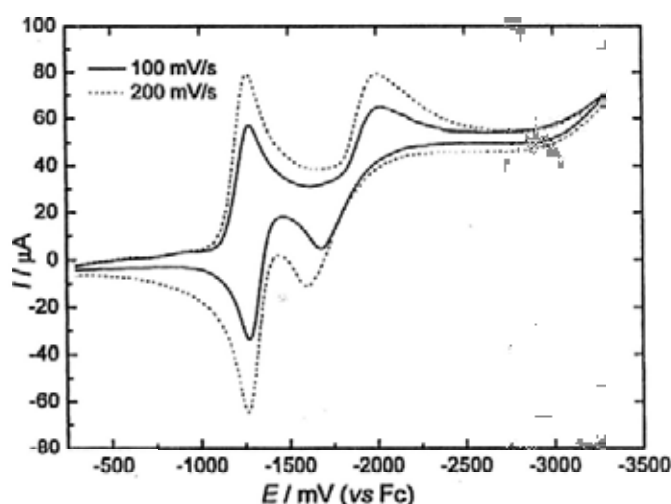
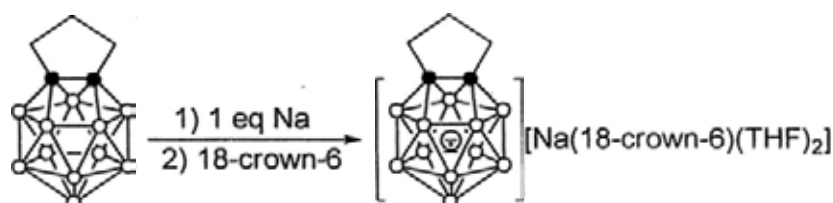


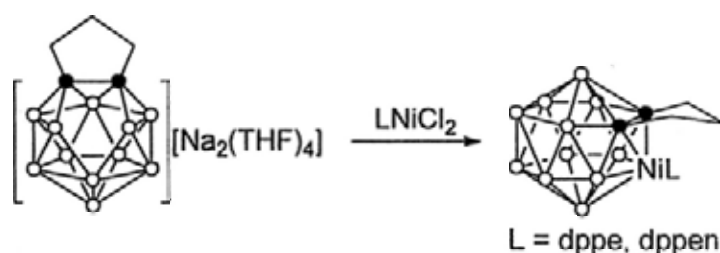
Figure 1.6. Cyclic voltammetry of μ -1,2-(CH₂)₃-1,2-C₂B₁₁H₁₁.

This paramagnetic species exhibits an EPR signal with $g = 1.994$ (line width = 23 G in solution and 5.5 G in solid-state) at room temperature, which is similar to those observed in $\cdot\text{CB}_{11}\text{Me}_{12}$ ⁷⁸ and $[\cdot\text{B}_{12}\text{R}_{12}]^-$.⁷⁹ Single-crystal X-ray analyses reveal that this radical monoanion has a geometry similar to that observed in CAD 13-vertex *closo* species with elongated C-B/B-B distances. This geometry is significantly different from that of CAD 13-vertex *nido*-carborane dianion. This is the first example of fully characterized carborane radical anion with $[2n+3]$ framework electrons. It is an intermediate between two well-established and abundant $2n+2$ (*closo*) and $2n+4$ (*nido*) systems.

1.3.4. Synthesis of 14-Vertex Metallocarboranes

Group 1 metal salts of 13-vertex *nido*-carborane dianions are useful synthons for the preparation of 14-vertex metallocarboranes. For example, reaction of CAD $[\mu\text{-}1,2\text{-}(\text{CH}_2)_3\text{-}1,2\text{-C}_2\text{B}_{11}\text{H}_{11}][\text{Na}_2(\text{THF})_4]$ with 1 equiv of $(\text{dppe})\text{NiCl}_2$ or $(\text{dppen})\text{NiCl}_2$ in THF affords CAD 14-vertex nickelacarboranes $8\text{-dppe-}\mu\text{-}2,3\text{-}(\text{CH}_2)_3\text{-}8,2,3\text{-NiC}_2\text{B}_{11}\text{H}_{11}$ or $8\text{-dppen-}\mu\text{-}2,3\text{-}(\text{CH}_2)_3\text{-}8,2,3\text{-NiC}_2\text{B}_{11}\text{H}_{11}$ in 34% or 45% isolated yield (Scheme 1.24).⁷⁴ These species are very air-sensitive and hygroscopic. They slowly decompose in solution at room temperature to regenerate the CAD 13-vertex *closo*-carborane $\mu\text{-}1,2\text{-}(\text{CH}_2)_3\text{-}1,2\text{-C}_2\text{B}_{11}\text{H}_{11}$ and Ni(0) complexes. Single-crystal X-ray analyses reveal that the two nickelacarboranes adopt a similar distorted bicapped hexagonal-antiprismatic geometry with two seven-coordinate boron atoms sitting in the apical positions. The geometry of the CAD *nido*-carborane segments are similar to those observed in group 1 metal salts. It is noted that bidentate phosphines are necessary to stabilize the above nickelacarboranes. Monophosphines often result in the decomposition of the resultant metal complexes, leading to the formation of CAD 13-vertex *closo*-carboranes and Ni(0) species.

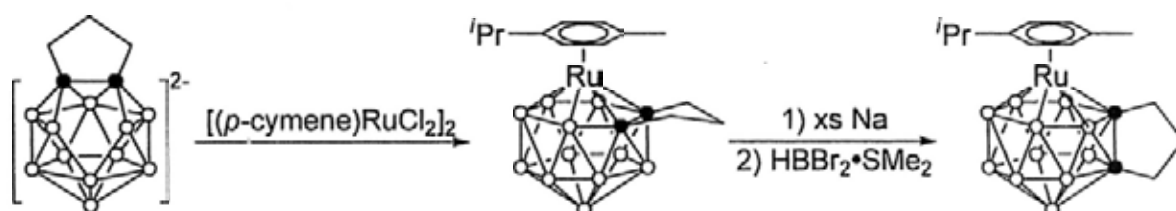
Scheme 1.24. Synthesis of CAD 14-Vertex Nickelacarboranes.



In sharp contrast, 14-vertex ruthenacarboranes are very stable to air and moisture. Treatment of CAD $[\mu\text{-}1,2\text{-}(\text{CH}_2)_3\text{-}1,2\text{-C}_2\text{B}_{11}\text{H}_{11}][\text{Na}_2(\text{THF})_4]$ with $[(p\text{-cymene})\text{RuCl}_2]_2$ in THF affords a CAD 14-vertex ruthenacarborane $1\text{-}(p\text{-cymene})\text{-}\mu\text{-}2,3\text{-}(\text{CH}_2)_3\text{-}1,2,3\text{-RuC}_2\text{B}_{11}\text{H}_{11}$ in 72% isolated yield. It reacts with excess Na metal, followed by

treatment with $\text{HBr}_2 \cdot \text{SMe}_2$ to give a regioisomer 1-(*p*-cymene)- μ -2,8-(CH_2)₃-1,2,8-RuC₂B₁₁H₁₁ in very low yield with the recovery of 2,3-isomer (Scheme 1.25).⁸⁰ Two isomers can be separated by column chromatography on silica gel. As confirmed by single-crystal X-ray analyses, both adopt a bicapped hexagonal antiprismatic geometry with the Ru atom occupying one of the apical vertices and the two cage carbons being located at the 2,3- and 2,8- positions, respectively. Notably the geometry of CAd *nido*-carborane unit in 14-vertex ruthenacarboranes is very different from those observed in the 14-vertex nickelacarborane and group 1 metal salts. The rearrangement of cage atoms clearly takes place in the capitation process to accommodate the larger Ru(II).

Scheme 1.25. Synthesis of CAd 14-Vertex Ruthenacarboranes.



1.3.5. Synthesis of 14-Vertex Carboranes

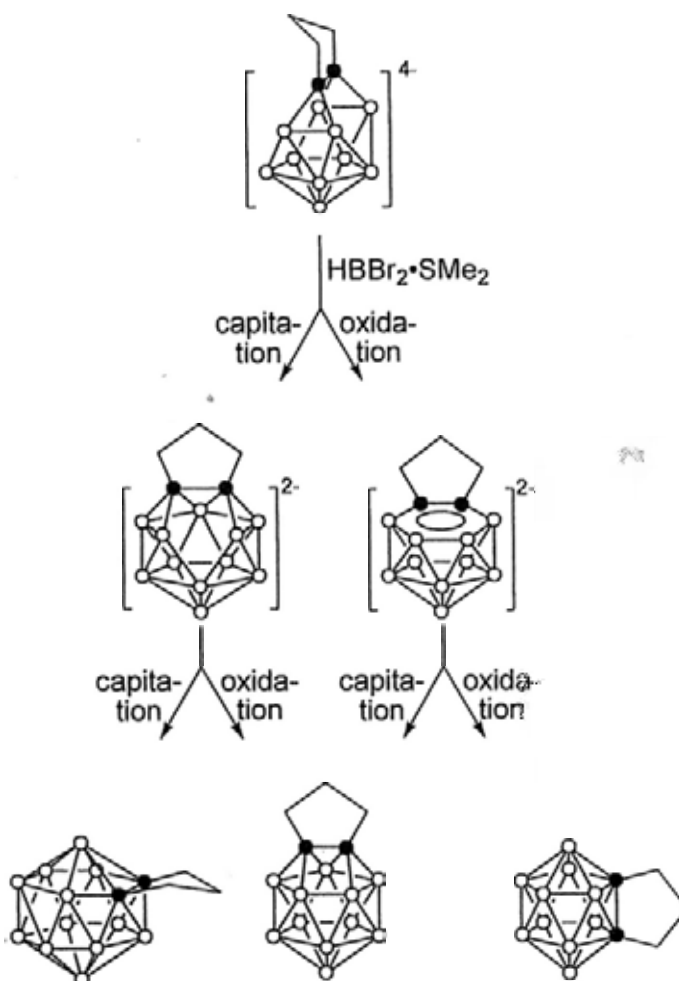
Polyhedral expansion methodology can also be applied to the synthesis of 14-vertex carboranes. Accordingly, two general approaches have been developed. One is the [12+2] protocol in which two $[\text{BH}]^{2+}$ vertices are added to one open hexagonal and one open pentagonal faces of a CAd 12-vertex *arachno*-carborane tetraanion, respectively. The other is called [13+1] protocol in which a $[\text{BH}]^{2+}$ fragment is incorporated into an open pentagonal face of a CAd 13-vertex *nido*-carborane dianion. The latter is more efficient than the former and offers a much higher yield of the 14-vertex carborane.

Reaction of CAd 12-vertex carborane μ -1,2-(CH₂)₃-1,2-C₂B₁₀H₁₀ with an excess amount of finely cut Li metal in THF gives a CAd 12-vertex *arachno*-[μ -1,2-(CH₂)₃-1,2-C₂B₁₀H₁₀][Li₄(THF)₅] which consists of two adjacent hexagonal and pentagonal bonding faces.^{45d} Treatment of this salt with 5 equiv of HBBr₂·SMe₂ in toluene affords the first CAd 14-vertex carborane μ -2,3-(CH₂)₃-2,3-C₂B₁₂H₁₂ in 7% isolated yield along with a CAd 13-vertex carborane μ -1,2-(CH₂)₃-1,2-C₂B₁₁H₁₁ (32% isolated yield) and a CAd 12-vertex carborane μ -1,2-(CH₂)₃-1,2-C₂B₁₀H₁₀ (2% isolated yield).⁸¹ Formation of the 14-vertex carborane indicates that two [BH]²⁺ vertices can be added into a pentagonal and a hexagonal faces of a CAd 12-vertex *arachno*-carborane in one reaction. Whether two capitation processes proceed simultaneously or sequentially is not clear yet. On the other hand, isolation of CAd 12-vertex *closo*-carborane suggests that HBBr₂ can oxidize *arachno*-[μ -1,2-(CH₂)₃-1,2-C₂B₁₀H₁₀]⁴⁻ to *nido*-[μ -1,2-(CH₂)₃-1,2-C₂B₁₀H₁₀]²⁻ and finally to *closo*- μ -1,2-(CH₂)₃-1,2-C₂B₁₀H₁₀. The 13-vertex carborane may be formed either via capitation reaction of HBBr₂ with *nido*-[μ -1,2-(CH₂)₃-1,2-C₂B₁₀H₁₀]²⁻ or oxidation of CAd 13-vertex *nido*-[μ -1,2-(CH₂)₃-1,2-C₂B₁₁H₁₁]²⁻ as shown in Scheme 1.26. It is noted that reaction of CAd 12-vertex *arachno*-carborane salt [μ -1,2-*o*-C₆H₄(CH₂)₂-1,2-C₂B₁₀H₁₀][Li₄(THF)₆]^{45b,c} with excess HBBr₂·SMe₂ only gives a CAd 13-vertex carborane μ -1,2-*o*-C₆H₄(CH₂)₂-1,2-C₂B₁₁H₁₁ and a CAd 12-vertex carborane μ -1,2-*o*-C₆H₄(CH₂)₂-1,2-C₂B₁₀H₁₀. No 14-vertex species is isolated (Scheme 1.27).⁷⁴ These results imply that the C,C'-linkages play an important role in the capitation process.

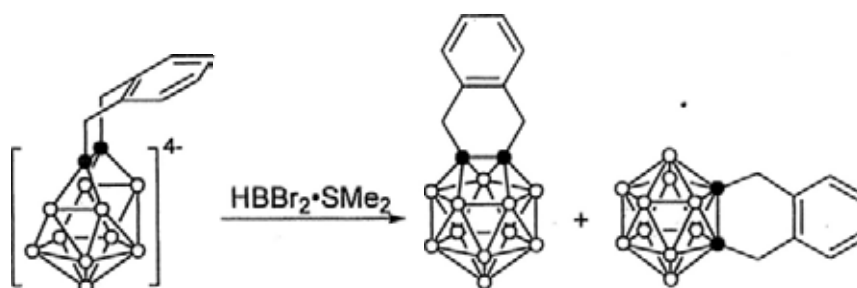
The CAd 14-vertex carborane μ -2,3-(CH₂)₃-2,3-C₂B₁₂H₁₂ is also synthesized from the reaction of CAd 13-vertex *nido*-carborane salt [μ -1,2-(CH₂)₃-1,2-C₂B₁₁H₁₁]-[Na₂(THF)₄] with 1.5 equiv of HBBr₂·SMe₂ in 30% isolated yield (Scheme 1.28). The 2,8-isomer of CAd 14-vertex carborane μ -2,8-(CH₂)₃-2,8-C₂B₁₂H₁₂ is prepared

from the oxidation of a CAd 14-vertex *nido*-carborane salt $[\mu-(\text{CH}_2)_3\text{C}_2\text{B}_{12}\text{H}_{12}]^-$ $[\text{Na}_2(\text{THF})_4]$ (Scheme 1.29). The 2,8-isomer has been structurally characterized to adopt a bicapped hexagonal antiprismatic geometry, similar to that calculated for $[\text{B}_{14}\text{H}_{14}]^{2-}$. All 24 faces are triangulated with two apical boron atoms being seven-coordinated.⁸¹

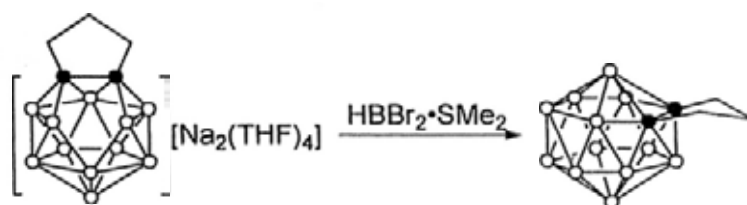
Scheme 1.26. Reaction of *arachno*- $[\mu-1,2-(\text{CH}_2)_3-1,2-\text{C}_2\text{B}_{10}\text{H}_{10}]^{4-}$ with HBrBr_2 .



Scheme 1.27. Reaction of *arachno*- $[\mu-1,2-o-\text{C}_6\text{H}_4(\text{CH}_2)_2-1,2-\text{C}_2\text{B}_{10}\text{H}_{10}]^{4-}$ with HBrBr_2 .



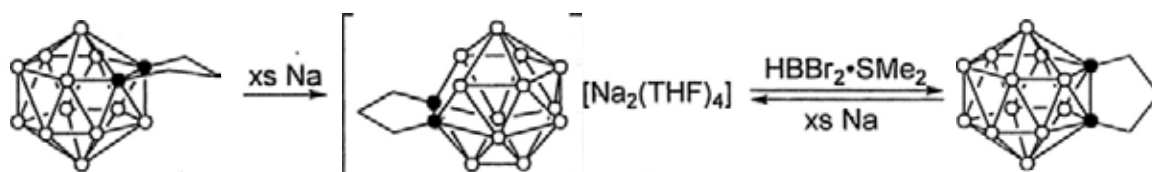
Scheme 1.28. Reaction of $nido-[\mu-1,2-(CH_2)_3-1,2-C_2B_{11}H_{11}]^{2-}$ with $HBrBr_2$.



1.3.6. Reduction of 14-Vertex Carboranes and Synthesis of 15-Vertex Metalla-carboranes

Like CAD 13-vertex carboranes, CAD 14-vertex *closo*-carboranes $\mu-2,3-(CH_2)_3-2,3-C_2B_{12}H_{12}$ or $\mu-2,8-(CH_2)_3-2,8-C_2B_{12}H_{12}$ react readily with excess Na metal in THF, to afford the same CAD 14-vertex *nido*-carborane salt $[\mu-1,2-(CH_2)_3-1,2-C_2B_{12}H_{12}][Na_2(THF)_4]$ (Scheme 1.29).⁸⁰ Single-crystal X-ray analyses reveal that it has a bent pentagonal open face which is larger and flatter than those observed in the CAD 13-vertex *nido*-carboranes. This five-membered open face is constructed by formally breaking a B-B bond in the B_5 belt after two-electron uptake from Na metal. Similar to the case of the CAD 13-vertex *nido*-carboranes, this CAD 14-vertex *nido*- $[\mu-1,2-(CH_2)_3-1,2-C_2B_{12}H_{12}]^{2-}$ dianion is also resistant to further reduction by Li metal.

Scheme 1.29. Two-Electron Reduction of $\mu-2,3-(CH_2)_3-2,3-C_2B_{12}H_{12}$ and Synthesis of $\mu-2,8-(CH_2)_3-2,8-C_2B_{12}H_{12}$.

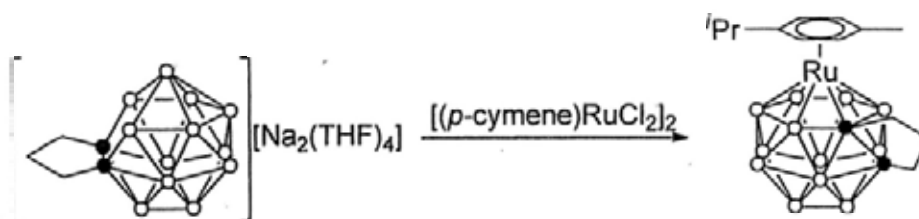


Treatment of CAD 14-vertex *nido*-carborane salt $[\mu-1,2-(CH_2)_3-1,2-C_2B_{12}H_{12}][Na_2(THF)_4]$ with 2 equiv of $HBBR_2 \cdot SMe_2$ does not give the desired 15-vertex carborane, rather affords CAD 14-vertex carborane $\mu-2,8-(CH_2)_3-2,8-C_2B_{12}H_{12}$.⁸¹ This re-

sult shows that polyhedral expansion methodology, which works well in the preparation of 13- and 14-vertex carboranes, has been unsuccessful when applied to the synthesis of 15-vertex carboranes. The reason could be ascribed to the stronger reducing power of CAd 14-vertex *nido*-carborane dianions over CAd 13-vertex *nido*- species.

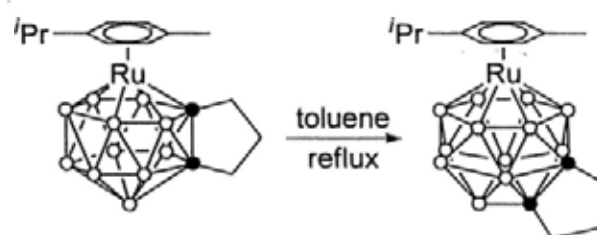
On the other hand, a metal fragment can be incorporated into a 14-vertex *nido*-carborane to form a 15-vertex metallocarborane. Reaction of CAd $[\mu-1,2-(\text{CH}_2)_3-1,2-\text{C}_2\text{B}_{12}\text{H}_{12}][\text{Na}_2(\text{THF})_4]$ with 0.5 equiv of $[(p\text{-cymene})\text{RuCl}_2]_2$ in THF gives a CAd 15-vertex ruthenacarborane $7-(p\text{-cymene})-\mu-1,4-(\text{CH}_2)_3-7,1,4\text{-RuC}_2\text{B}_{12}\text{H}_{12}$ in 62% isolated yield (Scheme 1.30).⁸⁰ It adopts a *closo*- structure bearing 26 triangulated faces, similar to that predicted for $[\text{B}_{15}\text{H}_{15}]^{2-}$ by theoretical calculations.^{66a,66c,d} It is noted that the cage geometry of CAd 14-vertex *nido*-carborane dianion in the sodium salt differs significantly from that observed in the 15-vertex ruthenacarborane, suggesting that cage rearrangements occur during the capitation reaction in order to accommodate the large Ru(II) ion.

Scheme 1.30. Synthesis of $7-(p\text{-cymene})-\mu-1,4-(\text{CH}_2)_3-7,1,4\text{-RuC}_2\text{B}_{12}\text{H}_{12}$.



Another CAd 15-vertex ruthenacarborane $7-(p\text{-cymene})-\mu-1,6-(\text{CH}_2)_3-7,1,6\text{-RuC}_2\text{B}_{12}\text{H}_{12}$ is prepared by the thermolysis of the CAd 14-vertex ruthenacarborane $1-(p\text{-cymene})-\mu-2,8-(\text{CH}_2)_3-1,2,8\text{-RuC}_2\text{B}_{11}\text{H}_{11}$ (Scheme 1.31).⁸² It is suggested that the formation of this 15-vertex species may involve adventitious capture of a BH fragment from the reaction system.

Scheme 1.31. Thermolysis Formation of 7-(*p*-cymene)- μ -1,6-(CH₂)₃-7,1,6-RuC₂B₁₂H₁₂.



1.4. Objectives

Compared to the well studied chemistry of icosahedral carboranes, that of supercarboranes is only at the beginning. The objectives of this dissertation are: 1) to study the role of the C,C'-linkage in the formation and stabilization of supercarboranes, 2) to synthesize other 13- and 14-vertex carboranes, and 3) to explore the nucleophilic reactions of supercarboranes.

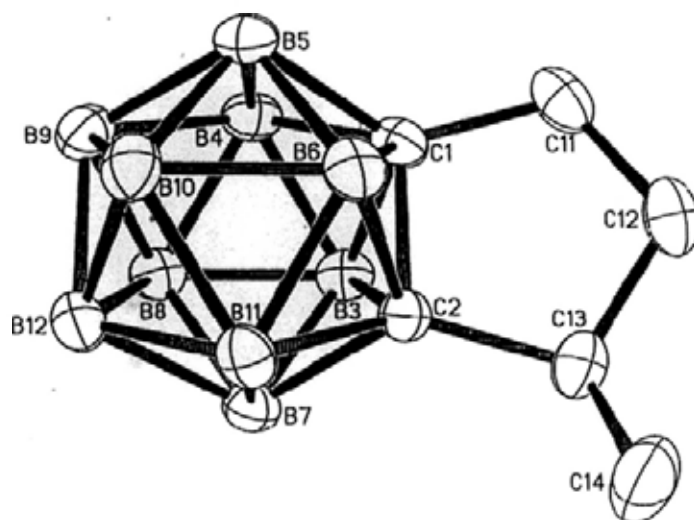
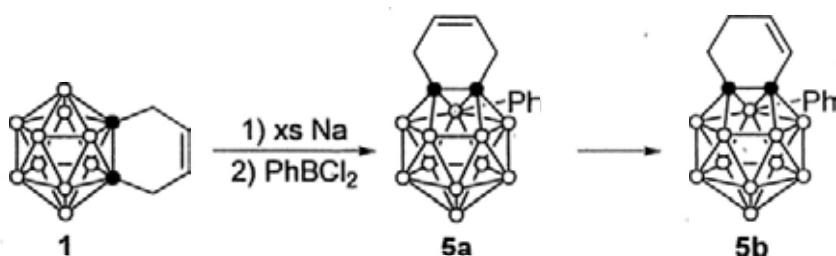


Figure 2.1. Molecular structure of μ -1,2-MeCH(CH₂)₂-1,2-C₂B₁₀H₁₀ (**4**).

Reaction of μ -1,2-(CH₂CH=CHCH₂)-1,2-C₂B₁₀H₁₀ (**1**) with excess of Na metal, followed by treatment with 2 equiv of PhBCl₂, afforded a 13-vertex carborane 3-Ph- μ -1,2-(CH₂CH=CHCH₂)-1,2-C₂B₁₁H₁₀ (**5a**) in 5% isolated yield after column chromatographic separation. Isomerization of **5a** to 3-Ph- μ -1,2-(CH=CHCH₂CH₂)-1,2-C₂B₁₁H₁₀ (**5b**) was observed after several months at room temperature (Scheme 2.2). The formation of **5b** might be due to the C=C double bond isomerization that was catalyzed by a very small amount of residual acid in **5a**.

Scheme 2.2. Synthesis of Two 13-Vertex Carborane Isomers.



Compounds **5a** and **5b** were characterized by several spectroscopic techniques, as well as HRMS, which confirmed their identical molecular mass. While **5a** exhibited a unique triplet at 5.69 ppm due to the splitting by the adjacent methylene group in the ¹H NMR spectrum and one peak at 122.9 ppm assigned to the CH unit in the ¹³C

NMR spectrum, **5b** showed two dt peaks at 6.74 and 6.41 ppm in the ^1H NMR spectrum and two peaks at 139.2 and 133.4 ppm in the ^{13}C NMR spectrum. The symmetric structure of **5a** in solution was also reflected by signals of only one type of methylene group at 3.41 ppm in the ^1H NMR spectrum and at 44.0 in the ^{13}C NMR spectrum, and cage carbon at 141.5 ppm, that were observed. The unsymmetric molecule **5b** showed two types of the corresponding signals, in the ^1H NMR spectrum at 2.81 (t) and 1.99 ppm (ddt) for the methylene units, and in the ^{13}C NMR spectrum at 39.1 and 20.4 ppm for the methylene units and at 136.0 and 135.2 ppm for the cage carbons. Their ^{11}B NMR spectra were also in different patterns.

Their structures were also determined by single-crystal X-ray analyses as shown in Figure 2.2. Although they are isomorphous and isostructural, the C12-C13 bond length of 1.319(2) Å in **5a** and C13-C14 bond length of 1.354(3) Å in **5b** clearly indicates the distinct C=C double bond locations in the 6-membered ring of the 13-vertex carboranes. This is consistent with their ^1H and ^{13}C NMR spectra.

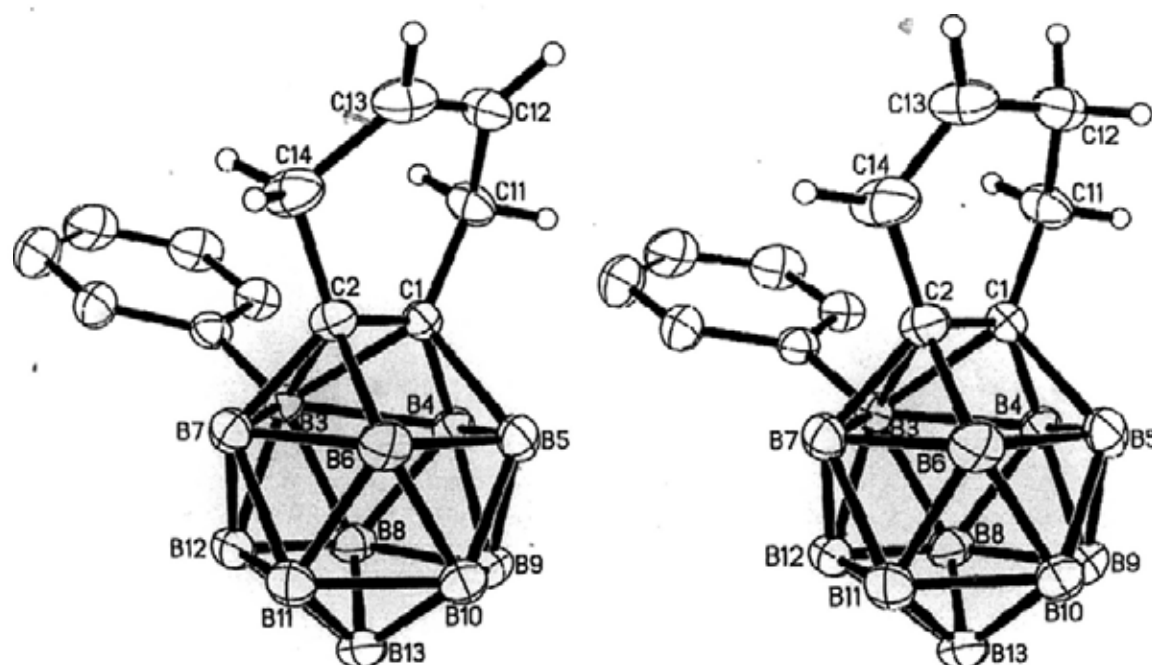
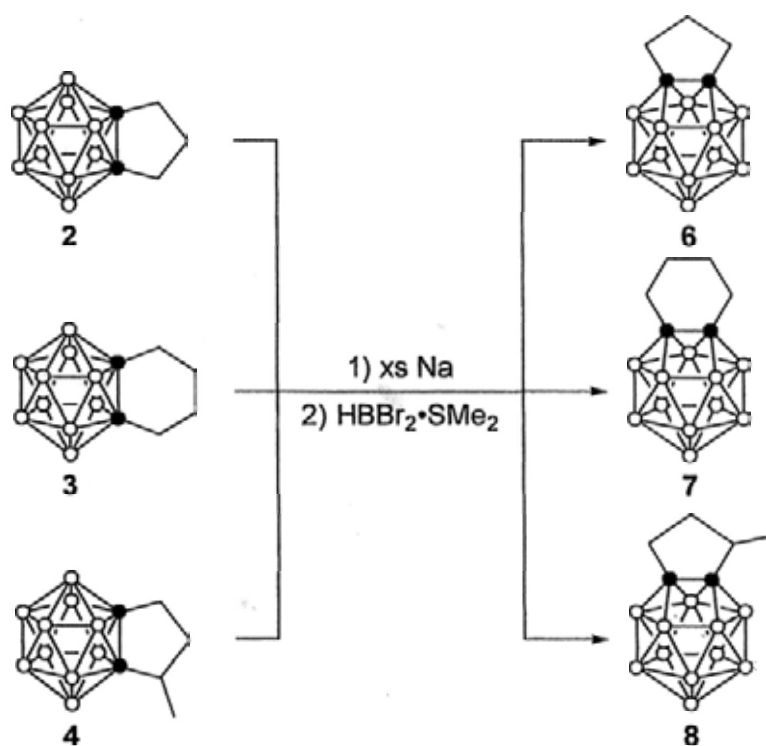


Figure 2.2. Molecular structures of 3-Ph- μ -1,2-(CH₂CH=CHCH₂)-1,2-C₂B₁₁H₁₀ (**5a**) (left) and 3-Ph- μ -1,2-(CH=CHCH₂CH₂)-1,2-C₂B₁₁H₁₀ (**5b**) (right).

The 13-vertex carborane μ -1,2-(CH₂)₃-1,2-C₂B₁₁H₁₁ (**6**) was synthesized according to the literature method from compound **2**.⁷⁴ In a similar manner, reaction of compounds **3** or **4** with excess Na metal in the presence of a catalytic amount of naphthalene followed by treatment of 2 equiv of HBrBr₂·SMe₂, gave the corresponding 13-vertex CAd carboranes μ -1,2-(CH₂)₄-1,2-C₂B₁₁H₁₁ (**7**), or μ -1,2-MeCH(CH₂)₂-1,2-C₂B₁₁H₁₁ (**8**) in 35% or 30% isolated yield after column chromatographic separation and recrystallization (Scheme 2.3).

Scheme 2.3. Synthesis of CAd 13-Vertex Carboranes.



Complexes **7** and **8** were characterized by several spectroscopic techniques as well as HRMS. Both of them showed a similar 1:5:5 pattern in the ¹¹B NMR, regardless of unsymmetric nature of compound **8**. The structures of compounds **6** and **7** were confirmed by single-crystal X-ray analyses as shown in Figures 2.3 and 2.4.

These reactions are not clean and contain many unidentified polar species that cannot be eluted by *n*-hexane, indicating that the reactions of CAd 12-vertex *nido*-carborane salts with HBrBr₂·SMe₂ are complicated, which is not limited to the capita-

tion processes and the redox reactions. Column chromatographic separation usually afforded 5% to 10% 12-vertex starting materials and a little amount of 14-vertex carborane isomers, in addition to 40% to 50% gross 13-vertex carboranes. These 14-vertex carboranes may be formed from the reduction of 13-vertex carboranes by the reductant, such as Na or $\text{NaC}_{10}\text{H}_8$ residue in the reaction system, followed by the capitation with borane reagent.

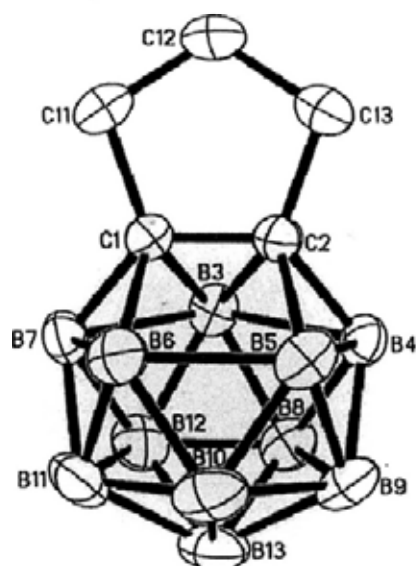


Figure 2.3. Molecular structure of $\mu\text{-1,2-(CH}_2\text{)}_4\text{-1,2-C}_2\text{B}_{11}\text{H}_{11}$ (6).

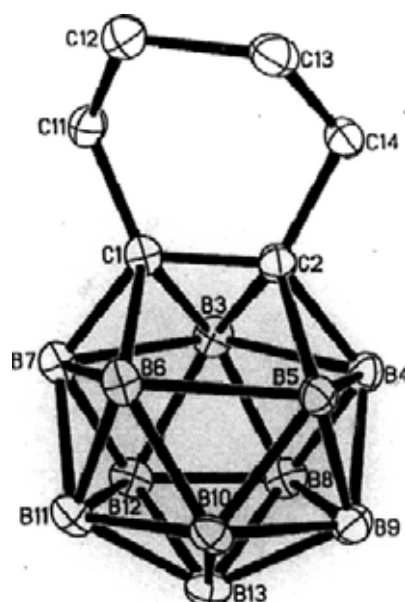


Figure 2.4. Molecular structure of $\mu\text{-1,2-(CH}_2\text{)}_4\text{-1,2-C}_2\text{B}_{11}\text{H}_{11}$ (7).

In the gross products of 13-vertex carboranes, we also observed a very small amount of 3-substituted 13-vertex carborane (cal. 5%) from ^{11}B NMR spectra. They were hard to purify by simple column chromatographic separation using *n*-hexane as elute, mainly because of the very similar polarities to the corresponding non-substituted ones. Complex 3-Me- μ -1,2-(CH₂)₃-1,2-C₂B₁₁H₁₀ (**6'**) was only distinguished from compound **6** in the ^1H NMR spectrum (Figure 2.5), in which the methyl group at 0.45 ppm was clearly observed. Fortunately, complex 3-Me- μ -1,2-(CH₂)₄-1,2-C₂B₁₁H₁₀ (**7'**) was able to be afforded in milligrams with more than 90% purity after repeated column chromatographic separation and recrystallization. It was characterized by several NMR spectroscopic techniques as well as HRMS. Its methyl signals also appeared in the high field, at 0.11 ppm in the ^1H NMR spectrum, and at 0.3 ppm (br) in the ^{13}C NMR spectrum. The structure of complex **7'** was confirmed by single-crystal X-ray analyses. As shown in Figure 2.6, it has similar cage geometry to those of other CA δ 13-vertex carboranes, and with the methyl group substituted on the B3 atom.

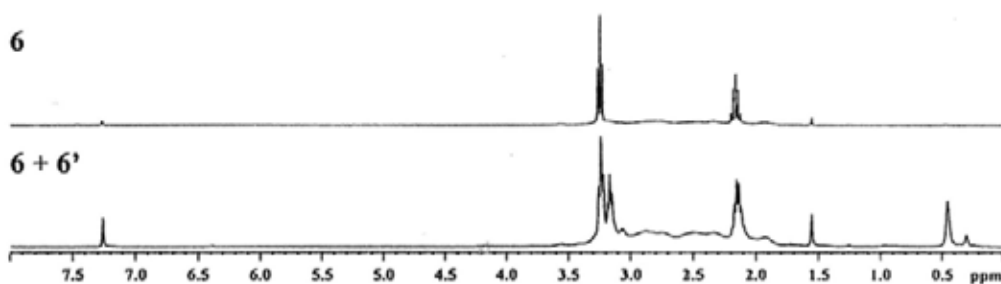


Figure 2.5. ^1H NMR spectra of **6** (top) and a mixture of **6** and **6'** (bottom).

The formation of 3-Me substituted 13-vertex carborane was unexpected. It would not likely be formed by electrophilic substitution reaction of a non-substituted 13-vertex carborane as 3-position is the least electron-rich site.⁷⁴ A possible pathway for its formation is via direct insertion of a $[\text{MeB}]^{2+}$ fragment into the 12-vertex *nido*-carborane dianion. On the other hand, we also found few crystals from the reaction

system, which was structurally characterized as $[\text{Me}_3\text{S}]\text{Br}$ (Figure 2.7). This result may suggest the possible formation of MeBBr_2 species in the reaction mixture via acid-base reactions.

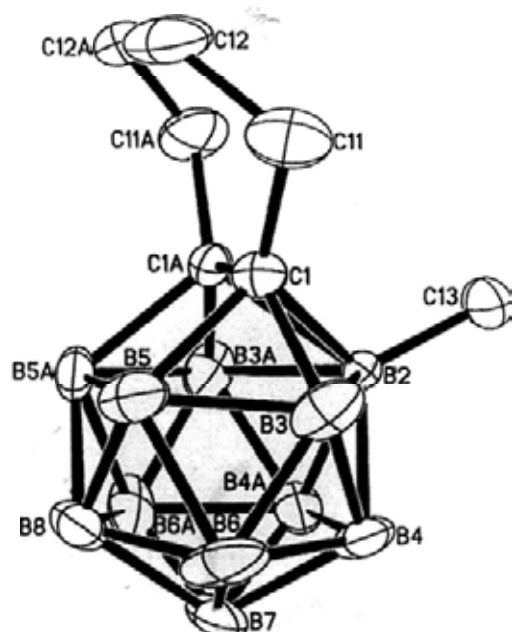


Figure 2.6. Molecular structure of 3-Me- μ -1,2-(CH₂)₄-1,2-C₂B₁₁H₁₀ (7').

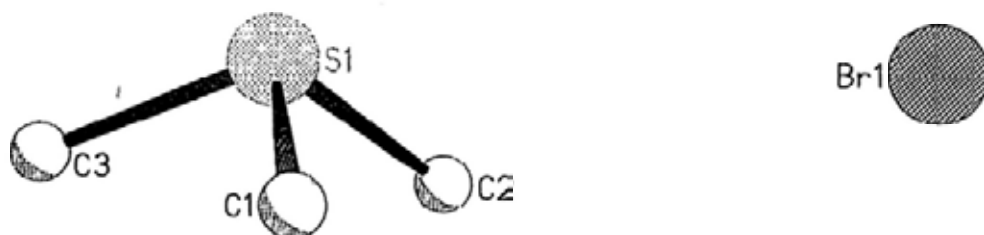


Figure 2.7. Molecular structure of $[\text{Me}_3\text{S}]\text{Br}$.

2.1.2. Structural and NMR Feature of CA_d 13-Vertex *closo*-Carboranes

All structurally characterized CA_d 13-vertex carboranes have a common henicosahedral geometry bearing one or two trapezoidal open faces constructed by the two cage carbons and two boron atoms of the B₅ belt. The more electronegative carbon atoms are less coordinated than the boron atoms. As a result, the cage C-C bond lengths in CA_d 13-vertex carboranes are remarkably shorter, ranging from 1.40 to 1.46 Å, than those found in 12-vertex *closo*-carboranes (Table 2.1). These distances

are even less than the normal C-C single bond,⁸⁴ indicative of increased bond order and more electrons filling in the bonding orbitals between them.

Table 2.1. Cage C-C Bond Lengths (Å) in CAd 13-Vertex Carboranes.

Compd.	C _{cage} -C _{cage} bond length
1,2-Me ₂ -1,2-C ₂ B ₁₁ H ₁₁ (17a)	1.421(5)
μ -1,2-(CH ₂) ₃ -1,2-C ₂ B ₁₁ H ₁₁ (6)	1.421(3)
3-Ph- μ -1,2-(CH ₂) ₃ -1,2-C ₂ B ₁₁ H ₁₀ ^a	1.443(2)
μ -1,2-Me ₂ Si(CH ₂) ₂ -1,2-C ₂ B ₁₁ H ₁₁ (16)	1.439(3)
μ -1,2-(CH ₂) ₄ -1,2-C ₂ B ₁₁ H ₁₁ (7)	1.425(4)
3-Me- μ -1,2-(CH ₂) ₄ -1,2-C ₂ B ₁₁ H ₁₀ (7')	1.408(4)
μ -1,2- <i>o</i> -C ₆ H ₄ (CH ₂) ₂ -1,2-C ₂ B ₁₁ H ₁₁ ^a	1.427(2)
5-Ph- μ -1,2- <i>o</i> -C ₆ H ₄ (CH ₂) ₂ -1,2-C ₂ B ₁₁ H ₁₀ ^b	1.427(2)
3-Ph- μ -1,2-CH ₂ CH=CHCH ₂ -1,2-C ₂ B ₁₁ H ₁₀ (5a)	1.414(2)
3-Ph- μ -1,2-CH=CHCH ₂ CH ₂ -1,2-C ₂ B ₁₁ H ₁₀ (5b)	1.404(2)
8,9,10,11,12,13-Me ₆ - μ -1,2-(CH ₂) ₃ -1,2-C ₂ B ₁₁ H ₅ ^a	1.461(9)
8,9,10,11,12,13-Br ₆ - μ -1,2-(CH ₂) ₃ -1,2-C ₂ B ₁₁ H ₅ ^a	1.420(10)
{ μ -1,2-(CH ₂) ₃ -1,2-C ₂ B ₁₁ H ₁₁ } ^{-c}	1.447(12)

^a Ref. 74. ^b Ref. 69. ^c Ref. 77.

The ¹¹B NMR spectra of all CAd 13-vertex carboranes without substituents on the B atoms show a similar 1:5:5 pattern spanning in a small range from 6 to -1 ppm except for μ -1,2-Me₂Si(CH₂)₂-1,2-C₂B₁₁H₁₁ (**16**), in which two peaks are overlapped to exhibit a 1:10 pattern. On the other hand, different substituents on cage carbons clearly influence the pattern and chemical shifts of ¹¹B NMR spectra of the 12-vertex carboranes. This implies that the C-substituents have less effect on the ¹¹B NMR spectra of 13-vertex carboranes.

The characteristic ^{13}C chemical shifts of the less coordinated cage carbons in these 13-vertex carboranes are observed at about 140 ppm, which are similar to those observed in benzene analogues, but downfield shifted by up to 70 ppm compared to the 12-vertex cousins (Table 2.2). The hybridization of a ^{13}C atom is of decisive importance for the chemical shift. sp^3 C atoms absorb at highest field, followed by sp C atoms and finally by sp^2 C atoms at lowest field.⁸⁵ In this regard, the cage carbons in the CAd 13-vertex carboranes can be formally viewed as sp^2 hybridized, while those in an icosahedron are sp hybridized (It is noted that despite of the sp hybridization bonding model of icosahedral carboranes, the calculated value is about $sp^{1.6}$ using ^{13}C - ^1H coupling constant.^{16g}).⁸⁶ This is in accordance with the C-C bond lengths, which can be ascribed to the (partial) overlap of the remaining p -orbitals. Thus a hypothetical bonding model of CAd 13-vertex carborane can be roughly described as shown in Figure 2.8. The two cage carbons are sp^2 hybridized and all cage borons are sp hybridized. A cage carbon would use one radial sp^2 orbital to bind with the *exo*-substituent, the second one to interact with another one on the other cage carbon in the same direction to form a σ -bond, and the last one to take part in the forming of bonding and anti-bonding MOs with the tangential p -orbitals of the boron atoms. π -Bonding interaction would be resulted from overlap of the remaining p -orbitals on the cage carbons. These two orbitals would also take part in the MOs formation in the whole cluster as a result of orbital overlap with the tangential p -orbitals of the boron atoms. In other words, it can be viewed that the π -electrons on the two cage carbons would delocalized to the boron-cage part (Figure 2.9), thus the C-C bond lengths are between a normal C-C single bond and a normal C=C double bond.

The anisotropic effect caused by this type of π -interaction on the cage carbons makes the peaks of the α -CH attached to cage carbons more deshielded and generally

shifted toward the low field, by 0.5 to 0.8 ppm, as the clusters change from 12-vertex to the 13-vertex ones. Meanwhile, the ^{13}C chemical shifts of the α -CH units are also downfielded by 10 to 15 ppm. This influence is a little bit weaker when there is a substituent on the B3 atom, probably as a result of the electronic effect. These data are also comparable with those of the benzene analogues, which are also shifted to the low field. It indicates that the outer substituents are more deshielded in the 13-vertex carboranes than those in the corresponding benzene derivatives. Thus, their cages can serve as strong electron-withdrawing groups.

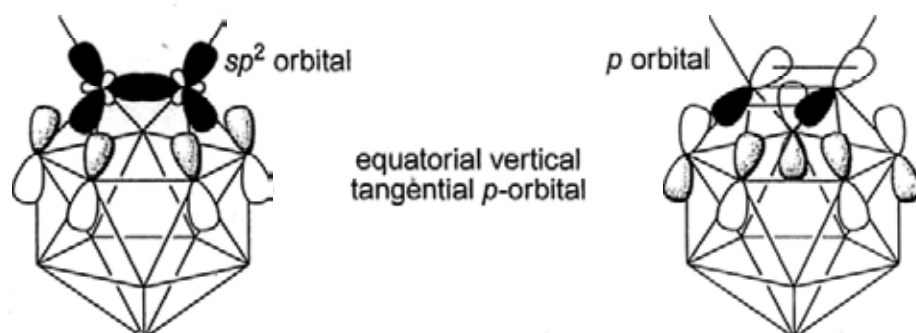
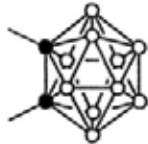
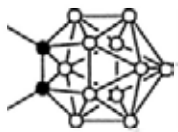
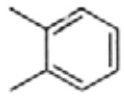
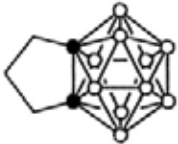
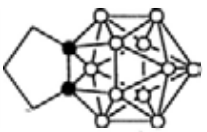
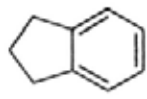
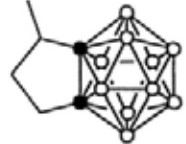
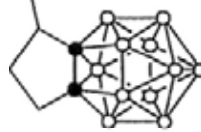
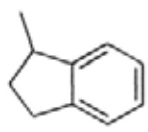


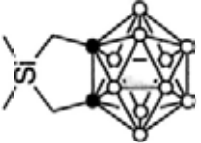
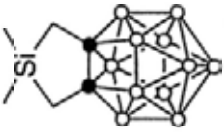
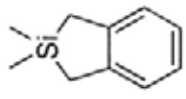

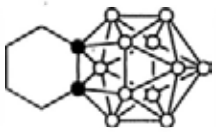
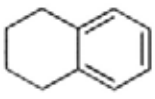

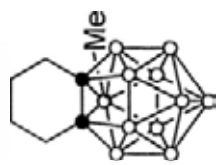

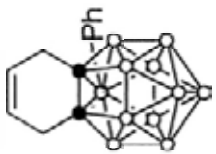
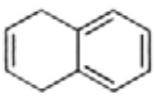
Figure 2.8. Hypothetic bonding model of a CAd 13-vertex carborane and possible overlap and interaction of sp^2 and p -orbitals on the sp^2 -hybridized cage carbons with equatorial vertical tangential p -orbitals on the sp -hybridized cage borons, for example.

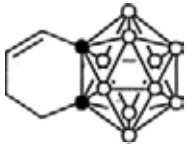
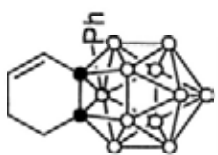
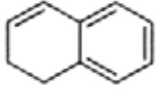
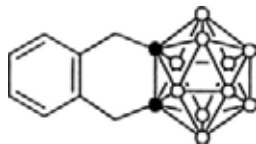
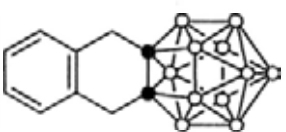
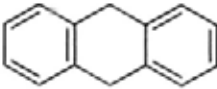
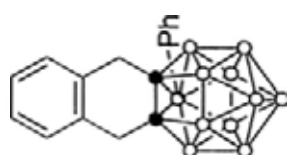


Figure 2.9. Formal electron delocalization between a two-dimensional fragment (cage carbons) and a three-dimensional fragment (cage borons) in a CAd 13-vertex carborane.

Table 2.2. Corresponding ^1H and ^{13}C Chemical Shifts (ppm) of 12-, 13-Vertex Carboranes and Their Benzene Analogues in CDCl_3 .

Compd.	12-Vertex carborane			13-Vertex carborane			Benzene analogue				
	$\alpha\text{-CH}$	$\alpha\text{-CH}$	Cage C	$\alpha\text{-CH}$	$\alpha\text{-CH}$	Cage C	Compd.	$\alpha\text{-CH}$	$\alpha\text{-CH}$	Quat C	
	2.03	23.4	73.5		2.73	34.9	140.7		^a 2.19	19.6	136.4
	2.50	34.8	84.0		3.24	49.3	136.4		^c 3.01	33.1	144.3
	2.91	41.0	88.0		3.22	53.9	142.3		^d 2.7-3.0	34.8	143.8
	2.42	34.1	84.2		3.23	47.8	136.1		3.0-3.4	39.6	148.7
					3.04						

12-Vertex carborane			13-Vertex carborane			Benzene analogue					
Compd.	α -CH	α -CH	Compd.	α -CH	α -CH	Compd.	α -CH	α -CH	Quat C		
		Cage C			Cage C						
	1.81	25.3	87.5		2.55	40.7	144.5		^e 2.15	21.3	142.2
	2.43	32.9	73.2		3.05	44.2	142.5		^f 2.77	29.4	137.1
					2.99	42.6	143.9				
	3.01	33.2	70.2		3.41	44.0	141.5		^g 3.40	29.8	134.2

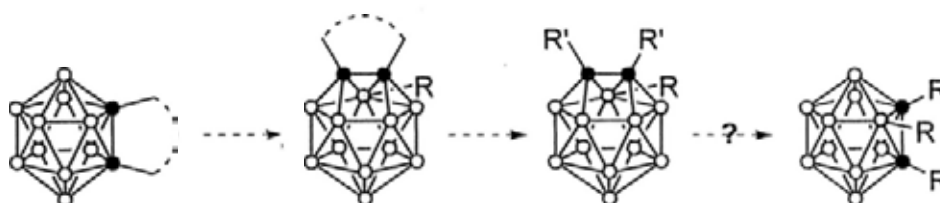
12-Vertex carborane				13-Vertex carborane				Benzene analogue				
Compd.	α -CH	α -CH	Cage C	Compd.	α -CH	α -CH	Cage C	Compd.	α -CH	α -CH	α -CH	Quat C
	/	/	/		2.81	39.1	136.0		^h 2.79	27.9	134.6	
	3.75	37.6	71.2		^b 4.35	50.8	/		^k 3.93	36.0	136.5	
					^j 3.91	48.7	140.2					

^a Ref. 87. ^b Ref. 74. ^c Ref. 88. ^d Ref. 89. ^e Ref. 90. ^f Ref. 91. ^g Ref. 92. ^h Ref. 93. ⁱ Ref. 45c. ^j Ref. 69. As the quat C of the phenyl group that is attached to B atom is hard to resolve, we arbitrarily assume the signal at 140.2 ppm should be of the cage C. ^k Ref. 94.

2.2. Synthesis and Structure of CAP 13-Vertex *closo*-Carboranes and *closo*-Metallacarboranes

The successful synthesis of supercarboranes relies on the use of CAd carborane anions with a short C,C'-linkage, which have relative low reducing power compared to their CAP counterparts.^{48y,z} It was reported that reactions of CAP *nido*-carborane anions with several RBX₂ reagents afforded only 12-vertex carboranes, which were believed to be thermal decomposition products of the newly formed 13-vertex carboranes.^{67,69} These results lead to an assumption that the C,C'-linkage is crucial to stabilize the 13-vertex carborane.^{68,69} To address the role of the C,C'-linkage in the formation and stabilization of 13-vertex carboranes, we intended to employ a 12-vertex carborane with a potentially removable linkage for the synthesis of a 13-vertex one by the polyhedral expansion method. The thermal stability of the 13-vertex carborane without linkage will be examined after removal of the linkage. (Scheme 2.4).

Scheme 2.4. Procedure to Investigate the Role of C,C'-Linkage in Stabilization of 13-Vertex Carboranes.



2.2.1. Screening the Ligand

To achieve the goal mentioned above, a 12-vertex carborane with a potentially removable linkage should be prepared, which must meet the following conditions: (1) it can be used to synthesize a CAd 13-vertex carborane; (2) its linkage is stable under normal conditions; and (3) its linkage can be easily removed. Thus we chose some

compounds with unsaturated bond or heteroatom in the cyclic ring as candidates for our purpose, such as μ -1,2-(CH₂CH=CHCH₂)-1,2-C₂B₁₀H₁₀ (**1**),⁸³ μ -1,2-O(CH₂)₂-1,2-C₂B₁₀H₁₀ (**9**),^{17a,b} μ -1,2-O(Me₂Si)₂-1,2-C₂B₁₀H₁₀ (**10**)⁹⁵ and μ -1,2-Me₂Si(CH₂)₂-1,2-C₂B₁₀H₁₀ (**11**),^{17a} which are shown in Figure 2.10. These complexes were prepared according to the literature methods.

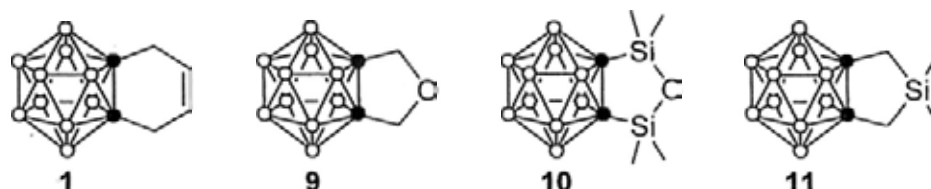
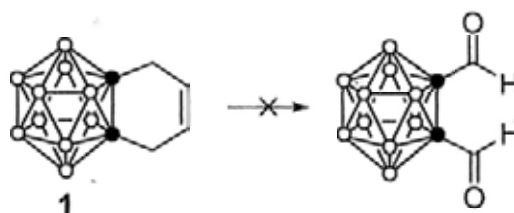


Figure 2.10. 12-Vertex carboranes with potentially removable linkage.

Compound μ -1,2-(CH₂CH=CHCH₂)-1,2-C₂B₁₀H₁₀ (**1**) can be used to synthesize a 13-vertex carborane 3-Ph- μ -1,2-(CH₂CH=CHCH₂)-1,2-C₂B₁₁H₁₀ (**5a**) as mentioned in Chapter 2.1. However, the C=C double bond in **1** was very stable under several reaction conditions examined. For example, it was unchanged in a 1:1 ClCH₂CH₂Cl/H₂O mixture in the presence of 2 equiv NaIO₄ and 0.1 equiv RuCl₃,⁹⁶ or in a 3:1 THF/H₂O solution in the presence of 2 equiv KMnO₄ at room temperature.⁹⁷ Although **1** did react with NaIO₄ in the presence of RuCl₃ in a 6:1 MeCN/H₂O mixture, the messy ¹H NMR spectrum indicated complicated products formation (Scheme 2.5). Compound **1** is not a good candidate.

Scheme 2.5. Proposed Oxidative Cleavage of C=C double Bond in μ -1,2-(CH₂CH=CHCH₂)-1,2-C₂B₁₀H₁₀ (**1**).



Compound μ -1,2-O(CH₂)₂-1,2-C₂B₁₀H₁₀ (**9**) reacted readily with Na metal to give a mixture of products. Treatment of **9** with excess Na metal in the presence of a catalytic amount of naphthalene in THF resulted in the formation of a dark red solution after one day. This solution was concentrated to afford some tiny yellow crystals, one of which was structurally characterized as [7,7'-(CH₂CH₂)-9,9'-Me₂-7,7',9,9'-(C₂B₁₀H₁₀)₂][Na₄(THF)₁₂] ([**12a**][Na₄(THF)₁₂]). On the other hand, addition of excess 18-crown-6 to this dark red solution with stirring gave some crystals which were determined by X-ray diffraction as [μ -7,8-O(CH₂)₂-7,8-C₂B₉H₉][Na₂(18-crown-6)] ([**12b**][Na₂(18-crown-6)]). Treatment of the same solution with 2 equiv of HBBBr₂·SMe₂ gave 1,2-Me₂-1,2-C₂B₁₀H₁₀ (**13**) in 5% isolated yield after column chromatography using *n*-hexane as elute (Scheme 2.6).

Scheme 2.6. Reaction of μ -1,2-O(CH₂)₂-1,2-C₂B₁₀H₁₀ (**9**) with Na Metal.

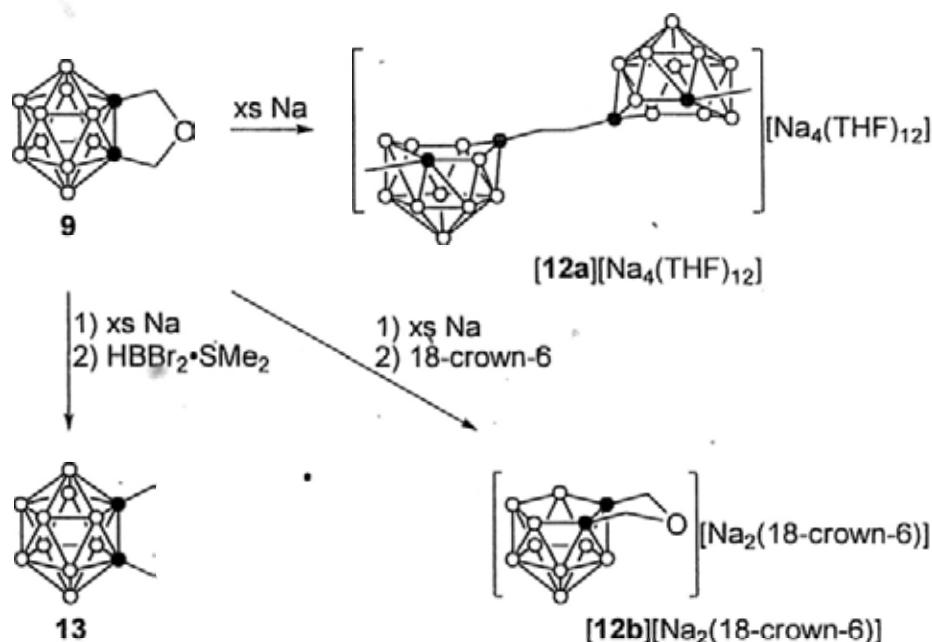


Figure 2.11 clearly shows the structure of [**12a**][Na₄(THF)₁₂], which bears two 12-vertex *nido*-carborane cages that are linked by an ethylene unit. The *exo*-substituents on the cage indicated the cage carbon atoms are in 7- and 9-positions. The C71-C71A distance of 1.419(7) Å cannot determine whether it is a single bond

or a double bond, due to the poor resolution of the crystal, but the C-O bonds cleavage is doubtless. **[12b]**[Na₂(18-crown-6)] exhibits two-dimensional polymeric structure, as shown in Figure 2.12, in which the cages are linked by three types of Na⁺ counterions in different coordination environment. It clearly shows the *nido*-C₂B₉²⁻ cage geometry with the C,C'-linkage being preserved.

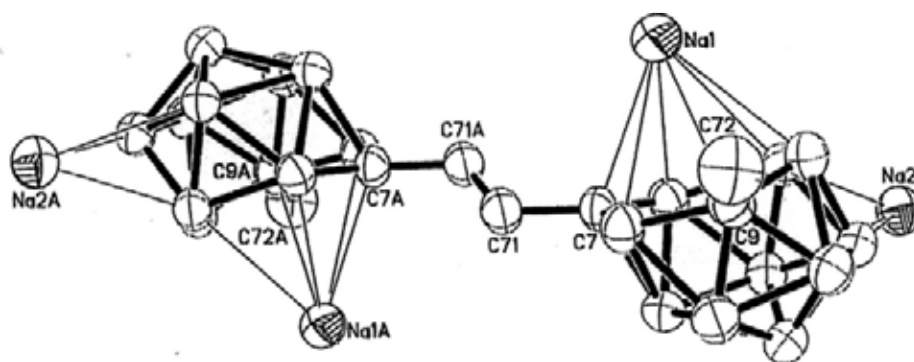


Figure 2.11. Molecular structure of [7,7'-(CH₂CH₂)-9,9'-Me₂-7,7',9,9'-(C₂B₁₀H₁₀)₂][Na₄(THF)₁₂] (**[12a]**[Na₄(THF)₁₂]). The THF molecules are omitted.

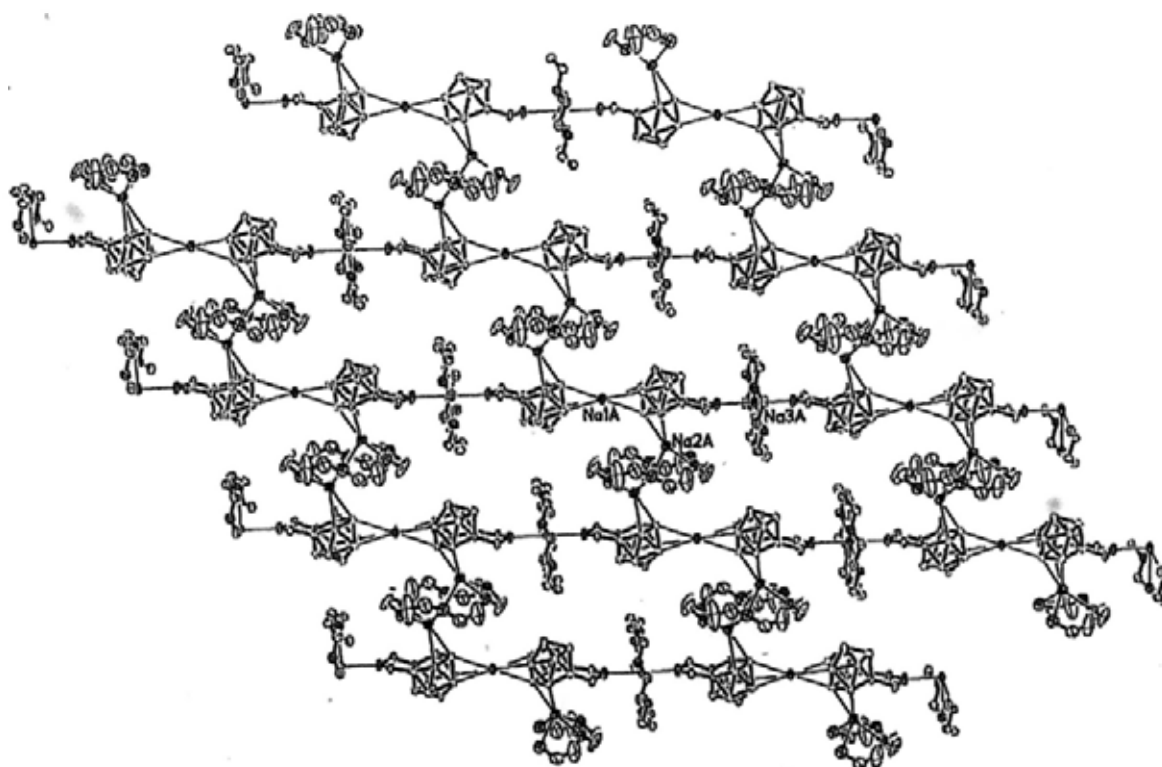
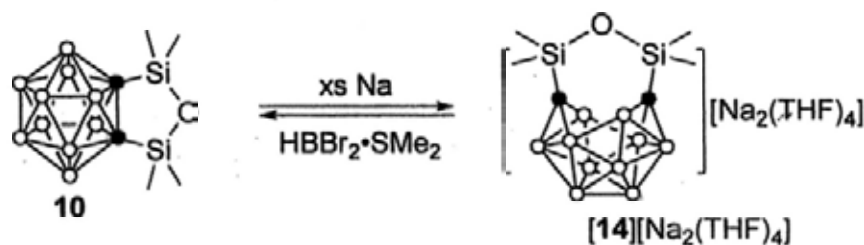


Figure 2.12. Two-dimensional polymeric structure of [μ-7,8-O(CH₂)₂-7,8-C₂B₉H₉][Na₂(18-crown-6)] (**[12b]**[Na₂(18-crown-6)]).

The structural identification of **[12a]**[Na₄(THF)₁₂] and **[12b]**[Na₂(18-crown-6)] suggested the complexity of reaction of **9** with Na metal. Cleavages of C-O bonds by alkali metals or alkali metal aromatic radical anions to the corresponding group 1 metal alkyls and alkoxides are well documented, and radical intermediates are regarded to be involved in the process, which are summarized in earlier reviews.⁹⁸ Thus, a possible mechanism can be proposed which involves several radical intermediate with the formation of Na₂O. Hydrogen abstraction or radical coupling leads to several 12-vertex carboranes which can be reduced to the corresponding *nido*- anions. Na₂O may cause deboration of **9** in THF to give *nido*-**[12b]**²⁻.

We then examined the suitability of μ -1,2-O(Me₂Si)₂-1,2-C₂B₁₀H₁₀ (**10**), as it is reported that C_{cage}-Si bonds of *o*-carboranes can be readily cleaved by TBAF to give the corresponding desilylated species in high yields.²⁰ Compound **10** reacted readily with excess Na metal in THF even without the presence of naphthalene to give a clear yellow green solution. Recrystallization from THF gave $[\mu$ -7,10-O(Me₂Si)₂-7,10-C₂B₁₀H₁₀][Na₂(THF)₄] (**[14]**[Na₂(THF)₄]) as yellow crystals in 90% isolated yield. Treatment of this *nido*-carborane salt with excess HBBR₂·SMe₂ in toluene/CH₂Cl₂ gave only **10** as observed from ¹¹B NMR spectrum, without isolation of any 13-vertex species (Scheme 2.7).

Scheme 2.7. Synthesis and Oxidation of a 12-Vertex *nido*-7,10-Carborane Salt.



Compound **[14]**[Na₂(THF)₄] was characterized by various spectroscopic techniques as well as elemental analyses. Its ¹¹B NMR spectrum shows 4 peaks in a ratio

of 2:2:4:2 at 13.0, -2.4, -17.7 and -20.8 ppm, which is significantly different from its precursor **10**. Single-crystal X-ray analyses showed that the cage carbons are in the 7,10-positions rather than in the 7,8-positions (Figure 2.13), making the 6-membered open-face of the *nido*-carborane anion highly distorted, which is similar to those reported for 12-vertex *nido*-carborane anions $[\mu\text{-}7,10\text{-R}_2\text{-}7,10\text{-C}_2\text{B}_{10}\text{H}_{10}]^{2-}$ with linkages ($\text{R}_2 = o\text{-C}_{12}\text{H}_8(\text{CH}_2)_2, (\text{CH}_2)_5, (\text{CH}_2)_6$).^{45c,d} The C...C separation of 2.763(7) Å is in the range of 2.69-2.97 Å that observed in these compounds. Formation of the 7,10-isomer rather than the 7,8- one is probably due to the large ring size, which is caused by two big Si atoms. This linkage is just seated over the open face of *nido*-carborane cage, which blocks the approach and insertion of a $[\text{BH}]^{2+}$ unit upon treatment of **[14]** $[\text{Na}_2(\text{THF})_4]$ with $\text{HBBR}_2\cdot\text{SMe}_2$.

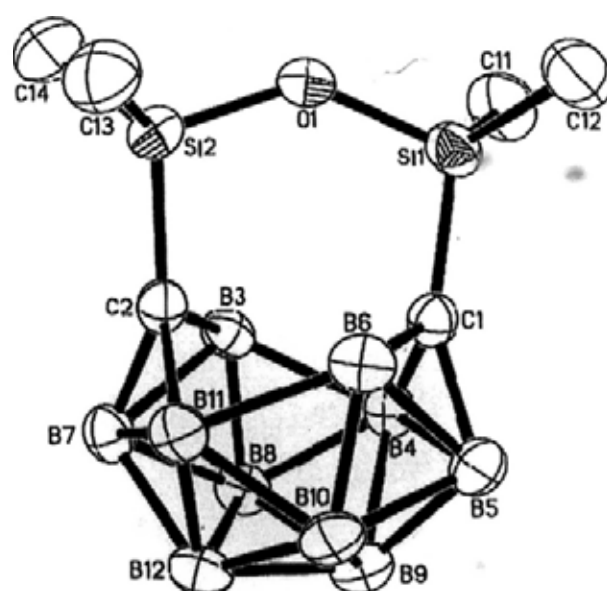
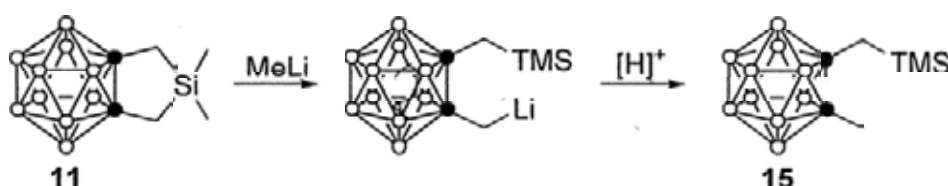


Figure 2.13. Structure of $[\mu\text{-}7,10\text{-O}(\text{Me}_2\text{Si})_2\text{-}7,10\text{-C}_2\text{B}_{10}\text{H}_{10}]^{2-}$ (**[14]**²⁻), in **[14]** $[\text{Na}_2(\text{THF})_4]$.

$\mu\text{-}1,2\text{-Me}_2\text{Si}(\text{CH}_2)_2\text{-}1,2\text{-C}_2\text{B}_{10}\text{H}_{10}$ (**11**), which bears a smaller ring than compound **10**, was selected for testing. Treatment of **11** with TBAF only afforded deboration products as monitored by ¹¹B NMR spectrum. On the other hand, it is documented that 1-R-2-TMSCH₂-1,2-C₂B₁₀H₁₀ can react with *n*-BuLi to cleave the C-Si bond,

affording the transmetallation product 1-R-2-LiCH₂-1,2-C₂B₁₀H₁₀.⁹⁹ In a similar manner, compound **11** was treated with 2 equiv MeLi in Et₂O at room temperature for one day, to afford intermediate 1-TMSCH₂-2-LiCH₂-1,2-C₂B₁₀H₁₀. Subsequent quenching of the reaction by HCl afforded 1-TMSCH₂-2-Me-1,2-C₂B₁₀H₁₀ (**15**) in almost quantitative yield (Scheme 2.8). It was noted that excess MeLi did not give the bis-metallated product 1,2-(LiCH₂)₂-1,2-C₂B₁₀H₁₀, making the reaction easy to handle.

Scheme 2.8. Cleavage of One C-Si Bond of μ -1,2-Me₂Si(CH₂)₂-1,2-C₂B₁₀H₁₀ (**11**).



Compound **15** was characterized by various spectroscopic methods as well as HRMS. Its ¹¹B NMR spectrum showed a pseudo 2:2:6 pattern which is similar to that of compound **11**, but their ¹H and ¹³C NMR spectra were distinct from each.

2.2.2. Synthesis of μ -1,2-Me₂Si(CH₂)₂-1,2-C₂B₁₁H₁₁ and Unprecedented C-Si Bond Cleavage

Compound **11** was readily reduced by excess Na metal in THF even in the absence of naphthalene, which gave the corresponding *nido*-carborane salt [μ -7,8-Me₂Si(CH₂)₂-7,8-C₂B₁₀H₁₀][Na₂(THF)_x] as viewed from ¹¹B NMR. Addition of 2 equiv of HBBBr₂·SMe₂ to a toluene suspension of this salt at -78°C to 0 °C gave a slurry yellow solution. The ¹¹B NMR spectrum of the solution phase showed two major peaks at about 3 and 0 ppm in a ratio of about 1:10, which were for those of the product μ -1,2-Me₂Si(CH₂)₂-1,2-C₂B₁₁H₁₁ (**16**). However, column chromatographic separation did not afford the desired product, rather gave a major species with 3 peaks in the region of 5 to 0 ppm in a molar ratio of 1:5:5 in the ¹¹B NMR,

which indicated the desired product is not stable toward silica gel. We reexamined the reaction. Recrystallization from $\text{CH}_2\text{Cl}_2/n$ -hexane was performed to afford compound **16** in 39% isolated yield after the solution stood at room temperature for one day (Scheme 2.9).

Scheme 2.9. Synthesis of a CAAd 13-Vertex Carborane.

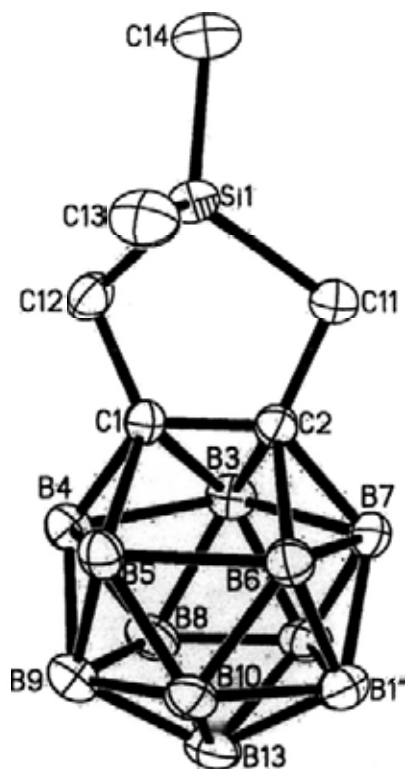


Figure 2.14. Molecular structure of μ -1,2- $\text{Me}_2\text{Si}(\text{CH}_2)_2$ -1,2- $\text{C}_2\text{B}_{11}\text{H}_{11}$ (**16**).

It was fully characterized by ^1H , ^{13}C , and ^{11}B NMR spectroscopy as well as HRMS. The ^{11}B NMR spectrum showed a 1:10 not a 1:5:5 pattern which may be caused by coincident overlap of the peaks. Two singlets at 2.55 and 0.31 ppm attributable to the methylene and methyl units, respectively, were observed in the ^1H

NMR spectrum. Single-crystal X-ray analyses confirmed that **16** has a hencosaedral structure which is similar to that of the known 13-vertex carboranes (Figure 2.14).

When subjected to column chromatography on SiO₂ using *n*-hexane as elute, compound **16** can be totally desilylated and 1,2-Me₂-1,2-C₂B₁₁H₁₁ (**17a**) and 1,12-Me₂-1,12-C₂B₁₁H₁₁ (**17b**) were isolated in 60% and 30% yields, respectively (Scheme 2.10). Compounds **17a** and **17b** have the identical HRMS, indicating that they are isomers. The ¹¹B NMR spectrum of **17a** showed a clear 1:5:5 pattern, while that of **17b** exhibited a *pseudo* 1:10 pattern where a broad peak is not well resolved. The ¹H NMR spectra displayed only one singlet of the methyl protons at 2.73 ppm for **17a** and two singlets at 2.63 and 1.89 ppm assignable to the two different methyl groups for **17b**. Accordingly, two resonances at 140.6 (cage C) and 34.8 ppm (CH₃) and four peaks at 120.7, 83.0 (cage C) and 35.6, 27.3 ppm (CH₃) were observed in the ¹³C NMR spectra of **17a** and **17b**, respectively. These spectroscopic data suggest that the two cage carbon atoms in **17b** have different coordination environments compared to **17a**: one may be more connected than the other. The molecular structure of **17a** was confirmed by single-crystal X-ray analyses, as shown in Figure 2.15. The cage geometry is almost the same as that observed in **16** with the two cage carbon atoms remaining in adjacent positions. Compound **17a** represents the first 13-vertex carborane without a C,C'-linkage.

Compound **17a** was not stable in solution and would slowly isomerize to **17b**. This process was favored upon heating in a toluene solution and quantitative conversion occurred within one day, suggesting that **17b** resulted from **17a** and was a thermodynamically stable product. No decomposition was observed during this process as evidenced by NMR spectra. These results show clearly that the C,C'-linkage does

not have any obvious effects on the stability of 13-vertex carboranes, and **17b** is thermodynamically more stable than its structural isomer **17a**, which is well consistent with the properties of 12-vertex carboranes.^{6,7}

Scheme 2.10. Unprecedented Disilylation of μ -1,2-Me₂Si(CH₂)₂-1,2-C₂B₁₁H₁₁ (**16**).

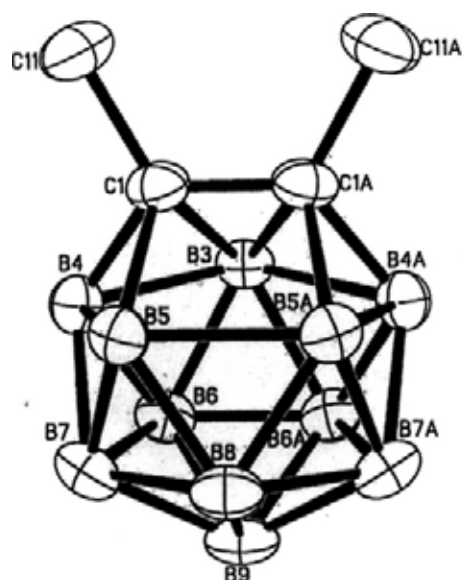
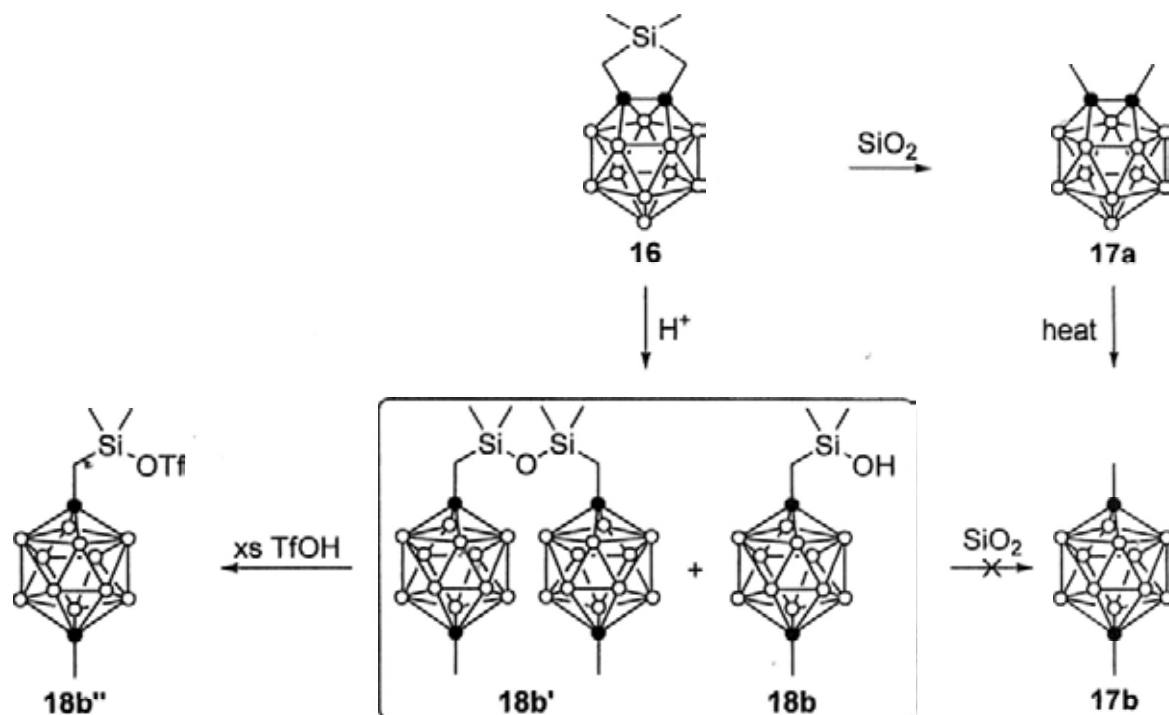


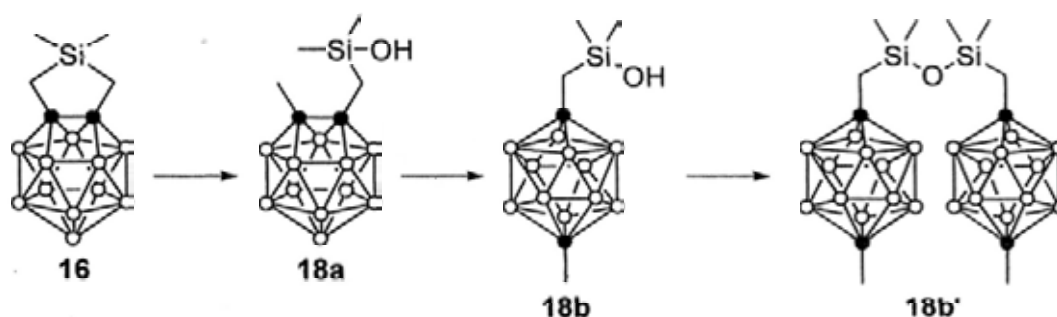
Figure 2.15. Molecular structure of 1,2-Me₂-1,2-C₂B₁₁H₁₁ (**17a**).

On the other hand, compound **16** can also undergo mono-desilylation. Although it

was stable in the solid state, it would slowly decompose in the *n*-hexane mother liquor to give a sticky oil after one week. Subsequent extraction by *n*-hexane afforded a mixture of **17b** (minor) and presumably, 1-HOMe₂SiCH₂-12-Me-1,12-C₂B₁₁H₁₁ (**18b**) and 1,1'-O(Me₂SiCH₂)₂-12,12'-Me₂-(1,12-C₂B₁₁H₁₁)₂ (**18b'**) (major), according to the NMR spectra. Compound **17b** can be removed by thoroughly drying at 60 °C via vacuum for 6 h, leaving a mixture of **18b** and **18b'** in about 60% yield. This mixture exhibited a very similar ¹¹B NMR spectrum to that of **17b**, although the signals were broadened, indicating the nature of CAp 13-vertex carborane. The ¹H NMR spectrum showed two different Me₂SiCH₂ units, while the Me substituents on the B12 atoms of the two complexes overlapped. Meanwhile, the ¹³C NMR spectrum also showed overlapping signals of **18b** and **18b'**. However, two signals at 4.6 and 3.0 ppm in a ratio of *ca.* 5:2 were observed in the ²⁹Si NMR spectrum. When treated with excess TfOH in a C₂D₂Cl₄ solution, the mixture can be converted to a single product 1-TfOMe₂SiCH₂-12-Me-1,12-C₂B₁₁H₁₁ (**18b''**) in situ as evidenced by ¹H, ¹³C and ²⁹Si NMR spectra. The ¹H and ¹³C signals of the Me₂SiCH₂ unit were upfield shifted by the influence of the strong electron withdrawing Tf group. Moreover, the corresponding ²⁹Si signal was observed at 37.3 ppm, which was comparable to that of 44.0 for TfOTMS.¹⁰⁰ This complex was very hygroscopic and converted to the mixture of **18b** and **18b'** upon contact with water and not isolated.

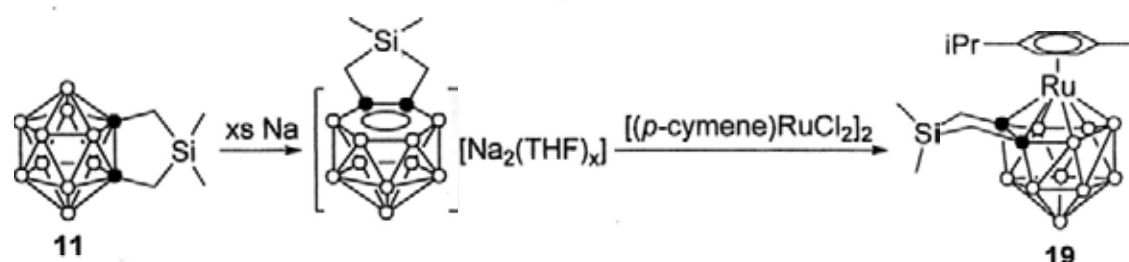
Formation of **18b** and **18b'** would result from mono-desilylation of **16** to form a CAp 13-vertex carborane intermediate **18a**. Complex **18a** would isomerize to **18b**, which then underwent partial dehydration to afford **18b'** in solution (Scheme 2.11). This mixture of **18b** and **18b'** was stable toward silica gel even in refluxing CDCl₃, without detection of **17b**, which indicated different desilylation pathways.

Scheme 2.11. Proposed Mechanism for the Formation of **18b** and **18b'**.



To understand the reasons for facile desilylation of compound **16** over silica gel, we examined the properties of a 13-vertex ruthenacarborane analogue of **16**. Reduction of compound **11** by excess Na metal in THF to afford its salt *nido*-[μ -7,8-Me₂Si(CH₂)₂-7,8-C₂B₁₀H₁₀][Na₂(THF)_x]. Treatment of this salt with 0.5 equiv of [(*p*-cymene)RuCl₂]₂ gave 4-(*p*-cymene)- μ -1,2-Me₂Si(CH₂)₂-4,1,2-RuC₂B₁₀H₁₀ (**19**) in about 50% isolated yield after column chromatographic separation on silica gel (Scheme 2.12).

Scheme 2.12. Synthesis of a 13-Vertex Ruthenacarborane.



Compound **19** was characterized by various spectroscopic techniques as well as HRMS. Its ¹¹B NMR shows a 2:2:1:1:2:2 pattern in the range 7 to -17 ppm, which is parallel to that observed in 4-(*p*-cymene)- μ -1,2-(CH₂)₃-4,1,2-RuC₂B₁₀H₁₀.^{57a} Its structure was unambiguously determined by single-crystal X-ray analyses as shown in Figure 2.16, which is also similar to that of 4-(*p*-cymene)- μ -1,2-(CH₂)₃-4,1,2-RuC₂B₁₀H₁₀. Also, it contains a trapezoidal open face like that of a CAd 13-vertex carborane.

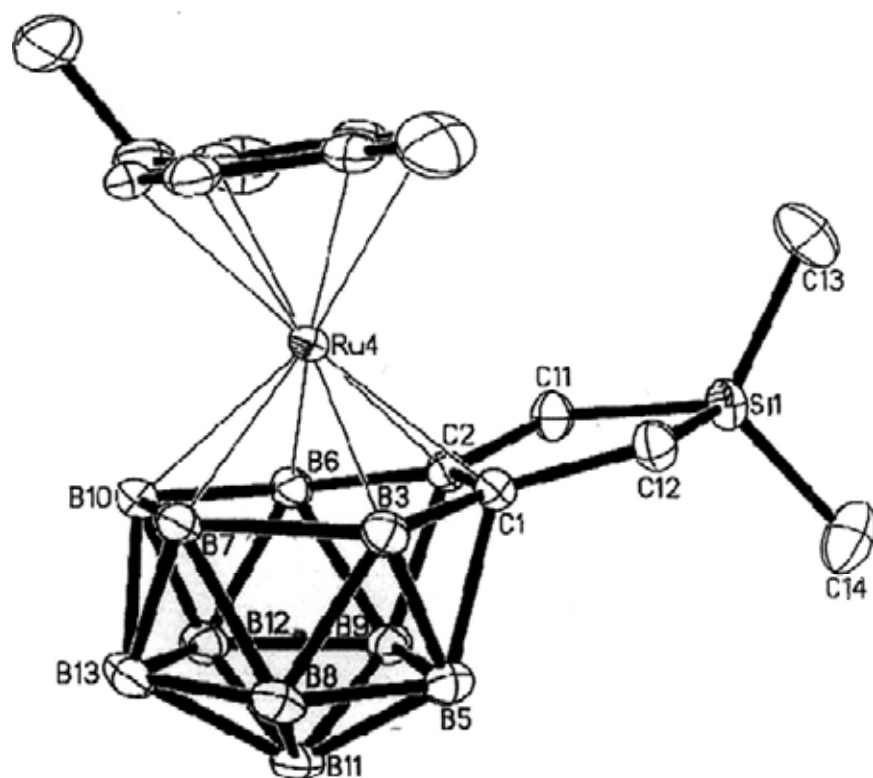

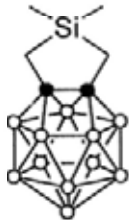
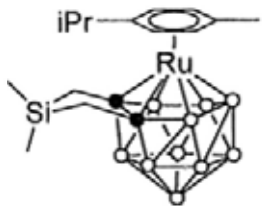
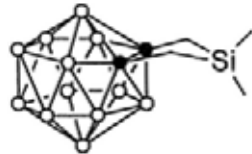
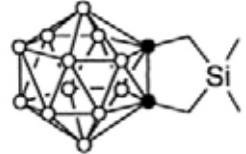
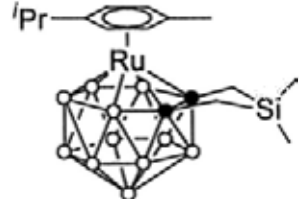
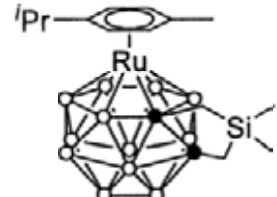


Figure 2.16. Molecular structure of 4-(*p*-cymene)- μ -1,2-Me₂Si(CH₂)₂-4,1,2-RuC₂B₁₀H₁₀ (**19**).

However, complex **19** was stable toward silica gel even when heated at 70 °C in CDCl₃. Besides, several 12- and 14-vertex carboranes, and 14- and 15-vertex ruthenacarboranes bearing the same Me₂Si(CH₂)₂ linkage, such as μ -1,2-Me₂Si(CH₂)₂-1,2-C₂B₁₀H₁₀ (**11**), μ -2,3-Me₂Si(CH₂)₂-2,3-C₂B₁₂H₁₂ (**28a**), μ -2,8-Me₂Si(CH₂)₂-2,8-C₂B₁₂H₁₂ (**28b**), 1-(*p*-cymene)- μ -2,3-Me₂Si(CH₂)₂-1,2,3-RuC₂B₁₁H₁₁ (**32a**), 1-(*p*-cymene)- μ -2,8-Me₂Si(CH₂)₂-1,2,8-RuC₂B₁₁H₁₁ (**32b**), and 7-(*p*-cymene)- μ -1,4-Me₂Si(CH₂)₂-7,1,4-RuC₂B₁₂H₁₂ (**35**), were also stable toward silica gel (Chapter 3). It gave an assumption that the nature of the cluster itself influences the desilylation process. In this regard, we compared several structural data of the corresponding carboranes or ruthenacarboranes as listed in Table 2.3. The structure of **11** was determined by single-crystal X-ray analyses and shown in Figure 2.17, although it is a known compound. It was hard to get X-ray quality crystals of **32b**, thus it was not

used for comparison.

Table 2.3. Comparison of Selected Bond Lengths (Å) and Bond Angles (°) of Carboranes or Ruthenacarboranes bearing Me₂Si(CH₂)₂ Linkage.

Compd.	No.	Vertex	C _{cage} -C _{cage}	C-Si-C (ring)
	11	12	1.702(5)	97.3(2)
	16	13	1.439(3)	89.5(1)
	19	13	1.459(7)	94.8(2)
	28a	14	1.648(3)	95.6(1)
	28b	14	1.663(5)	97.8(2)
	32a	14	1.702(7)	97.3(3)
	35	15	1.715(4)	96.6(1)

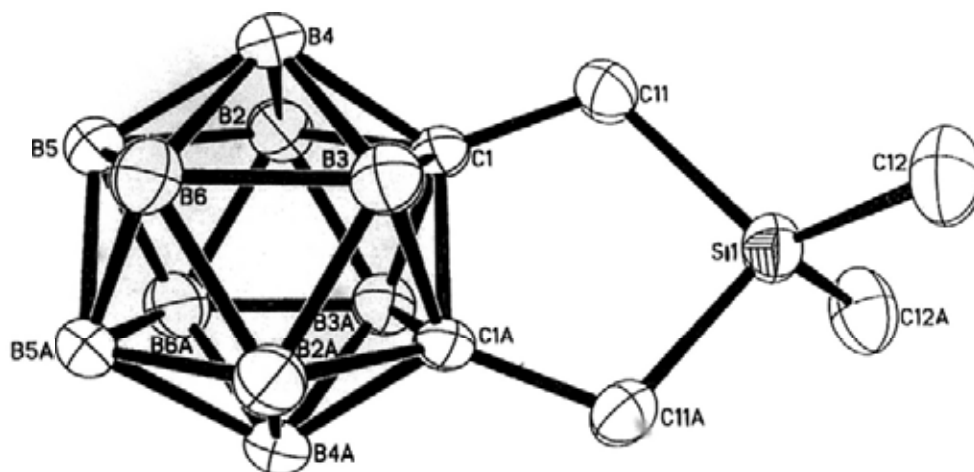


Figure 2.17. Molecular structure of μ -1,2-Me₂Si(CH₂)₂-1,2-C₂B₁₀H₁₀ (**11**).

The data listed in Table 2.3 give a general idea on the relationship of geometry of the cage and structure of the 5-membered silacyclopentane ring. We found that the corresponding CH₂-Si bond lengths of 1.887(3) Å and 1.888(3) Å in 13-vertex carborane **16** are in the range of 1.88 to 1.90 Å in these compounds but not elongated, indicating the bonds would not be specifically weakened. However, great distinctions are reflected in the C_{cage}-C_{cage} bond distances and the C-Si-C bond angles in the 5-membered ring. The corresponding values in the 13-vertex ruthenacarborane **19** and carborane **16** are remarkably reduced to 1.459(7) Å and 1.439(3) Å, and 89.5(1) ° for **16**, respectively. In this regard, we think that the specific structure of 13-vertex carborane with the short C_{cage}-C_{cage} bond leads to small C-Si-C angle in **16**. Such a ring-strain makes the Si atom easily attacked by nucleophiles, facilitating the C-Si bond cleavage and disilylation process (Figure 2.18).

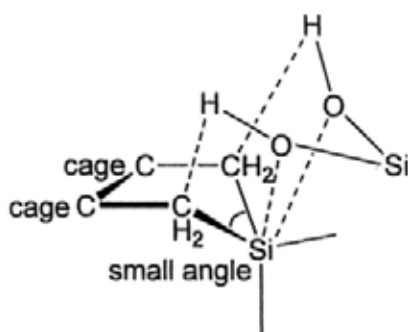
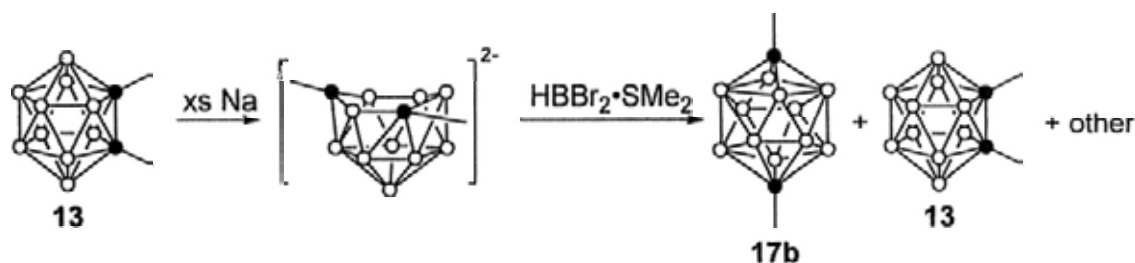


Figure 2.18. Proposed desilylation process facilitated by ring-strain.

2.2.3. Direct Synthesis of 13-Vertex CAP Carboranes and Structural Characterization

As the CAP 13-vertex carborane 1,12-Me₂-1,12-C₂B₁₁H₁₁ (**17b**) is much more stable than the CAD 13-vertex carborane 1,2-Me₂-1,2-C₂B₁₁H₁₁ (**17a**), we are prompted to re-examine the reaction of CAP *nido*-C₂B₁₀H₁₂²⁻ with RBX₂ reagent. Treatment of compound 1,2-Me₂-1,2-C₂B₁₀H₁₀ (**13**)¹⁰¹ with excess Na metal in the presence of a catalytic amount of naphthalene gave CAP [7,9-Me₂-7,9-C₂B₁₀H₁₀]²⁻,⁴² followed by reaction with 2 equiv of HBBr₂·SMe₂ in toluene/CH₂Cl₂, gave, after chromatographic separation, **17b** and **13** in 5% and 17% isolated yields, respectively (Scheme 2.13). The remaining product is a mixture of inseparable highly polar boron-containing species.

Scheme 2.13. Direct Synthesis of a CAP 13-Vertex Carborane.



Although the synthetic yield is rather low, this is the first time to show that CAP 13-vertex carborane can be directly prepared via capitation reaction of [*nido*-7,9-R₂-7,9-C₂B₁₀H₁₀]²⁻Na₂ with a dihaloborane reagent. It is reasonable to assume that the two cage carbon atoms in **17b** remain in *meta* positions after the capitation reaction, giving a thermodynamically more stable all-triangulated dicosahedral structure with the cage carbons being likely located in the 1,6-positions, that is, 1,6-Me₂-1,6-C₂B₁₁H₁₁, as shown in Figure 2.19, based on the reaction mentioned above. However,

X-ray diffraction studies failed.

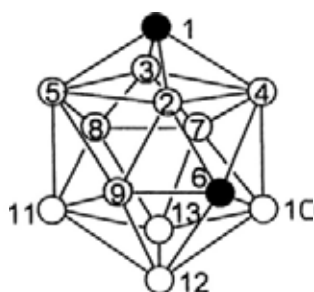
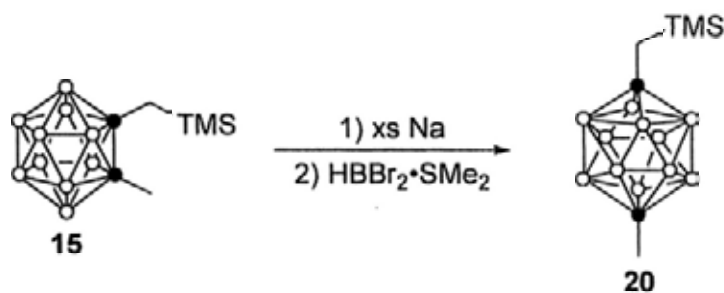


Figure 2.19. Previously proposed cage geometry of CAP 13-vertex carborane.

In order to get the unambiguous structure of the CAP 13-vertex carborane, several reactions were tried to directly synthesize the 13-vertex carboranes using CAP 12-vertex *nido*-carborane anions. Reaction of 1-TMSCH₂-2-Me-1,2-C₂B₁₀H₁₀ (**15**) with excess of Na metal followed by treatment with HBBr₂·SMe₂ afforded 1-TMSCH₂-12-Me-1,12-C₂B₁₁H₁₁ (**20**) in 5% isolated yield after chromatographic separation (Scheme 2.14).

Scheme 2.14. Synthesis of a 13-Vertex CAP Carborane.



Compound **20** was characterized by various spectroscopy and HRMS. It has common spectroscopic features with other 13-vertex CAP carboranes mentioned above, as listed in Table 2.4. Its ¹¹B NMR spectra showed a pseudo 1:10 pattern at 11.7 and -6.9 ppm, which was very similar to those of **17b** and **18b**, indicating they would have similar cluster structures. Two types of cage carbon signals were observed. One was in the lower field at about 125 ppm, which was close to that ob-

served for the CAd 13-vertex carborane at about 140 ppm, and regarded as the less coordinated carbon atom. The other kind in the higher field at about 80 ppm was comparable to that of a 12-vertex carborane, thus belonged to the more coordinated carbon. The two-dimensional ^1H - ^{13}C HMBC experiment indicated that the less coordinated cage carbon attached to the alkyl group with downfielded signal, while the 6-coordinate cage carbon attached to the methyl group at high field. This indicated the differences of electronic environment of the cage carbons and corresponding deshielding effect on the C-substituents. No products with opposite arrangement of the substituents were detected or isolated.

Table 2.4. Summary of ^{11}B , ^1H and ^{13}C Chemical Shifts (ppm) of CAP 13-Vertex Carboranes 1-R-12-R'-1,12- $\text{C}_2\text{B}_{11}\text{H}_{11}$.

Compd.		17b ^a	18b + 18b' ^a	18b'' ^b	20 ^a
		R = CH ₃ R' = CH ₃	R = CH ₂ SiMe ₂ OX R' = CH ₃		R = CH ₂ TMS R' = CH ₃
^{11}B NMR		13.3 (1)	11.8 (1)	14.5 (1)	11.7 (1)
		-6.6 (10)	-6.9 (10)	-5.1 (10)	-6.9 (10)
^1H NMR	R	2.63	2.72, 2.70 0.15, 0.14	2.99 0.58	2.70 0.07
	R'	1.89	1.89	1.91	1.89
^{13}C NMR	C1	120.6	127.8	121.5	129.7
	C12	83.2	83.3	84.0	83.1
	R	35.7	45.3 0.85	40.7 -0.9	44.4 -1.2
	R'	27.4	27.3	27.0	27.3

^a in CDCl_3 . ^b in $\text{C}_2\text{D}_2\text{Cl}_4$.

The structure of compound **20** was further confirmed by single-crystal X-ray ana-

lyses as shown in Figure 2.20. It adopts an all-triangulated dicosahedral geometry, which is similar to that predicted by theoretical calculations for $B_{13}H_{13}^{2-}$.^{66d} However, the cage carbons are not in the 1,6- positions, rather in the 1,12- positions. The distances between the 6-coordinated C12 atom and the neighboring 6-coordinated boron atoms are around 1.7 Å which are similar to those observed in the 12-vertex carboranes. On the other hand, the distances of 1.541(3) or 1.515(3) Å between the low-coordinated C1 atom and the 6-coordinated B2 or B3 atoms are much shorter, while the C1-B4 or C1-B5 bond lengths of 1.769(3) or 1.799(3) Å are a bit longer. The TMSCH₂ group is attached to the C1 atom while the Me group is attached to the C12 atom, which is well consistent with the spectroscopic feature.

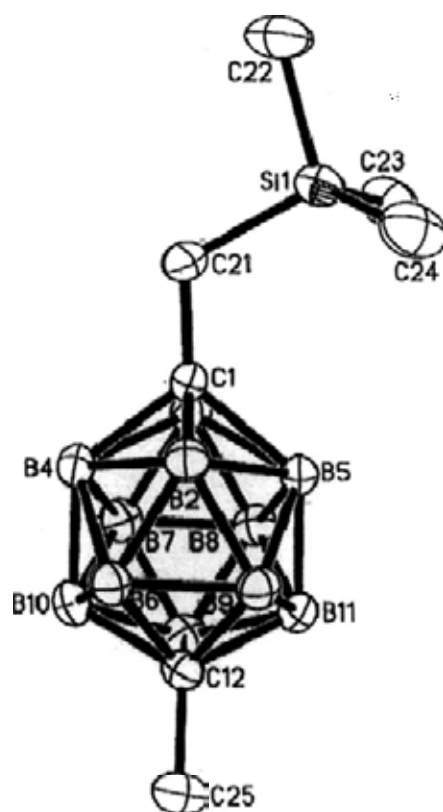
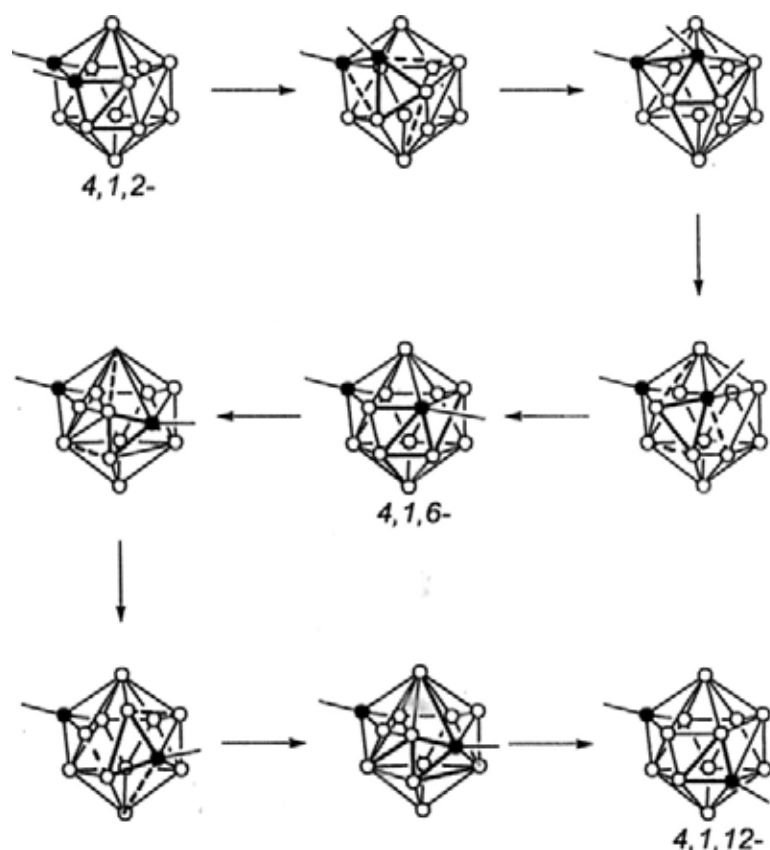


Figure 2.20. Molecular structure of 1-TMSCH₂-12-Me-1,12-C₂B₁₁H₁₁ (20).

A 1,6- isomer 1-R-6-R'-1,6-C₂B₁₁H₁₁ might be initially formed from the reaction, and 1,2- to 1,12-isomerization of Me₂C₂B₁₁H₁₁ might also involve the 1,6- isomer as an intermediate. This process can be explained by "Extended RTF" process (Scheme

2.15).^{10,13} However, we have not observed any spectroscopic evidence of 1,6-Me₂-1,6-C₂B₁₁ either in the isomerization process or in the capitation process, while 1,2-Me₂-1,2-C₂B₁₁H₁₁ (**17a**) can survive in solution for some time. Thus, the 1,2-isomer would be stable than the 1,6-isomer, which might be due to the additional stabilization caused by the preference of a hencosahedron geometry than a docosahedron. More exactly, it would like to say that the activation barrier for isomerization from the 1,2-isomer is higher than that for a 1,6- one, which is caused by the trapezoidal open face and the short C_{cage}-C_{cage} bond or enhanced bond strength. Thus the first step is slow and rate-determining while the latter one is quick so that the 1,6- intermediate is not observable.

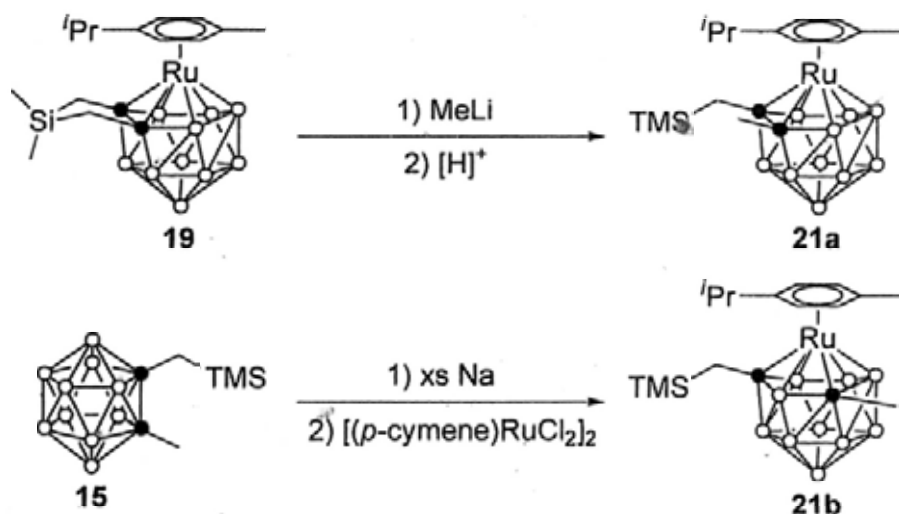
Scheme 2.15. Proposed Isomerization Process of 13-Vertex Carborane without Linkage.



A similar process of 4,1,6- to 4,1,12- isomerization in 13-vertex metallocarborane

system, where 4- position is the metal fragment had been reported.^{57b,60} In this regard, we would like to qualitatively examine thermal stability of the 4,1,2- and 4,1,6- 13-vertex metallacarborane analogues. Using the same transmetallation method in the reaction of μ -1,2-Me₂Si(CH₂)₂-1,2-C₂B₁₀H₁₀ with MeLi, treatment of 4-(*p*-cymene)- μ -1,2-Me₂Si(CH₂)₂-4,1,2-RuC₂B₁₀H₁₀ (**19**) with 2 equiv of MeLi in Et₂O for 2 d followed by quenching with excess HCl afforded a CAd 13-vertex metallacarborane 4-(*p*-cymene)-1-TMSCH₂-2-Me-4,1,2-RuC₂B₁₀H₁₀ (**21a**) in about 40% isolated yield after column chromatographic separation. Its 4,1,6-isomer 4-(*p*-cymene)-1-TMSCH₂-6-Me-4,1,6-RuC₂B₁₀H₁₀ (**21b**) was directly synthesized in 50% isolated yield from reduction of 1-TMSCH₂-2-Me-1,2-C₂B₁₀H₁₀ (**15**) by excess Na metal followed by treatment with 0.5 equiv of [(*p*-cymene)RuCl₂]₂ (Scheme 2.16).

Scheme 2.16. Synthesis of Two 13-Vertex Ruthenacarborane Isomers.



Compound **21a** and **21b** were characterized by several spectroscopic techniques and HRMS. They showed distinct ¹¹B NMR spectra indicative of different symmetry of the cage C atoms. Their molecular structures were determined by single-crystal X-ray analyses and shown in Figures 2.21 and 2.22, respectively. To our knowledge, compound **21a** represents the first 4,1,2- 13-vertex carborane without C,C'-linkage (Recently the Welch group has reported synthesis of 4-C₉H₇-1,2-(CH₃)₂-4,1,2-

$\text{CoC}_2\text{B}_{10}\text{H}_{10}$),^{57b} but its trapezoidal open face is somehow distorted compared to that of **19** (Figure 2.23). This phenomenon was also observed in some 4,1,2- 13-vertex metallocarborane with C,C-linkage.^{57a} Compound **21b** has a similar structure as those of 4,1,6- 13-vertex metallocarborane that have been reported.

Although **21a** also has a distorted trapezoidal open face, it is stable both in the solid state and in solution for several weeks. It is also resistant to change under heating up to 110 °C for several days in a $\text{C}_2\text{D}_2\text{Cl}_4$ solution as monitored by ^1H NMR. However, **21b** began to isomerize at 50 °C although the rate was rather slow. This implied that like the 13-vertex carboranes, the isomerization barriers in the 13-vertex ruthenacarborane system are also higher for a 4,1,6- one than for a 4,1,2- one.

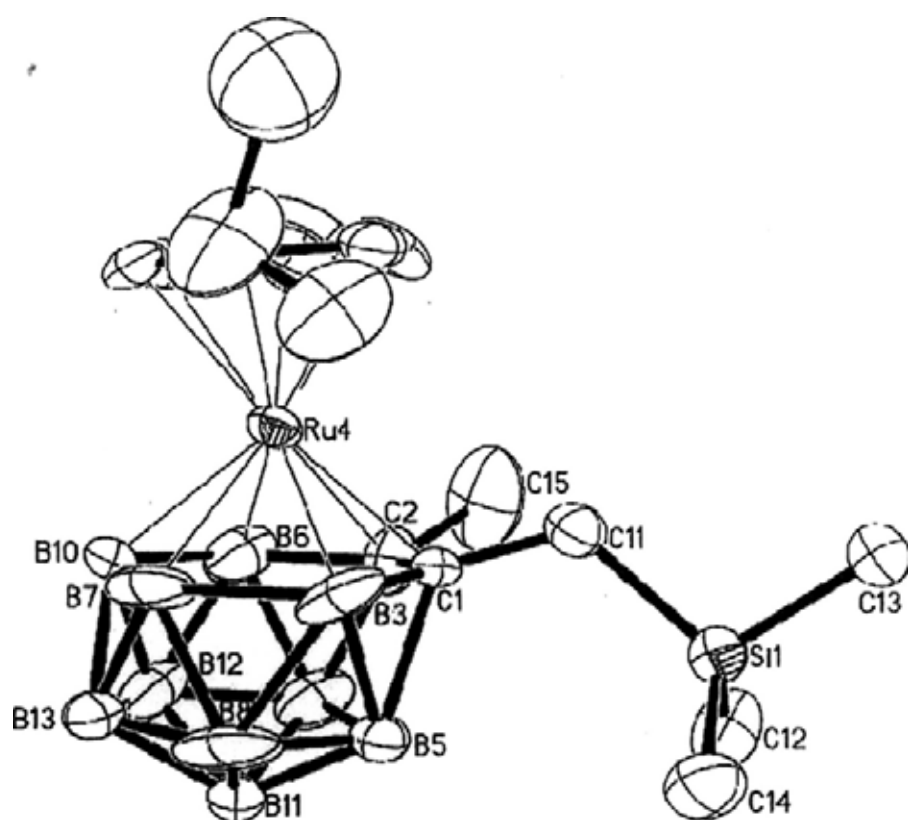


Figure 2.21. Molecular structure of 4-(*p*-cymene)-1-TMSCH₂-2-Me-4,1,2- $\text{RuC}_2\text{B}_{10}\text{H}_{10}$ (**21a**).

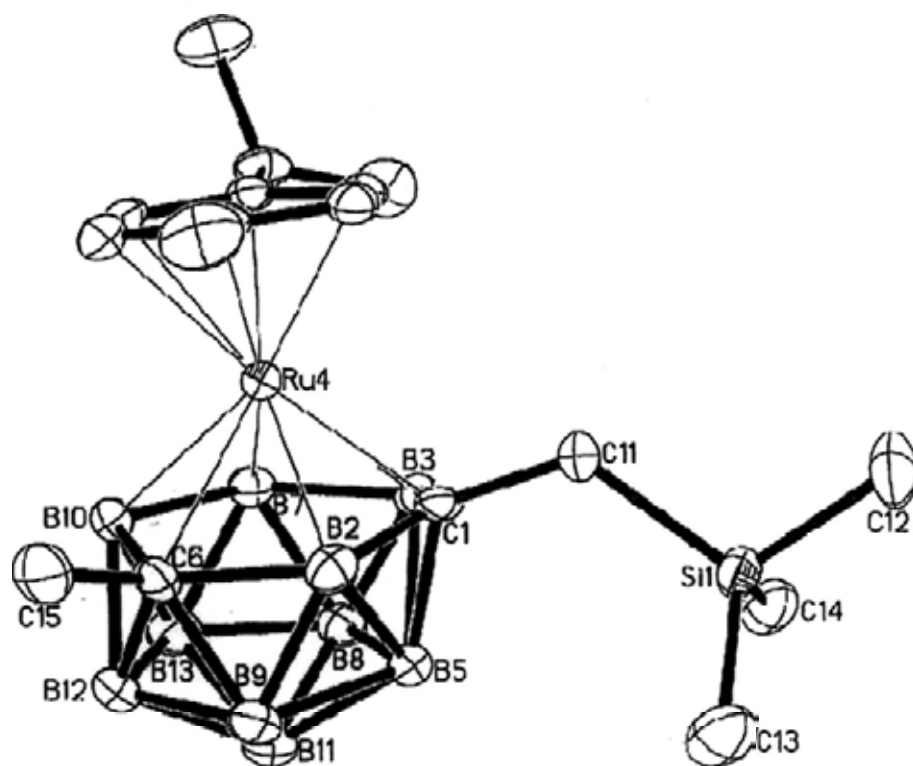


Figure 2.22. Molecular structure of 4-(*p*-cymene)-1-TMSCH₂-6-Me-4,1,6-RuC₂B₁₀H₁₀ (**21b**).

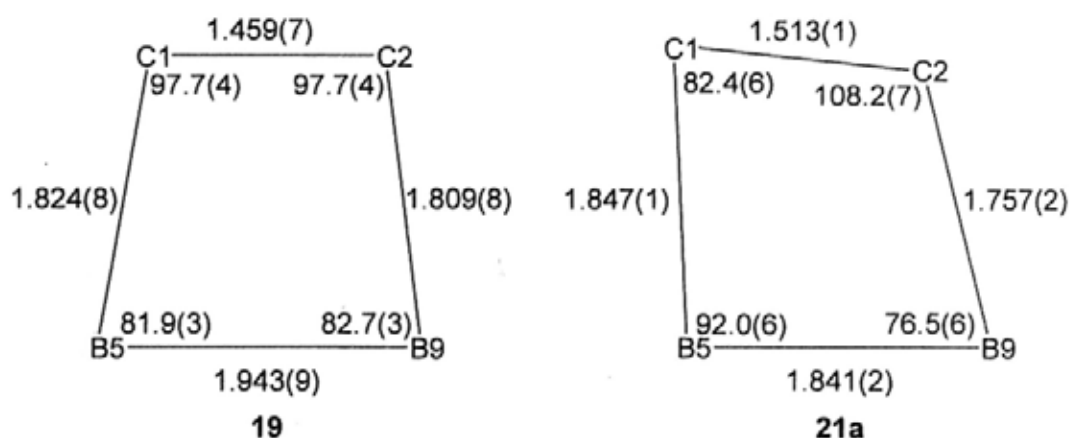


Figure 2.23. Trapezoidal open faces in compound **19** and **21a**, showing the differences in the bond lengths (Å) (outside) and internal angles (°) (inside).

2.3. Summary

Several CAd 13-vertex carboranes were synthesized and characterized using CAd 12-vertex *nido*-carborane anions. They had similar cage structures with short C_{cage}-C_{cage} bond lengths, which indicated increased electron delocalization between the

two cage carbons. The ^{13}C chemical shifts of the cage carbons are down fielded to about 140 ppm thus shows the " sp^2 " hybridization character. The ^1H and ^{13}C chemical shifts of the α -CH groups attached to the cage carbons are also down fielded, indicating the more deshielding effect of the 13-vertex carborane cages.

To study the role of C,C'-linkage in the formation and stabilization of 13-vertex carborane, a 12-vertex carborane with removable linkage was employed and lead to the formation of a 13-vertex carborane μ -1,2-Me₂Si(CH₂)₂-1,2-C₂B₁₁H₁₁. This carborane would undergo facile desilylation, which is believed to be induced by the special structure of 13-vertex carboranes, to afford CAd and CAp 13-vertex carboranes without linkage. This indicates C,C'-linkage does not have any obvious effects on the stability of 13-vertex carboranes. The CAp 13-vertex carborane can also be directly synthesized using CAp 12-vertex *nido*-carborane anions, but in much lower yield due to the very strong reducing power of the CAp *nido*-carborane dianions. The role of the linkages is just to lower the reducing power of the *nido*-carborane dianions, facilitating the capitation reaction.

The structure of CAp 13-vertex carborane was determined as 1,12-isomer but not 1,6-isomer. An initial formation of a 1,6-isomer followed is believed in the process but would subsequent isomerize to the 1,12-isomer and was not observed, which indicated the barrier of isomerization process is lower for the 1,2-isomer than for the 1,6-one. A similar phenomenon is also observed in the 13-vertex ruthenacarboranes, in which 4,1,2-isomer is thermo stable than the 4,1,6-one.

Chapter 3. Synthesis and Structure of *closo*-Carboranes and *closo*-Metallacarboranes with More than 13 Vertices

3.1. Synthesis and Characterization of 13-Vertex *nido*-Carborane Dianions

The 13-vertex *nido*-carborane dianions are potential synthons for the synthesis of 14-vertex *closo*-carboranes via insertion of a $[RB]^{2+}$ unit. Indeed, the first CAd 14-vertex carborane μ -2,3-(CH₂)₃-2,3-C₂B₁₂H₁₂ can be prepared from the corresponding $[\mu$ -1,2-(CH₂)₃-1,2-C₂B₁₁H₁₁][Na₂(THF)₄] salts and HBBr₂·SMe₂ reagent.⁸¹ However, the C,C'-linkages greatly influence the formation of 14-vertex carborane. When the linkage was changed from (CH₂)₃ to *o*-C₆H₄(CH₂)₂, no 14-vertex carborane was isolated by the same method, which is mainly regarded as the steric effect. And the knowledge of the 14-vertex *closo*-carboranes is only confined to two isomers bearing the (CH₂)₃ linkage. Thus other 14-vertex carboranes became our target molecules and are of great importance for more detailed and comprehensive understanding of their properties and potential applications. For this reason, synthesis of different 13-vertex *nido*-carborane dianions is the first step to pursue.

3.1.1. Synthesis

Our group has systematically studied the synthesis of CAd 13-vertex *nido*-carborane dianions via reduction of CAd 13-vertex carboranes by group 1 or group 2 metals.⁷⁴ These reduction processes take place very quickly even in the absence of naphthalene and usually finish within several hours. This easiness is usually ascribed to the existence of the trapezoidal open faces in the CAd 13-vertex *closo*-carboranes. Accordingly, $[\mu$ -1,2-(CH₂)₃-1,2-C₂B₁₁H₁₁][Na₂(THF)₄] (**[22]**[Na₂(THF)₄]) was pre-

pared based on the literature from compound μ -1,2-(CH₂)₃-1,2-C₂B₁₁H₁₁ (**6**).⁷⁴ Similarly, treatment of CAP 13-vertex carboranes μ -1,2-Me₂Si(CH₂)₂-1,2-C₂B₁₁H₁₁ (**16**), μ -1,2-(CH₂)₄-1,2-C₂B₁₁H₁₁ (**7**), μ -1,2-MeCH(CH₂)₂-1,2-C₂B₁₁H₁₁ (**8**) and 1,2-Me₂-1,2-C₂B₁₁H₁₁ (**17a**) with excess Na metal in THF gave dark red solutions at once, which indicated single-electron reduction processes.⁷⁷ The red solution was further stirred and faded to pale yellow or colorless within several hours demonstrating the completion of the two-electron reduction. After recrystallization, the corresponding 13-vertex *nido*-carborane salts [μ -1,2-Me₂Si(CH₂)₂-1,2-C₂B₁₁H₁₁][Na₂(THF)₄] (**[23]**), [μ -1,2-(CH₂)₄-1,2-C₂B₁₁H₁₁][Na₂(THF)₄] (**[24]**), [μ -1,2-MeCH(CH₂)₂-1,2-C₂B₁₁H₁₁][Na₂(THF)₄] (**[25]**) and [1,2-Me₂-1,2-C₂B₁₁H₁₁][Na₂(THF)₄] (**[26a]**) were isolated in almost quantitative yield as colorless crystals or white solids, as shown in Scheme 3.1, and the numbering system is shown in Figure 3.1.

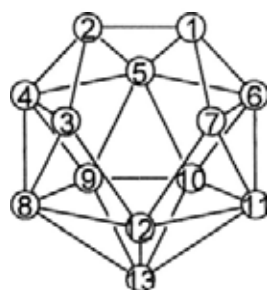
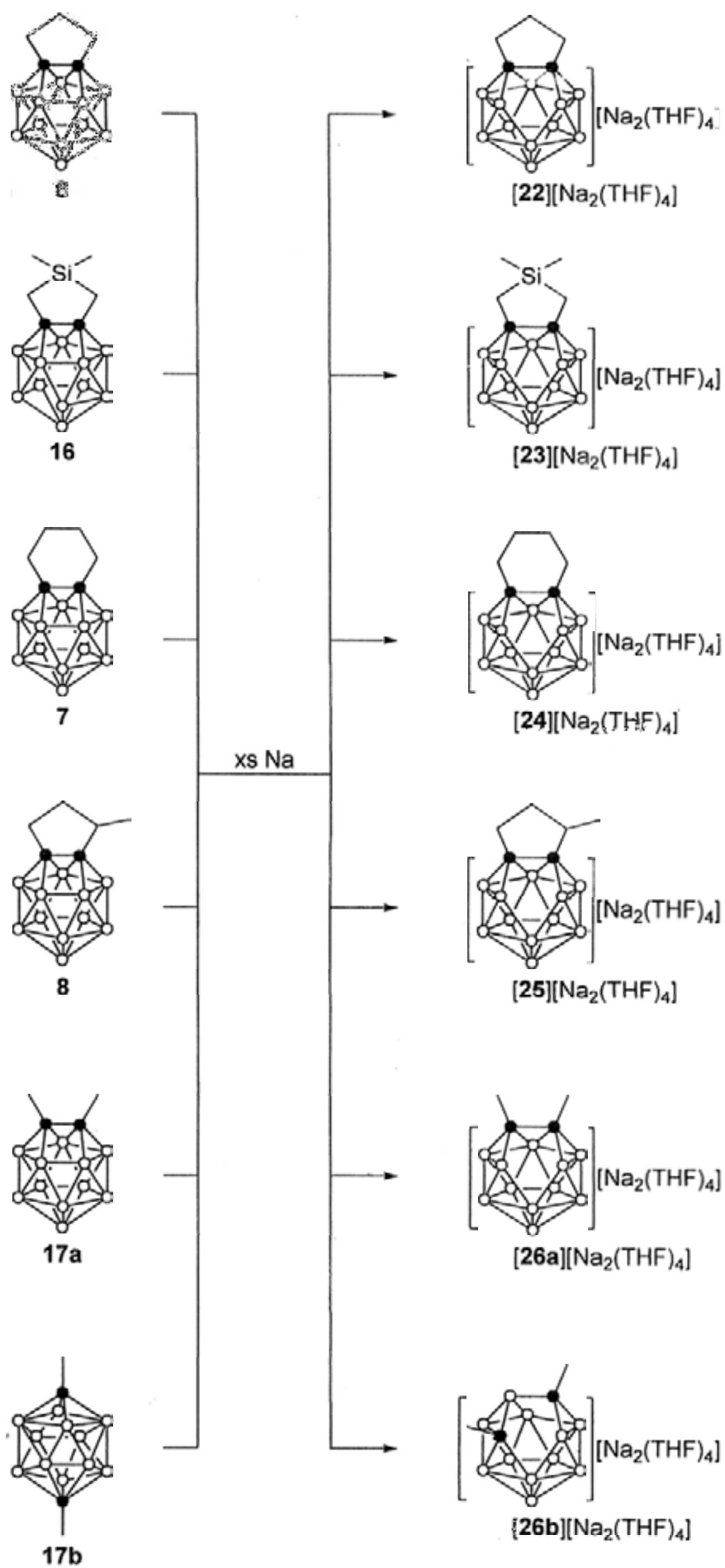


Figure 3.1. Numbering system for 13-vertex *nido*-carborane dianions.

The CAP 13-vertex carborane was also readily reduced by excess Na metal to afford the corresponding CAP 13-vertex *nido*-carborane salt. Treatment of 1,12-Me₂-1,12-C₂B₁₁H₁₁ (**17b**) with excess Na metal in THF also gave a red solution at the beginning and faded to pale yellow within several hours. Recrystallization from THF/*n*-hexane gave [1,3-Me₂-1,3-C₂B₁₁H₁₁][Na₂(THF)₄] (**[26b]**) as colorless crystals in about 80% isolated yield (Scheme 3.1).

Scheme 3.1. Synthesis of 13-Vertex *nido*-Carborane Salts.



3.1.2. Characterization

The molecular structures of CAd 13-vertex *nido*-carborane salts [23][Na₂(THF)₄] and [26a][Na₂(THF)₄] were determined by single-crystal X-ray analyses and shown in Figures 3.2 and 3.3, respectively. They are one dimensional coordination polymers in the solid state as those of other 13-vertex carboranes salts with [Na₂(THF)₄]²⁺ cation that were reported, in which the sodium ions link the *nido*-carborane cages via Na···H-B interaction.⁷⁴ The coordination environments of the two Na atoms are symmetric, one of which is coordinated to B3-H and B12-H of one *nido*-carborane unit, and to B10-H, B11-H and B13-H of another unit to form infinite zigzag polymeric chains. A typical one of [26a][Na₂(THF)₄] is shown in Figure 3.4.

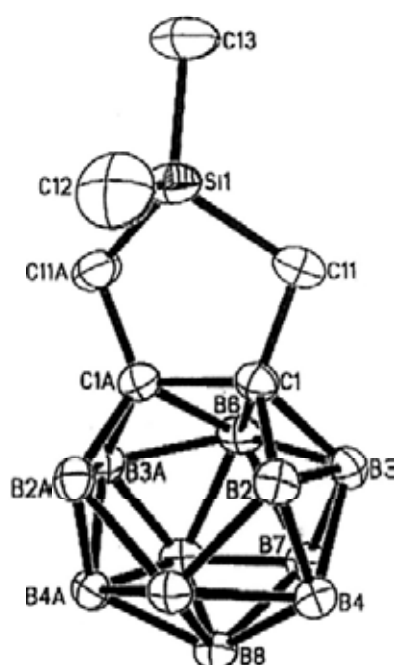


Figure 3.2. Structure of [μ -1,2-Me₂Si(CH₂)₂-1,2-C₂B₁₁H₁₁]²⁻ ([23]²⁻), in [23][Na₂(THF)₄].

The structural features of the dianions [23]²⁻ and [26a]²⁻ are also very similar to other structurally characterized CAd 13-vertex cousins and bear bent 5-membered open faces with long B3···B7 separations. The cage C-C bond lengths are elongated by more than 0.1 Å in these anions and the B3···B7 distances are elongated by more

than 1.0 Å, respectively, after taking up two electrons of the corresponding *closo*-species from the Na metal, and these data are listed in Table 3.1. It is noted that reduction of **17a**, a 13-vertex carborane without linkage, also gave the CAd 13-vertex *nido*-carborane anions, in which the cage B-B bond is broken but the cage C-C bond remains contact, although a little longer. This is very different from the reduction of the 12-vertex analogues, in which the cage C-C bond is usually broken and leads to the formation of a CAp 12-vertex *nido*-carborane dianion.⁴² This result further indicates that the trapezoidal open faces greatly influence the chemical properties of the 13-vertex CAd carboranes.

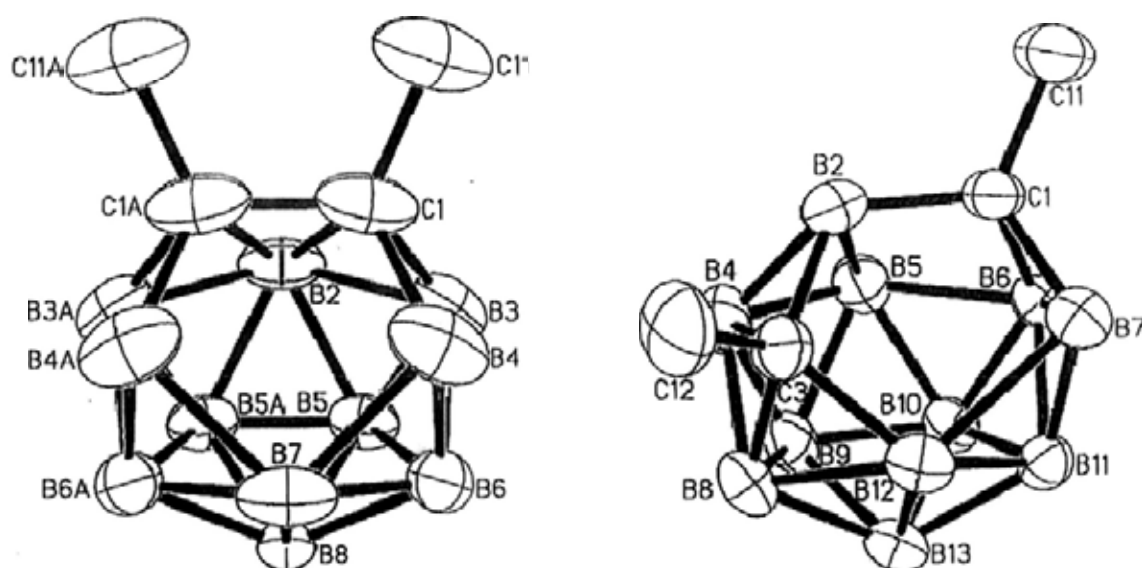


Figure 3.3. Structure of $[1,2\text{-Me}_2\text{-}1,2\text{-C}_2\text{B}_{11}\text{H}_{11}]^{2-}$ ($[\mathbf{26a}]^{2-}$) in $[\mathbf{26a}][\text{Na}_2(\text{THF})_4]$ (left) and $[1,3\text{-Me}_2\text{-}1,3\text{-C}_2\text{B}_{11}\text{H}_{11}]^{2-}$ ($[\mathbf{26b}]^{2-}$) in $[\mathbf{26b}][\text{Na}_2(\text{THF})_4]$ (right).

The structure of the CAp 13-vertex *nido*-carborane salt $[\mathbf{26b}][\text{Na}_2(\text{THF})_4]$ was also determined by X-ray diffraction and shown in Figure 3.3. The geometry of the anion is similar to that observed in its CAd isomer $[\mathbf{26a}]^{2-}$ with a five-membered open face on which the two cage carbons are located. However, these carbon atoms are separated and at the C1 and C3 positions. The formation of the *meta*- but not *para*- *nido*-carborane anions is consistent with that in a 12-vertex carborane system, in

which the *meta*-isomer is more stable.^{42,44} The C1...B5 distance is 2.379(10) Å and regarded as non-bonded, thus the C1 atom is 4-coordinated and a distorted trapezoidal open face also exists in the anion. The average C1-B bond length of 1.602(7) Å is shorter than the average C3-B bond distance of 1.666(8) Å, in which the C3 atom is 5-coordinated. This CAP 13-vertex *nido*-carborane salt also forms one-dimensional polymeric network in the solid state through Na...H-B interactions, but in an unsymmetric manner compared to its CAD isomer [26a][Na₂(THF)₄] (Figure 3.4).

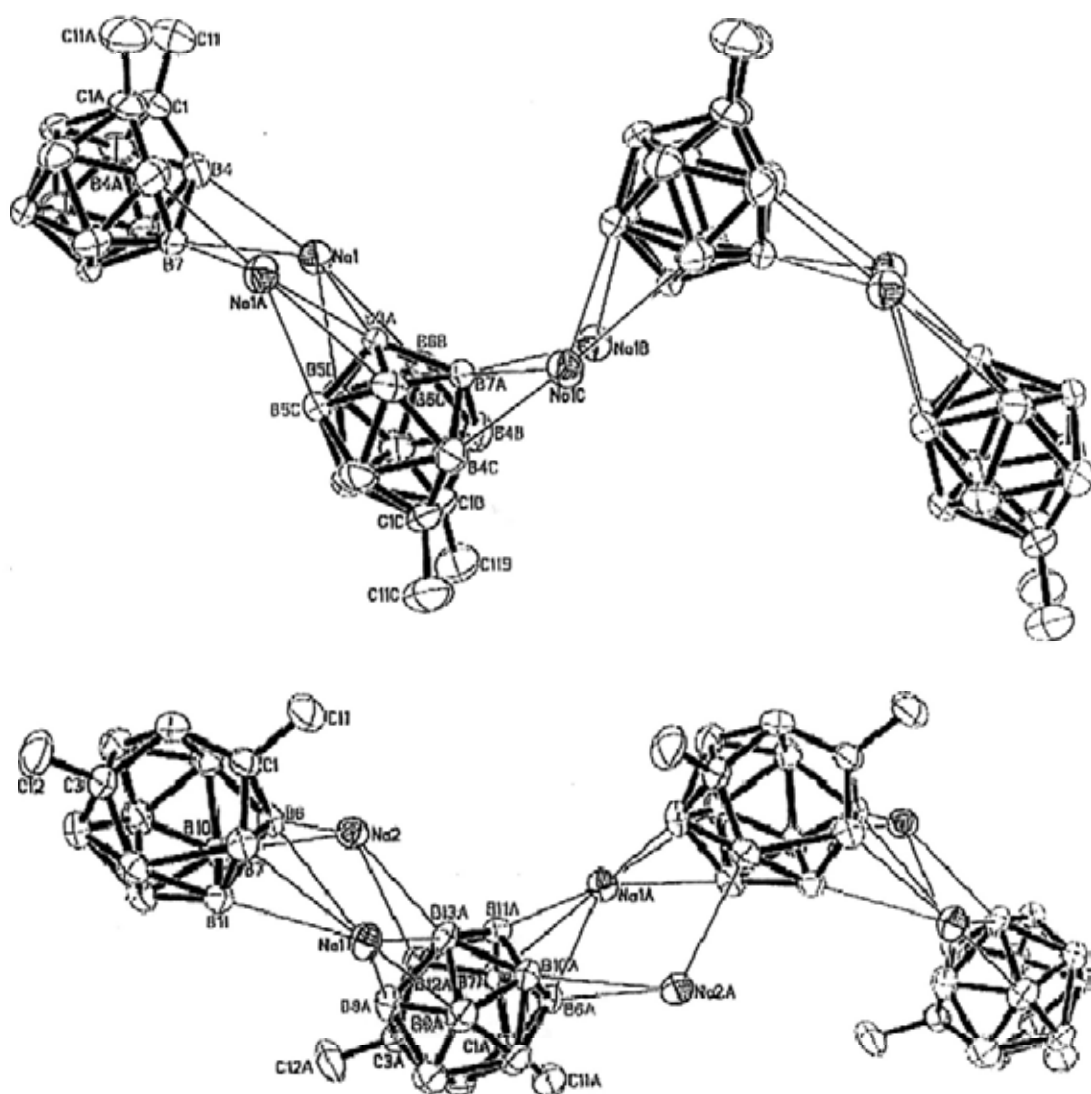


Figure 3.4. Na...H-B interactions in the one dimensional polymeric chains of [1,2-Me₂-1,2-C₂B₁₁H₁₁][Na₂(THF)₄] ([26a][Na₂(THF)₄]) (top) and [1,3-Me₂-1,3-C₂B₁₁H₁₁][Na₂(THF)₄] ([26b][Na₂(THF)₄]) (bottom). The THF molecules are omitted.

Table 3.1. C_{cage}-C_{cage} Bond Lengths (Å) and B···B Separations in 13-Vertex *closo*- and *nido*-Carboranes.

The 13-vertex <i>closo</i> -carborane	C _{cage} -C _{cage} bond lengths		B···B distances	
	<i>closo</i> -species	<i>nido</i> -species ^a	<i>closo</i> -species	<i>nido</i> -species ^a
μ -1,2-(CH ₂) ₃ -1,2-C ₂ B ₁₁ H ₁₁	1.421(3)	1.529(8) ^b	1.959(4)	2.677(6) ^b
μ -1,2-(CH ₂) ₃ -3-Ph-1,2-C ₂ B ₁₁ H ₁₀	1.443(2) ^c	1.552(6) ^c	1.940(4) ^c	2.653(6) ^c
μ -1,2- <i>o</i> -C ₆ H ₄ (CH ₂) ₂ -1,2-C ₂ B ₁₁ H ₁₁	1.427(2) ^c	1.553(5) ^c	1.975(2) ^c	2.584(8) ^c
μ -1,2-Me ₂ Si(CH ₂) ₂ -1,2-C ₂ B ₁₁ H ₁₁	1.439(3)	1.568(6)	1.964(5)	2.628(7)
1,2-Me ₂ -1,2-C ₂ B ₁₁ H ₁₁	1.421(5)	1.556(11)	1.937(5)	2.746(8)

^a The cation is [Na₂(THF)₄]²⁺. ^b Ref. 81. ^c Ref. 74.

These complexes were also characterized by several spectroscopic techniques as well as elemental analyses. The CAd 13-vertex *nido*-carborane salts all exhibited very similar ¹¹B NMR spectra in solution with peaks at about -10, -15 and -26 ppm in a ratio of 1:5:5, regardless of the substituents on the cage carbons, which was the same as those reported in literature.⁷⁴ This pattern was not consistent with the low symmetries observed in the solid-state structures. Even complex [25][Na₂(THF)₄], with an unsymmetric linkage on the cage carbons, showed the same pattern. And its ¹³C NMR indicated that only one set of signals was observed in solution. The ¹H NMR spectra of other compounds with symmetric linkages also showed no differentiation of the signals corresponding to the *exo*- and *endo*-H atoms referred to the five-membered open faces. Thus, it is reasonable to assume that these anions undergo rapid *dsd* processes in solution as shown in Figure 3.5.

The highfield signals of the cage borons indicate the influence of the negative charges on the cages of these CAd 13-vertex *nido*-carborane dianions. This effect is

also reflected in the chemical shifts of the cage carbons in their ^{13}C NMR spectra, which are significantly upfielded (at less than 20 ppm) compared to the corresponding 13-vertex *closo*-carboranes. These data are listed in Table 3.2.

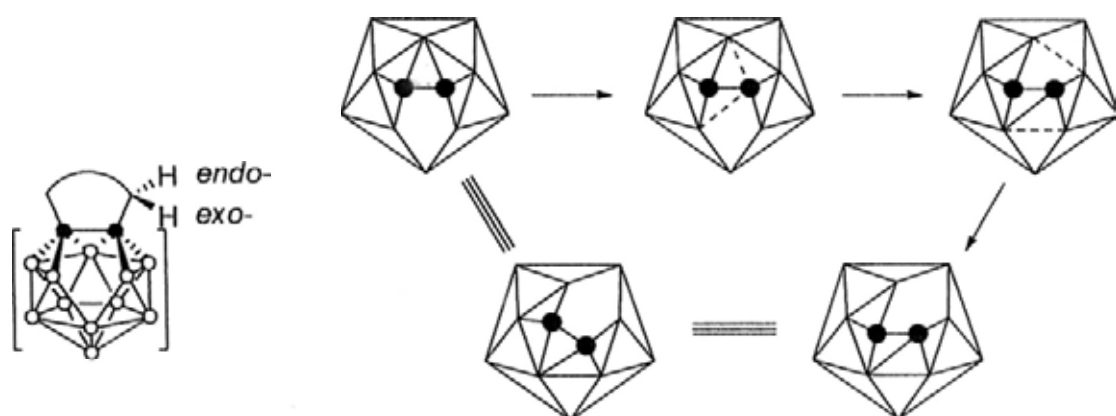


Figure 3.5. Topology representation of proposed *dsd* process of CAD 13-vertex *nido*-carborane dianion in solution (the *para*-B atom to the cage carbons are not presented). The *endo*-H atom is the one on the same side of 5-membered open face with the cage, while the *exo*-H atom is the opposite one.

Table 3.2. Comparison of the ^{13}C Chemical Shifts of the Cage Carbons in 13-Vertex *nido*-Carborane Dianions and Their Corresponding *closo*-Species.

13-Vertex <i>closo</i> -carborane	Chemical shifts of the cage carbons (ppm)	
	<i>closo</i> -species ^a	<i>nido</i> -species ^b
μ -1,2-(CH ₂) ₃ -1,2-C ₂ B ₁₁ H ₁₁	136.4	16.0
μ -1,2-Me ₂ Si(CH ₂) ₂ -1,2-C ₂ B ₁₁ H ₁₁	144.5	11.2
μ -1,2-(CH ₂) ₄ -1,2-C ₂ B ₁₁ H ₁₁	142.5	10.3
μ -1,2-MeCH(CH ₂) ₂ -1,2-C ₂ B ₁₁ H ₁₁	142.3, 136.1	19.2, 16.6
1,2-Me ₂ -1,2-C ₂ B ₁₁ H ₁₁	140.7	7.3
1,12-Me ₂ -1,12-C ₂ B ₁₁ H ₁₁	120.6, 83.2	44.4, 35.7

^a in CDCl₃. ^b in *d*₅-pyridine.

The CAP 13-vertex carborane salt [26b][Na₂(THF)₄] exhibited a 2:2:2:2:2:1 pat-

tern within -2.7 to -33.1 ppm in the ^{11}B NMR spectrum in a THF solution and this pattern changed to 2:1:5:2:1 in a solution of d_5 -pyridine. Its ^1H NMR showed two Me peaks in different environment at 2.47 and 2.11 ppm. Accordingly, two distinct peaks at 29.8 and 31.5 ppm were observed in the ^{13}C NMR spectrum together with 35.7 and 44.4 ppm corresponding to the two cage carbons, which were also upfielded compared to the *closo*- species **17b**.

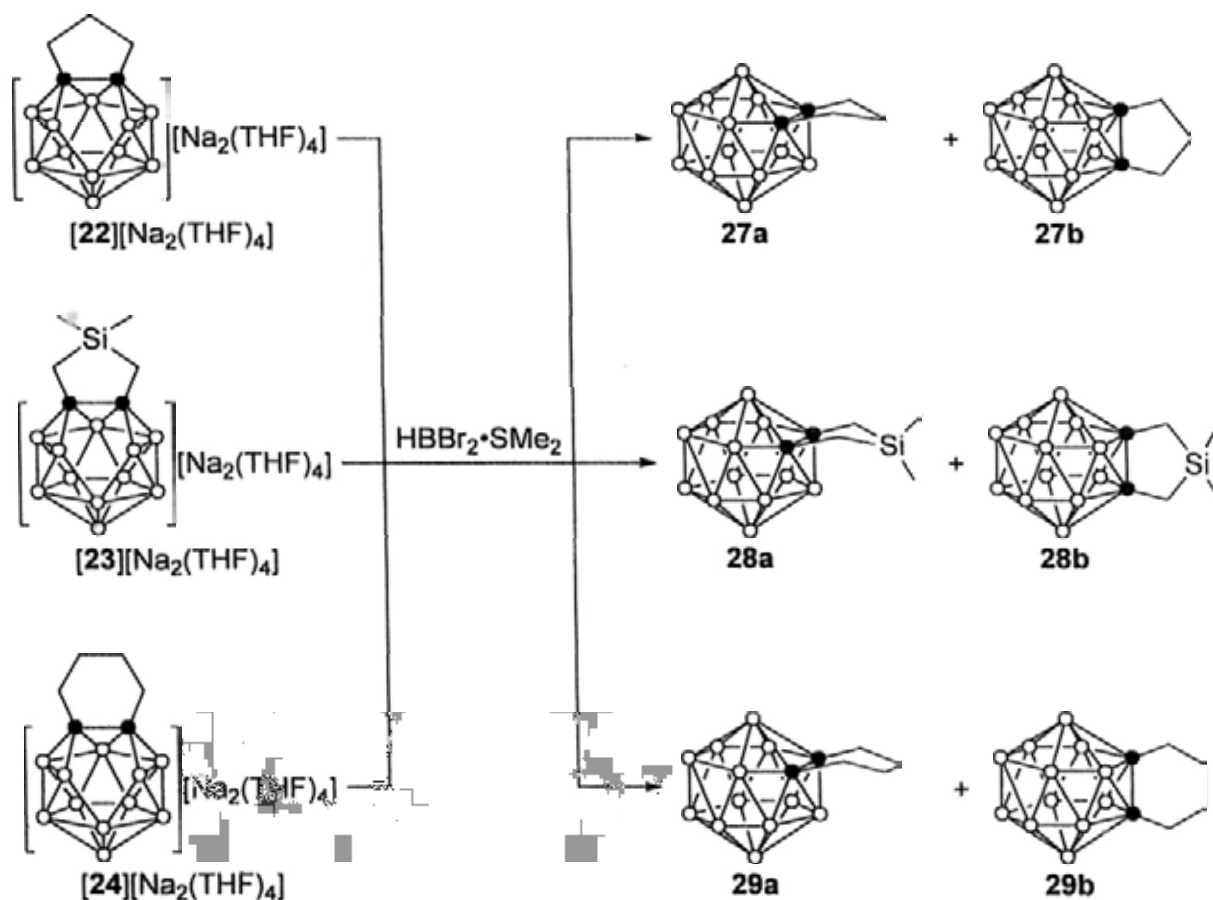
3.2. Synthesis and Structure of 14-Vertex Carboranes

3.2.1 Synthesis

With several 13-vertex *nido*-carborane salts in hand, we attempted the synthesis of desired 14-vertex carboranes. Following the [13+1] protocol, the 14-vertex carboranes μ -2,3-(CH_2)₃-2,3- $\text{C}_2\text{B}_{12}\text{H}_{12}$ (**27a**) was synthesized by treatment of [22][$\text{Na}_2(\text{THF})_4$] with 2 equiv of $\text{HBBr}_2 \cdot \text{SMe}_2$ in a toluene/ CH_2Cl_2 suspension, according to the literature, in 20% isolated yield after column chromatographic separation.⁸¹ Besides, its isomer μ -2,8-(CH_2)₃-2,8- $\text{C}_2\text{B}_{12}\text{H}_{12}$ (**27b**) was isolated in about 0.5% yield. Similarly, other 14-vertex carboranes with C,C'-linkage were also synthesized. Reaction of [23][$\text{Na}_2(\text{THF})_4$] with the same borane reagent lead to isolation of μ -2,3- $\text{Me}_2\text{Si}(\text{CH}_2)_2$ -2,3- $\text{C}_2\text{B}_{12}\text{H}_{12}$ (**28a**) in about 5% yield and μ -2,8- $\text{Me}_2\text{Si}(\text{CH}_2)_2$ -2,8- $\text{C}_2\text{B}_{12}\text{H}_{12}$ (**28b**) in about 1% yield, respectively. Interaction of [24][$\text{Na}_2(\text{THF})_4$] with $\text{HBBr}_2 \cdot \text{SMe}_2$ gave μ -2,3-(CH_2)₄-2,3- $\text{C}_2\text{B}_{12}\text{H}_{12}$ (**29a**) in about 0.5% yield and μ -2,8-(CH_2)₄-2,8- $\text{C}_2\text{B}_{12}\text{H}_{12}$ (**29b**) in about 10% yield (Scheme 3.2). It is noted that we only obtained a mixture containing **29a** and **29b** in a ratio of 2:1. Complex **29a** was not able to be further purified by column chromatography on silica gel, which may be due to the loss in the purification process. The same method also worked using [25][$\text{Na}_2(\text{THF})_4$] as evidenced by the ^{11}B NMR spectra of the reaction mixtures.

However, the products were hard to be purified and isolated, mainly because of the methyl substituent on the linkage, which would result in the formation of four possible isomers rather than two.

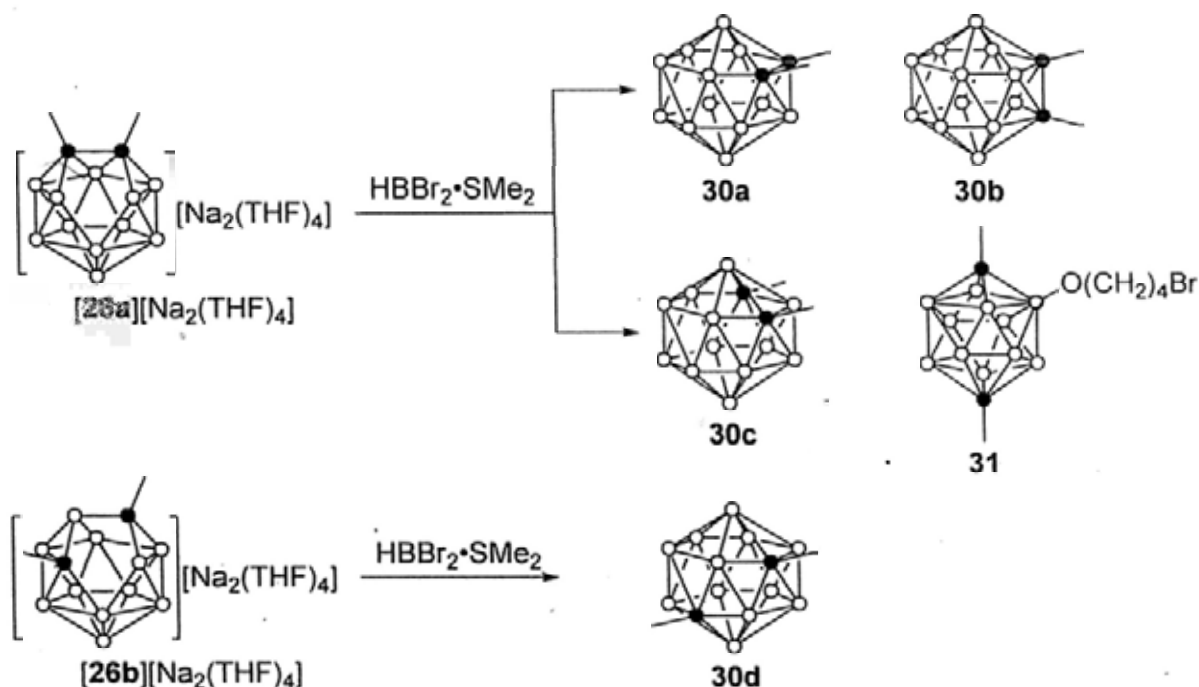
Scheme 3.2. Synthesis of 14-Vertex Carboranes with C,C'-Linkage via a [13+1] Protocol.



The same [13+1] methodology can also be used in the synthesis of 14-vertex carboranes without linkage. Treatment of CAD **[26a][Na₂(THF)₄]** with 2 equiv of $\text{HBr}_2 \cdot \text{SMe}_2$ in a toluene/ CH_2Cl_2 suspension resulted in the formation of several isomers of $\text{Me}_2\text{C}_2\text{B}_{12}\text{H}_{12}$, besides *cal.* 10% 13-vertex $\text{Me}_2\text{C}_2\text{B}_{11}\text{H}_{11}$ isomers **17a** and **17b** (Scheme 3.3). In these 14-vertex carborane isomers, a trace amount of 2,3-Me₂-2,3- $\text{C}_2\text{B}_{12}\text{H}_{12}$ (**30a**) was detected according to the ¹¹B NMR spectra, which had a similar pattern as that of 2,3-(CH₂)₃-2,3- $\text{C}_2\text{B}_{12}\text{H}_{12}$ (**26a**),⁸¹ but not isolable. About 2% 2,8-Me₂-2,8- $\text{C}_2\text{B}_{12}\text{H}_{12}$ (**30b**) was isolated as white solids, and *cal.* less than 0.5% 2,4-

Me₂-2,4-C₂B₁₂H₁₂ (**30c**), presumably, was also afforded, after repeated column chromatographic separation using *n*-hexane as elute. A 13-vertex CAP carborane B-O(CH₂)₄Br-C,C'-Me₂-C₂B₁₁H₁₀ (**31**), which might be 4-O(CH₂)₄Br-1,12-Me₂-1,12-C₂B₁₁H₁₀, was also isolated in about 5% yield as colorless liquid. Its ¹¹B NMR spectra showed three peaks in an 1:5:5 pattern at 17.0, -4.8 and -10.8 ppm, one of which was at the lowest field as a singlet in the ¹H coupled spectrum and linked to the oxygen atom. Four methylene units together with two diastereotopic methyl groups were observed in the ¹H and ¹³C NMR spectra. Two corresponding cage carbons were observed at 96.6 and 84.3 ppm. The EI MS spectrometry showed one signal group centered at *m/z* 199 corresponding to the Me₂C₂B₁₁H₁₀O fragment and two isotopic peaks at *m/z* 135 and 137 corresponding to the (CH₂)₄Br fragment.

Scheme 3.3. Synthesis of 14-Vertex Carboranes without C,C'-Linkage via a [13+1] Protocol.

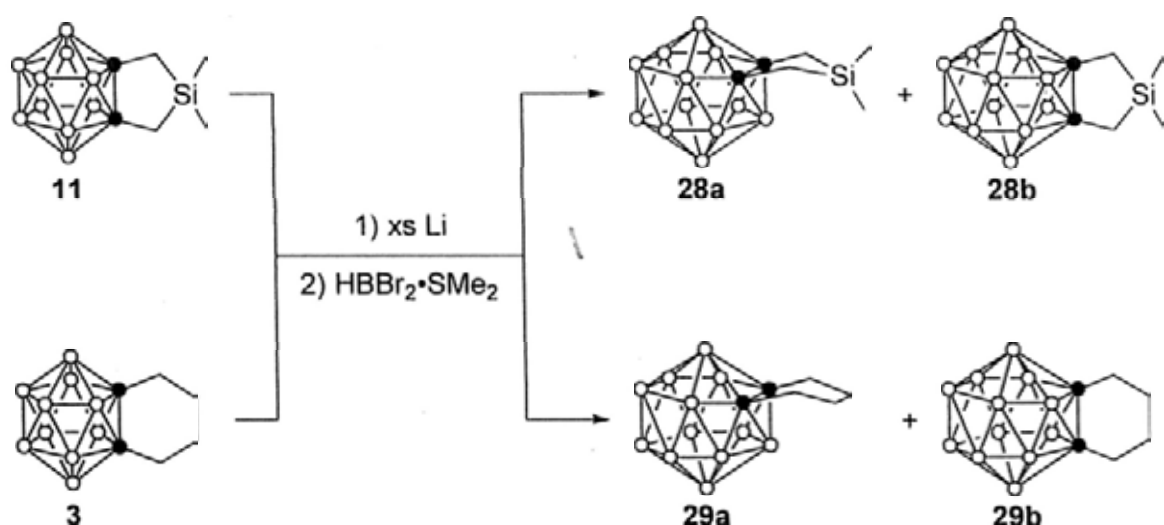


A CAP 14-vertex carborane can also be synthesized from CAP 13-vertex *nido*-carborane salt. Treatment of [1,3-Me₂-1,3-C₂B₁₁H₁₁][Na₂(THF)₄] (**[26b][Na₂(THF)₄]**)

with 2 equiv of $\text{HBr}_2 \cdot \text{SMe}_2$ in a toluene/ CH_2Cl_2 suspension gave 2,9- Me_2 -2,9- $\text{C}_2\text{B}_{12}\text{H}_{12}$ (**30d**) in 0.5% isolated yield (Scheme 3.3). In addition, the 13-vertex CAP carborane **17b** was recovered in 20% yield.

The [12+2] protocol, that is the capitation of a 12-vertex *arachno*-carborane with two $[\text{BH}]^{2+}$ units on both open faces, is introduced in the synthesis of the first 14-vertex CAD carborane **27a**. Indeed, this method is also useful in the synthesis of 14-vertex carboranes with C,C'-linkage **28a**, **28b**, **29a** and **29b**. Reduction of μ -1,2- $\text{Me}_2\text{Si}(\text{CH}_2)_2$ -1,2- $\text{C}_2\text{B}_{10}\text{H}_{10}$ (**11**) or μ -1,2- $(\text{CH}_2)_4$ -1,2- $\text{C}_2\text{B}_{10}\text{H}_{10}$ (**3**) with excess Li metal afforded the corresponding 12-vertex *arachno*-carborane salts $[\mu$ -1,2- $\text{Me}_2\text{Si}(\text{CH}_2)_2$ -1,2- $\text{C}_2\text{B}_{10}\text{H}_{10}][\text{Li}_4(\text{THF})_x]$ or $[\mu$ -1,2- $(\text{CH}_2)_4$ -1,2- $\text{C}_2\text{B}_{10}\text{H}_{10}][\text{Li}_4(\text{THF})_5]$.^{45d} Treatment of these two complexes with 3 equiv of $\text{HBr}_2 \cdot \text{SMe}_2$ in a toluene/ CH_2Cl_2 suspension gave **28a** in 3% isolated yield and **28b** in 0.5% isolated yield, and **29b** in 5% isolated yield (Scheme 3.4). Trace amount of **29a** was also observed in the gross product by ^{11}B NMR spectrum.

Scheme 3.4. Synthesis of 14-Vertex Carboranes with C,C'-Linkage via a [12+2] Protocol.



In these reactions, besides a small amount of the 12-vertex starting materials, lots

of 13-vertex carboranes were isolated, indicating that redox reactions dominated, thus leading to low yields of 14-vertex carboranes. This was the same as the preparation of **27a**. On the other hand, isolation of 4-O(CH₂)₄Br-1,12-Me₂-1,12-C₂B₁₁H₁₀ (**31**) in the reaction of [**26a**][Na₂(THF)₄] with HBBr₂·SMe₂ indicated that THF would also influence the reaction. C-O bond cleavage and ring-opening of THF by HBBr₂·SMe₂, which lead to the formation of R₂BO(CH₂)₄Br,¹⁰² would account for the formation of it. Thus donor solvent should be avoided as possible.

3.2.2. Characterization

The structures of **27a**, **28a**, **28b**, **29b** and **30d** were determined by single-crystal X-ray analyses, and are shown in Figures 3.6-3.10. Compound **27a** was cocrystallized with one equiv of naphthalene. They all adopt a bicapped hexagonal antiprismatic geometry as that predicted for [B₁₄H₁₄]²⁻ by theoretical calculation,^{66d} with two cage carbons located at 2- and 3- positions for **27a** and **28a**, or 2- and 8- positions for **28b** and **29b**, or 2- and 9- positions for **30d**.

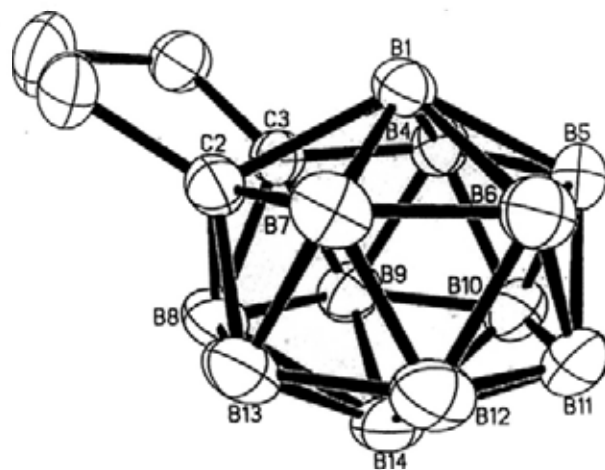


Figure 3.6. Molecular structure of μ -2,3-(CH₂)₃-2,3-C₂B₁₂H₁₂ (**27a**), in **27a**·C₁₀H₈.

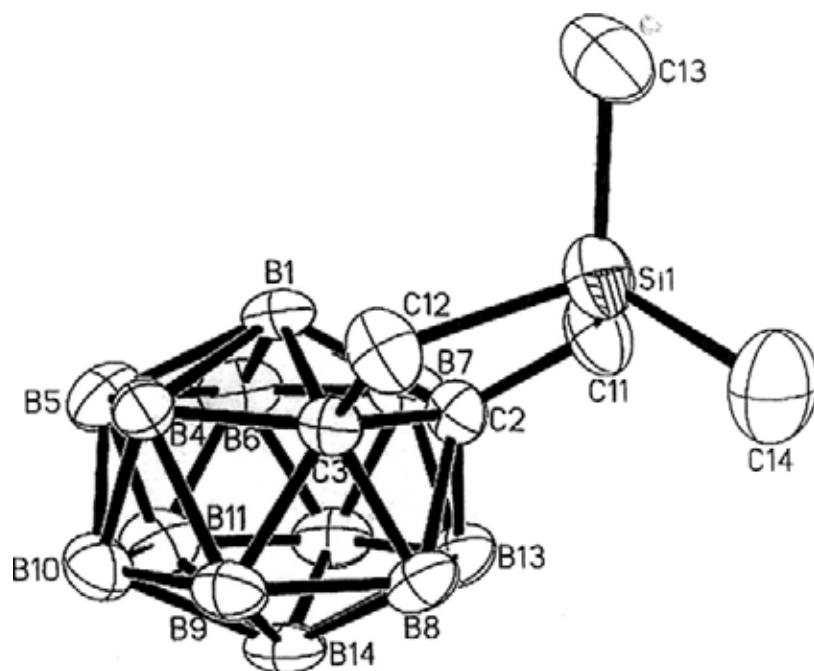


Figure 3.7. Molecular structure of μ -2,3-Me₂Si(CH₂)₂-2,3-C₂B₁₂H₁₂ (**28a**).

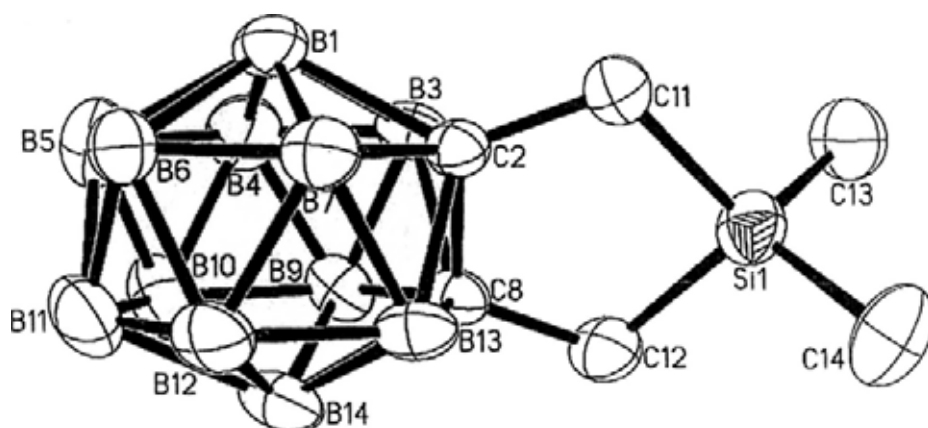


Figure 3.8. Molecular structure of μ -2,8-Me₂Si(CH₂)₂-2,8-C₂B₁₂H₁₂ (**28b**).

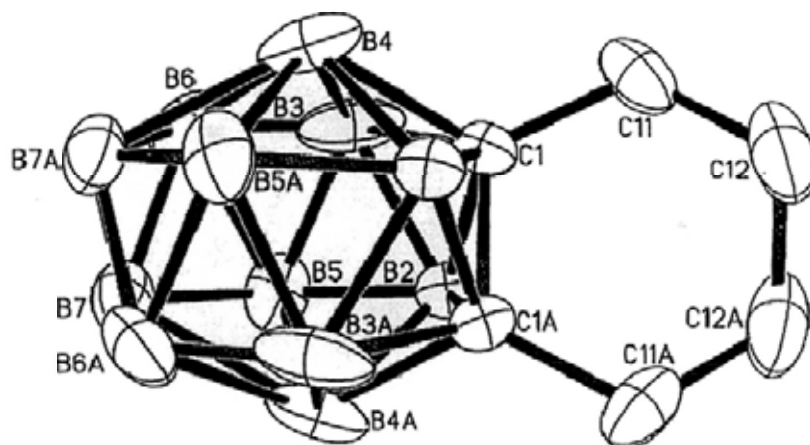


Figure 3.9. Molecular structure of μ -2,8-(CH₂)₄-2,8-C₂B₁₂H₁₂ (**29b**).

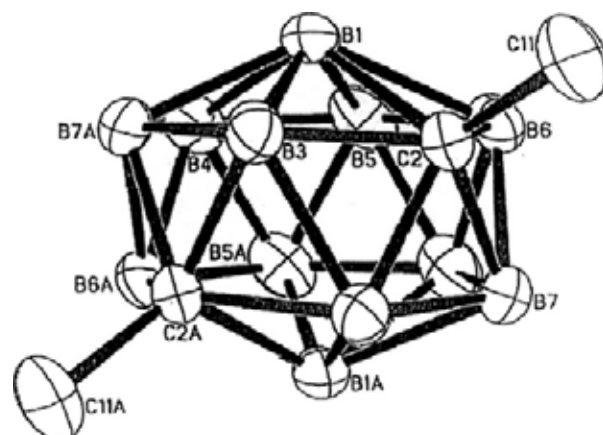


Figure 3.10. Molecular structure of 2,9-Me₂-2,9-C₂B₁₂H₁₂ (**30d**).

The relative bond distances of these 14-vertex *closo*-carboranes are listed in Table 3.3. The C-C bond lengths of CA_d 14-vertex carboranes are longer than their 13-vertex analogues but comparable to those observed in 12-vertex carboranes. The B1-Cent(up), Cent(up)-Cent(low) and Cent(low)-B14 distances are comparable among them.

Table 3.3. Relative Bond Distances (Å) in the 14-Vertex Carboranes.

Compd.	Cage C-C	B1-Cent(up)	Cent(up)-Cent(low)	Cent(low)-B14
27a	1.608(4)	0.848(6)	1.494(6)	0.831(6)
28a	1.648(3)	0.840(5)	1.489(5)	0.824(5)
27b ^a	1.599 (3)	0.841(3)	1.506(3)	0.841(3)
28b	1.663(5)	0.857(8)	1.501(8)	0.840(8)
29b	1.622(3)	0.899(8)	1.520(8)	0.899(8)
30d	/	0.837(5)	1.496(5)	0.837(5)

^a Ref. 81.

Compounds **28a**, **28b**, **29b**, **30b**, **30c** and **30d** were also characterized by spectroscopic techniques as well as HRMS. Complex **29a** was characterized from a mixture containing **29b**. The 2,3-isomers generally had low symmetry and the ¹¹B NMR

spectra of **28a** showed a accordant 1:2:2:1:2:1:2:1 pattern in the range 7 to -24 ppm. Complex **29a** showed a similar 1:2:2:2:1:2:1:1 (or 1:2:2:1:2:2:1:1 as it cannot be well resolved in the mixture) pattern in the 8 to -25 ppm range. The ^{11}B NMR spectra of **28b** exhibited a pseudo 2:6:2:2 pattern in the range 3 to -18 ppm, and for **29b**, it exhibited a 2:2:2:2:2:2 pattern in the range 5 to -17 ppm. For $\text{Me}_2\text{C}_2\text{B}_{12}\text{H}_{12}$ (**30**), there are 6 possible cage structures according to positions of the two cage carbon, in which the cage carbons taking up the 7-coordinated 1- or 14- position is not considered. The theoretical and observed ^{11}B NMR spectra patterns of these isomers are listed in Table 3.4.

Table 3.4. Theoretical and Observed ^{11}B NMR Spectra Patterns for Six Isomers of $\text{Me}_2\text{C}_2\text{B}_{12}\text{H}_{12}$.

Cage carbon positions	Theoretical pattern ^a	Observed pattern ^b	Range (ppm)
2,3-	1:1:1:1:2:2:2:2	1:2:2:1:2:1:2:1	8 to -26
2,4-	1:1:1:1:2:2:2:2	2:2:2:2:1:1:1:1	5 to -25
2,5-	1:1:2:4:4	/	/
2,8-	2:2:2:2:2:2	2:2:4:2:2	4 to -17
2,9-	2:2:2:2:2:2	2:4:4:2	4 to -19
2,10-	2:2:2:2:2:2	/	/

^a arrangement according to the relative intensities. ^b arrangement according to the chemical shifts.

The chemical shifts of the cage carbons in 14-vertex carboranes are generally observed at high field, compared to the corresponding 13-vertex carboranes and close to that of the 12-vertex analogues. These distinctions indicate the different electronic environments of the cage carbons in the clusters. Generally, the 5-coordinated carbon atoms in the 13-vertex carboranes are more electron-deficient than the 6-coordinated

carbon atoms in the 14- and 12-vertex carboranes. Moreover, cage carbon signals in the 2,3- (or 2,4-) isomers are always upfielded by about 12-18 ppm relative to those in the 2,8- (or 2,9-) isomers. These data are listed in Table 3.5. These differences can be ascribed to the electronic effects of which the cage carbons are on the same 6-membered belt or both of the belts.

Table 3.5. Cage Carbon Chemical Shifts (ppm) of 14-Vertex Carboranes in CDCl₃.

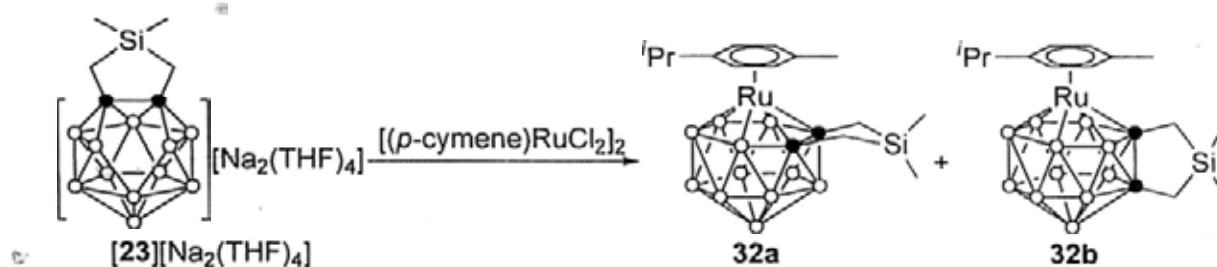
Compd.	C,C'-substituent	Cage C positions	δ (cage C)	$\Delta\delta$ (cage C)
27a	(CH ₂) ₃	2,3-	72.3	17.7
27b		2,8-	90.0	
28a	Me ₂ Si(CH ₂) ₂	2,3-	76.2	14.7
28b		2,8-	90.9	
29a	(CH ₂) ₄	2,3-	66.0	12.4
29b		2,8-	78.4	
30b ^a		2,8-	76.8	/
30c	Me ₂	2,4-	63.7	14.9
30d		2,9-	78.6	

^a The cage carbon signal overlapped with that of the CDCl₃ and was determined by HMBC experiment.

3.3. Synthesis and Structure of 14-Vertex Ruthenacarboranes

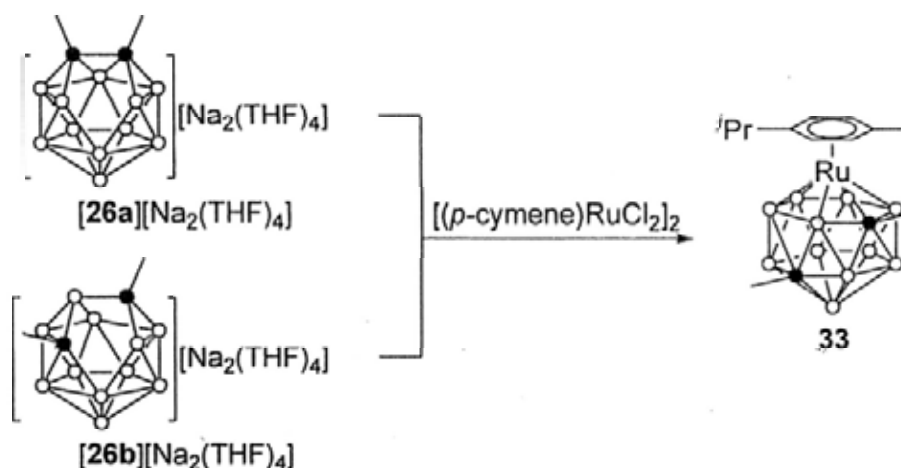
13-Vertex *nido*-carborane dianions are also useful synthons for the synthesis of 14-vertex metallocarboranes. Treatment of [23][Na₂(THF)₄] with 0.5 equiv of [(*p*-cymene)RuCl₂]₂ in THF gave 14-vertex ruthenacarborane isomers 1-(*p*-cymene)- μ -2,3-Me₂Si(CH₂)₂-1,2,3-RuC₂B₁₁H₁₁ (**32a**) as yellow crystals in 25% yield and 1-(*p*-cymene)- μ -2,8-Me₂Si(CH₂)₂-1,2,8-RuC₂B₁₁H₁₁ (**32b**) as cream-colored micro crystals in 20% isolated yield, respectively (Scheme 3.5).

Scheme 3.5. Synthesis of 14-Vertex Ruthenacarboranes.



The CAP 14-vertex ruthenacarborane was also synthesized in a similar manner. Treatment of $[26a][Na_2(THF)_4]$ or $[26b][Na_2(THF)_4]$ with 0.5 equiv of $[(p\text{-cymene})RuCl_2]_2$ in THF generated the same 14-vertex ruthenacarborane 1-(*p*-cymene)-2,9-Me₂-1,2,9-RuC₂B₁₁H₁₁ (**33**) in 19% (from $[26a]^{2-}$) and 75% yields (from $[26b]^{2-}$), respectively (Scheme 3.6). In addition, about 60% of 1,2-Me₂-1,2-C₂B₁₁H₁₁ (**17a**) was recovered from the former reaction as evidenced from ¹¹B NMR.

Scheme 3.6. Synthesis of a CAP 14-Vertex Ruthenacarborane.



The molecular structures of **32a** and **33** were confirmed by single-crystal X-ray analyses (Figures 3.11 and 3.12). They both adopt a bicapped hexagonal antiprism geometry with the Ru atom taking up one apical vertex, which is similar to 1-(*p*-cymene)- μ -2,3-(CH₂)₃-1,2,3-RuC₂B₁₁H₁₁ and 1-(*p*-cymene)- μ -2,8-(CH₂)₃-1,2,8-RuC₂B₁₁H₁₁,⁸⁰ but with the two cage carbons being located at different positions. The Ru1-cent(up), cent(up)-cent(low) and cent(low)-B14 distances are also comparable

to those observed in other 14-vertex ruthenacarboranes $\text{RuC}_2\text{B}_{11}$ and listed in Table 3.6.⁸⁰

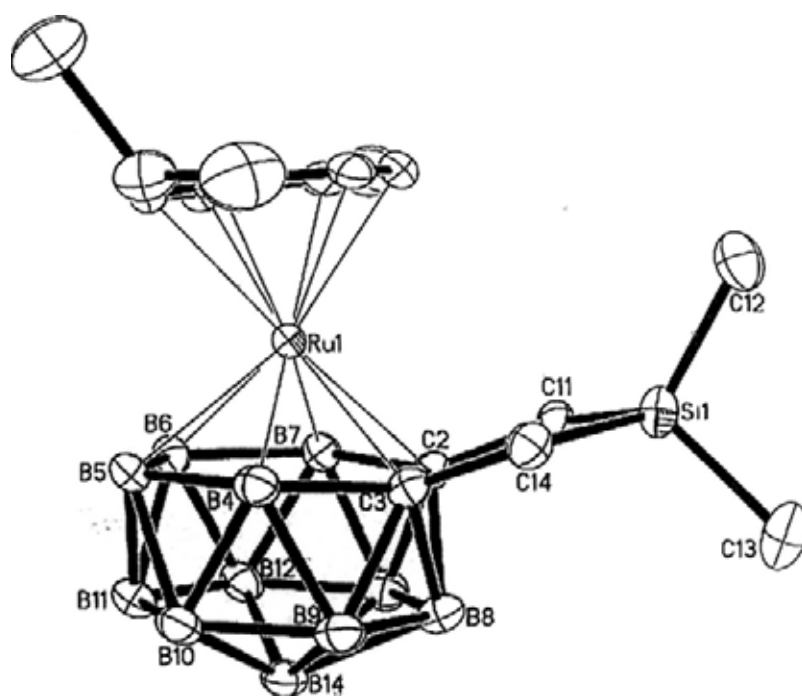


Figure 3.11. Molecular structure of 1-(*p*-cymene)- μ -2,3- $\text{Me}_2\text{Si}(\text{CH}_2)_2$ -1,2,3- $\text{RuC}_2\text{B}_{11}\text{H}_{11}$ (32a).

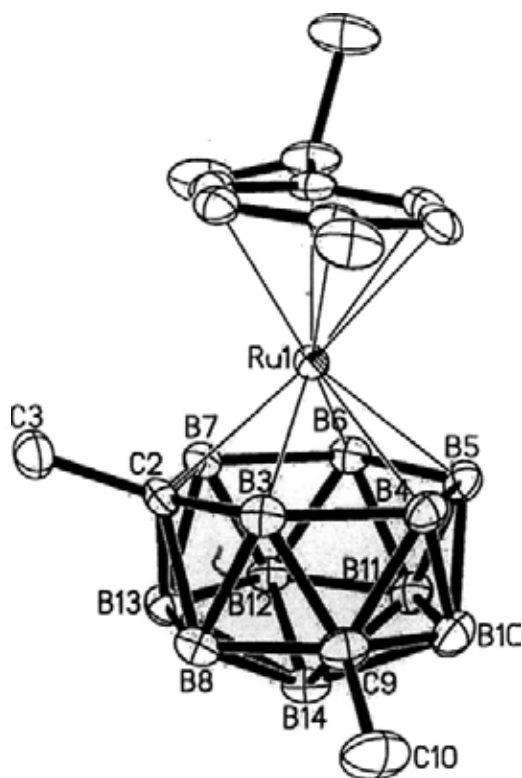
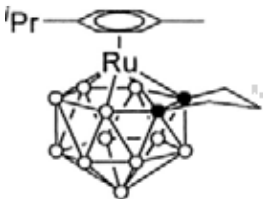
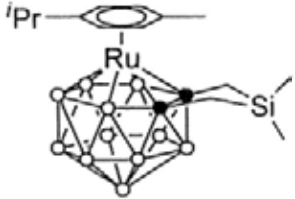
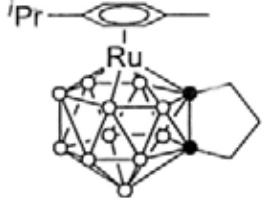
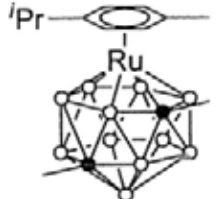


Figure 3.12. Molecular structure of 1-(*p*-cymene)-2,9- Me_2 -1,2,9- $\text{RuC}_2\text{B}_{11}\text{H}_{11}$ (33).

Table 3.6. Relative Bond Distances (Å) in the 14-Vertex Ruthenacarboranes.

Compd.	Ru1- Cent(Ar)	Ru- Cent(up)	Cent(up)- Cent(low)	Cent(low)- B14
	^a 1.776	1.455	1.498	0.835
	1.773	1.445	1.489	0.807
	^a 1.767	1.404	1.501	0.833
	1.769	1.410	1.496	0.824

^a Ref. 80.

Complexes **32a**, **32b** and **33** were also characterized by spectroscopic techniques as well as HRMS. The ¹¹B NMR spectrum of **32a** exhibited a 2:2:1:2:2:1:1 pattern in the range -6 to -23 ppm range, which was well consistent with its symmetry, while that of **32b** showed a 1:1:1:1:1:1:1:2 pattern in the range 0 to -24 ppm. On the other hand, that of complex **33** exhibited a 2:1:2:1:1:2:1:1 pattern in the range -3 to -27 ppm as a result of coincident overlap of the peaks. Compound **32a** showed two different types of chemical non-equivalent hydrogen atoms of the methylene units at 2.43 and 1.78 ppm, while its isomer **32b** exhibits four corresponding hydrogen atoms with different chemical shifts, which are consistent with their symmetry in solution.

Compound **33** showed two non-equivalent methyl groups in both the ^1H at 1.94 and 1.84 ppm, and ^{13}C NMR spectra at 34.5 and 34.7 ppm, respectively.

3.4. Reduction of 14-Vertex Carboranes and Synthesis of a 15-Vertex Ruthenacarborane

Reduction of the 14-vertex carboranes μ -2,3- $\text{Me}_2\text{Si}(\text{CH}_2)_2$ -2,3- $\text{C}_2\text{B}_{12}\text{H}_{12}$ (**28a**) and μ -2,8- $\text{Me}_2\text{Si}(\text{CH}_2)_2$ -2,8- $\text{C}_2\text{B}_{12}\text{H}_{12}$ (**28b**) can easily take place even in the absence of naphthalene, but give different products as suggested by the ^{11}B NMR spectra (Figure 3.13). Treatment of **28a** or **28b** with excess Na metal in THF gave the corresponding 14-vertex *nido*-carborane dianion $[\mathbf{34a}]^{2-}$ or $[\mathbf{34b}]^{2-}$, respectively. The ^{11}B NMR spectrum of $[\mathbf{34b}]^{2-}$ exhibits a 1:2:2:3:2:1:1 pattern in the range -1 to -47 ppm, which are similar to that of $[1,2-(\text{CH}_2)_3-1,2-\text{C}_2\text{B}_{11}\text{H}_{12}]^{2-}$. This result may indicate the similarity in structures. On the other hand, $[\mathbf{34a}]^{2-}$ shows a 1:1:1:3:1:1:1:1:1 pattern in the range 6 to -34 ppm, indicative of a more unsymmetric structure. The proposed structure is shown in Scheme 3.8. This phenomenon was different from the reduction process of the two 14-vertex carborane isomers **27a** and **27b** with a $(\text{CH}_2)_3$ linkage. However, it was observed that $[\mathbf{34a}]^{2-}$ would slowly isomerize to $[\mathbf{34b}]^{2-}$ as monitored by ^{11}B NMR spectra. This indicated that $[\mathbf{34b}]^{2-}$ was a thermodynamically more stable product. Both anions can be oxidized to a mixture of the 14-vertex carborane isomers **28a** and **28b** in a ratio of about 1:1 upon treatment with CuCl_2 (Scheme 3.7).¹⁰³

Treatment of $[\mathbf{34b}][\text{Na}_2(\text{THF})_x]$, which is directly prepared from reduction of **28b** by excess Na metal, with 0.5 equiv of $[(p\text{-cymene})\text{RuCl}_2]_2$ in a THF solution led to the isolation of a 15-vertex ruthenacarborane 7-(*p*-cymene)-1,4- $\text{Me}_2\text{Si}(\text{CH}_2)_2$ -7,1,4- $\text{RuC}_2\text{B}_{12}\text{H}_{12}$ (**35**) in 50% yield, after column chromatographic separation (Scheme

3.7).

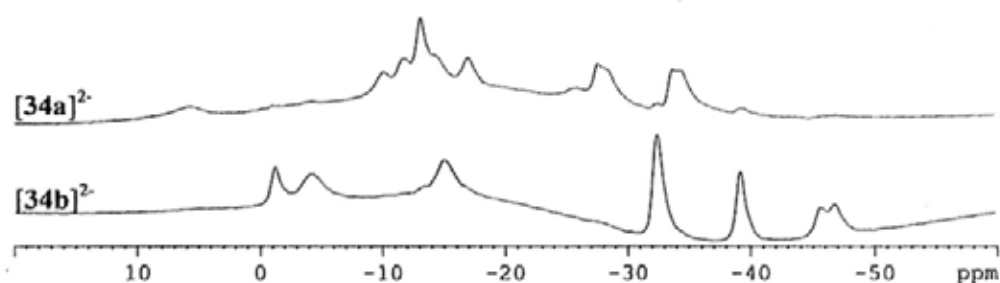
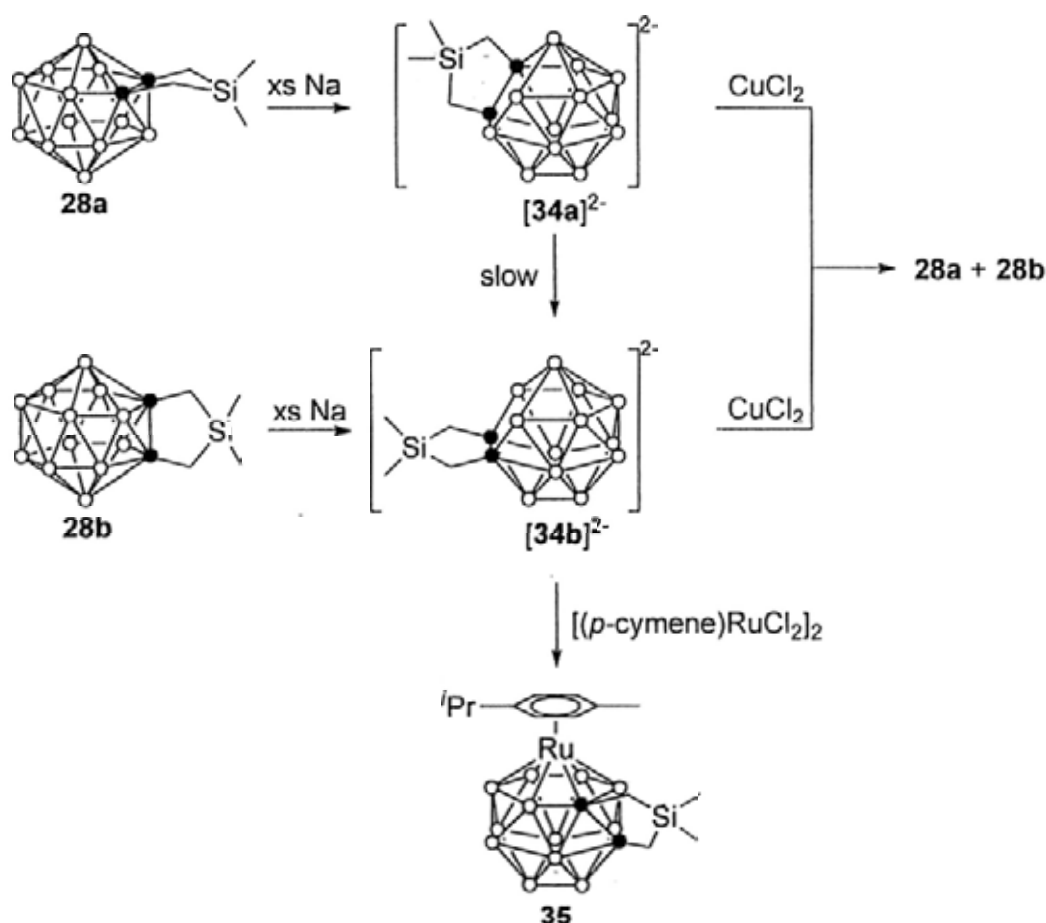


Figure 3.13. ^{11}B NMR spectra of different 14-vertex *nido*-carborane dianions formed by reduction of two 14-vertex carborane isomers with Na metal.

Scheme 3.7. Reduction of 14-Vertex Carboranes and Formation of a 15-Vertex Ruthenacarborane.



Complex **35** was characterized by various spectroscopic techniques as well as HRMS. Its ^{11}B NMR spectrum exhibited a 1:1:2:1:1:1:1:1:1:1 pattern in the range 14 to -30 ppm, which was similar to that of 7-(*p*-cymene)-1,4-(CH_2)₃-7,1,4-

$\text{RuC}_2\text{B}_{12}\text{H}_{12}$.⁸⁰ Four diastereotopic methylene protons were observed in the ^1H NMR spectrum. The structure of complex **35** was confirmed by single crystal X-ray analyses (Figure 3.14), with solvation of one equimolar CH_2Cl_2 , which was also very similar to that of 7-(*p*-cymene)-1,4-(CH_2)₃-7,1,4- $\text{RuC}_2\text{B}_{12}\text{H}_{12}$.⁸⁰

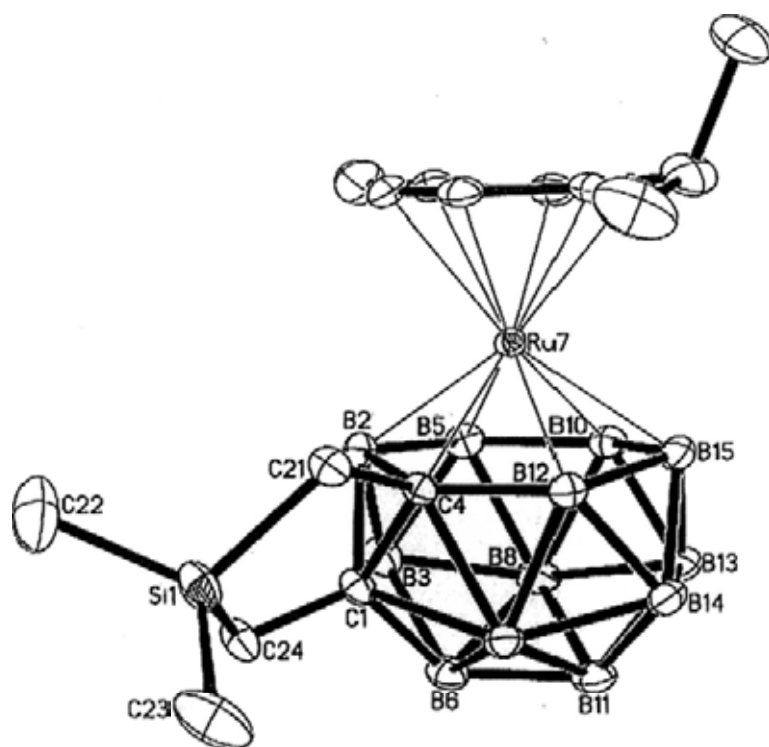


Figure 3.14. Molecular structure of 7-(*p*-cymene)-1,4- $\text{Me}_2\text{Si}(\text{CH}_2)_2$ -7,1,4- $\text{RuC}_2\text{B}_{12}\text{H}_{12}$ (**35**), in $35 \cdot \text{CH}_2\text{Cl}_2$.

3.5. Summary

13-Vertex CA_d and CA_p *nido*-carborane dianions can be easily synthesized from reduction of the corresponding CA_d and CA_p 13-vertex *closo*-carboranes by Na metal. They have similar structural features containing bent five-membered open faces with cage carbons at *ortho*- or *meta*- position. The cations are not coordinated to the open faces but to the *exo*- B-H bonds to form one dimensional polymeric network. Reduction of CA_d 13-vertex *closo*-carborane without C,C'-linkage also gave the CA_d *nido*-carborane anion with the cage C-C bond intact, which is significantly dif-

ferent from that of the 12-vertex carboranes, indicating the trapezoidal open face in the 13-vertex CAd carboranes greatly influences the reduction process. Their chemical shifts of the cage borons and carbons are greatly upfielded compared to the 12-vertex analogues after two-electron uptake.

These 13-vertex CAd and CAp *nido*-carborane dianions are useful synthons for the synthesis of 14-vertex CAd and CAp *closo*-carboranes via a [13+1] protocol. They can react with $\text{HBBr}_2 \cdot \text{SMe}_2$ to give 2,3- and 2,8- 14-vertex carborane isomers or 2,9- 14-vertex carborane. The yield is low and many 13-vertex *closo*-carboranes are recovered, indicative of the higher reducing power of these *nido*- anions, compared to the 12-vertex analogues. The same CAd 14-vertex carboranes can also be synthesized from 12-vertex *arachno*-carborane anions and $\text{HBBr}_2 \cdot \text{SMe}_2$ via a [12+2] protocol, but in much lower yields. The chemical properties of these 14-vertex carboranes are significantly different from their 13-vertex analogues but close to the 12-vertex ones. Moreover, the 13-vertex *nido*-carborane dianionic salts are also good synthons for the synthesis of CAd and CAp 14-vertex metallocarboranes.

The 14-vertex carborane isomers $\text{Me}_2\text{Si}(\text{CH}_2)_2\text{-}2,3\text{-C}_2\text{B}_{12}\text{H}_{12}$ (**28a**) and $\mu\text{-}2,8\text{-Me}_2\text{Si}(\text{CH}_2)_2\text{-}2,8\text{-C}_2\text{B}_{12}\text{H}_{12}$ (**28b**) can also be reduced by Na metal to give different 14-vertex carborane dianions, which leads to the synthesis of a 15-vertex ruthenacarborane by treatment with $[(p\text{-cymene})\text{RuCl}_2]_2$.

Chapter 4. Cage Carbon Extrusion Reaction of CAd

13-Vertex Carborane μ -1,2-(CH₂)₃-1,2-C₂B₁₁H₁₁

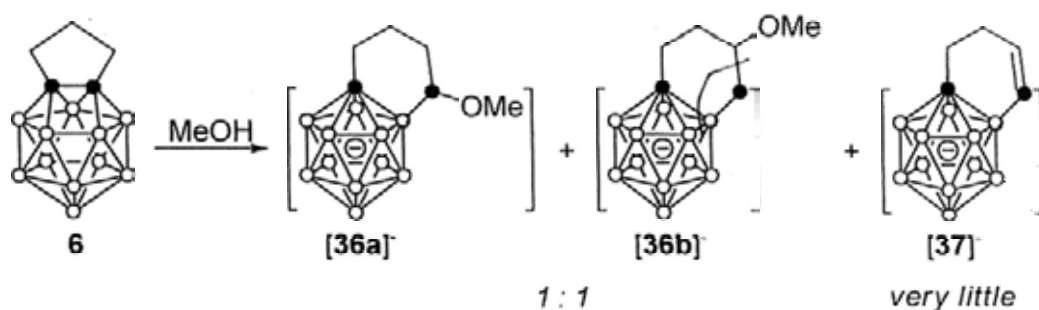
Nucleophilic reactions of icosahedral carboranes and subicosahedral carboranes were well studied in literature,^{2b,c,2f,3e} especially for the deboration reactions. As our group had studied electrophilic substitution reaction of CAd 13-vertex carborane μ -1,2-(CH₂)₃-1,2-C₂B₁₁H₁₁,⁷⁴ we were interested in the reaction of supercarboranes with nucleophiles. To our surprise, unprecedented cage carbon extrusion products were isolated instead of the expected deboration species after treatment of 13-vertex carborane with nucleophiles.

4.1. Reaction of μ -1,2-(CH₂)₃-1,2-C₂B₁₁H₁₁ with Alcohols

Followed by a routine procedure, reaction of μ -1,2-(CH₂)₃-1,2-C₂B₁₁H₁₁ (**6**) with MeOH was first attempted. When it was heated in refluxing MeOH in the presence of an excess amount of NaOH, a mixture of inseparable products was afforded. It was found that compound **6** was very reactive toward MeOH as evidenced by its ¹¹B NMR in a MeOH solution in the absence of base. In sharp contrast, its icosahedral cousin μ -1,2-(CH₂)₃-1,2-C₂B₁₀H₁₀ (**2**) is very stable in refluxing MeOH for several days without change. But it can be converted to *nido*- species [μ -7,8-(CH₂)₃-7,8-C₂B₉H₁₀]⁻ after NaOH was added to this refluxing MeOH solution. A MeOH solution of compound **6** was stirred at room temperature for 12h to give, after addition of [Me₃NH]Cl, [μ -1,2-(CH₂)₃CH(OMe)-1-CB₁₁H₁₀][Me₃NH] (**[36a]**[Me₃NH]) in 75% isolated yield. When the reaction was performed at room temperature in a prolonged time up to 4 d, or at 70 °C for 24 h, a mixture of **[36a]**[Me₃NH] and [μ -1,2-(CH₂)₂CH(OMe)CH₂-1-CB₁₁H₁₀][Me₃NH] (**[36b]**[Me₃NH]) was obtained in 80%

isolated yield in a ratio of about 1:1 with the observation of a very little amount of $[\mu\text{-}1,2\text{-}(\text{CH}_2)_2\text{CH}=\text{CH}\text{-}1\text{-CB}_{11}\text{H}_{10}][\text{Me}_3\text{NH}]$ (**[37]**)[Me_3NH] (Scheme 4.1). Complex **[36b]**[Me_3NH] was isolated in 35% yield after purification by thoroughly washing the mixture with water and repeated recrystallization from acetone. It was noted that the reaction would hardly proceed even when 10 equiv of MeOH was used in refluxing benzene.

Scheme 4.1. Reaction of **6** with MeOH.



Compound **[36a]**[Me_3NH] and **[36b]**[Me_3NH] were characterized by several NMR techniques as well as elemental analyses. The characteristic NMR data of these CB_{11}^- anions were summarized in Tables 4.1 and 4.2. The ^{11}B NMR spectra of **[36a]**[Me_3NH] showed a 1:1:6:3 pattern while that of **[36b]**[Me_3NH] exhibited a 1:1:7:1:1 one. The signal of substituted B2 atom in **[36a]**[Me_3NH] was clearly distinguished from others at -7.7 ppm as a singlet in ^{11}B NMR spectra, and that of **[36b]**[Me_3NH] was at -7.0 ppm. The $\alpha\text{-C}$ carbons bonded to the B2 atoms were unambiguously identified as they appeared to be broad signals caused by coupling of ^{11}B nucleus in the ^{13}C NMR spectra, at 74.2 ppm for **[36a]**[Me_3NH], and at 21.5 ppm for **[36b]**[Me_3NH], which indicated the different chemical environments.

Single-crystal X-ray analyses confirmed the molecular structures of **[36a]**[Me_3NH] and **[36b]**[Me_3NH] as shown in Figures 4.1 and 4.2, respectively. The icosahedral cages in these complexes have the same structural features of monocarba-*closo*-

dodecaborate anion.¹⁰⁴ The structural features of these CB_{11}^- anions are summarized and compared in Table 4.3. The C11-C1-B2-C14 atoms are almost coplanar and the 6-membered rings adopt a cyclohexene conformation with the bulky Nu substituents taking up the *e*-positions.

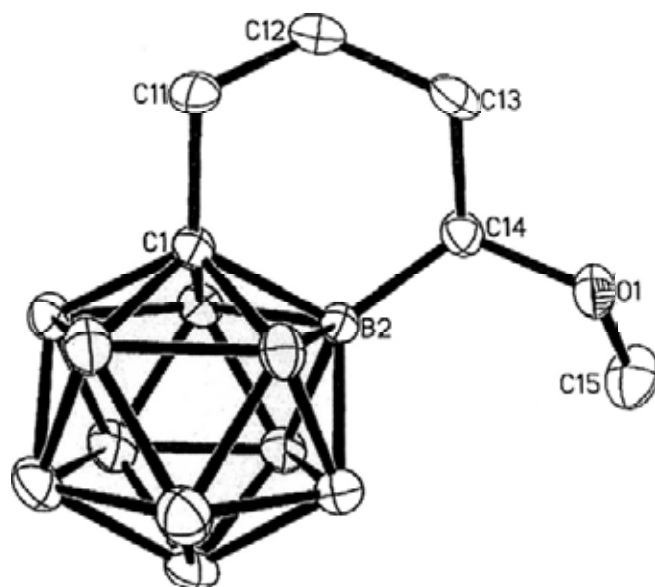


Figure 4.1. Structure of $[\mu\text{-}1,2\text{-(CH}_2\text{)}_3\text{CH(OMe)-}1\text{-CB}_{11}\text{H}_{10}]^-$ (**[36a]**), in **[36a]**- $[\text{Me}_3\text{NH}]$.

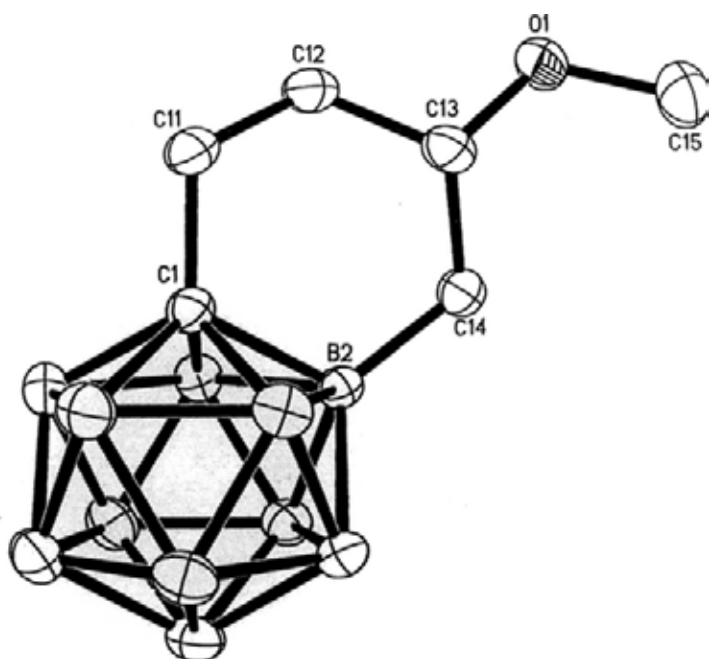


Figure 4.2. Structure of $[\mu\text{-}1,2\text{-(CH}_2\text{)}_2\text{CH(OMe)CH}_2\text{-}1\text{-CB}_{11}\text{H}_{10}]^-$ (**[36b]**), in **[36b]**- $[\text{Me}_3\text{NH}]$.

Table 4.1. Characteristic Chemical Shifts of $[\mu\text{-}1,2\text{-(CH}_2\text{)}_3\text{CH(Nu)-}1\text{-CB}_{11}\text{H}_{10}]^+$. ^a

Compd.	δ B2	δ α -CH	δ β -CH ₂	δ γ -CH ₂	δ δ -CH ₂	
Nu		δ α -CH	δ β -CH ₂	δ γ -CH ₂	δ δ -CH ₂	δ cage C
[36a] ^b	-7.7	3.11	1.68, 1.39	1.45, 1.21	1.81	
OMe		74.2	29.6	23.2	36.7	69.2
[38a] ^b	-7.7	3.19	1.68, 1.29	1.43, 1.17	1.77	
OEt		71.5	29.9	23.1	36.1	69.2
39	-9.4	3.36	2.01, 1.63	1.51, 1.39	1.85	
N ^t BuH ₂		44.5	29.3	23.2	35.1	68.9
40a	/	3.40	2.00, 1.53	1.68, 1.38	1.98, 1.79	
NEt ₂ H		54.4	24.7	24.5	35.5	69.1
41	/	3.73	2.13, 1.47	1.64, 1.57	1.99, 1.64	
PPh ₃		17.4	24.9	25.3	36.2	67.7
[42] ^c	-7.9	3.12	1.71, 1.38	1.55, 1.20	1.86	
S(4-MeC ₆ H ₄)		31.7	29.5	23.5	36.5	68.2
[43] ^d	-7.2	0.89	1.35	1.29	1.83	
H		14.2	22.8	26.0	36.5	67.9
46a	/	3.54	2.17, 1.63	1.72, 1.38	2.00, 1.81	
NEt ₃		66.0	24.5	25.5	36.3	69.4
53a	-8.7	4.73	2.30, 2.07	1.80, 1.54	2.08, 1.95	
NC ₅ H ₅		65.6	29.9	24.7	35.4	68.8

^a In *d*₆-acetone. ^b The cation is [Me₃NH]⁺. ^c The cation is [PPN]⁺. ^d The cation is [Me₄N]⁺.

Compound **6** can also react with EtOH in a similar manner, but the ratio of the products is different. A EtOH solution of **6** was stirred at room temperature for 24 h to give, after addition of [Me₃NH]Cl, a mixture of $[\mu\text{-}1,2\text{-(CH}_2\text{)}_3\text{CH(OEt)-}1\text{-CB}_{11}\text{H}_{10}][\text{Me}_3\text{NH}]$ (**[38a]**[Me₃NH]) and $[\mu\text{-}1,2\text{-(CH}_2\text{)}_2\text{CH=CH-}1\text{-CB}_{11}\text{H}_{10}][\text{Me}_3\text{NH}]$ (**[37]**[Me₃NH]) in a ratio of about 1:0.5 in 70% isolated yield with the observation of a little amount of $[\mu\text{-}1,2\text{-(CH}_2\text{)}_2\text{CH(OEt)CH}_2\text{-}1\text{-CB}_{11}\text{H}_{10}][\text{Me}_3\text{NH}]$ (**[38b]**[Me₃NH])

(Scheme 4.2). Several conditions were tried and compound [38a][Me₃NH] or [37][Me₃NH] cannot be isolated in the pure form by recrystallization from different solvents. The two products were not able to separate by column chromatography on silica gel or even by HPLC. Shortening the reaction time also gave a mixture of products. Thus the NMR spectra of the mixture were recorded and those signals of [38a][Me₃NH] and [38b][Me₃NH] were separated from [37][Me₃NH] according to the spectra of [37][PSH] and distinguished from each other by intensities of the peaks as well as COSY, HSQC and HMBC techniques.

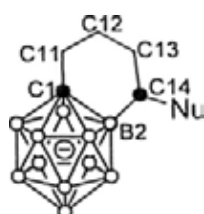
Several single-crystals were obtained from the reaction mixture after recrystallization from acetone and structures of [38a][Me₃NH] and [37][Me₃NH] were characterized by X-ray analyses and shown in Figures 4.3 and 4.4.

Table 4.2. Characteristic Chemical Shifts of $[\mu\text{-}1,2\text{-(CH}_2\text{)}_2\text{CH(Nu)CH}_2\text{-}1\text{-CB}_{11}\text{H}_{10}]^{\text{a}}$

Compd.	δ B2	δ α -CH ₂	δ β -CH	δ γ -CH ₂	δ δ -CH ₂	
Nu		δ α -CH ₂	δ β -CH	δ γ -CH ₂	δ δ -CH ₂	δ cage C
[36b] ^b	-7.0	1.49, 0.74	3.21	1.55, 1.28	2.02, 1.92	
OMe		21.5	79.9	31.9	36.1	67.7
[38b] ^b	/	1.41, 0.74	3.27	1.52, 1.24	1.97, 1.88	
OEt		22.2	77.7	32.0	35.8	67.5
40b	-8.2	1.39, 1.23	3.59	1.80, 1.70	2.16, 2.03	
NEt ₂ H		14.7	63.4	27.5	35.8	66.4
46b	-8.0	1.50, 1.37	3.54	2.07, 1.69	2.19, 2.03	
NEt ₃		15.5	72.7	27.0	36.8	66.3
47b ^c	/	1.28, 1.07	3.34	1.68, 1.53	2.10	
C ₁₄ H ₁₈ N ₂		22.6	35.3	32.3	36.0	66.8
53b	-8.1	1.74, 1.65	4.87	2.22, 1.96	2.24	
NC ₅ H ₅		24.6	73.6	33.1	36.2	66.2

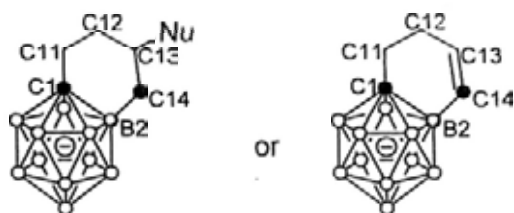
^a In *d*₆-acetone unless otherwise noted. ^b The cation is [Me₃NH]. ^c In *d*₆-DMSO.

Table 4.3. Corresponding Bond Lengths (Å) of the CB₁₁⁻ anions.



Compd.	[36a] ^{-a}	[38a] ^{-a,b}	39	40a	41
Nu	OMe	OEt	N ⁱ BuH ₂	NEt ₂ H	PPh ₃
C1-B2	1.721(4)	1.725(2)	1.709(2)	1.695(3)	1.724(4)
C1-C11	1.527(4)	1.532(2)	1.526(2)	1.515(3)	1.517(4)
C11-C12	1.519(5)	1.524(3)	1.526(3)	1.540(4)	1.532(5)
C12-C13	1.520(5)	1.527(2)	1.518(3)	1.504(5)	1.523(5)
C13-C14	1.527(4)	1.527(3)	1.534(2)	1.526(3)	1.560(4)
C14-B2	1.603(4)	1.599(3)	1.601(2)	1.601(3)	1.625(4)
C14-Nu	1.459(4)	1.464(2)	1.531(2)	1.521(3)	1.815(3)
av. C-B	1.714(4)	1.721(3)	1.715(3)	1.715(4)	1.717(5)
av. B-B	1.771(5)	1.780(3)	1.773(3)	1.770(4)	1.773(5)

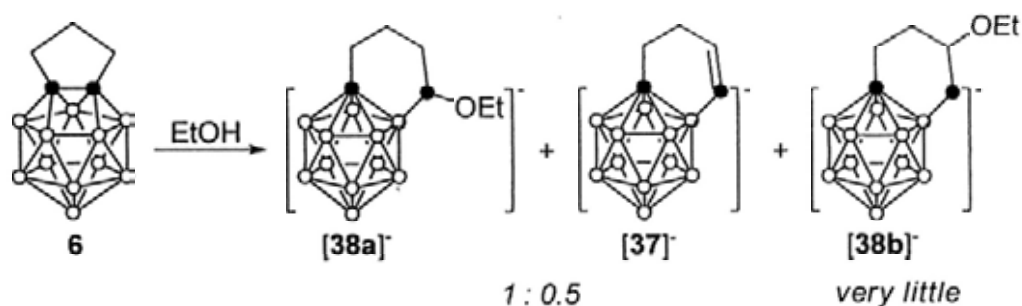
Compd.	[43] ^{-c,d}	46a ^d	53a	57a
Nu	H	NEt ₃	NC ₅ H ₅	NC ₅ H ₄ Me
C1-B2	1.700(6)	1.729(5)	1.714(3)	1.716(5)
C1-C11	1.507(9)	1.519(5)	1.525(3)	1.525(5)
C11-C12	1.528(8)	1.527(6)	1.520(4)	1.534(6)
C12-C13	1.517(9)	1.603(7)	1.541(3)	1.522(6)
C13-C14	1.527(9)	1.581(6)	1.536(3)	1.517(5)
C14-B2	1.681(10)	1.679(6)	1.612(3)	1.610(4)
C14-Nu	/	1.573(5)	1.507(2)	1.502(4)
av. C-B	1.718(7)	1.705(5)	1.717(3)	1.714(6)
av. B-B	1.740(11)	1.758(10)	1.774(4)	1.777(7)



Compd.	[36b] ^a	46b	47b	[37] ^e
Nu	OMe	NEt ₃	C ₁₄ H ₁₈ N ₂	/
C1-B2	1.718(3)	1.704(4)	1.715(11)	1.705(5)
C1-C11	1.528(3)	1.519(4)	1.521(10)	1.536(5)
C11-C12	1.520(3)	1.528(4)	1.509(10)	1.523(8)
C12-C13	1.510(4)	1.530(4)	1.516(11)	1.549(8)
C13-C14	1.517(3)	1.517(3)	1.519(9)	1.285(6)
C14-B2	1.594(3)	1.597(4)	1.597(11)	1.590(6)
C13-Nu	1.455(3)	1.561(3)	1.521(11)	/
av. C-B	1.714(4)	1.712(5)	1.702(12)	1.717(7)
av. B-B	1.774(4)	1.771(5)	1.767(14)	1.775(9)

^a The cation is [Me₃NH]⁺. ^b Space group is *Pna*2₁. ^c The cation is [Me₄N]⁺. ^d Disordered problems. ^e The cation is [PSH]⁺.

Scheme 4.2. Reaction of **6** with EtOH.



The short C13-C14 bond distances of 1.319(7) Å in [37]⁻ clearly indicates the C=C double bond character, which is in accordance with the resonances at 5.85 ppm in the ¹H NMR spectrum and a sharp signal at 131.8 and a broad one at 132.7 ppm in the ¹³C NMR spectrum, thus confirming the formation of the alkenyl product [37]⁻.

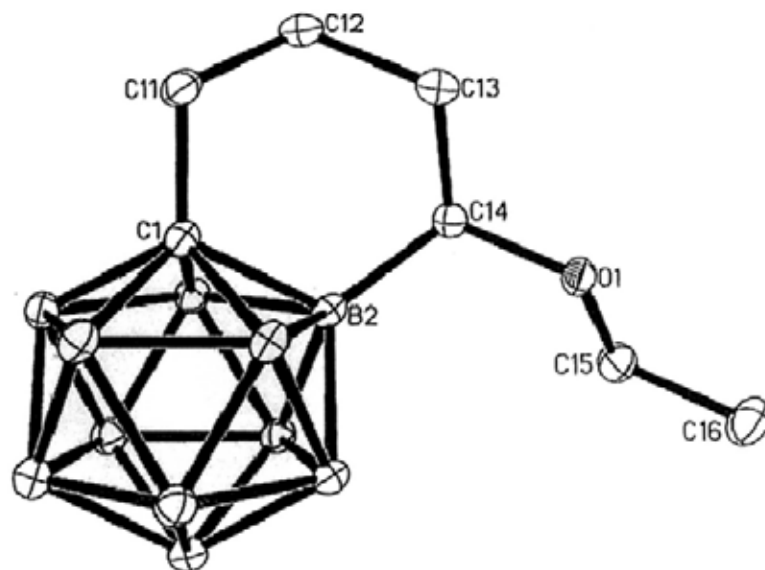


Figure 4.3. Structure of $[\mu\text{-}1,2\text{-(CH}_2\text{)}_3\text{CH(OEt)-}1\text{-CB}_{11}\text{H}_{10}]^-$ (**[38a]**⁻), in **[38a]**-**[Me₃NH]**.

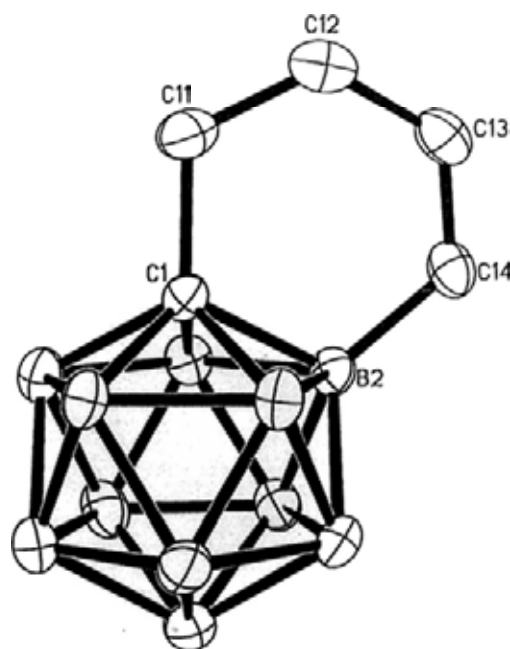
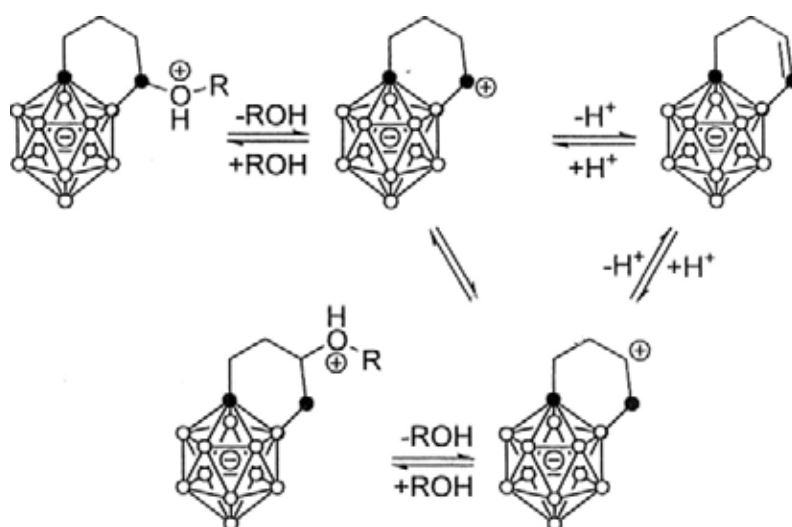


Figure 4.4. Structure of $[\mu\text{-}1,2\text{-(CH}_2\text{)}_2\text{CH=CH-}1\text{-CB}_{11}\text{H}_{10}]^-$ (**[37]**⁻), in **[37]****[Me₃NH]**.

In order to figure out how these products were formed, solvolysis of compound **6** using deuterated solvents was performed and closely monitored by ¹H and ¹³C NMR. It showed clearly that initial formation of **[36a]**⁻ or **[38a]**⁻ accompanied with decreasing of the starting material. Corresponding peaks of **[36b]**⁻ or **[37]**⁻ were observed after several hours and the mixture finally arrived at a ratio of about 1:1 or 1:0.5 at

room temperature. After heating these solutions for 24h at refluxing temperature, the spectra did not show obvious changes. With these results in hand, it would be expected that $[36a]^-$ or $[38a]^-$ is directly formed from compound **6**, which would undergo isomerization via alcohol elimination/addition under acidic media,^{98a} as shown in Scheme 4.3.

Scheme 4.3. Proposed Isomerization Mechanism.

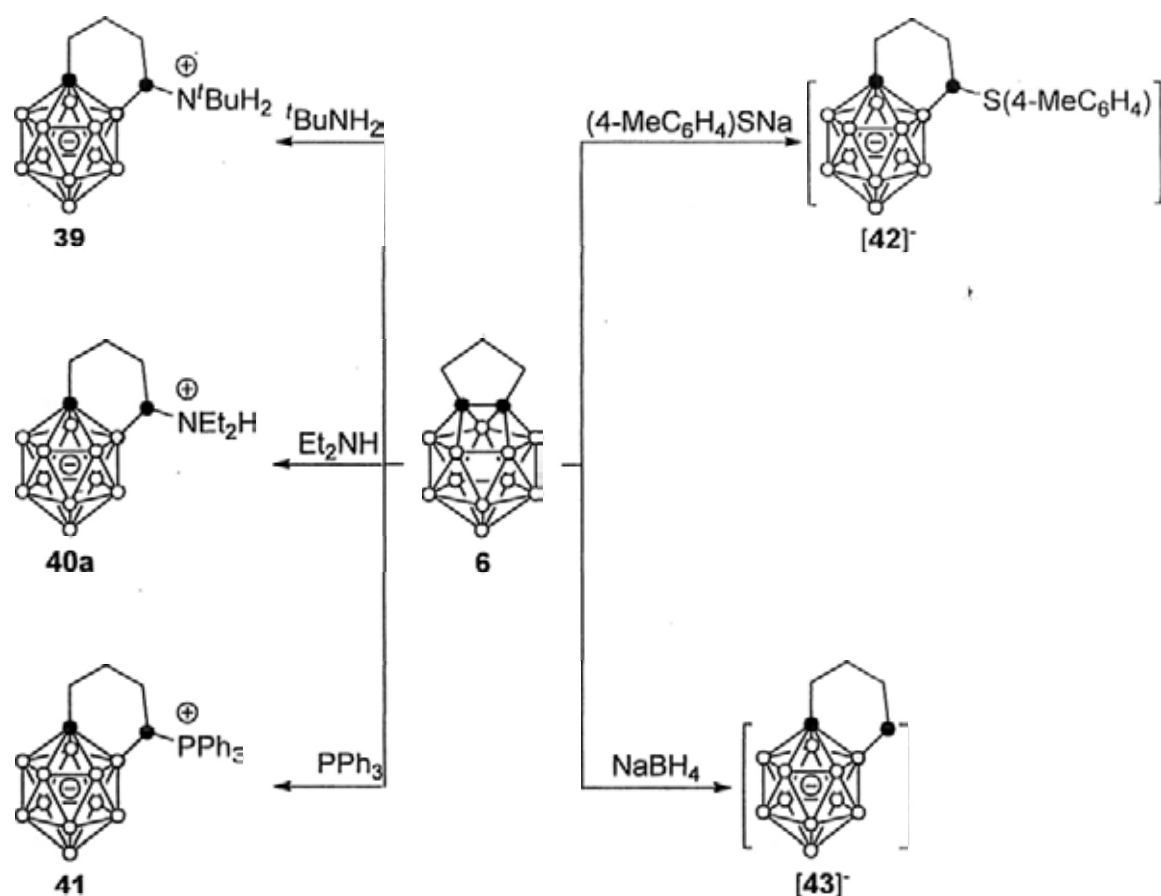


Several experiments were done to support this acid catalyzed elimination-/isomerization mechanism. 1) $[36a][Na]$, which was prepared in a MeOD solution by treatment of $[36a][Me_3NH]$ with excess of NaOH, was stable for several days under refluxing conditions without any detectable change in the 1H NMR, indicating the isomerization process would not proceed under basic media. 2) The diluted MeOD solutions of $[36a][Me_3NH]$ were heated at refluxing temperature in the presence of acids for 24 h. When conc. HCl was used, only about half conversion from $[36a]^-$ to $[36b]^-$ was observed from 1H NMR; while in the presence of TfOH, almost full conversion occurred. Thus acid catalyzed isomerization processes were confirmed and these evidences indicated that the ratio of the final products is greatly influenced by both of the acidity of the acid and ROH that used.

4.2. Reaction of μ -1,2-(CH₂)₃-1,2-C₂B₁₁H₁₁ with ^tBuNH₂, Et₂NH, PPh₃, (4-MeC₆H₄)SNa and NaBH₄

The 13-vertex carborane μ -1,2-(CH₂)₃-1,2-C₂B₁₁H₁₁ (**6**) reacted readily with several neutral nucleophiles to give the zwitterionic species. Treatment of **6** with 10 equiv of ^tBuNH₂ or Et₂NH in a toluene solution from 0 °C to room temperature with stirring for 12 h followed by removal of the volatile materials gave pale yellow solids. Recrystallization from CH₂Cl₂/hexane afforded zwitterionic species μ -1,2-(CH₂)₃CH(N^tBuH₂)-1-CB₁₁H₁₀ (**39**) or μ -1,2-(CH₂)₃CH(NEt₂H)-1-CB₁₁H₁₀ (**40a**) in 90% and 91% isolated yield. Compound **6** can also react with PPh₃ in toluene. The reaction was slow at room temperature but completed in 24 h at 110 °C. A zwitterionic compound μ -1,2-(CH₂)₃CH(PPh₃)-1-CB₁₁H₁₀ (**41**) can be isolated in 80% yield, after recrystallization from CH₂Cl₂ (Scheme 4.4).

Scheme 4.4. Reactions of **6** with ^tBuNH₂, Et₂NH, PPh₃, (4-MeC₆H₄)SNa and NaBH₄.



Complexes **39**, **40a** and **41** were characterized by several spectroscopic techniques as well as HRMS. The characteristic peaks of the B(2) atoms were observed at -9.4 ppm for **39**, as a singlet in the ^1H coupled ^{11}B NMR spectra, while those for **40a** and **41** overlapped with other cage B peaks, and were hardly resolved (Table 4.1). The ^{31}P NMR spectrum of **41** exhibits one sharp peak at 32.7 ppm, supportive of a tertiary phosphonium salt.¹⁰⁵ The structures of compound **39**, **40a**, **41**, were characterized by single-crystal X-ray analyses and shown in Figures 4.5 to 4.7.

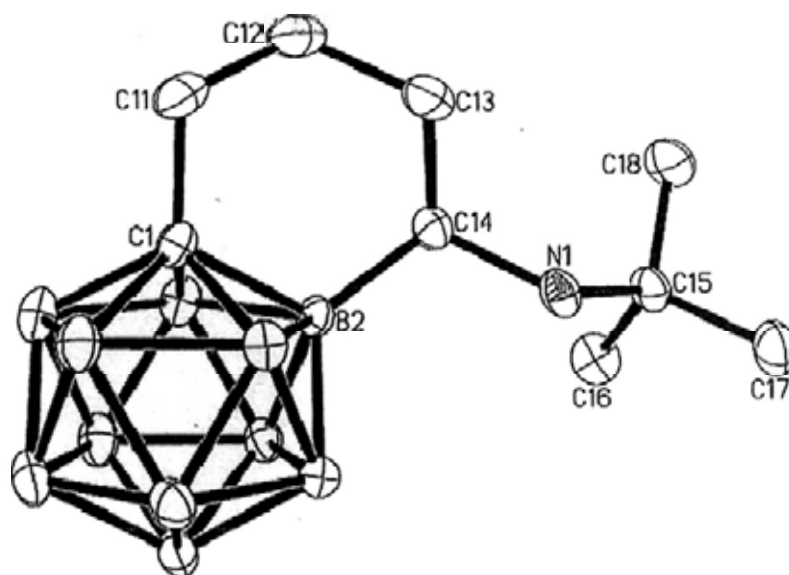


Figure 4.5. Molecular structure of μ -1,2-(CH_2) $_3\text{CH}(\text{N}^t\text{BuH}_2)$ -1- $\text{CB}_{11}\text{H}_{10}$ (**39**).

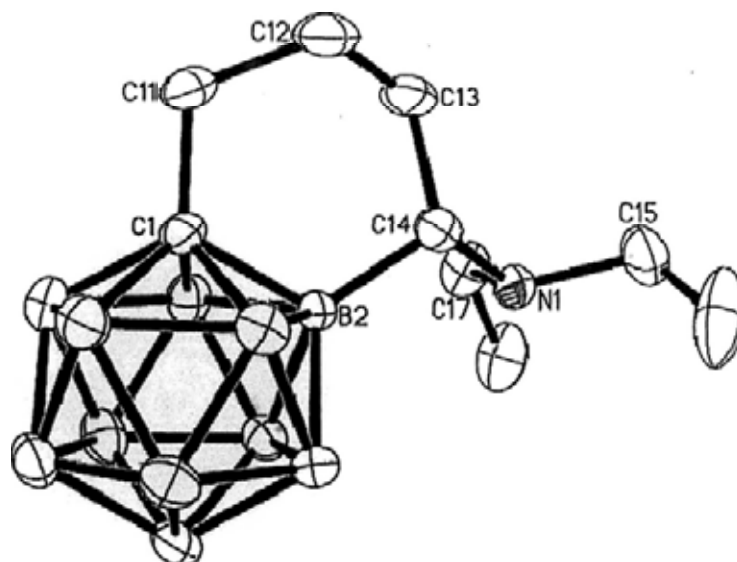


Figure 4.6. Molecular structure of μ -1,2-(CH_2) $_3\text{CH}(\text{NEt}_2\text{H})$ -1- $\text{CB}_{11}\text{H}_{10}$ (**40a**).

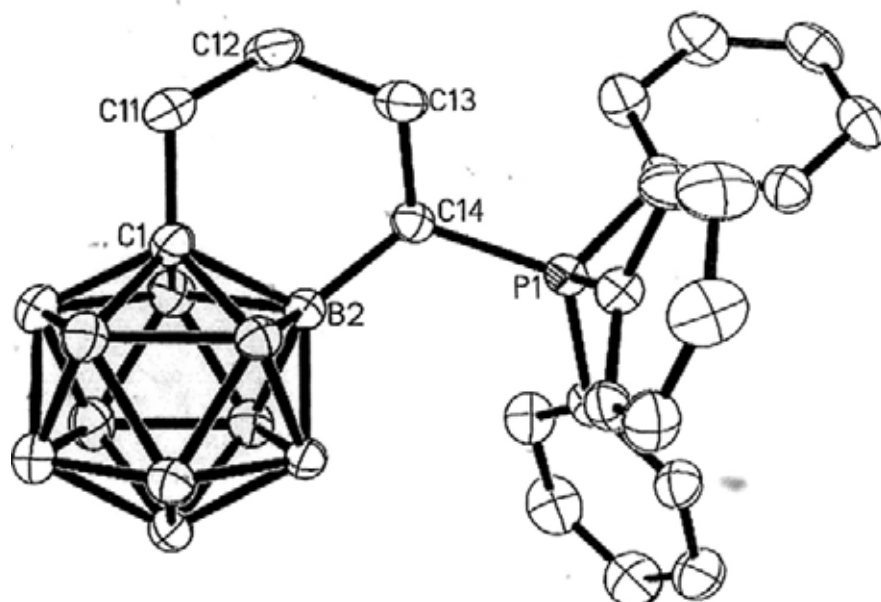


Figure 4.7. Molecular structure of μ -1,2-(CH₂)₃CH(PPh₃)-1-CB₁₁H₁₀ (**41**), in **41**·CH₂Cl₂.

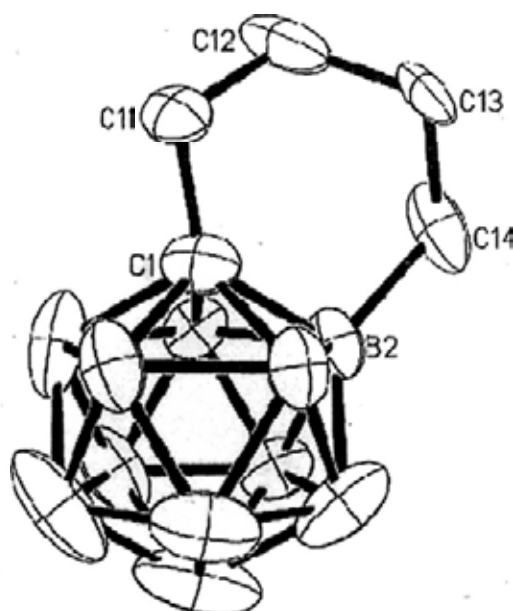


Figure 4.8. Structure of $[\mu$ -1,2-(CH₂)₄-1-CB₁₁H₁₀]⁺ (**[43]⁺**), in **[43]⁺**[Me₄N].

It can also react with some anionic nucleophiles to give similar results. Reaction of **6** with (4-MeC₆H₄)SNa in refluxing THF for 48 h, followed by addition of [PPN]Cl and recrystallization from MeOH, gave $[\mu$ -1,2-(CH₂)₃CH(S(4-MeC₆H₄))-1-CB₁₁H₁₀][PPN] (**[42]**[PPN]) in 80% yield. Complex **6** reacted with NaBH₄ in refluxing THF for 12 h to afford, after addition of 18-crown-6 or [Me₄N]Cl, $[\mu$ -1,2-(CH₂)₄-

1-CB₁₁H₁₀][Na(18-crown-6)(THF)₂] ([43][Na(18-crown-6)(THF)₂]) or [43][Me₄N] in 80% or 85% isolated yield after recrystallization (Scheme 4.4). [43][Na(18-crown-6)(THF)₂] suffered from poor resolution and [43][Me₄N] gave a much better result, although it suffered from disordered problems at the (CH₂)₄ unit. The structure of [43]⁻ was shown in Figure 4.8. Complexes [42][PPN] and [43][Me₄N] were characterized by several spectroscopic techniques as well as elemental analysis. The characteristic peaks of the B(2) atoms are observed at -7.9 ppm for [42]⁻ and -7.2 ppm for [43]⁻ as singlets in the ¹H coupled ¹¹B NMR spectra.

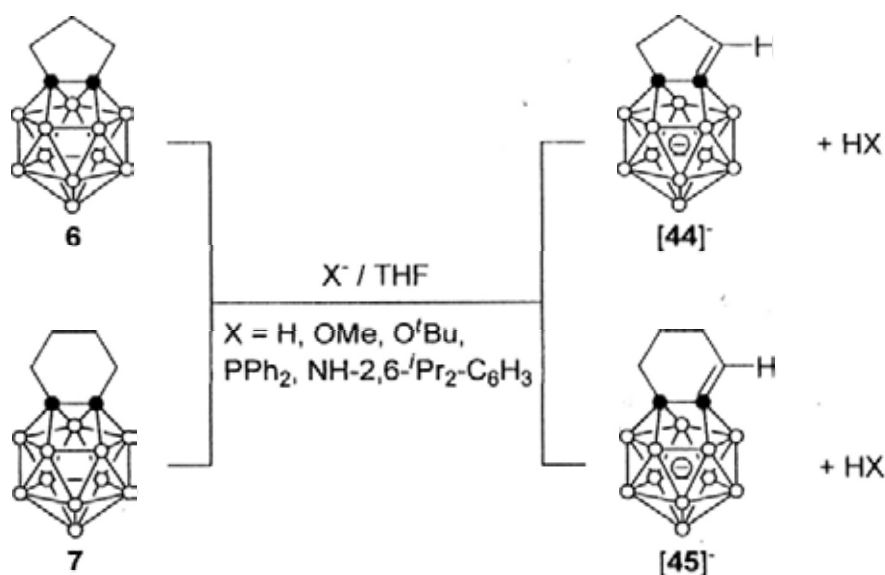
4.3. Reaction of μ -1,2-(CH₂)₃-1,2-C₂B₁₁H₁₁ with NaH—Unprecedented Deprotonation of α -CH

As BH₃·THF was a byproduct in the reaction of μ -1,2-(CH₂)₃-1,2-C₂B₁₁H₁₁ (6) with NaBH₄, we intended to get the desired product in an atomic economic manner thus the reaction of 6 with NaH was performed. However, the phenomenon and the product were totally different from the former. When NaH was added to a THF solution of 6, bubbles were gradually evolved indicating the generation of H₂ gas (Scheme 4.5), and solution was changed from colorless to brown. This process was completed within 2 h as no gas further came out. A very similar phenomenon was also observed in the reaction of μ -1,2-(CH₂)₄-1,2-C₂B₁₁H₁₁ (7) with NaH. The two solutions exhibited very similar ¹¹B NMR spectra. A 1:5:5 pattern was observed, which is the same as that observed in the CAd 13-vertex carboranes, but the chemical shifts were remarkably different with the peaks appearing at about 7, -1, -21 ppm.

In order to confirm the structures of the anions, several attempts were tried. Addition of 18-crown-6 to their THF solutions facilitated the crystallization. However, the crystals of [μ -1,2-(CH₂)₂CH-1,2-C₂B₁₁H₁₁][Na(18-crown-6)(THF)₂] ([44][Na(18-

crown-6)(THF)₂) were suffered from weak diffraction and those of [μ -1,2-(CH₂)₃CH-1,2-C₂B₁₁H₁₁][Na(18-crown-6)(THF)₂] ([45][Na(18-crown-6)(THF)₂]) were suffered from highly disordered problems. Cation exchange reaction of [PPN]Cl with the sodium salts afforded [44][PPN] or [45][PPN] as brown crystals in 50% or 90 % isolated yields, respectively. It is noted that although the deprotonation reactions were almost quantitative as monitored by ¹¹B NMR, [44][PPN] would be deteriorated in the process of purification, leading to low isolated yield whereas [45][PPN] is much more stable.

Scheme 4.5. Deprotonation of 13-Vertex Carboranes.



Both of them were characterized by several spectroscopic techniques as well as elemental analyses. Besides the very similar ¹¹B NMR spectra, their ¹H NMR and ¹³C NMR spectra also had common features. Two methylene units or three were observed for [44][PPN] or [45][PPN]. Besides, a characterized triplet at 5.45 ppm with $J = 3.1$ Hz in [44][PPN], and one at 5.76 ppm with $J = 4.8$ Hz in [45][PPN], were observed in the ¹H NMR spectra, indicative of the α -CH that were splitted by the neighboring methylene groups. Correspondingly, the ¹³C shifts of the α -CH, which was unambiguously determined by ¹H-¹³C HSQC experiments, was observed at

140.6 ppm in [44]⁻, and 150.1 ppm in [45]⁻, respectively. These data were in accordance with the sp^2 hybridization properties of the corresponding carbon atoms.

Their structures were determined by X-ray diffraction studies and the anions are shown in Figures 4.9 and 4.10. The preservation of the integrity of 13-vertex *closo*-cage geometry is unambiguously confirmed. The 5-membered ring of [44]⁻ is suffered from disordered problems, while the 6-membered ring in [45]⁻ are definitely determined. The C1-C11 bond length of 1.364(5) Å in [45]⁻ is much shorter than the other C-C bonds in the linkage (av. 1.519(5) Å), showing a typical C=C double bond character, which is in accordance with the NMR spectroscopic features. The C14-C2-C1-C11-C12 five atoms are almost coplanar with the C13 atom out of this plane. Another structural feature is that it contains two trapezoidal open faces, compared to only one observed in its precursor 7, as a result of the formation of C1=C11 double bond and pumping electron into the cage. The cage C1-C2 distance of 1.448(4) Å in [45]⁻ is only slightly longer than that of 1.425(4) Å in compound 7, indicating that π -bonding interaction still exists between the two cage carbons.

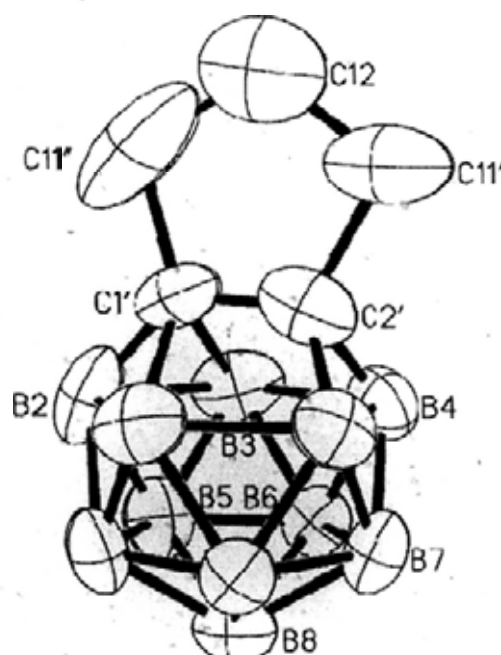


Figure 4.9. Structure of [μ -1,2-(CH₂)₂CH-1,2-C₂B₁₁H₁₁] ([44]⁻), in [44][PPN].

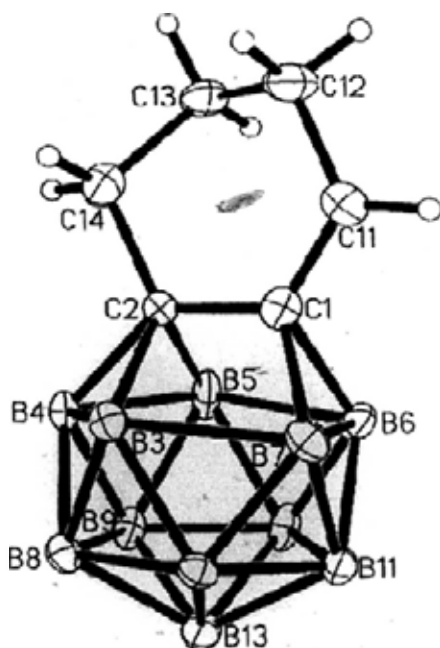


Figure 4.10. Structure of $[\mu\text{-}1,2\text{-(CH}_2\text{)}_2\text{CH-}1,2\text{-C}_2\text{B}_{11}\text{H}_{11}]$ ($[\mathbf{45}]^-$), in $[\mathbf{45}][\text{PPN}]$.

Formation of this type of 13-vertex *closo*-carborane anions can be ascribed to the negative charge delocalization into the cage cluster as shown in Figure 4.11. As discussed in Chapter 2, the NMR spectroscopic properties of 13-vertex carboranes indicated that they could serve as electron withdrawing group which induced strong deshielding effect. The alkyl anionic structure **IV-A**, which would be expected after deprotonation, was in resonance with the borate anionic structure **IV-B**, after donation of the lone pair electrons to the cage. As a result of the π -conjugation, a formally C=C double bond, together with an additional trapezoidal open face, was formed. As the negative charge is delocalized over the cluster, the anion is stabilized. Indeed, structure **IV-B** should be much more representative for the anions $[\mathbf{44}]^-$ and $[\mathbf{45}]^-$. The upfielded signals indicated this negative charge would mainly distributed on the two cage carbons and the five cage borons on the upper 5-membered belt.

We further found that this deprotonation proceeded not only by NaH, but also by other bases even not strong. Reactions of $\mu\text{-}1,2\text{-(CH}_2\text{)}_3\text{-}1,2\text{-C}_2\text{B}_{11}\text{H}_{11}$ (**6**) with $\text{NaNH-}2,6\text{-}^i\text{Pr}_2\text{-C}_6\text{H}_3$ or NaOMe in THF gave the deprotonation product $[\mathbf{44}]^-$ quantitatively

as evidenced by ^{11}B NMR. Treatment of μ -1,2-(CH_2)₄-1,2- $\text{C}_2\text{B}_{11}\text{H}_{11}$ (**7**) with KPPH_2 , $\text{NaNH}-2,6\text{-}^i\text{Pr}_2\text{-C}_6\text{H}_3$, NaOMe or KO^tBu also led to the formation of [45]. These primary results indicated that deprotonation of the α -CH proton would be a competing reaction to the carbon extrusion reaction when 13-vertex carborane is treated with anionic nucleophile. Which pathway the reaction undergoes would be dependent upon the relative nucleophilicity to the cage and basicity to the proton.

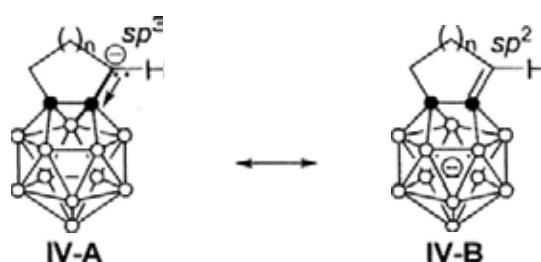


Figure 4.11. Resonance structures of deprotonated 13-vertex carborane.

4.4. Unusual Reaction of μ -1,2-(CH_2)₃-1,2- $\text{C}_2\text{B}_{11}\text{H}_{11}$ with Tertiary Amines

Reactions of **6** with tertiary amines are not as facile as those with primary or secondary amine. No obvious change was observed when a benzene solution of **6** and 10 equiv of Et_3N was heated to $90\text{ }^\circ\text{C}$ for several days. When compound **6** was dissolved in pure Et_3N , a yellow solution was formed immediately but without any change for several days at room temperature. When it was heated at $90\text{ }^\circ\text{C}$, a yellow solid was precipitated out and the reaction completed until no ^{11}B signal was detected within 48 h. After column chromatographic separation and recrystallization, μ -1,2-(CH_2)₃ $\text{CH}(\text{NEt}_3)$ -1- $\text{CB}_{11}\text{H}_{10}$ (**46a**), μ -1,2-(CH_2)₂ $\text{CH}(\text{NEt}_3)\text{CH}_2$ -1- $\text{CB}_{11}\text{H}_{10}$ (**46b**), and a mixture of [37][Et_3NH] and [43][Et_3NH] in a ratio of about 1:0.5, were afforded in 80%, 5%, and 10% yield, respectively (Scheme 4.6).

Complexes **46a** and **46b** were characterized by several spectroscopic techniques as well as HRMS. Their isomeric properties were confirmed by the identical molecular masses. The characteristic singlet B(2) resonance was observed at -8.0 ppm for

46b but cannot be distinguished for **46a** in the ^{11}B NMR spectra. The different broad peaks of $\alpha\text{-C}$ at 66.0 ppm for **46a** and 15.5 ppm for **46b** indicated the distinct groups attached to these carbon atoms. The structures of compounds **46a** and **46b** were further confirmed by single-crystal X-ray analyses and shown in Figures 4.12 and 4.13, which were consistent with their spectroscopic features. Compounds **[37][Et₃NH]** and **[43][Et₃NH]** were hard to separate, which were regarded as the similar polarities of the two species, but could be determined according to the known spectra of those containing the same anions.

Scheme 4.6. Reaction of **6** with Et_3N .

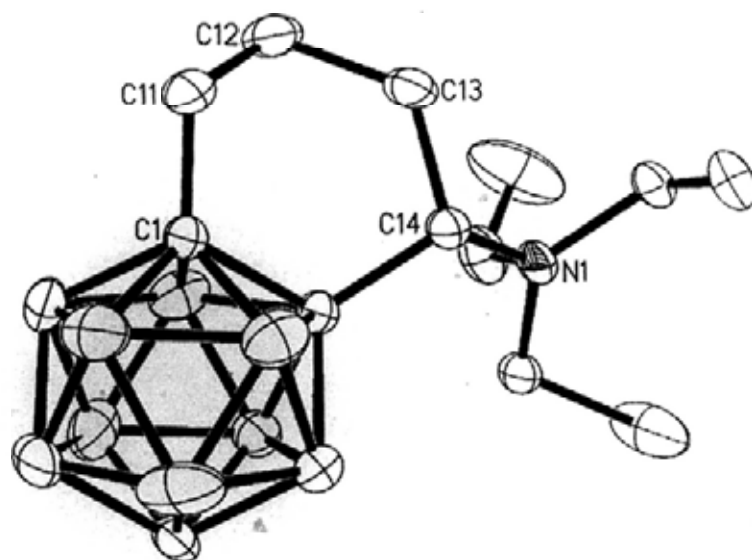
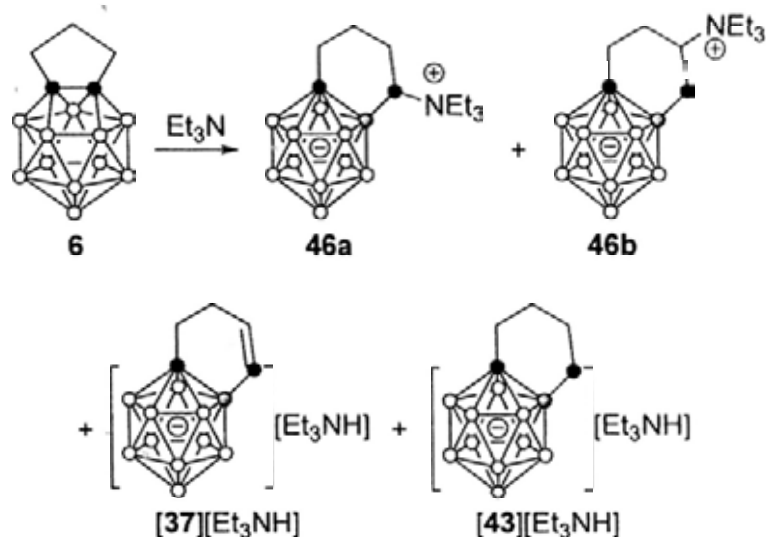


Figure 4.12. Molecular structure of $\mu\text{-1,2-(CH}_2\text{)}_3\text{CH(NEt}_3\text{)-1-CB}_{11}\text{H}_{10}$ (**46a**).

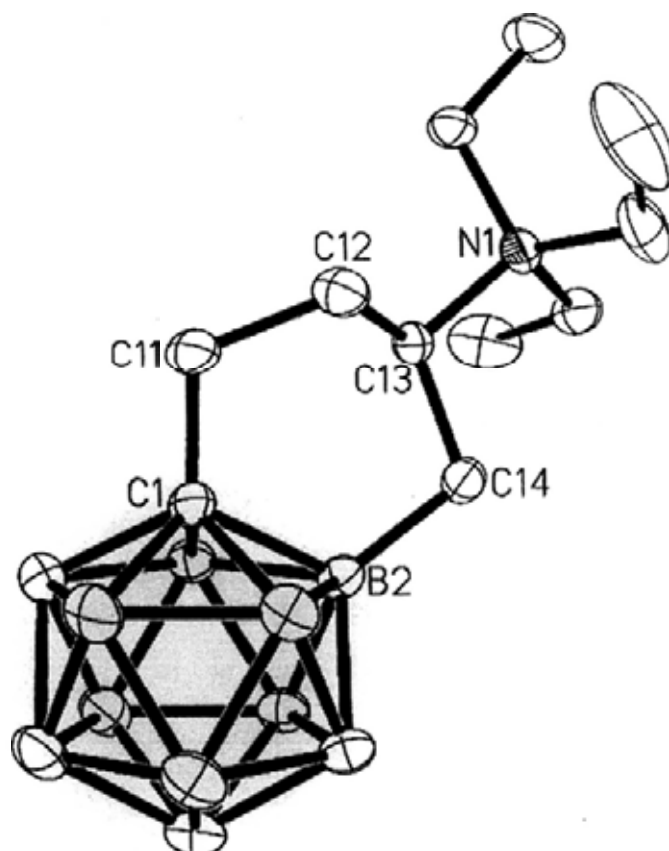


Figure 4.13. Molecular structure of μ -1,2-(CH₂)₂CH(NEt₃)CH₂-1-CB₁₁H₁₀ (**46b**).

Complex **6** can also react with PS (Proton Sponge, C₁₄H₁₈N₂), although the latter is not an N-nucleophile due to the steric effect but can serve as weak C-nucleophile to interact with strong electrophiles.¹⁰⁶ Compound **6** and 5 equiv of PS was dissolved in 10 mL of THF and the solution was heated at 90 °C. The reaction was very slow and even not completed after 28 d. The resulted yellow suspension was separated. The solid was collected affording μ -1,2-(CH₂)₂CH(4'-C₁₀H₅-1',8'-(NMe₂)₂H)CH₂-1-CB₁₁H₁₀ (**47b**) in 30% gross yield, which was purified by recrystallization from MeCN in 25% isolated yield. The liquid was dried and thoroughly washed with Et₂O to give [37][PSH] in 55% gross yield, which was purified by recrystallization from MeOH in 50% isolated yield (Scheme 4.7).

Scheme 4.7. Reaction of **6** with PS.

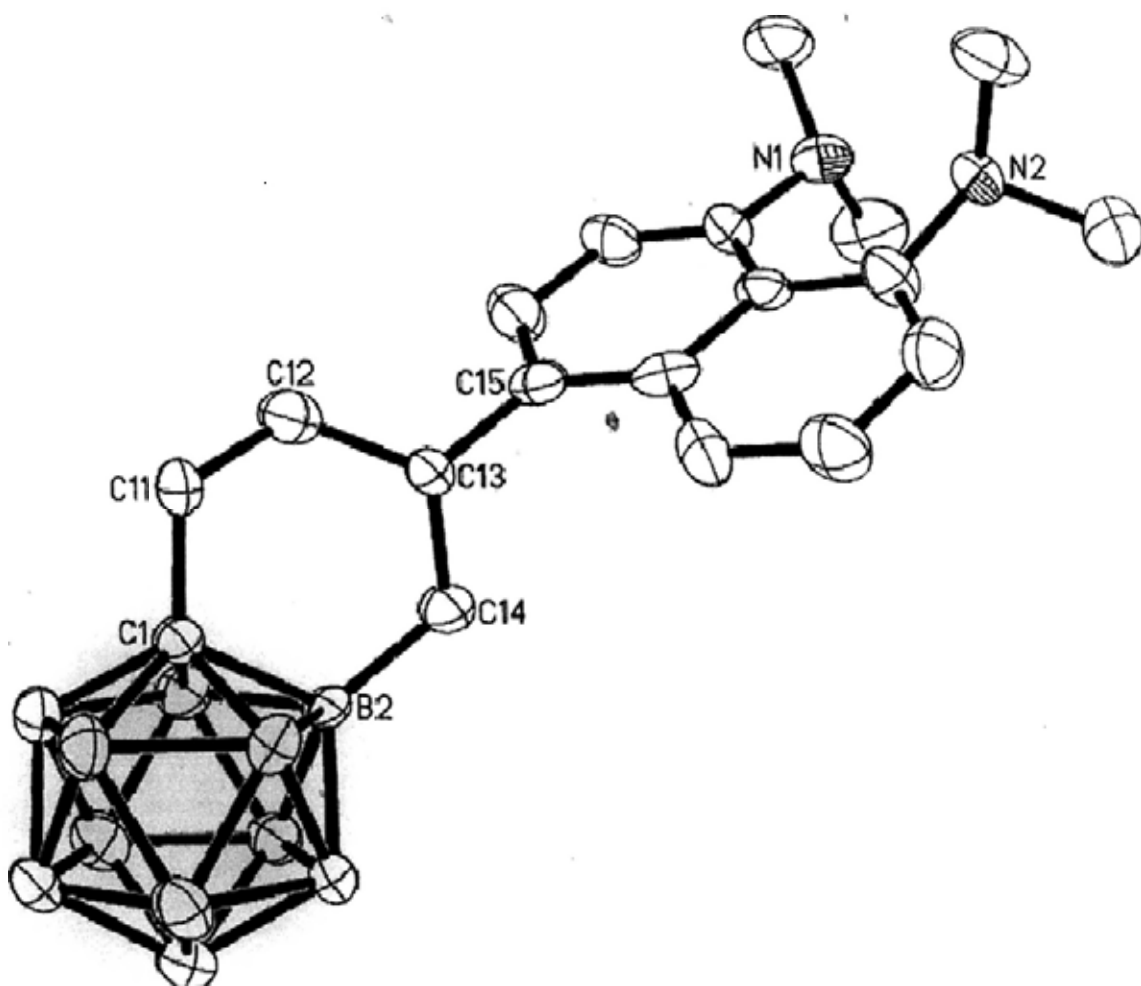
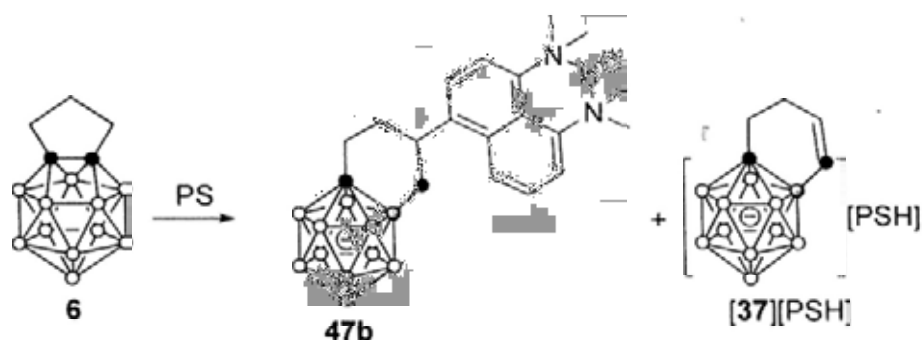


Figure 4.14. Molecular structure of μ -1,2-(CH₂)₂CH(4'-C₁₀H₅-1',8'-(NMe₂)₂H)CH₂-1-CB₁₁H₁₀ (**47b**).

Compounds **47b** and $[37][PSH]$ was characterized by several spectroscopic techniques as well as HRMS or elemental analyses. The solubility of **47b** is very low in *d*₆-acetone and other common polar organic solvents with low boiling point. Howev-

er, it is much more soluble in d_6 -DMSO thus facilitating the characterization. The ^{11}B NMR only shows one broad and sharp signal caused by overlap of the peaks. On the other hand, its ^1H NMR clearly shows 5 peaks with relative intensity of 1 for each in the aromatic region. Correspondingly, the ^{13}C and DEPT135 spectra indicated 5 CH and 3 tertiary carbon atoms in the aromatic region. The $\text{CH}_2\text{CH}_2\text{CHCH}_2$ linkage is determined by two-dimensional HSQC and COSY experiments. The ^1H NMR spectrum of [37][PSH] in d_6 -acetone was in accordance with that of [37][Me₃NH] and exhibiting a peak at 5.90 ppm with relative intensity of 2 in the alkene region and two peaks at 2.01 and 1.92 ppm indicative of the two CH_2 group. The two anisotropic CH unit can be distinguished from each other in a solution of CD_2Cl_2 , at 5.99 ppm for β -CH, and 5.93 ppm for α -CH. Their ^{13}C NMR spectra are also comparable. The structures of 47b and [37][PSH] were further confirmed by single-crystal X-ray analyses and shown in Figures 4.14 and 4.15.

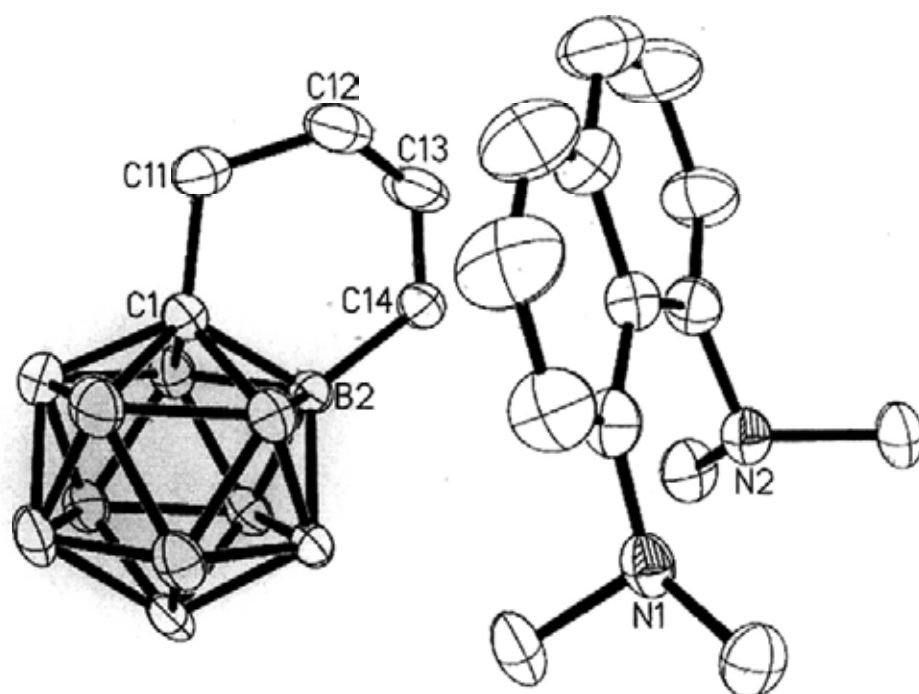
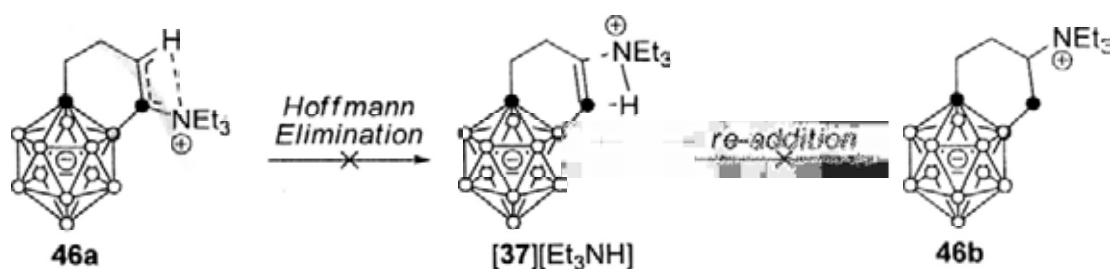


Figure 4.15. Molecular structure of $[\mu\text{-}1,2\text{-(CH}_2\text{)}_2\text{CH=CH-}1\text{-CB}_{11}\text{H}_{10}][\text{PSH}]$ ([37][PSH]).

Formation of the alkene product $[37]^-$ and the β -substituted product **46b** is very similar to the results of reactions of compound **6** with primary alcohol. It seems that the mixture was formed via a similar elimination/addition process from **46a** via the intermediate $[37]^-$. Considering the reaction media is basic but not acidic, a Hoffmann type elimination was proposed (Scheme 4.8).

Scheme 4.8. Proposed Mechanism for the Formation of $[37]^-$ and **46b**.



However, this mechanism was not supported by the following experiments. Compound **46a** was heated in refluxing acetone, or Et_3N or pyridine at $90\text{ }^\circ\text{C}$ for 48 h. In all cases no obvious changes were observed in the ^1H NMR. Under the same conditions, **46b** was also stable. We further heated the mixture of $[37][\text{Et}_3\text{NH}]$ and $[43][\text{Et}_3\text{NH}]$ in refluxing Et_3N , still no obvious formation of **46a** or **46b** was detected. Moreover, $[37][\text{PSH}]$ was heated at $90\text{ }^\circ\text{C}$ in THF either with or without the presence of 5 equiv PS giving no **47b** after 14 days. These results indicated that the formation of α -substituted, β -substituted and alkene products should be from different pathways and they are not interchangeable via elimination/isomerization process under the reaction conditions examined.

Formation of the $(\text{CH}_2)_4$ linked product $[43]^-$ is unexpected and the reason is not clear, but it might result from hydrogenation of $[37]^-$. Thermolysis of a mixture of $[36a][\text{Me}_3\text{NH}]$ and $[36b][\text{Me}_3\text{NH}]$ at $150\text{ }^\circ\text{C}$ for 24 h gave mainly $[43]^-$ as viewed from ^1H and ^{11}B NMR. But under the same condition, a mixture of $[36a][\text{Na}(18\text{-crown-6})]$ and $[36b][\text{Na}(18\text{-crown-6})]$ gave messy products. It would be expected

that [36a][H] and [36b][H] might be formed by thermal decomposition of the [Me₃NH]⁺ salts, but not the Na⁺ salts. Thus the formation of [43]⁻ from [37]⁻ would be possible.

4.5. Mechanistic Study of Carbon-Extrusion Reaction

The primary experimental results indicated that in the reactions of 13-vertex carborane μ -1,2-(CH₂)₃-1,2-C₂B₁₁H₁₁ (6) with several nucleophiles, one of the cage carbons is extruded to give monocarba-*closo*-dodecaborate anions in which the nucleophile is attached to the carbon atom or related species. This is significantly different from those of *o*-carboranes, in which the cage boron atoms are attacked by nucleophiles to give deboration products. Furthermore, cage carbon extrusion from carborane clusters is very rare although some examples are reported. A recent *closo*-to-*closo* example is the transformation of [1-H₂N-*closo*-CB₁₁F₁₁]⁻ to [3-NC-*closo*-B₁₁F₁₀]²⁻ via deprotonation, which is limited to highly fluorinated boron clusters.¹⁰⁷ Another one is the conversion of [7-R- μ -(9,10-HR'C)-7-*nido*-CB₁₀H₁₁]⁻ to [1-R-6-CH₂R'-1-*closo*-CB₉H₈]⁻, in which the cage carbon extrusion is suggested to proceed after removal of one BH vertex.¹⁰⁸ However, in both cases, although some viewpoints or mechanisms were prompted, no experimental evidences were given.

In our cases, most of the *closo*-CB₁₁⁻ products in the above reactions are the ones with nucleophiles bonding to the α -C to the cage B2 atom. Formally, it can be viewed both of the Nu group and one hydrogen atom attached to the cage boron adding to one of the cage carbons and pull it out of the cage. It gives a clue for the formation of the α -isomers but still cannot explain the formation of the β -isomers and the alkenyl product. Another problem is why the nucleophiles attack the cage carbon but not the boron which should be more electron-deficient than the former.

4.5.1. Reaction Intermediates

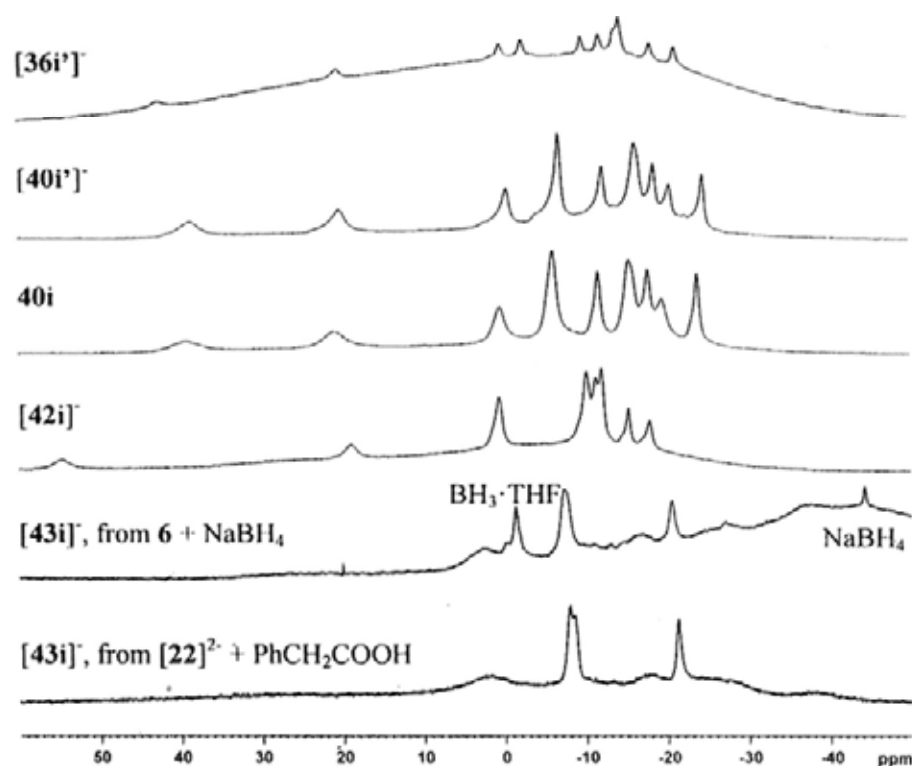


Figure 4.16. ^{11}B NMR spectra of observed and isolated intermediates.

With the above-mentioned questions in mind, we carefully monitored the reactions by ^{11}B NMR at room temperature. No detectable intermediate was observed in the reaction of compound **6** with PPh_3 , Et_3N or PS. The reaction with excess NaBH_4 in THF at room temperature gave, however, two sharp peaks at about -7 and -20 ppm together with some broad signals indicative of the formation of a possible intermediate $[\mathbf{43i}]^\bullet$ which increased gradually and reached its maximum amount usually in 20-24 h accompanying with the disappearance of complex **6**. These long-lived intermediate can survive in solution for a long time and slowly transfer to the final product $[\mathbf{43}]^\bullet$. A similar situation was observed in the reaction of **6** with $(4\text{-MeC}_6\text{H}_4)\text{SNa}$, but the reaction is much fast. The starting material disappeared within 10 min. At least two intermediates were observed at this stage: a short-lived one $[\mathbf{42i-1}]^\bullet$ with characteristic peaks at about 11, -28 and -38 ppm. These peaks almost disappeared

after 1 h. The other is a relatively stable intermediate **[42i]⁻** (Figure 4.16). Again, **[42i]⁻** disappeared within 2 d to give the final product. In the reaction with MeOH and EtOH, intermediates similar to **[42i-1]⁻** were detected with peaks at about -27 and -41 ppm in either case after 10 min besides a majority of the starting material. These peaks remained in relatively low intensities and finally disappeared until all the starting material was transferred to the CB₁₁⁻ anions. Intermediates similar to **[42i]⁻** were also detected, but the signals were even weaker. Under all circumstances mentioned above, we were not able to isolate the intermediates.

Finally, we found that the toluene solution of **6** and *ca* 10 equiv of Et₂NH showed within 10 min a species with distinct ¹¹B NMR spectrum from that of the product **40a** but similar to the observed **[42i]⁻**. This intermediate **40i** is stable up to 14 days at room temperature without obvious change. We thought it might be isolable. However, we repeated the experiment many times and every time only **40a** was isolated after workup. Since it was stable in solution, we intended to get structural information in solution. We reexamined this reaction: 8.5 equiv of Et₂NH was added to a 0.5 mL solution of 0.1 mmol of compound **19** in C₆D₆ in an NMR tube, and the solution was slowly warmed from 0 °C to rt with the formation of **40i** as evidenced by NMR spectra. It was characterized by ¹¹B, ¹H, ¹³C and various 2D NMR experiments. The ¹H-¹³C HSQC (Figure 4.17) and ¹H-¹H COSY experiments clearly illustrated the formation of a (CH₂)₃CH unit, suggesting that an H atom had migrated to one cage carbon. This CH group exhibited a characteristic signal at 1.87 ppm in the ¹H NMR spectrum and a peak at 12.7 ppm in the ¹³C NMR spectrum, which indicated that it is not attached to the N atom, thus the attack of the nucleophile should be after the migration of the H atom. An equimolar amount of Et₂N group was also seen in the ¹H spectrum with non-equivalent chemical shifts of the CH₂ and CH₃ units, showing it is attached

to the cage in an unsymmetric environment. The downfield signal at 39.8 ppm in the ^{11}B NMR indicated a low coordinated boron atom, which might be bound to the N atom. Reaction with $t\text{BuNH}_2$ also gave similar results, but the reaction is much faster. It was noted the formation of **39** made the NMR spectra more complex.

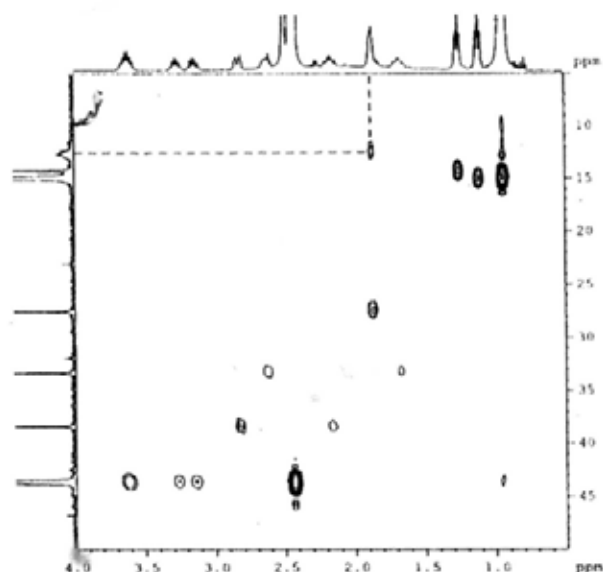
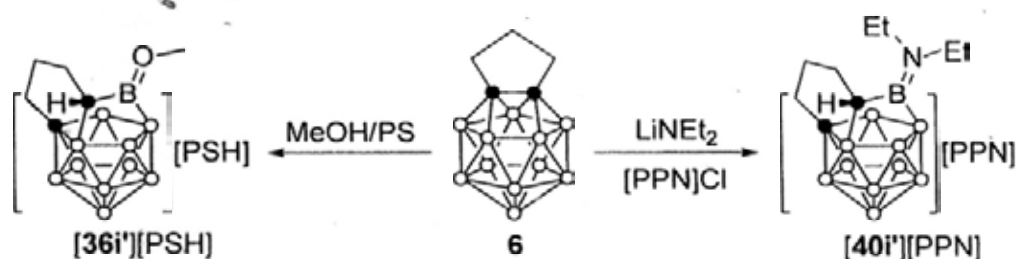


Figure 4.17. Two-dimensional ^1H - ^{13}C HSQC spectra of **40i**. The dashed lines indicate the correlation of the CH unit.

In order to structurally characterize the intermediate, several other attempts were tried. Finally, we found that treatment of **6** with one equiv of LiNEt_2 in THF afforded a species with a very similar ^{11}B NMR to that of **40i**. Cation exchange with 1 equiv of $[\text{PPN}]\text{Cl}$ gave, after recrystallization from CH_2Cl_2 , $[\mu\text{-}\eta\text{:}\eta\text{:}\eta\text{-}7,8,10\text{-}(\text{CH}_2)_3\text{CHB}(\text{NEt}_2)\text{-}7\text{-CB}_{10}\text{H}_{10}][\text{PPN}]$ (**[40i']** $[\text{PPN}]$) in 90% isolated yield. On the other hand, addition of compound **6** with 5 equiv of PS in MeOH also gave $[\mu\text{-}\eta\text{:}\eta\text{:}\eta\text{-}7,8,10\text{-}(\text{CH}_2)_3\text{CHB}(\text{OMe})\text{-}7\text{-CB}_{10}\text{H}_{10}][\text{PSH}]$ (**[36i']** $[\text{PSH}]$) as a white precipitate in 95% yield (Scheme 4.9). Product with the same anion cannot be prepared by reaction of **6** with NaOMe in THF, in which only the deprotonation product **[44] $^-$** was afforded, as viewed from the ^{11}B NMR spectrum.

Scheme 4.9. Reaction of **6** with Bases.



Compound $[\mathbf{40i}']][\text{PPN}]$ and $[\mathbf{36i}']][\text{PSH}]$ were characterized by several spectroscopic techniques as well as elemental analyses. The ^{11}B NMR spectra of $[\mathbf{40i}']][\text{PPN}]$ was almost the same as that observed for **40i**. Complex $[\mathbf{36i}']][\text{PSH}]$ also had a similar ^{11}B NMR spectra although with some differences. The specific boron atoms, which were adjacent to the heteroatoms, were observed at low field at 42.5 ppm for $[\mathbf{36i}']]$ and 38.8 ppm for $[\mathbf{40i}']]$. The ^1H and ^{13}C as well as various two-dimensional NMR spectra were well consistent with formation of $(\text{CH}_2)_3\text{CH}$, indicative of the H-transfer process.

The structures of compounds $[\mathbf{36i}']][\text{PSH}]$ and $[\mathbf{40i}']][\text{PPN}]$ were determined by single-crystal X-ray analyses and are shown in Figures 4.18 and 4.19. Anion $[\mathbf{36i}']]$ is composed by a *nido*- CB_{10} cage and a $(\text{CH}_2)_3\text{CHB}(\text{OMe})$ linkage, which is seated above the five-membered face of the CB_{10} part, bridging two of the boron atoms by CHB unit, and terminal bonding to the cage carbon by the trimethylene linkage. The sum of the C14-B12-O, O-B12-B10, B10-B12-C14 angles is $357.8(3)^\circ$ indicated that these atoms are almost coplanar and the B12 atoms can be regarded as three coordinated and sp^2 -hybridized. The B-O bond length of $1.377(5)\text{ \AA}$, falls in the range of 1.43 to 1.33 \AA , which is regarded to have double bond character.¹⁰⁹

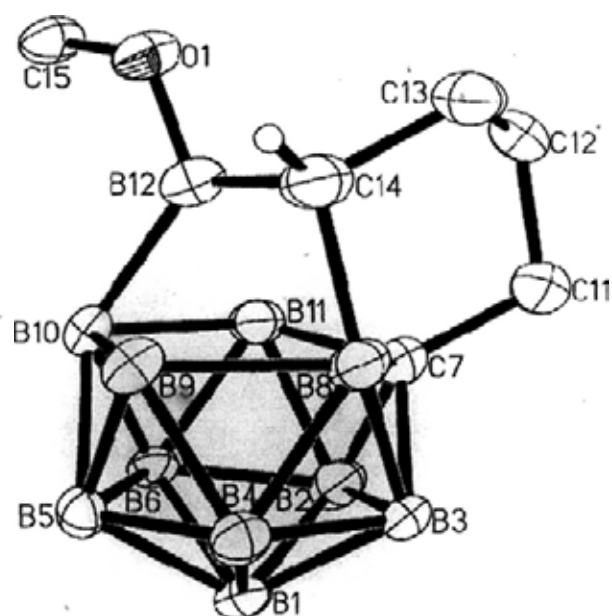


Figure 4.18. Structure of $[\mu\text{-}\eta:\eta:\eta\text{-}7,8,10\text{-(CH}_2\text{)}_3\text{CHB(OMe)-}7\text{-CB}_{10}\text{H}_{10}]^+$ (**[36i']**), in **[36i']**[PSH].

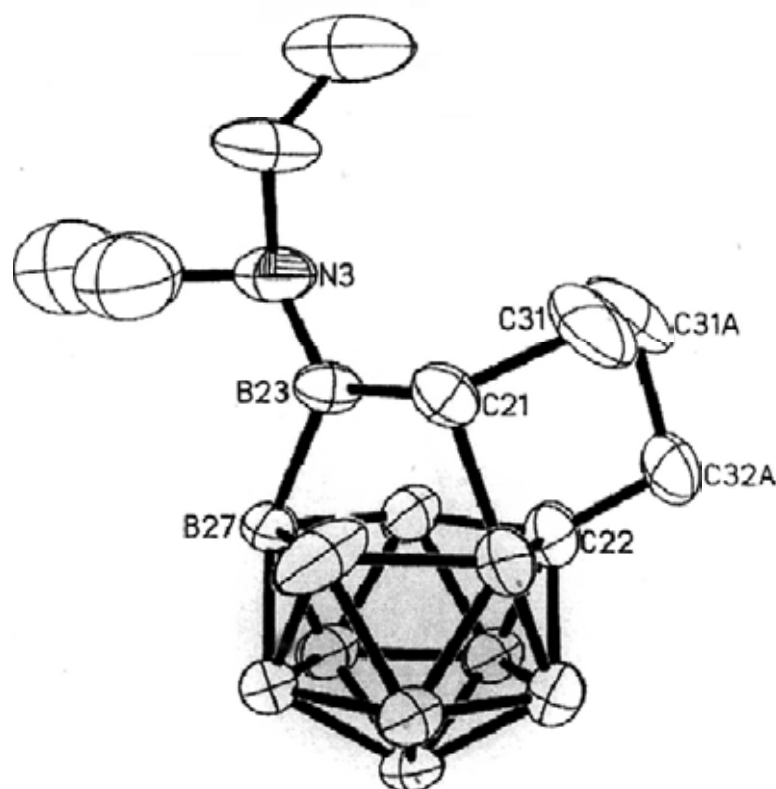


Figure 4.19. Structure of $[\mu\text{-}\eta:\eta:\eta\text{-}7,8,10\text{-(CH}_2\text{)}_3\text{CHB(NEt}_2\text{)-}7\text{-CB}_{10}\text{H}_{10}]^+$ (**[40i']**), in **[40i']**[PPN], showing one of the two crystallographic independent molecules.

There were two crystallographic independent molecules in the unit cell of **[40i']**[PPN], which also suffered from disordered problems. However, a similar

structure of the anion to that of $[36i']^-$ can be depicted. The average corresponding sum of bond angles around the boron atom of $359.8(8)^\circ$ and B-N bond lengths of $1.414(11) \text{ \AA}$, also support the sp^2 -hybridization of boron atom that was attached to the nitrogen atom and a B=N double bond character.¹¹⁰

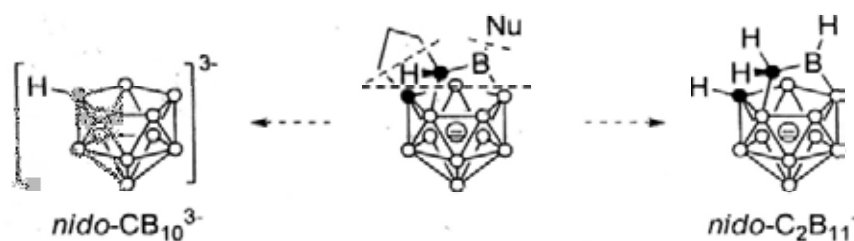


Figure 4.20. Two ways to describe the structure of the anion.



Figure 4.21. Compensation of electron-deficiency in classic boranes.

On the other hand, ambiguities exist in describing the structure of the cage, especially the bonding interaction around the boron atom bonded to the Nu group. Although the anion can be viewed as a derivative of an 11-vertex $nido-CB_{10}^{3-}$, it is also a type of 13-vertex $nido$ -carborane anion (Figure 4.20). In a classic borane compound, the three coordinate boron atom contains $6e^-$ in the valence orbitals. This electron-deficiency is usually compensated by electron donation from lone pair electrons of the adjacent heteroatom, or by forming 3c-2e bond (Figure 4.21). In this regard, both types of interaction would exist in the 13-vertex $nido$ -carborane $[\mu-\eta:\eta:\eta-7,8,10-(CH_2)_3CHB(NEt_2)-7-CB_{10}H_{10}]^-$, the relative strength of which is dependent upon the electron-donating ability of the heteroatom. In $[36i']^-$ and $[40i']^-$, the exact boron atom would tend to have a weak multicenter bonding interaction as a result of

strong π -interaction with the MeO or Et₂N group. B=S double bond would also exist in $[\mu-\eta:\eta:\eta-7,8,10-(\text{CH}_2)_3\text{CHB}(\text{S}(4\text{-MeC}_6\text{H}_4))-7\text{-CB}_{10}\text{H}_{10}]^-$ (**[42i]**), as a result of electron donation from one of the lone pair electrons on the sulfur atom.¹¹¹ However, no such interaction would be for the possible structure of **[43i]** ($[\mu-\eta:\eta:\eta-7,8,10-(\text{CH}_2)_3\text{CHBH}-7\text{-CB}_{10}\text{H}_{10}]^-$), and multicenter bond would be expected among the whole cage (Figure 4.22).

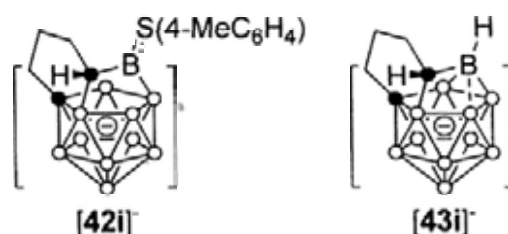


Figure 4.22. Possible structures of intermediate **[42i]** and **[43i]**.

4.5.2. Formation of the Intermediates

Formation of the intermediate $[\mu-\eta:\eta:\eta-7,8,10-(\text{CH}_2)_3\text{CHB}(\text{Nu})-7\text{-CB}_{10}\text{H}_{10}]^-$ indicated that attack of nucleophile on one of the cage borons and H-transfer from BH to cage carbon. It is well documented in literature, that neutral or anionic nucleophiles can attack cage boron atom of a *closo*-carborane or subicosahedral carborane, leading to cage opening and formation of zwitterionic or anionic *nido*-carborane species, after donation of $2e^-$ to the cage.^{2b,c,2f} The external Nu group is terminal bounded to the cage boron while the original terminal H atom is maintained, or changed to a bridging one, depending on the structure of the product. Two types of geometry are shown in Figure 4.23, taking a 5-membered open face for example. One is bridged structure, in which the HB(Nu) group is seated on an open face, while the other is a flattened structure in which the B(Nu) unit is a part of the open face. However, the definition of terminal and bridging is somehow ambiguous for these types of H atoms, which would be better described as non-*exo* ones, corresponding to the *exo*-

ones which point to the center of the cage along the B-H bond.

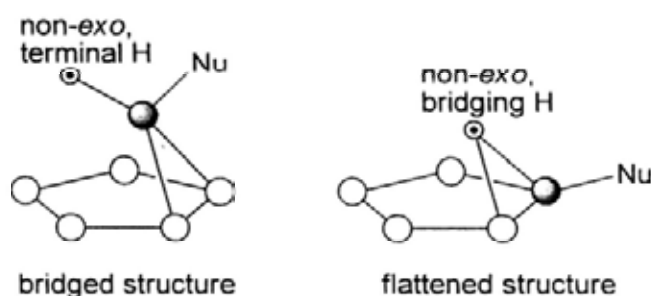


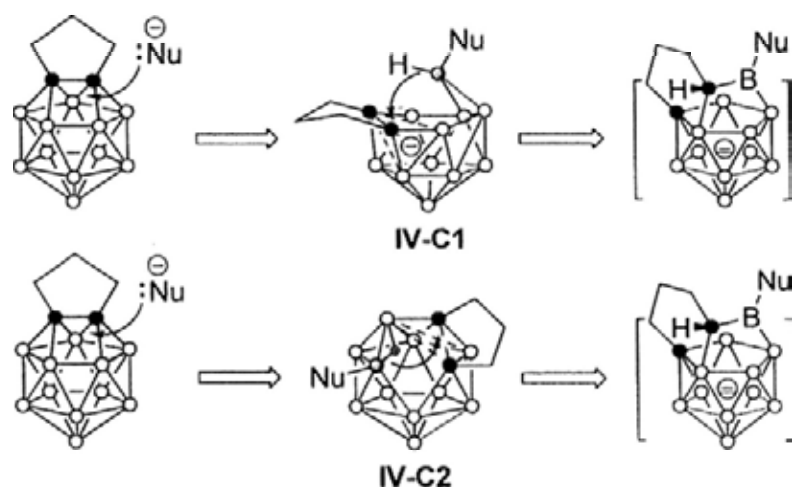
Figure 4.23. Two possible types of structures of *nido*- species that form from nucleophilic reaction of an icosahedral or subicosahedral carborane.

On the other hand, the transfer of non-*exo* (bridging) H atom to the cage carbon has been well established in the CAd 12-vertex *nido*-carborane monoanions, which is defined as kinetic to thermodynamic isomerization upon protonation of the corresponding *nido*-carborane dianions.⁴² That is isomerization from [7-R-9-R'-7,9-C₂B₁₀H₁₀H]⁻ to [7-R- μ -9,10-CR'H-7-CB₁₀H₁₀]⁻.¹¹² Although formation of the corresponding thermodynamic CAd *nido*- species only involves the cage rearrangement which still has a bridging hydrogen atom,^{45a,45c} the corresponding *arachno*- monoanion does undergo the H-transfer process.^{45c} While these are often described as "isomerization", the "H-migration" process is overlooked, to our knowledge. Despite of it, it offers a clue to reasonably assume the subsequent H-transfer in the formation of the [μ - η : η : η -7,8,10-(CH₂)₃CHB(Nu)-7-CB₁₀H₁₀]⁻ intermediate.

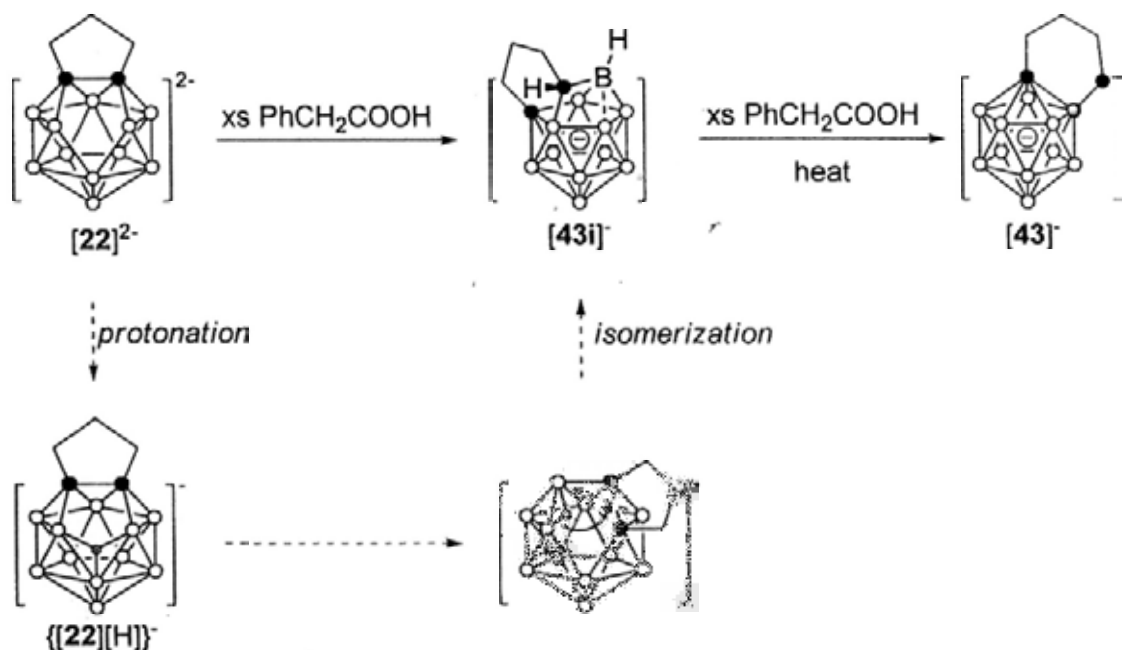
Two types of possible pathways are shown in Scheme 4.10, based on two possible "kinetic" structures of the nucleophilic adduct of 13-vertex carborane 6. Nucleophilic attack at the 7-coordinate cage boron atom gives a bridged intermediate **IV-C1**, which bears a 6-membered face, or a flattened one **IV-C2** that contains a 5-membered open face. Subsequent B-H addition to one of the cage carbons followed by several cage bonds cleavage and formation process give the [μ - η : η : η -7,8,10-

$(\text{CH}_2)_3\text{CHB}(\text{Nu})\text{-7-CB}_{10}\text{H}_{10}]^-$ intermediate. In either **IV-C1** or **IV-C2**, the cage carbon, to which the H atom transferred, may be regarded as a “carbenoid” as a result of a formal B-H insertion.

Scheme 4.10. Possible Pathways for the Formation of $[\mu\text{-}\eta\text{:}\eta\text{:}\eta\text{-7,8,10-}(\text{CH}_2)_3\text{CHB}(\text{Nu})\text{-7-CB}_{10}\text{H}_{10}]^-$ Intermediate.



Scheme 4.11. Protonation of $[1,2\text{-(CH}_2)_2\text{-1,2-C}_2\text{B}_{11}\text{H}_{11}]^{2-}$.



With the mechanism proposed above, we wondered whether protonation of the corresponding 13-vertex *nido*-carborane dianion $[1,2\text{-(CH}_2)_2\text{-1,2-C}_2\text{B}_{11}\text{H}_{11}]^{2-}$ (**[22]²⁻**) can give the similar “thermodynamic” product $[\mu\text{-}\eta\text{:}\eta\text{:}\eta\text{-7,8,10-}(\text{CH}_2)_3\text{CHBH-7-}$

$\text{CB}_{10}\text{H}_{10}]^-$ (**[43i]**). Treatment of **[22]** $[\text{Na}_2(\text{THF})_4]$ with excess PhCH_2COOH in THF gave **[43i]** at once (Figure 4.16), as evidenced by ^{11}B NMR spectrum (Scheme 4.11), which was partially converted to $[\mu\text{-}1,2\text{-(CH}_2\text{)}_4\text{-}1\text{-CB}_{11}\text{H}_{10}]^-$ (**[43]**) upon heating at 70°C . It indicates that structure **IV-C2**, which bears a five membered face as that of **[22]** $^{2-}$, might be preferred for the first-step intermediate. It is also supported by the structure of $3\text{-NEt}_2\text{H-}\mu\text{-}1,7\text{-(CH}_2\text{)}_4\text{-}1,7\text{-C}_2\text{B}_{11}\text{H}_{11}$ (**67**) (Chapter 6).

4.5.3. Formation of the α -isomer

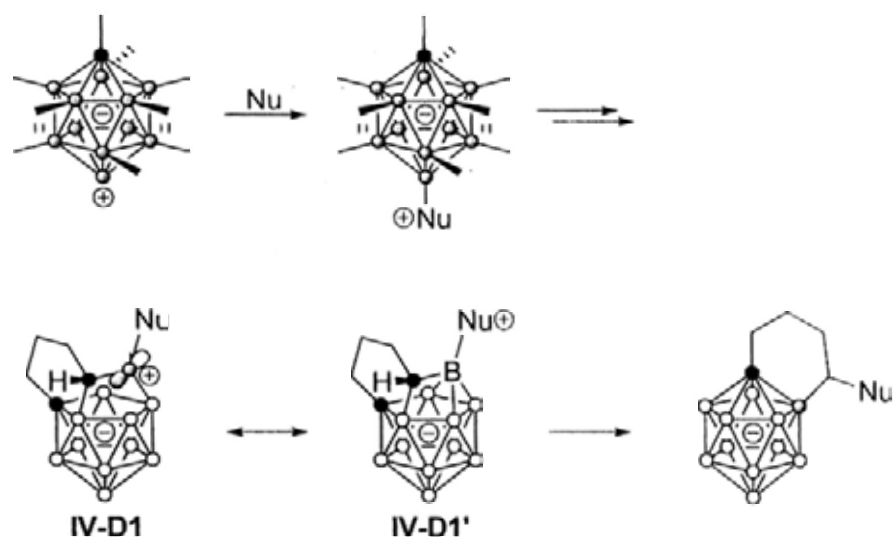
The structurally characterized two intermediate analogues were quite stable in CD_2Cl_2 solutions without any change for several weeks at room temperature. The **[40i']** $[\text{PPN}]$ was even resistance to heating at 70°C in THF for several days. However, protonation of these two anions by strong acid afforded the corresponding CB_{11}^- species immediately. Treatment of a CH_2Cl_2 solution of **[40i']** Li , which was directly prepared from **6** and equimolar amount of LiNEt_2 , with conc. HCl from 0°C to rt gave **40a** in 80% isolated yield after recrystallization. In a similar manner, to a CD_2Cl_2 solution of **[36i']** $[\text{PSH}]$ was added excess conc. HCl and a mixture of **[36a]** and **[36b]** was observed in the ^1H NMR (Scheme 4.12). Protonation would occur at the more basic site—the heteroatom N or O, leading to the possible formation of the reactive boron cation intermediate, which quickly isomerizes to the final product with substituent at the $\alpha\text{-C}$ position. In this regard, the observed long-lived intermediate **40i** in the reaction of **6** with Et_2NH would not be a real boron cation $\mu\text{-}\eta\text{:}\eta\text{:}\eta\text{-}7,8,10\text{-(CH}_2\text{)}_3\text{CHB(NEt}_2\text{H)-}7\text{-CB}_{10}\text{H}_{10}$ as it would not survive in solution but quickly convert to **40a** upon formation. It may be more likely $[\mu\text{-}\eta\text{:}\eta\text{:}\eta\text{-}7,8,10\text{-(CH}_2\text{)}_3\text{CHB(NEt}_2\text{)-}7\text{-CB}_{10}\text{H}_{10}][\text{H(NEt}_2\text{H)}_x]$ (**[40i']** $[\text{H(NEt}_2\text{H)}_x]$). This is also in accordance with the basicity of $\text{X}_2\text{B=NEt}_2$ and Et_2NH , the former is much weaker base due to the donation of the lone pair electrons to the empty p -orbital of the sp^2 -boron

ported, despite of more developed chemistry of classic boron cation.¹¹³ The 2:1 Nu adducts of *o*-carboranes, such as 10-BH(py)₂-7-Br-7,8-C₂B₉H₁₀ and 10-BH(NHC)₂-7-Br-7,8-C₂B₉H₁₀ (NHC = N-heterocarbene), which are deboration intermediate models, are almost the only examples of structurally characterized species.⁴¹ CB₁₁Me₁₁ Boronium ylide was reported by Michl group as an active intermediate.¹¹⁴ An analogy between the structure and reactivity of the boronium ylide and those of intermediate **IV-D1** is shown in Scheme 4.14. The boronium ylide has a naked boron vertex, in which the vacant *exo*- radial orbital can be arrested by nucleophile to compensate the charge. On the other hand, the boron cation intermediate **IV-D1**, classically as a borenium ion, is not electronically stabilized. Although its one *exo*- *sp*² orbital is filled by accepting a pair of electrons that is donated by the Nu group, the remaining empty *p* orbital is still vacant, thus multi-center bond would be formed with other cage boron atoms, in another resonance structure **IV-D1'**. It would be expected that this electron-deficiency at the boron center, would be one of the important factors governing the cage closure process. Saturation of the CH group, after the cleavage of C-B bond, would also be reformed by accepting the electrons from the Nu group.

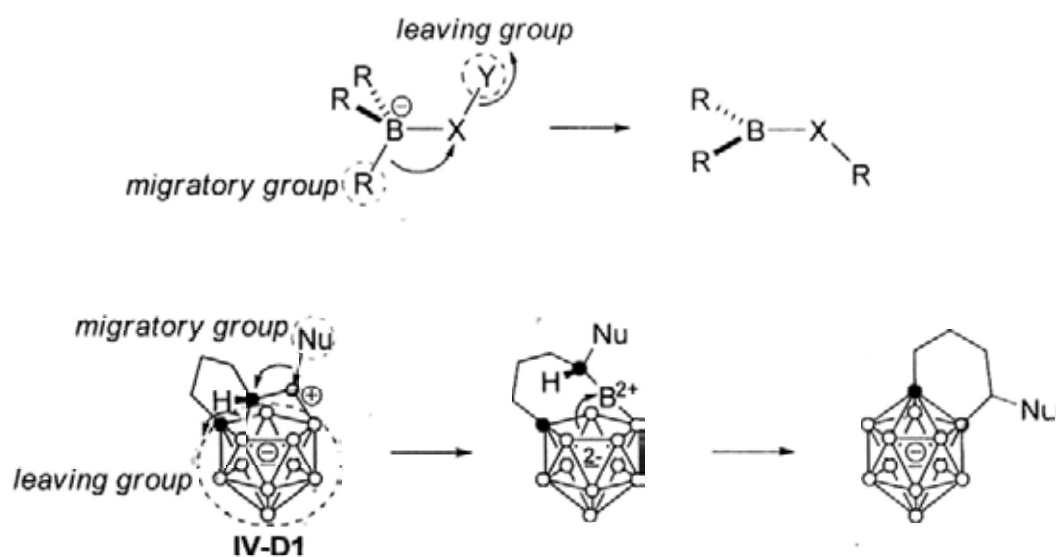
This boron cation mediated migration pathway would also be paralleled with reaction of organoborane. 1,2-Migration reactions dominate much of the reactivity of organoborates (Scheme 4.15).¹¹⁵ The tetrahedral borate species is formed by nucleophilic attack of XY on the empty *p* orbital on the boron atom of organoboranes. If Y is a leaving group, the 1,2-migration occurs very easily. And the product is usually stabilized as forming B=X double bond. In a similar manner, in the proposed 1,2-migration of intermediate **IV-D1**, the *nido*-CB₁₀ carborane cage can serve as the leaving group, which formally bears a dicationic boron center and a dianionic cage. Attack of the electron rich cage to the electron deficient boron atom gives the prod-

uct. It is noted that this step-by-step pathway is only to describe the *nido*-CB₁₀ cage as a leaving group but would not be the real process.

Scheme 4.14. Analogy between Boronium Ylide and Intermediate **IV-D1**.



Scheme 4.15. Analogy between Organicborate and Intermediate **IV-D1**.



In either analogy, the migratory ability of the Nu group and electron deficiency of the formal three coordinate boron is crucial to reconstruct a *closo*-cage. It would be the same in the reaction of compound **6** with anionic nucleophiles, despite of the organoborane property of the intermediate as shown in Scheme 4.13. We noted, that both intermediates [36i']⁻ and [40i']⁻ were very stable in solution for a long time

without any formation of the CB_{11}^- anions. Considering the electronic structure of these two species discussed earlier, formation of the B=O or B=N double bond, which is short and strong than a corresponding single bond, would inhibit the bond broken and migration process. Meanwhile, as the boron center is no longer electron deficient, forming multicenter bond with other atoms on the cage is also not possible, which means that attack of electrons on the anionic carborane cage to that boron atom is also prohibited. Thus, both factors would make the 1,2-migration hard to occur.

On the other hand, intermediate $[\mu-\eta:\eta:\eta-7,8,10-(\text{CH}_2)_3\text{CHB}(\text{S}(4\text{-MeC}_6\text{H}_4))\text{-7-CB}_{10}\text{H}_{10}]^-$ (**[42i]**), which would be expected to have a similar structure as that of **[36i']** or **[40i']**, was not stable in solution and isomerized to CB_{11}^- anion **[42]**. In order to exclude the possibility that the migration was from a boron cation center which was catalyzed by trace amount of acid $(4\text{-MeC}_6\text{H}_4)\text{SH}$ in the $(4\text{-MeC}_6\text{H}_4)\text{SNa}$, the reagent was treated with excess NaH in a suspension of THF, then the saturated solution of $(4\text{-MeC}_6\text{H}_4)\text{SNa}$ in THF was added to excess $\mu\text{-1,2-(CH}_2)_3\text{-1,2-C}_2\text{B}_{11}\text{H}_{11}$ (**6**). In this circumstance, formation of intermediate **[42i]** and subsequent migration were still observed as usual. Therefore it is suggested that the migration took place from a borane center but not a boron cation. In this regard, the possible B=S double bond in **[42i]**, would not as strong as a B=N or B=O double bond. Although it seems probable that the strengths of the B-O and B-S π bonds are very similar in $\text{R}_2\text{B-E'R}$ ($\text{E}' = \text{O, S}$) compounds,¹¹¹ the overall bond strength would be much weaker for the heavier sulfur atom.¹¹⁶ The soft base nature of the sulfur atom makes the thiolate both a good leaving group and a nucleophilic reagent. These might account for the instability of **[42i]** and its easiness to convert to **[42]**. Thus, the migratory ability of a nucleophile in the intermediate **IV-D** would be neutral Nu (MeOH, Et₂NH, etc.) >

soft anionic Nu (SR^-) > hard anionic Nu ($\text{H}^- \gg \text{NEt}_2^-, \text{OMe}^-$).

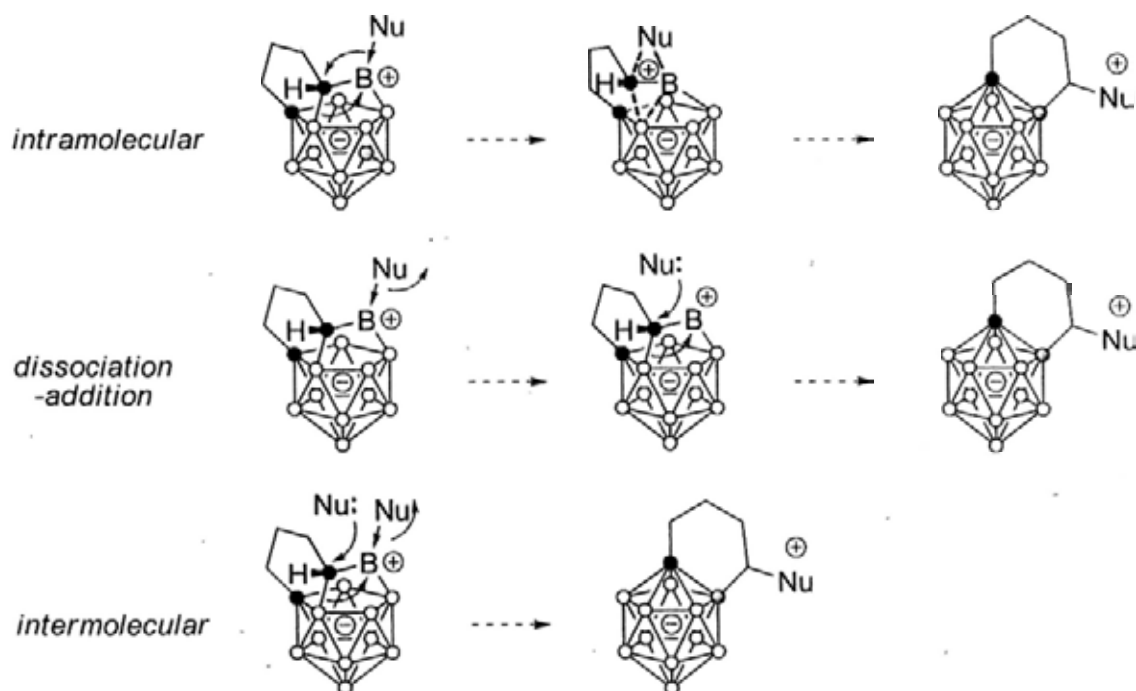
This sequence is different from that of nucleophilicity, the latter of which would determine the easiness for the attack of Nu to the cage boron and be reflected on the rate of intermediate formation. For those reactions with MeOH, EtOH, PPh_3 , NEt_3 and PS, in which trace amount or no intermediate was detected, subsequent reactions took place very quickly and happened as soon as the intermediate was formed, thus the rate-determining step(s) should be the formation of the intermediate. In the reactions with anionic compounds NaBH_4 , $(4\text{-MeC}_6\text{H}_4)\text{SNa}$, MeOH/PS, or Et_2NLi , migration is much slower than the intermediate formation, especially for the latter two cases, the anionic intermediates are even stable. In the reactions with Et_2NH or $t\text{-BuNH}_2$, both steps are quick in each case. Given to the observed reaction rates, the nucleophilicity toward 13-vertex carboranes is suggested as follows: Et_2N^- , MeO^- (MeOH/PS), $t\text{-BuNH}_2$, $\text{Et}_2\text{NH} > (4\text{-MeC}_6\text{H}_4)\text{S}^- > \text{BH}_4^- > \text{PPh}_3 > \text{MeOH}$, $\text{EtOH} > \text{NEt}_3 > \text{PS}$. The anionic nucleophiles are generally more reactive than the neutral species. It is noted that compound **6** reacts quickly with MeOH and EtOH if they are used as solvent, but no reaction is observed in C_6D_6 .

Lastly, this proposed migration/cage closure mechanism can proceed via three possible manners, at least: 1) intramolecular pathway, in which the migration and cage closure take place simultaneously; 2) dissociation-addition pathway, in which the Nu dissociates from the cationic boron center, then attacks the $\alpha\text{-C}$; 3) intermolecular process, in which another Nu attacks the $\alpha\text{-C}$ concurrently with the Nu elimination from boron cation, as shown in Scheme 4.16.

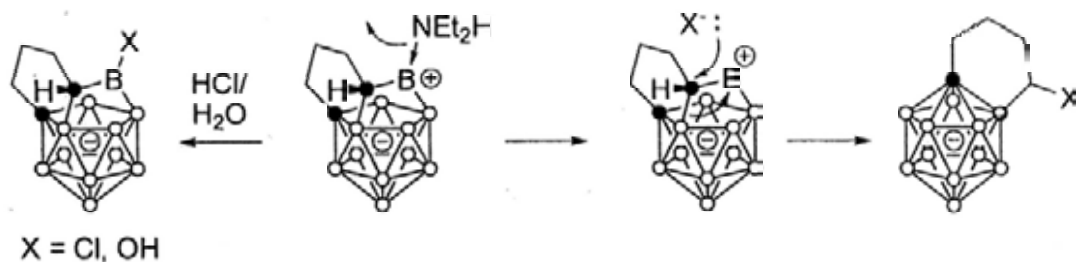
The dissociation-addition pathway seems unlikely to happen in the formation of **40a** from Et_2NLi followed by protonation of $[\mathbf{40i}']$ with HCl. Otherwise, the free Et_2NH , dissociated from the boron cation, would be further protonated by the large

excess amount of HCl, to afford $[\text{Et}_2\text{NH}_2]\text{Cl}$ and other possible boron-containing products (Scheme 4.17). They are not detected by ^1H and ^{11}B NMR spectra. Also, formation of a naked boron cation without stabilization is energetically highly unfavorable. In the same case, intermolecular process is also infeasible as there is no excess Et_2NH in solution. We also monitored the reaction of **6** with insufficient amount (less than 0.1 equiv) of $(4\text{-MeC}_6\text{H}_4)\text{SNa}$, the transformation from intermediate $[\mathbf{42i}]^-$ to $[\mathbf{42}]^-$ took place as usual, which also diminishes the possibility of the intermolecular pathway. Hence the intramolecular pathway is reasonable.

Scheme 4.16. Possible Pathways for the Nucleophile Migration.



Scheme 4.17. Possible Products Formation via Dissociation-Addition Pathway.

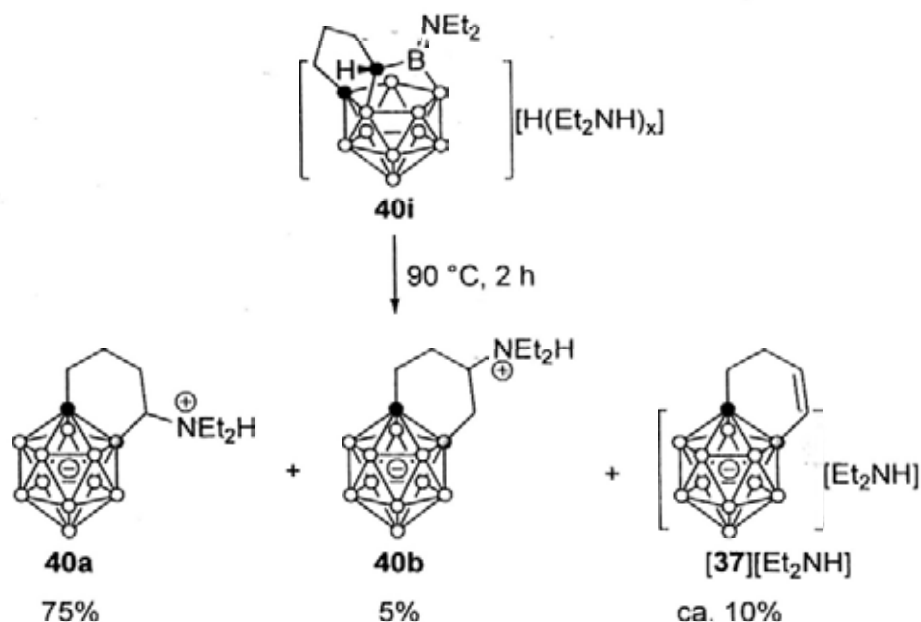


4.5.4. Formation of the β -isomer and alkenyl CB_{11}^- anions

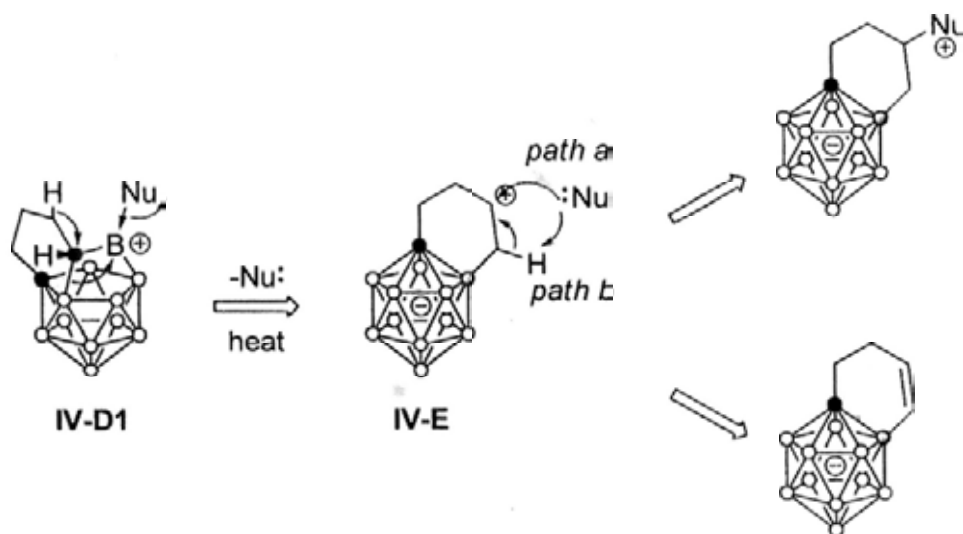
On the other hand, the formation of the β -substituted and the alkenyl CB_{11}^- anions is still not clear. As the α - CH_2 group to the cage carbon in the 13-vertex carboranes can be deprotonated under basic conditions, which is the β -position to the B2 atom in the CB_{11}^- , we initially thought that the $[\mu\text{-}1,2\text{-(CH}_2\text{)}_2\text{CH-}1,2\text{-C}_2\text{B}_{11}\text{H}_{11}]^-$ (**[44]**) might be the source of the two kinds of products. But when a freshly prepared **[22]**[Na] was heated in Et_3N or THF with 5 equiv of PS under the same conditions, no desired products after quenching the reaction by 1M HCl were detected from ^1H NMR spectrum in the mixture. Such an assumption should be incorrect.

We then turned our attention back to the boron cation intermediate **IV-D1** and thought why it would not act as the intermediate. We found that the reaction of **6** with Et_2NH in C_6D_6 was exoergic when it was repeated at room temperature, and besides those for **40a**, peaks at about 6 ppm in the ^1H NMR spectrum were observed indicative of the formation of alkene product **[37]**. We then freshly prepared the solution of **40i** in C_6D_6 at 0 °C and heated this solution at 90 °C for 2h. Two phases appeared and the ^{11}B NMR spectrum exhibited only one sharp and broad signal at about -11 ppm, indicative of the disappearance of **40i**. After removal of C_6D_6 and Et_2NH , d_6 -acetone was added. This time, the ^1H and ^{13}C NMR spectra clearly showed the formation of **[37]** and $\mu\text{-}1,2\text{-(CH}_2\text{)}_2\text{CH(NEt}_2\text{H)CH}_2\text{-}1\text{-CB}_{11}\text{H}_{10}$ (**40b**) with **40a** as a major product. The preparative experiment was performed under a similar condition in toluene from 1 mmol of **6**. After column chromatographic separation and recrystallization, **40a** was afforded in 75% isolated yield and **40b** was in 5% yield (Scheme 4.18). **[37]**[Et_2NH_2] was not isolated from the column as it is an ionic salt.

Scheme 4.18. Thermolysis of **40i**.



Scheme 4.19. Proposed Mechanism for the Formation of β -Substituted and Alkenyl CB_{11}^- Anions.



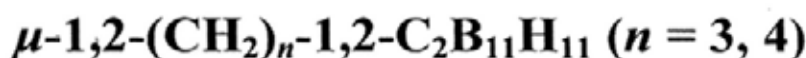
4.5. Summary

The 13-vertex carborane $\mu\text{-1,2-(CH}_2\text{)}_3\text{-1,2-C}_2\text{B}_{11}\text{H}_{11}$ can react with several nucleophiles to give monocarba-*closo*-dodecaborate anions $[\mu\text{-1,2-(CH}_2\text{)}_3\text{CH(Nu)-1-CB}_{11}\text{H}_{10}]^-$, $[\mu\text{-1,2-(CH}_2\text{)}_2\text{CH(Nu)CH}_2\text{-1-CB}_{11}\text{H}_{10}]^-$, and $[\mu\text{-1,2-(CH}_2\text{)}_2\text{CH=CH-1-CB}_{11}\text{H}_{10}]^-$. Mechanistic study indicated the formation of the boron cation or borane intermediate $[\mu\text{-}\eta\text{:}\eta\text{:}\eta\text{-7,8,10-(CH}_2\text{)}_3\text{CHB(Nu)-7-CB}_{10}\text{H}_{10}]^-$. While intramolecular Nu-migration gives α -substituted product $[\mu\text{-1,2-(CH}_2\text{)}_3\text{CH(Nu)-1-CB}_{11}\text{H}_{10}]^-$, H-

migration would give β -substituted product $[\mu-1,2-(\text{CH}_2)_2\text{CH}(\text{Nu})\text{CH}_2-1-\text{CB}_{11}\text{H}_{10}]^-$, and alkenyl $[\mu-1,2-(\text{CH}_2)_2\text{CH}=\text{CH}-1-\text{CB}_{11}\text{H}_{10}]^-$. In the reactions of $\mu-1,2-(\text{CH}_2)_3-1,2-\text{C}_2\text{B}_{11}\text{H}_{11}$ with ROH (R = Me, Et), $[\mu-1,2-(\text{CH}_2)_2\text{CH}(\text{Nu})\text{CH}_2-1-\text{CB}_{11}\text{H}_{10}]^-$ and $[\mu-1,2-(\text{CH}_2)_2\text{CH}=\text{CH}-1-\text{CB}_{11}\text{H}_{10}]^-$ can also be obtained via acid catalyzed isomerization. The ratio of the products in these reactions is dependent on the nucleophiles and the reaction conditions.

The 13-vertex carborane $\mu-1,2-(\text{CH}_2)_n-1,2-\text{C}_2\text{B}_{11}\text{H}_{11}$ ($n = 3, 4$) can also be deprotonated by several bases in dry THF to afford anions $[\mu-1,2-(\text{CH}_2)_{n-1}\text{CH}-1,2-\text{C}_2\text{B}_{11}\text{H}_{11}]^-$. This indicated competition between the nucleophilic attack on the cage boron atom and on the α -CH of the cage carbon.

Chapter 5. Cage Boron Extrusion Reaction of CAd 13-Vertex Carboranes

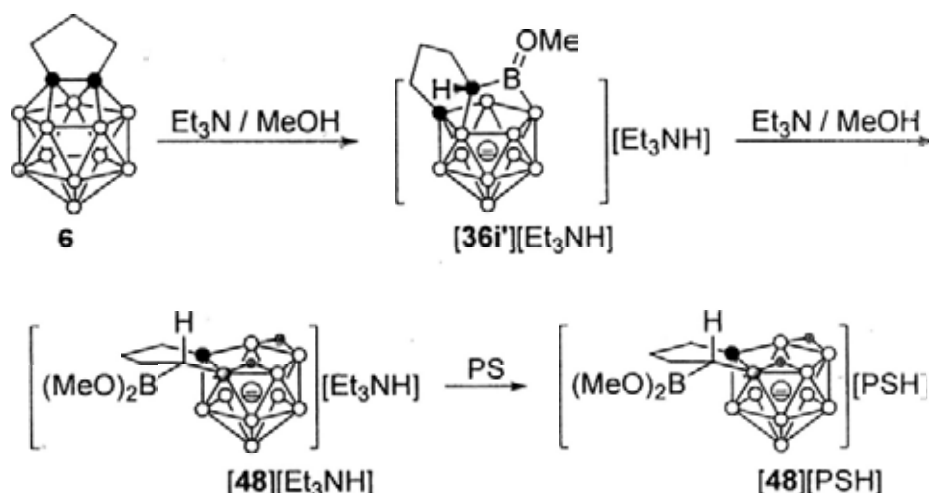


5.1. Reaction of 13-Vertex Carborane $\mu\text{-}1,2\text{-(CH}_2\text{)}_n\text{-}1,2\text{-C}_2\text{B}_{11}\text{H}_{11}$ ($n = 3, 4$) with Basic MeOH

As mentioned in Chapter 4, formation of messy products was observed in the initially attempted reaction of $\mu\text{-}1,2\text{-(CH}_2\text{)}_3\text{-}1,2\text{-C}_2\text{B}_{11}\text{H}_{11}$ (**6**) with hot MeOH in the presence of excess amount of NaOH. Later, several weaker bases were tried to control the reaction. When the reaction was performed in a closed vessel in the presence of Na_2CO_3 in a 10:1 MeOH/ H_2O solution after one day, the ^{11}B NMR spectra showed clearly one singlet and nine doublets, suggesting the formation of a single product. Similar results were also observed if K_2CO_3 or Et_3N was used instead. This pattern, which is distinct from those of *closo*- CB_{11}^- anions, was regarded to belong to *nido*-species as there are two characteristic peaks observed at about -30 and -34 ppm. This result led to an assumption that one boron vertex had been removed from the 13-vertex cluster. However, when the reaction mixture was treated in the open air, messy products were detected. Two new doublets at about -31 and -33 ppm were observed besides the original ones at -30 and -34 ppm in the ^1H coupled ^{11}B NMR spectrum. An 11-vertex *nido*- CB_{10}^- salt was isolated, after addition of $[\text{Me}_3\text{NH}]\text{Cl}$, from the above solution and structurally characterized as $[\mu\text{-}7,8\text{-(CH}_2\text{)}_3\text{CHOH-}7\text{-CB}_{10}\text{H}_{11}][\text{Me}_3\text{NH}]$. It was believed that this is the oxidative or hydrolysis product of the initially formed air-sensitive or hygroscopic species. Another experiment was performed to isolate such a compound.

The reaction of compound **6** in a dry MeOH suspension of Na₂CO₃ proceeded a little slower, which might be due to the low solubility of the solid base. Use of Et₃N gave a better result and also facilitated purification under inert atmosphere. In either case, the intermediate [μ - η : η : η -7,8,10-(CH₂)₃CHB(OMe)-7-CB₁₀H₁₀]⁻ (**[36i']**) was initially observed in the ¹¹B NMR spectra, and gradually turned to the desired product. Heating was not necessary but much better for a preparative reaction to guarantee the completion of the reaction within 24h. After removal of the volatile materials, the 11-vertex *nido*-CB₁₀⁻ salt [*endo*- μ -7,8-(CH₂)₃CHB(OMe)₂-7-CB₁₀H₁₁][Et₃NH] (**[48]**[Et₃NH]) was obtained as a sticky solid. In order to structurally characterize the product, cation exchange was performed by addition of excess amount of PS to give [*endo*- μ -7,8-(CH₂)₃CHB(OMe)₂-7-CB₁₀H₁₁][PSH] (**[48]**[PSH]) as a white solid in about 90% yield (Scheme 5.1). Recrystallization from THF gave the product as colorless crystals.

Scheme 5.1. Reaction of μ -1,2-(CH₂)₃-1,2-C₂B₁₁H₁₁ (**6**) with Et₃N/MeOH.



Complex **[48][PSH]** was characterized by several spectroscopic techniques as well as elemental analyses. Its ¹¹B NMR spectrum clearly exhibited a broad signal at about 32 ppm indicative of the RB(OMe)₂ unit, a singlet at about -2.1 ppm assignable to the boron atom attached to the *exo*-alkyl group, and 9 doublets. The broad signal

of α -C that attached to the cage boron atom was observed at about 11.4 ppm in the ^{13}C NMR spectrum. The corresponding signal of α -CH was observed at about 0.5 ppm in the ^1H NMR spectrum, together with a broad signal at about -3.2 ppm with a relative intensity of 2 indicating two bridging H atoms on the 5-membered open face of the *nido*- anion. These spectroscopic data of *nido*- CB_{10}^- anions are summarized in Table 5.1.

The structure of [48][PSH] was confirmed by single-crystal X-ray analyses and shown in Figure 5.1. The cage geometry of the anion is very similar to those of the known *nido*- CB_{10}^- anions.¹¹⁷ The *exo*-6-membered ring is in a pseudo half-chair conformation like a cyclohexene. A planar $(\text{OMe})_2\text{B}$ group is attached to the C14 atom at the *e*-position, which is directly attached to the cage B8 atom. As this boryl group and the cage are on the same side of the 6-membered plain, an “*endo*” configuration is assigned. The corresponding bond distances are listed in Table 5.2.

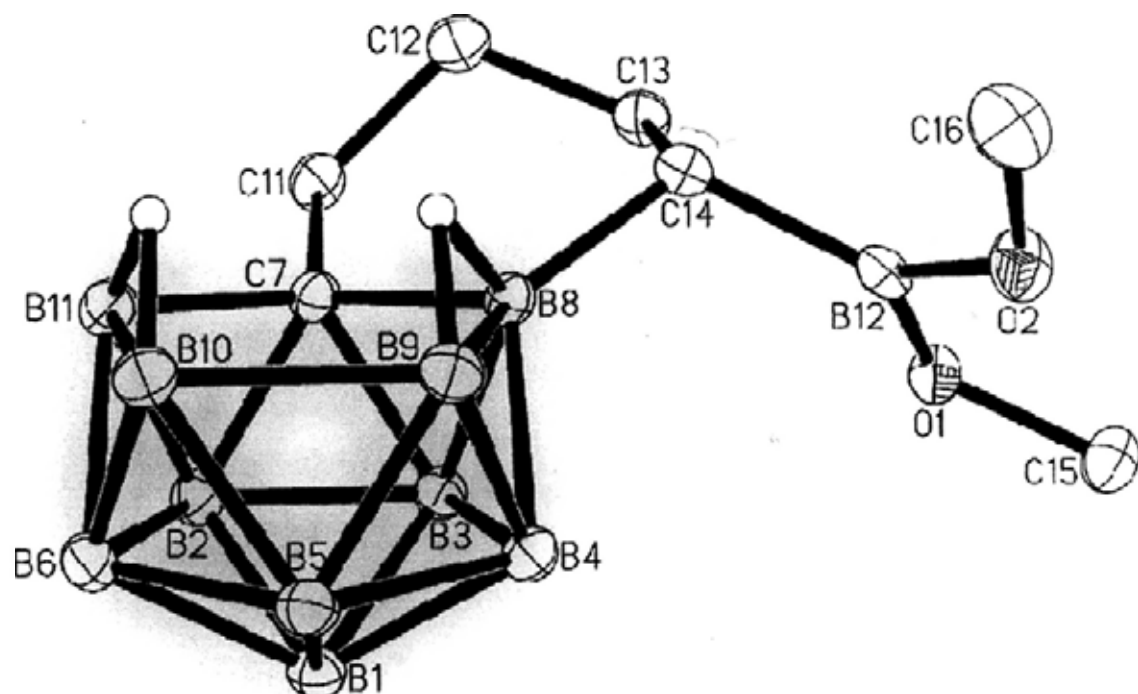


Figure 5.1. Structure of [*endo*- μ -7,8-(CH_2)₃CHB(OMe)₂-7-*nido*- $\text{CB}_{10}\text{H}_{11}$]⁻ ([48]⁻), in [48][PSH].

Table 5.1. Characteristic Chemical Shifts (ppm) of [*endo-μ-7,8*-(CH₂)_nCH(R)-7-*nido*-CB₁₀H₁₁]^a

Compd.	δ B7	δ α-CH	δ β-CH ₂	δ γ-CH ₂	δ δ-CH ₂	δ ε-CH ₂	δ cage C
R	δ α-CH	δ β-CH ₂	δ γ-CH ₂	δ δ-CH ₂	δ ε-CH ₂	δ cage C	
48	-2.1	0.80	1.50, 1.33	1.56, 1.19	2.22, 1.61	/	
B(OMe) ₂		11.4	25.8	28.5	39.1	/	52.2
48'	-2.0	0.57	1.65, 1.22	1.48, 1.27	2.23, 1.61	/	
B(OH) ₂		14.3	26.1	28.5	38.7	/	51.5
51	-1.4	3.41	1.67, 1.37	1.51, 1.24	2.13, 1.67	/	
OH		61.9	34.0	24.0	37.2	/	53.4
50	0.6	0.85	1.71, 1.49	1.81, 1.31	1.56	2.07, 1.90	
B(OMe) ₂		15.1	28.8	31.2	30.5	37.8	57.5
50'	1.5	0.70	1.89, 1.46	1.62	1.66, 1.41	1.99, 1.72	
B(OH) ₂		18.9	31.1	31.6	31.9	41.0	57.8
52	0.3	3.41	1.92, 1.53	1.66, 1.46	1.68, 1.36	2.04, 1.77	
OH		65.8	37.8	27.0	31.1	40.9	56.0

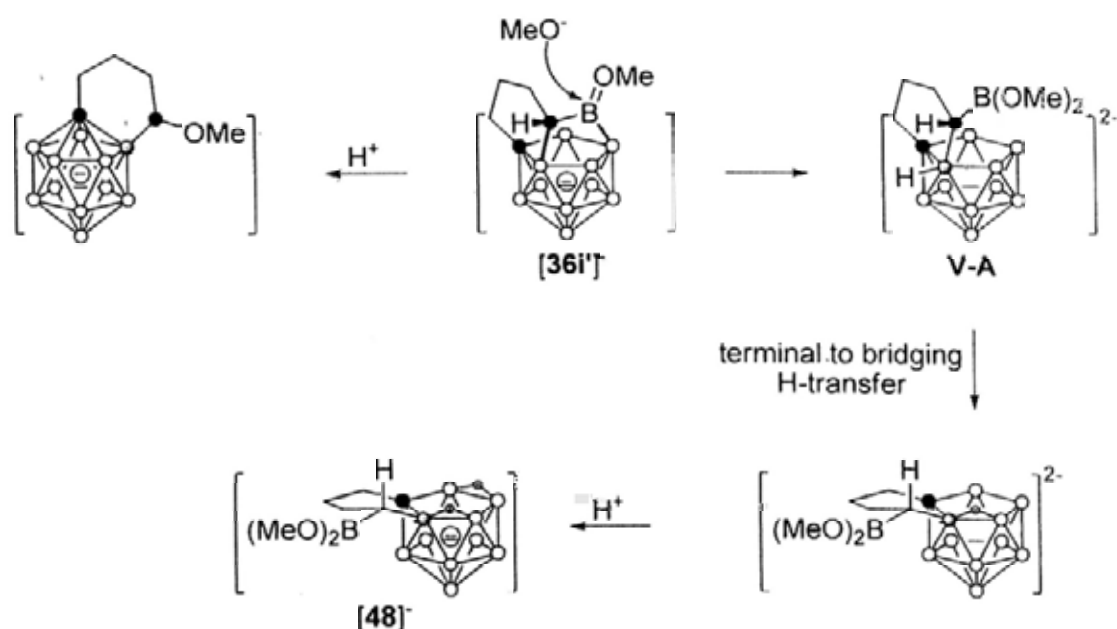
^a in CD₂Cl₂

Table 5.2. Selected Bond Distances (Å) of $[\mu\text{-}7,8\text{-(CH}_2)_n\text{CH(R)-}7\text{-nido-CB}_{10}\text{H}_{11}]^-$ ($n = 3, 4$) Anions.

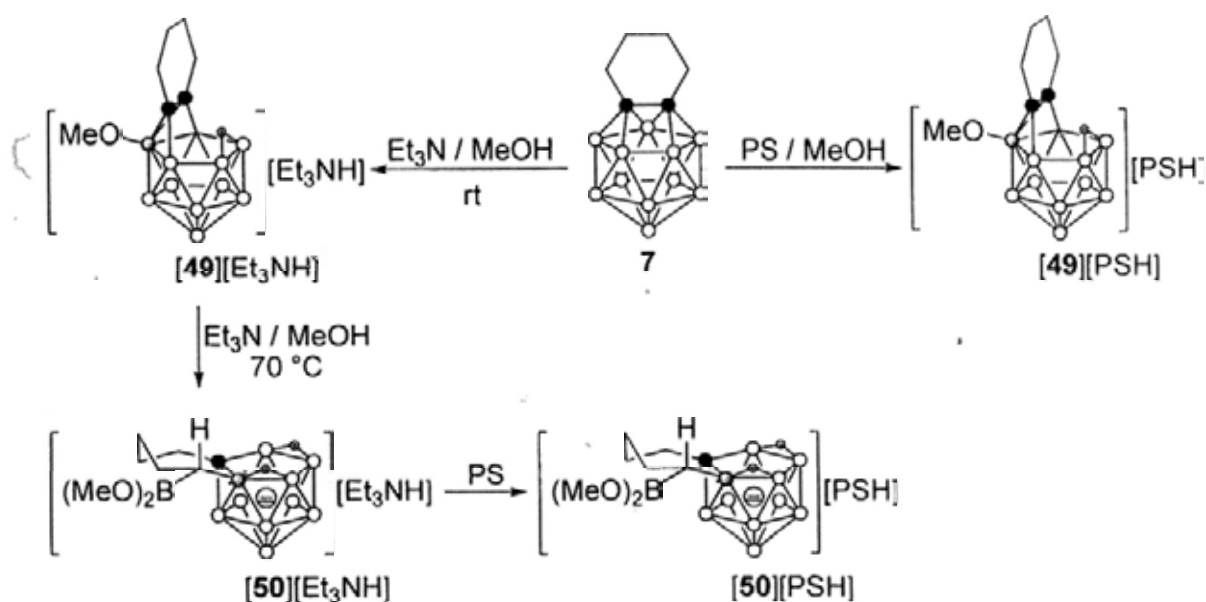
Bond	48	48'	51	50	52
C7-B11	1.660(3)	1.665(4)	1.658(5)	1.633(9)	1.665(3)
C7-B8	1.669(3)	1.654(4)	1.656(4)	1.615(9)	1.650(3)
C7-C11	1.531(3)	1.525(4)	1.529(4)	1.520(8)	1.534(3)
C11-C12	1.518(3)	1.516(4)	1.525(5)	1.534(9)	1.520(3)
C12-C13	1.521(3)	1.516(5)	1.510(5)	1.501(10)	1.517(3)
C13-C14	1.548(3)	1.553(4)	1.522(4)	1.368(9)	1.516(4)
C14-C15	/	/	/	1.553(7)	1.519(4)
C14(15)-B8	1.619(3)	1.616(4)	1.590(4)	1.676(8)	1.606(3)
C14(15)-X	1.569(3)	1.558(4)	1.453(3)	1.531(10)	1.450(3)
X	B	B	O	B	O
av. Cage C-B	1.675(3)	1.674(4)	1.679(5)	1.663(9)	1.674(3)
av. Cage B-B	1.793(3)	1.789(5)	1.786(6)	1.758(13)	1.787(4)

The above experimental results indicated that the intermediate $[\mathbf{36i}']^-$ would undergo different reaction pathways based on the acidity/basicity of the reaction media and a proposed mechanism was shown in Scheme 5.2. While acidic media resulted in the C-B bond cleavage to form *closo*-CB₁₁⁻ anion, basic media would lead to nucleophilic attack at the *sp*² boron center and B-B bond cleavage to form intermediate **V-A**. A possible reason for controlling the reaction pathway is that the acidic media would weaken the nucleophilicity of MeOH and facilitate it as a leaving group. On the other hand, bases would increase the nucleophilicity of MeOH as MeO⁻ and prevent the migration of the methoxy group. The intermediate **V-A** would undergo terminal-to-bridging H-transfer and protonation to afford monoanion $[\mathbf{48}]^-$.

Scheme 5.2. Possible Mechanism for the Formation of [48]⁻.



Scheme 5.3. Reaction of μ -1,2-(CH₂)₄-1,2-C₂B₁₁H₁₁ (7) with Et₃N/MeOH.



In a similar manner, treatment of μ -1,2-(CH₂)₄-1,2-C₂B₁₁H₁₁ (7) with excess Et₃N in MeOH at room temperature gave a 13-vertex *nido*-carborane salt [3-OMe- μ -1,2-(CH₂)₄-1,2-C₂B₁₁H₁₁][Et₃NH] ([49][Et₃NH]) immediately that was isolated as a white powder after removal of the volatile materials in almost quantitative yield (Scheme 5.3). Unlike [36i]⁻ which under the same condition would quickly convert to the *nido*-CB₁₀⁻ anion [48]⁻, complex [49][Et₃NH] is much more stable, although it

would also be decomposed at a much slower rate. However, when it was heated at 70 °C in the MeOH solution in the presence of excess amount of Et₃N for 24 h in a sealed tube, the *nido*-CB₁₀⁻ salt [*endo*- μ -7,8-(CH₂)₄CHB(OMe)₂-7-CB₁₀H₁₁][Et₃NH] ([50][Et₃NH]) was formed. Cation exchange with 5 equiv of PS followed by subsequent purification gave [*endo*- μ -7,8-(CH₂)₄CHB(OMe)₂-7-CB₁₀H₁₁][PSH] ([50][PSH]) as a white solid in about 80% isolated yield (Scheme 5.3).

Single-crystal of [49][Et₃NH] was grown from a CH₂Cl₂ solution, but its resolution was very poor. When PS was used instead of Et₃N, [49][PSH] was isolated as a white solid after purification in about 90% yield (Scheme 5.3). Single-crystal of [49][PSH] was grown from a THF solution. Its structure was confirmed by single-crystal X-ray analyses, and that of the anion was shown in Figure 5.2. It is significantly different from the general structures of the *nido*-carborane anions, which are formed by nucleophilic addition reactions of a *closo*-carborane with the nucleophiles bound to a bridging BH unit or a boron vertex on the planar open face.^{2b,c,2f} The structure of [49]⁻ bears a bent 6-membered C₂B₄ open face with a dihedral angle of 119.4(3) °. It is regarded that the bridging H atom is located on the B5 and B6 atoms. This cage geometry is also different from the 13-vertex *nido*-carborane dianions. The MeO group is attached to the 7-coordinated B3 atom, which is not on the open face. The B-O distances of 1.437(5) Å falls in the range 1.37 – 1.41 Å normally observed in alkoxy-substituted carboranes.^{32,75,118}

Complexes [49][Et₃NH] and [49][PSH] were also characterized by several spectroscopic techniques as well as elemental analyses. For [49][PSH], its ¹¹B NMR spectrum exhibited a 1:2:1:4:2:1 pattern in the range 1.7 to -26.0 ppm, in which the signal of the B3 atom that attached to the external methoxy group was unambiguously confirmed as a singlet at 1.7 ppm. The chemical shift of the “tertiary” cage car-

bonds was found at 140.7 ppm in the ^{13}C NMR spectrum, which was close to 142.5 ppm observed in its parent complex **7**, indicative of their electron deficient nature.

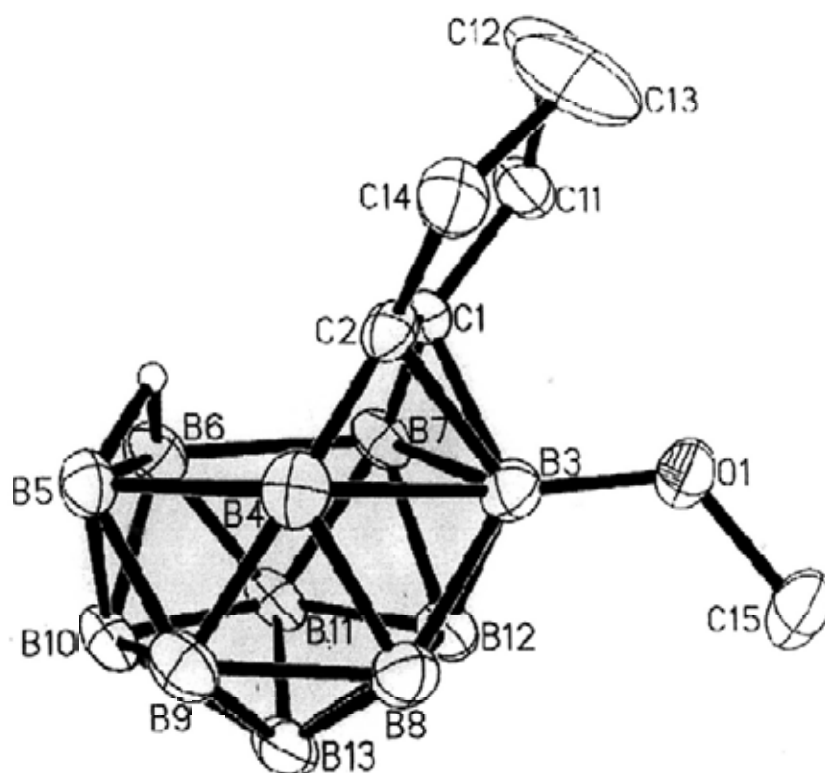


Figure 5.2. Structure of $[3\text{-OMe-}\mu\text{-}1,2\text{-(CH}_2\text{)}_4\text{-}1,2\text{-C}_2\text{B}_{11}\text{H}_{11}]^-$ (**[49]** $^-$), in **[49][PSH]**.

Complex **[50][PSH]** was characterized by several NMR spectroscopic techniques as well as elemental analyses. Its spectroscopic properties were very similar to those of **[48][PSH]**. Its $^{11}\text{B}\{^1\text{H}\}$ NMR spectrum clearly exhibited a broad signal at about 32.2 ppm indicative of the presence of an RB(OMe)_2 unit, a singlet at about 0.6 ppm assignable to the *B8* atom and other 9 doublets. The broad signal of $\alpha\text{-C}$ that attached to the cage *B8* atom was observed at about 15.1 ppm in the ^{13}C NMR spectrum. A broad signal at about -3.3 ppm with relative intensity of 2 was detected in the ^1H NMR spectrum, indicating two bridging H atoms on the 5-membered open face of the *nido*- anion.

Single-crystal of **[50][PSH]** was grown from a THF solution. X-ray diffraction studies indicated that the anion adopts a similar structure as that of **[48]** $^-$, although the

resolution is poor (Figure 5.3). An “endo” configuration is observed for the B(OMe)₂ group and the cage. However, this boryl group takes up the α -position not the ϵ -position in the twist-chair conformation of the 7-membered ring.

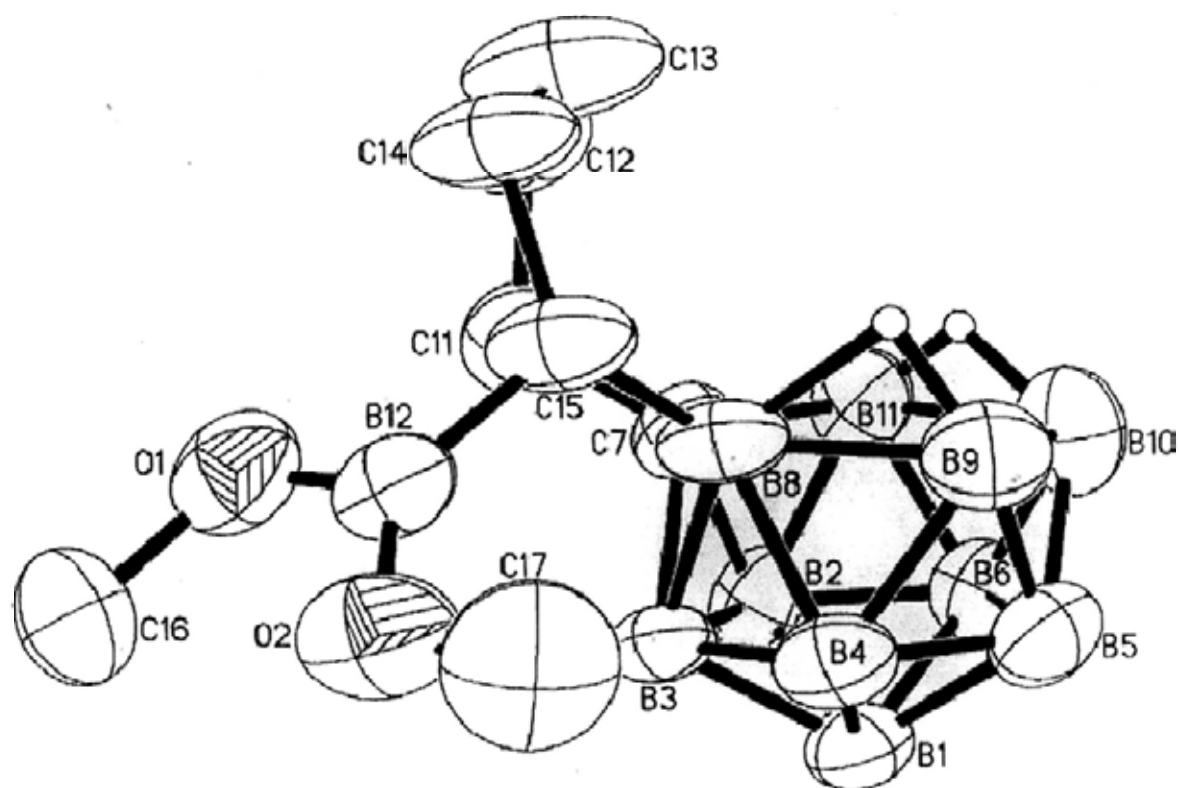
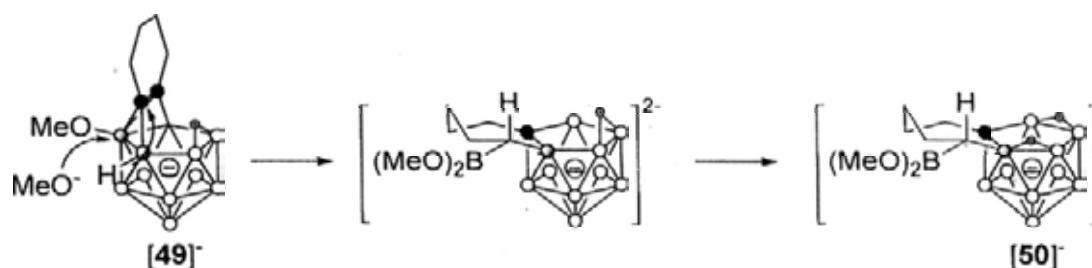


Figure 5.3. Structure of [*endo*- μ -7,8-(CH₂)₄CHB(OMe)₂-7-CB₁₀H₁₁]⁻ ([50]⁻), in [50][PSH].

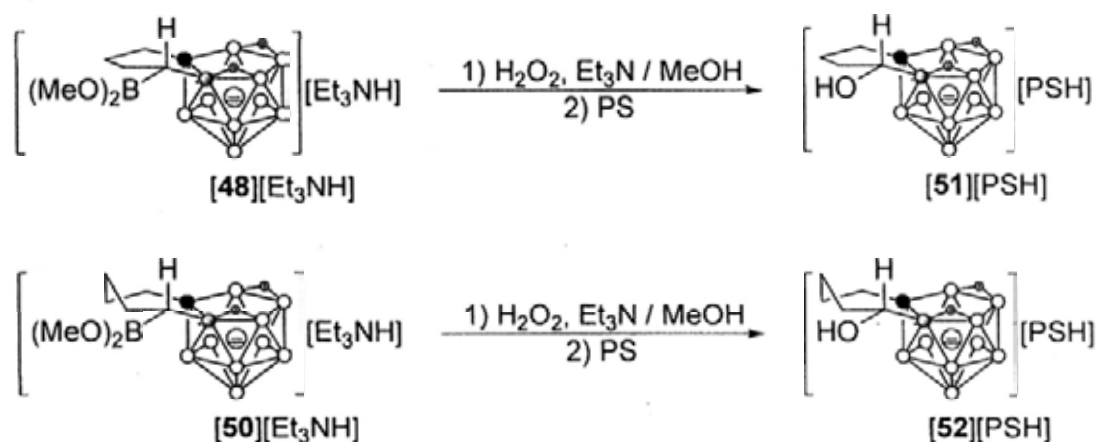
The above results indicated that the 13-vertex carborane **7** with a tetramethylene linkage can be converted to the 11-vertex *nido*-CB₁₀⁻ anions as that of 13-vertex carborane **6** with a trimethylene linkage. Isolation of the stable intermediate [49]⁻, in which the cage carbons were not attached to any H atom, showed that the H-migration was difficult to occur at room temperature in the 6-membered carbon ring system. It suggests that the reaction of 13-vertex carboranes with nucleophiles is also affected by the length of the C,C'-linkage. At this stage, it was hard to tell whether the attack of another MeO⁻ at the B3 atom and H-migration proceed stepwise or simultaneously. A proposed mechanism is depicted in Scheme 5.4.

Scheme 5.4. Possible Mechanism for the Formation of [50].



As boronic esters, complexes [48][PSH] and [50][PSH] are air sensitive. The C-B bonds would be slowly oxidized in the presence of a little amount of base such as Et_3N or Na_2CO_3 , which explained why messy products were afforded when the reactions were treated in the open air. These processes could be accelerated by using H_2O_2 as an oxidant. Treatment of [48][Et_3NH] or [50][Et_3NH], which was prepared in situ without separation, with excess amount of H_2O_2 followed by cation exchange with PS, gave [*endo*- μ -7,8-(CH_2) $_3$ CHOH-7- $\text{CB}_{10}\text{H}_{11}$][PSH] ([51][PSH]) or [*endo*- μ -7,8-(CH_2) $_4$ CHOH-7- $\text{CB}_{10}\text{H}_{11}$][PSH] ([52][PSH]) as a white powder in about 75% isolated yield, respectively (Scheme 5.5).

Scheme 5.5. Oxidation of Boronic Esters [48] and [50].



These two complexes were characterized by several spectroscopies and elemental analyses. They showed similar patterns in the ^{11}B NMR spectra (Figure 5.4), with disappearing of the original low field broad peaks of the boryl group. The characte-

istic singlets of the *B8* atoms were detected at -1.4 ppm for [51][PSH] and 0.3 ppm for [52][PSH], respectively. Owing to the effect of neighboring hydroxy group, the broad signals of the α -CH were downfielded at 3.41 ppm for both complexes in the ^1H NMR spectra, and the corresponding carbons were observed at 61.9 ppm for [51][PSH] and 65.8 ppm for [52][PSH], respectively.

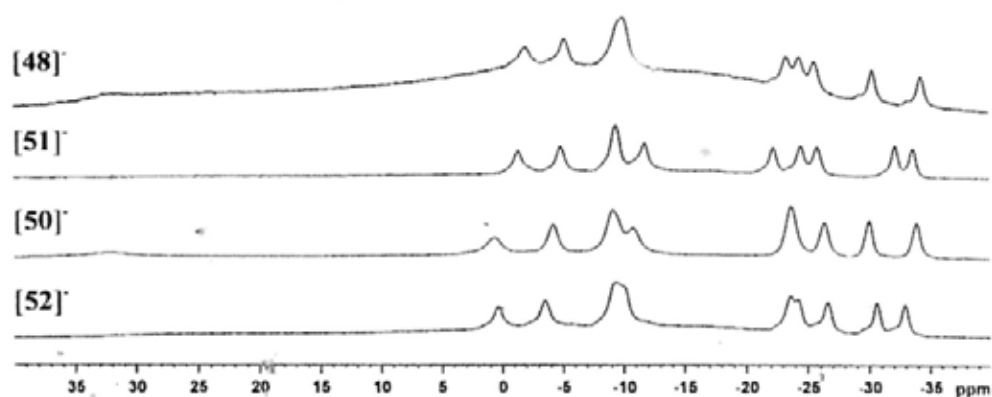


Figure 5.4. $^{11}\text{B}\{^1\text{H}\}$ NMR spectra of anions [48] $^-$, [50] $^-$, [51] $^-$ and [52] $^-$.

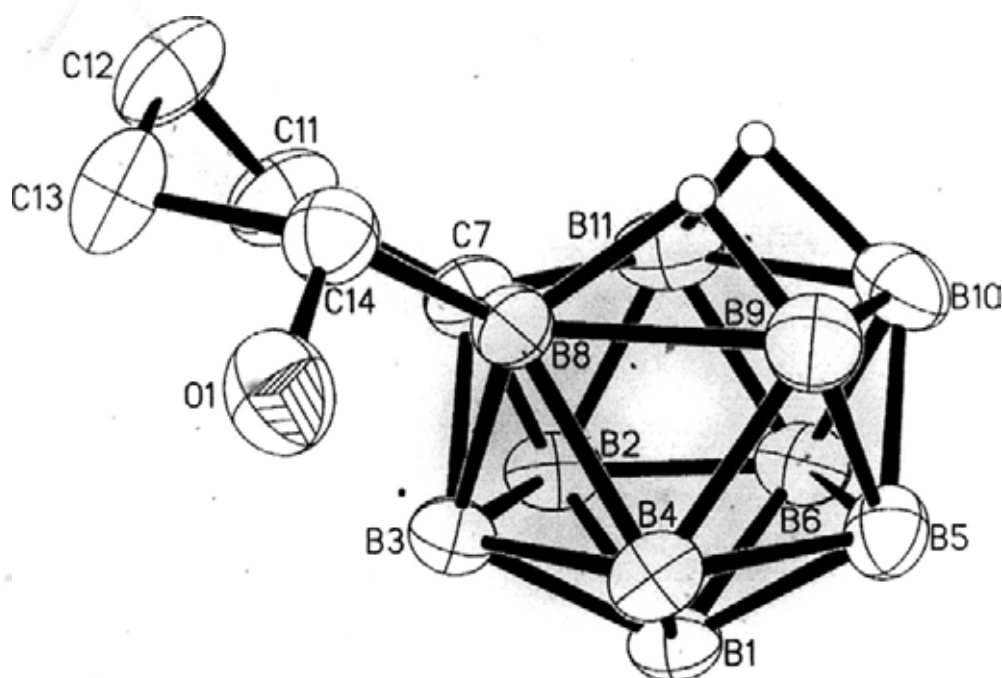


Figure 5.5. Structure of [endo- μ -7,8-(CH_2) $_3$ CHOH-7- $\text{CB}_{10}\text{H}_{11}$] $^-$ ([51] $^-$), in [51][PSH].

Single-crystal X-ray analyses confirmed the structures of the anions as shown in Figures 5.5 and 5.6. Anions [51] $^-$ and [52] $^-$ have very similar cage geometries compared to their precursors. The hydroxyl group still takes up the original *e*-positions of

the boryl group in [51] in a half-chair conformation, and *a*-positions in [52] in a chair conformation, respectively.

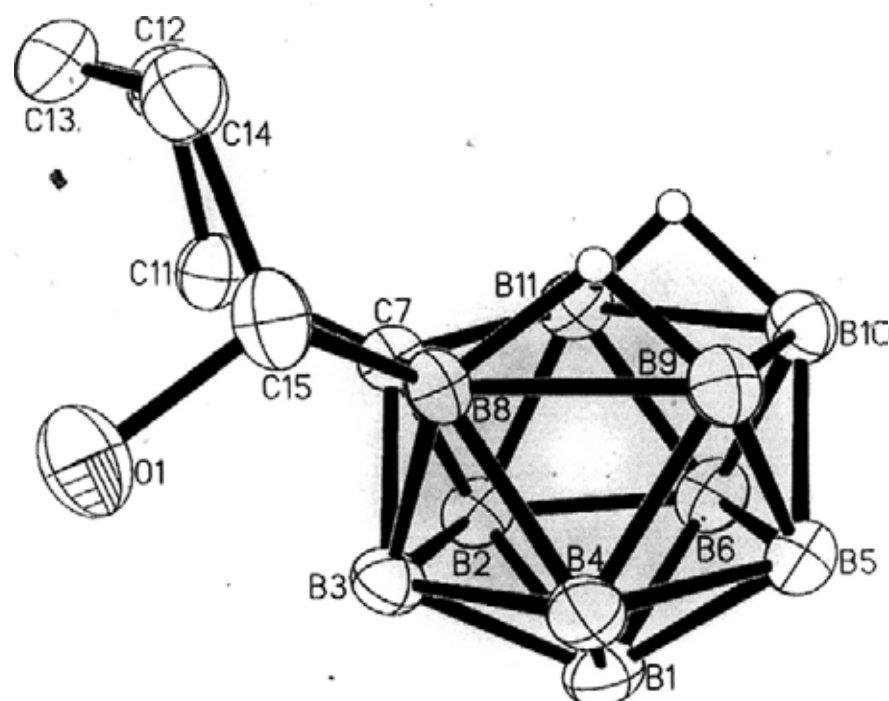
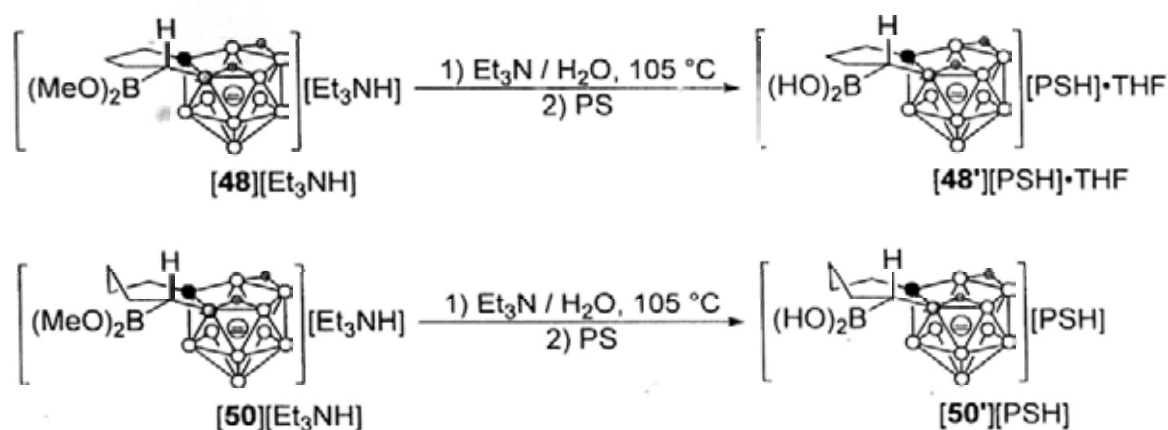


Figure 5.6. Structure of [*endo*- μ -7,8-(CH₂)₄CHOH-7-CB₁₀H₁₁] ([52]'), in [52][PSH].

On the other hand, the C-B bonds of the boronic esters were stable toward H₂O. Treatment of [48][Et₃NH] or [50][Et₃NH] with an excess amount of Et₃N in H₂O at 105 °C for 24 h in a sealed tube, followed by cation exchange with PS, only gave the hydrolysis products [*endo*- μ -7,8-(CH₂)₃CHB(OH)₂-7-CB₁₀H₁₁][PSH]·THF ([48'] [PSH]·THF) as colorless crystals, or [*endo*- μ -7,8-(CH₂)₄CHB(OH)₂-7-CB₁₀H₁₁][PSH] ([50'] [PSH]) as a white powder, respectively, in about 60% isolated yield (Scheme 5.6).

These two boronic acids were also characterized by various spectroscopic techniques and elemental analyses. Their ¹¹B NMR spectra were almost the same as those of their parent boronic esters [48][PSH] and [50][PSH]. The ¹H and ¹³C NMR spectra were also very similar, except that in the boronic acids [48'] [PSH]·THF and [50'] [PSH], the peaks of the MeO groups disappeared.

Scheme 5.6. Hydrolysis of Boronic Esters [48]⁻ and [50]⁻.



Cleavage of the B-O bonds rather than B-C bonds was confirmed by single-crystal X-ray diffraction study of [48'] [PSH]·THF, as shown in Figure 5.7. The anion adopts the dimeric structure via O-H···O hydrogen bonds from two boronic acid parts, each of which is also linked to a THF molecule through O-H···O interactions. Thus the real formula of [48'] [PSH]·THF should be best described as [{48'·THF}₂]²⁻ [PSH]₂. The geometry of the [48']⁻ is very similar to that of [48]⁻.

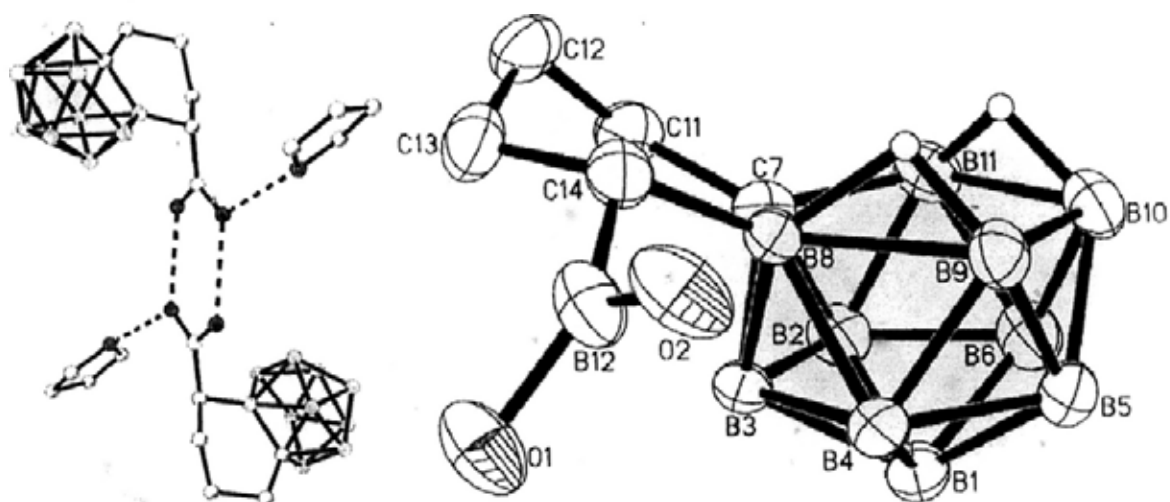


Figure 5.7. Dimeric structure of [*endo*- μ -7,8-(CH₂)₃CHB(OH)₂-7-CB₁₀H₁₁·THF]₂²⁻ ([{48'·THF}₂]²⁻) (left) and monomeric unit of [48']⁻ (right), in [48'] [PSH]·THF.

5.2. Reaction of 13-Vertex Carborane μ -1,2-(CH₂)₃-1,2-C₂B₁₁H₁₁ with Pyridine

13-Vertex carborane μ -1,2-(CH₂)₃-1,2-C₂B₁₁H₁₁ (**6**) was highly reactive toward pyridine. Unlike the reaction of compound **6** with tertiary amine Et₃N, which was almost undetectable at room temperature, compound **6** reacted readily with pyridine at room temperature under an inert atmosphere to give a red-brown then dark-blue and finally a brownish yellow solution. The reaction was extremely exoergic with boiling of the solution when pyridine was gradually added. The ¹¹B NMR spectra suggested the formation of the CB₁₁⁻ anion(s). However, the ¹H (Figure 5.8) and ¹³C NMR spectra illustrated a mixture of products, in which some were identifiable. The characteristic peaks at 6.59 (d) and 6.24 (br) ppm in the ¹H NMR and 132.3 ppm in the ¹³C NMR indicated the possible formation of [μ -1,2-(CH₂)₂CH=CH-1-CB₁₁H₁₀] ([**37**]). The peak at 4.89 ppm was regarded the α -CH that attached to N atom in *closo*- μ -1,2-(CH₂)₃CH(NC₅D₅)-1-CB₁₁H₁₀ (*d*₅-**53a**) and that at 5.01 ppm is the β -CH in *closo*- μ -1,2-(CH₂)₂CH(NC₅D₅)CH₂-1-CB₁₁H₁₀ (*d*₅-**53b**). These are normal carbon extrusion products of the 13-vertex carborane **6** and the ratio of **53a**/**53b**/[**37**] is about 3.4:1.4:1 as indicated by ¹H NMR. In the ¹H NMR spectrum, another set of peaks was also observed with a ratio of about 1:1 to [*d*₅-**53a**]. We intended to isolate this unexpected product.

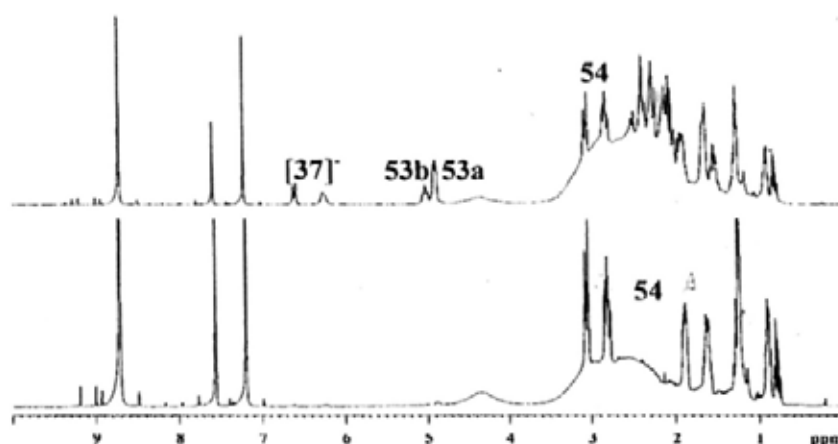
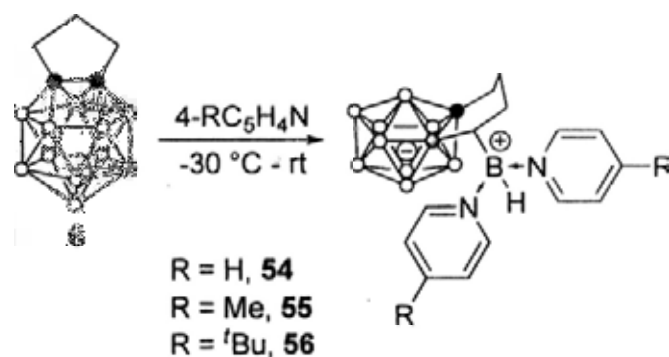


Figure 5.8. ¹H NMR spectra of **6** in *d*₅-pyridine: mixture (top); single product (bottom).

With these regards, an NMR tube reaction was performed at $-30\text{ }^{\circ}\text{C}$. Compound **6** was slowly added to d_5 -pyridine. It was noted that the surface of the solid turned to red-brown upon contacting with d_5 -pyridine. The color of the solution was gradually darkened to purple blue soon and finally to brownish yellow. The ^1H NMR spectrum indicated the formation of a single product (Figure 5.8). This species was not a *closo*- CB_{11}^- anion as the two-dimensional HSQC and COSY experiments indicated the formation of a $(\text{CH}_2)_3\text{CH}$ unit and that the CH unit was not attached to the N atom. Its ^{13}C NMR confirmed that this compound contained two $\text{C}_5\text{D}_5\text{N}$ units.

A preparative scale experiment was performed under the same reaction condition from $-30\text{ }^{\circ}\text{C}$ to room temperature. A *closo*- complex μ -2,4- $(\text{CH}_2)_3\text{CHBH}(\text{C}_5\text{H}_5\text{N})_2$ -2- CB_{10}H_9 (**54**) was isolated in about 50% yield as a white powder after removal of pyridine and thoroughly washed with THF (Scheme 5.7).

Scheme 5.7. Controlled Reaction of **6** with Pyridines.



In a similar manner, reaction of **6** with 4-Me $\text{C}_5\text{H}_4\text{N}$ and 4- $\text{tBuC}_5\text{H}_4\text{N}$ afforded μ -2,4- $(\text{CH}_2)_3\text{CHBH}(\text{MeC}_5\text{H}_4\text{N})_2$ -2- CB_{10}H_9 (**55**) as a pale pink powder in about 50% isolated yield and μ -2,4- $(\text{CH}_2)_3\text{CHBH}(\text{tBuC}_5\text{H}_4\text{N})_2$ -2- $\text{CB}_{10}\text{H}_9 \cdot \text{THF}$ (**56**·THF) as a white powder in about 30% isolated yield.

These complexes showed low solubilities in common polar solvents such as CH_2Cl_2 , MeOH, THF or acetone. Complex **54** was even hard to dissolve in d_5 -

pyridine after it precipitated out from the solution. They displayed a reasonable solubility in *d*₆-DMSO. Accordingly, the spectroscopic data were collected. These three complexes exhibited similar spectroscopic features. Their ¹¹B NMR spectra were almost identical, each of which contains a broad and sharp peak at about -11 ppm assignable to the cage borons and a broad signal at about -6 ppm corresponding to the cationic RBH group. The ¹H and ¹³C NMR spectra confirmed two chemically non-equivalent pyridine units in each complex.

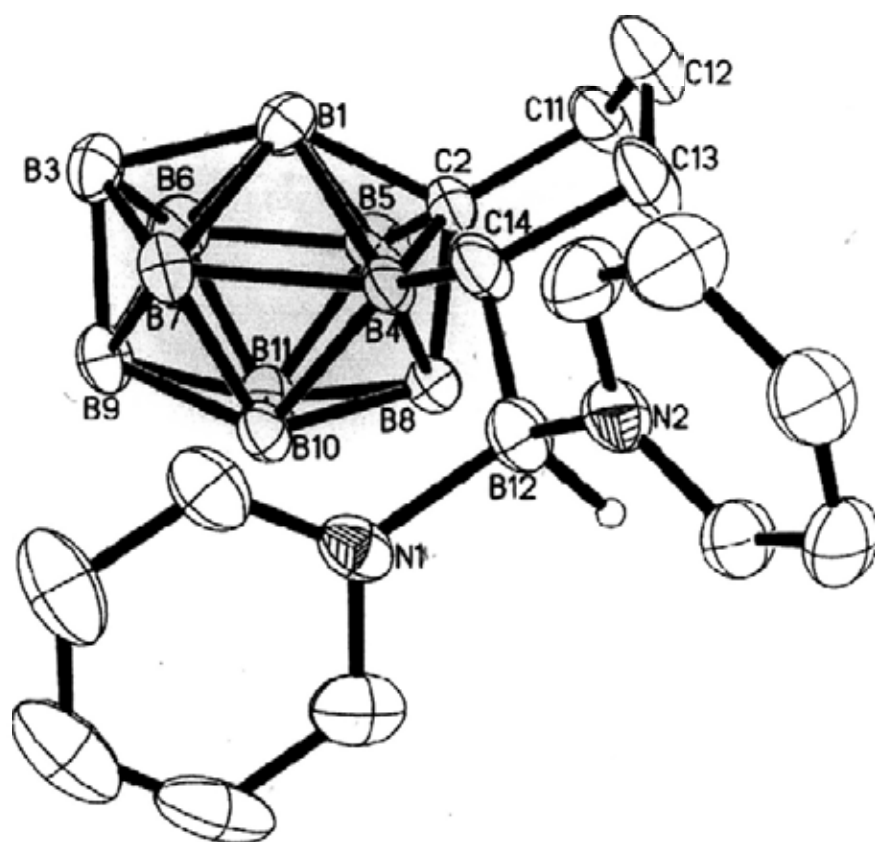


Figure 5.9. Molecular structure of μ -2,4-(CH₂)₃CHBH(C₅H₅N)₂-2-CB₁₀H₉ (**54**).

After many attempts, it was found that they were able to be crystallized via vapor diffusion of MeOH into a DMSO solution within 12 to 24 h. Single crystal X-ray analyses indicated that complex **54** has an 11-vertex *closo*-cage geometry (Figure 5.9). Its structural features are very similar to those of known monocarba-*closo*-undecaborate anions.^{117g,h,119} The carbon atom takes up the lowest coordination posi-

tion and a $(\text{CH}_2)_3\text{CH}$ unit links this C2 atom and the adjacent B4 atom. A boron atom is attached to the α -C atom that is adjacent to the B4 atom, which is also attached to two pyridine units. The B12 atom adopts a distorted tetrahedral geometry with the corresponding C14-B12-N1, C14-B12-N2, N1-B12-N2 angles of $115.4(3)^\circ$, $113.4(3)^\circ$ and $103.0(3)^\circ$, respectively. The B12-N1 and B12-N2 bond lengths of $1.604(4)$ and $1.634(4)$ Å, are close to 1.58 Å of averaged B-N single bond.¹¹⁰ Indeed, these properties are in supportive of a zwitterionic boronium cation of complex **54**.¹¹³

The resolution of **55** structures is poor. Nevertheless, the atom connectivities are unambiguously determined, as shown in Figures 5.10. There are two crystallographically independent molecules in the unit cell of **56**, and a typical one is shown in Figure 5.11. Both complexes have very similar structures to that of complex **54**.

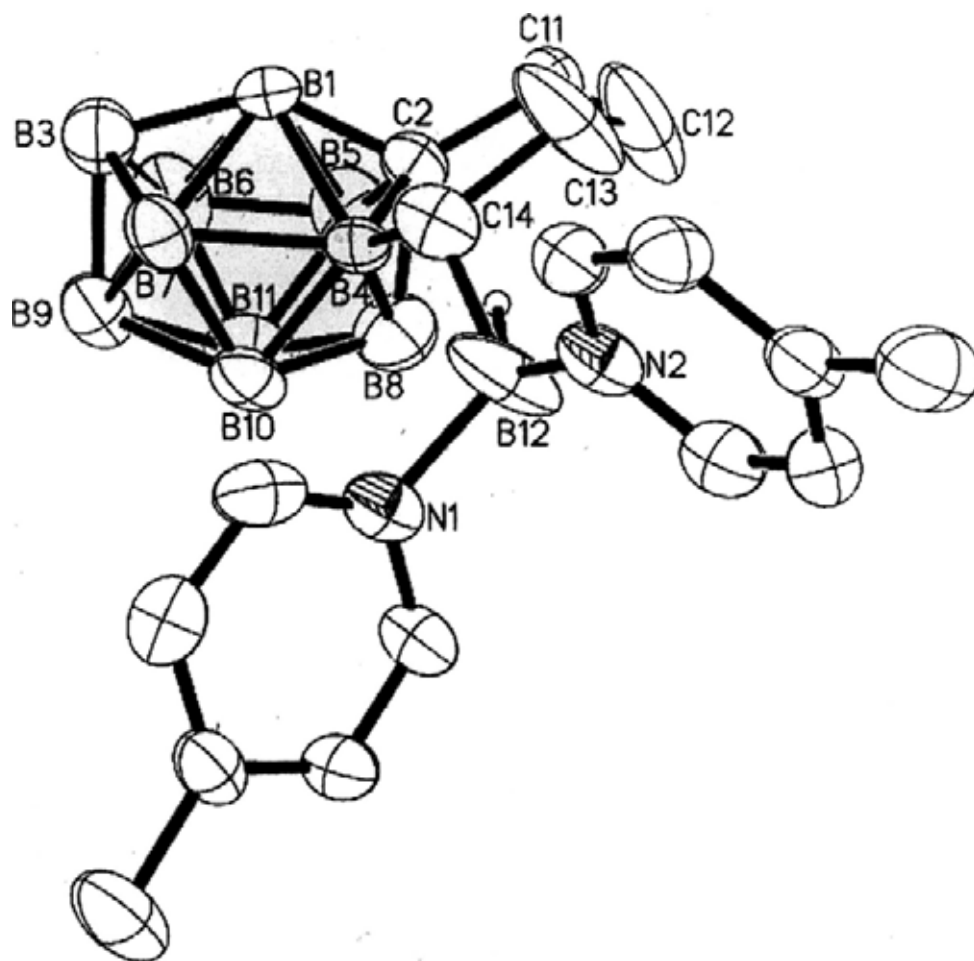


Figure 5.10. Molecular structure of μ -2,4- $(\text{CH}_2)_3\text{CHBH}(\text{CH}_3\text{C}_5\text{H}_4\text{N})_2$ -2- CB_{10}H_9 (**55**).

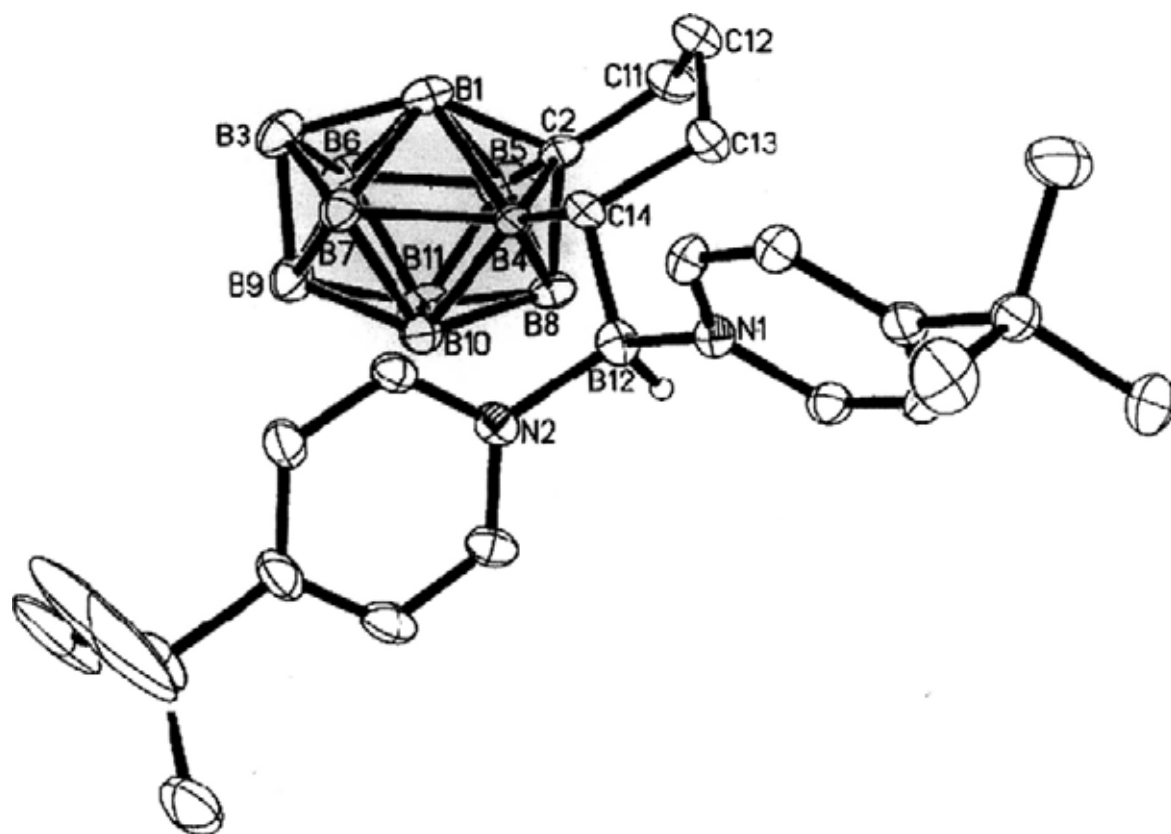


Figure 5.11. Molecular structure of μ -2,4-(CH₂)₃CHBH(^tBuC₅H₄N)₂-2-CB₁₀H₉ (**56**), showing one of two crystallographically independent molecules.

We performed the reaction of **6** with pyridine at room temperature on a preparative scale. After column chromatographic separation and repeated recrystallization from CH₂Cl₂ and acetone, zwitterionic *closo*-CB₁₁⁻ complexes μ -1,2-(CH₂)₃CH(NC₅H₅)-1-CB₁₁H₁₀ (**53a**) and μ -1,2-(CH₂)₂CH(NC₅H₅)CH₂-1-CB₁₁H₁₀ (**53b**) were isolated in about 20% and 5% yield (Scheme 5.8). [μ -1,2-(CH₂)₂CH=CH-1-CB₁₁H₁₀][C₅H₅NH] (**37**)[C₅H₅NH]) could hardly be purified in pure form. The two complexes were characterized by various spectroscopic techniques as well as HRMS. Their spectroscopic features were very similar to those complexes reported in Chapter 4 (Table 4.1 and 4.2). The structure of **53a** was confirmed by single-crystal X-ray analyses and shown in Figure 5.12.

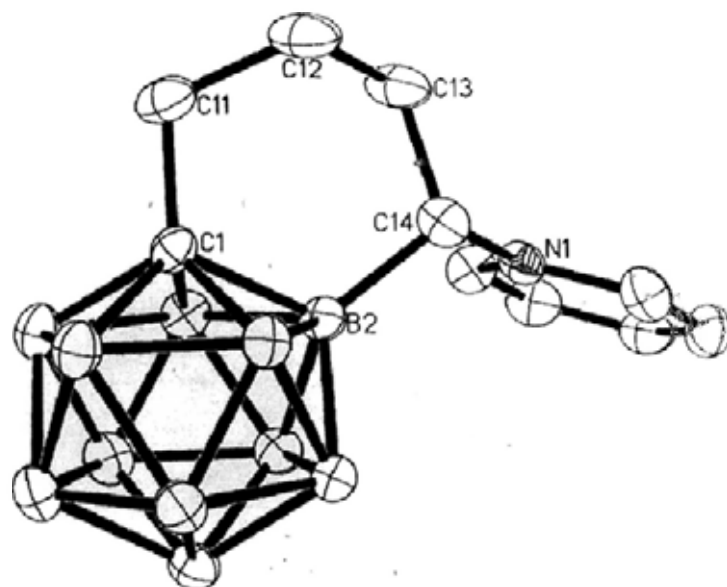
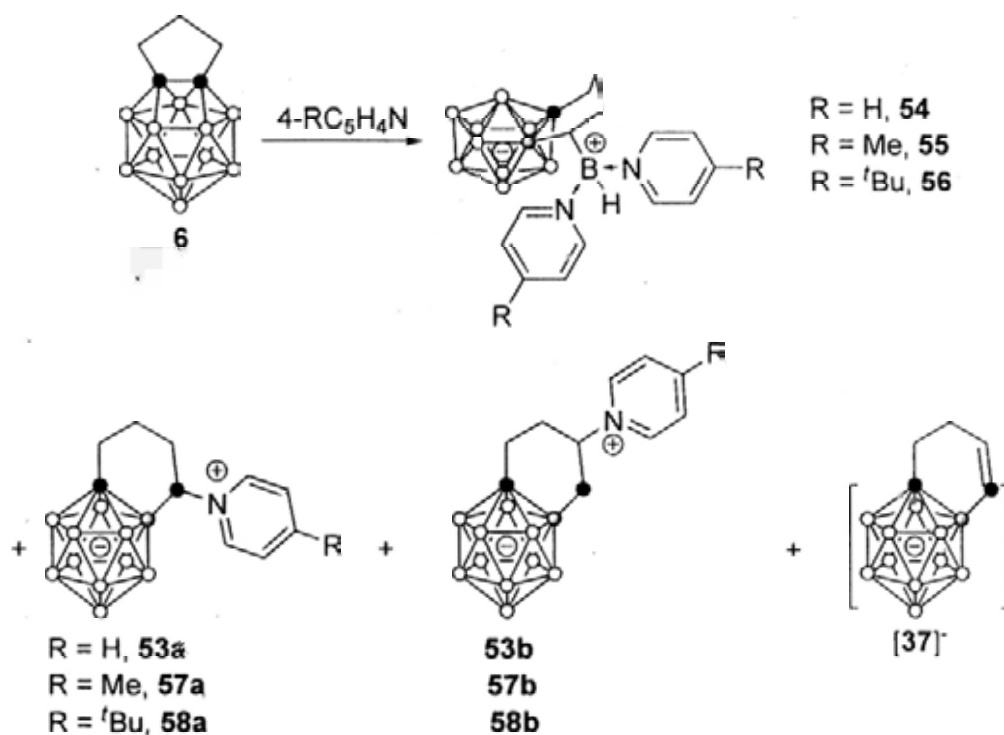


Figure 5.12. Molecular structure of μ -1,2-(CH₂)₃CH(NC₅H₅)-1-CB₁₁H₁₀ (**53a**).

Scheme 5.8. Reaction of **6** with Pyridines at Room Temperature.



Similarly, reactions of **6** with excess 4-MeC₅H₄N or 4-^tBuC₅H₄N also gave a mixture of products in C₆D₆ at room temperature as evidenced from ¹H NMR spectra. Besides 11-vertex *closo*-CB₁₀⁻ complexes μ -2,4-(CH₂)₃CHBH(4-RC₅H₄N)₂-2-CB₁₀H₉ (R = Me, **55**; R = ^tBu, **56**), 12-vertex *closo*-CB₁₁⁻ anions [μ -1,2-(CH₂)₂CH=CH-1-CB₁₁H₁₀]⁻ (**[37]**), μ -1,2-(CH₂)₃CH(4-RC₅H₄N)-1-CB₁₁H₁₀ (R = Me,

57a; R = ^tBu, **58a**) and μ -1,2-(CH₂)₂CH(4-RC₅H₄N)CH₂-1-CB₁₁H₁₀ (R = Me, **57b**; R = ^tBu, **58b**) were observed in the reactions (Scheme 5.8). The gross ¹H NMR spectra of these two reactions were shown in Figure 5.13.

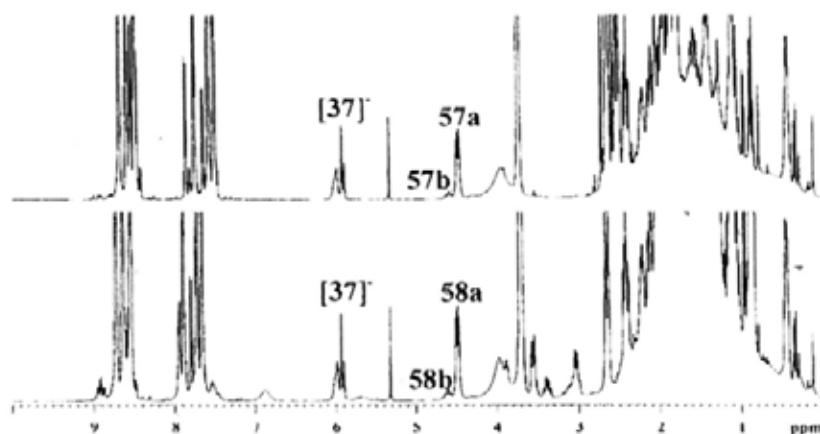


Figure 5.13. ¹H NMR spectra of the reaction mixture of compound **6** with 4-MeC₅H₄N (top), and 4-^tBuC₅H₄N (bottom).

One of the complexes **57a** was crystallized out from a CH₂Cl₂ solution of the reaction mixture of 4-MeC₅H₄N, which was structurally characterized as μ -1,2-(CH₂)₃CH(MeC₅H₄N)-1-CB₁₁H₁₀·CH₂Cl₂ (**57a**·CH₂Cl₂) (Figure 5.14). This result further confirmed the formation of CB₁₁⁻ zwitterions.

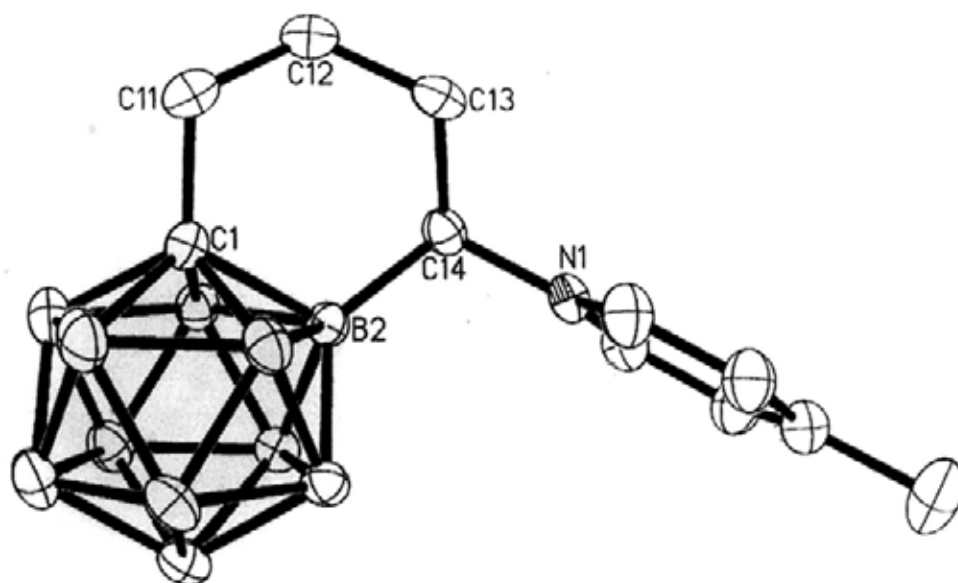
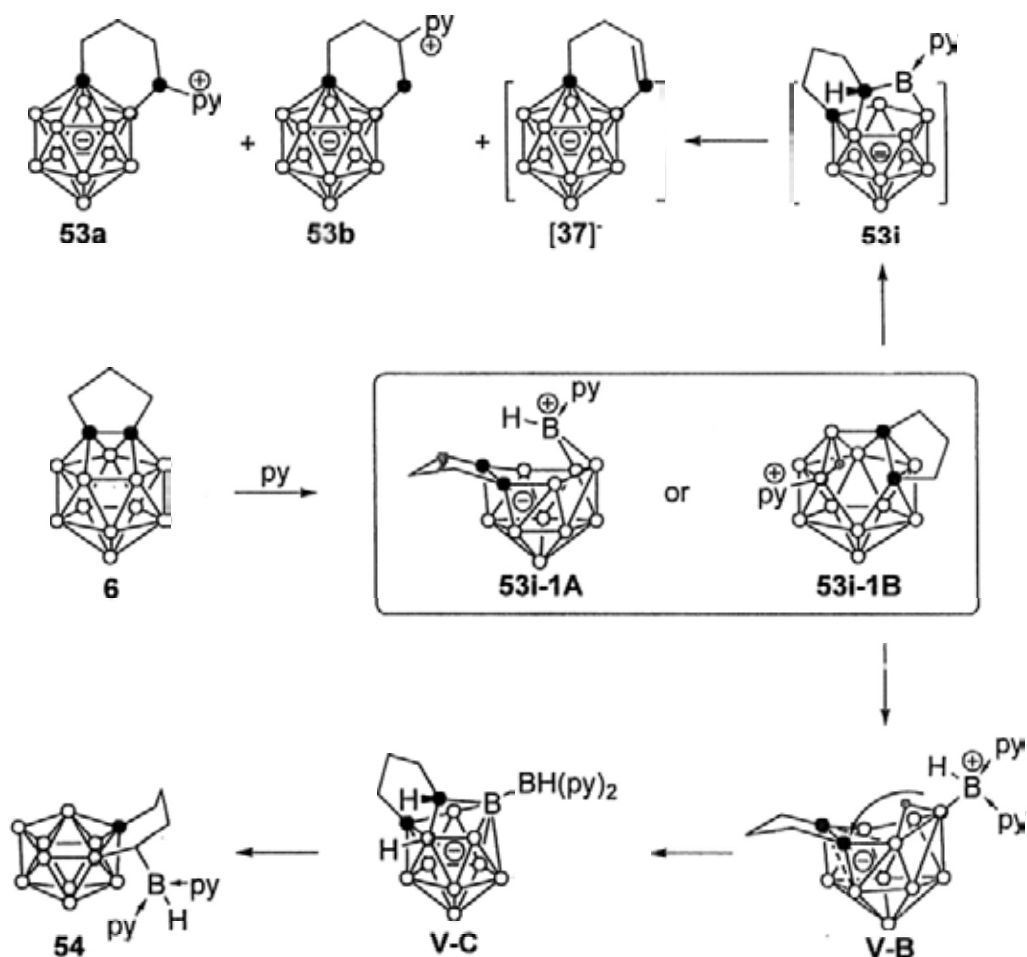


Figure 5.14. Molecular structure of μ -1,2-(CH₂)₃CH(MeC₅H₄N)-1-CB₁₁H₁₀ (**57a**), in

Scheme 5.9. Possible Mechanism for the Formation of Boronium Ion 54.

The above results indicated that formation of *closo*-CB₁₀⁻ and *closo*-CB₁₁⁻ species were via competitive reactions. While low temperature and high concentration of the reagents facilitated the formation of *closo*-CB₁₀⁻ anions, high temperature or low concentration would lead to the formation of both *closo*-CB₁₀⁻ and *closo*-CB₁₁⁻ anions. These reactions may proceed from the same intermediate and a proposed mechanism is shown in Scheme 5.9. Compound **6** reacts with one equimolar of pyridine to give the first intermediate **53i-1A** or **53i-1B**, which would give intermediate **V-B** upon attack of another pyridine molecule, followed by B-H addition to one of the cage carbons to give intermediate **V-C**. Migration of the BH(py)₂ group and cage closure affords the *closo*-CB₁₀⁻ product **54**. On the other hand, **53i-1** may undergo B-

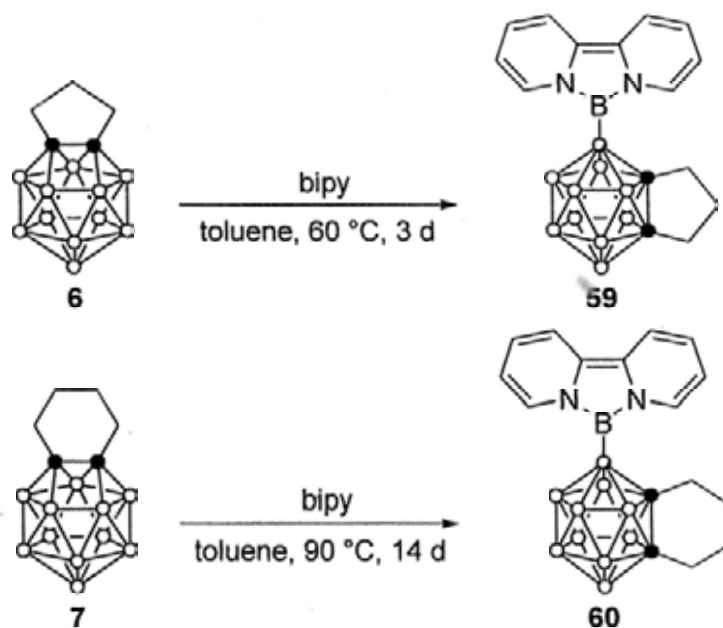
H addition to one of the cage carbons to give intermediate $\mu\text{-}\eta\text{:}\eta\text{:}\eta\text{-}7,8,10\text{-}(\text{CH}_2)_3\text{CHB}(\text{C}_5\text{H}_5\text{N})\text{-}7\text{-CB}_{10}\text{H}_{10}$ (**53i**), and finally to form the CB_{11}^- anions. As we did not observe any intermediate, we can not totally exclude the possibility that complex **54** is also formed from **53i**.

5.3. Reaction of 13-Vertex Carboranes $\mu\text{-}1,2\text{-}(\text{CH}_2)_n\text{-}1,2\text{-C}_2\text{B}_{11}\text{H}_{11}$ ($n = 3, 4$) with Bipyridines

Bidentate reagents may have different reactivities compared to the monodentate nucleophiles. In this regard, several reagents, such as TMEDA and dppe, were examined in the reaction with 13-vertex carborane $\mu\text{-}1,2\text{-}(\text{CH}_2)_3\text{-}1,2\text{-C}_2\text{B}_{11}\text{H}_{11}$ (**6**). The ^1H , ^{13}C and ^{11}B NMR spectra indicated that the major products were 12-vertex *closo*- CB_{11}^- anions $\mu\text{-}1,2\text{-}(\text{CH}_2)_3\text{CH}(\text{NMe}_2\text{CH}_2\text{CH}_2\text{NMe}_2)\text{-}1\text{-CB}_{11}\text{H}_{10}$ or $\mu\text{-}1,2\text{-}(\text{CH}_2)_3\text{CH}(\text{PPh}_2\text{CH}_2\text{CH}_2\text{PPh}_2)\text{-}1\text{-CB}_{11}\text{H}_{10}$.

On the other hand, reaction of compound **6** with 1 equiv of 2,2'-bipyridine (bipy) was examined in C_6D_6 at room temperature. The color of the solution was quickly changed to yellow, but the ^1H NMR spectrum indicated that the reaction was rather slow and gradually became messy at room temperature. However, a major species gradually appeared upon heating at 60 °C, and the reaction was completed within 3 d. The color of the solution was finally changed to dark red. Accordingly, the preparative scale reaction was performed in toluene. After recrystallization from CH_2Cl_2 , 4-(2,2'- $\text{C}_{10}\text{H}_8\text{N}_2\text{B}$)- $\mu\text{-}1,2\text{-}(\text{CH}_2)_3\text{-}1,2\text{-C}_2\text{B}_{10}\text{H}_9$ (**59**) was isolated as red crystals in about 70% isolated yield. Treatment of $\mu\text{-}1,2\text{-}(\text{CH}_2)_4\text{-}1,2\text{-C}_2\text{B}_{11}\text{H}_{11}$ (**7**) with 1 equiv of bipy in toluene at 90 °C for 14 days gave 4-(2,2'- $\text{C}_{10}\text{H}_8\text{N}_2\text{B}$)- $\mu\text{-}1,2\text{-}(\text{CH}_2)_4\text{-}1,2\text{-C}_2\text{B}_{10}\text{H}_9$ (**60**) as red crystals in about 60% isolated yield, after recrystallization from CH_2Cl_2 (Scheme 5.10).

Scheme 5.10. Reaction of Bipy with 13-vertex Carboranes μ -1,2-(CH₂)_n-1,2-C₂B₁₁H₁₁ ($n = 3, 4$).



Both complexes were characterized by several spectroscopic techniques as well as HRMS. The broad signals of the boron atom that attached to two nitrogen atoms were observed in the low field at about 30 ppm in the ¹¹B NMR spectra. The ¹H and ¹³C chemical shifts of the bipy units were up fielded compared to the free ligand (Figure 5.15).

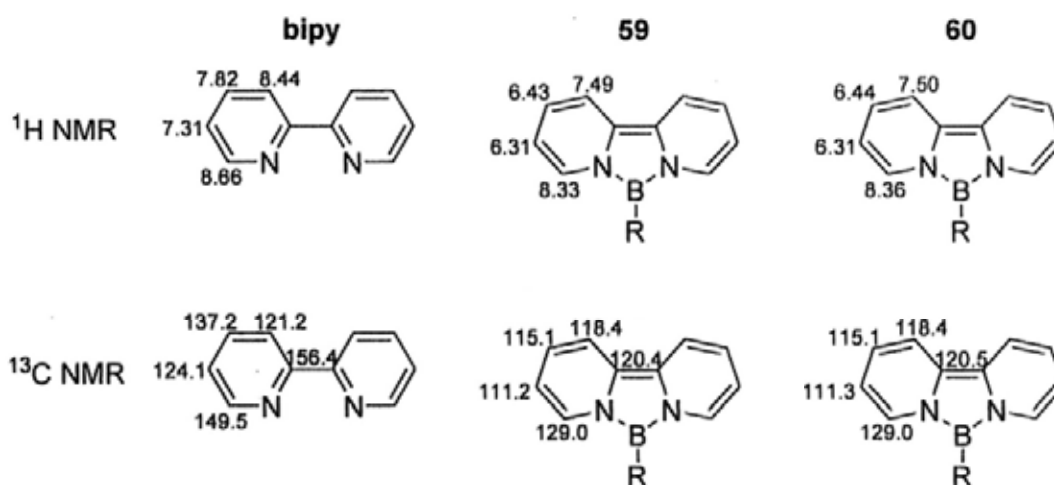


Figure 5.15. ¹H and ¹³C chemical shifts of the bipy units in the free ligand and complexes **59** and **60**.

These 2 complexes represent new species bearing both boron/nitrogen heterocycles and carborane unit. To the best of our knowledge, only two earlier reports demonstrated formation and characterization of (bipy)BX ($X = N^iPr_2, Ph, Cl$),¹²⁰ which have the similar (bipy)B unit as **59** and **60**. Besides their similar spectroscopic properties, they also have similar structural features.^{120b} The structures of complexes **59** and **60** were confirmed by single-crystal X-ray analyses. There are three crystallographically independent molecules in the unit cell of **59** and a representative one was shown in Figure 5.16. The molecular structure of **60** is shown in Figure 5.17. In both complexes, a 2,2'-C₁₀H₈N₂B- boryl group is linked to the B4 atom in the 12-vertex carborane with retain of the original linkage. The boryl group is almost coplanar and forms a conjugated system. It is noted that the newly formed B-N bonds are very short at a distance of about 1.44 Å. As shown in Table 5.3, the most dramatic change is that the *i* bond is shortened, from a single bond of 1.50 Å in the free bipy,¹²¹ to a double bond of about 1.37 Å.

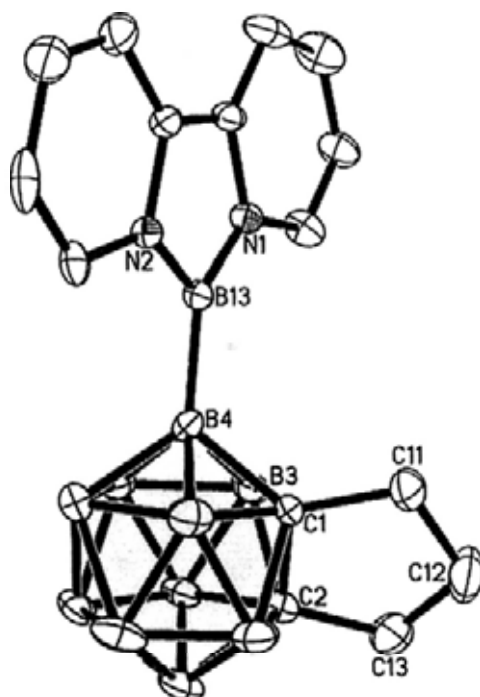
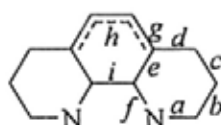


Figure 5.16. Molecular structure of 4-(2,2'-C₁₀H₈N₂B)- μ -1,2-(CH₂)₃-1,2-C₂B₁₀H₉ (**59**), showing one of the crystallographically independent molecules.

Table 5.3. Comparison of Average Bond Lengths of the Bipy and Phen Units in the Free Ligand and Complexes **59**, **60**, **61** and **62**.



Bond	bipy	59	60	phen	61	62
<i>a</i>	1.337(2)	1.408(9)	1.390(4)	1.313(5)	1.416(5)	1.408(4)
<i>b</i>	1.381(2)	1.360(14)	1.343(5)	1.396(7)	1.346(6)	1.342(5)
<i>c</i>	1.382(2)	1.419(14)	1.419(7)	1.356(7)	1.473(7)	1.489(5)
<i>d</i>	1.382(2)	1.356(14)	1.343(7)	1.417(6)	1.497(7)	1.500(5)
<i>e</i>	1.392(2)	1.429(10)	1.417(5)	1.406(5)	1.384(5)	1.383(4)
<i>f</i>	1.344(2)	1.410(9)	1.407(4)	1.359(5)	1.396(5)	1.398(3)
<i>g</i>	/	/	/	1.426(6)	1.391(7)	1.395(5)
<i>h</i>	/	/	/	1.331(9)	1.383(7)	1.383(5)
<i>i</i>	1.488(2)	1.371(11)	1.377(5)	1.454(6)	1.364(6)	1.372(4)
B-N	/	1.439(9)	1.443(4)	/	1.448(5)	1.452(4)
B-B(cage)	/	1.693(10)	1.688(5)	/	1.689(6)	1.684(4)

The 13-vertex carboranes 1,2-(CH₂)₃-1,2-C₂B₁₁H₁₁ (**6**) and 1,2-(CH₂)₄-1,2-C₂B₁₁H₁₁ (**7**) can also react with 1,10-phenanthroline (phen) under the similar reaction condition, but the reactions were much slower. Treatment of **6** with 1 equiv of phen in toluene at 90 °C for 7 d in a sealed tube gave a brown suspension. The solution phase was separated and dried. Recrystallization from CH₂Cl₂ gave 4-(4',7'-2*H*-1',10'-C₁₀H₈N₂B)-μ-1,2-(CH₂)₃-1,2-C₂B₁₀H₉ (**61**) in about 10% isolated yield. Reaction of **7** with 1 equiv of phen was even slower and not completed after 28 d at 110 °C as monitored by ¹¹B NMR spectra. The 4-(4',7'-2*H*-1',10'-C₁₀H₈N₂B)-μ-1,2-(CH₂)₄-1,2-C₂B₁₀H₉ (**62**) was isolated in about 10% yield.

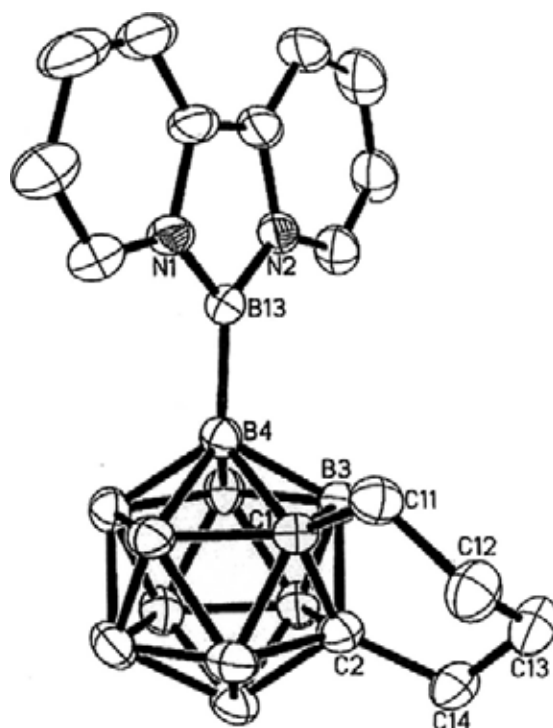
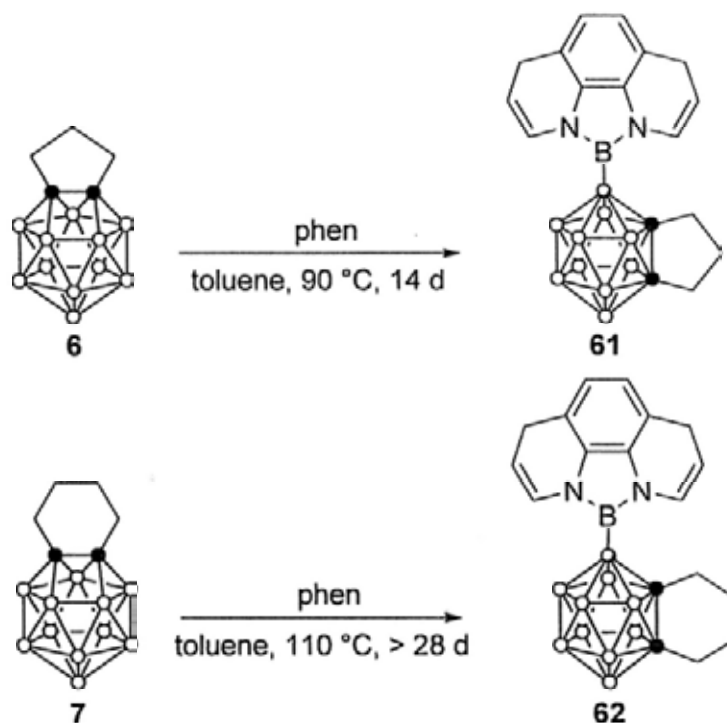


Figure 5.17. Molecular structure of 4-(2,2'-C₁₀H₈N₂B)-μ-1,2-(CH₂)₄-1,2-C₂B₁₀H₉ (60).

Scheme 5.11. Reaction of 13-Vertex Carboranes 1,2-(CH₂)_n-1,2-C₂B₁₁H₁₁ (*n* = 3, 4) with Phen.



These two complexes were characterized by various spectroscopic techniques as

well as HRMS. The broad signals of the boron atom that attached to two nitrogen atoms were observed in the low field at about 20 ppm in the ^{11}B NMR spectra. The unique signals of benzylic CH_2 groups were observed at 3.60 ppm for **61**, 3.61 ppm for **62** in the ^1H NMR spectra, and 25.3 ppm for both in the ^{13}C NMR spectra. Similarly, the ^1H and ^{13}C chemical shifts of the unsaturated units were also up-field shifted, compared to the free ligand (Figure 5.18).

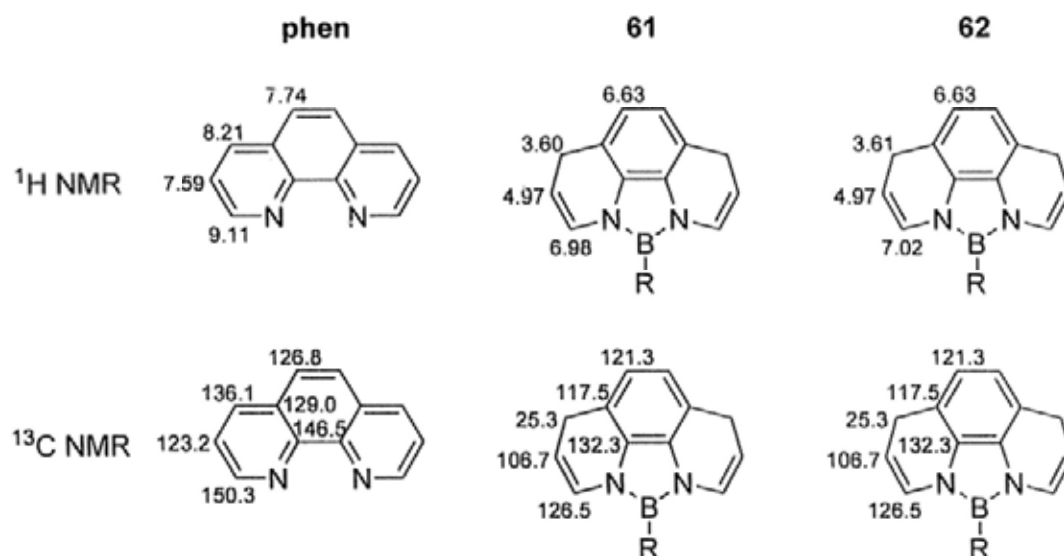


Figure 5.18. ^1H and ^{13}C chemical shifts of the phen units in the free ligand and complexes **61** and **62**.

The structures of complexes **61** and **62** were confirmed by single-crystal X-ray analyses. In both cases, there are two crystallographically independent molecules in the unit cell and the representative ones are shown in Figures 5.19 and 5.20. Again, dramatic change of bond distances is observed between complexes **61** and **62**, and free phen (Table 5.3).¹²² However, different from that of bipy, the aromaticity with the pyridine was lost. It is note that the C23 and C28 atoms in **61** (Figure 5.19), and C17 and C18 atoms in **62** (Figure 5.20) are converted to sp^3 from sp^2 hybridization after taking up two H atoms. Thus a $\text{H}_2(\text{phen})\text{B}$ heterocycle rather than a $(\text{phen})\text{B}$ one was formed. Although no compound containing $\text{H}_2(\text{phen})\text{B}$ unit has been ob-

served as that in **61** or **62**, there have been a handful of 1,3,2-diazaboriline species.¹²³ The *i* bond is shortened by about 0.09 Å in **61** and 0.08 Å in **62**. Meanwhile, the *e*, *g*, *h*, *i* bond distances are close to each other. The average bond lengths of 1.50 (*d*) and 1.47 Å (*c*) in **61**, and 1.50 (*d*) and 1.49 (*c*) Å in **62** confirm the *sp*³ hybridized property of the corresponding carbon atoms.

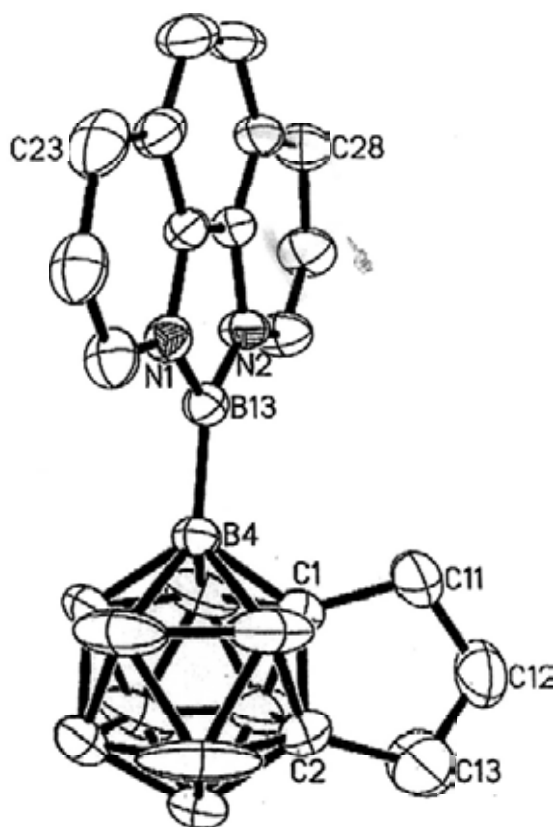


Figure 5.19. Molecular structure of 4-(4',7'-2*H*-1',10'-C₁₀H₈N₂B)- μ -1,2-(CH₂)₃-1,2-C₂B₁₀H₉ (**61**), showing one of the crystallographically independent molecules.

These 4 complexes stand for boranes/carboranes bearing *exo*- B-B bond between a non-classic and a classic boron atom. To the best of our knowledge, these species are very rare in literature, such as 1-BX₂-B₅H₈ (X = F, Cl, Br)¹²⁴ and 2-Br₂B-1,6-C₂B₄H₅.¹²⁵ Formation of complexes **59-62** offers a good opportunity for B-B bond activation study in the field of carborane.

This type of reactions is very different from those observed previously in the nucleophilic reactions of 13-vertex carboranes 1,2-(CH₂)₃-1,2-C₂B₁₁H₁₁ (**6**), in which

closo-CB₁₁⁻, *nido*-CB₁₀⁻ or *closo*-CB₁₀⁻ anions were formed via the cage carbon extrusion reaction. The product can be formally viewed as one boron atom was pulled out of the cage by the bipy or phen with the retention of the cage carbons (Scheme 5.12). Indeed these bidentate ligands play important roles.

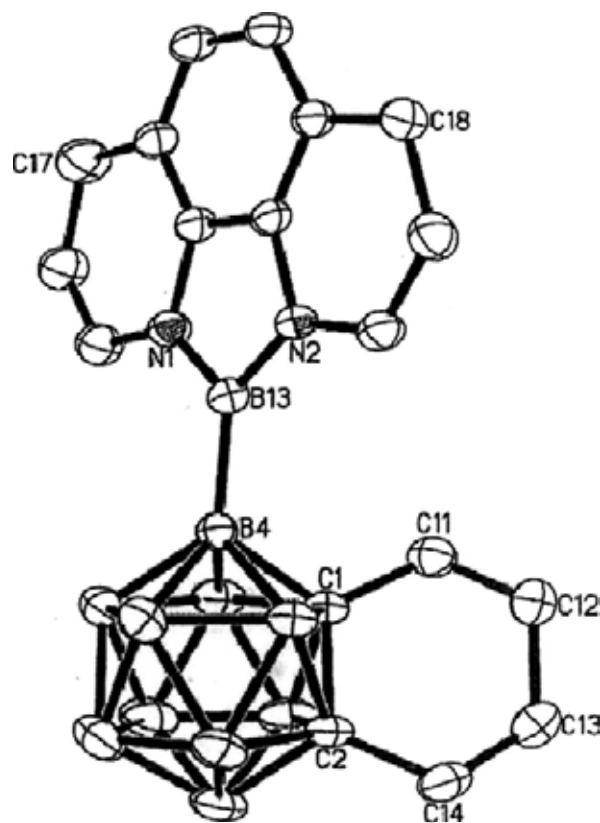
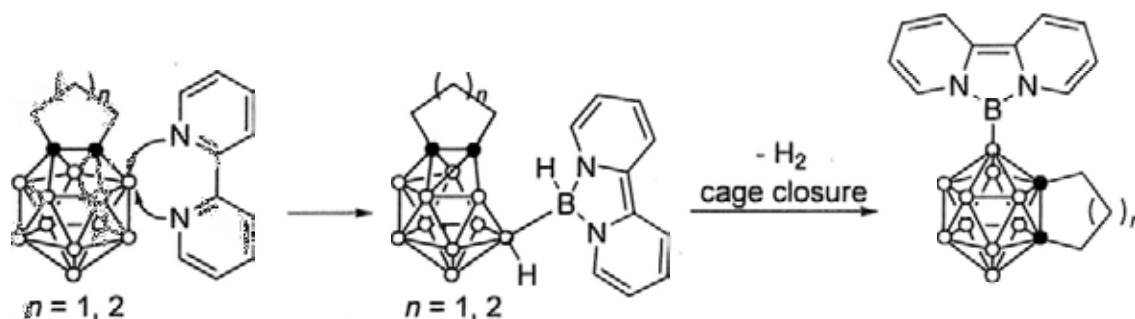


Figure 5.20. Molecular structure of 4-(4',7'-2H-1',10'-C₁₀H₈N₂B)- μ -1,2-(CH₂)₄-1,2-C₂B₁₀H₉ (**62**), showing one of the crystallographically independent molecules.

Scheme 5.12. Formal Formation of *closo*-C₂B₁₀ Products.



However, this would not represent the real process. We noticed that the reaction rate was much slower in the case of phen than in the case of bipy. But it was reported

the basicity of phen is a little bit stronger than bipy,¹²⁶ which indicated the reaction with phen would be quicker. In this regard, it would be presumed that this electronic effect did not govern the reaction rate. On the other hand, in the bipy ligand, the two pyridine units can rotate around the C-C axis, while this rotation is restricted in the phen. Thus, we proposed that simultaneous attack of two N atoms of the bipy or phen ligand might be sterically hindered (Figure 5.21). Moreover, the differences between the reaction rates of **6** and **7** suggest that the deformation of the cage is not only confined by the boron atoms but also by the cage carbon atoms. Thus, a similar boron cation intermediate, as those in the carbon extrusion reactions, may be involved, taking the reaction of **6** with bipy for example (Schem 5.13). A boron cation intermediate **V-D** was initially formed, which underwent electron transfer to give the boryl species **V-E**. Then H-tautomerization gave intermediate **V-F**, which eliminated one molecular of H₂ to give the product **59**.

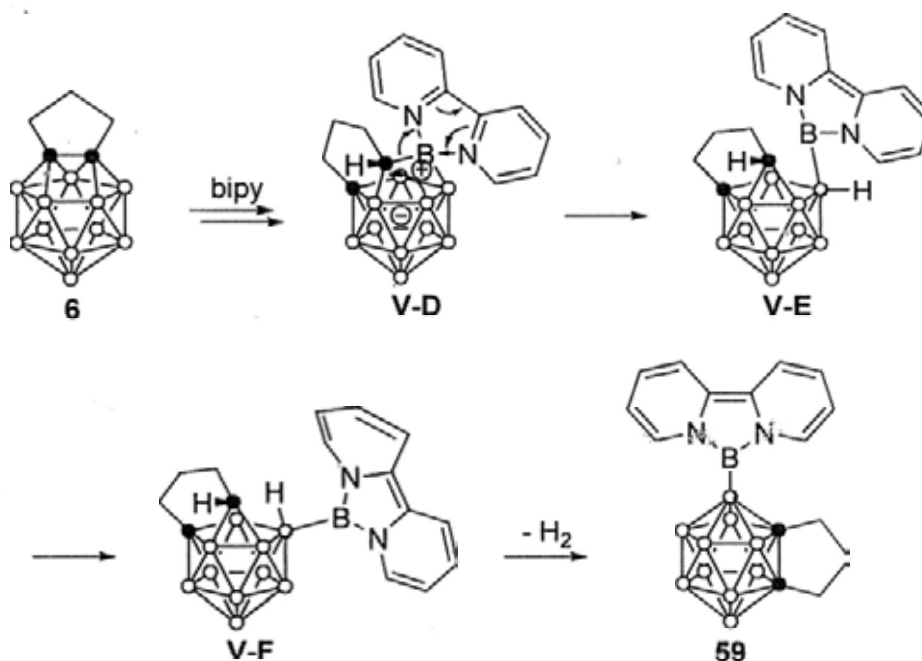


Figure 5.21. Proposed steric hindrance in the reaction of 13-vertex carboranes with bipy and phen.

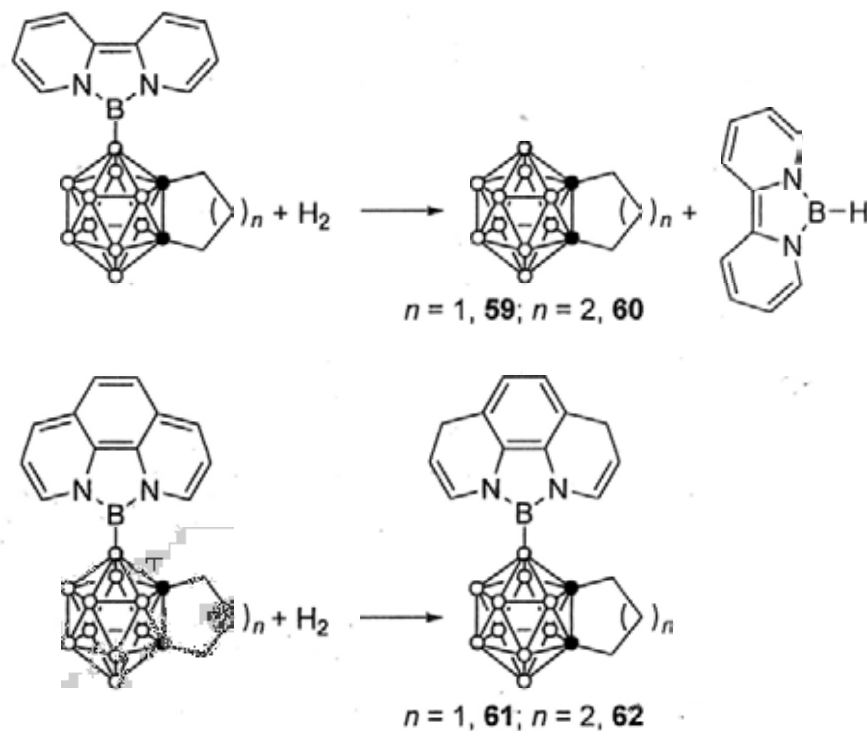
On the other hand, the heterocyclic rings formed in the reactions are different. Two additional H atoms were added to the phen ring, while it did not happen in the bipy case. We observed that at higher temperatures, the reaction rate of 1,2-(CH₂)_n-1,2-C₂B₁₁H₁₁ (*n* = 3, 4) with bipy was much faster, leading to the formation of by-products (bipy)BH and 1,2-(CH₂)_n-1,2-C₂B₁₀H₁₀ (*n* = 3, 4) as suggested by ¹¹B and

^1H NMR spectra. It gave an assumption that similar products were initially formed, which reacted with H_2 at high temperatures in different ways (Scheme 5.14). This might be ascribed to the different reactivity of the macrocyclic systems.

Scheme 5.13. Proposed Mechanism for the Formation of **59** and **60**.



Scheme 5.14. Proposed Formation of **61** and **62**.



5.4. Summary

Besides cage carbon extrusion reaction, cage boron atoms can also be extruded from 13-vertex carboranes under several reaction conditions.

Under basic conditions, μ -1,2-(CH₂)_n-1,2-C₂B₁₁H₁₁ ($n = 3, 4$) can react with MeOH to afford 11-vertex *nido*-CB₁₀⁻ anions [*endo*- μ -7,8-(CH₂)_nCHB(OMe)₂-1-CB₁₀H₁₁]⁻, via different intermediates [μ - η : η : η -7,8,10-(CH₂)₃CHB(OMe)-7-CB₁₀H₁₀]⁻ ($n = 3$) or [3-OMe- μ -1,2-(CH₂)₄-1,2-C₂B₁₁H₁₁]⁻ ($n = 4$). The boronic esters [*endo*- μ -7,8-(CH₂)_nCHB(OMe)₂-1-CB₁₀H₁₁]⁻ can be oxidized to give [*endo*- μ -7,8-(CH₂)_nCHOH-1-CB₁₀H₁₁]⁻, or hydrolyzed to afford [*endo*- μ -7,8-(CH₂)_nCHB(OH)₂-1-CB₁₀H₁₁]⁻ anions.

13-Vertex carborane μ -1,2-(CH₂)₃-1,2-C₂B₁₁H₁₁ can react with pyridines to afford zwitterionic boronium species μ -2,4-(CH₂)₃CHBH(4-RC₅H₄N)₂-2-CB₁₀H₉ (R = H, Me, ^tBu), at low temperatures, whereas a mixture of products containing *closo*-CB₁₁⁻ and *closo*-CB₁₀⁻ complexes was formed at room temperature.

μ -1,2-(CH₂)_n-1,2-C₂B₁₁H₁₁ ($n = 3, 4$) can react with 2,2'-bipyridine or 1,10-phenanthroline to afford 4-(2,2'-C₁₀H₈N₂B)- μ -1,2-(CH₂)_n-1,2-C₂B₁₀H₉ or 4-(4',7'-2H-1',10'-C₁₀H₈N₂B)- μ -1,2-(CH₂)_n-1,2-C₂B₁₀H₉, respectively.

Chapter 6. Nucleophilic Reaction of Other 13- and 14-Vertex Carboranes

The studies mentioned in the previous chapters indicated that the 13-vertex carborane μ -1,2-(CH₂)₃-1,2-C₂B₁₁H₁₁ (**6**) exhibited high reactivities toward nucleophiles, compared to its 12-vertex analogue. Most of the reactions afforded cage carbon extrusion products *closo*-CB₁₁⁻, or cage carbon together with cage boron extrusion products *nido*-CB₁₀⁻ or *closo*-CB₁₀⁻. Most of the reactions were regarded to proceed via the same intermediates [μ - η : η : η -7,8,10-(CH₂)₃CHB(Nu)-7-CB₁₀H₁₀]⁻, and formation of the products was dependent upon the nature of reagents and reaction conditions. Bidentate bipyridine ligands afforded the cage boron extrusion products with cage carbons retention as major products. Deprotonation of the α -CH proton in **6** was also observed by treatment with several kinds of bases in THF. On the other hand, linkage effects of 13-vertex carboranes were noted. To further explore the reactivity pattern of supercarboranes, we have extended our research to include other 13- and 14-vertex carboranes. Reactions of 13-vertex CAd carborane μ -1,2-(CH₂)₄-1,2-C₂B₁₁H₁₁ (**7**), 13-vertex CAp carborane 1,12-Me₂-1,12-C₂B₁₁H₁₁ (**17b**) and 14-vertex carboranes μ -2,3(8)-(CH₂)₃-2,3(8)-C₂B₁₁H₁₁ (**27**) with nucleophiles will be described.

6.1. Nucleophilic Reaction of 13-Vertex Carborane μ -1,2-(CH₂)₄-1,2-C₂B₁₁H₁₁

6.1.1. Reaction with Group 16 Nucleophiles

As mentioned in Chapter 5, reaction of μ -1,2-(CH₂)₄-1,2-C₂B₁₁H₁₁ (**7**) with MeOH in the presence of base such as Et₃N or PS at room temperature gave the 13-vertex *nido*-carborane anion [μ -1,2-(CH₂)₄-1,2-C₂B₁₁H₁₁]⁻ (**[49]**), in which the methoxy group was attached to a 7-coordinated cage boron and the terminal H

was converted to a bridging one. Reaction of **7** with pure MeOH, however, was not as facile and proceeded very slow at room temperature. This reaction was closely monitored by ^1H and ^{11}B NMR spectra in CD_3OD . An initial partial formation of $[\mathbf{49}]^-$ was observed, which finally disappeared after 28 d. Species like *closo*- CB_{11}^- and C_2B_{10} were formed as evidenced by the ^{11}B NMR spectra, and the peak of $\text{B}(\text{OMe})_3$ was detected at 18 ppm. During the whole process, two weak but characteristic signals at about 5.82 (br) and 5.66 (d, $J = 13.9$ Hz) ppm were observed, which almost disappeared after prolonged reaction, indicative of the formation of $[\mu\text{-}1,2\text{-}(\text{CH}_2)_3\text{CH}=\text{CH}\text{-}1\text{-CB}_{11}\text{H}_{10}]^-$ ($[\mathbf{63}]^-$). Compound $\mu\text{-}1,2\text{-}(\text{CH}_2)_4\text{-}1,2\text{-C}_2\text{B}_{10}\text{H}_{10}$ (**3**) was also detected from the ^1H NMR, besides messy peaks which were observed but hard to resolve. We also found that the ratio of the products was temperature dependent. Generally, at higher temperatures the reaction proceeded much faster with the formation of more deboration product **3**.

In this regard, a typical reaction was attempted at 40 °C to minimize the deboration reaction. A MeOH solution of 1 mmol of **7** was heated at 40 °C in a sealed tube for 14 d. After addition of an excess amount of PS, a mixture of ionic complexes was produced in about 70% total yield, besides the isolation of 10% compound **3**. They were not separable, but can be identified by ^1H , ^{13}C NMR and two-dimensional NMR techniques.

A mixture containing about 50% $[\mu\text{-}1,2\text{-}(\text{CH}_2)_3\text{CH}(\text{CH}_2\text{OMe})\text{-}1\text{-CB}_{11}\text{H}_{10}][\text{PSH}]$ ($[\mathbf{64}][\text{PSH}]$) and about 20% $[\mu\text{-}1,2\text{-}(\text{CH}_2)_5\text{-}1\text{-CB}_{11}\text{H}_{10}][\text{PSH}]$ ($[\mathbf{65}][\text{PSH}]$) were obtained (Scheme 6.1). As shown in Figure 6.1, the signals of the methylene and methyl group that were attached to the O atom in $[\mathbf{64}]^-$ were observed at 79.0 and 68.6 ppm, respectively, in the ^{13}C NMR spectra. Other three sharp peaks of the methylene groups were at 35.8, 25.7 and 23.9 ppm, respectively. The four sharp signals of the

methylene units in **[65]**⁻, were observed at 40.9, 33.3, 28.0 and 27.6 ppm, respectively. Other two minor products were regarded as $[\mu\text{-}1,2\text{-(CH}_2\text{)}_4\text{CHOMe-}1\text{-CB}_{11}\text{H}_{10}\text{]PSH}$ (**[66a]**⁻) and $[\mu\text{-}1,2\text{-(CH}_2\text{)}_3\text{CHOMeCH}_2\text{-}1\text{-CB}_{11}\text{H}_{10}\text{]PSH}$ (**[66b]**⁻), as two methyl groups were observed at 55.0 and 57.6 ppm in the ¹³C NMR spectra. Besides, the unique methyldene signal in **[66b]**⁻ was observed at 82.1 ppm.

Scheme 6.1. Reaction of $\mu\text{-}1,2\text{-(CH}_2\text{)}_4\text{-}1,2\text{-C}_2\text{B}_{11}\text{H}_{11}$ (**7**) with MeOH at 40 °C.

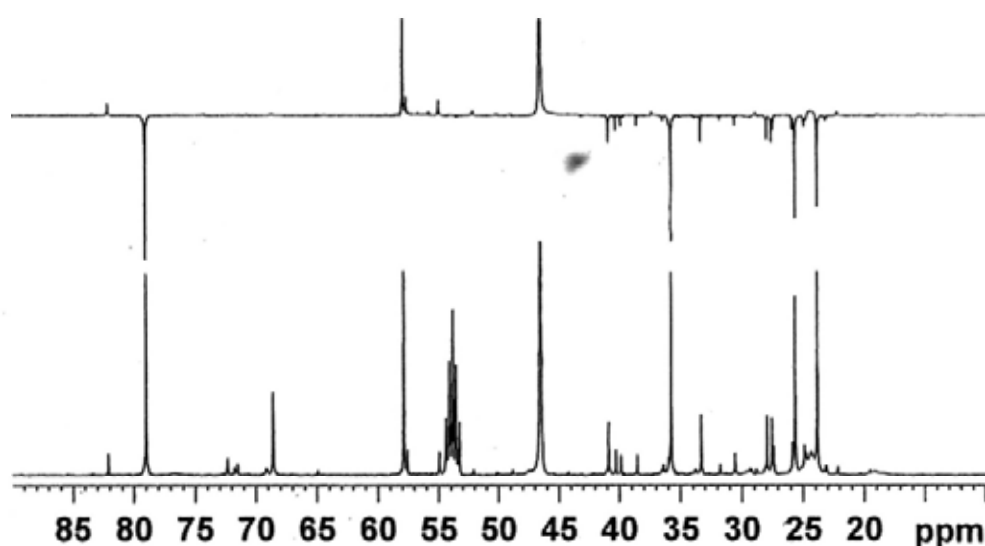
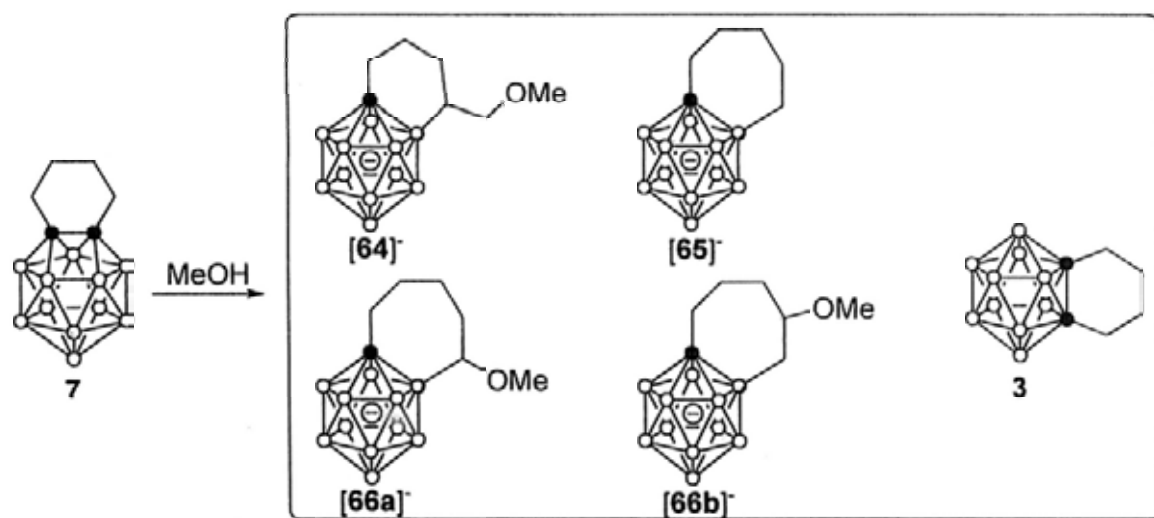


Figure 6.1. ¹³C (bottom) and DEPT135 (top) NMR spectra (partial) of the mixture.

Formation of these anions was also confirmed by negative FAB MS spectrometry (Figure 6.2). It displayed one signal group centered at m/z 241 corresponding to the

anion $[64]^-$ and another at m/z 211 attributable to the anion $[65]^-$. Recrystallization from a CH_2Cl_2 solution afforded some crystals which were structurally characterized as $[65][\text{PSH}]$, although its resolution was not good. The geometry of the anion is similar to those of *closo*- CB_{11}^- anions (Figure 6.3).

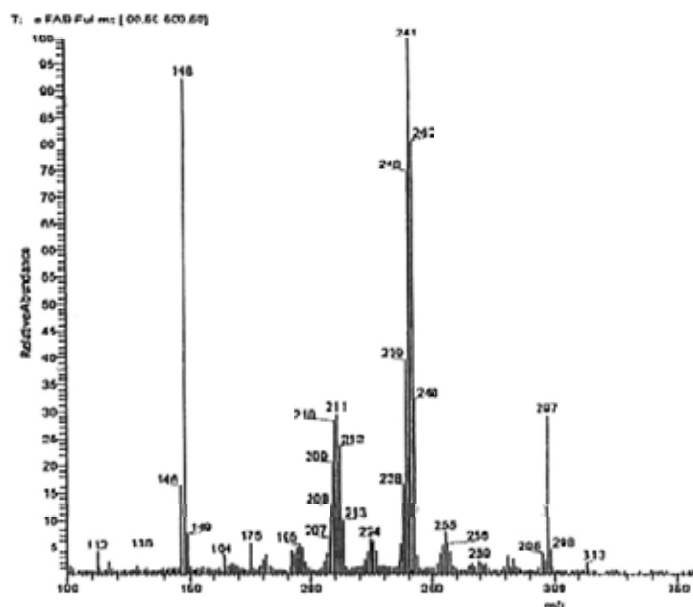


Figure 6.2. Negative FAB MS spectrometry of the mixture.

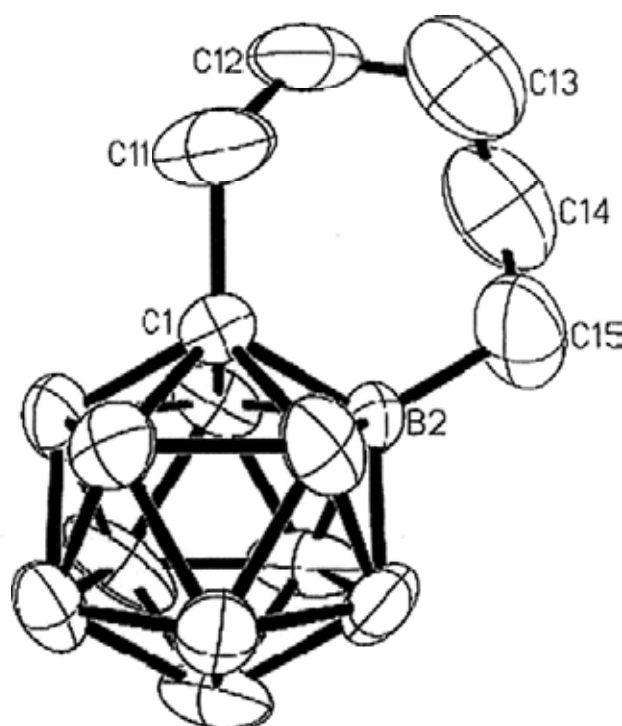
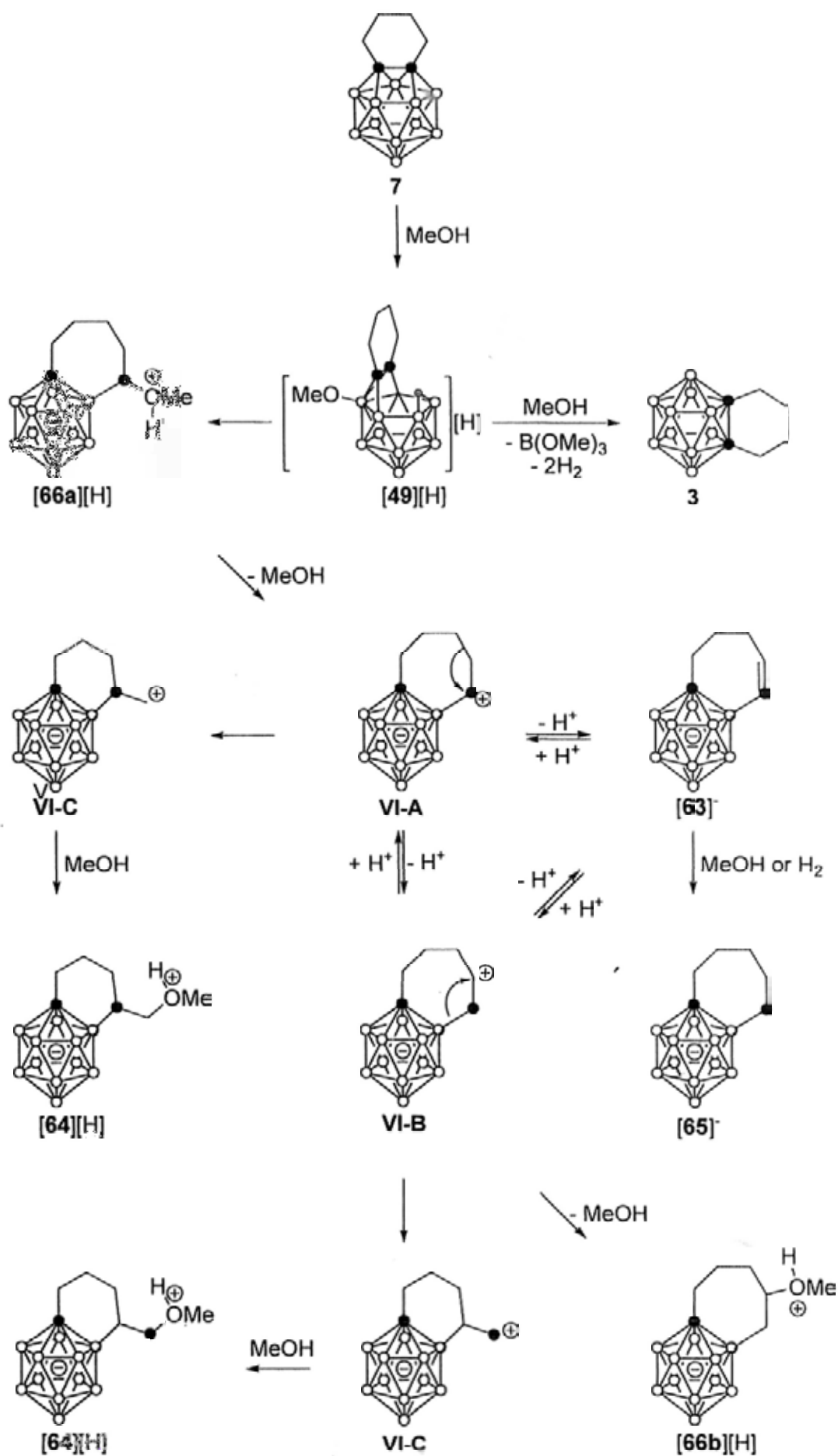


Figure 6.3. Structure of $[\mu\text{-}1,2\text{-(CH}_2\text{)}_5\text{-}1\text{-CB}_{11}\text{H}_{10}]^-$ ($[65]^-$), in $[65][\text{PSH}]$, showing one of the two crystallographic independent molecules.

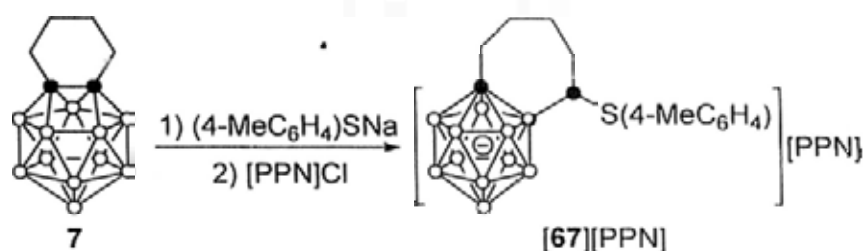
Scheme 6.2. Possible Reaction Pathway of Compound 7 with MeOH.



The above results gave a possible reaction pathway of compound **7** and MeOH (Scheme 6.2), although the cage transformation process was not clear. MeOH would attack one of the cage boron atoms in **7** to give **[49][H]**. Deboration of this intermediate affords compound **3** and B(OMe)₃ together with H₂, although it is still uncertain why *closo*- species was formed rather than the normal *nido*- species.³⁴ On the other hand, carbon extrusion can occur to give anion **[66a]**⁻. Acid promoted isomerization leads to the formation of **[63]**⁻ and **[66b]**⁻, via the carbocation intermediates **VI-A** and **VI-B**. **VI-C** may result from alkyl migration from **VI-A**, or boryl migration from **VI-B**, then give **[64]**⁻. Indeed, formation of this product with 6-membered ring could be ascribed to the relative stability compared to that of a 7-membered ring. **[65]**⁻ may be formed from hydrogenation of **[63]**⁻ by either MeOH as that in Chapter 4 or by H₂ that released from the reaction.

Compound **7** can also react with (4-MeC₆H₄)SNa to give CB₁₁⁻ anion. Treatment of **7** with 1 equiv of (4-MeC₆H₄)SNa in THF overnight, followed by salt metathesis with [PPN]Cl gave a pale yellow solution. Although the ¹¹B NMR spectra showed a mixture of products formation, a single product was generated after 60 d which was identified as [μ -1,2-(CH₂)₄CHS(4-MeC₆H₄)-1-CB₁₁H₁₀][PPN] (**[67][PPN]**) in about 80% isolated yield (Scheme 6.3). Closely monitoring the reaction by ¹¹B NMR showed that the starting material **7** quickly disappeared to give an unidentified intermediate. Many attempts to isolate this product failed. Conversion of this intermediate to **[67]**⁻ was very slow at room temperature and even not completed within one month. This process can be, however, accelerated by heating the solution at 70 °C and completed in one day. Its formation may be ascribed to that the thiolate is a better nucleophile than MeOH, and acidic media is crucial for the deboration and isomerization processes.

Scheme 6.3. Reaction of μ -1,2-(CH₂)₄-1,2-C₂B₁₁H₁₁ (**7**) with (4-MeC₆H₄)SNa.



Complex [67][PPN] was characterized by several spectroscopic techniques as well as elemental analyses. Its B atom with alkyl substituent was unambiguously determined at -6.6 ppm in the ¹¹B NMR spectra as a singlet. The C atom that attached to it was observed as a broad signal at 35.9 ppm in the ¹³C NMR spectrum. Single crystals suitable for X-ray diffraction study were grown from a solution of THF/DME. X-ray analysis confirmed its ionic nature with solvation of a THF molecule. The structure of the anion is shown in Figure 6.4.

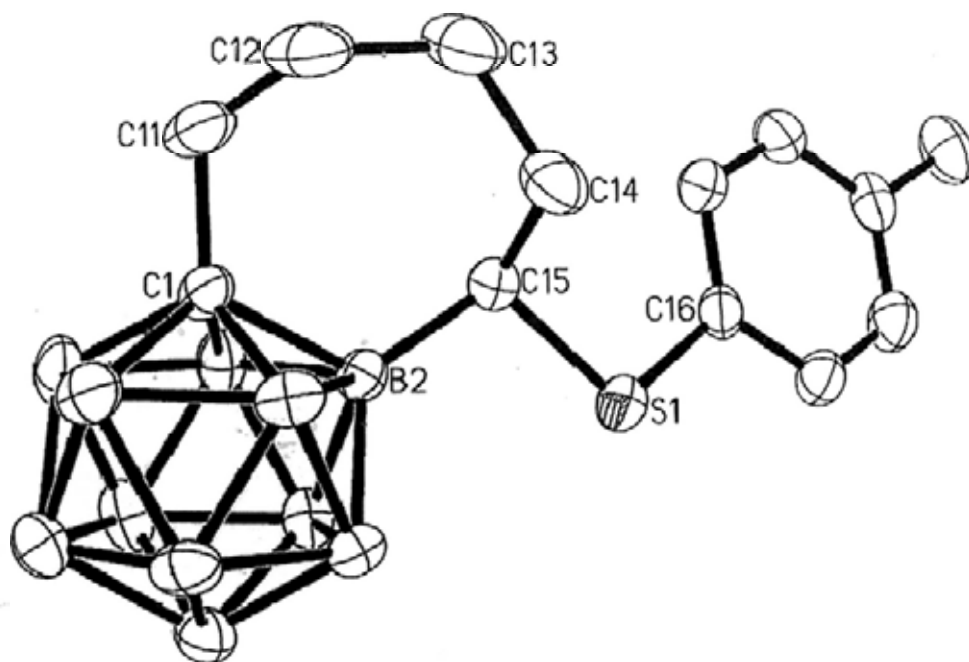


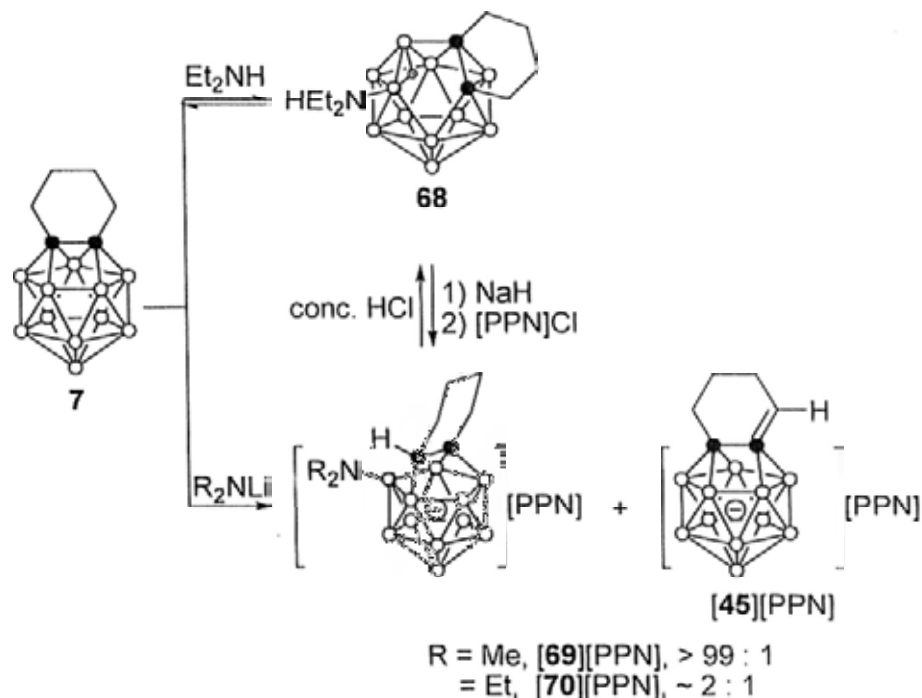
Figure 6.4. Structure of $[\mu$ -1,2-(CH₂)₄CHS(4-MeC₆H₄)-1-CB₁₁H₁₀]⁻ ([67]⁻), in [67][PPN]·THF.

6.1.2. Reactions with Nitrogen Nucleophiles

Reactions of 13-vertex carborane μ -1,2-(CH₂)₄-1,2-C₂B₁₁H₁₁ (**7**) with nitrogen

nucleophiles were very different from those described in the previous section. Et₂NH, a secondary amine, reacted with **7** much more smoothly than with MeOH. Treatment of compound **7** with excess Et₂NH in toluene afforded, after recrystallization from CH₂Cl₂, a zwitterionic *nido*- species 3-NEt₂H- μ -1,7-(CH₂)₄-1,7-C₂B₁₁H₁₁ (**68**) in > 90% isolated yield, (Scheme 6.4).

Scheme 6.4. Reactions of μ -1,2-(CH₂)₄-1,2-C₂B₁₁H₁₁ (**7**) with Nitrogen Nucleophiles.



Dynamic processes were observed in solution, which made characterization of **68** difficult. Its ¹¹B NMR exhibited a 2:2:4:2:1 pattern in the range 4.1 to -33 ppm. In addition, the peaks of 13-vertex carborane μ -1,2-(CH₂)₄-1,2-C₂B₁₁H₁₁ (**7**) at 0.2 and -0.6 ppm were observed. Moreover, the peaks of free Et₂NH and **7** were also found in the ¹H and ¹³C NMR spectra. These data indicated that the formation of **68** in solution would be reversible. Its ¹H and ¹³C NMR spectra exhibited broad signals of the methylene group that attached to the N atom or the cage carbons. Only two of four hydrogens of the CCH₂ unit were well defined in the ¹H NMR spectrum at 2.11 ppm, whereas the other two were broadened signals. The corresponding carbon atoms

were also observed as a very broad signal at about 38 ppm. The cage carbons were not observed in CD_2Cl_2 .

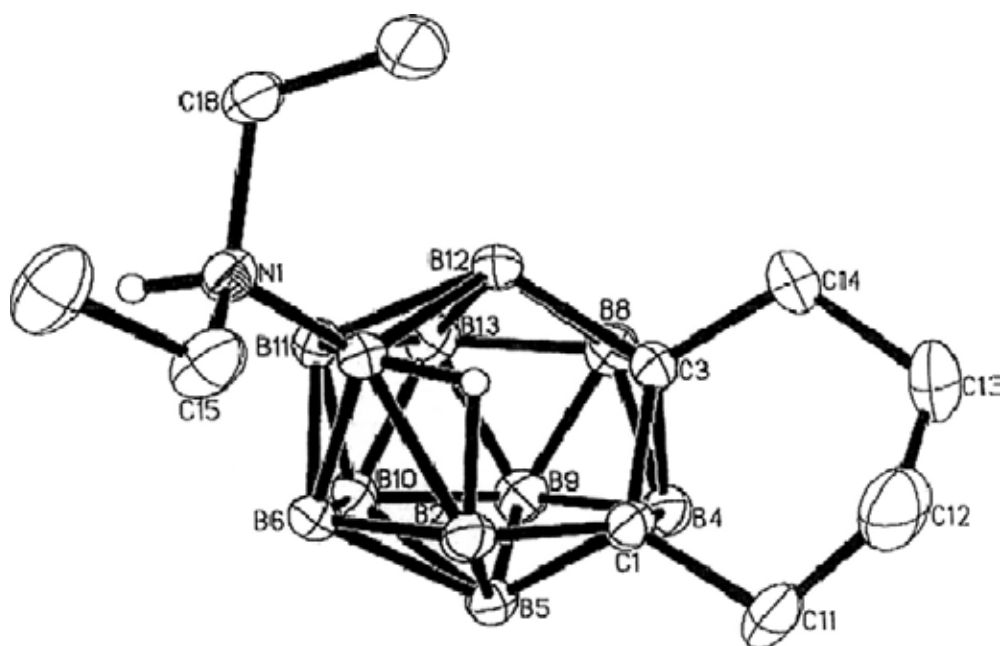


Figure 6.5. Molecular structure of 3- NEt_2H - μ -1,7- $(\text{CH}_2)_4$ -1,7- $\text{C}_2\text{B}_{11}\text{H}_{11}$ (**68**).

On the other hand, its solid-state structure was unambiguously confirmed by single-crystal X-ray analyses and shown in Figure 6.5. Its cage geometry is very similar to those of 13-vertex *nido*-carborane dianions that are formed from reduction of 13-vertex *closo*-carboranes, and can be viewed as removal of one vertex from a 14-vertex *closo*-carborane. However, its cage carbons are located on 2,3- but not on 1,2-positions. The NEt_2H group is attached to the B7 atom, which is opposite to two cage carbons in the 5-membered open face. This B-N bond length of 1.580(2) Å indicates a normal single bond and π - π conjugation would not exist.¹¹⁰ Moreover, the corresponding C-N-C, C-N-B and B-N-C bond angles of 114.4(1)°, 111.9(1)° and 111.6(1)° indicative of the sp^3 -hybridized property of the N atom. The two ethyl groups on the N atom and the cage are in the *trans*-conformation around the N1-B7 bond, which would be ascribed to both of the stereo repulsion of big substituents and electronic repulsion of the two protonic H atoms (Figure 6.6).

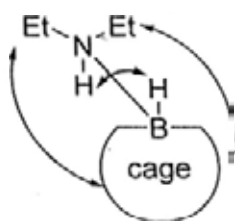


Figure 6.6. Stereo and electronic repulsion in **68**.

The cage geometry of **68** would represent the first intermediate in the reaction of nucleophiles with 13-vertex CAd carboranes. However, complex **68** was hard to convert to $[\mu-\eta:\eta:\eta-7,8,10-(\text{CH}_2)_4\text{CHB}(\text{Nu})-7\text{-CB}_{10}\text{H}_{10}]^-$, as monitored by ^{11}B NMR spectra, but slow formation of CB_{11}^- species would be expected. And messy products formation was detected in the ^1H NMR. Heating would promote this transformation process but single product was not isolated from mixture. This further indicated that ring expansion from a 6-membered ring to a 7-membered one was not as facile as that from a 5-membered one to a 6-membered one, in the cage carbon extrusion reaction of 13-vertex carboranes.

Reactions of **7** with amide gave products with different cage geometry. Treatment of **7** with 1 equiv of Me_2NLi in toluene followed by cation exchange with $[\text{PPN}]\text{Cl}$ afforded $[\mu-9\text{-NMe}_2-7,8,10-(\text{CH}_2)_4\text{CCH-B}_{11}\text{H}_{10}][\text{PPN}]$ (**[69]** $[\text{PPN}]$) as pale yellow crystals in about 80% isolated yield. On the other hand, when Et_2NLi was used, a mixture of $[\mu-9\text{-NEt}_2-7,8,10-(\text{CH}_2)_4\text{CCH-B}_{11}\text{H}_{10}][\text{PPN}]$ (**[70]** $[\text{PPN}]$) and deprotonated species **[45]** $[\text{PPN}]$ was afforded in a ratio of about 2:1. Attempted purification of **[70]** $[\text{PPN}]$ failed. However, when **68** was deprotonated by NaH , **[70]** $^-$ was formed almost quantitatively as evidenced by ^{11}B NMR. Cation exchange with $[\text{PPN}]\text{Cl}$ followed by recrystallization from CH_2Cl_2 gave **[70]** $[\text{PPN}]$ as a pale yellow solid in about 95% isolated yield (Scheme 6.4).

Complexes **[69]** $[\text{PPN}]$ and **[70]** $[\text{PPN}]$ were characterized by several spectroscopic techniques as well as elemental analyses. They exhibited very similar ^{11}B NMR spec-

tra, in which the downfield-shifted signals of the B atoms that attached to the N atoms were observed at about 50 ppm as singlet for each. The peaks of the α -CH were observed at 1.26 ppm for [69]⁻ and 1.32 ppm for [70]⁻ in the ¹H NMR spectra, and the corresponding ¹³C signals were observed at 6.8 ppm and 8.5 ppm, respectively, which suggested the H-migration from boron to carbon.

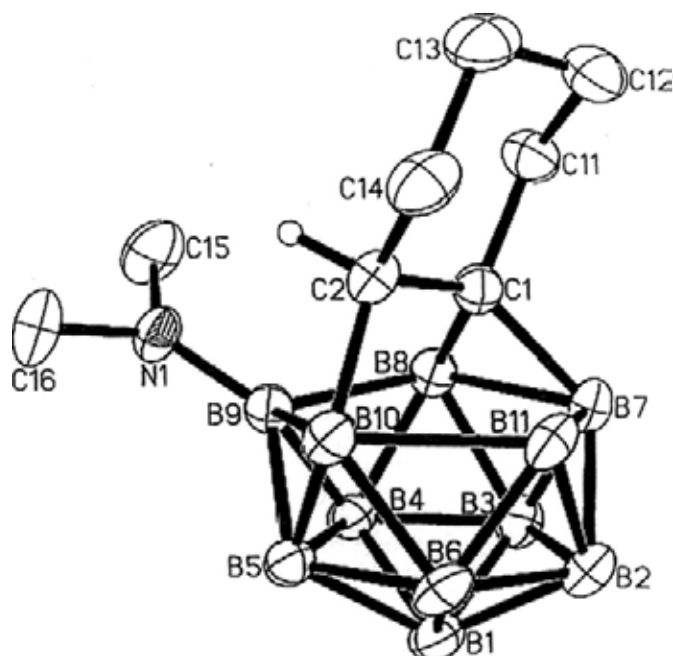


Figure 6.7. Structure of [9-NMe₂-μ-7,8,10-(CH₂)₄CCH-B₁₁H₁₀]⁻ ([69]⁻), in [69][PPN].

Molecule structure of [69][PPN] and [70][PPN] were confirmed by single-crystal X-ray analyses and the anions were shown in Figures 6.7 and 6.8. The geometry of these 13-vertex *nido*-carborane anions can be viewed as an 11-vertex *nido*-B₁₁ cage that was capped with a bridging (CH₂)₄CCH unit. The amido group was terminally bound to the cage B₉ atom with a bond length of 1.405(5) Å in [69]⁻ and 1.411(6) Å in [70]⁻, and showed B=N double bond characters.¹¹⁰ This N atom and the B atom and two C atoms around it are almost coplanar with a sum of bond angles around N atom of 359.7(4)° in [69]⁻ and 360.0(4)° in [70]⁻, confirming the *sp*² hybridization of the N atom. The cage C1 and C2 atoms are still bonded with a distance of 1.535(5)

Å in [69]⁻ and 1.542(6) Å in [70]⁻. The sum of angles around the C2 atom indicates that it bounds to a hydrogen atom, in each case.

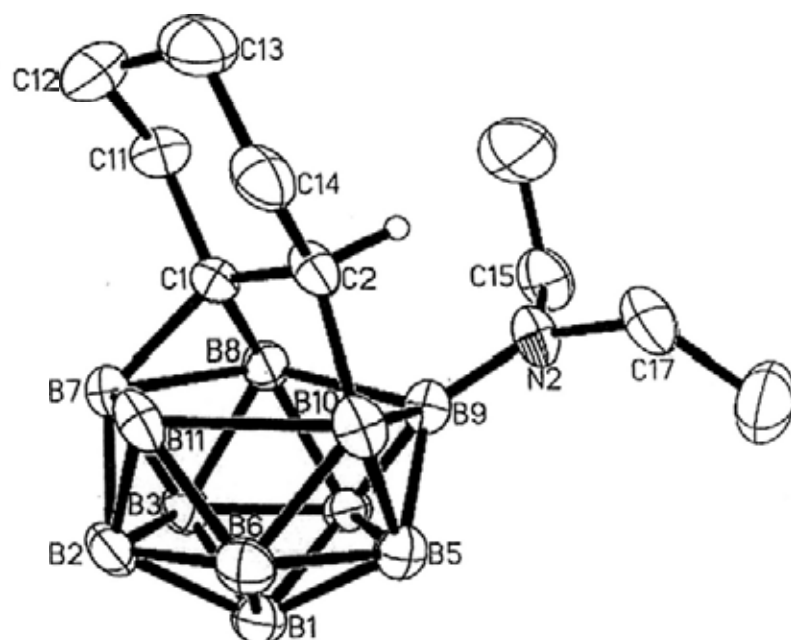


Figure 6.8. Structure of [9-NEt₂-μ-7,8,10-(CH₂)₄CCH-B₁₁H₁₀]⁻ ([70]⁻), in [70][PPN].

Heteroboranes bearing exopolyhedral dative B=N bonds have been reported by Paetzold¹²⁷ and Sneddon,¹²⁸ and the geometries were optimized by theoretical calculations. The calculated values are 1.398 Å for 6-(Me₂N)-*nido*-5,7-C₂B₈H₁₁, 1.398 Å for 6-(^tBuNH)-*nido*-5,7-C₂B₈H₁₁, 1.386 Å for 6-ClC₆H₄-9-(^tPr₂N)-*nido*-6-NB₉H₁₀, and 1.381 Å for 6-ClC₆H₄-9-(^tBuHN)-*nido*-6-NB₉H₁₀.¹²⁸ These short B-N bond distances are close to those of [69]⁻ and [70]⁻. Similarly, the B=N double bond in these two complexes would be formed by donating the lone pair electrons of the N atom to the vacant orbital on B9 atom, as shown in Figure 6.9. Besides, a hybrid *nido*-*dolarachno* structural formulation arising from the increased cage skeletal electron count resulting from the electron-pair donation of the amino group would also be envisaged.

On the other hand, the formation of [70]⁻ from complex **68** was reversible. Upon addition of excess amount of conc. HCl, [70]⁻ was converted to **68** immediately as

evidenced by ^{11}B and ^1H NMR spectra. These results clearly indicated the influences of the substituents' electronic properties on the products formation. While the electron deficient unit R_4N^+ cannot donate electrons to the cage, the bridging H atom, which was positive charged, preferred to reside on the electron rich boron atom(s). Addition of the H^- source would deprotonate the more acidic proton on the ammonium ion, leading to the formation of a lone pair of electrons on the N atom. Donation of lone-pair electrons to the cage causes electron redistribution of the cage. In this case, the protic H atom would no longer reside on the less basic B atoms, promoting H-migration to one of the cage carbons. This influence was further proved by the reversibility of the H-migration process.

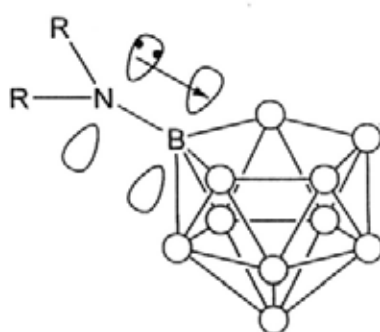
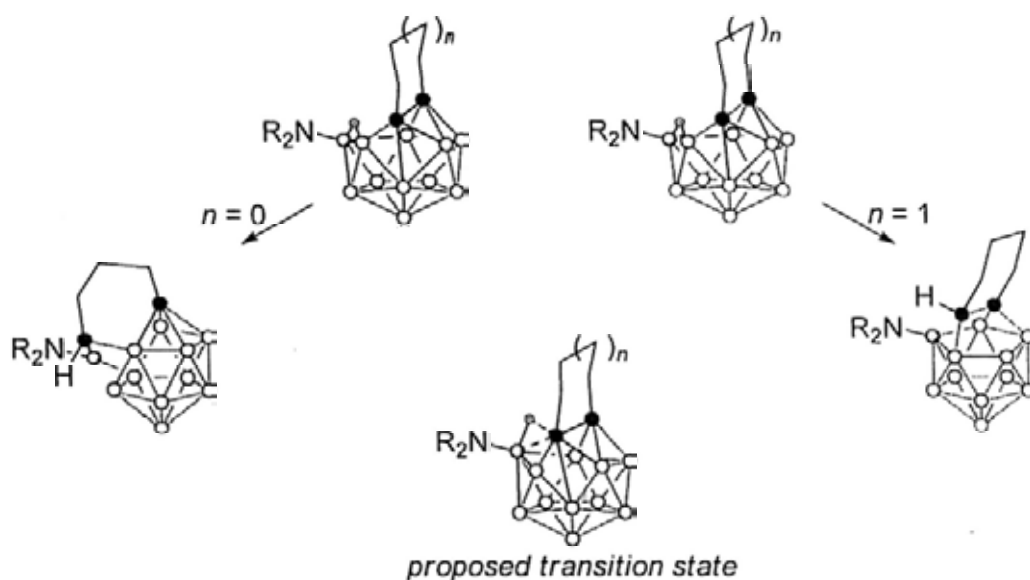


Figure 6.9. Possible B=N bond formation by electron donation from the lone pair electrons to the vacant orbital on the B atom in [69]⁻ and [70]⁻. The cage carbons were not shown.

This cage transformation process is shown in Scheme 6.5. In the proposed transition state, the boron atom bearing a bridging H atom and an amino group would approach one of the cage carbons. The major differences between a 5-membered and a 6-membered carbon ring system were, that in the former case the C-C bond was broken and a new C-B bond was formed, while in the latter case the C-C bond remained with no C-B bond formation. One possible reason was that ring expansion from 6- to 7-membered ring would be energetically not favorable as that from 5- to 6-

membered one.

Scheme 6.5. Proposed Cage Transformation Process of 13-Vertex Carborane-Nucleophile Adduct.



Moreover, the above results indicated that the reaction of nucleophiles with μ -1,2-(CH₂)₄-1,2-C₂B₁₁H₁₁ (**7**) was highly dependent upon the reagents used. Different cluster formation was observed when the nature of the nucleophiles was changed.

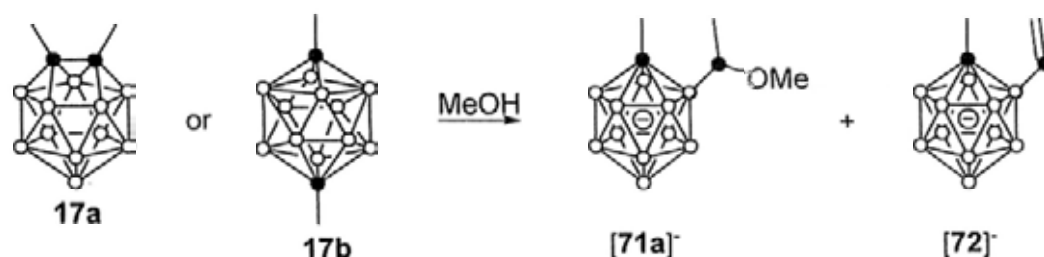
6.2. Nucleophilic Reactions of CAP 13-Vertex Carborane 1,12-Me₂-1,12-C₂B₁₁H₁₁

6.2.1. Reaction with Group 16 Nucleophiles

Reaction of CAP 13-vertex carborane 1,12-Me₂-1,12-C₂B₁₁H₁₁ (**17b**) with pure MeOH gave a similar result as that of CAD one μ -1,2-(CH₂)₃-1,2-C₂B₁₁H₁₁ (**6**), although at a little slower rate. A MeOH solution of **17b** was stirred at room temperature for 24 h, followed by addition of [Me₃NH]Cl to give [1-Me-2-CH(OMe)Me-1-CB₁₁H₁₀][Me₃NH] (**[71a][Me₃NH]**) as colorless crystals in about 50% yield (Scheme 6.6). If the reaction was further stirred for several days, or heated at 70 °C for 24 h, a mixture containing **[71a][Me₃NH]** and [1-Me-2-CH₂=CH-1-CB₁₁H₁₀][Me₃NH]

([72][Me₃NH]) in a ratio of about 1.4:1 was obtained which was hard to be separated. The formation of anion [72]⁻ would proceed via a similar acid promoted MeOH elimination process.

Scheme 6.6. Reaction of 13-Vertex Carboranes without C,C'-Linkage with MeOH.



Complex [71a][Me₃NH] was characterized by several spectroscopic techniques as well as elemental analyses. Complex [72][Me₃NH], however, was only identified from [71a][Me₃NH] in the mixture. In [71a]⁻, the unique boron atom with *exo*-substituent was unambiguously determined in the ¹¹B NMR at -5.0 ppm, while that in [72]⁻ was observed at -6.6 ppm. The broad signal of α -C attached to this boron atom is observed at 74.0 ppm in the ¹³C NMR. On the other hand, three characteristic peaks of the vinyl group in [72]⁻ were observed at 6.04 (dd), 5.47 (d) and 5.38 (br) ppm, respectively, in the ¹H NMR spectra. The corresponding carbon signals appeared at 141.4 (br) and 125.2 ppm in the ¹³C NMR spectra.

The icosahedral cage geometry of [71a][Me₃NH] was determined by single-crystal X-ray analyses and shown in Figure 6.10, which has similar structural features of monocarba-*closo*-dodecaborate anions. The N-H \cdots O hydrogen bonding interactions were observed between the ammonium cation and methoxy group. Meanwhile, some tiny crystals were found among other crystals, which was structurally characterized as [72][Me₃NH] (Figure 6.11). The C12-C13 bond length of 1.298(4) Å in [72]⁻ clear indicates a double bond character.

The CAD analogue 1,12-Me₂-1,12-C₂B₁₁H₁₁ (17a) also gave the same products

mixture as that of **17b** as monitored by ^1H and ^{11}B NMR in CD_3OD (Scheme 6.5). Comparing to that only starting material and products were observed in the reaction of **17b** with MeOH in the ^{11}B NMR spectra, the reaction of **17a** with CD_3OD was more complicated, with gradual formation of **17b** and CB_{11}^- anions [**71a**] $^-$ and [**72**] $^-$ with other messy peaks. They were finally converted to the [**71a**] $^-$ and [**72**] $^-$ mixture as monitored by ^{11}B and ^1H NMR.

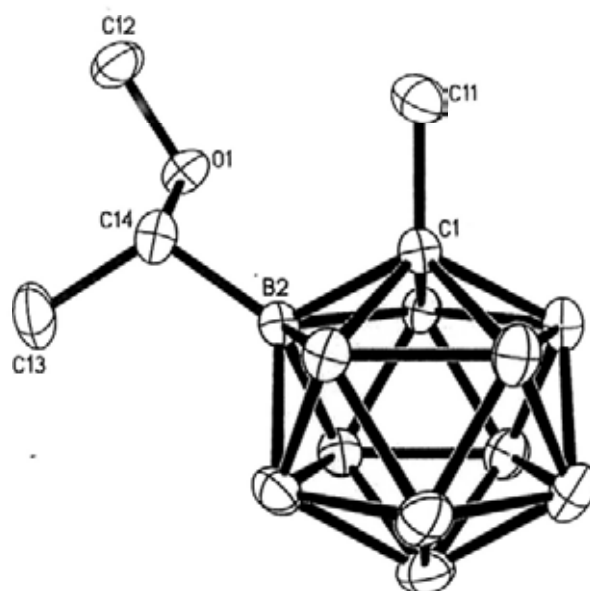


Figure 6.10. Structure of $[\text{1-Me-2-CH}(\text{OMe})\text{Me-1-CB}_{11}\text{H}_{10}]^-$ (**[71a]**), in **[71a][Me₃NH]**.

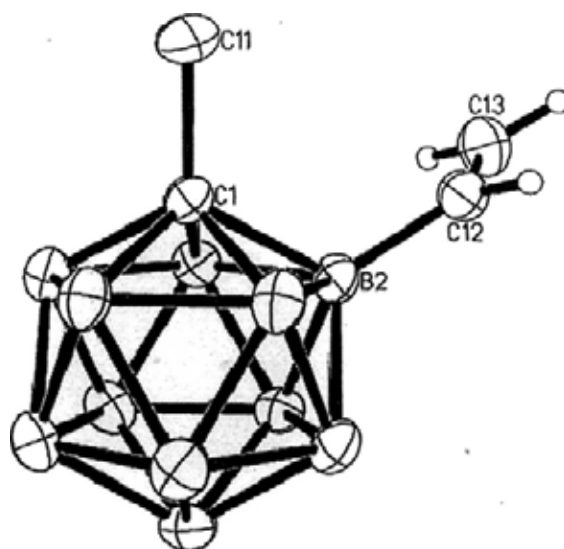


Figure 6.11. Structure of $[\text{1-Me-2-CH}_2=\text{CH-1-CB}_{11}\text{H}_{10}]^-$ (**[72]**), in **[72][Me₃NH]**.

We were interested in the possible intermediate in the reaction of **17b** with MeOH, as the remarkable cage carbon shifts and cage deformation took place. We tried to trap this intermediate by using excess amount of PS in MeOH. An intermediate $[71i']^-$, which might be $[7\text{-Me-}\mu\text{-}\eta\text{:}\eta\text{-}8,10\text{-MeCHB(OMe)-}7\text{-CB}_{10}\text{H}_{10}]$ as that of $[36i']^-$, or species with similar structure, was detected from ^{11}B (Figure 6.12) and ^1H NMR spectra as soon as CD_3OD was added to **17b**. The singlet at about 46 ppm in the ^{11}B NMR spectra together with a doublet at about 1.00 ppm of the methyl group in the ^1H NMR spectra indicated that H-migration from cage boron to cage carbon would take place.

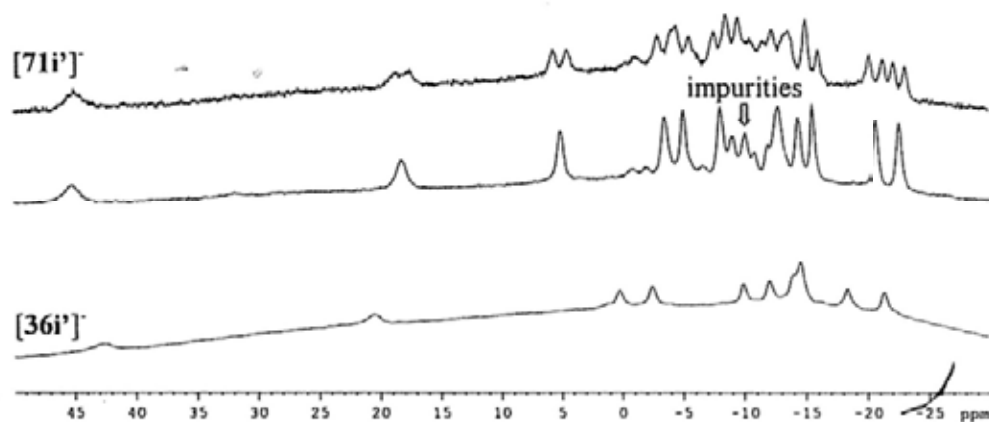
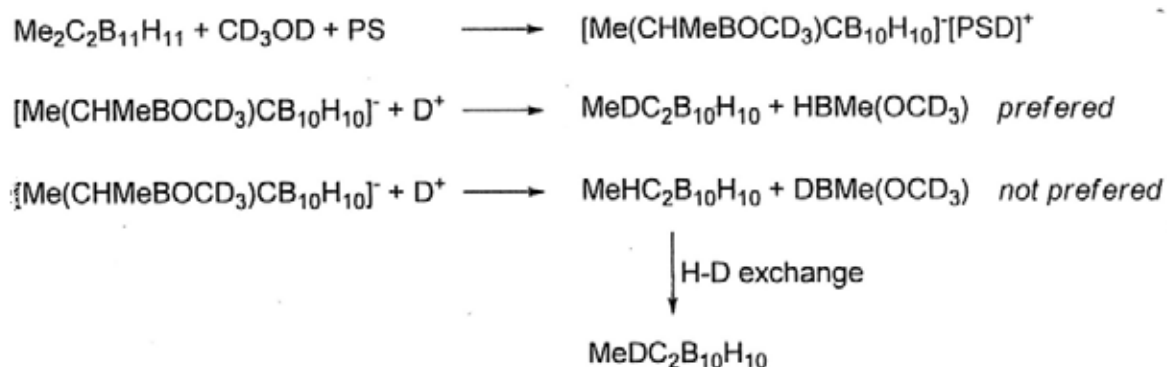
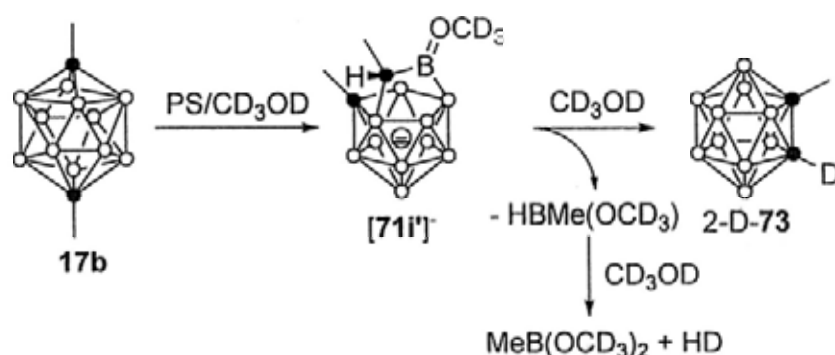


Figure 6.12. Comparison of the ^{11}B NMR spectra of $[71i']^-$ (top: ^1H -coupled; middle: ^1H -decoupled) and $[36i']^-$ (bottom).

But unlike $[36i']^-[\text{PSH}]$, which was much more stable in MeOH, $[71i']^-[\text{PSH}]$ quickly decomposed in solution and could not be isolated. After one day, a major species was identified as 1-Me-2-D-1,2- $\text{C}_2\text{B}_{10}\text{H}_{10}$ [2-D-**73**] from ^{11}B , ^1H and ^{13}C NMR spectra of the reaction mixture. Besides, $\text{MeB(OCD}_3)_2$ was also detected. After column chromatographic separation, [2-D-**73**] was isolated in about 50% yield with about 75% deuteration, which was characterized by several spectroscopic techniques and in coincidence with that of 1-Me-1,2- $\text{C}_2\text{B}_{10}\text{H}_{11}$ (**73**). Controlled experiment indicated that H-D exchange of **73** in CD_3OD could be promoted by PS. Thus, we won-

dered whether the deuterium was directly protonated from CD₃OD, or via indirect H-D exchange from **73**. Monitoring the reaction by ¹H NMR spectra indicated that a borane HBMe(OCD₃) or HBMe(OCD₃)R⁻ rather than DBMe(OCD₃) or DBMe(OCD₃)R⁻ was formed as the methyl group was observed as a doublet. It gradually disappeared with formation of MeB(OCD₃)₂. Considering the mass balance in the reaction, [2-D-**73**] would be directly formed (Scheme 6.7).

Scheme 6.7. Reaction of CAP 13-Vertex Carborane 1,12-Me₂-1,12-C₂B₁₁H₁₁ (**17b**) with CD₃OD/PS.



Reaction of **17b** with (4-MeC₆H₄)SNa was also attempted. Treatment of **17b** with 1 equiv of (4-MeC₆H₄)SNa, followed by cation exchange with [PPN]Cl gave new species which seemed like C₂B₁₀ or CB₁₁ from the ¹¹B NMR spectra. Recrystallization from THF did not give any pure product. However, recrystallization from hot MeOH gave [7-Me-7,8-C₂B₉H₁₁][PPN] (**[74]**[PPN]) in about 25% isolated yield as colorless crystals (Scheme 6.8). Compound **[74]**[PPN] was characterized by several

spectroscopic techniques and elemental analyses, which is in coincidence with that of [74]Cs in literature.^{37a} Single-crystal X-ray analyses of [74][PPN] suffered from poor crystal quality, but the preliminary results confirmed its cage geometry (Figure 6.13).

Scheme 6.8. Reaction of 17b with (4-MeC₆H₄)SNa.

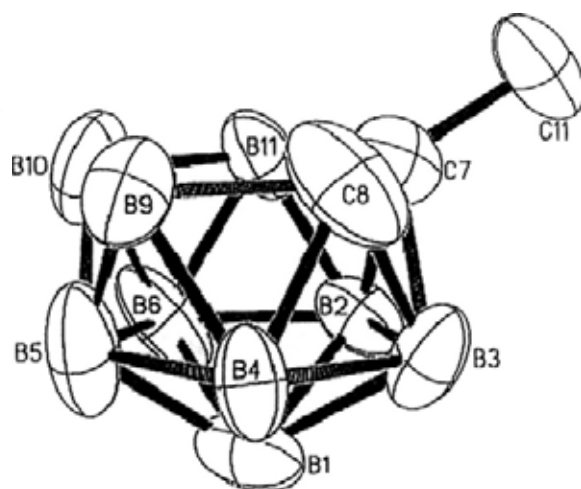
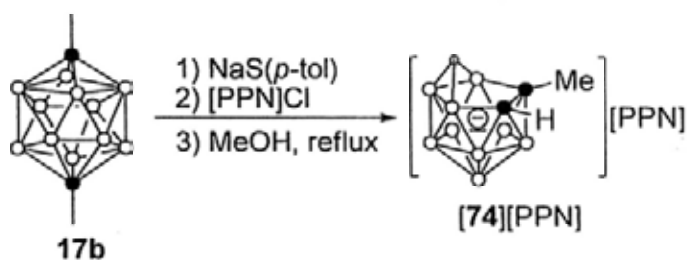


Figure 6.13. Structure of [7-Me-7,8-C₂B₉H₁₁]⁻ ([74]⁻), in [74][PPN].

Formation of the deborated C₂B₉⁻ anion [74]⁻ gave a hypothesis that 1-Me-1,2-C₂B₁₀H₁₁ (73) was initially formed, which would be deborated in the presence of (4-MeC₆H₄)SNa in MeOH. With this in mind, we reexamined the reaction mixture without addition of MeOH under inert atmosphere. The ¹H NMR spectrum showed two doublets at about 0 ppm corresponding to the methyl groups attached to BH group(s), two singlets at about 2.0 ppm assignable to the methyl groups that attached to the cage carbon(s), and a singlet at about 2.2 ppm indicative of the methyl group on the thiolate, in a ratio of about 3:3:3:3 (Figure 6.14). We noted that three peaks gradually decreased with the increase of the other two peaks and release of the “free”

thiolate. This process can be accelerated by heating a CD_2Cl_2 solution at $60\text{ }^\circ\text{C}$ and completed within 8 h. The NMR data suggested that the major carborane containing complexes in the reaction mixture were $[\text{1-Me-2-HBMeS(4-MeC}_6\text{H}_4\text{)-1,2-C}_2\text{B}_{10}\text{H}_{10}]^-$ (**[75]⁻**) and $\text{1-Me-2-HBMe-1,2-C}_2\text{B}_{10}\text{H}_{10}$ (**76**). The former would eliminate the thiolate in solution to afford the latter. Quenching the mixture by 1M HCl gave $\text{1-Me-1,2-C}_2\text{B}_{10}\text{H}_{11}$ (**73**) as monitored by ^1H and ^{11}B NMR spectra. Deboration of **73** to $[\text{74}]^-$ can be promoted by $(\text{4-MeC}_6\text{H}_4)\text{SNa}$ in the solution of CD_3OD (Scheme 6.9). However, this process was hard for completion probably due to the weak basicity of the thiolate.

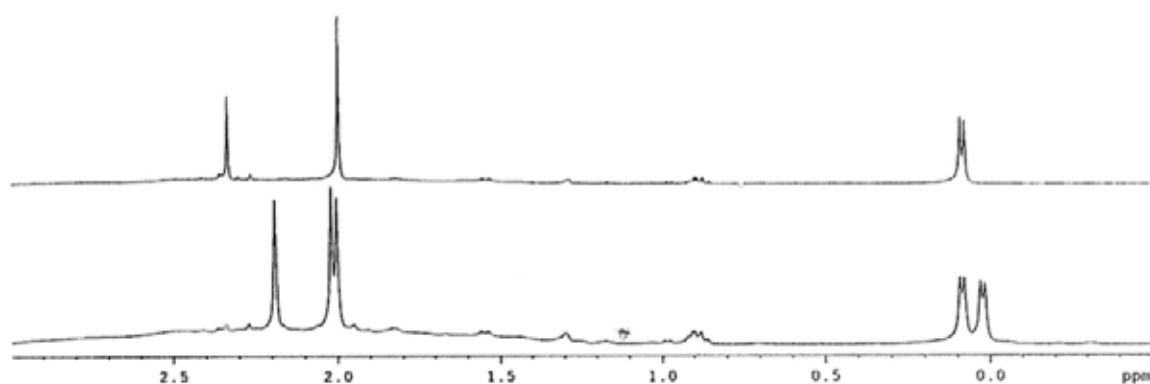
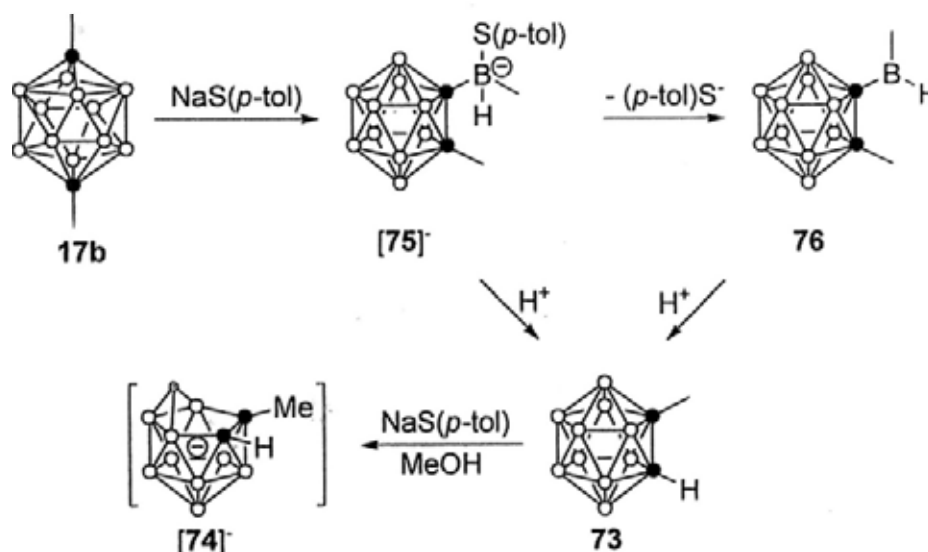


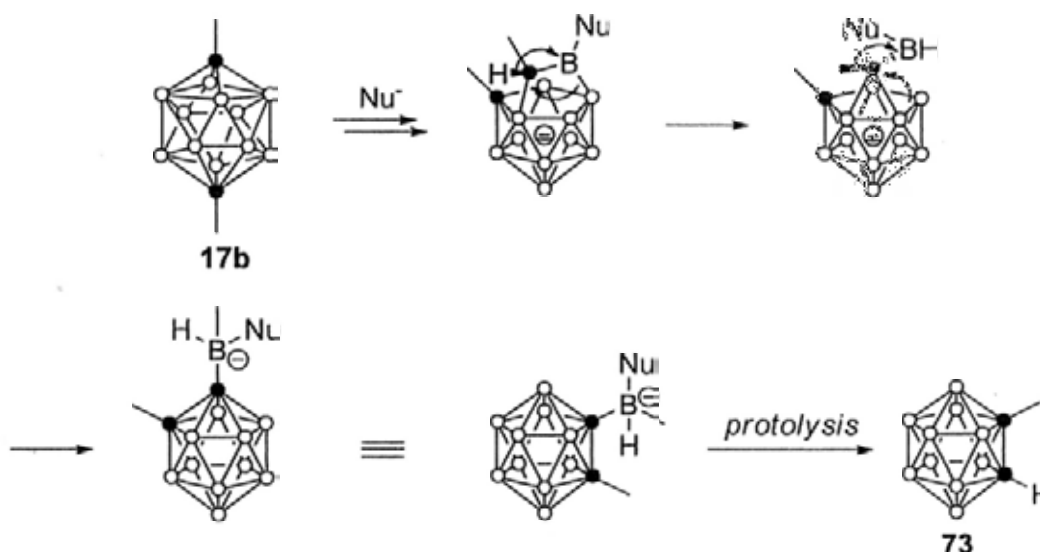
Figure 6.14. ^1H NMR spectra of the reaction mixture of **17b** with $(\text{4-MeC}_6\text{H}_4)\text{SNa}$ at room temperature: 1:1 mixture (bottom); after heating (top).

Scheme 6.9. Reaction Pathway of **17b** with $(\text{4-MeC}_6\text{H}_4)\text{SNa}$.



The results afore-mentioned suggest a possible pathway for the cage boron extrusion reaction of CAp 13-vertex carborane 1,12-Me₂-1,12-C₂B₁₁H₁₁. This reaction may involve both C-H and C-CH₃ bond cleavage, and B-H and B-CH₃ bond formation. This reaction type is very different from the formation of CB₁₁⁻ complexes, which involves the sequential migration of the H atom and CH₃ group to the boron atom, or vice versa. Given to the observed intermediate and products in the above reactions, a possible mechanism for this C-H and C-CH₃ bond cleavage process is proposed in Scheme 6.10.

Scheme 6.10. Possible Mechanism.



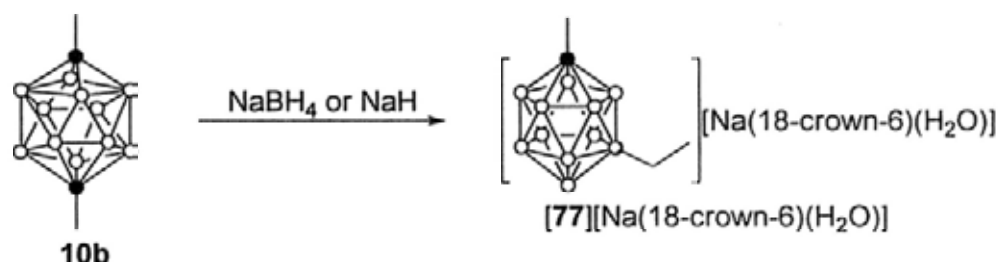
The H-migration from cage boron to carbon then to boron has been observed and confirmed in the reaction system of μ -1,2-(CH₂)₄-1,2-C₂B₁₁H₁₁ (7) with amine (amide), but C-C bond cleavage was unexpected. It is reported that 1-Hal(CH₂)_n-1-CB₁₁Me₁₁⁻ ($n = 2, 5, \text{ or } 6$) can undergo Grob fragmentation to lose the alkyl chain in the form of a terminal alkene to give a naked carbonium ylide intermediate which was then captured by nucleophiles.¹²⁹ However, no reaction was observed under the same conditions when the substituent at the carbon vertex was a plain alkyl group. Another example is that functionalized *o*-carboranyl methanol¹³⁰ or carboxylate¹³¹

can undergo decarboranylation under basic conditions. To our knowledge, the non-functionalized $C_{\text{alkyl}}-C_{\text{cage}}$ bond is very strong and hard to cleave.

6.2.2. Reaction with NaBH_4 or NaH

Reaction of **17b** with NaBH_4 or NaH gave primarily CB_{11}^- anion. Treatment of **17b** with NaBH_4 in THF overnight gave a mixture of products as well as $\text{BH}_3 \cdot \text{THF}$, as evidenced by the ^{11}B NMR spectra. Reaction of **17b** with NaH was a little slower but completed within several hours when heating at 70°C , giving a mixture of products which is similar to that of the reaction with NaBH_4 . The latter did not give $\text{BH}_3 \cdot \text{THF}$. After addition of excess amount of 18-crown-6, a single product [1-Me-7-Et-1- $\text{CB}_{11}\text{H}_{10}$][$\text{Na}(18\text{-crown-6})(\text{H}_2\text{O})$] (**[77]**[$\text{Na}(18\text{-crown-6})(\text{H}_2\text{O})$]) was isolated in about 30% yield as colorless crystals (Scheme 6.11).

Scheme 6.11. Reaction of 13-vertex Carborane **17b** with NaBH_4 or NaH .



Compound **[77]**[$\text{Na}(18\text{-crown-6})(\text{H}_2\text{O})$] was characterized by several spectroscopic techniques as well as elemental analyses. Its ^{11}B NMR spectrum exhibited a singlet at -1.0 ppm (B7), four doublets at -9.5 (B12), -11.7 (B2, 3, 8, 11), -12.7 (B4, 6, 9, 10), -15.5 (B5), as determined by $^{11}\text{B}\{^1\text{H}\}-^{11}\text{B}\{^1\text{H}\}$ COSY NMR spectrum (Figure 6.15), suggesting that the Et group is attached to the B7 atom not B2 atom. Its methylene group was unambiguously determined at 0.64 ppm in the ^1H NMR spectrum, and at 11.0 ppm in the ^{13}C NMR spectrum, respectively. Single-crystal X-ray analyses further confirmed its structure. As shown in Figure 6.16, the methyl group is attached to C1 atom, and the ethyl group is attached to the B7 atom, in the icosahedral

CB₁₁⁻ cage.

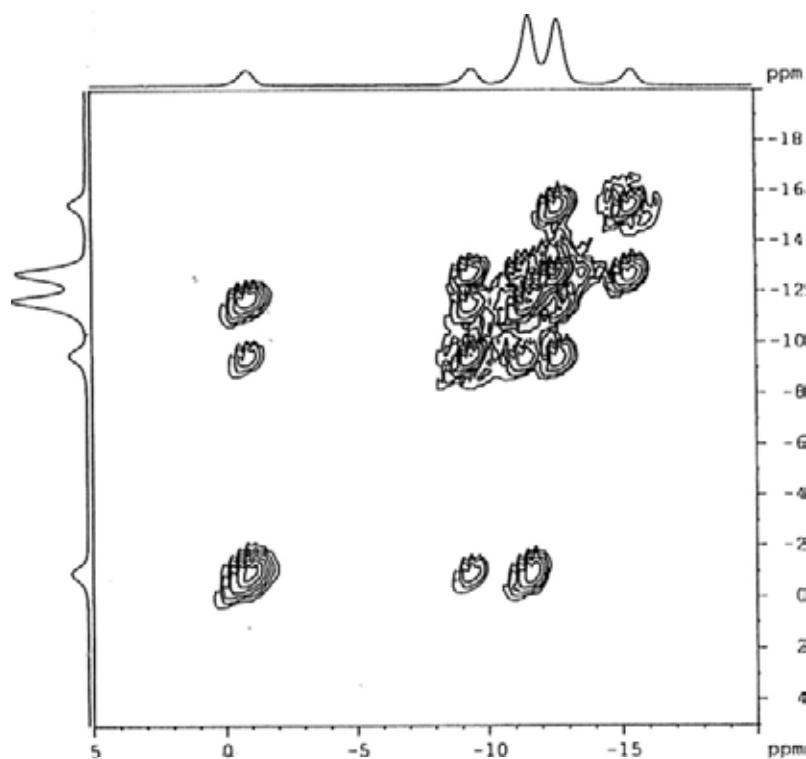


Figure 6.15. Two-dimensional $^{11}\text{B}\{^1\text{H}\}\text{-}^{11}\text{B}\{^1\text{H}\}$ COSY NMR spectrum of $[\text{77}][\text{Na}(\text{18-crown-6})(\text{H}_2\text{O})]$.

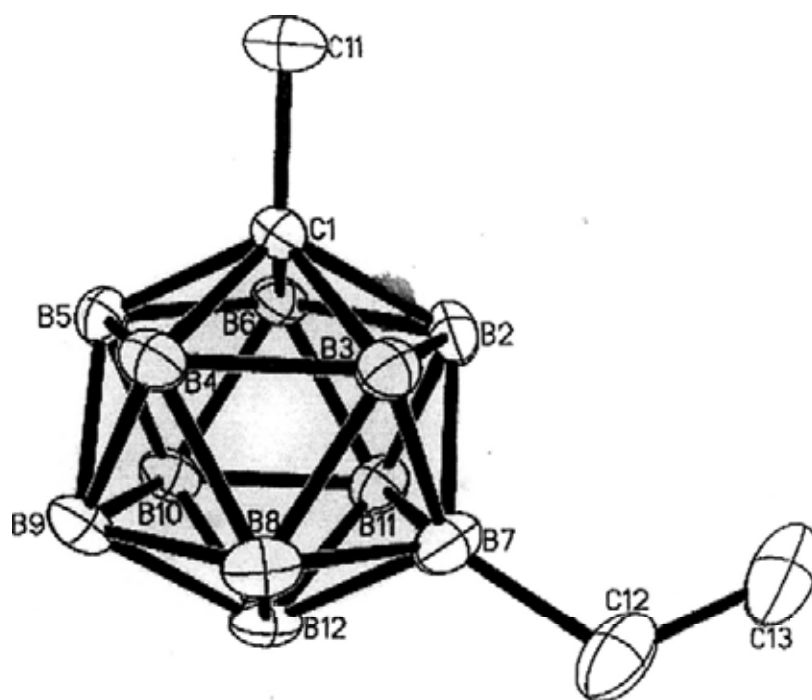
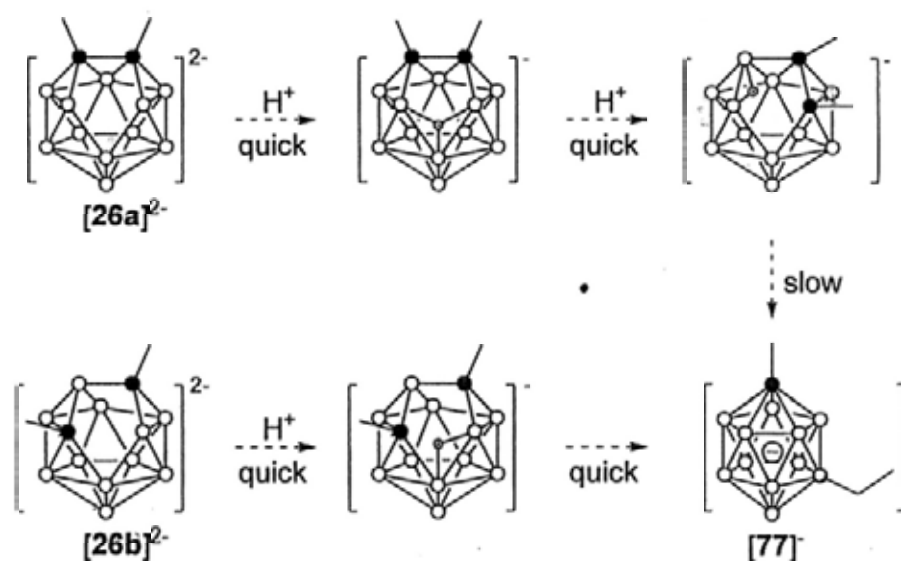


Figure 6.16. Structure of $[\text{1-Me-7-Et-1-CB}_{11}\text{H}_{10}]^-$ (**[77]**), in $[\text{77}][\text{Na}(\text{18-crown-6})(\text{H}_2\text{O})]$, showing one of the two crystallographically independent molecules.

The byproduct, which was not isolated, might be $[1\text{-Me-2-H}_2\text{BMe-1,2-C}_2\text{B}_{10}\text{H}_{10}]^-$, as a triplet at about -20 ppm was observed in the ^{11}B NMR spectrum of the reaction mixture. Characteristic peaks of 1-Me-1,2-C₂B₁₀H₁₁ at about -1 and -7 ppm were detected, after quenching the mixture by HCl. This phenomenon further suggested that reaction of CAP 13-vertex carborane with nucleophiles was more complicated than that of CAD 13-vertex carborane **6**, which was probably due to the absence of the linkage to confine the two cage carbons.

Scheme 6.12. Protonation of 13-Vertex *nido*-Carborane Dianions.



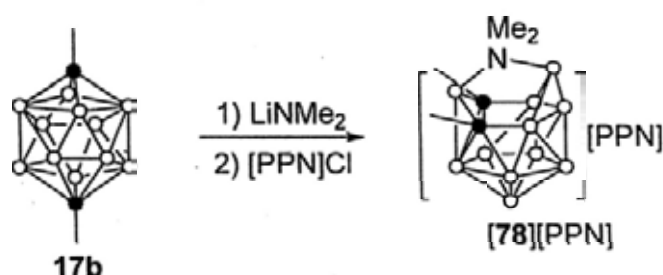
It was hard to explain why ethyl substituent is not on B2 but on B7 position, after extrusion of one cage carbon and cage closure. Monitoring the reaction by ^{11}B NMR spectra did not give any evidence of the intermediate. On the other hand, protonation of the corresponding 13-vertex *nido*-carborane dianions would give some clue on the nucleophilic attack of the cage (Scheme 6.12). Addition of excess amount of PhCH₂COOH to a THF solution of $[1,3\text{-Me}_2\text{-C}_2\text{B}_{11}\text{H}_{11}][\text{Na}_2(\text{THF})_4]$ ([26b][Na₂(THF)₄]) gave quickly the anion [77]⁻ as the major product as evidenced by ^{11}B NMR spectra. Treatment of the same phenylacetic acid with a THF solution of $[1,2\text{-Me}_2\text{-C}_2\text{B}_{11}\text{H}_{11}][\text{Na}_2(\text{THF})_4]$ ([26a][Na₂(THF)₄]) gave immediately a 13-

vertex *nido*-carborane monoanion, which was then slowly converted to [77]⁻ as a major product at room temperature. Thus, it seemed that {[26b][H]}⁻ may be the first intermediate in the reaction of NaH (or NaBH₄) with 17b, which underwent fast H-transfer processes to give the carbon extrusion product. Formation of [77]⁻ from [26a][Na₂(THF)₄] was also observed, but at a much slower rate. The protonated *nido*- species {[26a][H]}⁻ was detected as a long-lived intermediate which would not totally disappeared within a month at room temperature.

6.2.3. Reaction with Me₂NLi

Reaction of 13-vertex CAP carborane 17b with Me₂NLi afforded a 14-vertex *arachno*-azacarborane as the major product. Treatment of 17b with 1 equiv of Me₂NLi in THF, followed by addition of an equimolar amount of [PPN]Cl, gave [C,C',N,N'-Me₄-NC₂B₁₁H₁₁][PPN] ([78][PPN]) in about 5% isolated yield, after repeated recrystallization (Scheme 6.13). It was note that the gross yield of [78]⁻ was about 40% from the ¹¹B NMR spectrum, however, the messy products formation made it very difficult to be purified.

Scheme 6.13. Reaction of 17b with LiNMe₂.



Complex [78][PPN] was characterized by several spectroscopic techniques as well as elemental analyses. It exhibited a 1:4:1:1:3:1 pattern in the range 49 to -31 ppm in the ¹¹B NMR spectrum. Two types of methyl groups were observed at 2.78 and 1.52 ppm in the ¹H NMR spectrum, and 46.0 and 36.9 ppm in the ¹³C NMR spectrum, respectively. The signal of the cage carbons was found at 26.0 ppm.

The structure of the azacarborane cage was unambiguously determined by single-crystal X-ray analyses (Figure 6.17). It bears two open faces which share a common B12-N2-B13 edge. This geometry, however, cannot be derived directly from a 16-vertex *closo*-cluster that was calculated by theoretical calculation, by simply removing two vertices. It can be generated via *DSD* transformation, as shown in Figure 6.18. The two cage carbons are separated by one boron atom. The B12-N2 bond distance of 1.611(7) Å is a little longer than the B13-N2 bond length of 1.539(7) Å, indicative of an unsymmetric coordination environment of the cage N atom.

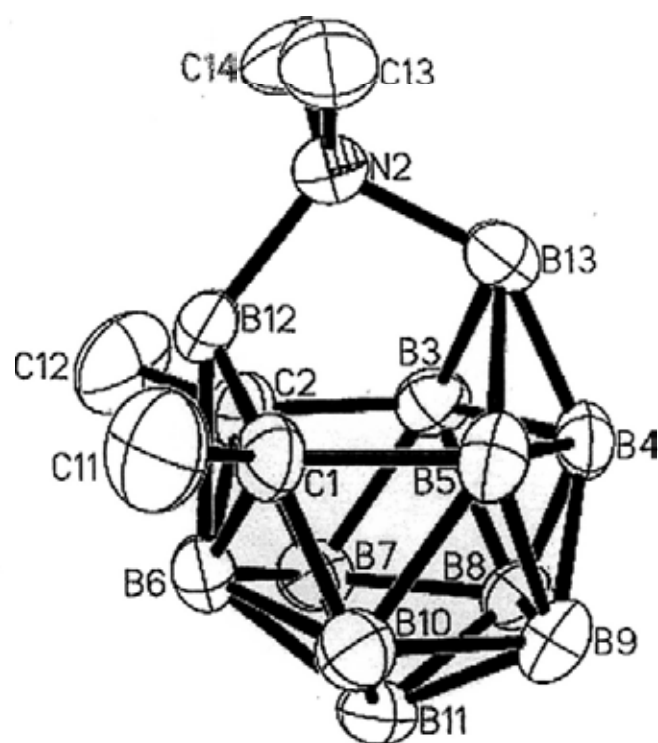


Figure 6.17. Structure of $[C,C',N,N'-Me_4-NC_2B_{11}H_{11}]^-$ ([78]⁻), in [78][PPN].

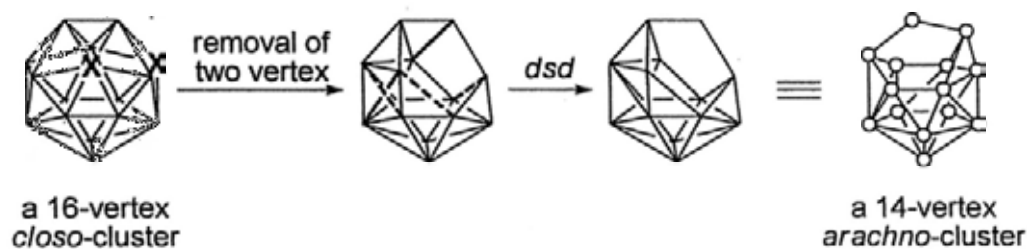


Figure 6.18. Cage conversion from a 16-vertex *closo*-cluster to a 14-vertex *arachno*-cluster.

This cluster represents the first 14-vertex *arachno*-azacarborane, which is synthesized by formal insertion of a hetero atom into the 13-vertex carborane cage. A similar method was reported for the synthesis of neutral 11-vertex *arachno*-azacarboranes 1,6,9-NC₂B₁₀ from the reaction of 10-vertex *closo*-carborane 1,2-C₂B₈H₁₀ with amines R₁R₂NH.¹³² The product also bear two 5-membered open face sharing a common B-N-B edge, and the two cage carbons are in the 5-membered ring and in adjacent positions. Meanwhile, the two B-N bonds are symmetrical.

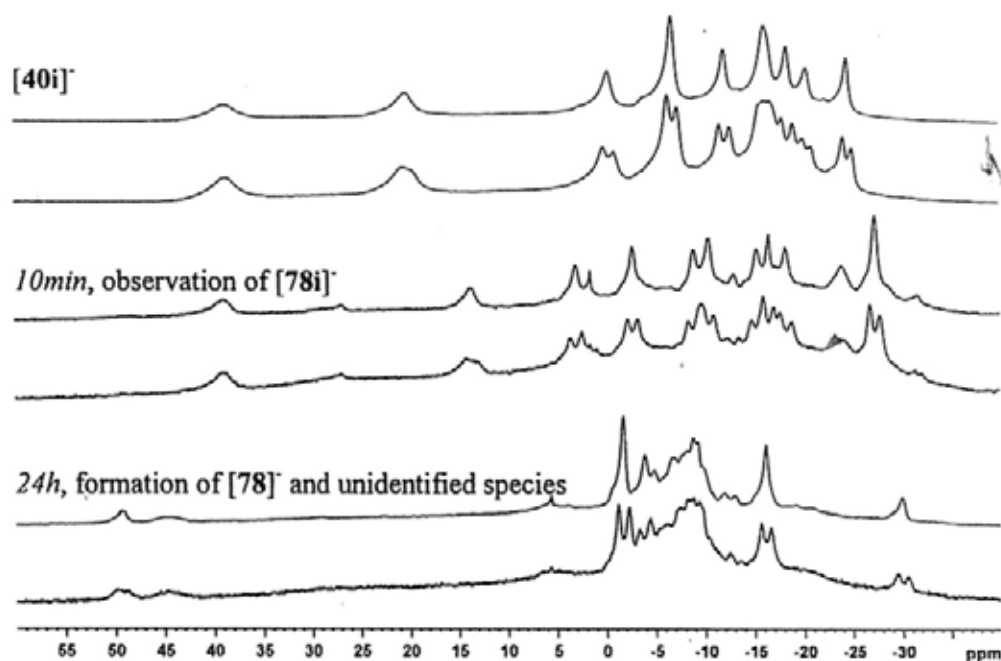
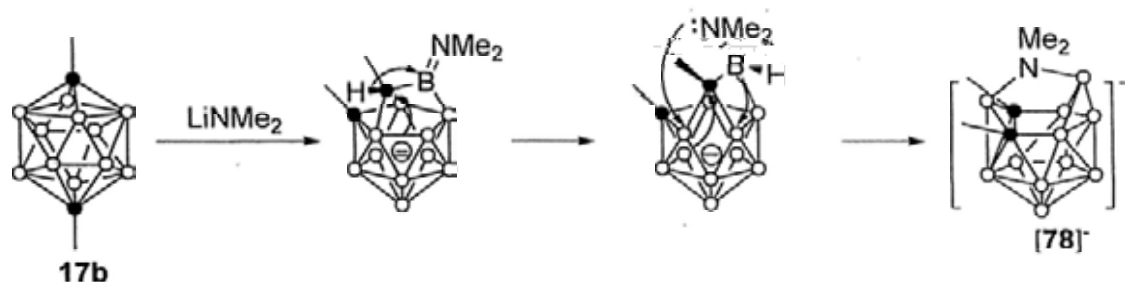


Figure 6.19. Comparison of ¹¹B{¹H} and ¹H-coupled ¹¹B NMR spectrum of [40i]⁻ (top), reaction of 17b with LiNMe₂ after 10min (middle), and the reaction after 24 h (bottom).

Monitoring the reaction by ¹¹B NMR spectrum clearly indicated a H-migration product formation, which might be [7-Me-μ-η:η-8,10-MeCHB(NMe₂)-7-CB₁₀H₁₀] ([78i]⁻) or species with a similar structure (Figure 6.19). Thus the formation of [78]⁻ might involve a BH to CH to BH migration process, and a proposed mechanism was shown in Scheme 6.14. After the formation of the intermediate [78i]⁻, 1,2- H-migration led to the formation of another intermediate, which contains an amino

group with a lone-pair electrons. Nucleophilic attack of the N atom on the cage boron atom between the two cage carbons resulted in the cage conversion and formation of the product.

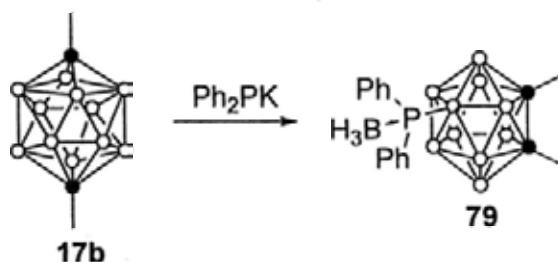
Scheme 6.14. Proposed Mechanism for the Formation of [78].



6.2.4. Reaction with Ph_2PK

Reaction of **17b** with Ph_2PK , however, gave a neutral species as a major product. Treatment of **17b** with 1 equiv of Ph_2PK , which is directly prepared from Ph_2PH and potassium metal in THF,¹³³ followed by repeated recrystallization from $\text{Et}_2\text{O}/n$ -hexane, gave 8- BH_3PPh_2 -1,2- Me_2 -1,2- $\text{C}_2\text{B}_{10}\text{H}_9$ (**79**) as a white powder in 10% isolated yield (Scheme 6.15). Similarly, the gross yield of **79** was about 30-40% according to the ^{31}P NMR spectrum of the reaction mixture, but it was hard to be purified.

Scheme 6.15. Reaction of **17b** with Ph_2PK .



Complex **79** was characterized by various spectroscopic techniques as well as HRMS. The methyl group was observed at 2.02 ppm in the ^1H NMR spectrum and 23.6 ppm in the ^{13}C NMR spectrum. The chemical shift of the cage carbons was observed at 75.6 ppm. These data are similar to those observed in 1,2- Me_2 -1,1-

$C_2B_{10}H_{10}$. The ^{11}B NMR spectrum showed a unique dq peak at -36 ppm ($J_{BH} \approx 94\text{Hz}$, $J_{BH} \approx 50\text{Hz}$), which is similar to other phosphine borane adducts.¹³⁴ The ^{31}P NMR spectrum showed a broad peak at -23 ppm. Its structure was confirmed by single-crystal analyses as shown in Figure 6.20. The P- B_{cage} bond distance of 1.937(3) Å is close to that of 1.928(7) Å in $[PdCl(7-PPh_2-8-Me-11-PPh_2-7,8-C_2B_9H_9)(PPh_3)]$.¹³⁵

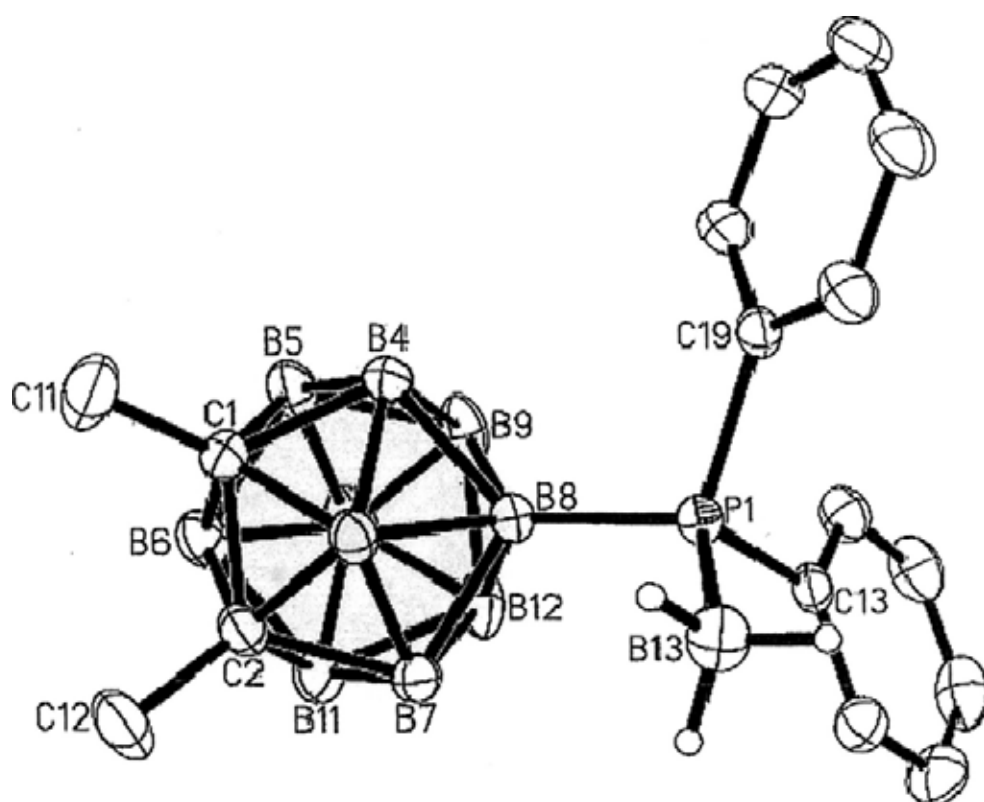


Figure 6.20. Molecular structure of 8-BH₃PPh₂-1,2-Me₂-1,2-C₂B₁₀H₉ (79).

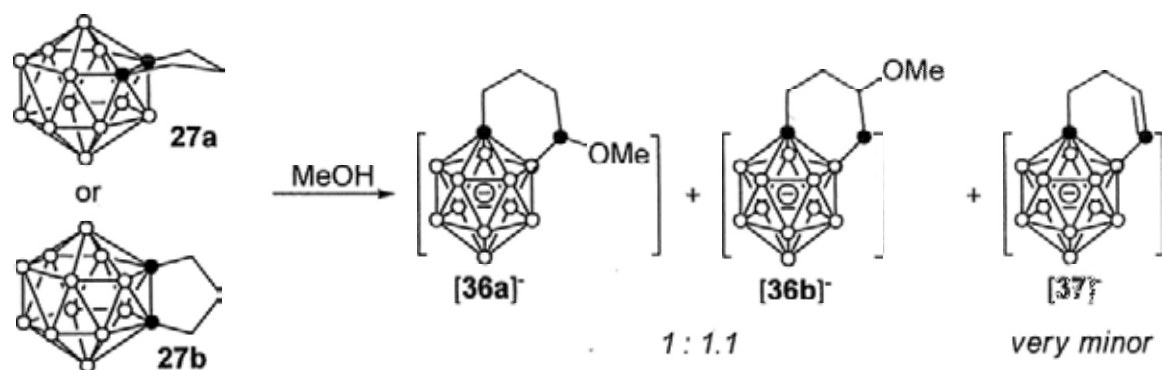
Formation of this neutral species is unexpected, as it formally needs an additional H atom. It was noted that no reaction took place when **17b** was heated in refluxing C₆D₆ in the presence of excess amount of PPh₂H. A possible source of the proton might be from the possible intermediate which bears a bridging hydrogen atom.

6.3. Nucleophilic Reaction of 14-Vertex Carborane $\mu-(CH_2)_3-C_2B_{12}H_{12}$

To make a comparison between 13- and 14-vertex carboranes in reaction with nucleophiles, the reaction of μ -2,3-(CH₂)₃-2,3-C₂B₁₂H₁₂ (**27a**) with MeOH was first

attempted and closely monitored by ^{11}B NMR spectroscopy. It was found that this reaction proceeded very slowly at room temperature and was not completed in one month. However, the ^{11}B NMR spectrum clearly showed the formation of $\text{B}(\text{OMe})_3$ and *closo*- CB_{11}^- with the gradual disappearance of **27a**. This reaction was accelerated by heating to reflux at 70°C in a closed vessel and almost completed in 48 h. Addition of $[\text{Me}_3\text{NH}]\text{Cl}$ to the reaction solution gave a mixture of $[\mu\text{-}1,2\text{-}(\text{CH}_2)_3\text{CH}(\text{OMe})\text{-}1\text{-CB}_{11}\text{H}_{10}][\text{Me}_3\text{NH}]$ (**[36a]** $[\text{Me}_3\text{NH}]$) and $[\mu\text{-}1,2\text{-}(\text{CH}_2)_2\text{CH}(\text{OMe})\text{CH}_2\text{-}1\text{-CB}_{11}\text{H}_{10}][\text{Me}_3\text{NH}]$ (**[36b]** $[\text{Me}_3\text{NH}]$) in a molar ratio of *ca.* 1:1.1, together with a small amount of $[\mu\text{-}1,2\text{-}(\text{CH}_2)_2\text{CH}=\text{CH}\text{-}1\text{-CB}_{11}\text{H}_{10}][\text{Me}_3\text{NH}]$ (**[37]** $[\text{Me}_3\text{NH}]$), as measured by ^1H NMR spectrum (Scheme 6.16). The 14-vertex carborane isomer $\mu\text{-}2,8\text{-}(\text{CH}_2)_3\text{-}2,8\text{-C}_2\text{B}_{12}\text{H}_{12}$ (**27b**) also gave a similar result as evidenced by ^{11}B NMR, when reacted with MeOH.

Scheme 6.16. Reaction of 14-Vertex Carborane $\mu\text{-}(\text{CH}_2)_3\text{-C}_2\text{B}_{12}\text{H}_{12}$ (**27**) with MeOH.



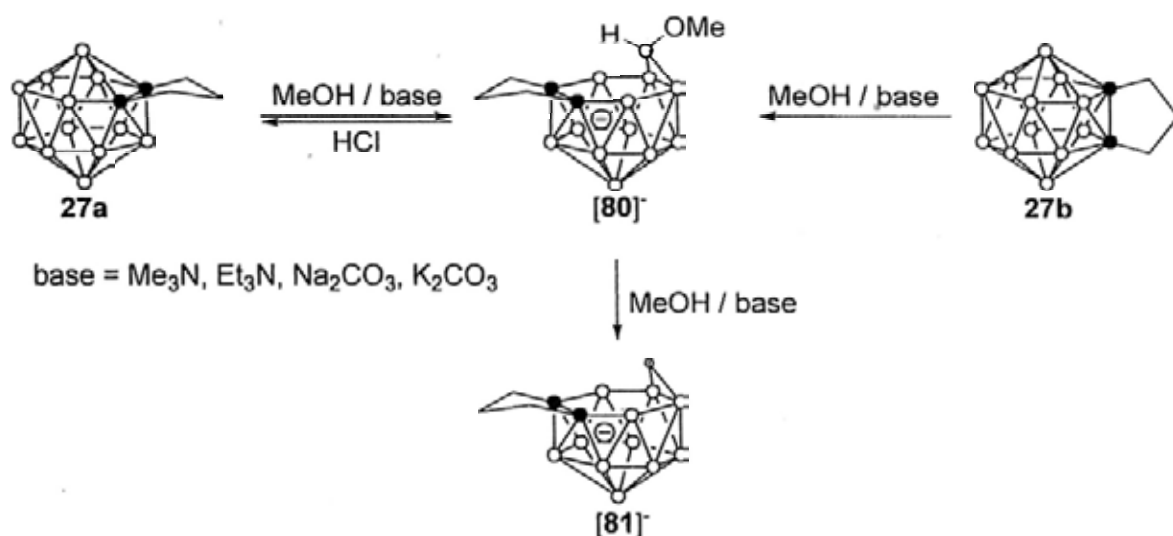
It was noteworthy that reaction of **27** with EtOH, however, was even much slower than that with MeOH, and not completed within a week at 70°C . But it clearly showed the formation of $\text{B}(\text{OEt})_3$ and CB_{11}^- anions in the ^{11}B NMR spectra. Compound **27** did not react with PPh_3 even in refluxing toluene whereas the 13-vertex one reacts readily with PPh_3 to give the zwitterionic compound $\mu\text{-}1,2\text{-}(\text{CH}_2)_3\text{CH}(\text{PPh}_3)\text{-}1\text{-CB}_{11}\text{H}_{10}$ (**41**). These results indicate that 13-vertex carborane is

more reactive than 14-vertex one, which can be ascribed to the presence of a trapezoidal face in the 13-vertex carborane while the 14-vertex carboranes have only triangulated faces, and the reaction is highly dependent on the nature of the nucleophiles.

The aforementioned results raise a question on the mechanism by which the *closo*-CB₁₁⁻ anions [36a]⁻, [36b]⁻ and [37]⁻ are formed, although formation of the latter two is much clear and can be ascribed to the isomerization from [36a]⁻ in the acidic reaction media. The formation of B(OMe)₃ suggests that a boron atom must be removed from the cage by attack of the MeOH, which could explain why PPh₃ did not react with 14-vertex carborane as it could not serve as a deboration reagent. In this regard, we tried to trap the deboration intermediates.

Similar to the procedures used in the reactions of 13-vertex carboranes with basic MeOH, several bases, such as Me₃N, Et₃N, K₂CO₃ or KHCO₃ were added in excess amount to a freshly prepared MeOH solution of 27a or 27b. In either case, the same species was initially observed within 5 min and slowly turned messy in solution, as indicated by ¹¹B NMR spectrum. After many attempts, mixing 27 with MeOH and excess Me₃N aqueous solution at room temperature followed by quick removal of the volatile substrates, gave the salt of *nido*-C₂B₁₂⁻ anion [μ -8,9-(CH₂)₃- μ -11,12-BH(OMe)-8,9-C₂B₁₁H₁₁][Me₃NH] ([80][Me₃NH]) as a white solid in almost quantitative yield (Scheme 6.17). On the other hand, the ¹¹B experiments showed that it can be converted to 27a immediately, after addition of concentrated HCl to the solution at room temperature. This result suggests that such reaction is pH dependent. Heating a MeOH solution of [80][Me₃NH] gave primarily *closo*-CB₁₁⁻ anions and B(OMe)₃ as evidenced by ¹¹B NMR.

Scheme 6.17. Reaction of 14-Vertex Carborane $\mu\text{-(CH}_2\text{)}_3\text{-C}_2\text{B}_{12}\text{H}_{12}$ (**27**) with basic MeOH.



Compound **[80][Me₃NH]** was fully characterized by ¹H, ¹³C and ¹¹B NMR spectroscopy as well as elemental analyses. It exhibited a 1:2:1:2:2:3(1:2):1 pattern in the 22 to -28 ppm range in the ¹¹B NMR spectrum, which is in accordance with its symmetry in solution. The downfield doublet at 22.2 ppm is assigned the signal for the bridging boron atom which is attached to the O atom. The signal of the H atom attached to this boron appeared at about -1.1 ppm as a broad quartet in the ¹H NMR spectrum.

Single-crystal of **[80][Me₃NH]** suitable for X-ray analyses was quickly grown from a solution of CH₂Cl₂. Although it suffers from poor resolution, the connectivity is unambiguously determined. There are two crystallographically independent molecules in the unit cell and a typical one is shown in Figure 6.21. It has a 13-vertex *nido*-C₂B₁₁ geometry which contains a 6-membered open face composed by two carbon atoms and four boron atoms, on which a bridging BH group attached to B11 and B12 atoms. The nucleophile MeO group is bound to this bridging boron atom, which should be the most electrophilic site in compound **27a**. It was noted that the cage

geometry transformation took place in the reaction of **27b** with basic MeOH (Scheme 6.17). The B-O bond distance of 1.418(12) Å is close to the range 1.37 – 1.41 Å normally observed in alkoxy-substituted carboranes, indicative of partial π -backdonation from the oxygen atom.^{32,75,118} The N \cdots O distance of 2.793(12) Å suggests a N-H \cdots O hydrogen bond between the MeO group and the ammonium counterion.

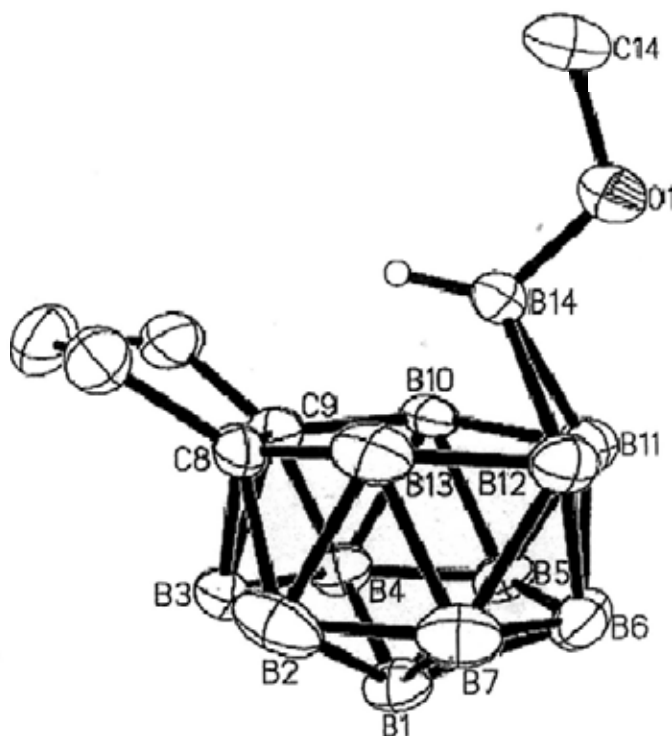


Figure 6.21. Structure of $[\mu\text{-}8,9\text{-(CH}_2\text{)}_3\text{-}\mu\text{-}11,12\text{-BH(OMe)-}8,9\text{-C}_2\text{B}_{11}\text{H}_{11}]^-$ (**[80]**⁻), in **[80]**[Me₃NH], showing one of the two crystallographically independent molecules.

We also monitored further decomposition of this 14-vertex *nido*-carborane anion **[80]**⁻ in MeOH in the presence of an excess amount of bases, such as Me₃N, Et₃N, K₂CO₃ or KHCO₃. Deboration occurred and a 13-vertex *nido*-carborane anion $[\mu\text{-}8,9\text{-(CH}_2\text{)}_3\text{-}8,9\text{-C}_2\text{B}_{11}\text{H}_{12}]^-$ (**[81]**⁻) was observed in the ¹¹B NMR spectrum (Scheme 6.17). The same anion can also be obtained using CsF as deboration reagents. Treatment of a large excess amount of CsF with **27** in a wet THF solution for a week, followed by addition of [Me₃NH]Cl and recrystallization from acetone, gave

[81][(Me₃NH)₂Cl] as colorless crystals in about 60% isolated yield (Scheme 6.18).

Scheme 6.18. Reaction of 14-Vertex Carborane μ -(CH₂)₃-C₂B₁₂H₁₂ (**27**) with CsF.

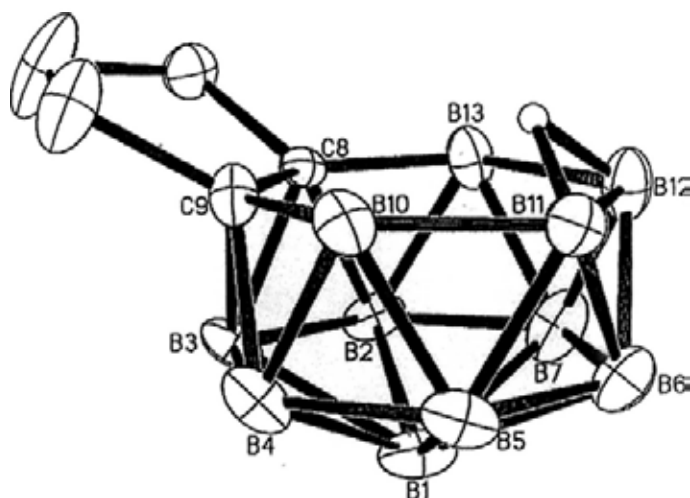
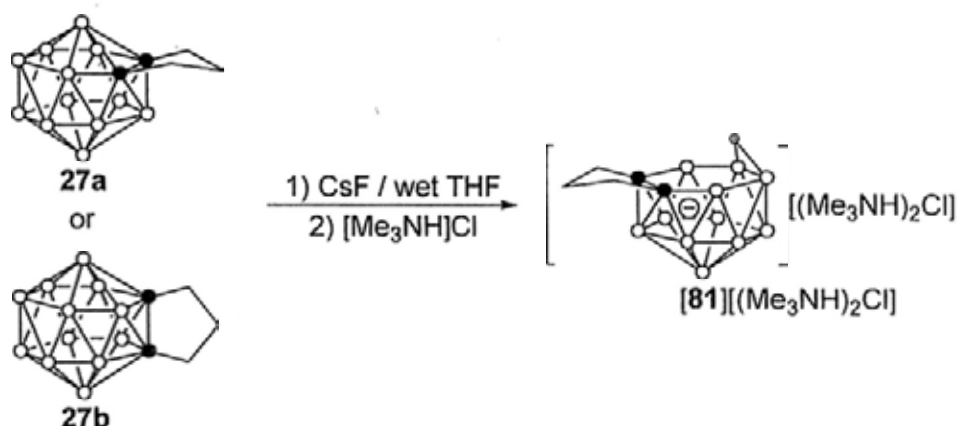


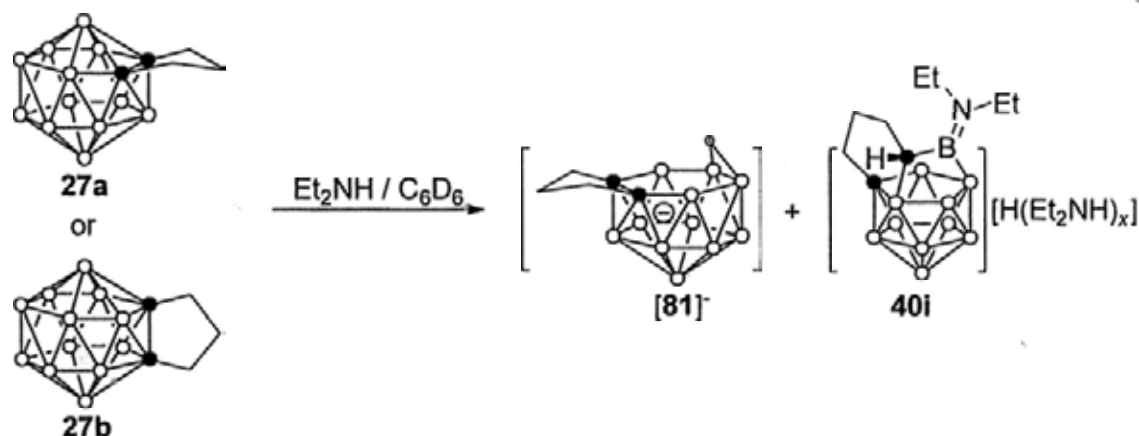
Figure 6.22. Structure of [μ -8,9-(CH₂)₃-8,9-C₂B₁₁H₁₂]⁻ ([81]⁻), in [81][(Me₃NH)₂Cl], showing one of the two crystallographically independent molecules.

Complex [81][(Me₃NH)₂Cl] was characterized by several spectroscopic techniques as well as elemental analyses. Its ¹¹B NMR spectrum exhibited a 2:3:2:2:1:1 pattern in the range 1 to -33 ppm. Its ¹H NMR spectrum clearly showed the bridging H at about -1.27 ppm. The structure of [81][(Me₃NH)₂Cl] was determined by single-crystal X-ray analyses, which is suffered from poor resolution. There are also two crystallographically independent molecules in the unit cell and a typical one is shown in Figure 6.22. The geometry of [81]⁻ can be regarded as removal of the bridging

BH(OMe) group in [80]⁻. This is very different from that of 13-vertex *nido*-carborane dianions generated by the reduction of *closo* species with group 1 or 2 metals, but is very similar to that observed in 14-vertex ruthenacarboranes.

With these results, there are at least two pathways for the deboronative degradation of 14-vertex carborane, both of which proceed via the 14-vertex *nido*-carborane anion. One product is *closo*-CB₁₁⁻ anion and the other is *nido*-C₂B₁₁⁻ anions. We wondered whether the latter can be converted to the former in the acidic media. However, [81][Me₃NH₂Cl] is stable in refluxing MeOH even in the presence of concentrated HCl. Therefore [81]⁻ is not the possible intermediate in the transformation from a *closo*-C₂B₁₂ species to *closo*-CB₁₁⁻ anions. On the other hand, treatment of about 10 equiv of Et₂NH with 27 in a C₆D₆ solution gave a colorless solution. The ¹¹B NMR spectrum clearly showed the formation of [μ-η:η:η-7,8,10-(CH₂)₃CHB(NEt₂)-7-CB₁₀H₁₀][H(NEt₂H)_x] ([40i]). Besides, the characteristic peak at about -33 ppm of deborated species [81]⁻ was also observed (Scheme 6.19). With these data, a general pathway for the reaction of 14-vertex carboranes with nucleophile HY was described in Scheme 6.20.

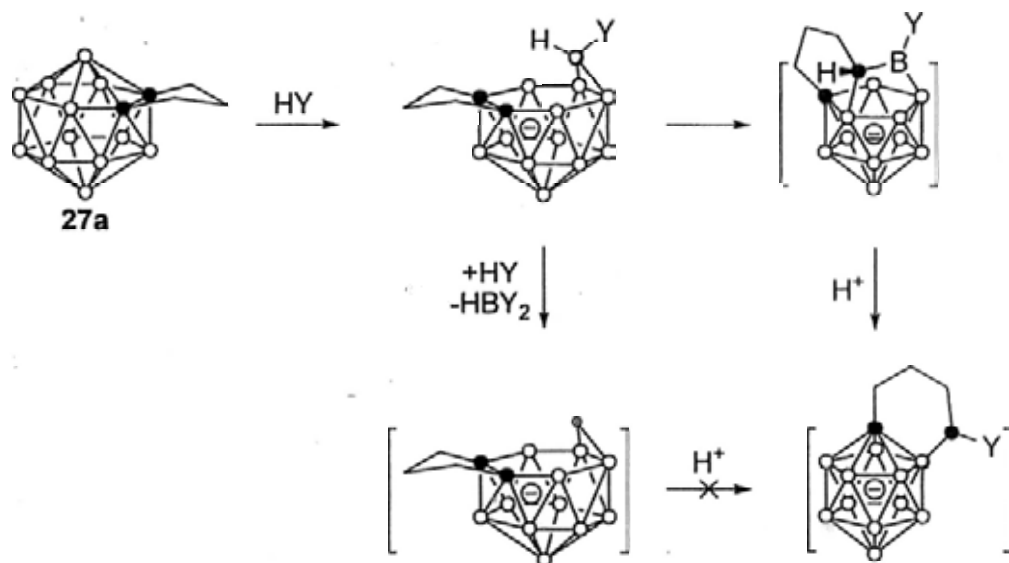
Scheme 6.19. Reaction of 14-Vertex Carborane μ-(CH₂)₃-C₂B₁₂H₁₂ (27) with Et₂NH.



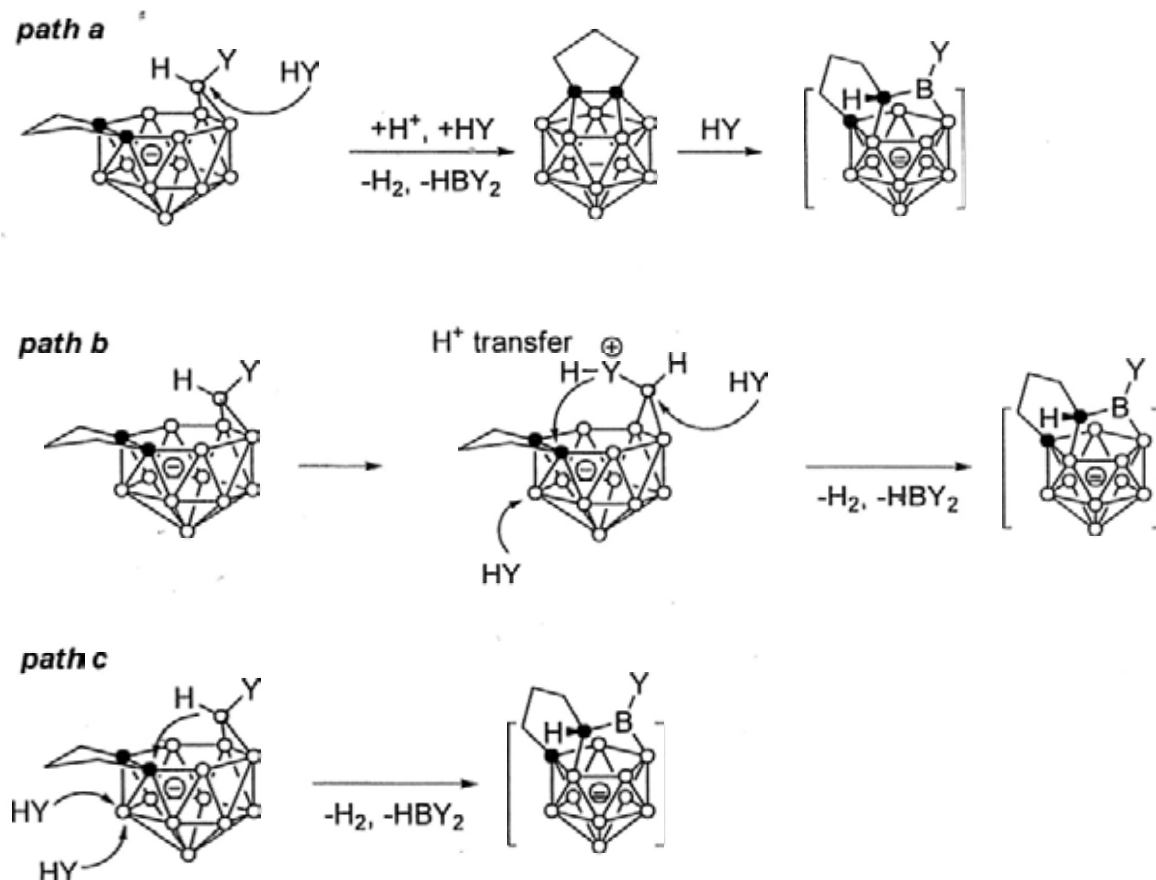
How is the [μ-η:η:η-7,8,10-(CH₂)₃CHB(Y)-7-CB₁₀H₁₀]⁻ formed from [μ-8,9-

$(\text{CH}_2)_3\text{-}\mu\text{-11,12\text{-BH(Y)-8,9-C}_2\text{B}_{11}\text{H}_{11}]$? Depending on the possibility of the boron atom that was removed from the cluster and the H atom that migrated to the cage carbon, there are three possible types of mechanism for this process (Scheme 6.21): (a) Removal of the boron vertex that attached to the Y group to afford the 13-vertex carborane, followed by another nucleophilic attack; (b) H-migration of the B-H vertex to the cage carbon followed by deboration at another BH vertex; (c) H-migration of the proton from the nucleophile to the cage carbon coupled with the nucleophilic attack on another cage boron adjacent to two cage carbons as well as on the bridging boron atom. Although CD_3OD was used as a reagent, the H/D exchange on cage BH vertices and isomerization of the CB_{11}^- anions did not offer useful information on the H-transfer process.

Scheme 6.20. Reaction Pathway of 14-Vertex Carborane $\mu\text{-(CH}_2\text{)}_3\text{-C}_2\text{B}_{12}\text{H}_{12}$ (27) with Nucleophile HY.



Scheme 6.21. Three Possible Pathway for the Formation of $[\mu\text{-}\eta\text{:}\eta\text{:}\eta\text{-}7,8,10\text{-}(\text{CH}_2)_3\text{CHB}(\text{Y})\text{-}7\text{-CB}_{10}\text{H}_{10}]^-$.



6.4. Summary

The reactivities of 13-vertex carborane $\mu\text{-}1,2\text{-}(\text{CH}_2)_4\text{-}1,2\text{-C}_2\text{B}_{11}\text{H}_{11}$ (**7**), 1,12-Me₂-1,12-C₂B₁₁H₁₁ (**17b**) and 14-vertex carboranes $\mu\text{-}2,3(8)\text{-}(\text{CH}_2)_3\text{-}2,3(8)\text{-C}_2\text{B}_{11}\text{H}_{11}$ (**27**) toward nucleophiles are lower than that of $\mu\text{-}1,2\text{-}(\text{CH}_2)_3\text{-}1,2\text{-C}_2\text{B}_{11}\text{H}_{11}$ (**6**), but more diverse reactivity patterns are observed with compounds **7** and **17a,b**.

Carbon extrusion reaction of $\mu\text{-}1,2\text{-}(\text{CH}_2)_4\text{-}1,2\text{-C}_2\text{B}_{11}\text{H}_{11}$ (**7**) is hard, but can occur under some conditions. Reaction of **7** with pure MeOH gives a mixture of CB₁₁⁻ anions as well as deboration product $\mu\text{-}1,2\text{-}(\text{CH}_2)_4\text{-}1,2\text{-C}_2\text{B}_{10}\text{H}_{10}$ (**3**). Use of (4-MeC₆H₄)SNa can give pure product $[\mu\text{-}1,2\text{-}(\text{CH}_2)_4\text{CHS}(4\text{-MeC}_6\text{H}_4)\text{-}1\text{-CB}_{11}\text{H}_{10}]^-$ (**[67]**), but at a much slower rate than that with compound **6**. On the other hand, treatment of **7** with Et₂NH gives nucleophilic adduct of 13-vertex carborane, which

can undergo H-migration upon deprotonation. The similar anions can also be synthesized by reaction of **7** with R_2NLi , in which deprotonation of the α -CH of the 13-vertex *closo*-carborane is a competing reaction, and the ratio of the product is related to nature of the R group.

Compound 1,12-Me₂-1,12-C₂B₁₁H₁₁ (**17b**) can undergo carbon extrusion reaction to give 2-substituted CB₁₁⁻ anions with MeOH, or 7-substituted CB₁₁⁻ anion with NaBH₄ or NaH. Under some conditions, C-C bond activation product 1-Me-1,2-C₂B₁₀H₁₁ is also observed, which is regarded to via the proposed intermediate 1-Me-2-BHMe(Nu)-1,2-C₂B₁₀H₁₀⁻ and 1-Me-2-BHMe-1,2-C₂B₁₀H₁₀. Reaction of **17b** with Me₂NLi, give the first 14-vertex *arachno*-azacarborane. 1,2-Me₂-1,2-C₂B₁₁H₁₁ (**17a**) has similar reactivities to those of **17b**.

μ -(CH₂)₃-C₂B₁₂H₁₂ (**27**) reacts with MeOH at 70 °C to give *closo*-CB₁₁ anions. Treatment of **27** with MeOH/Me₃N affords *nido*-C₂B₁₂ species [8,9-(CH₂)₃- μ -11,12-(OMe)BH-8,9-C₂B₁₁H₁₁]⁻ (**[80]**). In the presence of acid such as HCl, anions **[80]**⁻ are converted to **27a**. However, **[80]**⁻ undergo deboration reaction, in the presence of excess Me₃N, to generate a *nido*-C₂B₁₁ anion [8,9-(CH₂)₃-8,9-C₂B₁₁H₁₂]⁻ (**[81]**) that can also be directly formed from the reaction of **27** with excess CsF. Compound **27** can also react with Et₂NH in C₆D₆ to afford **[81]**⁻ and **[40i]** as evidenced by ¹¹B NMR spectrum. Mechanistic studies show that **[80]**⁻ is the first intermediate in the reaction of **27** with MeOH and **[81]**⁻ is unlikely an intermediate.

Chapter 7. Conclusion

Several CAd (Carbon-Atoms-Adjacent) 13-vertex carboranes bearing different C,C'-linkages were synthesized from the reaction of the corresponding CAd 12-vertex *nido*-carborane dianionic salts with dihaloborane reagents. These 13-vertex carboranes have short C-C bond lengths around 1.4 Å. The ^{13}C chemical shifts of the cage carbons in these molecules are downfield shifted to about 140 ppm compared to their 12-vertex analogues, indicative of their electron-deficient properties. As a result, the corresponding ^1H and ^{13}C chemical shifts of the CH_n ($n = 1, 2, 3$) groups adjacent to the cage carbons were also observed at lower field.

In order to understand the role of the linkage in the formation and stabilization of 13-vertex carboranes, the 12-vertex carborane $1,2\text{-Me}_2\text{Si}(\text{CH}_2)_2\text{-}1,2\text{-C}_2\text{B}_{10}\text{H}_{10}$ was selected as the starting material. Following the same synthetic route, a 13-vertex CAd carborane $\mu\text{-}1,2\text{-Me}_2\text{Si}(\text{CH}_2)_2\text{-}1,2\text{-C}_2\text{B}_{11}\text{H}_{11}$ was synthesized. This 13-vertex carborane underwent unprecedented desilylation on silica gel to give two 13-vertex carborane isomers without linkage— $1,2\text{-Me}_2\text{-}1,2\text{-C}_2\text{B}_{11}\text{H}_{11}$ and $1,12\text{-Me}_2\text{-}1,12\text{-C}_2\text{B}_{11}\text{H}_{11}$. The former slowly isomerized to its CAp (Carbon-Atoms-Apart) isomer $1,12\text{-Me}_2\text{-}1,12\text{-C}_2\text{B}_{11}\text{H}_{11}$ in solution without decomposition. This result indicated that the C,C'-linkage does not have any obvious effects on the stability of 13-vertex carboranes. The structural data showed that the $\text{C}_{\text{cage}}\text{-C}_{\text{cage}}$ bond of the 13-vertex carborane $\mu\text{-}1,2\text{-Me}_2\text{Si}(\text{CH}_2)_2\text{-}1,2\text{-C}_2\text{B}_{11}\text{H}_{11}$ is very short at 1.439(3) Å and the C-Si-C bond angle in the silacyclopentane ring is reduced to 89.5(1)°. Such a ring-strain makes the Si atom easily attacked by nucleophiles, facilitating the C-Si bond cleavage and desilylation process.

The 13-vertex CAp carboranes were also directly synthesized from the reaction of

CAP 12-vertex *nido*-carborane anions and $\text{HBBr}_2 \cdot \text{SMe}_2$, but in much lower yields. X-ray analyses indicated the cage carbons are at the 1,12- positions in an all-triangulated dicosahedron, not at the 1,6-positions proposed initially. It indicated that a thermal isomerization process would be involved, and the barrier is greater for the 1,2- to 1,6- isomerization than for the 1,6- to 1,12- process. This phenomenon was also observed in the thermolysis of two 13-vertex ruthenacarborane isomers 4-(*p*-cymene)-1-TMSCH₂-2-Me-4,1,2-RuC₂B₁₀H₁₀ and 4-(*p*-cymene)-1-TMSCH₂-6-Me-4,1,6-RuC₂B₁₀H₁₀. The latter began to rearrange at a lower temperatures.

Reduction of CAd 13-vertex carboranes with Na metal resulted in the formation of the corresponding CAd 13-vertex *nido*-carborane salts, regardless of the linkages. These species displayed common spectroscopic and structural features, with upfield shifted ¹³C chemical shifts of the cage carbons and elongated C_{cage}-C_{cage} distances, which are significantly different from their parent molecules. In a similar manner, reduction of CAp 13-vertex carborane 1,12-Me₂-1,12-C₂B₁₁H₁₁ gave [1,3-Me₂-1,3-C₂B₁₁H₁₁]²⁻. These 13-vertex *nido*-carborane salts were good synthons for the synthesis of a number of 14-vertex carboranes a [13+1] protocol. The CAd 14-vertex carboranes with C,C'-linkages were also directly synthesized via a [12+2] protocol from the reaction of CAd 12-vertex *arachno*-carborane tetraanions with $\text{HBBr}_2 \cdot \text{SMe}_2$.

14- and 15-vertex ruthenacarboranes were also synthesized. Reaction of [1,2-Me₂Si(CH₂)₂-1,2-C₂B₁₁H₁₁][Na₂(THF)₄] with [(*p*-cymene)RuCl₂]₂ gave two 14-vertex ruthenacarboranes 1,2,3- and 1,2,8-(*p*-cymene)Me₂Si(CH₂)₂-RuC₂B₁₁H₁₁. Treatment of 1,2- or 1,3-[Me₂-C₂B₁₁H₁₁][Na₂(THF)₄] with [(*p*-cymene)RuCl₂]₂ gave the same product 1,2,9-(*p*-cymene)Me₂-RuC₂B₁₁H₁₁. Reduction of a 14-vertex carborane 2,8-Me₂Si(CH₂)₂-C₂B₁₂H₁₂ followed by treatment with [(*p*-cymene)RuCl₂]₂ afforded a 15-vertex ruthenacarborane 7,1,4-(*p*-cymene)Me₂Si(CH₂)₂-RuC₂B₁₂H₁₂.

13-vertex CAD carborane $1,2-(\text{CH}_2)_3-1,2-\text{C}_2\text{B}_{11}\text{H}_{11}$ showed high reactivities toward nucleophiles, leading to the formation of the cage carbon extrusion products—12-vertex *closo*- CB_{11}^- anions $1,2-(\text{CH}_2)_3\text{CH}(\text{Nu})-1-\text{CB}_{11}\text{H}_{10}^-$, $1,2-(\text{CH}_2)_2\text{CH}(\text{Nu})\text{CH}_2-1-\text{CB}_{11}\text{H}_{10}^-$ and $1,2-(\text{CH}_2)_2\text{CH}=\text{CH}-1-\text{CB}_{11}\text{H}_{10}^-$, which are significantly different from that of its 12-vertex analogues. The key intermediates $[\mu-7,8,10-(\text{CH}_2)_3\text{CHBX}-7-\text{CB}_{10}\text{H}_{10}]^-$ ($\text{X} = \text{OMe}, \text{NEt}_2$) were synthesized and structurally characterized from reaction of $1,2-(\text{CH}_2)_3-1,2-\text{C}_2\text{B}_{11}\text{H}_{11}$ with MeOH/PS or LiNEt_2 .

Cage boron extrusion was also observed in the reactions of 13-vertex carboranes with some nucleophiles. $1,2-(\text{CH}_2)_n-1,2-\text{C}_2\text{B}_{11}\text{H}_{11}$ ($n = 3, 4$) reacted with MeOH in the presence of inorganic or organic base to afford 11-vertex *nido*- CB_{10}^- anions $[\mu-7,8-(\text{CH}_2)_n\text{CHB}(\text{OMe})_2-7-\text{CB}_{10}\text{H}_{11}]^-$, via $[\mu-7,8,10-(\text{CH}_2)_3\text{CHBOMe}-7-\text{CB}_{10}\text{H}_{10}]^-$ ($n = 3$) or $[3-\text{MeO}-\mu-1,2-(\text{CH}_2)_4-1,2-\text{C}_2\text{B}_{11}\text{H}_{11}]^-$ ($n = 4$) intermediate. These anions are boronic esters in nature and underwent oxidization reaction to give $[\mu-7,8-(\text{CH}_2)_n\text{CHOH}-7-\text{CB}_{10}\text{H}_{11}]^-$ or hydrolysis to $[\mu-7,8-(\text{CH}_2)_n\text{CHB}(\text{OH})_2-7-\text{CB}_{10}\text{H}_{11}]^-$. Reaction of $1,2-(\text{CH}_2)_3-1,2-\text{C}_2\text{B}_{11}\text{H}_{11}$ with 4-substituted pyridines ($4-\text{RC}_5\text{H}_4\text{N}$) at low temperature gave 11-vertex *closo*- CB_{10}^- anions $\mu-2,4-(\text{CH}_2)_3\text{CHBH}(4-\text{RC}_5\text{H}_4\text{N})_2-2-\text{CB}_{10}\text{H}_9$. $1,2-(\text{CH}_2)_n-1,2-\text{C}_2\text{B}_{11}\text{H}_{11}$ ($n = 3, 4$) reacted with bipy or phen to yield 12-vertex *closo*- C_2B_{10} molecules $4-(\text{bipy})\text{B}-1,2-(\text{CH}_2)_n-1,2-\text{C}_2\text{B}_{10}\text{H}_9$ or $4-(\text{H}_2\text{phen})\text{B}-1,2-(\text{CH}_2)_n-1,2-\text{C}_2\text{B}_{10}\text{H}_9$.

The linkage showed some effects on the products formation. Reaction of 13-vertex carborane $1,2-(\text{CH}_2)_4-1,2-\text{C}_2\text{B}_{11}\text{H}_{11}$ with MeOH afforded a mixture of cage carbon extrusion products 12-vertex *closo*- CB_{11}^- anions and deboration product 12-vertex *closo*- C_2B_{10} species $1,2-(\text{CH}_2)_4-1,2-\text{C}_2\text{B}_{10}\text{H}_{10}$. It also reacted with $(4-\text{MeC}_6\text{H}_4)\text{SNa}$ to yield the CB_{11}^- product $[\mu-1,2-(\text{CH}_2)_4\text{CHS}(4-\text{MeC}_6\text{H}_4)-1-\text{CB}_{11}\text{H}_{10}]^-$. On the other hand, reaction of $1,2-(\text{CH}_2)_4-1,2-\text{C}_2\text{B}_{11}\text{H}_{11}$ with Et_2NH gave $3-\text{NEt}_2\text{H}-\mu-$

1,7-(CH₂)₄-1,7-C₂B₁₁H₁₁. This product was deprotonated by NaH to afford [9-NEt₂-μ-7,8,10-(CH₂)₄CCH-B₁₁H₁₀]⁻ with an exopolyhedral B=N double bond. This process was reversible upon addition of HCl. The same anions were also directly formed by reaction of 1,2-(CH₂)₄-1,2-C₂B₁₁H₁₁ with LiNR₂ (R = Me, Et). These results indicated that the nature of the nucleophile greatly influenced the formation and structure of the products.

13-Vertex C_{Ap} carborane 1,12-Me₂-1,12-C₂B₁₁H₁₁ reacted with MeOH to give 2-substituted CB₁₁⁻ anions. However, it reacted with NaBH₄ or NaH to yield 7-substituted CB₁₁⁻ anion [1-Me-7-Et-1-CB₁₁H₁₀]⁻. The same anion can also be prepared by deprotonation of the 13-vertex *nido*-carborane dianions 1,2- or 1,3-[Me₂C₂B₁₁H₁₁]²⁻. Treatment of 1,12-Me₂-1,12-C₂B₁₁H₁₁ with Me₂NLi generated a 14-vertex *arachno*-azacarborane [C,C',N,N'-Me₄-NC₂B₁₁H₁₁]⁻ whereas a 12-vertex carborane 8-BH₃PPh₂-1,2-Me₂-1,2-C₂B₁₀H₉ was isolated in the reaction with PPh₂K.

Reactions of 14-vertex *closo*-carboranes 2,3- or 2,8-(CH₂)₃-C₂B₁₂H₁₂ with MeOH at 70 °C gave 12-vertex *closo*-CB₁₁⁻ anions. In the presence of Me₃N, the above reaction afforded [8,9-(CH₂)₃-μ-11,12-(MeO)BH-8,9-C₂B₁₁H₁₁]⁻ at room temperature, which was converted to the 2,3-isomer of 14-vertex carborane in the presence of acid such as HCl, or underwent further deboration to give [8,9-(CH₂)₃-8,9-C₂B₁₁H₁₂]⁻. Mechanistic studies showed that [8,9-(CH₂)₃-μ-11,12-(MeO)BH-8,9-C₂B₁₁H₁₁]⁻ is the first intermediate in the reaction of 14-vertex carborane with MeOH and [8,9-(CH₂)₃-8,9-C₂B₁₁H₁₂]⁻ is unlikely an intermediate.

This work clearly demonstrated that the chemistry of supercarboranes is very different from that of 12-vertex ones.

Chapter 8. Experimental Section

General Procedures. Unless otherwise noted, all experiments were performed under an atmosphere of dry dinitrogen or argon with the rigid exclusion of air and moisture using standard Schlenk or cannula techniques, or in a glovebox. CH_2Cl_2 and MeCN were refluxed over CaH_2 for several days and distilled immediately prior to use. Other organic solvents were refluxed over sodium benzophenone ketyl for several days and freshly distilled prior to use. All chemicals were purchased from either Aldrich or Acros Chemical Co. and used as received unless otherwise noted. μ -1,2-($\text{CH}_2\text{CH}=\text{CHCH}_2$)-1,2- $\text{C}_2\text{B}_{10}\text{H}_{10}$ (1),⁸³ μ -1,2-(CH_2)₃-1,2- $\text{C}_2\text{B}_{10}\text{H}_{10}$ (2),⁷³ μ -1,2-(CH_2)₄-1,2- $\text{C}_2\text{B}_{10}\text{H}_{10}$ (3),^{73a} μ -1,2-(CH_2)₃-1,2- $\text{C}_2\text{B}_{11}\text{H}_{11}$ (6),⁷⁴ μ -1,2-O(CH_2)₂-1,2- $\text{C}_2\text{B}_{10}\text{H}_{10}$ (9),^{17a,b} μ -1,2-O(Me_2Si)₂-1,2- $\text{C}_2\text{B}_{10}\text{H}_{10}$ (10),⁹⁵ μ -1,2-Me₂Si(CH_2)₂-1,2- $\text{C}_2\text{B}_{10}\text{H}_{10}$ (11),^{17a} 1,2-Me₂-1,2- $\text{C}_2\text{B}_{10}\text{H}_{10}$ (13),¹⁰¹ [μ -1,2-(CH_2)₃-1,2- $\text{C}_2\text{B}_{11}\text{H}_{11}$][$\text{Na}_2(\text{THF})_4$] ([22][$\text{Na}_2(\text{THF})_4$]),⁷⁴ μ -2,3-(CH_2)₃-2,3- $\text{C}_2\text{B}_{12}\text{H}_{12}$ (27a),⁸¹ μ -2,8-(CH_2)₃-2,8- $\text{C}_2\text{B}_{12}\text{H}_{12}$ (27b),⁸¹ 1-Me-1,2- $\text{C}_2\text{B}_{10}\text{H}_{11}$ (73),^{20a} and $\text{Ph}_2\text{PK}^{133}$ were prepared according to literature methods. Infrared spectra were obtained from KBr pellets (prepared in the glovebox if the complex was hygroscopic or air sensitive) on a Perkin-Elmer 1600 Fourier transform spectrometer. The ¹H and ¹³C NMR spectra were recorded on a Bruker DPX 300 spectrometer at 300.13 and 75.47 MHz, or a Varian Inova 400 spectrometer, or a Bruker DPX 400 spectrometer or a Bruker DPX 400Q spectrometer at 400.16 and 100.6 MHz, respectively. The ¹¹B NMR spectra and ³¹P NMR spectra were recorded on a Bruker DPX 300 spectrometer at 96.29 and 121.49 MHz, or a Varian Inova 400 spectrometer, or a Bruker DPX 400 spectrometer or a Bruker DPX 400Q spectrometer at 128.4 and 162.0 MHz, respectively. The ²⁹Si NMR spectra were recorded on a Varian Inova 400 spectrometer or a Bruker DPX

400Q spectrometer at 79.5 MHz. All chemical shifts are reported in δ units with references to the residual protons of the deuterated solvents for proton chemical shifts, to the carbons of the deuterated solvents for carbon chemical shifts according to the literature, to external $\text{BF}_3 \cdot \text{OEt}_2$ (0.0 ppm) for boron chemical shifts, to external 85% H_3PO_4 (0.0 ppm) for phosphorous chemical shifts, and to external or internal Me_4Si (0.0 ppm) for silicon chemical shifts. Mass spectra were recorded on a Thermo Finnigan MAT 95 XL spectrometry. Elemental analyses were performed by MEDAC Ltd., Brunel University, Middlesex, U.K. or Shanghai Institute of Organic Chemistry, SIOC, Shanghai, China.

NMR Data of Compounds Prepared According to Literature Methods

μ -1,2-($\text{CH}_2\text{CH}=\text{CHCH}_2$)-1,2- $\text{C}_2\text{B}_{10}\text{H}_{10}$ (1). ^1H NMR (400 MHz, CDCl_3): δ 5.66 (t, $J = 1.3$ Hz, 2H, CH), 3.01 (br, 4H, CH_2). $^{13}\text{C}\{^1\text{H}\}$ NMR (100 MHz, CDCl_3): δ 119.9 (CH), 70.2 (cage C), 33.2 (CH_2). ^{11}B NMR (128 MHz, CDCl_3): δ -6.0 (d, $J_{\text{BH}} = 148$ Hz, 2B), -9.5 (d, $J_{\text{BH}} = 142$ Hz, 2B), -10.1 (d, $J_{\text{BH}} = 165$ Hz, 4B), -11.8 (d, $J_{\text{BH}} = 218$ Hz, 2B).

μ -1,2-(CH_2)₃-1,2- $\text{C}_2\text{B}_{10}\text{H}_{10}$ (2). ^1H NMR (400 MHz, CDCl_3): δ 2.50 (m, 4H, CCH_2), 2.41 (m, 2H, CCH_2CH_2). $^{13}\text{C}\{^1\text{H}\}$ NMR (100 MHz, CDCl_3): δ 84.0 (cage C), 34.8 (CCH_2), 32.2 (CCH_2CH_2). ^{11}B NMR (96 MHz, CDCl_3): δ -7.1 (d, $J_{\text{BH}} = 140$ Hz, 2B), -8.4 (d, $J_{\text{BH}} = 129$ Hz, 2B), -9.2 (d, $J_{\text{BH}} = 100$ Hz, 2B), -11.9 (d, $J_{\text{BH}} = 164$ Hz, 4B).

μ -1,2-(CH_2)₄-1,2- $\text{C}_2\text{B}_{10}\text{H}_{10}$ (3). ^1H NMR (400 MHz, CDCl_3): δ 2.43 (m, 4H, CCH_2), 1.58 (m, 4H, CCH_2CH_2). $^{13}\text{C}\{^1\text{H}\}$ NMR (100 MHz, CDCl_3): δ 73.2 (cage C), 32.9 (CCH_2), 19.8 (CCH_2CH_2). ^{11}B NMR (96 MHz, CDCl_3): δ -6.1 (d, $J_{\text{BH}} = 148$ Hz, 2B), -9.8 (d, $J_{\text{BH}} = 169$ Hz, 6B), -11.8 (d, $J_{\text{BH}} = 195$ Hz, 2B).

μ -1,2-(CH₂)₃-1,2-C₂B₁₁H₁₁ (6). ¹H NMR (400 MHz, CDCl₃): δ 3.24 (t, J = 7.4 Hz, 4H, CCH₂), 2.16 (m, J = 7.4 Hz, 2H, CCH₂CH₂). ¹³C{¹H} NMR (100 MHz, CDCl₃): δ 136.4 (cage C), 49.3 (CCH₂), 25.7 (CCH₂CH₂). ¹¹B NMR (96 MHz, CDCl₃): δ 3.2 (d, $J_{\text{BH}} \approx 148$ Hz, 1B), 0.7 (d, $J_{\text{BH}} = 168$ Hz, 5B), -1.4 (d, $J_{\text{BH}} = 189$ Hz, 5B).

μ -1,2-O(CH₂)₂-1,2-C₂B₁₀H₁₀ (9). ¹H NMR (400 MHz, CDCl₃): δ 4.27 (s, 4H, CH₂). ¹³C{¹H} NMR (100 MHz, CDCl₃): δ 78.9 (cage C), 73.7 (CH₂). ¹¹B NMR (128 MHz, CDCl₃): δ -6.0 (d, $J_{\text{BH}} = 149$ Hz, 2B), -8.2 (d, $J_{\text{BH}} = 145$ Hz, 2B), -8.7 (d, $J_{\text{BH}} = 175$ Hz, 2B), -12.9 (d, $J_{\text{BH}} = 164$ Hz, 4B).

μ -1,2-O(Me₂Si)₂-1,2-C₂B₁₀H₁₀ (10). ¹H NMR (400 MHz, CDCl₃): δ 0.38 (s, 12H, CH₃). ¹³C{¹H} NMR (100 MHz, CDCl₃): δ 73.4 (cage C), -1.0 (CH₃). ¹¹B NMR (128 MHz, CDCl₃): δ -0.8 (d, $J_{\text{BH}} = 143$ Hz, 2B), -4.1 (d, $J_{\text{BH}} = 146$ Hz, 2B), -11.1 (d, $J_{\text{BH}} = 162$ Hz, 4B), -12.9 (d, $J_{\text{BH}} \approx 226$ Hz, 2B).

μ -1,2-Me₂Si(CH₂)₂-1,2-C₂B₁₀H₁₀ (11). ¹H NMR (400 MHz, CDCl₃): δ 1.81 (s, 4H, CH₂), 0.33 (s, 6H, CH₃). ¹³C{¹H} NMR (100 MHz, CDCl₃): δ 87.5 (cage C), 25.3 (CH₂), 0.1 (CH₃). ¹¹B NMR (96 MHz, CDCl₃): δ -6.8 (d, $J_{\text{BH}} = 157$ Hz, 2B), -8.5 (d, $J_{\text{BH}} = 162$ Hz, 2B), -10.2 (d, $J_{\text{BH}} = 165$ Hz, 6B).

1,2-Me₂-1,2-C₂B₁₀H₁₀ (13). ¹H NMR (400 MHz, CDCl₃): δ 2.03 (s, 6H, CH₃). ¹³C{¹H} NMR (100 MHz, CDCl₃): δ 73.5 (cage C), 23.4 (CH₃). ¹¹B NMR (96 MHz, CDCl₃): δ -5.4 (d, $J_{\text{BH}} = 148$ Hz, 2B), -8.4 (d, $J_{\text{BH}} = 141$ Hz, 2B), -9.7 (d, $J_{\text{BH}} = 150$ Hz, 4B), -10.6 (d, $J_{\text{BH}} \approx 79$ Hz, 2B).

[μ -1,2-(CH₂)₃-1,2-C₂B₁₁H₁₁][Na₂(THF)₄] ([22][Na₂(THF)₄]). ¹H NMR (400 MHz, pyridine-*d*₅): δ 3.66 (m, 16H, THF), 2.37 (t, J = 6.5 Hz, 4H, CCH₂), 2.21 (m, J = 6.6 Hz, 2H, CCH₂CH₂), 1.64 (m, 16H, THF). ¹³C{¹H} NMR (100 MHz, pyridine-*d*₅): δ 67.9 (THF), 43.4 (CCH₂), 29.8 (CCH₂CH₂), 25.8 (THF), 16.0 (cage C). ¹¹B NMR (128 MHz, pyridine-*d*₅): δ -9.6 (d, $J_{\text{BH}} = 114$ Hz, 1B), -15.1 (br, 5B), -25.2 (d,

$J_{\text{BH}} \approx 77$ Hz, 5B).

μ -2,3-(CH₂)₃-2,3-C₂B₁₂H₁₂ (27a). ¹H NMR (400 MHz, CDCl₃): δ 3.15 (m, 2H, CCH₂), 2.38 (m, 1H, CCH₂CH₂), 2.28 (m, 2H, CCH₂), 2.03 (m, 1H, CCH₂CH₂). ¹³C{¹H} NMR (100 MHz, CDCl₃): δ 72.3 (cage C), 40.7 (CCH₂), 26.0 (CCH₂CH₂). ¹¹B NMR (128 MHz, CDCl₃): δ 7.4 (d, $J_{\text{BH}} = 156$ Hz, 1B), 5.4 (d, $J_{\text{BH}} = 152$ Hz, 2B), 2.8 (d, $J_{\text{BH}} = 166$ Hz, 2B), -4.2 (d, $J_{\text{BH}} = 177$ Hz, 1B), -6.5 (d, $J_{\text{BH}} = 151$ Hz, 2B), -9.5 (d, $J_{\text{BH}} = 165$ Hz, 1B), -12.4 (d, $J_{\text{BH}} = 162$ Hz, 2B), -24.8 (d, $J_{\text{BH}} = 143$ Hz, 1B).

μ -2,8-(CH₂)₃-2,8-C₂B₁₂H₁₂ (27b). ¹H NMR (400 MHz, CDCl₃): δ 2.89 (br, 4H, CCH₂), 2.25 (br, 2H, CCH₂CH₂). ¹³C{¹H} NMR (100 MHz, CDCl₃): δ 90.0 (cage C), 43.1 (CCH₂), 29.0 (CCH₂CH₂).

1-Me-1,2-C₂B₁₀H₁₁ (73). ¹H NMR (400 MHz, CDCl₃): δ 3.58 (s, 1H, CH), 2.04 (s, 3H, CH₃). ¹³C{¹H} NMR (100 MHz, CDCl₃): δ 70.6 (cage CCH₃), 61.7 (cage CH), 26.0 (CH₃). ¹¹B NMR (128 MHz, CDCl₃): δ -2.2 (d, $J_{\text{BH}} = 149$ Hz, 1B), -7.1 (d, $J_{\text{BH}} = 151$ Hz, 1B), -9.5 (d, $J_{\text{BH}} = 162$ Hz, 2B), -10.9 (d, $J_{\text{BH}} = 168$ Hz, 2B), -11.6 (d, $J_{\text{BH}} = 183$ Hz, 2B), -13.0 (d, $J_{\text{BH}} = 170$ Hz, 2B).

Chapter 2

Preparation of μ -1,2-MeCH(CH₂)₂-1,2-C₂B₁₀H₁₀ (4). To a solution of 1,2-C₂B₁₀H₁₂ (4.327 g, 30.0 mmol) in toluene/Et₂O (2:1, 60 mL) was added dropwise a 1.60 M solution of *n*-BuLi in *n*-hexane (38.4 mL, 61.4 mmol) at 0°C with stirring. The mixture was allowed to warm to room temperature and further stirred for 2 h to give a pale yellow suspension of 1,2-Li₂-1,2-C₂B₁₀H₁₀. This suspension was then cooled to 0°C, and BrCH₂CH₂CHBrMe (3.9 mL, $d = 1.8$, 97%, 31.5 mmol) was slowly added with stirring. The mixture was heated to reflux overnight and then quenched with 50 mL of water. After removal of the precipitate by filtration, the or-

ganic layer was separated, and the aqueous layer was extracted with Et₂O (25 mL x 3). The organic layers were combined and dried over Na₂SO₄. After removal of the solvent, the resultant solid was subjected to column chromatographic separation (SiO₂, 300 - 400 mesh) using *n*-hexane as eluent to give **4** as white powder (4.80 g, 24.2 mmol, 81 %). X-ray-quality crystals of **4** were obtained by recrystallization from *n*-hexane. ¹H NMR (400 MHz, CDCl₃): δ 2.91 (m, 1H, CH), 2.47(m, 1H, CHCH₂), 2.42 (m, 2H, CCH₂), 1.93 (m, 1H, CHCH₂), 1.17 (d, *J* = 6.7 Hz, 3H, CH₃). ¹³C NMR (100 MHz, CDCl₃): δ 88.0 (cage CCH), 84.2 (cage CCH₂), 41.0 (CH), 40.9 (CHCH₂), 34.1 (CCH₂), 19.6 (CH₃). ¹¹B NMR (96 MHz, CDCl₃): δ -6.4 (d, *J*_{BH} ≈ 168 Hz, 1B), -7.3 (d, *J*_{BH} = 136 Hz, 3B), -9.9 (d, *J*_{BH} = 147 Hz, 1B), -10.8 (d, *J*_{BH} = 142 Hz, 1B), -12.3 (d, *J*_{BH} ≈ 133 Hz, 1B), -13.4 (d, *J*_{BH} = 163 Hz, 3B). IR (KBr) ν_{\max} (cm⁻¹): 2588, 2570 (vs, BH). HRMS (EI): *m/z* calcd for C₆H₁₆¹¹B₈¹⁰B₂ [M - 2H]⁺: 196.2250; Found: 196.2242.

Preparation of 3-Ph- μ -1,2-(CH₂CH=CHCH₂)-1,2-C₂B₁₁H₁₀ (5a). To a THF (20 mL) solution of **1** (982 mg, 5.0 mmol) was added finely cut Na metal (460 mg, 20.0 mmol) and a catalytic amount of naphthalene (64 mg, 0.5 mmol), and the mixture was stirred at room temperature for 3 days. After removal of excess Na metal and THF, toluene (10 mL) was then added. PhBCl₂ (1.4 mL, *d* = 1.224, 97%, 10.5 mmol) was slowly added to the above suspension at -78 °C and the mixture was stirred at this temperature for 1 h and at room temperature overnight. Removal of the precipitate and solvents, followed by column chromatographic separation (SiO₂, 300-400 mesh, *n*-hexane) afforded **5a** as a yellow solid (70 mg, 0.25 mmol, 5%). X-ray-quality crystals of **5a** were obtained by recrystallization from CH₂Cl₂. ¹H NMR (400 MHz, CDCl₃): δ 7.32 (m, 5H, C₆H₅), 5.69 (t, *J* = 2.1 Hz, 2H, CH), 3.41 (d, *J* = 2.0 Hz, 4H, CH₂). ¹³C{¹H} NMR (100 MHz, CDCl₃): δ 141.5 (cage C), 134.5, 129.7,

128.2 (C₆H₅), 122.9 (CH), 44.0 (CH₂). ¹¹B NMR (96 MHz, CDCl₃): δ 5.5 (d, *J*_{BH} ≈ 150 Hz, 2B), 3.2 (d, *J*_{BH} = 182 Hz, 2B), 1.4 (d, *J*_{BH} = 132 Hz, 2B), 0.4 (d, *J*_{BH} ≈ 124 Hz, 2B), -2.1 (d, *J*_{BH} = 175 Hz, 2B), -4.3 (d, *J*_{BH} = 177 Hz, 1B). IR (KBr) *v*_{max} (cm⁻¹): 2561, 2551 (vs, BH). HRMS (EI): *m/z* calcd for C₁₂H₁₉¹¹B₉¹⁰B₂ [M - 2H]⁺: 282.2578; Found: 282.2580.

Isolation of 3-Ph- μ -1,2-(CH=CHCH₂CH₂)-1,2-C₂B₁₁H₁₀ (5b). Compound **5a** (114 mg, 0.40 mmol) was kept in the open air for 2 years. Column chromatographic separation (SiO₂, 300-400 mesh, *n*-hexane) afforded **5a** (87 mg, 76%) and **5b** (21 mg, 0.074 mmol, 18%) as a yellow solid. X-ray-quality crystals of **5b** were obtained by recrystallization from CH₂Cl₂. ¹H NMR (400 MHz, CDCl₃): δ 7.39 (m, 2H, C₆H₅), 7.32 (m, 1H, C₆H₅), 7.24 (m, 2H, C₆H₅), 6.74 (dt, *J*₁ = 9.4 Hz, *J*₂ = 1.8 Hz, 1H, CCH), 6.41 (dt, *J*₁ = 9.4 Hz, *J*₂ = 4.5 Hz, 1H, CCH=CH), 2.81 (t, *J* = 7.5 Hz, 2H, CCH₂), 1.99 (ddt, *J*₁ = 1.9 Hz, *J*₂ = 4.5 Hz, *J*₃ = 7.5 Hz, 2H, CHCH₂). ¹³C{¹H} NMR (100 MHz, CDCl₃): δ 139.1 (CCH=CH), 136.0 (cage CCH), 135.2 (cage CCH₂), 134.4 (C₆H₅), 133.4 (CCH), 129.8, 128.1 (C₆H₅), 39.1 (CCH₂), 20.4 (CHCH₂). ¹¹B NMR (96 MHz, CDCl₃): δ 8.4 (s, 1B), 5.2 (d, *J*_{BH} = 156 Hz, 1B), 2.2 (d, *J*_{BH} = 162 Hz, 4B), 0.3 (d, *J*_{BH} ≈ 183 Hz, 2B), -1.6 (d, *J*_{BH} ≈ 185 Hz, 1B), -4.9 (d, *J*_{BH} = 146 Hz, 1B). IR (KBr) *v*_{max} (cm⁻¹): 2554 (vs, BH). HRMS (EI): *m/z* calcd for C₁₂H₁₉¹¹B₉¹⁰B₂ [M - 2H]⁺: 282.2578; Found: 282.2579.

Preparation of μ -1,2-(CH₂)₄-1,2-C₂B₁₁H₁₁ (7) and 3-Me- μ -1,2-(CH₂)₄-1,2-C₂B₁₁H₁₀ (7'). To a THF (40 mL) solution of **3** (4.958 g, 25.0 mmol) was added finely cut Na metal (2.299 g, 100.0 mmol) and a catalytic amount of naphthalene (320 mg, 2.5 mmol), and the mixture was stirred at room temperature overnight. After removal of excess Na metal and THF, toluene (30 mL) was then added. A 1.0 M solution of HBBBr₂·SMe₂ in CH₂Cl₂ (50.0 mL, 50.0 mmol) was slowly added to the above

suspension at $-78\text{ }^{\circ}\text{C}$ and the mixture was stirred at this temperature for 1 h and at room temperature overnight. Removal of the precipitate and solvents, followed by column chromatographic separation (SiO_2 , 300-400 mesh, *n*-hexane) afforded **7** in about 45% yield. Recrystallization from *n*-hexane gave **7** as a white solid (1.900 g, 9.0 mmol, 36%). X-ray-quality crystals of **7** were obtained by slowly evaporation of a saturated *n*-hexane solution. Compound **7'** was obtained as a mixture of a white solid with **7** in about 1:1 ratio (490 mg, 1.13 mmol, 4.5%). Repeated column chromatographic separation (SiO_2 , 300-400 mesh, *n*-hexane) gave **7'** as a white solid (5 mg, >95%, 0.022 mmol, 0.89%). X-ray-quality crystals of **7'** were obtained by slowly evaporation of a saturated *n*-hexane solution. **7**: ^1H NMR (400 MHz, CDCl_3): δ 3.05 (m, 4H, CH_2), 1.78 (m, 4H, CH_2). $^{13}\text{C}\{^1\text{H}\}$ NMR (100 MHz, CDCl_3): δ 142.5 (cage C), 44.2 (CCH_2), 20.4 (CCH_2CH_2). ^{11}B NMR (96 MHz, CDCl_3): δ 4.3 (d, $J_{\text{BH}} = 149\text{ Hz}$, 1B), 0.4 (d, $J_{\text{BH}} = 145\text{ Hz}$, 5B), -0.4 (d, $J_{\text{BH}} = 164\text{ Hz}$, 5B). IR (KBr) ν_{max} (cm^{-1}): 2566, 2556 (vs, BH). HRMS (EI): m/z calcd for $\text{C}_6\text{H}_{18}^{11}\text{B}_9^{10}\text{B}_2$ $[\text{M} - \text{H}]^+$: 209.2499; Found: 209.2495. **7'**: ^1H NMR (400 MHz, CDCl_3): δ 2.99 (m, 4H, CCH_2), 1.77 (m, 4H, CCH_2CH_2), 0.11 (s, 3H, CH_3). $^{13}\text{C}\{^1\text{H}\}$ NMR (100 MHz, CDCl_3): δ 143.9 (cage C), 42.6 (CCH_2), 20.6 (CCH_2CH_2), 0.3 (CH_3). ^{11}B NMR (128 MHz, CDCl_3): δ 5.6 (d, $J_{\text{BH}} = 167\text{ Hz}$, 2B), 4.0 (d, $J_{\text{BH}} \approx 212\text{ Hz}$, 1B), 3.2 (s, 1B), 2.1 (d, $J_{\text{BH}} = 151\text{ Hz}$, 2B), 1.1 (d, $J_{\text{BH}} = 136\text{ Hz}$, 2B), -2.3 (d, $J_{\text{BH}} = 169\text{ Hz}$, 2B), -5.5 (d, $J_{\text{BH}} = 151\text{ Hz}$, 1B). IR (KBr) ν_{max} (cm^{-1}): 2558 (vs, BH). HRMS (EI): m/z calcd for $\text{C}_7\text{H}_{20}^{11}\text{B}_9^{10}\text{B}_2$ $[\text{M} - \text{H}]^+$: 223.2656; Found: 223.2654.

Preparation of μ -1,2-MeCH(CH₂)₂-1,2-C₂B₁₁H₁₁ (8). To a THF (40 mL) solution of **4** (4.958 g, 25.0 mmol) was added finely cut Na metal (2.299 g, 100.0 mmol) and a catalytic amount of naphthalene (320 mg, 2.5 mmol), and the mixture was stirred at room temperature overnight. After removal of excess Na metal and THF,

toluene (30 mL) was then added. A 1.0 M solution of $\text{HBBBr}_2 \cdot \text{SMe}_2$ in CH_2Cl_2 (50.0 mL, 50.0 mmol) was slowly added to the above suspension at -78°C and the mixture was stirred at this temperature for 1 h and at room temperature overnight. Removal of the precipitate and solvents, followed by column chromatographic separation (SiO_2 , 300-400 mesh, *n*-hexane) afforded gross **8** in about 40% yield. Recrystallization from *n*-hexane gave **8** as a white solid (1.700 g, 8.1 mmol, 32%). ^1H NMR (400 MHz, CDCl_3): δ 3.23 (m, 1H, CCH_2), 3.22 (m, 1H, CH), 3.04 (ddd, $J_1 = 7.6$ Hz, $J_2 = 10.1$ Hz, $J_3 = 16.7$ Hz, 1H, CCH_2), 2.42 (ddt, $J_1 = 3.6$ Hz, $J_2 = 13.1$ Hz, $J_3 = 7.4$ Hz, 1H, CHCH_2), 1.72 (ddt, $J_1 = 7.9$ Hz, $J_2 = 13.1$ Hz, $J_3 = 9.9$ Hz, 1H, CHCH_2), 1.47 (d, $J = 7.0$ Hz, 3H, CH_3). $^{13}\text{C}\{^1\text{H}\}$ NMR (100 MHz, CDCl_3): δ 142.3 (cage CCH), 136.1 (cage CCH_2), 53.9 (CH), 47.8 (CCH_2), 34.8 (CHCH_2), 17.6 (CH_3). ^{11}B NMR (128 MHz, CDCl_3): δ 3.3 (d, $J_{\text{BH}} = 159$ Hz, 1B), 0.7 (d, $J_{\text{BH}} = 151$ Hz, 5B), -2.1 (d, $J_{\text{BH}} = 166$ Hz, 5B). IR (KBr) ν_{max} (cm^{-1}): 2570 (vs, BH). HRMS (EI): m/z calcd for $\text{C}_6\text{H}_{18}^{11}\text{B}_9^{10}\text{B}_2 [\text{M} - \text{H}]^+$: 209.2503; Found: 209.2502.

Reduction of μ -1,2- $\text{O}(\text{CH}_2)_2$ -1,2- $\text{C}_2\text{B}_{10}\text{H}_{10}$ (9**) with Na metal.** To a THF (10 mL) solution of compound **2** (745 mg, 4.00 mmol) was added finely cut Na metal (920 mg, 40.0 mmol) and naphthalene (51 mg, 0.40 mmol). The reaction mixture was stirred overnight to give a dark red suspension. After filtration on Celite, a dark red solution was collected. After concentration of this solution to about 1 mL, some yellow crystals was obtained after standing for 2 weeks, from which [9,9'- Me_2 -7,7'-($\text{CH}=\text{CH}$)-(7,9- $\text{C}_2\text{B}_{10}\text{H}_{10}$) $_2$][$\text{Na}_4(\text{THF})_{12}$] (**[12a]**[$\text{Na}_4(\text{THF})_{12}$]) was structurally characterized by single-crystal X-ray analyses.

Addition of 18-crown-6 (2.115 g, 8.00 mmol) to the above red solution mentioned above with stirring gave a yellow suspension. After filtration, the colorless filtrate was separated from the yellow solid. This colorless solution was stood for two weeks

to give some colorless crystals, from which $[\mu\text{-}7,8\text{-O}(\text{CH}_2)_2\text{-}7,8\text{-C}_2\text{B}_9\text{H}_9][\text{Na}_2(18\text{-crown-}6)]$ (**[12b]** $[\text{Na}_2(18\text{-crown-}6)]$) was structurally characterized by single-crystal X-ray analyses.

The red solution mentioned above was dried via vacuum and 20 mL toluene was added. To this suspension was added 1.0 M solution of $\text{HBBr}_2 \cdot \text{SMe}_2$ in CH_2Cl_2 (8.0 mL, 8.0 mmol) at -78°C with stirring then slowly warmed to room temperature, and stirred overnight. The resulting suspension was quenched with 20 mL of water. The organic layer was separated and the water phase was extracted with CH_2Cl_2 (10 mL x 3). The organic layer was combined and dried over Na_2SO_4 . Column chromatographic separation (SiO_2 , 300-400 mesh, *n*-hexane) gave **13** as a white powder (30 mg, 0.17 mmol, 4.4%), together with other unidentified species.

Preparation of $[\mu\text{-}7,10\text{-O}(\text{Me}_2\text{Si})_2\text{-}7,10\text{-C}_2\text{B}_{10}\text{H}_{10}][\text{Na}_2(\text{THF})_4]$ ([14]** $[\text{Na}_2(\text{THF})_4]$).** To a THF (10 mL) solution of compound **10** (275 mg, 1.00 mmol) was added finely cut Na metal (230 mg, 10.0 mmol) and mixture was stirred overnight to give a yellow green suspension. After filtration on Celite, a yellow green solution was collected and concentrated to about 2 mL. The sticky solution was stood for two weeks to give **[14]** $[\text{Na}_2(\text{THF})_4]$ as yellow crystals (570 mg, 0.94 mmol, 94%). ^1H NMR (400 MHz, pyridine-*d*₅): δ 3.66 (m, 16H, THF), 1.65 (m, 16H, THF), 0.81 (s, 12H, CH_3). $^{13}\text{C}\{^1\text{H}\}$ NMR (100 MHz, pyridine-*d*₅): δ 94.9 (cage C), 67.9, 25.8 (THF), 4.22 (CH_3). ^{11}B NMR (96 MHz, pyridine-*d*₅): δ 13.0 (br, 2B), -2.4 (d, $J_{\text{BH}} = 109$ Hz, 2B), -17.7 (d, $J_{\text{BH}} \approx 98$ Hz, 4B), -20.8 (d, $J_{\text{BH}} = 114$ Hz, 2B). IR (KBr) ν_{max} (cm^{-1}): 2574 (vs, BH). Anal. Calcd for $\text{C}_{19}\text{H}_{48}\text{B}_{10}\text{Na}_2\text{O}_{4.25}\text{Si}_2$ (M - 0.75 THF): C, 41.13; H, 8.72. Found: C, 41.42; H, 8.89.

Preparation of 1-TMSCH₂-2-Me-1,2-C₂B₁₀H₁₀ (15). To an Et₂O (40 mL) suspension of **11** (4.568 g, 20.0 mmol) was added a 1.6 M solution of MeLi in Et₂O

(25.0 mL, 40.0 mmol) at $-78\text{ }^{\circ}\text{C}$ with stirring. Then the suspension was slowly warmed to room temperature to give a colorless solution and further stirred overnight. The solution was cooled to $0\text{ }^{\circ}\text{C}$ and a 1.0 M solution of HCl in H_2O (50.0 mL, 50.0 mmol) was added. The mixture was further stirred at room temperature for 30 min then the organic layer was separated. The aqueous layer was extracted with Et_2O (10 mL x 3). The organic layers were combined and dried over Na_2SO_4 . Flash chromatographic separation (SiO_2 , 300-400 mesh, *n*-hexane) gave **15** as a white solid (4.840 g, 19.8 mmol, 99%). ^1H NMR (400 MHz, CDCl_3): δ 2.04 (s, 3H, CCH_3), 1.61 (s, 2H, CH_2), 0.17 (s, 9H, SiCH_3). $^{13}\text{C}\{^1\text{H}\}$ NMR (100 MHz, CDCl_3): δ 78.2 (cage CCH_2), 76.7 (cage CCH_3), 26.1 (CH_2), 23.6 (CCH_3), -0.5 (SiCH_3). ^{11}B NMR (96 MHz, CDCl_3): δ -5.4 (d, $J_{\text{BH}} = 150\text{ Hz}$, 2B), -8.1 (d, $J_{\text{BH}} \approx 185\text{ Hz}$, 2B), -9.9 (d, $J_{\text{BH}} \approx 158\text{ Hz}$, 2B), -10.5 (d, $J_{\text{BH}} = 156\text{ Hz}$, 4B). IR (KBr) ν_{max} (cm^{-1}): 2588, 2572 (vs, BH). HRMS (EI): m/z calcd for $\text{C}_7\text{H}_{24}\text{Si}_1^{11}\text{B}_8^{10}\text{B}_2$ [M] $^+$: 244.2645; Found: 244.2652.

Preparation of μ -1,2- $\text{Me}_2\text{Si}(\text{CH}_2)_2$ -1,2- $\text{C}_2\text{B}_{11}\text{H}_{11}$ (16**).** To a THF (30 mL) solution of **11** (2.284 g, 10.0 mmol) was added finely cut Na metal (1.000 g, 43.5 mmol), and the mixture was stirred at room temperature for 3 days. After removal of excess Na metal and THF, toluene (20 mL) was then added. To this suspension was slowly added a 1.0 M solution of $\text{HBBR}_2 \cdot \text{SMe}_2$ in CH_2Cl_2 (20.0 mL, 20.0 mmol) at $-78\text{ }^{\circ}\text{C}$, and the mixture was stirred at this temperature for 1 h and at room temperature overnight. The precipitate was filtered off and washed with *n*-hexane (3 x 30 mL). The combined organic solutions were concentrated to yield a white solid. Recrystallization from *n*-hexane/ CH_2Cl_2 gave **16** as colorless crystals (0.937 g, 39%). ^1H NMR (400 MHz, CDCl_3): δ 2.55 (s, 4H, CH_2), 0.31 (s, 6H, CH_3). $^{13}\text{C}\{^1\text{H}\}$ NMR (100 MHz, CDCl_3): δ 144.5 (cage C), 40.7 (CH_2), -2.9 (CH_3). ^{11}B NMR (96 MHz, CDCl_3): δ 4.3 (d, $J_{\text{BH}} = 152\text{ Hz}$, 1B), 0.4 (d, $J_{\text{BH}} = 153\text{ Hz}$, 10B). IR (KBr) ν_{max} (cm^{-1}): 2577 (vs,

BH). HRMS (CI): m/z calcd for $C_6H_{22}Si_1^{11}B_9^{10}B_2 [M + H]^+$: 241.2582; Found: 241.2582.

Preparation of 1,2-Me₂-1,2-C₂B₁₁H₁₁ (17a) and 1,12-Me₂-1,12-C₂B₁₁H₁₁ (17b).

Compound **16** (721 mg, 3.0 mmol) was subjected to column chromatographic separation (SiO₂, 300-400 mesh, *n*-hexane) affording **17a** (331 mg, 60%) and **17b** (166 mg, 30%) as a white solid. X-ray-quality crystals of **17a** were obtained by recrystallization from *n*-hexane. **17a**: ¹H NMR (400 MHz, CDCl₃): δ 2.73(s, 6H, CH₃). ¹³C{¹H} NMR (100 MHz, CDCl₃): δ 140.7 (cage C), 34.9 (CH₃). ¹¹B NMR (96 MHz, CDCl₃): δ 4.3 (d, J_{BH} = 160 Hz, 1B), 1.6 (d, J_{BH} = 157 Hz, 5B), -0.2 (d, J_{BH} = 169 Hz, 5B). IR (KBr) ν_{max} (cm⁻¹): 2574 (vs, BH). HRMS (EI): m/z calcd for $C_4H_{16}^{11}B_9^{10}B_2 [M - H]^+$: 183.2343; Found: 183.2343. **17b**: ¹H NMR (400 MHz, CDCl₃): δ 2.63 (s, 3H, CH₃), 1.89 (s, 3H, CH₃). ¹³C{¹H} NMR (100 MHz, CDCl₃): δ 120.6, 83.2 (cage C), 35.7, 27.4 (CH₃). ¹¹B NMR (128 MHz, CDCl₃): δ 13.3 (d, J_{BH} = 164 Hz, 1B), -5.5 (br, overlap, 5B), -6.6 (d, J_{BH} = 162 Hz, 5B). IR (KBr) ν_{max} (cm⁻¹): 2581 (vs, BH). HRMS (EI): m/z calcd for $C_4H_{16}^{11}B_9^{10}B_2 [M - H]^+$: 183.2343; Found: 183.2344.

Preparation of 1-HOMe₂SiCH₂-12-Me-1,12-C₂B₁₁H₁₁ (18b) and 1,1'-O(Me₂SiCH₂)₂-12,12'-Me₂-(1,12-C₂B₁₁H₁₁)₂ (18b'). The gross **16**, prepared from **11** (4.568 g, 20.0 mmol), was stood in the mother liquor (10 mL) in the open air for two weeks. Flash chromatographic separation (SiO₂, 300-400 mesh, *n*-hexane) gave a mixture of **17b** (minor), **18b** and **18b'** (major). After removal of **17b** via sublimation at 60 °C under vacuum, a mixture of **18b** and **18b'** was obtained as a white solid (1.250 g, 2.5 mmol, 25%). ¹H NMR (400 MHz, CDCl₃): δ 2.72, 2.70 (2H, CH₂), 1.89 (3H, CH₃), 0.15, 0.14 (6H, SiCH₃). ¹³C{¹H} NMR (100 MHz, CDCl₃): δ 127.8, 83.3 (cage C), 45.3 (CH₂), 27.3 (CH₃), 0.9 (SiCH₃). ¹¹B NMR (128 MHz, CDCl₃): δ 11.8 (br, J_{BH} ≈ 132 Hz, 1B), -6.9 (br, J_{BH} ≈ 134 Hz, 10B). ²⁹Si NMR (80 MHz, CDCl₃): δ

4.0, 2.4. IR (KBr) ν_{\max} (cm^{-1}): 2576 (vs, BH). Anal. Calcd for $\text{C}_{12}\text{H}_{44}\text{B}_{22}\text{OSi}_2$ (**18b'**): C, 28.91; H, 8.90. Found: C, 28.75; H, 9.08. HRMS (EI): m/z calcd for $\text{C}_{11}\text{H}_{41}^{11}\text{B}_{18}^{10}\text{B}_4\text{OSi}_2$ [**18b'** - CH_3] $^+$: 483.4895; Found: 483.4890.

Preparation of 1-TfOMe₂SiCH₂-12-Me-1,12-C₂B₁₁H₁₁ (18b''**).** To a $\text{C}_2\text{D}_2\text{Cl}_4$ (0.5 mL) solution of a mixture of **18b** and **18b'** (80 mg) in an NMR tube was added 0.1 mL of TfOH to give a solution of **18b''** in situ, which would turn back to the mixture of **18b** and **18b'** upon washing with water. ^1H NMR (400 MHz, $\text{C}_2\text{D}_2\text{Cl}_4$): δ 2.99 (2H, CH_2), 1.91 (3H, CH_3), 0.58 (6H, SiCH_3). $^{13}\text{C}\{^1\text{H}\}$ NMR (100 MHz, $\text{C}_2\text{D}_2\text{Cl}_4$): δ 121.5 (cage C), 117.9 (q, $J_{\text{CF}} = 318$ Hz, CF_3), 84.0 (cage C), 40.7 (CH_2), 27.0 (CH_3), -0.9 (SiCH_3). ^{11}B NMR (128 MHz, $\text{C}_2\text{D}_2\text{Cl}_4$): δ 14.5 (br, 1B), -5.1 (br, 10B). ^{29}Si NMR (80 MHz, $\text{C}_2\text{D}_2\text{Cl}_4$): δ 37.3.

Preparation of 4-(*p*-cymene)- μ -1,2-Me₂Si(CH₂)₂-4,1,2-RuC₂B₁₀H₁₀ (19**).** To a THF (20 mL) solution of **11** (1.142 g, 5.0 mmol) was added finely cut Na metal (460 mg, 20.0 mmol), and the mixture was stirred at room temperature for 3 days. After removal of excess Na metal, the filtrate was cooled to -30 °C and [(*p*-cymene)RuCl₂]₂ (1.531 g, 2.5 mmol) was slowly added with stirring. The mixture was slowly warmed up to room temperature and further stirred overnight to give a dark red suspension. After filtration, the red solution was concentrated. Chromatographic separation (SiO_2 , 300-400 mesh, *n*-hexane/ CH_2Cl_2 2:1) gave gross **19** in about 60% yield. Further washing with cold CH_2Cl_2 gave **19** as a yellow powder (1.159 g, 2.5 mmol, 50%). X-ray-quality crystals of **19** were obtained by recrystallization from CH_2Cl_2 . ^1H NMR (400 MHz, CD_2Cl_2): δ 5.73 (d, $J = 6.2$ Hz, 2H, C_6H_4), 5.64 (d, $J = 6.2$ Hz, 2H, C_6H_4), 2.93 (m, $J = 6.9$ Hz, 1H, CH), 2.28 (s, 3H, $\text{CH}_3\text{C}_6\text{H}_4$), 2.12 (d, $J = 17.1$ Hz, 2H, CH_2), 1.99 (d, $J = 17.1$ Hz, 2H, CH_2), 1.30 (d, $J = 6.9$ Hz, 6H, CH_3CH), 0.39 (s, 3H, CH_3Si), -0.20 (s, 3H, CH_3Si). $^{13}\text{C}\{^1\text{H}\}$ NMR (100 MHz,

CD₂Cl₂): δ 119.9, 110.3, 97.6, 95.2 (C₆H₄), 87.0 (cage C), 34.7 (CH₂), 30.6 (CH), 22.9 (CH₃CH), 17.8 (CH₃C₆H₄), -1.2, -1.4 (CH₃Si). ¹¹B NMR (96 MHz, CD₂Cl₂): δ 6.9 (d, $J_{\text{BH}} \approx 108$ Hz, 2B), 6.2 (d, $J_{\text{BH}} = 116$ Hz, 2B), -0.2 (d, $J_{\text{BH}} = 123$ Hz, 2B), -1.4 (d, $J_{\text{BH}} = 123$ Hz, 2B), -9.4 (d, $J_{\text{BH}} = 143$ Hz, 2B), -16.6 (d, $J_{\text{BH}} = 143$ Hz, 2B). IR (KBr) ν_{max} (cm⁻¹): 2516 (vs, BH). HRMS (ESI): m/z calcd for C₁₆H₃₄Si₁Ru₁¹⁰B₈¹¹B₂ [M]⁺: 464.2471; Found: 464.2467.

Alternative Method for the Preparation of 1,12-Me₂-1,12-C₂B₁₀H₁₀ (17b). To a THF (10 mL) solution of **13** (517 mg, 3.0 mmol) was added finely cut Na metal (300 mg, 13.0 mmol) and a catalytic amount of naphthalene (39 mg, 0.3 mmol), and the mixture was stirred at room temperature overnight. After removal of excess Na metal and THF, toluene (10 mL) was then added. A 1.0 M solution of HBBr₂·SMe₂ in CH₂Cl₂ (6.0 mL, 6.0 mmol) was slowly added to the above suspension at -78 °C and the mixture was stirred at this temperature for 1 h and at room temperature overnight. Removal of the precipitate and solvents, followed by column chromatographic separation (SiO₂, 300-400 mesh, *n*-hexane) afforded **17b** (28 mg, 5%) and **13** (88 mg, 17%).

Preparation of 1-TMSCH₂-12-Me-1,12-C₂B₁₁H₁₁ (20). To a THF (30 mL) solution of **15** (4.889 g, 20.0 mmol) was added finely cut Na metal (1.379 g, 60.0 mmol), and the mixture was stirred at room temperature for one week. After removal of excess Na metal and THF, toluene (20 mL) was then added. A 1.0 M solution of HBBr₂·SMe₂ in CH₂Cl₂ (40.0 mL, 40.0 mmol) was slowly added to the above suspension at -78 °C and the mixture was stirred at this temperature for 1 h and at room temperature overnight. Removal of the precipitate and solvents, followed by column chromatographic separation (SiO₂, 300-400 mesh, *n*-hexane) afforded **20** as a white solid (240 mg, 0.94 mmol, 4.7%). X-ray-quality crystals of **20** were obtained by re-

crystallization from *n*-hexane. ^1H NMR (400 MHz, CDCl_3): δ 2.70 (s, 2H, CH_2), 1.89 (s, CCH_3), 0.07 (s, SiCH_3). $^{13}\text{C}\{^1\text{H}\}$ NMR (100 MHz, CDCl_3): δ 129.7 (cage CCH_2), 83.1 (cage CCH_3), 44.4 (CH_2), 27.3 (CCH_3), -1.2 (SiCH_3). ^{11}B NMR (96 MHz, CDCl_3): δ 11.7 (d, $J_{\text{BH}} = 159$ Hz, 1B), -5.4 (not well resolved, 4B), -6.9 (d, $J_{\text{BH}} = 161$ Hz, 6B). IR (KBr) ν_{max} (cm^{-1}): 2580 (vs, BH). HRMS (EI): m/z calcd for $\text{C}_7\text{H}_{25}\text{Si}_1^{11}\text{B}_9^{10}\text{B}_2 [\text{M}]^+$: 256.2816; Found: 256.2817.

Preparation of 4-(*p*-cymene)-1-TMSCH₂-2-Me-4,1,2-RuC₂B₁₀H₁₀ (21a). To an Et₂O (20 mL) suspension of **19** (1.159 g, 2.5 mmol) was added 1.6 M solution of MeLi in Et₂O (7.5 mL, 12 mmol) at -78 °C with stirring. Then the suspension was slowly warmed to room temperature to give a clear yellow solution and further stirred overnight. The solution was cooled to 0 °C, and a 1.0 M solution of HCl in H₂O (15.0 mL, 15.0 mmol) was added. The mixture was further stirred at room temperature for 30 min, then the organic layer was separated. The aqueous layer was extracted with CH₂Cl₂ (10 mL x 3). The organic layers were combined and dried over Na₂SO₄. Chromatographic separation (SiO₂, 300-400 mesh, *n*-hexane/CH₂Cl₂ 2:1) gave **21a** as a yellow solid (500 mg, 1.04 mmol, 42%). X-ray-quality crystals of **21a** were obtained by recrystallization from CH₂Cl₂. ^1H NMR (400 MHz, CD_2Cl_2): δ 5.80 (d, $J = 5.8$ Hz, 2H, C_6H_4), 5.74 (d, $J = 6.0$ Hz, 2H, C_6H_4), 2.93 (m, $J = 6.9$ Hz, 1H, CH), 2.31 (d, $J = 13.2$ Hz, 1H, CH_2), 2.28 (s, 3H, $\text{C}_6\text{H}_4\text{CH}_3$), 2.22 (d, $J = 13.4$ Hz, 1H, CH_2), 2.19 (s, 3H, CCH_3), 1.30 (d, $J = 6.1$ Hz, 3H, $\text{C}_6\text{H}_4\text{CH}_3$), 1.29 (d, $J = 6.2$ Hz, 3H, $\text{C}_6\text{H}_4\text{CH}_3$), 0.17 (s, 9H, SiCH_3). $^{13}\text{C}\{^1\text{H}\}$ NMR (100 MHz, CD_2Cl_2): δ 120.6, 110.8, 98.3, 96.4, 95.6, 94.0 (C_6H_4), 85.4, 80.5 (cage C), 38.2 (CH_2), 31.4 (CCH_3), 30.8 (CH), 23.7, 22.2 (CHCH_3), 18.1 ($\text{C}_6\text{H}_4\text{CH}_3$), 0.7 (SiCH_3). ^{11}B NMR (96 MHz, CD_2Cl_2): δ 10.2 (d, $J_{\text{BH}} = 153$ Hz, 1B), 7.7 (d, $J_{\text{BH}} = 127$ Hz, 2B), 4.9 (d, $J_{\text{BH}} = 157$ Hz, 1B), 0.7 (d, $J_{\text{BH}} = 141$ Hz, 1B), -1.6 (d, $J_{\text{BH}} = 152$ Hz, 1B), -8.8 (d, $J_{\text{BH}} = 132$

Hz, 1B), -12.5 (d, $J_{\text{BH}} = 147$ Hz, 1B), -15.7 (d, $J_{\text{BH}} = 141$ Hz, 1B), -18.6 (d, $J_{\text{BH}} = 143$ Hz, 1B). IR (KBr) ν_{max} (cm^{-1}): 2505 (vs, BH). HRMS (EI): m/z calcd for $\text{C}_{17}\text{H}_{38}\text{Ru}_1\text{Si}_1^{11}\text{B}_8^{10}\text{B}_2$ $[\text{M}]^+$: 480.2784; Found: 480.2782.

Preparation of 4-(*p*-cymene)-1-TMSCH₂-6-Me-4,1,6-RuC₂B₁₀H₁₀ (21b). To a THF (20 mL) solution of **15** (1.222 g, 5.0 mmol) was added finely cut Na metal (460 mg, 20.0 mmol), and the mixture was stirred at room temperature for 3 days. After removal of excess Na metal, the filtrate was cooled to -30 °C and [(*p*-cymene)RuCl₂]₂ (1.531 g, 2.5 mmol) was slowly added with stirring. The mixture was slowly warmed up to room temperature and further stirred overnight to give a dark red suspension. After filtration, the red solution was concentrated. Chromatographic separation (SiO₂, 300-400 mesh, *n*-hexane/CH₂Cl₂ 2:1) gave gross **21b** in about 50% yield. Recrystallization from CH₂Cl₂ gave **21b** as yellow crystals (959 mg, 2.0 mmol, 40%). ¹H NMR (400 MHz, CD₂Cl₂): δ 5.78 (dd, $J_1 = 6.2$ Hz, $J_2 = 1.1$ Hz, 1H, C₆H₄), 5.72 (dd, $J_1 = 6.1$ Hz, $J_2 = 0.8$ Hz, 1H, C₆H₄), 5.40 (dd, $J_1 = 6.2$ Hz, $J_2 = 1.1$ Hz, 1H, C₆H₄), 5.35 (dd, $J_1 = 6.3$ Hz, $J_2 = 0.9$ Hz, 1H, C₆H₄), 2.92 (m, $J = 6.9$ Hz, 1H, CH), 2.48 (d, $J = 11.9$ Hz, 1H, CH₂), 2.37 (s, 3H, C₆H₄CH₃), 2.19 (d, $J = 11.9$ Hz, 1H, CH₂), 1.84 (s, 3H, CCH₃), 1.38 (d, $J = 6.9$ Hz, 3H, CHCH₃), 1.27 (d, $J = 6.9$ Hz, 3H, CHCH₃), 0.05 (s, 9H, SiCH₃). ¹³C{¹H} NMR (100 MHz, CD₂Cl₂): δ 121.5, 110.8, 95.9, 92.1, 89.7, 86.2 (C₆H₄), 77.4 (cage CCH₃), 72.9 (cage CCH₂), 42.2 (CH₂), 35.3 (CCH₃), 31.4 (CH), 23.2, 22.6 (CHCH₃), 19.2 (C₆H₄CH₃), -0.5 (SiCH₃). ¹¹B NMR (96 MHz, CD₂Cl₂): δ 10.4 (d, $J_{\text{BH}} = 121$ Hz, 1B), 0.4 (d, $J_{\text{BH}} \approx 138$ Hz, 2B), -7.5 (d, $J_{\text{BH}} \approx 140$ Hz, 5B), -12.6 (d, $J_{\text{BH}} = 140$ Hz, 1B), -17.9 (d, $J_{\text{BH}} = 154$ Hz, 1B). IR (KBr) ν_{max} (cm^{-1}): 2516, 2575 (vs, BH). HRMS (EI): m/z calcd for $\text{C}_{17}\text{H}_{38}\text{Ru}_1\text{Si}_1^{11}\text{B}_8^{10}\text{B}_2$ $[\text{M}]^+$: 480.2784; Found: 480.2772.

Chapter 3

Preparation of $[\mu\text{-}1,2\text{-Me}_2\text{Si}(\text{CH}_2)_2\text{-}1,2\text{-C}_2\text{B}_{11}\text{H}_{11}][\text{Na}_2(\text{THF})_4]$ ([23][Na₂(THF)₄]). To a THF (20 mL) solution of **16** (1.201 g, 5.0 mmol) was added finely cut Na metal (460 mg, 20.0 mmol), and the mixture was stirred at room temperature overnight. After removal of excess Na metal, the pale yellow solution was concentrated to about 5 mL. *n*-Hexane layering gave [23][Na₂(THF)₄] as colorless crystals (270 mg, 4.7 mmol, 94%). ¹H NMR (400 MHz, pyridine-*d*₅): δ 3.64 (m, 4H, THF), 1.61 (m, 8H, CH₂ + THF), 0.50 (s, 6H, CH₃). ¹³C{¹H} NMR (100 MHz, pyridine-*d*₅): δ 67.8 (THF), 32.4 (CH₂), 25.7 (THF), 11.2 (cage C), -1.3 (CH₃). ¹¹B NMR (96 MHz, pyridine-*d*₅): δ -8.9 (d, *J*_{BH} = 112 Hz, 1B), -13.4 (br, 5B), -25.6 (d, *J*_{BH} = 102 Hz, 5B). IR (KBr) *v*_{max} (cm⁻¹): 2536 (vs, BH). Anal. Calcd for C₁₀H₂₉B₁₁Na₂OSi (M - 3THF): C, 33.52; H, 8.16. Found: C, 33.36; H, 7.78.

Preparation of $[\mu\text{-}1,2\text{-(CH}_2)_4\text{-}1,2\text{-C}_2\text{B}_{11}\text{H}_{11}][\text{Na}_2(\text{THF})_4]$ ([24][Na₂(THF)₄]). To a THF (20 mL) solution of **7** (1.051 g, 5.0 mmol) was added finely cut Na metal (460 mg, 20.0 mmol), and the mixture was stirred at room temperature overnight. After removal of excess Na metal, the pale yellow solution was concentrated to about 5 mL. *n*-Hexane layering gave [24][Na₂(THF)₄] as a white powder (250 mg, 4.6 mmol, 92%). ¹H NMR (400 MHz, pyridine-*d*₅): δ 3.67 (m, 16H, THF), 2.25 (br, 4H, CCH₂CH₂), 2.17 (br, 4H, CCH₂), 1.65 (m, 16H, THF). ¹³C{¹H} NMR (100 MHz, pyridine-*d*₅): δ 67.9 (THF), 38.1 (CCH₂), 25.8 (THF), 25.2 (CCH₂CH₂), 10.3 (cage C). ¹¹B NMR (128 MHz, pyridine-*d*₅): δ -9.8 (d, *J*_{BH} ≈ 120 Hz, 1B), -15.2 (br, 5B), -26.0 (d, *J*_{BH} ≈ 72 Hz, 1B). IR (KBr) *v*_{max} (cm⁻¹): 2499 (vs, BH). Anal. Calcd for C₁₃H₃₃B₁₁Na₂O_{1.75} (M - 2.25THF): C, 40.84; H, 8.70. Found: C, 40.76; H, 8.53.

Preparation of $[\mu\text{-}1,2\text{-MeCH}(\text{CH}_2)_2\text{-}1,2\text{-C}_2\text{B}_{11}\text{H}_{11}][\text{Na}_2(\text{THF})_4]$ ([25][Na₂(THF)₄]). To a THF (20 mL) solution of **8** (1.051 g, 5.0 mmol) was added

finely cut Na metal (460 mg, 20.0 mmol), and the mixture was stirred at room temperature overnight. After removal of excess Na metal, the pale yellow solution was concentrated to about 5 mL. *n*-Hexane layering gave **[25][Na₂(THF)₄]** as a white powder (230 mg, 4.2 mmol, 84%). ¹H NMR (400 MHz, pyridine-*d*₅): δ 3.67 (m, 16H, THF), 2.35 (m, 2H, CH + CCH₂), 2.22 (m, 1H, CCH₂), 2.14 (m, 2H, CHCH₂), 1.66 (THF), 1.36 (d, *J* = 6.7 Hz, 3H, CH₃). ¹³C{¹H} NMR (100 MHz, pyridine-*d*₅): δ 68.0 (THF), 45.4 (CH), 42.1 (CCH₂), 39.4 (CHCH₂), 25.8 (THF), 19.2 (cage CCH), 18.5 (CH₃), 16.6 (cage CCH₂). ¹¹B NMR (128 MHz, pyridine-*d*₅): δ -9.0 (d, *J*_{BH} = 110 Hz, 1B), -15.8 (br, 5B), -25.6 (d, *J*_{BH} ≈ 86 Hz, 5B). IR (KBr) ν_{\max} (cm⁻¹): 2520 (vs, BH). Anal. Calcd for C₇H₂₁B₁₁Na₂O_{0.25} (M - 3.75THF): C, 30.67; H, 7.72. Found: C, 30.97; H, 7.31.

Preparation of [1,2-Me₂-1,2-C₂B₁₁H₁₁][Na₂(THF)₄] ([26a][Na₂(THF)₄]). To a THF (20 mL) solution of **17a** (920 mg, 5.0 mmol) was added finely cut Na metal (460 mg, 20.0 mmol), and the mixture was stirred at room temperature overnight. After removal of excess Na metal, the pale yellow solution was concentrated to about 5 mL. *n*-Hexane layering gave **[26a][Na₂(THF)₄]** as colorless crystals (240 mg, 4.6 mmol, 93%). ¹H NMR (400 MHz, pyridine-*d*₅): δ 3.64 (m, 8H, THF), 2.09 (s, 6H, CH₃), 1.61 (m, 8H, THF). ¹³C{¹H} NMR (100 MHz, pyridine-*d*₅): δ 67.8 (THF), 29.5 (CH₃), 25.8 (THF), 7.3 (cage C). ¹¹B NMR (96 MHz, pyridine-*d*₅): δ -8.5 (d, *J*_{BH} = 123 Hz, 1B), -13.7 (br, 5B), -25.0 (d, *J*_{BH} = 114 Hz, 5B). IR (KBr) ν_{\max} (cm⁻¹): 2522 (vs, BH). Anal. Calcd for C₁₂H₃₃B₁₁Na₂O₂ (M - 2THF): C, 38.51; H, 8.89. Found: C, 39.00; H, 9.04.

Preparation of [1,3-Me₂-1,3-C₂B₁₁H₁₁][Na₂(THF)₄] ([26b][Na₂(THF)₄]). To a THF (20 mL) solution of **17b** (920 mg, 5.0 mmol) was added finely cut Na metal (460 mg, 20.0 mmol), and the mixture was stirred at room temperature overnight.

After removal of excess Na metal, the pale yellow solution was concentrated to about 5 mL. *n*-Hexane layering gave [26b][Na₂(THF)₄] as colorless crystals (200 mg, 3.9 mmol, 77%). ¹H NMR (400 MHz, pyridine-*d*₅): δ 3.65 (m, 16H, THF), 2.47 (s, 3H, CH₃), 2.11 (s, 3H, CH₃), 1.63 (m, 16H, THF). ¹³C{¹H} NMR (100 MHz, pyridine-*d*₅): δ 67.9 (THF), 44.4, 35.7 (cage C), 31.5, 29.8 (CH₃), 25.8 (THF). ¹¹B NMR (128 MHz, pyridine-*d*₅): δ -1.5 (d, *J*_{BH} = 106 Hz, 2B), -12.0 (d, *J*_{BH} = 109 Hz, 1B), -16.9 (br, 5B), -28.6 (br, 2B), -32.6 (d, *J*_{BH} = 124 Hz, 1B). IR (KBr) *v*_{max} (cm⁻¹): 2526 (vs, BH). Anal. Calcd for C₈H₂₅B₁₁Na₂O (M - 3THF): C, 31.80; H, 8.34. Found: C, 31.79; H, 8.06.

Preparation of μ -2,3-Me₂Si(CH₂)₂-2,3-C₂B₁₂H₁₂ (28a) and μ -2,8-Me₂Si(CH₂)₂-2,8-C₂B₁₂H₁₂ (28b). To a toluene (20 mL) suspension of [23][Na₂(THF)₄], which is prepared from 16 (1.201 g, 5.0 mmol), was added a 1.0 M solution of HBBr₂·SMe₂ in CH₂Cl₂ (10.0 mL, 10.0 mmol) at -78 °C and the mixture was stirred at this temperature for 1 h and at room temperature overnight. Removal of the precipitate and solvents, followed by repeated column chromatographic separation (SiO₂, 300-400 mesh, *n*-hexane) afforded 28a (63 mg, 0.25 mmol, 5%) and 28b (13 mg, 0.05 mmol, 1%) as a white solid. X-ray-quality crystals of 28a and 28b were obtained by slowly evaporation of a saturated *n*-hexane solution. 28a: ¹H NMR (400 MHz, CDCl₃): δ 2.46 (d, *J* = 16.6 Hz, 2H, CH₂), 2.08 (d, *J* = 16.6 Hz, 2H, CH₂), 0.45 (s, 3H, CH₃), 0.13 (s, 3H, CH₃). ¹³C{¹H} NMR (100 MHz, CDCl₃): δ 76.2 (cage C), 31.9 (CH₂), -0.5, -0.7 (CH₃). ¹¹B NMR (128 MHz, CDCl₃): δ 7.4 (d, *J*_{BH} = 151 Hz, 1B), 4.5 (d, *J*_{BH} = 151 Hz, 2B), 2.0 (d, *J*_{BH} = 164 Hz, 2B), -1.8 (d, *J*_{BH} = 172 Hz, 1B), -6.6 (d, *J*_{BH} = 157 Hz, 2B), -8.4 (d, *J*_{BH} = 168 Hz, 2B), -13.0 (d, *J*_{BH} = 161 Hz, 1B), -23.6 (d, *J*_{BH} = 143 Hz, 1B). IR (KBr) *v*_{max} (cm⁻¹): 2571 (vs, BH). HRMS (EI): *m/z* calcd for C₆H₂₂Si₁¹¹B₁₀¹⁰B₂ [M]⁺: 252.2675; Found: 252.2680. 28b: ¹H NMR (400 MHz,

CDCl₃): δ 2.52 (d, $J = 13.9$ Hz, 2H, CH₂), 2.17 (d, $J = 13.9$ Hz, 2H, CH₂), 0.56 (s, 6H, CH₃). ¹³C{¹H} NMR (100 MHz, CDCl₃): δ 90.9 (cage C), 35.2 (CH₂), 1.1 (CH₃). ¹¹B NMR (128 MHz, CDCl₃): δ 2.9 (d, $J_{\text{BH}} = 153$ Hz, 2B), -1.7 (d, $J_{\text{BH}} = 154$ Hz, 6B), -5.1 (d, $J_{\text{BH}} = 173$ Hz, 2B), -17.5 (d, $J_{\text{BH}} = 148$ Hz, 2B). IR (KBr) ν_{max} (cm⁻¹): 2562 (vs, BH). HRMS (EI): m/z calcd for C₆H₂₂Si₁¹¹B₁₀¹⁰B₂ [M]⁺: 252.2675; Found: 252.2683.

Alternative Method for the Preparation of μ -2,3-Me₂Si(CH₂)₂-2,3-C₂B₁₂H₁₂ (28a) and μ -2,8-Me₂Si(CH₂)₂-2,8-C₂B₁₂H₁₂ (28b). To a THF (30 mL) solution of **11** (2.284 g, 10.0 mmol) was added finely cut Li metal (694 mg, 100 mmol), and the mixture was stirred at room temperature for 3 days. After removal of excess Li metal and THF, toluene (20 mL) was then added. To this suspension was slowly added a 1.0 M solution of HBBr₂·SMe₂ in CH₂Cl₂ (50.0 mL, 50.0 mmol) at -78 °C, and the mixture was stirred at this temperature for 1 h and at room temperature overnight. Removal of the precipitate and solvents, followed by repeated column chromatographic separation (SiO₂, 300-400 mesh, *n*-hexane) afforded **28a** (76 mg, 0.30 mmol, 3%) and **28b** (13 mg, 0.05 mmol, 0.5%) as white solids.

Preparation of μ -2,3-(CH₂)₄-2,3-C₂B₁₂H₁₂ (29a) and μ -2,8-(CH₂)₄-2,8-C₂B₁₂H₁₂ (29b). To a toluene (30 mL) suspension of [24][Na₂(THF)₄], which is prepared from **7** (2.101 g, 10.0 mmol), was added a 1.0 M solution of HBBr₂·SMe₂ in CH₂Cl₂ (20.0 mL, 20.0 mmol) at -78 °C and the mixture was stirred at this temperature for 1 h and at room temperature overnight. Removal of the precipitate and solvents, followed by column chromatographic separation (SiO₂, 300-400 mesh, *n*-hexane) afforded a mixture of **29a** (17 mg, ~66% purity, 0.05 mmol, 0.5%) which contained about 33% of **29b**, and **29b** (222 mg, 1.0 mmol, 10%) as a white solid. X-ray-quality crystals of **29b** were obtained by slowly evaporation of a saturated

CH₂Cl₂ solution. **29a**: ¹H NMR (400 MHz, CDCl₃): δ 3.02 (m, 2H, CCH₂), 2.64 (m, 2H, CCH₂), 1.86 (m, 2H, CCH₂CH₂), 1.50 (m, 2H, CCH₂CH₂). ¹³C{¹H} NMR (100 MHz, CDCl₃): δ 66.0 (cage C), 39.6 (CCH₂), 20.3 (CCH₂CH₂). ¹¹B NMR (128 MHz, CDCl₃): δ 8.2 (1B), 5.8 (2B), 3.3 (2B), -2.1 (1B), -6.9 (2B) -9.5 (1B), -11.0 (2B), -25.2 (1B). **29b**: ¹H NMR (400 MHz, CDCl₃): δ 3.15 (br, 2H, CCH₂), 2.36 (d, *J* = 14.2 Hz, 2H, CCH₂), 2.07 (br, 2H, CCH₂CH₂), 1.97 (br, 2H, CCH₂CH₂). ¹³C{¹H} NMR (100 MHz, CDCl₃): δ 78.4 (cage C), 39.3 (CCH₂), 19.2 (CCH₂CH₂). ¹¹B NMR (128 MHz, CDCl₃): δ 4.5 (d, *J*_{BH} = 152 Hz, 2B), -1.3 (d, *J*_{BH} = 151 Hz, 2B), -2.3 (d, *J*_{BH} = 119 Hz, 2B), -3.2 (d, *J*_{BH} = 133 Hz, 2B), -7.0 (d, *J*_{BH} = 174 Hz, 2B), -16.6 (d, *J*_{BH} = 154 Hz, 2B). IR (KBr) ν_{max} (cm⁻¹): 2558 (vs, BH). HRMS (EI): *m/z* calcd for C₆H₂₀¹¹B₁₀¹⁰B₂ [M]⁺: 222.2749; Found: 222.2757.

Alternative Method for the Preparation of μ-2,3-(CH₂)₄-2,3-C₂B₁₂H₁₂ (29a) and μ-2,8-(CH₂)₄-2,8-C₂B₁₂H₁₂ (29b). To a THF (30 mL) solution of **3** (1.983 g, 10.0 mmol) was added finely cut Li metal (694 mg, 100 mmol), and the mixture was stirred at room temperature for 3 days. After removal of excess Li metal and THF, toluene (20 mL) was then added. To this suspension was slowly added a 1.0 M solution of HBBBr₂·SMe₂ in CH₂Cl₂ (50.0 mL, 50.0 mmol) at -78 °C, and the mixture was stirred at this temperature for 1 h and at room temperature overnight. Removal of the precipitate and solvents, followed by repeated column chromatographic separation (SiO₂, 300-400 mesh, *n*-hexane) afforded **29b** (111 mg, 0.5 mmol, 5%) as a white solid. Compound **29a** was observed in very minor amount in the ¹¹B NMR spectrum of the products.

Reaction of [1,2-Me₂-1,2-C₂B₁₁H₁₁][Na₂(THF)₄] ([26a][Na₂(THF)₄]) with HBBBr₂·SMe₂. To a toluene (30 mL) suspension of [26a][Na₂(THF)₄], which is prepared from **17a** (1.840 g, 10.0 mmol), was added a 1.0 M solution of HBBBr₂·SMe₂ in

CH_2Cl_2 (20.0 mL, 20.0 mmol) at $-78\text{ }^\circ\text{C}$, and the mixture was stirred at this temperature for 1 h and at room temperature overnight. Removal of the precipitate and solvents, followed by repeated column chromatographic separation (SiO_2 , 300-400 mesh, *n*-hexane) afforded 2,8- Me_2 -2,8- $\text{C}_2\text{B}_{12}\text{H}_{12}$ (**30b**) (20 mg, 0.05 mmol, 1%) and 2,4- Me_2 -2,4- $\text{C}_2\text{B}_{12}\text{H}_{12}$ (**30c**) (10 mg, 0.05 mmol, 0.5%) as a white solid, and 4- $\text{Br}(\text{CH}_2)_4\text{O}$ -1,12- Me_2 -1,12- $\text{C}_2\text{B}_{11}\text{H}_{10}$ (**31**) (80 mg, 0.24 mmol, 2.4%) as colorless oil. Some 2,3- Me_2 -2,3- $\text{C}_2\text{B}_{12}\text{H}_{12}$ (**30a**) was observed from the ^{11}B NMR spectra. **30b**: ^1H NMR (400 MHz, CDCl_3): δ 2.47 (s, 6H, CH_3). $^{13}\text{C}\{^1\text{H}\}$ NMR (100 MHz, CDCl_3): δ 76.8 (cage C), 31.2 (CH_3). ^{11}B NMR (96 MHz, CDCl_3): δ 4.4 (d, $J_{\text{BH}} = 150$ Hz, 2B), -0.9 (d, $J_{\text{BH}} = 167$ Hz, 2B), -3.1 (d, $J_{\text{BH}} = 167$ Hz, 4B), -6.0 (d, $J_{\text{BH}} \approx 193$ Hz, 2B), -17.4 (d, $J_{\text{BH}} = 155$ Hz, 2B). HRMS (EI): m/z calcd for $\text{C}_4\text{H}_{16}^{11}\text{B}_{10}^{10}\text{B}_2 [\text{M} - 2\text{H}]^+$: 194.2438; Found: 194.2436. **30c**: ^1H NMR (400 MHz, CDCl_3): δ 2.18 (s, 6H, CH_3). $^{13}\text{C}\{^1\text{H}\}$ NMR (100 MHz, CDCl_3): δ 63.7 (cage C), 32.1 (CH_3). ^{11}B NMR (96 MHz, CDCl_3): δ 5.1 (d, $J_{\text{BH}} = 151$ Hz, 2B), 1.9 (d, $J_{\text{BH}} = 164$ Hz, 2B), 1.1 (d, $J_{\text{BH}} = 158$ Hz, 2B), -6.1 (d, $J_{\text{BH}} = 161$ Hz, 2B), -11.5 (d, $J_{\text{BH}} = 173$ Hz, 2B), -15.4 (d, $J_{\text{BH}} = 164$ Hz, 1B), -25.1 (d, $J_{\text{BH}} = 144$ Hz, 1B). ^1H NMR (400 MHz, CD_2Cl_2): δ 2.19 (s, 6H, CH_3). $^{13}\text{C}\{^1\text{H}\}$ NMR (100 MHz, CD_2Cl_2): δ 64.3 (cage C), 32.2 (CH_3). ^{11}B NMR (96 MHz, CD_2Cl_2): δ 5.0 (d, $J_{\text{BH}} = 148$ Hz, 2B), 1.9 (d, $J_{\text{BH}} = 163$ Hz, 2B), 1.2 (d, $J_{\text{BH}} = 163$ Hz, 2B), -6.0 (d, $J_{\text{BH}} = 165$ Hz, 2B), -11.2 (d, $J_{\text{BH}} = 177$ Hz, 1B), -11.7 (d, $J_{\text{BH}} = 149$ Hz, 1B), -15.3 (d, $J_{\text{BH}} = 166$ Hz, 1B), -25.1 (d, $J_{\text{BH}} = 142$ Hz, 1B). HRMS (EI): m/z calcd for $\text{C}_4\text{H}_{16}^{11}\text{B}_{10}^{10}\text{B}_2 [\text{M} - 2\text{H}]^+$: 194.2438; Found: 194.2434. **31**: ^1H NMR (400 MHz, CDCl_3): δ 4.10 (t, $J = 6.2$ Hz, 2H, OCH_2), 3.46 (t, $J = 6.7$ Hz, 2H, BrCH_2), 2.05 (s, 3H, CH_3), 1.97 (m, 2H, BrCH_2CH_2), 1.84 (s, 3H, CH_3), 1.76 (m, 2H, OCH_2CH_2). $^{13}\text{C}\{^1\text{H}\}$ NMR (100 MHz, CDCl_3): δ 96.7, 84.3 (cage C), 65.0 (OCH_2), 33.7 (BrCH_2), 29.9 (OCH_2CH_2), 29.5 (BrCH_2CH_2), 27.3, 27.1 (CH_3). ^{11}B NMR (96 MHz, CDCl_3):

δ 17.0 (s, 1B), -4.5 (d, $J_{\text{BH}} = 149$ Hz, 5B), -10.8 (d, $J_{\text{BH}} = 159$ Hz, 5B). HRMS (ESI): m/z calcd for $\text{C}_8\text{H}_{25}^{11}\text{B}_9^{10}\text{B}_2^{79}\text{BrO} [\text{M} + \text{H}]^+$: 335.2197; found: 335.2195.

Preparation of 2,9-Me₂-2,9-C₂B₁₂H₁₂ (30d). To a toluene (30 mL) suspension of [26b][Na₂(THF)₄], which is prepared from 17b (1.840 g, 10.0 mmol), was added a 1.0 M solution of HBBr₂·SMe₂ in CH₂Cl₂ (20.0 mL, 20.0 mmol) at -78 °C, and the mixture was stirred at this temperature for 1 h and at room temperature overnight. Removal of the precipitate and solvents, followed by repeated column chromatographic separation (SiO₂, 300-400 mesh, *n*-hexane) afforded 30d as a white solid (6 mg, 0.03 mmol, 0.3%). X-ray-quality crystals of 30d were obtained by slow evaporation of a saturated *n*-hexane solution. ¹H NMR (400 MHz, CDCl₃): δ 2.22 (s, 6H, CH₃). ¹³C{¹H} NMR (100 MHz, CDCl₃): δ 78.6 (cage C), 33.5 (CH₃). ¹¹B NMR (96 MHz, CDCl₃): δ 3.8 (d, $J_{\text{BH}} = 154$ Hz, 2B), -3.5 (d, $J_{\text{BH}} = 157$ Hz, 4B), -7.4 (d, $J_{\text{BH}} = 178$ Hz, 4B), -18.7 (d, $J_{\text{BH}} = 156$ Hz, 2B). IR (KBr) ν_{max} (cm⁻¹): 2578, 2566 (vs, BH). HRMS (EI): m/z calcd for $\text{C}_4\text{H}_{16}^{11}\text{B}_{10}^{10}\text{B}_2 [\text{M} - 2\text{H}]^+$: 194.2436; Found: 194.2434.

Preparation of 1-(*p*-cymene)- μ -2,3-Me₂Si(CH₂)₂-1,2,3-RuC₂B₁₁H₁₁ (32a) and 1-(*p*-cymene)- μ -2,8-Me₂Si(CH₂)₂-1,2,8-RuC₂B₁₁H₁₁ (32b). To a THF (10 mL) solution of [23][Na₂(THF)₄], which is prepared from 16 (721 mg, 3.0 mmol), was slowly added [(*p*-cymene)RuCl₂]₂ (919 mg, 1.5 mmol) at -30 °C. The mixture was slowly warmed up to room temperature and further stirred overnight to give a dark red suspension. After filtration, the red solution was concentrated. Repeated chromatographic separation (SiO₂, 300-400 mesh, *n*-hexane/CH₂Cl₂ 2:1) gave 32a (350 mg, 0.74 mmol, 25%) as a yellow solid and 32b (285 mg, 0.60 mmol 20%) as a beige solid. X-ray-quality crystals of 32a were obtained by recrystallization from CH₂Cl₂. 32a: ¹H NMR (400 MHz, CD₂Cl₂): δ 5.51 (d, $J = 6.4$ Hz, 2H, C₆H₄), 5.45 (d, $J = 6.4$ Hz, 2H, C₆H₄), 2.96 (m, $J = 6.9$ Hz, 1H, CH), 2.43 (d, $J = 16.1$ Hz, 2H, CH₂), 2.27 (s, 3H,

$C_6H_4CH_3$), 1.78 (d, $J = 16.1$ Hz, 2H, CH_2), 1.30 (d, $J = 7.0$ Hz, 6H, $CHCH_3$), 0.40 (s, 3H, $SiCH_3$), 0.33 (s, 3H, $SiCH_3$). $^{13}C\{^1H\}$ NMR (100 MHz, CD_2Cl_2): δ 117.8, 108.4, 95.3, 92.6 (C_6H_4), 67.2 (cage C), 33.3 (CH_2), 30.6 (CH), 22.7 ($CHCH_3$), 18.8 ($C_6H_4CH_3$), 1.8 -0.1 ($SiCH_3$). ^{11}B NMR (96 MHz, CD_2Cl_2): δ -6.4 (d, $J_{BH} = 131$ Hz, 2B), -12.1 (d, $J_{BH} = 171$ Hz, 2B), -14.2 (d, $J_{BH} = 159$ Hz, 1B), -14.8 (d, $J_{BH} = 134$ Hz, 2B), -17.1 (d, $J_{BH} = 155$ Hz, 2B), -22.0 (d, $J_{BH} = 126$ Hz, 1B), -23.4 (d, $J_{BH} = 157$ Hz, 1B). IR (KBr) ν_{max} (cm^{-1}): 2514 (vs, BH). HRMS (EI): m/z calcd for $C_{16}H_{35}Ru_1Si_1^{11}B_9^{10}B_2 [M]^+$: 476.2642; Found: 476.2641. **32b**: 1H NMR (400 MHz, CD_2Cl_2): δ 5.55 (d, $J = 6.4$ Hz, 1H, C_6H_4), 5.46 (d, $J \approx 7.2$ Hz, 1H, C_6H_4), 5.44 (d, $J \approx 7.2$ Hz, 1H, C_6H_4), 5.35 (d, $J = 6.4$ Hz, 1H, C_6H_4) 2.99 (m, $J = 7.0$ Hz, 1H, CH), 2.28 (s, 3H, $C_6H_4CH_3$), 2.16 (d, $J = 13.4$ Hz, 1H, CH_2), 1.96 (d, $J = 13.6$ Hz, 1H, CH_2), 1.85 (d, $J = 13.8$ Hz, 1H, CH_2), 1.42 (d, $J = 13.4$ Hz, 1H, CH_2), 1.29 (d, $J = 7.3$ Hz, 3H, $CHCH_3$), 1.27 (d, $J = 7.3$ Hz, 3H, $CHCH_3$), 0.40 (s, 3H, $SiCH_3$), 0.32 (s, 3H, $SiCH_3$). $^{13}C\{^1H\}$ NMR (100 MHz, CD_2Cl_2): δ 119.3, 109.7, 96.3, 96.0, 93.3, 92.7 (C_6H_4), 73.7, 48.4 (cage C), 35.7, 33.2 (CH_2), 30.6 (CH), 23.3, 22.3 ($CHCH_3$), 18.5 ($C_6H_4CH_3$), 1.5, 0.9 ($SiCH_3$). ^{11}B NMR (96 MHz, CD_2Cl_2): δ 0.0 (d, $J_{BH} = 129$ Hz, 1B), -2.5 (d, $J_{BH} = 138$ Hz, 1B), -6.5 (d, $J_{BH} \approx 116$ Hz, 1B), -7.1 (d, $J_{BH} \approx 116$ Hz, 1B), -10.7 (d, $J_{BH} = 169$ Hz, 1B), -13.3 (d, $J_{BH} = 132$ Hz, 1B), -20.5 (d, $J_{BH} = 148$ Hz, 1B), -22.9 (d, $J_{BH} = 124$ Hz, 1B), -24.0 (d, $J_{BH} = 135$ Hz, 1B). IR (KBr) ν_{max} (cm^{-1}): 2509 (vs, BH). HRMS (EI): m/z calcd for $C_{16}H_{35}Ru_1Si_1^{11}B_9^{10}B_2 [M]^+$: 476.2642; Found: 476.2639.

Preparation of 1-(*p*-cymene)-2,9-Me₂-1,2,9-RuC₂B₁₁H₁₁ (33). To a THF (10 mL) solution of [26b][Na₂(THF)₄], which is prepared from 17b (92 mg, 0.50 mmol), was added [(*p*-cymene)RuCl₂]₂ (153 mg, 0.25 mmol) at -30 °C, and the mixture was stirred at room temperature overnight. After filtration, the red solution was concen-

trated. Chromatographic separation (SiO₂, 300-400 mesh, *n*-hexane/CH₂Cl₂ 2:1) gave **33** as a pale yellow solid (157 mg, 0.37 mmol, 75%). X-ray-quality crystals were obtained by recrystallization from CH₂Cl₂. ¹H NMR (400 MHz, CD₂Cl₂): δ 5.60 (dd, *J*₁ = 1.1 Hz, *J*₂ = 6.4 Hz, 1H, C₆H₄), 5.50 (dd, *J*₁ = 1.1 Hz, *J*₂ = 6.4 Hz, 1H, C₆H₄), 5.47 (dd, *J*₁ = 1.2 Hz, *J*₂ = 6.4 Hz, 1H, C₆H₄), 5.36 (dd, *J*₁ = 0.9 Hz, *J*₂ = 6.4 Hz, 1H, C₆H₄), 2.99 (m, *J* = 6.9 Hz, 1H, C₆H₄CH), 2.29 (s, 3H, C₆H₄CH₃), 1.94 (s, 3H, CCH₃), 1.84 (s, 3H, CCH₃), 1.31 (d, *J* = 7.0 Hz, 3H, CHCH₃), 1.28 (d, *J* = 7.0 Hz, 3H, CHCH₃). ¹³C{¹H} NMR (100 MHz, CD₂Cl₂): δ 119.4, 109.9, 95.7, 95.6, 92.6, 92.3 (C₆H₄), 60.3, 38.2 (cage C), 34.7, 34.5 (CCH₃), 30.7 (C₆H₄CH), 22.8, 22.6 (CHCH₃), 18.5 (C₆H₄CH₃). ¹¹B NMR (96 MHz, CD₂Cl₂): δ -3.1 (d, *J*_{BH} = 142 Hz, 2B), -4.6 (d, *J*_{BH} = 136 Hz, 1B), -9.5 (d, *J*_{BH} = 157 Hz, 2B), -13.7 (d, *J*_{BH} = 137 Hz, 1B), -21.3 (d, *J*_{BH} = 144 Hz, 1B), -24.1 (d, *J*_{BH} = 141 Hz, 2B), -25.5 (d, *J*_{BH} = 134 Hz, 1B), -26.5 (d, *J*_{BH} = 109 Hz, 1B). IR (KBr) *v*_{max} (cm⁻¹): 2521 (vs, BH). HRMS (EI): *m/z* calcd for C₁₄H₃₁¹¹B₉¹⁰B₂Ru₁ [M]⁺, 420.2560; Found: 420.2556.

Alternative Method for the Preparation of 1-(*p*-cymene)-2,9-Me₂-1,2,9-RuC₂B₁₁H₁₁ (33**).** To a THF (10 mL) solution of [26a][Na₂(THF)₄], which is prepared from **17a** (92 mg, 0.50 mmol), was added [(*p*-cymene)RuCl₂]₂ (153 mg, 0.25 mmol) at -30 °C, and the mixture was stirred at room temperature overnight. After filtration, the red solution was concentrated. Chromatographic separation (SiO₂, 300-400 mesh, *n*-hexane/CH₂Cl₂ 2:1) gave **33** as a pale yellow solid (20 mg, 0.048 mmol, 19%).

Preparation of 7-(*p*-cymene)- μ -1,4-Me₂Si(CH₂)₂-7,1,4-RuC₂B₁₂H₁₂ (35**).** To a THF (10 mL) solution of **28a** (20 mg, 0.079 mmol) was added finely cut Na metal (23 mg, 1.0 mmol), and the mixture was stirred at room temperature for 3 days. Removal of excess Na metal gave a THF solution of [μ -2,3-Me₂Si(CH₂)₂-2,3-

$C_2B_{12}H_{12}[Na_2(THF)_4]$ (**[34a]** $[Na_2(THF)_4]$) in situ, which would slowly isomerize to **[34b]** $[Na_2(THF)_4]$ in solution. To a THF (10 mL) solution of **28b** (20 mg, 0.079 mmol) was added finely cut Na metal (23 mg, 1.0 mmol), and the mixture was stirred at room temperature for 3 days. Removal of excess Na metal gave a THF solution of $[\mu-1,2-Me_2Si(CH_2)_2-1,2-C_2B_{12}H_{12}][Na_2(THF)_4]$ (**[34b]** $[Na_2(THF)_4]$) in situ. To this solution of **[34b]** $[Na_2(THF)_4]$ was added [*p*-cymene) $RuCl_2$] $_2$ (98 mg, 0.16 mmol) at $-30\text{ }^\circ\text{C}$, and the mixture was stirred at room temperature overnight. After filtration, the red solution was concentrated. Chromatographic separation (SiO_2 , 300-400 mesh, *n*-hexane/ CH_2Cl_2 2:1) gave **35** as an orange solid (20 mg, 0.041 mmol, 52%). X-ray-quality crystals were obtained by recrystallization from CH_2Cl_2 as **35** $\cdot CH_2Cl_2$.

[34a] $[Na_2(THF)_4]$: ^{11}B NMR (128 MHz, THF): δ 5.4 (1B), -10.2 (1B), -11.9 (1B), -13.2 (3B), -14.4 (1B), -17.0 (1B), -27.6 (1B), -28.3 (1B), -33.7 (1B), -34.4 (1B).

[34b] $[Na_2(THF)_4]$: ^{11}B NMR (128 MHz, THF): δ -1.3 (1B), -4.3 (2B), -15.0 (2B), -32.4 (3B), -39.2 (2B), -45.6 (1B), -46.9 (1B).

35: 1H NMR (400 MHz, CD_2Cl_2): δ 5.85 (dd, $J_1 = 6.4$ Hz, $J_2 = 1.4$ Hz, 1H, C_6H_4), 5.78 (dd, $J_1 = 6.4$ Hz, $J_2 = 1.2$ Hz, 1H, C_6H_4), 5.44 (dd, $J_1 = 6.4$ Hz, $J_2 = 1.3$ Hz, 1H, C_6H_4), 5.29 (dd, $J_1 = 6.4$ Hz, $J_2 = 1.2$ Hz, 1H, C_6H_4), 3.10 (m, $J = 6.9$ Hz, 1H, $CHCH_3$), 2.77 (d, $J = 14.7$ Hz, 1H, CH_2), 2.33 (s, 3H, $CH_3C_6H_4$), 2.17 (d, $J = 14.8$ Hz, 1H, CH_2), 1.89 (d, $J = 15.3$ Hz, 1H, CH_2), 1.52 (d, $J = 15.3$ Hz, 1H, CH_2), 1.33 (d, $J = 7.0$ Hz, 3H, $CHCH_3$), 1.26 (d, $J = 6.9$ Hz, 3H, $CHCH_3$), 0.33 (s, 3H, $SiCH_3$), 0.21 (s, 3H, $SiCH_3$).

$^{13}C\{^1H\}$ NMR (100 MHz, CD_2Cl_2): δ 124.3, 114.6, 100.9, 97.6, 97.0, 93.6 (C_6H_4), 39.8 (CH_2), 38.6, 38.3 (cage C), 30.5 ($CHCH_3$), 27.5 (CH_2), 23.4, 22.2 ($CHCH_3$), 18.2 ($CH_3C_6H_4$), 0.1 -0.3 ($SiCH_3$).

^{11}B NMR (128 MHz, CD_2Cl_2): δ 13.9(d, $J_{BH} = 134$ Hz, 1B), 2.7 (d, $J_{BH} = 150$ Hz, 1B), -0.7 (d, $J_{BH} = 130$ Hz, 2B), -7.4 (d, $J_{BH} = 138$ Hz, 1B), -9.4 (not well resolved, 1B), -11.6 (d, $J_{BH} = 167$ Hz, 1B), -12.8 (d, $J_{BH} = 130$ Hz, 1B), -15.4 (d, J_{BH}

= 148 Hz, 1B), -16.7 (d, $J_{\text{BH}} = 176$ Hz, 1B), -26.9 (d, $J_{\text{BH}} = 134$ Hz, 1B), -30.4 (d, $J_{\text{BH}} = 145$ Hz, 1B). HRMS (EI): m/z calcd for $\text{C}_{16}\text{H}_{36}\text{Ru}_1\text{Si}_1^{11}\text{B}_{10}^{10}\text{B}_2$ $[\text{M}]^+$: 488.2814; Found: 488.2814.

Chapter 4

Reaction of 6 with MeOH. Method A: Compound 6 (196 mg, 1.00 mmol) was dissolved in MeOH (10 mL), and the solution was stirred at room temperature for 12 h. After addition of $[\text{Me}_3\text{NH}]\text{Cl}$ (191 mg, 2.00 mmol), the mixture was further stirred for 1 h. MeOH was then pumped off, and the residue was thoroughly washed with water to give a white solid. Recrystallization from acetone gave $[\mu\text{-}1,2\text{-}(\text{CH}_2)_3\text{CH}(\text{OMe})\text{-}1\text{-CB}_{11}\text{H}_{10}][\text{Me}_3\text{NH}]$ (**[36a]** $[\text{Me}_3\text{NH}]$) as colorless crystals (215 mg, 75%). **Method B:** Compound 6 (196 mg, 1.00 mmol) was dissolved in MeOH (10 mL) in a sealed tube, and the solution was stirred at 70 °C for 24 h. After addition of $[\text{Me}_3\text{NH}]\text{Cl}$ (191 mg, 2.00 mmol), the mixture was further stirred for 1 h. Removal of the volatile materials gave a white solid that was washed with cold water to remove the excess amount of $[\text{Me}_3\text{NH}]\text{Cl}$. The ^1H NMR of the crude product showed the molar ratio of **[36a]** $[\text{Me}_3\text{NH}]$ and $[\mu\text{-}1,2\text{-}(\text{CH}_2)_2\text{CH}(\text{OMe})\text{CH}_2\text{-}1\text{-CB}_{11}\text{H}_{10}][\text{Me}_3\text{NH}]$ (**[36b]** $[\text{Me}_3\text{NH}]$) was about 1:1, together with the observation of a small amount of $[\mu\text{-}1,2\text{-}(\text{CH}_2)_2\text{CH}=\text{CH}\text{-}1\text{-CB}_{11}\text{H}_{10}][\text{Me}_3\text{NH}]$ (**[37]** $[\text{Me}_3\text{NH}]$). Thoroughly washing with water followed by recrystallization from acetone afforded **[36b]** $[\text{Me}_3\text{NH}]$ as colorless crystals (38 mg, 35%). **[36a]** $[\text{Me}_3\text{NH}]$: ^1H NMR (400 MHz, acetone- d_6): δ 3.34 (s, 3H, OCH_3), 3.20 (s, 9H, NCH_3), 3.11 (t, $J \approx 6.9$ Hz, 1H, $\alpha\text{-CH}$), 1.81 (m, 2H, $\delta\text{-CH}_2$), 1.68 (m, 1H, $\beta\text{-CH}_2$), 1.45 (m, 1H, $\gamma\text{-CH}_2$), 1.39 (m, 1H, $\beta\text{-CH}_2$), 1.21 (m, 1H, $\gamma\text{-CH}_2$). $^{13}\text{C}\{^1\text{H}\}$ NMR (100 MHz, acetone- d_6): δ 74.2 (br, $\alpha\text{-CH}$), 69.2 (cage C), 57.7 (OCH_3), 46.2 (NCH_3), 36.7 ($\delta\text{-CH}_2$), 29.6 ($\beta\text{-CH}_2$), 23.2 ($\gamma\text{-CH}_2$).

CH₂). ¹¹B NMR (96 MHz, acetone-*d*₆): δ -7.7 (s, 1B), -9.3 (d, *J*_{BH} = 144 Hz, 1B), -12.4 (d, *J*_{BH} = 113 Hz, 6B), -13.5 (d, *J*_{BH} ≈ 104 Hz, 1B), -14.0 (d, *J*_{BH} ≈ 178 Hz, 2B). IR (KBr) *v*_{max} (cm⁻¹): 2539 (vs, BH). Anal. Calcd for C₉H₃₀B₁₁NO [M]: C, 37.63; H, 10.53; N, 4.88. Found: C, 37.98; H, 11.05; N, 4.79. [36b][Me₃NH]: ¹H NMR (400 MHz, acetone-*d*₆): δ 3.21 (m, 1H, β-CH), 3.185 (s, 9H, NCH₃), 3.177 (s, 3H, OCH₃), 2.02 (m, 1H, δ-CH₂), 1.92 (m, 1H, δ-CH₂), 1.55 (m, 1H, γ-CH₂), 1.49 (m, 1H, α-CH₂), 1.28 (m, 1H, γ-CH₂), 0.74 (m, 1H, α-CH₂). ¹³C{¹H} NMR (100 MHz, acetone-*d*₆): δ 79.9 (β-CH), 67.7 (cage C), 54.7 (OCH₃), 46.0 (NCH₃), 36.1 (δ-CH₂), 31.9 (γ-CH₂), 21.5 (br, α-CH₂). ¹¹B NMR (96 MHz, acetone-*d*₆): δ -7.0 (s, 1B), -9.9 (d, *J*_{BH} ≈ 146 Hz, 1B), -12.1 (d, *J*_{BH} = 123 Hz, 7B), -13.5 (d, *J*_{BH} = 148 Hz, 1B), -15.6 (d, *J*_{BH} ≈ 142 Hz, 1B). IR (KBr) *v*_{max} (cm⁻¹): 2522 (vs, BH). Anal. Calcd for C₉H₃₀B₁₁NO [M]: C, 37.63; H, 10.53; N, 4.88. Found: C, 38.10; H, 10.77; N, 4.68.

Reaction of 19 with EtOH. Compound 6 (196 mg, 1.00 mmol) was dissolved in EtOH (10 mL) in a sealed tube, and the solution was stirred at 70 °C for 24 h. After addition of [Me₃NH]Cl (191 mg, 2.00 mmol), the mixture was further stirred for 1 h. Removal of the volatile materials gave a white solid that was washed with cold water to remove the excess amount of [Me₃NH]Cl. The ¹H NMR of the crude product showed that the molar ratio of [μ-1,2-(CH₂)₃CH(OEt)-1-CB₁₁H₁₀][Me₃NH] ([38a][Me₃NH]) and [37][Me₃NH] is about 1:0.5, together with the observation of a very small amount of [μ-1,2-(CH₂)₂CH(OEt)CH₂-1-CB₁₁H₁₀][Me₃NH] ([38b][Me₃NH]). Recrystallization from acetone afforded some crystals of [38a][Me₃NH]. Concentration of the mother liquor yielded few colorless X-ray-quality-crystals identified as [37][Me₃NH]. [37][Me₃NH]: ¹H NMR (400 MHz, acetone-*d*₆): δ 5.85 (m, 2H, CH=CH), 3.13 (s, 9H, NCH₃), 1.98 (dt, *J*₁ = 2.9 Hz, *J*₂ = 6.4 Hz, 2H, γ-CH₂), 1.87 (t, *J* = 6.7 Hz, 2H, δ-CH₂). ¹³C{¹H} NMR (100 MHz, acetone-

d_6): δ 132.7 (br, α -CH), 131.8 (β -CH), 66.7 (cage C), 45.9 (NCH₃), 33.0 (δ -CH₂), 26.0 (γ -CH₂). [38a][Me₃NH]: ¹H NMR (400 MHz, acetone- d_6): δ 3.69 (dq, $J_1 = 9.5$ Hz, $J_2 = 7.0$ Hz, 1H, OCH₂), 3.44 (dq, $J_1 = 9.5$ Hz, $J_2 = 7.0$ Hz, 1H, OCH₂), 3.19 (dd, $J_1 = 6.1$ Hz, $J_2 = 9.1$ Hz, 1H, α -CH), 3.13 (s, 9H, NCH₃), 1.77 (m, 2H, δ -CH₂), 1.68 (m, 1H, β -CH₂), 1.43 (m, 1H, γ -CH₂), 1.29 (m, 1H, β -CH₂), 1.17 (m, 1H, γ -CH₂), 1.07 (t, $J = 7.0$ Hz, 3H, CH₂CH₃). ¹³C{¹H} NMR (100 MHz, acetone- d_6): δ 71.5 (br, α -CH₂), 69.2 (cage C), 64.7 (OCH₂), 45.9 (NCH₃), 36.1 (δ -CH₂), 29.9 (β -CH₂), 23.1 (γ -CH₂), 15.9 (CH₂CH₃). [38b][Me₃NH]: ¹H NMR (400 MHz, acetone- d_6): δ 3.41 (1H, OCH₂), 3.31 (1H, OCH₂), 3.27 (1H, β -CH), 3.13 (9H, NCH₃), 1.97 (1H, δ -CH₂), 1.88 (1H, δ -CH₂), 1.52 (1H, γ -CH₂), 1.41 (1H, α -CH₂), 1.24 (1H, γ -CH₂), 1.05 (t, $J = 7.0$ Hz, 3H, CH₂CH₃), 0.74 (1H, α -CH₂). ¹³C{¹H} NMR (100 MHz, acetone- d_6): δ 77.7 (β -CH), 67.5 (cage C), 62.3 (OCH₂), 45.9 (NCH₃), 35.8 (δ -CH₂), 32.0 (γ -CH₂), 22.2 (br, α -CH₂), 15.9 (CH₂CH₃).

Preparation of μ -1,2-(CH₂)₃CH(N^tBuH₂)-1-CB₁₁H₁₀ (39). To a toluene (10 mL) solution of **6** (98mg, 0.50 mmol) was added ^tBuNH₂ (1.0 mL, 696 mg, 9.5 mmol) at 0 °C, and the mixture was further stirred overnight. Removal of the volatile materials gave a pale yellow solid. Recrystallization from CH₂Cl₂ afforded **39** as colorless crystals (121 mg, 0.45 mmol, 90%). ¹H NMR (400 MHz, acetone- d_6): δ 3.36 (t, $J = 7.3$ Hz, 1H, α -CH), 2.01 (m, 1H, β -CH₂), 1.85 (m, 2H, δ -CH₂), 1.63 (m, 1H, β -CH₂), 1.57 (s, 9H, CCH₃), 1.51 (m, 1H, γ -CH₂), 1.39 (m, 1H, γ -CH₂). ¹³C{¹H} NMR (100 MHz, acetone- d_6): δ 68.9 (cage C), 60.7 (CCH₃), 44.5 (br, α -CH), 35.1 (δ -CH₂), 29.3 (β -CH₂), 26.4 (CCH₃), 23.2 (γ -CH₂). ¹¹B NMR (96 MHz, acetone- d_6): δ -8.9 (d, $J_{\text{BH}} = 137$ Hz, 1B), -9.4 (s, 1B), -11.6 (d, $J_{\text{BH}} = 159$ Hz, 5B), -13.8 (d, $J_{\text{BH}} = 170$ Hz, 4B). IR (KBr) ν_{max} (cm⁻¹): 2546 (vs, BH). HRMS (EI): m/z calcd for C₉H₂₈¹¹B₉¹⁰B₂N [M]⁺: 269.3312; Found: 269.3312.

Preparation of μ -1,2-(CH₂)₃CH(NEt₂H)-1-CB₁₁H₁₀ (40a). To a toluene (10 mL) solution of **6** (98mg, 0.50 mmol) was added Et₂NH (1.0 mL, 707 mg, 9.7 mmol) at 0 °C, and the mixture was further stirred overnight. Removal of the volatile materials gave a pale yellow solid. Recrystallization from CH₂Cl₂ afforded **40a** as colorless crystals (121 mg, 0.45 mmol, 90%). ¹H NMR (400 MHz, acetone-*d*₆): δ 3.78 (m, 2H, NCH₂), 3.52 (m, 1H, NCH₂), 3.40 (m, 2H, NCH₂ + α -CH), 2.00 (m, 1H, β -CH₂), 1.98 (m, 1H, δ -CH₂), 1.79 (m, 1H, δ -CH₂), 1.68 (m, 1H, γ -CH₂), 1.53 (m, 1H, β -CH₂), 1.43 (t, *J* = 7.3 Hz, 6H, CH₃), 1.38 (m, 1H, γ -CH₂). ¹³C{¹H} NMR (100 MHz, acetone-*d*₆): δ 69.1 (cage C), 54.4 (br, α -CH), 47.1 (NCH₂), 35.5 (δ -CH₂), 24.7 (β -CH₂), 24.5 (γ -CH₂), 11.2, 10.0 (CH₃). ¹¹B NMR (96 MHz, acetone-*d*₆): δ -8.5 (d, *J*_{BH} = 153 Hz, 1B), -10.8 (d, *J*_{BH} = 159 Hz, 2B), -11.8 (d, *J*_{BH} = 146 Hz, 4B), -13.0 (d, *J*_{BH} \approx 124 Hz, 4B). IR (KBr) ν_{\max} (cm⁻¹): 2549 (vs, BH). HRMS (EI): *m/z* calcd for C₉H₂₈¹¹B₉¹⁰B₂N [M]⁺: 269.3312; Found: 269.3310.

Preparation of μ -1,2-(CH₂)₃CH(PPh₃)-1-CB₁₁H₁₀·CH₂Cl₂ (41·CH₂Cl₂). PPh₃ (276 mg, 1.05 mmol) was added to a solution of **6** (196 mg, 1.00 mmol) in toluene (20 mL), and the reaction vessel was closed. The mixture was heated at 110 °C for 12 h to give a white suspension. After removal of toluene, the white solid was recrystallized from CH₂Cl₂ to give **41·CH₂Cl₂** as colorless crystals (435 mg, 80%). ¹H NMR (400 MHz, acetone-*d*₆): δ 8.08 (m, 6H, C₆H₅), 7.80 (m, 3H, C₆H₅), 7.70 (m, 6H, C₆H₅), 5.62 (s, 2H; CH₂Cl₂), 3.73 (m, 1H, α -CH), 2.13 (m, 1H, β -CH₂), 1.99 (m, 1H, δ -CH₂), 1.64 (m, 2H, δ -CH₂ + γ -CH₂), 1.57 (m, 1H, γ -CH₂), 1.47 (m, 1H, β -CH₂). ¹³C{¹H} NMR (100 MHz, acetone-*d*₆): δ 135.2 (d, *J*_{PC} = 9.1 Hz), 134.8 (d, *J*_{PC} = 2.0 Hz), 130.4 (d, *J*_{PC} = 12.1 Hz), 121.6 (d, *J*_{PC} = 83.1 Hz) (C₆H₅), 67.7 (cage C), 55.0 (CH₂Cl₂), 36.2 (δ -CH₂), 25.3 (d, *J*_{PC} = 14.3 Hz, γ -CH₂), 24.9 (d, *J*_{PC} = 2.8 Hz, β -CH₂), 17.4 (br, α -CH). ¹¹B NMR (96 MHz, acetone-*d*₆): δ -8.4 (d, *J*_{BH} = 151 Hz, 1B), -11.1

(d, $J_{\text{BH}} = 151$ Hz, 3B), -12.4 (d, $J_{\text{BH}} = 123$ Hz, 7B). ^{31}P NMR (121 MHz, acetone- d_6): δ 32.7. IR (KBr) ν_{max} (cm^{-1}): 2539 (vs, BH). Anal. Calcd for $\text{C}_{23}\text{H}_{32}\text{B}_{11}\text{P}$ [$\text{M} - \text{CH}_2\text{Cl}_2$]: C 60.26, H 7.04; found: C 60.38, H 6.81.

Preparation of $[\mu\text{-}1,2\text{-(CH}_2\text{)}_3\text{CHS(4-Me-C}_6\text{H}_4\text{)-}1\text{-CB}_{11}\text{H}_{10}][\text{PPN}]$ ([42][PPN]).

To a THF (10 mL) solution of **6** (98mg, 0.50 mmol) was added (4-Me- C_6H_4)SNa (76 mg, 0.52 mmol) in a sealed tube and the mixture was heated at 70 °C for 48 h. [PPN]Cl (287 mg, 0.50 mmol) was added and the mixture was further stirred for 6 h. After filtration, THF was removed. The residue was recrystallized from MeOH to give [42][PPN] as a white solid (343 mg, 0.40 mmol, 80%). ^1H NMR (400 MHz, acetone- d_6): δ 7.70 (m, 18H, PPN), 7.56 (m, 12H, PPN), 7.19 (d, $J = 8.1$ Hz, 2H, C_6H_4), 7.03 (d, $J = 8.0$ Hz, 2H, C_6H_4), 3.12 (t, $J = 5.8$ Hz, 1H, $\alpha\text{-CH}$), 2.23 (s, 3H, CH_3), 1.86 (m, 2H, $\delta\text{-CH}_2$), 1.71 (m, 1H, $\beta\text{-CH}_2$), 1.55 (m, 1H, $\gamma\text{-CH}_2$), 1.38 (m, 1H, $\beta\text{-CH}_2$), 1.20 (m, 1H, $\gamma\text{-CH}_2$). $^{13}\text{C}\{^1\text{H}\}$ NMR (100 MHz, acetone- d_6): δ 137.0, 134.9 (C_6H_4), 134.4, 133.0, 130.3 (PPN), 129.9 (C_6H_4), 128.0 (PPN), 68.2 (cage C), 36.5 ($\delta\text{-CH}_2$), 31.7 (br, $\alpha\text{-CH}_2$), 29.5 ($\beta\text{-CH}_2$), 23.5 ($\gamma\text{-CH}_2$), 20.9 (CH_3). ^{11}B NMR (128 MHz, acetone- d_6): δ -7.9 (s, 1B), -9.7 (d, $J_{\text{BH}} \approx 142$ Hz, 2B), -12.1 (d, $J_{\text{BH}} \approx 129$ Hz, 6B), -14.4 (d, $J_{\text{BH}} \approx 202$ Hz, 2B). IR (KBr) ν_{max} (cm^{-1}): 2532 (vs, BH). Anal. Calcd for $\text{C}_{48}\text{H}_{54}\text{B}_{11}\text{NP}_2\text{S}$ (M): C, 67.20; H, 6.34; N, 1.63. Found: C, 67.21; H, 6.32; N, 1.52.

Preparation of $[\mu\text{-}1,2\text{-(CH}_2\text{)}_4\text{-}1\text{-CB}_{11}\text{H}_{10}][\text{Na(18-crown-6)}]$ ([43][Na(18-crown-6)]) and $[\mu\text{-}1,2\text{-(CH}_2\text{)}_4\text{-}1\text{-CB}_{11}\text{H}_{10}][\text{NMe}_4]$ ([43][NMe₄]). To a THF (10 mL) solution of **6** (98mg, 0.50 mmol) was added NaBH_4 (38 mg, 1.0 mmol) in a closed vessel and the mixture was heated at 70 °C overnight. After filtration, a solution of [43][Na(THF)_x] was afforded. To this solution was added 18-crown-6 (264 mg, 1.0 mmol). After removal of the solvent, the residue was thoroughly washed with water

to give **[43][Na(18-crown-6)]** as a white solid (194 mg, 0.40 mmol, 80%). X-ray-quality crystals were obtained by recrystallization from THF as **[43][Na(18-crown-6)(THF)₂]**. To the above solution of **[43][Na(THF)_x]** was added **[NMe₄]Cl** (110 mg, 1.0 mmol). After removal of the solvent, the residue was washed with water and recrystallization from acetone to give **[43][NMe₄]** as colorless crystals (115 mg, 0.42 mmol, 85%). **[43][Na(18-crown-6)]**: ¹H NMR (400 MHz, acetone-*d*₆): δ 3.65 (s, 24H, OCH₂), 1.84 (t, *J* = 5.7 Hz, 2H, CH₂), 1.36 (br, 2H, CH₂), 1.29 (br, 2H, CH₂), 0.90 (br, 2H, CH₂). ¹³C{¹H} NMR (100 MHz, acetone-*d*₆): δ 70.2 (OCH₂), 67.8 (cage C), 36.6, 26.1, 22.9, 14.4 (CH₂). ¹¹B NMR (96 MHz, acetone-*d*₆): δ -7.2 (s, 1B), -9.5 (d, *J*_{BH} = 185 Hz, 1B), -11.5 (d, *J*_{BH} = 140 Hz, 4B), -12.8 (d, *J*_{BH} = 135 Hz, 4B), -15.7 (d, *J*_{BH} = 138 Hz, 1B). **[43][NMe₄]**: ¹H NMR (400 MHz, acetone-*d*₆): δ 3.41 (s, 12H, CH₃), 1.83 (t, *J* = 6.2 Hz, 2H, δ-CH₂), 1.35 (br, 2H, β-CH₂), 1.29 (m, 2H, γ-CH₂), 0.89 (br, 2H, α-CH₂). ¹³C{¹H} NMR (128 MHz, acetone-*d*₆): δ 67.9 (cage C), 55.9 (CH₃), 36.5 (δ-CH₂), 26.0 (γ-CH₂), 22.8 (β-CH₂), 14.2 (br, α-CH₂). ¹¹B NMR (96 MHz, acetone-*d*₆): δ -7.2 (s, 1B), -9.7 (d, *J*_{BH} = 177 Hz, 1B), -11.6 (d, *J*_{BH} = 140 Hz, 4B), -12.9 (d, *J*_{BH} = 135 Hz, 4B), -15.9 (d, *J*_{BH} = 137 Hz, 1B). IR (KBr) $\tilde{\nu}_{\max}$ (cm⁻¹): 2512 (vs, BH). Anal. Calcd for C₉H₃₀B₁₁N [M]: C, 39.85; H, 11.15; N, 5.16. Found: C, 40.09; H, 11.32; N, 4.93.

Preparation of [μ-1,2-CH(CH₂)₂-1,2-C₂B₁₁H₁₁][PPN] ([44][PPN]). To a THF (20 mL) solution of **6** (98 mg, 0.50 mmol) was added NaH (48 mg, 2.0 mmol) at room temperature and the mixture was stirred until no gas was evolved. After filtration, **[PPN]Cl** (287 mg, 0.50 mmol) was added to the brown filtrate and further stirred overnight. After filtration, the filtrate was concentrated to about 5 mL and *n*-hexane layering gave **[44][PPN]** as brown crystals (190 mg, 0.26 mmol, 52%). ¹H NMR (400 MHz, CD₂Cl₂): δ 7.68 (m, 6H, PPN), 7.49 (m, 24H, PPN), 5.45 (t, *J* = 3.1

Hz, 1H, CH), 2.65 (m, 2H, CHCH₂), 2.39 (t, *J* = 10.5, 2H, CCH₂). ¹³C{¹H} NMR (100 MHz, CD₂Cl₂): δ 140.8 (CH), 133.1, 131.0, 128.9, 125.6 (PPN), 87.1 (cage CCH), 60.2 (cage CCH₂), 40.9 (CCH₂), 33.0 (CHCH₂). ¹¹B NMR (96 MHz, CD₂Cl₂): δ 7.1 (d, *J*_{BH} = 135 Hz, 1B), 0.4 (d, *J*_{BH} = 150 Hz, 5B), -20.4 (d, *J*_{BH} = 135 Hz, 5B). IR (KBr) *v*_{max} (cm⁻¹): 2519 (vs, BH). Anal. Calcd for C₄₁H₄₆B₁₁NP₂ (M): C, 67.12; H, 6.32; N, 1.91. Found: C, 67.47; H, 6.45; N, 1.59.

Preparation of [μ-1,2-CH(CH₂)₃-1,2-C₂B₁₁H₁₁][PPN] ([45][PPN]). To a THF (20 mL) solution of **7** (105 mg, 0.50 mmol) was added NaH (48 mg, 2.0 mmol) at room temperature and the mixture was stirred until no gas was evolved. After filtration, [PPN]Cl (287 mg, 0.50 mmol) was added to the brown filtrate and further stirred overnight. After filtration, the filtrate was concentrated to about 5 mL, and *n*-hexane layering gave [45][PPN] as brown crystals (350 mg, 0.47 mmol, 94%). ¹H NMR (400 MHz, CD₂Cl₂): δ 7.69 (m, 6H, PPN), 7.54 (m, 24H, PPN), 5.76 (t, *J* = 4.8 Hz, 1H, CH), 2.14 (m, 2H, CHCH₂), 2.11 (t, *J* = 6.1 Hz, 2H, CCH₂), 1.56 (m, *J* = 6.0 Hz, 2H, CH₂CH₂CH₂). ¹³C{¹H} NMR (100 MHz, CD₂Cl₂): δ 150.3 (CH), 134.2, 132.6, 129.9, 127.4 (PPN), 80.4 (cage CCH), 53.5 (cage CCH₂), 42.3 (CCH₂), 29.0 (CHCH₂), 19.4 (CH₂CH₂CH₂). ¹¹B NMR (96 MHz, CD₂Cl₂): δ 6.6 (d, *J*_{BH} = 134 Hz, 1B), -1.4 (d, *J*_{BH} = 148 Hz, 5B), -21.4 (d, *J*_{BH} = 135 Hz, 5B). IR (KBr) *v*_{max} (cm⁻¹): 2526 (vs, BH). Anal. Calcd for C₄₂H₄₈B₁₁NP₂ (M): C, 67.47; H, 6.47; N, 1.87. Found: C, 67.13; H, 6.40; N, 1.96.

Reaction of **6 with Et₃N.** A Et₃N (10 mL) solution of **6** (196 mg, 1.00 mmol) was heated at 90 °C in a sealed tube for 48 h to give a pale yellow suspension. Column chromatographic separation (SiO₂, 300-400 mesh, CH₂Cl₂) followed by recrystallization from CH₂Cl₂ afforded μ-1,2-(CH₂)₃CH(NEt₃)-1-CB₁₁H₁₀ (**46a**) (223 mg, 0.75 mmol, 75%) and μ-1,2-(CH₂)₂CH(NEt₃)CH₂-1-CB₁₁H₁₀ (**46b**) (15 mg, 0.05 mmol,

5%) as colorless crystals each. **46a**: ^1H NMR (400 MHz, acetone- d_6): δ 3.89 (m, 3H, NCH_2), 3.74 (m, 3H, NCH_2), 3.54 (d, $J = 10.5$ Hz, 1H, $\alpha\text{-CH}$), 2.17 (br, 1H, $\beta\text{-CH}_2$), 2.00 (m, 1H, $\delta\text{-CH}_2$), 1.81 (m, 1H, $\delta\text{-CH}_2$), 1.72 (m, 1H, $\gamma\text{-CH}_2$), 1.63 (m, 1H, $\beta\text{-CH}_2$), 1.44 (m, 9H, CH_3), 1.38 (m, 1H, $\gamma\text{-CH}_2$). $^{13}\text{C}\{^1\text{H}\}$ NMR (100 MHz, acetone- d_6): δ 69.4 (cage C), 66.0 ($\alpha\text{-CH}$), 54.1 (NCH_2), 36.3 ($\delta\text{-CH}_2$), 25.5 ($\gamma\text{-CH}_2$), 24.5 ($\beta\text{-CH}_2$), 10.1 (CH_3). ^{11}B NMR (96 MHz, acetone- d_6): δ -8.1 (d, $J_{\text{BH}} = 152$ Hz, 1B), -10.0 (d, $J_{\text{BH}} = 195$ Hz, 1B), -11.0 (d, $J_{\text{BH}} \approx 141$ Hz, 2B), -12.0 (d, $J_{\text{BH}} \approx 141$ Hz, 6B), -13.8 (d, $J_{\text{BH}} = 163$ Hz, 1B). IR (KBr) ν_{max} (cm^{-1}): 2544, 2521 (vs, BH). HRMS (EI): m/z calcd for $\text{C}_{11}\text{H}_{32}^{11}\text{B}_9^{10}\text{B}_2\text{N}$ $[\text{M}]^+$: 297.3626; Found: 297.3617. **46b**: ^1H NMR (400 MHz, acetone- d_6): δ 3.54 (m, 7H, $\text{NCH}_2 + \beta\text{-CH}$), 2.19 (m, 1H, $\delta\text{-CH}_2$), 2.07 (m, 1H, $\gamma\text{-CH}_2$), 2.03 (m, 1H, $\delta\text{-CH}_2$), 1.69 (m, 1H, $\gamma\text{-CH}_2$), 1.50 (m, 1H, $\alpha\text{-CH}_2$), 1.41 (m, 9H, CH_3), 1.37 (m, 1H, $\alpha\text{-CH}_2$). $^{13}\text{C}\{^1\text{H}\}$ NMR (100 MHz, acetone- d_6): δ 72.7 ($\beta\text{-CH}$), 66.3 (cage C), 53.1 (NCH_2), 36.8 ($\delta\text{-CH}_2$), 27.0 ($\gamma\text{-CH}_2$), 15.5 ($\alpha\text{-CH}_2$), 9.5 (CH_3). ^{11}B NMR (96 MHz, acetone- d_6): δ -8.0 (s, 1B), -9.3 (d, $J_{\text{BH}} = 140$ Hz, 1B), -11.5 (d, $J_{\text{BH}} = 127$ Hz, 5B), -12.7 (d, $J_{\text{BH}} = 119$ Hz, 2B), -13.8 (d, $J_{\text{BH}} \approx 94$ Hz, 1B), -14.9 (d, $J_{\text{BH}} = 129$ Hz, 1B). IR (KBr) ν_{max} (cm^{-1}): 2537 (vs, BH). HRMS (EI): m/z calcd for $\text{C}_{11}\text{H}_{32}^{11}\text{B}_9^{10}\text{B}_2\text{N}$ $[\text{M}]^+$: 297.3626; Found: 297.3620.

Reaction of 6 with PS. To a THF (10 mL) solution of **6** (196 mg, 1.00 mmol) was added PS (1.072 g, 5.00 mmol) and the mixture was heated at 90 °C in a sealed tube for 28 d to give a pale yellow suspension. After filtration, the pale yellow solid was thoroughly washed with CH_2Cl_2 to give gross $\mu\text{-1,2-(CH}_2\text{)}_2\text{CH(4'-C}_{10}\text{H}_5\text{-1',8'-(NMe}_2\text{)}_2\text{H)CH}_2\text{-1-CB}_{11}\text{H}_{10}$ (**47b**) (100 mg, 0.24 mmol, 24%). Recrystallization from MeCN afforded **47b** as colorless crystals (50mg, 0.12 mmol, 12%). Removal of the solvent from the filtrate and thoroughly washing with Et_2O gave gross $[\mu\text{-1,2-(CH}_2\text{)}_2\text{CH=CH-1-CB}_{11}\text{H}_{10}][\text{PSH}]$ (**[37][PSH]**) as a pale yellow solid (240 mg, 0.58

mmol, 58%). Recrystallization from CH_2Cl_2 afforded [37][PSH] as colorless crystals (220 mg, 0.54 mmol, 54%). [37][PSH]: ^1H NMR (400 MHz, acetone- d_6): δ 8.12 (m, 4H, C_{10}H_6), 7.77 (t, $J = 7.9$ Hz, 2H, C_{10}H_6), 5.90 (br, 2H, $\text{CH}=\text{CH}$), 3.34 (d, $J = 2.6$ Hz, 12H, NCH_3), 2.01 (m, 2H, $\delta\text{-CH}_2$), 1.92 (t, $J = 6.6$ Hz, $\gamma\text{-CH}_2$). $^{13}\text{C}\{^1\text{H}\}$ NMR (100 MHz, acetone- d_6): δ 145.3, 136.2 (C_{10}H_6), 133.2 (br, $\alpha\text{-CH}$), 131.8 ($\beta\text{-CH}$), 130.1, 127.9, 122.5, 120.0 (C_{10}H_6), 66.9 (cage C), 46.6 (NCH_3), 33.4 ($\delta\text{-CH}_2$), 26.4 ($\gamma\text{-CH}_2$). ^{11}B NMR (96 MHz, acetone- d_6): δ -9.1 (d, $J_{\text{BH}} = 168$ Hz, 1B), -10.9 (d, $J_{\text{BH}} = 146$ Hz, 3B), -12.2 (d, $J_{\text{BH}} = 121$ Hz, 4B), -13.6 (d, $J_{\text{BH}} = 133$ Hz, 3B). ^1H NMR (400 MHz, CD_2Cl_2): δ 8.04 (d, $J = 8.2$ Hz, 2H, C_{10}H_6), 7.80 (d, $J = 7.4$ Hz, 2H, C_{10}H_6), 7.73 (t, $J = 7.9$ Hz, 2H, C_{10}H_6), 5.99 (br, 1H, $\beta\text{-CH}$), 5.93 (d, $J = 12.7$ Hz, 1H, $\alpha\text{-CH}$), 3.18 (d, $J = 2.7$ Hz, 12H, NCH_3), 2.05 (m, 2H, $\delta\text{-CH}_2$), 1.96 (t, $J = 6.6$ Hz, $\gamma\text{-CH}_2$). $^{13}\text{C}\{^1\text{H}\}$ NMR (100 MHz, CD_2Cl_2): δ 144.0, 136.1 (C_{10}H_6), 133.1 ($\beta\text{-CH}$), 131.9 (br, $\alpha\text{-CH}$), 130.4, 127.8, 121.8, 119.1 (C_{10}H_6), 67.7 (cage C), 47.1 (NCH_3), 33.0 ($\delta\text{-CH}_2$), 26.3 ($\gamma\text{-CH}_2$). ^{11}B NMR (96 MHz, CD_2Cl_2): δ -10.3 (d, $J_{\text{BH}} = 132$ Hz, 1B), -11.5 (d, $J_{\text{BH}} = 150$ Hz, 2B), -12.8 (d, $J_{\text{BH}} = 167$ Hz, 2B), -13.5 (d, $J_{\text{BH}} = 130$ Hz, 2B), -14.6 (d, $J_{\text{BH}} = 129$ Hz, 3B). IR (KBr) ν_{max} (cm^{-1}): 2534, 2516 (vs, BH). Anal. Calcd for $\text{C}_{19}\text{H}_{35}\text{B}_{11}\text{N}_2$ [M]: C, 55.60; H, 8.60; N, 6.83. Found: C, 55.13; H, 8.30; N, 7.33. **47b**: ^1H NMR (400 MHz, DMSO- d_6): δ 8.15 (d, $J = 8.7$ Hz, 1H, C_{10}H_5), 8.07 (d, $J = 7.5$ Hz, 1H, C_{10}H_5), 8.00 (d, $J = 8.1$ Hz, 1H, C_{10}H_5), 7.80 (t, $J = 8.1$ Hz, 1H, C_{10}H_5), 7.58 (d, $J = 8.0$ Hz, 1H, C_{10}H_5), 3.34 (m, 1H, $\beta\text{-CH}$), 3.14 (d, $J = 2.2$ Hz, 3H, CH_3), 3.12 (m, 6H, CH_3), 3.10 (d, $J = 1.7$ Hz, 3H, CH_3), 2.10 (m, 2H, $\delta\text{-CH}_2$), 1.68 (m, 1H, $\gamma\text{-CH}_2$), 1.53 (m, 1H, $\gamma\text{-CH}_2$), 1.28 (m, 1H, $\alpha\text{-CH}_2$), 1.07 (m, 1H, $\alpha\text{-CH}_2$). $^{13}\text{C}\{^1\text{H}\}$ NMR (100 MHz, DMSO- d_6): δ 147.4, 145.6, 141.9, 132.3, 126.9, 123.7, 123.1, 121.5, 121.4, 119.2 (C_{10}H_5), 66.8 (cage C), 45.7, 45.6 (CH_3), 36.0 ($\delta\text{-CH}_2$), 35.3 ($\beta\text{-CH}_2$), 32.3 ($\gamma\text{-CH}_2$), 22.6 ($\alpha\text{-CH}_2$). ^{11}B NMR (96 MHz, DMSO- d_6): δ -12.5

(br, 11B). IR (KBr) ν_{\max} (cm⁻¹): 2536 (vs, BH). HRMS (EI): m/z calcd for C₁₉H₃₅¹¹B₉¹⁰B₂N₂ [M]⁺: 410.3891; Found: 410.3886.

Preparation of $[\mu-\eta:\eta:\eta-7,8,10-(\text{CH}_2)_3\text{CHB}(\text{NEt}_2)-7\text{-CB}_{10}\text{H}_{10}][\text{H}(\text{Et}_2\text{NH})_x]$ (40i). To a C₆D₆ (0.5 mL) solution of **6** (9.8 mg, 0.05 mmol) was added Et₂NH (~0.05 mL, 70.7 mg, ~0.48 mmol) at -30 °C and slowly warmed to room temperature to afford **40i** in situ. ¹H NMR (400 MHz, C₆D₆): δ 3.61 (m, 2H, NCH₂), 3.26 (m, 1H, NCH₂), 3.13 (m, 1H, NCH₂), 2.82 (m, 1H, δ -CH₂), 2.62 (m, 1H, β -CH₂), 2.16 (m, 1H, δ -CH₂), 1.87 (m, 2H, α -CH + δ -CH₂), 1.82 (m, 1H, δ -CH₂), 1.67 (m, 1H, β -CH₂), 1.26 (t, J = 6.9 Hz, 3H, CH₃), 1.11 (t, J = 6.9 Hz, 3H, CH₃). ¹³C{¹H} NMR (100 MHz, C₆D₆): δ 93.6 (cage C), 43.6 (NCH₂), 38.4 (δ -CH₂), 33.4 (β -CH₂), 27.6 (γ -CH₂), 15.1, 14.3 (CH₃), 12.7 (α -CH). ¹¹B NMR (128 MHz, C₆D₆): δ 39.8 (s, 1B), 21.1 (br, 1B), 0.5 (d, J_{BH} = 113 Hz, 1B), -6.0 (d, J_{BH} = 97 Hz, 2B), -11.6 (d, J_{BH} = 131 Hz, 1B), -15.4 (d, J_{BH} \approx 191 Hz, 2B), -17.7 (d, J_{BH} = 148 Hz, 1B), -19.4 (d, J_{BH} \approx 192 Hz, 1B), -23.8 (d, J_{BH} = 115 Hz, 1B).

Preparation of $[\mu-\eta:\eta:\eta-7,8,10-(\text{CH}_2)_3\text{CHB}(\text{NEt}_2)-7\text{-CB}_{10}\text{H}_{10}][\text{PPN}]$ ([40i'] [PPN]). To a THF (10 mL) solution of **6** (98 mg, 0.50 mmol) was added Et₂NLi (40 mg, 0.50 mmol) at room temperature and the mixture was stirred overnight to give a solution of $[\mu-\eta:\eta:\eta-7,8,10-(\text{CH}_2)_3\text{CHB}(\text{NEt}_2)-7\text{-CB}_{10}\text{H}_{10}]\text{Li}$ ([40i'] Li). [PPN]Cl was added and the mixture was further stirred for 6 h. After removal of the solvent, the residue was recrystallized from CH₂Cl₂ to afford [40i'] [PPN] as pale yellow crystals (363 mg, 0.45 mmol, 90%). ¹H NMR (400 MHz, CD₂Cl₂): δ 7.69 (m, 12H, PPN), 7.53 (m, 18H, PPN), 3.46 (m, 1H, NCH₂), 3.33 (m, 1H, NCH₂), 3.09 (m, 2H, NCH₂), 2.35 (m, 1H, δ -CH₂), 2.33 (m, 1H, β -CH₂), 1.66 (m, 1H, δ -CH₂), 1.56 (m, 1H, γ -CH₂), 1.43 (m, 1H, γ -CH₂), 1.41 (m, 1H, α -CH), 1.24 (m, 1H, β -CH₂), 1.09 (t, J = 7.0 Hz, 3H, CH₃), 1.06 (t, J = 7.1 Hz, 3H, CH₃). ¹³C{¹H}

NMR (100 MHz, CD₂Cl₂): δ 134.2, 132.6, 129.9, 127.4 (PPN), 92.9 (cage C), 43.4, 43.3 (NCH₂), 38.0 (δ -CH₂), 33.0 (β -CH₂), 27.3 (γ -CH₂), 15.0, 14.1 (CH₃), 12.2 (α -CH). ¹¹B NMR (128 MHz, CD₂Cl₂): δ 38.8 (, $J_{\text{BH}} = \text{Hz}$, 1B), 20.2 (br, 1B), -0.4 (d, $J_{\text{BH}} = 141 \text{ Hz}$, 1B), -6.9 (d, $J_{\text{BH}} = 127 \text{ Hz}$, 2B), -12.2 (d, $J_{\text{BH}} = 128 \text{ Hz}$, 1B), -16.3 (d, $J_{\text{BH}} = 123 \text{ Hz}$, 2B), -18.5 (d, $J_{\text{BH}} = 141 \text{ Hz}$, 1B), -20.4 (d, $J_{\text{BH}} = 113 \text{ Hz}$, 1B), -24.6 (d, $J_{\text{BH}} = 118 \text{ Hz}$, 1B). IR (KBr) ν_{max} (cm⁻¹): 2510 (vs, BH). Anal. Calcd for C₄₅H₅₇B₁₁N₂P₂ [M]: C, 66.99; H, 7.12; N, 3.47. Found: C, 67.18; H, 7.08; N, 3.50.

Preparation of $[\mu\text{-}\eta\text{:}\eta\text{:}\eta\text{-}7,8,10\text{-(CH}_2\text{)}_3\text{CHB(OMe)-7-CB}_{10}\text{H}_{10}][\text{PSH}]$ ([36i'] [PSH]). PS (118 mg, 0.55 mmol) was dissolved in MeOH (5 mL) and this solution was added to **6** (98 mg, 0.50 mmol) with stirring and a white suspension was formed in 5 min. After removal of the solvent, the residue was thoroughly washed with Et₂O to afford [36i'] [PSH] as a white solid (199 mg, 0.45 mmol, 90%). X-ray-quality crystals were obtained by recrystallization from THF. ¹H NMR (400 MHz, CD₂Cl₂): δ 8.04 (d, $J = 8.2 \text{ Hz}$, 2H, C₁₀H₆), 7.85 (d, $J = 7.6 \text{ Hz}$, 2H, C₁₀H₆), 7.74 (dd, av. $J = 7.9 \text{ Hz}$, 2H, C₁₀H₆), 3.70 (s, 3H, OCH₃), 3.20 (d, $J = 2.4 \text{ Hz}$, 12H, NCH₃), 2.45 (m, 1H, δ -CH₂), 2.30 (m, 1H, β -CH₂), 1.74 (m, 1H, δ -CH₂), 1.66 (m, 1H, γ -CH₂), 1.59 (br, 1H, CH), 1.32 (m, 1H, γ -CH₂), 1.16 (m, 1H, β -CH₂). ¹³C {¹H} NMR (100 MHz, CD₂Cl₂): δ 143.9, 135.9, 130.2, 127.7, 121.8, 119.0 (C₁₀H₆), 104.3 (cage C), 55.5 (OCH₃), 46.9 (NCH₃), 37.5 (δ -CH₂), 30.0 (β -CH₂), 27.2 (γ -CH₂), 15.9 (α -CH). ¹¹B NMR (96 MHz, CD₂Cl₂): δ 42.5 (s, 1B), 20.4 (d, $J_{\text{BH}} = 144 \text{ Hz}$, 1B), 0.2 (d, $J_{\text{BH}} = 166 \text{ Hz}$, 1B), -2.5 (d, $J_{\text{BH}} = 132 \text{ Hz}$, 1B), -9.9 (d, $J_{\text{BH}} = 128 \text{ Hz}$, 1B), -12.0 (d, $J_{\text{BH}} = 139 \text{ Hz}$, 1B), -14.0 (d, $J_{\text{BH}} \approx 106 \text{ Hz}$, 1B), -14.6 (d, $J_{\text{BH}} = 115 \text{ Hz}$, 2B), -18.3 (d, $J_{\text{BH}} = 115 \text{ Hz}$, 1B), -21.3 (d, $J_{\text{BH}} = 117 \text{ Hz}$, 1B). IR (KBr) ν_{max} (cm⁻¹): 2514 (vs, BH). Anal. Calcd for C₂₀H₃₉B₁₁N₂O (M): C, 54.29; H, 8.88; N, 6.33. Found: C, 54.40; H, 8.60; N, 6.53.

Alternative Method for the Preparation of μ -1,2-(CH₂)₃CH(NEt₂H)-1-CB₁₁H₁₀ (40a). A THF solution of [40i']⁺[PPN]⁻ was prepared from **6** (196 mg, 1.00 mmol) and Et₂NLi (80 mg, 1.00 mmol). After removal of THF, CH₂Cl₂ (10 mL) and a 1.0 M solution of HCl (5 mL, 5.0 mmol) was added, respectively, at 0 °C. The mixture was stirred at room temperature for 30 min. The organic layer was separated. The aqueous layer was extracted with CH₂Cl₂ (10 mL x 3). The organic layers were combined and dried over Na₂SO₄. Recrystallization from CH₂Cl₂ afforded **40a** as colorless crystals (215 mg, 0.80 mmol, 80%).

Thermolysis of 40i. To a toluene (20 mL) solution of **6** (196 mg, 1.00 mmol) was added Et₂NH (2 mL, 1.414 mg, 19.2 mmol) at -30 °C and slowly warmed to room temperature to afford **40i** in situ. The mixture was heated at 90 °C for 2 h in a sealed tube. Column chromatographic separation (SiO₂, 300-400 mesh, CH₂Cl₂) followed by recrystallization from CH₂Cl₂ afforded **40a** (215 mg, 0.80 mmol, 80%) as colorless crystals and μ -1,2-(CH₂)₂CH(NEt₂H)CH₂-1-CB₁₁H₁₀ (**40b**) as a white solid (10 mg, 0.037 mmol, 3.7%). **40b**: ¹H NMR (400 MHz, acetone-*d*₆): δ 3.59 (m, 1H, β -CH), 3.40 (m, 4H, NCH₂), 2.16 (m, 1H, δ -CH₂), 2.03 (m, 1H, δ -CH₂), 1.80 (m, 1H, γ -CH₂), 1.70 (m, 1H, γ -CH₂), 1.42 (t, *J* = 7.3 Hz, 6H, CH₃), 1.39 (m, 1H, α -CH₂), 1.23 (m, 1H, α -CH₂). ¹³C{¹H} NMR (100 MHz, acetone-*d*₆): δ 66.4 (cage C), 63.4 (β -CH), 46.1 (NCH₂), 35.8 (δ -CH₂), 27.5 (γ -CH₂), 14.7 (br, α -CH₂), 11.0 (CH₃). ¹¹B NMR (128 MHz, acetone-*d*₆): δ -8.2 (s, 1B), -9.3 (d, *J*_{BH} = 151 Hz, 1B), -11.6 (d, *J*_{BH} = 131 Hz, 7B), -13.8 (d, *J*_{BH} = 165 Hz, 1B), -15.0 (d, *J*_{BH} = 142 Hz, 1B). IR (KBr) ν_{\max} (cm⁻¹): 2534 (vs, BH). HRMS (EI): *m/z* calcd for C₉H₂₆¹¹B₉¹⁰B₂N [M - 2H]⁺: 267.3156; Found: 269.3152.

Chapter 5

Preparation of [*endo*- μ -7,8-(CH₂)₃CHB(OMe)₂-7-CB₁₀H₁₁][PSH] ([48][PSH]).

Et₃N (1 mL, 726 mg, 7.2 mmol) and MeOH (10 mL) were added to **6** (98 mg, 0.50 mmol) at 0 °C, respectively. The mixture was stirred at room temperature for 1 h then heated at 70 °C in a sealed tube for 24 h to give a solution of [μ -7,8-(CH₂)₃CHB(OMe)₂-7-CB₁₀H₁₁][Et₃NH] ([48][Et₃NH]) in situ. A 0.25 M PS solution in MeOH (10 mL, 2.5 mmol) was added to give a white suspension in 5 min. After removal of the volatile materials, the residue was thoroughly washed with Et₂O to afford [48][PSH] as a white solid (214 mg, 0.45 mmol, 90%). X-ray-quality crystals were obtained by recrystallization from THF. ¹H NMR (400 MHz, CD₂Cl₂): δ 8.03 (dd, $J_1 = 8.3$ Hz, $J_2 = 0.9$ Hz, 2H, C₁₀H₆), 7.79 (dd, $J_1 = 7.6$ Hz, $J_2 = 1.0$ Hz, 2H, C₁₀H₆), 7.72 (t, $J = 7.9$ Hz, 2H, C₁₀H₆), 3.49 (s, 6H, OCH₃), 3.19 (d, $J = 2.7$ Hz, 12H, NCH₃), 2.22 (m, 1H, δ -CH₂), 1.61 (m, 1H, δ -CH₂), 1.56 (m, 1H, γ -CH₂), 1.50 (m, 1H, β -CH₂), 1.33 (m, 1H, β -CH₂), 1.19 (m, 1H, γ -CH₂), 0.80 (br, 1H, α -CH). ¹³C{¹H} NMR (100 MHz, CD₂Cl₂): δ 144.1, 136.1, 130.4, 127.8, 121.8, 119.2 (C₁₀H₆), 52.2 (br, cage C), 51.6 (OCH₃), 47.2 (NCH₃), 39.1 (δ -CH₂), 28.5 (γ -CH₂), 25.8 (β -CH₂), 11.4 (br, α -CH). ¹¹B NMR (128 MHz, CD₂Cl₂): δ 32.0 (s, 1B), -2.1 (s, 1B), -5.3 (d, $J_{BH} = 142$ Hz, 1B), -10.1 (d, $J_{BH} = 119$ Hz, 3B), -23.4 (d, $J_{BH} = 132$ Hz, 1B), -24.5 (d, $J_{BH} = 162$ Hz, 1B), -25.7 (d, $J_{BH} = 140$ Hz, 1B), -30.4 (d, $J_{BH} = 142$ Hz, 1B), -34.4 (d, $J_{BH} = 127$ Hz, 1B). IR (KBr) ν_{max} (cm⁻¹): 2519 (vs, BH). Anal. Calcd for C₂₁H₄₃B₁₁N₂O₂ [M]: C, 53.16; H, 9.13; N, 5.90. Found: C, 53.58; H, 9.14; N, 5.82.

Preparation of [3-OMe- μ -1,2-(CH₂)₄-1,2-C₂B₁₁H₁₁][Et₃NH] ([49][Et₃NH]).

Et₃N (1 mL, 726 mg, 7.2 mmol) and MeOH (10 mL) were added to **7** (105 mg, 0.50 mmol) at 0 °C, respectively. The mixture was stirred for 5 min to give a MeOH solution of [49][Et₃NH] in situ. After removal of the volatile materials, the residue was thoroughly washed with Et₂O to afford [49][Et₃NH] as a white solid (191 mg, 0.45

mmol, 90%). X-ray-quality crystals were obtained by recrystallization from CH_2Cl_2 . ^1H NMR (400 MHz, CD_2Cl_2): δ 6.17 (s, 1H, NH), 3.29 (t, $J = 7.3$ Hz, 6H, NCH_2), 3.21 (s, 3H, OCH_3), 2.79 (m, 2H, CCH_2), 2.59 (m, 2H, CCH_2), 1.58 (m, 4H, CCH_2CH_2), 1.42 (d, $J = 7.3$ Hz, 9H, CH_3). $^{13}\text{C}\{^1\text{H}\}$ NMR (100 MHz, CD_2Cl_2): δ 141.4 (cage C), 52.6 (OCH_3), 48.7 (NCH_2), 36.4 (CCH_2), 23.5 (CCH_2CH_2), 9.4 (CH_3). ^{11}B NMR (128 MHz, CD_2Cl_2): δ 1.7 (s, 1B), -3.4 (d, $J_{\text{BH}} = 112$ Hz, 2B), -6.2 (d, $J_{\text{BH}} = 142$ Hz, 1B), -8.6 (d, $J_{\text{BH}} = 116$ Hz, 4B), -19.0 (d, $J_{\text{BH}} = 130$ Hz, 2B), -26.0 (d, $J_{\text{BH}} = 139$ Hz, 1B). IR (KBr) ν_{max} (cm^{-1}): 2511 (vs, BH). Anal. Calcd for $\text{C}_{13}\text{H}_{38}\text{B}_{11}\text{NO}$ [M]: C, 45.47; H, 11.15; N, 4.08. Found: C, 45.28; H, 11.26; N, 4.24.

Preparation of [3-OMe- μ -1,2-(CH_2)₄-1,2- $\text{C}_2\text{B}_{11}\text{H}_{11}$][PSH] ([49][PSH]). To **7** (105 mg, 0.50 mmol) was added a 0.25 M PS solution in MeOH (10 mL, 2.5 mmol) to give a white suspension in 5 min. After removal of the volatile materials, the residue was thoroughly washed with Et_2O to afford [49][PSH] as a white solid (206 mg, 0.45 mmol, 90%). ^1H NMR (400 MHz, CD_2Cl_2): δ 8.04 (d, $J = 8.2$ Hz, 2H, C_{10}H_6), 7.86, (d, $J = 7.5$ Hz, 2H, C_{10}H_6), 7.74 (d, $J = 7.9$ Hz, 2H, C_{10}H_6), 3.23 (d, $J = 1.6$ Hz, 12H, NCH_3), 3.21 (s, 3H, OCH_3), 2.79 (m, 2H, CCH_2), 2.60 (m, 2H, CCH_2), 1.57 (m, 4H, CCH_2CH_2). $^{13}\text{C}\{^1\text{H}\}$ NMR (100 MHz, CD_2Cl_2): δ 144.0 (C_{10}H_6), 140.7 (cage C), 136.0, 130.2, 127.7, 121.9, 119.1 (C_{10}H_6), 52.4 (OCH_3), 47.0 (NCH_3), 36.4 (CCH_2), 23.6 (CCH_2CH_2). ^{11}B NMR (128 MHz, CD_2Cl_2): δ 1.7 (s, 1B), -3.4 (d, $J_{\text{BH}} = 109$ Hz, 2B), -6.1 (d, $J_{\text{BH}} = 136$ Hz, 1B), -8.6 (d, $J_{\text{BH}} = 123$ Hz, 4B), -19.0 (d, $J_{\text{BH}} = 132$ Hz, 2B), -26.0 (d, $J_{\text{BH}} = 139$ Hz, 1B). IR (KBr) ν_{max} (cm^{-1}): 2508 (vs, BH). Anal. Calcd for $\text{C}_{21}\text{H}_{41}\text{B}_{11}\text{N}_2\text{O}$: C, 55.25; H, 9.05; N, 6.14. Found: C, 54.78; H, 8.84; N, 6.10.

Preparation of [endo- μ -7,8-(CH_2)₄CHB(OMe)₂-7- $\text{CB}_{10}\text{H}_{11}$][PSH] ([50][PSH]). A MeOH (10 mL) solution of [49][Et_3NH], which was prepared in situ from Et_3N (1 mL, 726 mg, 7.2 mmol) and **7** (105 mg, 0.50 mmol), was heated at 70 °C for 24 h to

give a solution of **[50][Et₃NH]**. A 0.25 M PS solution in MeOH (10 mL, 2.5 mmol) was added. After removal of the volatile materials, the residue was thoroughly washed with Et₂O to afford **[50][PSH]** as a white solid (220 mg, 0.45 mmol, 90%). X-ray-quality crystals were obtained by recrystallization from THF. ¹H NMR (400 MHz, CD₂Cl₂): δ 8.05 (d, *J* = 8.3 Hz, 2H, C₁₀H₆), 7.84 (d, *J* = 7.6 Hz, 2H, C₁₀H₆), 7.74 (d, *J* = 7.9 Hz, 2H, C₁₀H₆), 3.49 (s, 6H, OCH₃), 3.21 (d, *J* = 2.7 Hz, 12H, NCH₃), 2.07 (m, 1H, ε-CH₂), 1.90 (m, 1H, ε-CH₂), 1.81 (m, 1H, γ-CH₂), 1.71 (m, 1H, β-CH₂), 1.56 (m, 2H, δ-CH₂), 1.49 (m, 1H, β-CH₂), 1.31 (m, 1H, γ-CH₂), 0.85 (m, 1H, α-CH). ¹³C{¹H} NMR (100 MHz, CD₂Cl₂): δ 143.9, 136.0, 130.3, 127.7, 121.8, 119.0 (C₁₀H₆), 57.5 (cage C), 51.4 (OCH₃), 47.0 (NCH₃), 37.8 (ε-CH₂), 31.2 (γ-CH₂), 30.5 (δ-CH₂), 28.8 (β-CH₂), 15.1 (α-CH). ¹¹B NMR (128 MHz, CD₂Cl₂): δ 32.2 (s, 1B), 0.6 (s, 1B), -4.2 (d, *J*_{BH} = 120 Hz, 1B), -9.2 (d, *J*_{BH} = 140 Hz, 2B), -10.8 (d, *J*_{BH} = 189 Hz, 1B), -23.8 (d, *J*_{BH} = 92 Hz, 2B), -26.4 (d, *J*_{BH} = 131 Hz, 1B), -30.1 (d, *J*_{BH} = 136 Hz, 1B), -33.9 (d, *J*_{BH} = 134 Hz, 1B). IR (KBr) ν_{max} (cm⁻¹): 2519 (vs, BH). Anal. Calcd for C₂₂H₄₅B₁₁N₂O₂ [M]: C, 54.09; H, 9.28; N, 5.73. Found: C, 53.92; H, 9.13; N, 6.23.

Preparation of [*endo*-μ-7,8-(CH₂)₃CHOH-7-CB₁₀H₁₁][PSH] ([51][PSH]). To a MeOH (10 mL) solution of **[48][Et₃NH]**, which was prepared in situ from Et₃N (1 mL, 726 mg, 7.2 mmol) and **6** (98 mg, 0.50 mmol), was added H₂O₂ (1 mL, 30%, 300 mg, 8.8 mmol) at 0 °C. The mixture was stirred at room temperature for 1 h. A 0.25 M PS solution in MeOH (10 mL, 2.5 mmol) was then added. After removal of the volatile materials, the residue was thoroughly washed with Et₂O to afford **[51][PSH]** as a white solid (188 mg, 0.45 mmol, 90%). X-ray-quality crystals were obtained by recrystallization from CH₂Cl₂. ¹H NMR (400 MHz, CD₂Cl₂): δ 8.04 (d, *J* = 8.1 Hz, 2H, C₁₀H₆), 7.82 (d, *J* = 7.5 Hz, 2H, C₁₀H₆), 7.73 (t, *J* = 7.9 Hz, 2H, C₁₀H₆),

3.41 (m, 1H, α -CH), 3.19 (d, $J = 2.6$ Hz, 12H, NCH₃), 2.13 (m, 1H, δ -CH₂), 1.67 (m, 2H, β -CH₂ + δ -CH₂), 1.51 (m, 1H, γ -CH₂), 1.37 (m, 1H, β -CH₂), 1.24 (m, 1H, γ -CH₂). ¹³C{¹H} NMR (100 MHz, CD₂Cl₂): δ 143.9, 136.0, 130.3, 127.7, 121.8, 119.1 (C₁₀H₆), 61.9 (α -CH), 53.4 (cage C), 47.0 (NCH₃), 37.2 (δ -CH₂), 34.0 (β -CH₂), 24.0 (γ -CH₂). ¹¹B NMR (128 MHz, CD₂Cl₂): δ -1.4 (s, 1B), -4.9 (d, $J_{BH} = 138$ Hz, 1B), -9.4 (d, $J_{BH} = 141$ Hz, 2B), -11.8 (d, $J_{BH} = 140$ Hz, 1B), -22.3 (d, $J_{BH} = 140$ Hz, 1B), -24.5 (d, $J_{BH} = 139$ Hz, 1B), -25.9 (d, $J_{BH} = 142$ Hz, 1B), -32.2 (d, $J_{BH} = 147$ Hz, 1B), -33.7 (d, $J_{BH} = 141$ Hz, 1B). IR (KBr) ν_{max} (cm⁻¹): 2526 (vs, BH). Anal. Calcd for C₁₉H₃₈B₁₀N₂O [M]: C, 54.51; H, 9.15; N, 6.69. Found: C, 54.38; H, 8.92; N, 6.54.

Preparation of [endo- μ -7,8-(CH₂)₄CHOH-7-CB₁₀H₁₁][PSH] ([52][PSH]). To a MeOH (10 mL) solution of [50][Et₃NH], which was prepared in situ from Et₃N (1 mL, 726 mg, 7.2 mmol) and 7 (105 mg, 0.50 mmol), was added H₂O₂ (1 mL, 30%, 300mg, 8.8 mmol) at 0 °C. The mixture was stirred at room temperature for 1 h. A 0.25 M PS solution in MeOH (10 mL, 2.5 mmol) was added. After removal of the volatile materials, the residue was thoroughly washed with Et₂O to afford [52][PSH] as a white solid (195 mg, 0.45 mmol, 90%). X-ray-quality crystals were obtained by recrystallization from CH₂Cl₂. ¹H NMR (400 MHz, CD₂Cl₂): δ 8.04 (dd, $J_1 = 8.3$ Hz, $J_2 = 0.8$ Hz, 2H, C₁₀H₆), 7.81 (dd, $J_1 = 7.6$ Hz, $J_2 = 0.9$ Hz, 2H, C₁₀H₆), 7.73 (t, $J = 7.9$ Hz, 2H, C₁₀H₆), 3.41 (d, $J = 8.4$ Hz, 1H, α -CH), 3.19 (d, $J = 2.7$ Hz, 12H, NCH₃), 2.04 (m, 1H, ϵ -CH₂), 1.92 (m, 1H, β -CH₂), 1.77 (m, 1H, ϵ -CH₂), 1.68 (m, 1H, δ -CH₂), 1.66 (m, 1H, γ -CH₂), 1.53 (m, 1H, β -CH₂), 1.46 (m, 1H, γ -CH₂), 1.36 (m, 1H, δ -CH₂). ¹³C{¹H} NMR (100 MHz, CD₂Cl₂): δ 143.9, 136.0, 130.4, 127.8, 121.8, 119.1 (C₁₀H₆), 65.8 (CH), 56.0 (cage C), 47.1 (NCH₃), 40.9 (ϵ -CH₂), 37.8 (β -CH₂), 31.1 (δ -CH₂), 27.0 (γ -CH₂). ¹¹B NMR (128 MHz, CD₂Cl₂): δ 0.3 (s, 1B), -3.5 (d, $J_{BH} = 123$ Hz, 1B), -9.3 (overlap, 3B), -23.6 (overlap, 1B), -24.3 (overlap, 1B), -26.7 (d, $J_{BH} =$

139 Hz, 1B), -30.7 (d, $J_{\text{BH}} = 143$ Hz, 1B), -32.9 (d, $J_{\text{BH}} = 132$ Hz, 1B). IR (KBr) ν_{max} (cm^{-1}): 2518, 2495 (vs, BH). Anal. Calcd for $\text{C}_{20}\text{H}_{40}\text{B}_{10}\text{N}_2\text{O}$ [M]: C, 55.52; H, 9.32; N, 6.47. Found: C, 55.55; H, 9.57; N, 6.40.

Preparation of $[\text{endo-}\mu\text{-7,8-(CH}_2\text{)}_3\text{CHB(OH)}_2\text{-7-CB}_{10}\text{H}_{11}][\text{PSH}]\cdot\text{THF}$ ([48'] $[\text{PSH}]\cdot\text{THF}$). A MeOH (10 mL) solution of [48] $[\text{Et}_3\text{NH}]$ was prepared in situ from Et_3N (1 mL, 726 mg, 7.2 mmol) and **6** (98 mg, 0.50 mmol). After removal of the volatile materials, Et_3N (1 mL, 726 mg, 7.2 mmol) and H_2O (10 mL) was added. The mixture was heated at 105 °C in a sealed tube for 24 h. A 0.25 M PS solution in MeOH (10 mL, 2.5 mmol) was then added. After removal of the volatile materials, the residue was thoroughly washed with Et_2O . Recrystallization from THF gave [48'] $[\text{PSH}]\cdot\text{THF}$ as colorless crystals (130 mg, 0.25 mmol, 50%). ^1H NMR (400 MHz, CD_2Cl_2): δ 8.03 (dd, $J_1 = 8.3$ Hz, $J_2 = 0.8$ Hz, 2H, C_{10}H_6), 7.81 (dd, $J_1 = 7.6$ Hz, $J_2 = 0.8$ Hz, 2H, C_{10}H_6), 7.72 (t, $J = 7.9$ Hz, 2H, C_{10}H_6), 4.64 (brs, 2H, OH), 3.67 (m, 4H, THF), 3.19 (d, $J = 2.7$ Hz, 12H, NCH_3), 2.23 (m, 1H, $\delta\text{-CH}_2$), 1.82 (m, 4H, THF), 1.65 (m, 1H, $\beta\text{-CH}_2$), 1.61 (m, 1H, $\delta\text{-CH}_2$), 1.48 (m, 1H, $\gamma\text{-CH}_2$), 1.27 (m, 1H, $\gamma\text{-CH}_2$), 1.22 (m, 1H, $\beta\text{-CH}_2$), 0.57 (m, 1H, $\alpha\text{-CH}$). $^{13}\text{C}\{^1\text{H}\}$ NMR (100 MHz, CD_2Cl_2): δ 144.1, 136.1, 130.3, 127.8, 121.8, 119.2 (C_{10}H_6), 68.3 (THF), 51.5 (cage C), 47.2 (NCH_3), 38.7 ($\delta\text{-CH}_2$), 28.5 ($\gamma\text{-CH}_2$), 26.1 ($\beta\text{-CH}_2 + \text{THF}$), 14.3 ($\alpha\text{-CH}$). ^{11}B NMR (128 MHz, CD_2Cl_2): δ 33.6 (s, 1B), -2.0 (s, 1B), -5.4 (d, $J_{\text{BH}} = 139$ Hz, 2B), -9.9 (d, $J_{\text{BH}} = 114$ Hz, 1B), -10.6 (d, $J_{\text{BH}} = 137$ Hz, 1B), -22.4 (d, $J_{\text{BH}} = 107$ Hz, 1B), -25.4 (d, $J_{\text{BH}} = 130$ Hz, 2B), -30.5 (d, $J_{\text{BH}} = 124$ Hz, 1B), -34.6 (d, $J_{\text{BH}} = 138$ Hz, 1B). IR (KBr) ν_{max} (cm^{-1}): 2521 (vs, BH). Anal. Calcd for $\text{C}_{21}\text{H}_{43}\text{B}_{11}\text{N}_2\text{O}_{2.5}$ (M - 0.5THF): C, 52.27; H, 8.98; N, 5.81. Found: C, 52.29; H, 9.00; N, 5.80.

Preparation of $[\text{endo-}\mu\text{-7,8-(CH}_2\text{)}_4\text{CHB(OH)}_2\text{-7-CB}_{10}\text{H}_{11}][\text{PSH}]$ ([50'] $[\text{PSH}]$). A MeOH (10 mL) solution of [50] $[\text{Et}_3\text{NH}]$ was prepared in situ from Et_3N (1 mL,

726 mg, 7.2 mmol) and **7** (105 mg, 0.50 mmol). After removal of the volatile materials, Et₃N (1 mL, 726 mg, 7.2 mmol) and H₂O (10 mL) were added. The mixture was heated at 105 °C in a sealed tube for 24 h. A 0.25 M PS solution in MeOH (10 mL, 2.5 mmol) was then added. After removal of the volatile materials, the residue was thoroughly washed with Et₂O to give [**50'**][PSH] as a white solid (115 mg, 0.25 mmol, 25%). ¹H NMR (400 MHz, CD₂Cl₂): δ 8.04 (d, *J* = 8.2 Hz, 2H, C₁₀H₆), 7.83 (d, *J* = 7.5 Hz, 2H, C₁₀H₆), 7.73 (t, *J* = 7.9 Hz, 2H, C₁₀H₆), 5.0 (brs, 2H, OH), 3.19 (d, *J* = 2.6 Hz, 2H, NCH₃), 1.99 (m, 1H, ε-CH₂), 1.89 (m, 1H, β-CH₂), 1.72 (m, 1H, ε-CH₂), 1.66 (m, 1H, δ-CH₂), 1.62 (m, 2H, γ-CH₂), 1.46 (m, 1H, β-CH₂), 1.41 (m, 1H, δ-CH₂), 0.70 (br, 1H, α-CH). ¹³C{¹H} NMR (100 MHz, CD₂Cl₂): δ 143.9, 136.0, 130.3, 127.7, 121.8, 119.0 (C₁₀H₆), 57.8 (cage C), 47.0 (NCH₃), 41.0 (ε-CH₂), 31.9 (δ-CH₂), 31.6 (γ-CH₂), 31.1 (β-CH₂), 18.9 (α-CH). ¹¹B NMR (128 MHz, CD₂Cl₂): δ 33.6 (s, 1B), 1.5 (s, 1B), -4.3 (d, *J*_{BH} = 116 Hz, 1B), -8.0 (d, *J*_{BH} = 138 Hz, 1B), -8.8 (d, *J*_{BH} = 141 Hz, 1B), -10.6 (d, *J*_{BH} ≈ 228 Hz, 1B), -23.5 (d, *J*_{BH} = 96 Hz, 2B), -26.3 (d, *J*_{BH} = 129 Hz, 1B), -30.2 (d, *J*_{BH} = 129 Hz, 1B), -33.8 (d, *J*_{BH} = 135 Hz, 1B). IR (KBr) ν_{max} (cm⁻¹): 2514 (vs, BH). Anal. Calcd for C₂₀H₄₁B₁₁N₂O₂ [**M**]: C, 52.17; H, 8.97; N, 6.08. Found: C, 52.22; H, 8.60; N, 5.90.

Reaction of 6 with C₅H₅N. Method A: To C₅H₅N (5 mL) was slowly added **6** (98 mg, 0.50 mmol) in batches at -30 °C. The resulting dark blue solution was stirred at room temperature overnight and gradually turned to a clear brown solution. After removal of the solvent, the residue was washed with THF to give μ-2,4-(CH₂)₃CHBH(C₅H₅N)₂-2-CB₁₀H₉ (**54**) as a white powder (200 mg, 0.28 mmol, 56%). X-ray-quality crystals were obtained by recrystallization from DMSO/MeOH. **Method B:** C₅H₅N (5 mL) was slowly added to **6** (196 mg, 1.00 mmol) at room temperature with vigorously boiling. After removal of the solvent, column chromatographic

separation (SiO₂, 300-400 mesh, CH₂Cl₂) gave 50% gross μ -1,2-(CH₂)₃CH(NC₅H₅)-1-CB₁₁H₁₀ (**53a**) and 10% gross μ -1,2-(CH₂)₂CH(NC₅H₅)CH₂-1-CB₁₁H₁₀ (**53b**), with observation of μ -2,4-(CH₂)₃CHBH(C₅H₅N)₂-2-CB₁₀H₉ (**54**). Repeated recrystallization from CH₂Cl₂ and acetone afforded **53a** (100 mg, 0.36 mmol, 36%) and **53b** (12 mg, 0.05 mmol, 5%) as a white solid each. X-ray quality crystals of **53a** were grown from slow evaporation of an acetone solution. **53a**: ¹H NMR (400 MHz, acetone-*d*₆): δ 9.11 (d, *J* = 5.7 Hz, 2H, C₅H₅N), 8.63 (t, *J* = 7.8 Hz, 1H, C₅H₅N), 8.22 (d, *J* = 6.7 Hz, 2H, C₅H₅N), 4.73 (d, *J* = 6.3 Hz, 1H, α -CH), 2.30 (br, 1H, β -CH₂), 2.08 (m, 1H, δ -CH₂), 2.07 (m, 1H, β -CH₂), 1.95 (m, 1H, δ -CH₂), 1.80 (m, 1H, γ -CH₂), 1.54 (m, 1H, γ -CH₂). ¹³C{¹H} NMR (100 MHz, acetone-*d*₆): δ 145.2, 144.5, 128.9 (C₅H₅N), 68.8 (cage C), 65.6 (br, α -CH), 35.4 (δ -CH₂), 29.9 (β -CH₂), 24.7 (γ -CH₂). ¹¹B NMR (128 MHz, acetone-*d*₆): δ -8.7 (s, 1B), -8.8 (d, *J*_{BH} = 139 Hz, 1B), -10.5 (d, *J*_{BH} = 174 Hz, 1B), -11.8 (d, *J*_{BH} = 161 Hz, 4B), -13.6 (br, 4B). HRMS (EI): *m/z* calcd for C₁₀H₂₀¹¹B₉¹⁰B₂N [M - 2H]⁺: 273.2692; Found: 273.2691. **53b**: ¹H NMR (400 MHz, acetone-*d*₆): δ 9.29 (d, *J* = 5.8 Hz, 2H, C₅H₅N), 8.70 (t, *J* = 7.7 Hz, 1H, C₅H₅N), 8.25 (t, *J* = 6.7 Hz, 2H, C₅H₅N), 4.87 (m, 1H, β -CH), 2.24 (m, 2H, δ -CH₂), 2.22 (m, 1H, γ -CH₂), 1.96 (m, 1H, γ -CH₂), 1.74 (m, 1H, α -CH₂), 1.65 (m, 1H, α -CH₂). ¹³C{¹H} NMR (100 MHz, acetone-*d*₆): δ 146.4, 144.1, 129.3 (C₅H₅N), 73.6 (β -CH), 66.2 (cage C), 36.2 (δ -CH₂), 33.1 (γ -CH₂), 24.6 (br, α -CH₂). ¹¹B NMR (128 MHz, acetone-*d*₆): δ -8.1 (s, 1B), -9.0 (d, *J*_{BH} = 193 Hz, 1B), -10.3 (d, *J*_{BH} = 155 Hz, 1B), -11.4 (d, *J*_{BH} = 128 Hz, 4B), -12.3 (d, *J*_{BH} = 134 Hz, 2B), -13.5 (d, *J*_{BH} = 150 Hz, 1B), -14.7 (d, *J*_{BH} = 150 Hz, 1B). HRMS (ESI): *m/z* calcd for C₁₀H₂₂¹¹B₉¹⁰B₂NNa [M + Na]⁺: 298.2741; Found: 298.2742. **54**: ¹H NMR (400 MHz, DMSO-*d*₆): δ 9.07 (d, *J* = 5.4 Hz, 2H, C₅H₅N), 9.00 (d, *J* = 5.4 Hz, 2H, C₅H₅N), 8.35 (t, *J* = 7.6 Hz, 1H, C₅H₅N), 8.32 (t, *J* = 7.7 Hz, 1H, C₅H₅N), 7.90 (t, *J* = 7.0 Hz, 2H, C₅H₅N), 7.84 (t, *J* =

7.0 Hz, 2H, C₅H₅N), 2.53 (m, 1H, δ-CH₂), 2.28 (m, 1H, δ-CH₂), 1.69 (m, 1H, γ-CH₂), 1.28 (m, 1H, γ-CH₂), 0.94 (m, 2H, β-CH₂), 0.52 (m, 1H, α-CH₂). ¹³C{¹H} NMR (100 MHz, DMSO-*d*₆): δ 147.7, 146.3, 143.9, 143.7, 127.3, 126.4 (C₅H₅N), 72.8 (cage C), 34.8 (δ-CH₂), 27.1 (β-CH₂), 26.5 (γ-CH₂), 14.9 (α-CH). ¹¹B NMR (128 MHz, DMSO-*d*₆): δ 1.9 (br, 1B), -10.2 (br, 9B), -15.5 (br, 1B). Anal. Calcd for C₁₅H₂₇B₁₁N₂ [M]: C, 50.85; H, 7.68; N, 7.91. Found: C, 50.59; H, 7.85; N, 7.57.

Reaction of 6 with *p*-MeC₅H₄N. Method A: To *p*-MeC₅H₄N (5 mL) was slowly added 6 (98 mg, 0.50 mmol) in batches at -30 °C. The resulting dark blue solution was stirred at room temperature overnight and gradually turned to a clear brown solution. After removal of the solvent, the residue was washed with THF to give μ-2,4-(CH₂)₃CHBH(MeC₅H₄N)₂-2-CB₁₀H₉ (**55**) as a white powder (100 mg, 0.26 mmol, 52%). X-ray-quality crystals were obtained by recrystallization from DMSO/MeOH.

Method B: To a C₆D₆ (0.5 mL) solution of 6 (10 mg, 0.05 mmol) was slowly added *p*-MeC₅H₄N (0.1 mL) at room temperature to afford a mixture of **54**, μ-1,2-(CH₂)₃CH(MeC₅H₄N)-1-CB₁₁H₁₀ (**57a**), μ-1,2-(CH₂)₂CH(MeC₅H₄N)CH₂-1-CB₁₁H₁₀ (**57b**) and [37][MeC₅H₄NH]. Some crystals were grown from a CH₂Cl₂ solution and structurally characterized as **57a**·CH₂Cl₂. **55**: ¹H NMR (400 MHz, DMSO-*d*₆): δ 8.87 (d, *J* = 5.7 Hz, 2H, C₄H₅N), 8.80 (d, *J* = 5.7 Hz, 2H, C₄H₅N), 7.69 (d, *J* = 5.4 Hz, 2H, C₄H₅N), 7.81 (d, *J* = 5.6 Hz, 2H, C₄H₅N), 2.52 (m, 1H, δ-CH₂), 2.47 (s, 6H, CH₃), 2.28 (m, 1H, δ-CH₂), 1.68 (m, 1H, γ-CH₂), 1.27 (m, 1H, γ-CH₂), 0.94 (m, 2H, β-CH₂), 0.47 (m, 1H, α-CH₂). ¹³C{¹H} NMR (100 MHz, DMSO-*d*₆): δ 156.3, 146.8, 145.4, 127.6, 126.7 (C₄H₅N), 72.7 (cage C), 34.8 (δ-CH₂), 27.2 (β-CH₂), 26.4 (γ-CH₂), 21.0 (CH₃), 14.8 (α-CH). ¹¹B NMR (128 MHz, DMSO-*d*₆): δ 2.7 (br, 1B), -10.2 (br, 8B), -15.9 (br, 2B). Anal. Calcd for C₁₇H₃₁B₁₁N₂ [M]: C, 53.40; H, 8.17; N, 7.33. Found: C, 53.29; H, 8.44; N, 7.22.

Reaction of 6 with *p*-^tBuC₅H₄N. Method A: To *p*-^tBuC₅H₄N (5 mL) was slowly added **6** (98 mg, 0.50 mmol) in batches at -30 °C. The dark blue solution was stirred at room temperature overnight and gradually turned to a clear brown solution. After removal of the solvent, the residue was washed with THF to give μ-2,4-(CH₂)₃CHBH(^tBuC₅H₄N)₂-2-CB₁₀H₉·THF (**56**·THF) as a white powder (70 mg, 0.13 mmol, 26%). X-ray-quality crystals were obtained by recrystallization from DMSO/MeOH as **56**. **Method B:** To a C₆D₆ (0.5 mL) solution of **19** (10 mg, 0.05 mmol) was slowly added *p*-^tBuC₅H₄N (0.1 mL) at room temperature to afford a mixture of **54**, μ-1,2-(CH₂)₃CH(^tBuC₅H₄N)-1-CB₁₁H₁₀ (**58a**), μ-1,2-(CH₂)₂CH(^tBuC₅H₄N)CH₂-1-CB₁₁H₁₀ (**58b**) and [37][^tBuC₅H₄NH]. **56**·THF: ¹H NMR (400 MHz, DMSO-*d*₆): δ 8.93 (d, *J* = 5.8 Hz, 2H, C₄H₅N), 8.87 (d, *J* = 5.8 Hz, 2H, C₄H₅N), 7.87 (d, *J* = 5.8 Hz, 2H, C₄H₅N), 7.81 (d, *J* = 5.8 Hz, 2H, C₄H₅N), 3.59 (br, 4H, THF), 2.52 (m, 1H, δ-CH₂), 2.28 (m, 1H, δ-CH₂), 1.75 (br, 2H, THF), 1.69 (m, 1H, γ-CH₂), 1.30 (s, 9H, CH₃), 1.28 (m, 10H, CH₃ + γ-CH₂), 0.94 (m, 2H, β-CH₂), 0.51 (m, 1H, α-CH₂). ¹³C{¹H} NMR (100 MHz, DMSO-*d*₆): δ 167.8, 167.6, 147.2, 145.8, 124.1, 123.1 (C₄H₅N), 72.7 (cage C), 67.0 (THF), 35.63, 35.59 (CCH₃), 34.8 (δ-CH₂), 29.64, 29.59 (CH₃), 27.2 (β-CH₂), 26.4 (γ-CH₂), 25.1 (THF), 15.1 (α-CH). ¹¹B NMR (128 MHz, DMSO-*d*₆): δ 3.2 (br, 1B), -10.2 (br, 8B), -15.9 (br, 2B). Anal. Calcd for C₂₃H₄₃B₁₁N₂ [M - THF]: C, 59.21; H, 9.29; N, 6.00. Found: C, 59.13; H, 9.26; N, 5.55.

Preparation of 4-(2,2'-C₁₀H₈N₂B)-μ-1,2-(CH₂)₃-1,2-C₂B₁₀H₉ (59**).** To a toluene (10 mL) solution of **6** (98 mg, 0.50 mmol) was added bipyridine (78 mg, 0.50 mmol) and the mixture was heated at 60 °C for 72 h in a sealed tube to give a red solution. After filtration, toluene was removed and 1 mL of CH₂Cl₂ was added to dissolve the red solid, to which a 50 of mL *n*-hexane was added. After filtration and removal of

the volatile materials, the residue was washed with a minimum amount of Et₂O to give gross **59** as a red solid (122 mg, 0.35 mmol, 70%). X-ray-quality crystals were obtained by recrystallization from Et₂O. ¹H NMR (400 MHz, CD₂Cl₂): δ 8.33 (d, *J* = 7.3 Hz, 2H, C₁₀H₈N₂B), 7.49 (dt, *J* = 9.1 Hz, 2H, C₁₀H₈N₂B), 6.43 (m, 2H, C₁₀H₈N₂B), 6.31 (m, 2H, C₁₀H₈N₂B), 2.53 (m, 2H, CH₂), 2.38 (m, 3H, CH₂), 2.20 (m, 1H, CH₂). ¹³C{¹H} NMR (100 MHz, CD₂Cl₂): δ 129.0, 120.4, 118.4, 115.1, 111.2 (aromatic C), 86.6 (cage C), 35.3, 35.1 (CCH₂), 32.6 (CCH₂CH₂). ¹¹B NMR (128 MHz, CD₂Cl₂): δ 19.7 (brs, 1B), -6.2 (br, 2B), -7.0 (br, 1B), -7.4 (br, 1B), -8.3 (br, 1B), -8.9 (br, 1B), -11.1 (br, 4B). HRMS (EI): *m/z* calcd for C₁₅H₂₃¹¹B₉¹⁰B₂N₂ [M]⁺: 350.2952; Found: 350.2960.

Preparation of 4-(2,2'-C₁₀H₈N₂B)-μ-1,2-(CH₂)₄-1,2-C₂B₁₀H₉ (60). To a toluene (10 mL) solution of **7** (105 mg, 0.50 mmol) was added bipyridine (78 mg, 0.50 mmol) and the mixture was heated at 90 °C for two weeks in a sealed tube to give a red solution. After filtration, toluene was removed and 1 mL of CH₂Cl₂ was added to dissolve the red solid, to which a 50 mL of *n*-hexane was added. After filtration and removal of the volatile materials, the residue was washed with a minimum amount of Et₂O to give gross **60** as a red solid (109 mg, 0.30 mmol, 60%). X-ray-quality crystals were obtained by recrystallization from toluene. ¹H NMR (400 MHz, CD₂Cl₂): δ 8.36 (d, *J* = 7.3 Hz, 2H, C₁₀H₈N₂B), 7.50 (dt, *J*₁ = 9.1 Hz, *J*₂ = 1.2 Hz, 2H, C₁₀H₈N₂B), 6.44 (ddd, *J*₁ = 9.1 Hz, *J*₂ = 6.1 Hz, *J*₃ = 0.8 Hz, 2H, C₁₀H₈N₂B), 6.31 (ddd, *J*₁ = 7.2 Hz, *J*₂ = 6.2 Hz, *J*₃ = 1.3 Hz, 2H, C₁₀H₈N₂B), 2.50 (m, 2H, CH₂), 2.30 (m, 1H, CH₂), 2.09 (m, 1H, CH₂), 1.55 (m, 2H, CH₂), 1.47 (m, 2H, CH₂). ¹³C{¹H} NMR (100 MHz, CD₂Cl₂): δ 129.0, 120.5, 118.4, 115.1, 111.3 (aromatic C), 75.6 (cage C), 33.7, 33.0 (CCH₂), 20.1, 19.9 (CCH₂CH₂). ¹¹B NMR (128 MHz, CD₂Cl₂): δ 20.0 (brs, 1B), -5.0 (d, *J*_{BH} = 143 Hz, 2B), -8.7 (br, 6B), -11.3 (br, 2B). HRMS (EI):

m/z calcd for $C_{16}H_{25}^{11}B_9^{10}B_2N_2 [M]^+$: 364.3108; Found: 364.3107.

Preparation of 4-(4',7'-2H-1',10'-C₁₀H₈N₂B)- μ -1,2-(CH₂)₃-1,2-C₂B₁₀H₉ (61).

To a toluene (10 mL) solution of **6** (98 mg, 0.50 mmol) was added phenanthroline (90 mg, 0.50 mmol) and the mixture was heated at 90 °C for two weeks in a sealed tube to give a red solution. After filtration, toluene was removed and 1 mL of CH₂Cl₂ was added to dissolve the red solid, to which a 30 mL of *n*-hexane was added. After filtration and removal of the volatile materials, the residue was washed with a minimum amount of Et₂O to give gross **61** as a brown solid (19 mg, 0.05 mmol, 10%). X-ray-quality crystals were obtained by recrystallization from toluene. ¹H NMR (400 MHz, CD₂Cl₂): δ 6.98 (dt, $J_1 = 8.2$ Hz, $J_2 = 1.9$ Hz, 2H, CH=CH-CH₂), 6.63 (s, 2H, CH), 4.97 (dt, $J_1 = 8.2$ Hz, $J_2 = 3.4$ Hz, 2H, CH=CH-CH₂), 3.60 (br, 4H, CH=CHCH₂), 2.51 (m, 3H, CH₂), 2.40 (m, 3H, CH₂). ¹³C{¹H} NMR (100 MHz, CD₂Cl₂): δ 132.3 (aromatic C), 126.5 (CH=CHCH₂), 121.3, 117.5 (aromatic C), 106.7 (CH=CHCH₂), 87.0, 86.4 (cage C), 35.20, 35.15, 32.7 (CH₂), 25.3 (CH=CHCH₂). ¹¹B NMR (128 MHz, CD₂Cl₂): δ 27.0 (brs, 1B), -5.9 (d, $J_{BH} = 129$ Hz, 2B), -7.0 (d, $J_{BH} = 145$ Hz, 2B), -8.0 (br, 1B), -8.8 (br, 1B), -10.0 (br, 1B), -10.9 (br, 3B). HRMS (EI): m/z calcd for $C_{17}H_{24}^{11}B_9^{10}B_2N_2 [M - H]^+$: 375.3030; Found: 375.3039.

Preparation of 4-(4',7'-2H-1',10'-C₁₀H₈N₂B)- μ -1,2-(CH₂)₄-1,2-C₂B₁₀H₉ (62).

To a toluene (10 mL) solution of **7** (105 mg, 0.50 mmol) was added phenanthroline (90 mg, 0.50 mmol) and the mixture was heated at 1100 °C for four weeks in a sealed tube to give a red solution. After filtration, toluene was removed and 1 mL of CH₂Cl₂ was added to dissolve the red solid, to which a 30 mL of *n*-hexane was added. After filtration and removal of the volatile materials, the residue was washed with a minimum amount of Et₂O to give gross **62** as a brown solid (16 mg, 0.04 mmol, 8%).

X-ray-quality crystals were obtained by recrystallization from CH_2Cl_2 . ^1H NMR (400 MHz, CD_2Cl_2): δ 7.02 (d, $J = 8.1$ Hz, 2H, $\text{CH}=\text{CH}-\text{CH}_2$), 6.63 (s, 2H, CH), 4.97 (dt, $J_1 = 8.0$ Hz, $J_2 = 3.2$ Hz, 2H, $\text{CH}=\text{CH}-\text{CH}_2$), 3.61 (br, 4H, $\text{CH}=\text{CHCH}_2$), 2.47 (m, 2H, CH_2), 2.37 (m, 1H, CH_2), 2.28 (m, 1H, CH_2), 1.55 (m, 4H, CH_2). $^{13}\text{C}\{^1\text{H}\}$ NMR (100 MHz, CD_2Cl_2): δ 132.3 (aromatic C), 126.5 ($\text{CH}=\text{CHCH}_2$), 121.3, 117.5 (aromatic C), 106.7 ($\text{CH}=\text{CHCH}_2$), 75.9, 75.5 (cage C), 33.6, 33.3 (CCH_2), 25.3 ($\text{CH}=\text{CHCH}_2$), 20.2, 19.9 (CCH_2CH_2). ^{11}B NMR (128 MHz, CD_2Cl_2): δ 26.7 (brs, 1B), -4.8 (d, $J_{\text{BH}} = 143$ Hz, 2B), -8.3 (br, 6B), -10.8 (br, 1B), -11.3 (br, 1B). HRMS (EI): m/z calcd for $\text{C}_{18}\text{H}_{26}^{11}\text{B}_9^{10}\text{B}_2\text{N}_2$ $[\text{M} - \text{H}]^+$: 389.3187; Found: 389.3193.

Chapter 6

Reaction of 7 with MeOH. A MeOH (10 mL) solution of 7 (210 mg, 1.00 mmol) was heated at 40 °C in a sealed tube for 14 days. PS (428 mg, 2.00 mmol) was then added and the mixture was stirred for 1 h at room temperature. After removal of the volatile materials, the residue was thoroughly washed with Et_2O to give a mixture of white solid. ^1H and ^{13}C NMR spectra indicated that it contained about 50% $[\mu-1,2-(\text{CH}_2)_3\text{CH}(\text{CH}_2\text{OMe})-1-\text{CB}_{11}\text{H}_{10}][\text{PSH}]$ (**[64]**[PSH]) and about 20% $[\mu-1,2-(\text{CH}_2)_5-1-\text{CB}_{11}\text{H}_{10}][\text{PSH}]$ (**[65]**[PSH]). Some crystals were grown from a CH_2Cl_2 solution and structurally characterized as **[65]**[PSH]. The Et_2O solution was concentrated. Column chromatographic separation (SiO_2 , 300-400 mesh, *n*-hexane) gave 7 as a white solid (20mg, 10%). **[64]**[PSH]: ^1H NMR (400 MHz, CD_2Cl_2): δ 8.04 (d, $J = 8.2$ Hz, 2H, C_{10}H_6), 7.95 (d, $J = 7.1$ Hz, 2H, C_{10}H_6), 7.76 (t, $J = 7.9$ Hz, 2H, C_{10}H_6), 3.62 (dd, $J_1 = 4.0$ Hz, $J_2 = 9.7$ Hz, 1H, OCH_2), 3.30 (m, 1H, OCH_2), 3.27 (s, 3H, OCH_3), 3.25 (d, $J = 2.0$ Hz, 12H, NCH_3), 1.90 (m, 1H, $\delta\text{-CH}_2$), 1.74 (m, 1H, $\delta\text{-CH}_2$), 1.69 (m, 1H, $\beta\text{-CH}_2$), 1.44 (m, 1H, $\alpha\text{-CH}$), 1.42 (m, 1H, $\gamma\text{-CH}_2$), 1.24 (m, 1H, $\gamma\text{-CH}_2$), 0.99 (m, 1H,

β -CH₂). ¹³C{¹H} NMR (100 MHz, CD₂Cl₂): δ 143.8, 135.6, 129.9, 127.5, 121.8, 118.8 (C₁₀H₆), 68.8 (cage C), 79.2 (OCH₂), 58.0 (OCH₃), 35.9 (δ -CH₂), 25.8 (β -CH₂), 24.5 (br, α -CH), 24.0 (γ -CH₂). HRMS (FAB): m/z calcd for C₇H₂₂¹¹B₉¹⁰B₂O [anion]⁻: 241.2765; Found: 241.2767. [65][PSH]: ¹H NMR (400 MHz, CD₂Cl₂): δ 8.04 (d, J = 8.2 Hz, 2H, C₁₀H₆), 7.95 (d, J = 7.1 Hz, 2H, C₁₀H₆), 7.76 (t, J = 7.9 Hz, 2H, C₁₀H₆), 3.25 (d, J = 2.0 Hz, 12H, NCH₃), 2.00 (m, 2H, ϵ -CH₂), 1.58 (m, 2H, β -CH₂), 1.46 (m, 2H, δ -CH₂), 1.39 (m, 2H, γ -CH₂), 1.04 (m, 2H, α -CH₂). ¹³C{¹H} NMR (100 MHz, CD₂Cl₂): δ 143.8, 135.6, 129.9, 127.5, 121.8, 118.8 (C₁₀H₆), 72.5 (cage C), 41.1 (ϵ -CH₂), 33.5 (γ -CH₂), 28.1 (δ -CH₂), 27.7 (β -CH₂), 19.3 (br, α -CH₂). HRMS (FAB): m/z calcd for C₆H₂₀¹¹B₉¹⁰B₂ [anion]⁻: 211.2659; Found: 211.2653.

Preparation of [μ -1,2-(CH₂)₄CH(SC₇H₇)-1-CB₁₁H₁₀][PPN] ([67][PPN]). To a THF (10 mL) solution of 7 (105 mg, 0.50 mmol) was added NaSC₇H₇ (73 mg, 0.50 mmol) and the mixture was stirred overnight. [PPN]Cl (287mg, 0.50 mmol) was then added and the mixture was further stirred for 6 h. After filtration, the colorless solution was concentrated to about 3 mL, to which a 5 mL of DME was added. *n*-Hexane layering afforded [67][PPN]·THF as colorless crystals after 60 days. The crystals were thoroughly washed with Et₂O and dried to give [67][PPN] as a pale yellow solid (350 mg, 0.40 mmol, 80%). ¹H NMR (400 MHz, CD₂Cl₂): δ 7.69 (m, 6H, PPN), 7.52 (m, 24H, PPN), 7.22 (d, J = 8.1 Hz, 2H, C₆H₄), 7.04 (d, J = 8.0 Hz, 2H, C₆H₄), 3.10 (d, J = 8.1 Hz, 1H, α -CH), 2.28 (s, 3H, CH₃), 2.15 (m, 1H, ϵ -CH₂), 2.04 (m, 1H, ϵ -CH₂), 1.90 (m, 1H, β -CH₂), 1.77 (m, 2H, β -CH₂ + γ -CH₂), 1.53 (m, 2H, δ -CH₂), 1.19 (m, 1H, γ -CH₂). ¹³C{¹H} NMR (100 MHz, CD₂Cl₂): δ 136.8, 134.8 (C₆H₄), 134.2, 132.6, 130.0 (PPN), 129.62, 129.60 (C₆H₄), 127.5 (PPN), 72.0 (cage C), 40.8 (ϵ -CH₂), 35.9 (br, α -CH), 33.0 (β -CH₂), 29.8 (γ -CH₂), 27.5 (δ -CH₂), 21.2 (CH₃). ¹¹B NMR (128 MHz, CD₂Cl₂): δ -6.6 (s, 1B), -9.9 (d, J_{BH} = 148 Hz, 1B), -11.8 (d, J_{BH} =

135 Hz, 5B), -15.2 (d, $J_{\text{BH}} = 131$ Hz, 4B). IR (KBr) ν_{max} (cm^{-1}): 2541, 2527 (vs, BH). Calcd for $\text{C}_{49}\text{H}_{56}\text{B}_{11}\text{NP}_2\text{S}$ [M]: C, 67.50; H, 6.47; N, 1.61. Found: C, 67.23; H, 6.55; N, 1.38.

Preparation of 3-NEt₂H- μ -1,7-(CH₂)₄-1,7-C₂B₁₁H₁₁ (68). To a toluene (10 mL) solution of **7** (420 μmol , 2.00 mmol) was added Et₂NH (2.0 mL, 1.414 mg, 19.4 mmol) and the solution was stirred at room temperature overnight. After removal of the volatile materials, the pale yellow residue was recrystallized from CH₂Cl₂/*n*-hexane to afford **68** as colorless crystals (500 mg, 1.76 mmol, 88%). ¹H NMR (400 MHz, CD₂Cl₂): δ (m, 4H, NCH₂), 2.24 (br, 2H, CCH₂), 2.11 (m, 2H, CCH₂), 1.63 (br, CCH₂CH₂), 1.38 (t, $J = 7.3$ Hz, 6H, CH₃). ¹³C{¹H} NMR (100 MHz, CD₂Cl₂): δ 46.1 (NCH₂), 38.2 (br, CCH₂), 22.1 (CCH₂CH₂), 10.6 (CH₃), the cage carbons were not observed. ¹¹B NMR (96 MHz, CD₂Cl₂): δ 4.1 (d, $J_{\text{BH}} = 73$ Hz, 2B), -5.7 (d, $J_{\text{BH}} = 140$ Hz, 2B), -16.9 (d, $J_{\text{BH}} = 142$ Hz, 4B), -24.8 (d, $J_{\text{BH}} = 142$ Hz, 2B), -33.0 (br, 1B). IR (KBr) ν_{max} (cm^{-1}): 2580 (vs, BH). Anal. Calcd for C₁₀H₃₀B₁₁N [M]: C, 42.40; H, 10.67; N, 4.94. Found: C, 42.70; H, 10.42; N, 5.01.

Preparation of [9-NMe₂- μ -7,8,10-(CH₂)₄CCH-B₁₁H₁₀][PPN] ([69][PPN]). To a toluene (10 mL) solution of **7** (105 mg, 0.50 mmol) was added LiNMe₂ (26 mg, 0.50 mmol) at -30 °C, then the solution was stirred at room temperature overnight. After addition of [PPN]Cl (287mg, 0.50 mmol), the suspension was further stirred for 6 h then filtered. After removal of the solvent, the solid residue was extracted with CH₂Cl₂ (10 mL). Recrystallization from CH₂Cl₂/*n*-Hexane gave [69][PPN] as pale yellow crystals (360 mg, 91%). ¹H NMR (400 MHz, CD₂Cl₂): δ 7.69 (m, 6H, PPN), 7.51 (m, 24H, PPN), 3.00 (s, 6H, NCH₃), 1.88 (m, 1H, β -CH₂), 1.81 (m, 3H, β -CH₂ + δ -CH₂ + ϵ -CH₂), 1.67 (m, 1H, δ -CH₂), 1.54 (m, 2H, γ -CH₂ + ϵ -CH₂), 1.45 (m, 1H, γ -CH₂), 1.26 (m, 1H, α -CH). ¹³C{¹H} NMR (100 MHz, CD₂Cl₂): δ 134.1, 132.4, 129.8,

127.3 (PPN), 63.5 (cage C), 51.8 (δ -CH₂), 43.5 (NCH₃), 40.5 (β -CH₂), 28.8 (ϵ -CH₂), 25.2 (γ -CH₂), 6.8 (α -CH). ¹¹B NMR (96 MHz, CD₂Cl₂): δ 48.8 (s, 1B), 25.5 (d, $J_{\text{BH}} = 103$ Hz, 1B), 9.6 (d, $J_{\text{BH}} = 131$ Hz, 1B), -6.8 (d, $J_{\text{BH}} = 117$ Hz, 1B), -8.6 (d, $J_{\text{BH}} = 146$ Hz, 1B), -11.1 (d, $J_{\text{BH}} = 137$ Hz, 1B), -18.5 (d, $J_{\text{BH}} = 131$ Hz, 1B), -20.3 (d, $J_{\text{BH}} = 136$ Hz, 1B), -23.0 (d, $J_{\text{BH}} = 134$ Hz, 2B), -32.6 (d, $J_{\text{BH}} = 138$ Hz, 1B). IR (KBr) ν_{max} (cm⁻¹): 2502 (vs, BH). Anal. Calcd for C₄₄H₅₅B₁₁N₂P₂ [M]: C, 66.66; H, 6.99; N, 3.53. Found: C, 66.69; H, 7.26; N, 3.15.

Preparation of [9-NEt₂- μ -7,8,10-(CH₂)₄CCH-B₁₁H₁₀][PPN] ([70][PPN]). To a CH₂Cl₂ (10 mL) solution of **68** (283 mg, 1.00 mmol) was added excess NaH (80 mg, 3.30 mmol) at room temperature, then the suspension was stirred for 2 h until no gas evolved. After addition of [PPN]Cl (287mg, 0.50 mmol), the suspension was further stirred for 6 h then filtered. After filtration, the solution was concentrated to about 10 mL and *n*-hexane layering gave **[70][PPN]** as pale yellow micro crystals (390 mg, 95%). ¹H NMR (400 MHz, CD₂Cl₂): δ 7.69 (m, 6H, PPN), 7.52 (m, 24H, PPN), 3.47 (m, 1H, NCH₂), 3.27 (m, 3H, NCH₂), 1.85 (m, 1H, β -CH₂), 1.80 (m, 3H, β -CH₂ + δ -CH₂ + ϵ -CH₂), 1.61 (m, 2H, γ -CH₂ + δ -CH₂), 1.50 (m, 1H, ϵ -CH₂), 1.47 (m, 1H, γ -CH₂), 1.32 (m, 1H, α -CH), 1.13 (m, 6H, CH₃). ¹³C{¹H} NMR (100 MHz, CD₂Cl₂): δ 134.1, 132.4, 129.8, 127.3 (PPN), 60.7 (cage C), 51.2 (δ -CH₂), 46.2, 46.1 (NCH₂), 40.1 (β -CH₂), 29.0 (ϵ -CH₂), 25.1 (γ -CH₂), 15.6, 15.3 (NCH₃), 8.5 (α -CH). ¹¹B NMR (96 MHz, CD₂Cl₂): δ 49.4 (s, 1B), 24.6 (d, $J_{\text{BH}} = 103$ Hz, 1B), 9.8 (d, $J_{\text{BH}} = 126$ Hz, 1B), -7.2 (d, $J_{\text{BH}} = 125$ Hz, 1B), -8.8 (d, $J_{\text{BH}} = 146$ Hz, 1B), -11.6 (d, $J_{\text{BH}} = 136$ Hz, 1B), -18.2 (d, $J_{\text{BH}} = 134$ Hz, 1B), -20.7 (d, $J_{\text{BH}} = 130$ Hz, 1B), -22.9 (d, $J_{\text{BH}} = 130$ Hz, 2B), -32.7 (d, $J_{\text{BH}} = 136$ Hz, 1B). IR (KBr) ν_{max} (cm⁻¹): 2502 (vs, BH). Anal. Calcd for C₄₆H₅₉B₁₁N₂P₂ [M]: C, 67.31; H, 7.24; N, 3.41. Found: C, 67.47; H, 7.31; N, 3.30.

Reaction of 17b with MeOH. Method A: Compound **17b** (184 mg, 1.00 mmol)

was dissolved in MeOH (10 mL), and the solution was stirred at room temperature for 1 d. After addition of [Me₃NH]Cl (191 mg, 2.00 mmol), the mixture was stirred for another 1 h. MeOH was pumped off and the residue was thoroughly washed with water to give a white solid. Recrystallization from acetone gave [1-Me-2-CH(OMe)Me-1-CB₁₁H₁₀][Me₃NH] (**[71a][Me₃NH]**) as colorless crystals (152 mg, 55%). **Method B:** Compound **17b** (184 mg, 1.00 mmol) was dissolved in MeOH (10 mL), and the solution was stirred at 70 °C for 1 d. After addition of [Me₃NH]Cl (191 mg, 2.00 mmol), the mixture was stirred for another 1 h. MeOH was pumped off and the residue was thoroughly washed with water to give a white solid as a mixture of **[71a][Me₃NH]** and [1-Me-2-CH₂=CH-1-CB₁₁H₁₀][Me₃NH] (**[72][Me₃NH]**). Some crystals were grown from the mother liquor which was structurally characterized as **[72][Me₃NH]**. **[71a][Me₃NH]**: ¹H NMR (400 MHz, acetone-*d*₆): δ 3.23 (s, 3H, OCH₃), 3.13 (s, 9H, NCH₃), 3.03 (m, 1H, CH), 1.51 (s, 3H, CCH₃), 1.28 (d, *J* = 6.7 Hz, 3H, CHCH₃). ¹³C{¹H} NMR (100 MHz, acetone-*d*₆): δ 72.2 (br, CH), 65.2 (cage C), 57.1 (OCH₃), 46.1 (NCH₃), 25.0 (CCH₃), 19.6 (CHCH₃). ¹¹B NMR (96 MHz, acetone-*d*₆): δ -5.1 (s, 1B), -9.2 (d, *J*_{BH} = 208 Hz, 1B), -11.4 (d, *J*_{BH} = 166 Hz, 6B), -13.6 (d, *J*_{BH} = 182 Hz, 2B). IR (KBr) *v*_{max} (cm⁻¹): 2530 (vs, BH). Anal. Calcd for C₈H₃₀B₁₁NO [M]: C, 34.91; H, 10.99; N, 5.09. Found: C, 34.63; H, 10.52; N, 4.65. **[72][Me₃NH]**: ¹H NMR (400 MHz, acetone-*d*₆): δ 6.04 (dd, *J*₁ = 13.1 Hz, *J*₂ = 19.2 Hz, 1H, CH=CH₂), 5.47 (d, *J* = 19.4 Hz, 1H, CH=CH₂), 5.38 (br, 1H, CH=CH₂), 3.14 (s, 9H, NCH₃), 1.43 (CCH₃). ¹³C{¹H} NMR (100 MHz, acetone-*d*₆): δ 141.4 (br, CH), 125.2 (CH₂), 65.1 (cage C), 46.0 (NCH₃), 25.1 (CCH₃).

Reaction of 17b with MeOH in the presence of PS. **17b** (18.4 mg, 0.10 mmol) was dissolved in a CD₃OD solution (0.5 mL) of PS (86 mg, 0.40 mmol) in an sealed NMR tube. After 1 d, 1-Me-2-D-C₂B₁₀H₁₀ (**2-D-73**) was observed. After removal of

MeOH, the residue was subjected to column chromatographic separation (SiO₂, 300-400 mesh, *n*-hexane) and **2-D-73** was isolated as a white solid (8 mg, 50%) with 75% D incorporation. ¹H NMR (400 MHz, CDCl₃): δ 3.56 (s, 0.26H, residual CH), 2.03 (s, 3H, CH₃). ¹³C{¹H} NMR (100 MHz, CDCl₃): δ 70.4 (cage CCH₃), 61.7 (residual cage CH), 61.4 (t, *J*_{CD} ≈ 30 Hz), 26.0 (CH₃). ¹¹B NMR (128 MHz, CDCl₃): δ -1.9 (d, *J*_{BH} = 152 Hz, 1B), -6.8 (d, *J*_{BH} = 155 Hz, 1B), -9.3 (d, *J*_{BH} = 166 Hz, 2B), -10.7 (d, *J*_{BH} = 170 Hz, 2B), -11.4 (d, *J*_{BH} = 178 Hz, 2B), -12.8 (d, *J*_{BH} = 167 Hz, 2B).

Reaction of 17b with (4-Me-C₆H₄)SNa. To a THF (10 mL) solution of **17b** (92 mg, 0.50 mol) was added (4-Me-C₆H₄)SNa (73 mg, 0.50 mol), and the solution was stirred at room temperature overnight. After addition of PPNCl (287mg, 0.50 mmol), the suspension was further stirred for 6 h. After filtration, the solution was concentrated to about 10 mL, and *n*-hexane layering gave a mixture of [1-Me-2-HBMeS(4-Me-C₆H₄)-1,2-C₂B₁₀H₁₀]⁻ (**[75]**) and 1-Me-2-HBMe-1,2-C₂B₁₀H₁₀ (**76**). Repeated recrystallization of this mixture in refluxing MeOH gave [7-Me-7,8-C₂B₉H₁₁][PPN] (**[74]**[PPN]) as colorless crystals (90 mg, 26%). **[75]**: ¹H NMR (400 MHz, CD₂Cl₂): δ 7.26 (d, *J* = 8.1 Hz, 2H, SC₆H₄), 6.84 (d, *J* = 8.0 Hz, 2H, SC₆H₄), 2.19 (s, 3H, C₆H₄CH₃), 2.00 (s, 3H, CCH₃), -0.04 (d, *J* = 5.6 Hz, 3H, BCH₃). ¹³C{¹H} NMR (100 MHz, CD₂Cl₂): δ 142.6, 130.8, 128.4 (C₆H₄), 90.8 (br, cage CBHCH₃), 76.5 (cage CCH₃), 24.5 (CCH₃), 20.9 (C₆H₄CH₃), 8.9 (br, BHCH₃). **76**: ¹H NMR (400 MHz, CD₂Cl₂): δ 1.98 (s, 3H, CCH₃), 0.05 (d, *J* = 5.3 Hz, 3H, BCH₃). ¹³C{¹H} NMR (100 MHz, CD₂Cl₂): δ 89.4 (br, cage CBHCH₃), 76.2 (cage CCH₃), 24.4 (CCH₃), 11.3 (br, BHCH₃). ¹¹B NMR (128 MHz, CD₂Cl₂): δ -4.6 (s+d, 2B), -6.4 (d, *J*_{BH} = 148 Hz, 1B), -9.3 (d, 2B), -9.9 (d, 2B), -10.7 (d, 3B), -12.6 (m, 1B). **[74]**[PPN]: ¹H NMR (400 MHz, acetone-*d*₆): δ 7.72 (m, 18H, PPN), 7.57 (m, 12H, PPN), 1.56 (s, 1H, CH), 1.33 (s, 3H, CH₃). ¹³C{¹H} NMR (100 MHz, acetone-*d*₆): δ 134.5, 133.1, 130.3,

128.1 (PPN), 54.1 (br, cage CCH₃), 49.0 (cage CH), 25.8 (CCH₃). ¹¹B NMR (128 MHz, acetone-*d*₆): δ -9.4 (d, *J*_{BH} = 123 Hz, 1B), -10.3 (d, *J*_{BH} = 127 Hz, 1B), -12.7 (d, *J*_{BH} = 158 Hz, 1B), -16.6 (d, *J*_{BH} = 120 Hz, 1B), -17.5 (d, *J*_{BH} ≈ 114 Hz, 1B), -18.0 (d, *J*_{BH} ≈ 149 Hz, 1B), -21.7 (d, *J*_{BH} = 147 Hz, 1B), -32.8 (d, *J*_{BH} ≈ 118 Hz, 1B), -36.0 (d, *J*_{BH} = 141 Hz, 1B). Anal. Calcd for C₃₉H₄₄B₉NP₂ [M]: C, 68.28; H, 6.46; N, 2.04. Found: C, 68.36; H, 6.28; N, 1.81.

Preparation of [1-Me-7-Et-1-CB₁₁H₁₀][Na(18-crown-6)(H₂O)] ([77][Na(18-crown-6)(H₂O)]). To a THF solution (10 mL) of **17b** (92 mg, 0.50 mol) was added NaBH₄ (80 mg, 2.11 mol), and the suspension was stirred at room temperature overnight. After filtration, 18-crown-6 (132 mg, 0.50 mmol) was added and solvent was removed in vacuum. The residue was washed with water and Et₂O. Recrystallization from acetone gave [77][Na(18-crown-6)(H₂O)] as colorless crystals. ¹H NMR (400 MHz, acetone-*d*₆): δ 3.63 (s, 24H, OCH₂), 1.47 (s, 3H, CCH₃), 0.85 (br, 3H, CH₂CH₃), 0.64 (br, 2H, CH₂CH₃). ¹³C{¹H} NMR (100 MHz, acetone-*d*₆): δ 70.1 (OCH₂), 63.8 (cage C), 27.9 (CCH₃), 15.1 (CH₂CH₃), 11.0 (br, CH₂CH₃). ¹¹B NMR (128 MHz, acetone-*d*₆): δ -1.0 (s, 1B), -9.5 (d, *J*_{BH} = 141 Hz, 1B), -11.7 (d, *J*_{BH} = 137 Hz, 4B), -12.7 (d, *J*_{BH} = 141 Hz, 4B), -15.5 (d, *J*_{BH} = 151 Hz, 1B). IR (KBr) ν_{max} (cm⁻¹): 2519 (vs, BH). Anal. Calcd for C₁₆H₄₄B₁₁NaO₇ [M]: C, 39.18; H, 9.04. Found: C, 39.36; H, 8.99.

Preparation of [C,C',N,N-Me₄-NC₂B₁₁H₁₁][PPN] ([78][PPN]). To a THF solution (10 mL) of **17b** (184 mg, 1.00 mol) was added LiNMe₂ (51 mg, 1.00 mmol) and the solution was stirred at room temperature overnight. The ¹¹B NMR spectrum indicated [78]⁻ was in about 50%. After addition of [PPN]Cl (574 mg, 0.50 mmol), the suspension was further stirred for 6 h. After filtration, THF was removed from the solution in vacuum, and the residue was extracted with CH₂Cl₂. Repeated recrystalli-

zation from THF/*n*-hexane gave **[78][PPN]** as colorless crystals (40 mg, 5%). ^1H NMR (400 MHz, CD_2Cl_2): δ 7.67 (m, 6H, PPN), 7.49 (m, 24H, PPN), 2.78 (s, 6H, NCH_3), 1.52 (s, 6H, CCH_3). $^{13}\text{C}\{^1\text{H}\}$ NMR (100 MHz, CD_2Cl_2): δ 134.1, 132.5, 139.8, 127.5 (PPN), 45.8 (NCH_3), 36.8 (CCH_3), 26.4 (cage C). ^{11}B NMR (96 MHz, CD_2Cl_2): δ 48.9 (d, $J_{\text{BH}} \approx 101$ Hz, 1B), -2.8 (d, $J_{\text{BH}} = 138$ Hz, 4B), -5.8 (d, $J_{\text{BH}} = 147$ Hz, 1B), -10.1 (d, $J_{\text{BH}} = 117$ Hz, 1B), -16.9 (d, $J_{\text{BH}} = 123$ Hz, 3B), -30.9 (d, $J_{\text{BH}} = 132$ Hz, 1B). Anal. Calcd for $\text{C}_{42}\text{H}_{53}\text{B}_{11}\text{N}_2\text{P}_2$ [M]: C, 65.79; H, 6.97; N, 3.65. Found: C, 65.72; H, 7.02; N, 3.41.

Preparation of 8-BH₃PPh₂-1,2-Me₂-1,2-C₂B₁₀H₉ (79). To a THF solution (10 mL) of Ph_2PH (93 mg, 0.50 mmol) was added finely cut K metal (40 mg, 1.00 mmol) and the solution was stirred at room temperature overnight. After filtration, the filtrate was slowly added to a THF solution (10 mL) of **17b** (92 mg, 0.50 mol), and the solution was further stirred for one day. After removal of THF, the residue was extracted with Et_2O . Repeated recrystallization from $\text{Et}_2\text{O}/n$ -hexane gave **79** as colorless crystals (20 mg, 11%). ^1H NMR (400 MHz, CD_2Cl_2): δ 7.79 (m, 4H, C_6H_5), 7.43 (m, 6H, C_6H_5), 2.02 (s, 6H, CH_3). $^{13}\text{C}\{^1\text{H}\}$ NMR (100 MHz, CD_2Cl_2): δ 133.9 (d, $J_{\text{PC}} = 8.5$ Hz), 130.60 (d, $J_{\text{PC}} = 2.1$ Hz), 130.55 (d, $J_{\text{PC}} = 52$ Hz), 128.6 (d, $J_{\text{PC}} = 9.9$ Hz) (C_6H_5), 75.6 (cage C), 23.6 (CH_3). ^{11}B NMR (128 MHz, CD_2Cl_2): δ -4.9 (2B), -6.4 (1B), -7.4 (1B), -8.1 (1B), -9.2 (5B), -36.2 (dt, $J_{\text{BH}} \approx 94\text{Hz}$, $J_{\text{BH}} \approx 50$ Hz, 1B). ^{31}P NMR (162 MHz, CD_2Cl_2): δ -23.1 (br). HRMS (ESI): m/z calcd for $\text{C}_6\text{H}_{28}^{11}\text{B}_9^{10}\text{B}_2\text{PNa}$ [M + Na] $^+$: 393.2917; Found: 393.2916.

Reaction of 27a with MeOH. A MeOH solution (5 mL) of **27a** (78 mg, 0.38 mmol) in a closed Schlenk flask was heated to reflux at 70 °C for 48 h. After addition of $[\text{Me}_3\text{NH}]\text{Cl}$ (72 mg, 0.75 mmol), the mixture was stirred for another 1 h at room temperature. Removal of the volatile materials and washing with water gave a mix-

ture of [36a][Me₃NH] and [36b][Me₃NH].

Preparation of [μ -8,9-(CH₂)₃- μ -11,12-BH(OMe)-8,9-C₂B₁₁H₁₁][Me₃NH] ([80][Me₃NH]). To a MeOH solution (5 mL) of **27a** (54 mg, 0.26 mmol) was added an aqueous solution of Me₃N (45%, 0.5 mL, 7.00 mmol), and the reaction mixture was stirred at room temperature for 1 min. After removal of solvents under vacuum, the solid residue was thoroughly washed with *n*-hexane and Et₂O to give [80][Me₃NH] as a white solid (75 mg, 96%). Recrystallization from a CH₂Cl₂ solution afforded colorless crystals. ¹H NMR (400 MHz, CD₂Cl₂): δ 3.35 (s, 3H, OCH₃), 2.97 (s, 9H, NCH₃), 2.58 (m, 2H, CCH₂), 1.95 (m, 2H, CCH₂), 1.88 (m, 1H, CCH₂CH₂), 1.60 (m, 1H, CCH₂CH₂). ¹³C{¹H} NMR (100 MHz, CD₂Cl₂): δ 86.0 (cage C), 60.1 (OCH₃), 46.7 (NCH₃), 41.0 (CCH₂), 24.9 (CCH₂CH₂). ¹¹B NMR (96 MHz, CD₂Cl₂): δ 22.2 (d, *J*_{BH} = 127 Hz, 1B), 9.8 (d, *J*_{BH} = 150 Hz, 2B), 4.5 (d, *J*_{BH} = 134 Hz, 1B), -1.3 (d, *J*_{BH} = 137 Hz, 2B), -4.1 (d, *J*_{BH} = 149 Hz, 2B), -8.5 (d, *J*_{BH} = 121 Hz, 3B), -28.3 (d, *J*_{BH} = 138 Hz, 1B). IR (KBr) ν_{\max} (cm⁻¹): 2507 (vs, BH). Anal. Calcd for C₉H₃₁B₁₂NO [M]: C, 36.14; H, 10.45; N, 4.68. Found: C, 36.41; H, 10.53; N, 4.77.

Preparation of [μ -8,9-(CH₂)₃-8,9-C₂B₁₁H₁₁][(Me₃NH)₂Cl] ([80][(Me₃NH)₂Cl]). To a THF solution (5 mL) of **27a** (50 mg, 0.24 mmol) was added CsF (185 mg, 1.22 mmol), and the mixture was stirred at room temperature for 7 d. After addition of [Me₃NH]Cl (120 mg, 1.25 mmol), the mixture was stirred for another 1 h at room temperature. Removal of the precipitate and the solvent gave a white solid that was recrystallized from acetone to afford [80][(Me₃NH)₂Cl] as colorless crystals (51 mg, 60%). ¹H NMR (400 MHz, acetone-*d*₆): δ 3.02 (s, 18H, CH₃), 2.34 (m, 2H, CCH₂), 2.07 (m, 2H, CCH₂), 1.69 (m, 1H, CCH₂CH₂), 1.48 (m, 1H, CCH₂CH₂). ¹³C{¹H} NMR (100 MHz, acetone-*d*₆): δ 82.3 (cage C), 45.2 (CH₃), 40.2 (CCH₂), 26.4

(CCH₂CH₂). ¹¹B NMR (96 MHz, acetone-*d*₆): δ 0.5 (d, *J*_{BH} = 133 Hz, 2B), -1.1 (d, *J*_{BH} = 158 Hz, 3B), -8.2 (d, *J*_{BH} = 150 Hz, 2B), -11.5 (d, *J*_{BH} = 139 Hz, 2B), -15.1 (d, *J*_{BH} = 126 Hz, 1B), -33.3 (d, *J*_{BH} = 127 Hz, 1B). IR (KBr) *v*_{max} (cm⁻¹): 2517 (vs, BH). Anal. Calcd for C₁₁H₃₈B₁₁ClN₂ [M]: C, 37.45; H, 10.86; N, 7.94. Found: C, 37.59; H, 10.32; N, 7.50.

X-ray Structure Determination. All single crystals were immersed in Paraton-N oil and sealed under N₂ in thin-walled glass capillaries. Data were collected on a Bruker SMART 1000 CCD diffractometer or a Bruker AXS kappa Apex II Duo diffractometer using Mo-K α or Cu-K α radiation. An empirical absorption correction was applied using the SADABS program.¹³⁶ All structures were solved by direct methods and subsequent Fourier difference techniques and refined anisotropically for all non-hydrogen atoms by full-matrix least squares calculations on *F*² using the SHELXTL program package.¹³⁷ For noncentrosymmetric structures, the appropriate enantiomorph was chosen by refining Flack's parameter *x* toward zero.¹³⁸ All hydrogen atoms were geometrically fixed using the riding model. Crystal data and details of data collection and structure refinements are given in Appendix II. CIF files are given in Appendix III in electronic format.

References

- (1) (a) Williams, R. E. *Inorg. Chem.* **1971**, *10*, 210-214. (b) Wade, K. *J. Chem. Soc. D: Chem. Commun.* **1971**, 792-793. (c) Rudolph, R. W.; Pretzer, W. R. *Inorg. Chem.* **1972**, *11*, 1974-1978. (d) Wade, K. *Adv. Inorg. Chem. Radiochem.* **1976**, *18*, 1-66. (e) Williams, R. E. *Adv. Inorg. Chem. Radiochem.* **1976**, *18*, 67-142. (f) Rudolph, R. W. *Acc. Chem. Res.* **1976**, *9*, 446-452. (g) O'Neill, M. E.; Wade, K. In *Comprehensive Organometallic Chemistry*; Wilkinson, G., Stone, F. G. A., Abel, E. W., Eds.; Pergamon: Oxford, 1982; Vol. 1, pp 1-42. (h) Williams, R. E. *Chem. Rev.* **1992**, *92*, 177-207.
- (2) (a) Grimes, R. N. *Carboranes*; Academic Press: New York, 1970. (b) Onak, T. In *Comprehensive Organometallic Chemistry*; Wilkinson, G., Stone, F. G. A., Abel, E. W., Eds.; Pergamon: Oxford, 1982; Vol. 1, pp 411-457. (c) Onak, T. In *Comprehensive Organometallic Chemistry II*; Abel, E. W., Stone, F. G. A., Wilkinson, G., Eds.; Elsevier: Oxford, 1995; Vol. 1, pp 217-255. (d) Davidson, M.; Hughes, A. K.; Marder, T. B.; Wade, K. *Contemporary Boron Chemistry*; RSC: Cambridge, UK, 2000. (e) Bubnov, Yu. N. *Boron Chemistry at the Beginning of the 21st Century*; Russian Academy of Sciences: Moscow, Russia, 2003. (f) Fox, M. A. In *Comprehensive Organometallic Chemistry III*; Crabtree, R. H., Mingos, D. M. P., Eds.; Elsevier: Oxford, 2007; Vol. 3, pp 49-112.
- (3) (a) Zakharkin, L. I. *Pure Appl. Chem.* **1972**, *29*, 513-526. (b) Dunks, G. B.; Hawthorne, M. F. *Acc. Chem. Res.* **1973**, *6*, 124-131. (c) Bregadze, V. I. *Chem. Rev.* **1992**, *92*, 209-223. (d) Štíbr, B. *Chem. Rev.* **1992**, *92*, 225-250. (e) Kalinin, V. N.; Ol'shevskaya, V. A. *Russ. Chem. Bull.* **2008**, *57*, 815-836.
- (4) (a) Heying, T. L.; Ager, J. W., Jr.; Clark, S. L.; Mangold, D. J.; Goldstein, H.

- L.; Hillman, M.; Polak, R. J.; Szymanski, J. W. *Inorg. Chem.* **1963**, *2*, 1089-1092. (b) Fein, M. M.; Bobinski, J.; Mayes, N.; Schwartz, N.; Cohen, M. S. *Inorg. Chem.* **1963**, *2*, 1111-1115. (c) Fein, M. M.; Grafstein, D.; Paustian, J. E.; Bobinski, J.; Lichstein, B. M.; Mayes, N.; Schwartz, N. N.; Cohen, M. S. *Inorg. Chem.* **1963**, *2*, 1115-1119. (d) Jiang, W.; Knobler, C. B.; Hawthorne, M. F. *Inorg. Chem.* **1996**, *35*, 3056-3058. (e) Causey, P. W.; Besanger, T. R.; Valliant, J. F. *J. Med. Chem.* **2008**, *51*, 2833-2844.
- (5) (a) Kusari, U.; Li, Y.; Bradley, M. G.; Sneddon, L. G. *J. Am. Chem. Soc.* **2004**, *126*, 8662-8663. (b) Li, Y.; Carroll, P. J.; Sneddon, L. G. *Inorg. Chem.* **2008**, *47*, 9193-9202.
- (6) Grafstein, D.; Dvorak, J. *Inorg. Chem.* **1963**, *2*, 1128-1133.
- (7) Papetti, S.; Heying, T. L. *J. Am. Chem. Soc.* **1964**, *86*, 2295.
- (8) (a) Hoffmann, R.; Lipscomb, W. N. *Inorg. Chem.* **1963**, *2*, 231-232. (b) Lipscomb, W. N. *Science* **1966**, *153*, 373-378.
- (9) Zakharkin, L. I.; Kalinin, V. N. *Dokl. Akad. Nauk SSSR* **1966**, *169*, 590-593.
- (10) (a) Muetterties, E. L.; Knoth, W. H. *Polyhedral Boranes*; Marcel Dekker: New York, 1968. (b) Muetterties, E. L. *J. Am. Chem. Soc.* **1969**, *91*, 1636-1643.
- (11) (a) Kaesz, H. D.; Bau, R.; Beall, H. A.; Lipscomb, W. N. *J. Am. Chem. Soc.* **1967**, *89*, 4218-4220. (b) Hart, H. V.; Lipscomb, W. N. *J. Am. Chem. Soc.* **1969**, *91*, 771-772. (c) Hart, H. V.; Lipscomb, W. N. *Inorg. Chem.* **1973**, *12*, 2644-2649.
- (12) (a) Wong, H. S.; Lipscomb, W. N. *Inorg. Chem.* **1975**, *14*, 1350-1357. (b) Edverson, G. M.; Gaines, D. F. *Inorg. Chem.* **1990**, *29*, 1210-1216.
- (13) (a) Wu, S.-H.; Jones, M., Jr. *J. Am. Chem. Soc.* **1989**, *111*, 5373-5384. (b)

- Gimarc, B. M.; Warren, D. S.; Ott, J. J.; Brown, C. *Inorg. Chem.* **1991**, *30*, 1598-1605.
- (14) Brown, C. A.; McKee, M. L. *J. Mol. Model.* **2006**, *12*, 653-664.
- (15) Hawthorne, M. F.; Wegner, P. A. *J. Am. Chem. Soc.* **1965**, *87*, 4392-4393.
- (16) (a) Mikhailov, B. M.; Potapova, T. V. *Izv. Akad. Nauk SSSR, Ser. Khim.* **1967**, 1629. (b) Potapova, T. V.; Mikhailov, B. M. *Izv. Akad. Nauk SSSR, Ser. Khim.* **1967**, 2367. (c) Hawthorne, M. F.; Wegner, P. A. *J. Am. Chem. Soc.* **1968**, *90*, 896-901. (d) Roscoe, J. S.; Kongpricha, S.; Papetti, S. *Inorg. Chem.* **1970**, *9*, 1561-1563. (e) Li, J.; Jones, M., Jr. *Inorg. Chem.* **1990**, *29*, 4162-4163. (f) Li, J.; Logan, C. F.; Jones, M., Jr. *Inorg. Chem.* **1991**, *30*, 4866-4868. (g) Colella, S. M.; Li, J.; Jones, M., Jr. *Organometallics* **1992**, *11*, 4346-4347. (h) Chen, W.; Rockwell, J. J.; Knobler, C. B.; Harwell, D. E.; Hawthorne, M. F. *Polyhedron* **1999**, *18*, 1725-1734. (i) Viñas, C.; Barberà, G.; Oliva, J. M.; Teixidor, F.; Welch, A. J.; Rosair, G. M. *Inorg. Chem.* **2001**, *40*, 6555-6562. (j) Robertson, S.; Ellis, D.; McGrath, T. D.; Rosair, G. M.; Welch, A. J. *Polyhedron* **2003**, *22*, 1293-1301. (k) Yamazaki, H.; Ohta, K.; Endo, Y. *Tetrahedron Lett.* **2005**, *46*, 3119-3122. (l) Ramachandran, B. M.; Knobler, C. B.; Hawthorne, M. F. *Inorg. Chem.* **2006**, *45*, 336-340.
- (17) (a) Heying, T. L.; Ager, J. W., Jr.; Clark, S. L.; Alexander, R. P.; Papetti, S.; Reid, J. A.; Trotz, S. I. *Inorg. Chem.* **1963**, *2*, 1097-1105. (b) Grafstein, D.; Bobinski, J.; Dvorak, J.; Smith, H.; Schwartz, N.; Cohen, M. S.; Fein, M. M. *Inorg. Chem.* **1963**, *2*, 1120-1125. (c) Zakharkin, L. I.; Stanko, V. I.; Klimova, A. I.; Chapovskii, Yu. A. *Izv. Akad. Nauk SSSR, Ser. Khim.* **1963**, 2236-2237.
- (18) Zakharkin, L. I.; Grebennikov, A. V.; Kazantsev, A. V. *Izv. Akad. Nauk SSSR, Ser. Khim.* **1967**, 2077-2078.

- (19) Viñas, C.; Benakki, R.; Teixidor, F.; Casabó, J. *Inorg. Chem.* **1995**, *34*, 3844-3845.
- (20) (a) Gomez, F. A.; Johnson, S. E.; Hawthorne, M. F. *J. Am. Chem. Soc.* **1991**, *113*, 5915-5917. (b) Gomez, F. A.; Hawthorne, M. F. *J. Org. Chem.* **1992**, *57*, 1384-1390.
- (21) (a) Gingrich, H. L.; Ghosh, T.; Huang, Q.; Jones, M., Jr. *J. Am. Chem. Soc.* **1990**, *112*, 4082-4083. (b) Huang, Q.; Gingrich, H. L.; Jones, M., Jr. *Inorg. Chem.* **1991**, *30*, 3254-3257. (c) Cunningham, R. J.; Bian, N.; Jones, M., Jr. *Inorg. Chem.* **1994**, *33*, 4811-4812. (d) Atkins, J. H.; Ho, D. M.; Jones, M., Jr. *Tetrahedron Lett.* **1996**, *37*, 7217-7220. (e) Barnett-Thamattoor, L.; Zheng, G.-X.; Ho, D. M.; Jones, M., Jr.; Jackson, J. E. *Inorg. Chem.* **1996**, *35*, 7311-7315. (f) Jeon, J.; Kitamura, T.; Yoo, B.-W.; Kang, S. O.; Ko, J. *Chem. Commun.* **2001**, 2110-2111. (g) Lee, T.; Jeon, J.; Song, K. H.; Jung, I.; Baik, C.; Park, K.-M.; Lee, S. S.; Kang, S. O.; Ko, J. *Dalton Trans.* **2004**, 933-937. (h) Wang, S. R.; Qiu, Z.; Xie, Z. *J. Am. Chem. Soc.* **2010**, *132*, 9988-9989.
- (22) (a) Deng, L.; Chan, H.-S.; Xie, Z. *J. Am. Chem. Soc.* **2006**, *128*, 7728-7729. (b) Qiu, Z.; Xie, Z. *Angew. Chem. Int. Ed.* **2008**, *47*, 6572-6575. (c) Qiu, Z.; Xie, Z. *J. Am. Chem. Soc.* **2009**, *131*, 2084-2085. (d) Qiu, Z.; Wang, S. R.; Xie, Z. *Angew. Chem. Int. Ed.* **2010**, *49*, 4649-4652.
- (23) Ren, S.; Chan, H.-S.; Xie, Z. *J. Am. Chem. Soc.* **2009**, *131*, 3862-3863.
- (24) (a) Zakharkin, L. I.; Kalinin, V. N. *Izv. Akad. Nauk SSSR, Ser. Khim.* **1965**, 1311. (b) Zakharkin, L. I.; Kalinin, V. N. *Dokl. Akad. Nauk SSSR* **1966**, *170*, 92-95. (c) Zakharkin, L. I.; Kalinin, V. N. *Izv. Akad. Nauk SSSR, Ser. Khim.* **1966**, 575-577. (d) Potenza, J. A.; Lipscomb, W. N.; Vickers, G. D.; Schroeder, H. *J. Am. Chem. Soc.* **1966**, *88*, 628-629. (e) Stanko, V. I.;

- Struchkov, Yu. T.; Klimova, A. I.; Bryukhova, L. V.; Semin, G. K. *Zh. Obshch. Khim.* **1966**, *36*, 1707. (f) Stanko, V. I.; Klimova, A. I. *Zh. Obshch. Khim.* **1968**, *38*, 1194. (g) Stanko, V. I.; Brattsev, V. A.; Vostrikova, T. N.; Danilova, G. N. *Zh. Obshch. Khim.* **1968**, *38*, 1348-1352. (h) Zakharkin, L. I.; Kalinin, V. N.; Lozovskaya, V. S. *Izv. Akad. Nauk SSSR, Ser. Khim.* **1968**, 1780-1786. (i) Merkushev, E. B.; Simakhina, N. D.; Grigor'ev, M. G. *Izv. Akad. Nauk SSSR, Ser. Khim.* **1980**, 2649. (j) Andrews, J. S.; Zayas, J.; Jones, M., Jr. *Inorg. Chem.* **1985**, *24*, 3715-3716. (k) Lebedev, V. N.; Zakharkin, L. I. *Izv. Akad. Nauk SSSR, Ser. Khim.* **1986**, 253-254. (l) Zakharkin, L. I.; Ol'shevskaya, V. A.; Poroshina, T. Y.; Balagurova, E. V. *Zh. Obshch. Khim.* **1987**, *57*, 2012-2016. (m) Lebedev, V. N.; Balagurova, E. V.; Polyakov, A. V.; Yanovskii, A. I.; Struchkov, Yu. T.; Zakharkin, L. I. *J. Organomet. Chem.* **1990**, *385*, 307-318. (n) Zheng, Z.; Jiang, W.; Zinn, A. A.; Knobler, C. B.; Hawthorne, M. F. *Inorg. Chem.* **1995**, *34*, 2095-2100.
- (25) (a) Zakharkin, L. I.; Kovredov, A. I.; Ol'shevskaya, V. A.; Shaugumbekova, Z. S. *Izv. Akad. Nauk SSSR, Ser. Khim.* **1980**, 1691. (b) Zakharkin, L. I.; Kovredov, A. I.; Ol'shevskaya, V. A. *Izv. Akad. Nauk SSSR, Ser. Khim.* **1981**, 2159-2161. (c) Zakharkin, L. I.; Kovredov, A. I.; Savel'eva, I. S.; Safronova, E. V. *Zh. Obshch. Khim.* **1981**, *51*, 2383. (d) Zakharkin, L. I.; Kovredov, A. I.; Ol'shevskaya, V. A. *Zh. Obshch. Khim.* **1981**, *51*, 2807-2808. (e) Zakharkin, L. I.; Kovredov, A. I.; Ol'shevskaya, V. A.; Shaugumbekova, Z. S. *J. Organomet. Chem.* **1982**, *226*, 217-222. (f) Zakharkin, L. I.; Kovredov, A. I.; Ol'shevskaya, V. A.; Antonovich, V. A. *J. Organomet. Chem.* **1984**, *267*, 81-91. (g) Zakharkin, L. I.; Kovredov, A. I.; Ol'shevskaya, V. A. *Izv. Akad. Nauk SSSR, Ser. Khim.* **1985**, 888-892. (h) Kovredov, A. I.; Shaugumbekova, Z. S.;

- Petrovskii, P. V.; Zakharkin, L. I. *Zh. Obshch. Khim.* **1989**, *59*, 607-611. (i) Gal'chenko, G. L.; Tamm, N. B.; Pavlovich, V. K.; Ol'shevskaya, V. A.; Zakharkin, L. I. *Metalloorg. Khim.* **1990**, *3*, 259-263. (j) Gal'chenko, G. L.; Tamm, N. B.; Pavlovich, V. K.; Ol'shevskaya, V. A.; Zakharkin, L. I. *Metalloorg. Khim.* **1990**, *3*, 414-218. (k) Jiang, W.; Knobler, C. B.; Curtis, C. E.; Mortimer, M. D.; Hawthorne, M. F. *Inorg. Chem.* **1995**, *34*, 3491-3498. (l) Harakas, G.; Vu, T.; Knobler, C. B.; Hawthorne, M. F. *J. Am. Chem. Soc.* **1998**, *120*, 6405-6406. (m) Zakharkin, L. I.; Ol'shevskaya, V. A.; Balagurova, E. V.; Petrovskii, P. V. *Russ. J. Gen. Chem.* **2000**, *70*, 550-551. (n) Lee, H.; Knobler, C. B.; Hawthorne, M. F. *Chem. Commun.* **2000**, 2485-2486. (o) Bayer, M. J.; Herzog, A.; Diaz, M.; Harakas, G. A.; Lee, H.; Knobler, C. B.; Hawthorne, M. F. *Chem.--Eur. J.* **2003**, *9*, 2732-2744. (p) Beletskaya, I. P.; Bregadze, V. I.; Ivushkin, V. A.; Petrovskii, P. V.; Sivaev, I. B.; Sjöberg, S.; Zhigareva, G. G. *J. Organomet. Chem.* **2004**, *689*, 2920-2929. (q) Beletskaya, I. P.; Bregadze, V. I.; Ivushkin, V. A.; Zhigareva, G. G.; Petrovskii, P. V.; Sivaev, I. B. *Russ. J. Org. Chem.* **2005**, *41*, 1359-1366. (r) Barberà, G.; Vaca, A.; Teixidor, F.; Sillanpää, R.; Kivekäs, R.; Viñas, C. *Inorg. Chem.* **2008**, *47*, 7309-7316.
- (26) (a) Zakharkin, L. I.; Balagurova, E. V.; Lebedev, V. N. *Russ. J. Gen. Chem.* **1998**, *68*, 922-924. (b) Eriksson, L.; Beletskaya, I. P.; Bregadze, V. I.; Sivaev, I. B.; Sjöberg, S. *J. Organomet. Chem.* **2002**, *657*, 267-272. (c) Aizawa, K.; Ohta, K.; Endo, Y. *Heterocycles* **2010**, *80*, 369-377.
- (27) (a) Zakharkin, L. I.; Ol'shevskaya, V. A. *Synth. React. Inorg. Met.-Org. Chem.* **1991**, *21*, 1041-1046. (b) Zakharkin, L. I.; Ol'shevskaya, V. A.; Guseva, V. V. *Russ. Chem. Bull.* **1998**, *47*, 524-525. (c) Zakharkin, L. I.; Ol'shevskaya, V.

- A.; Zhigareva, G. G. *Russ. J. Gen. Chem.* **1998**, *68*, 925-927.
- (28) Jiang, W.; Harwell, D. E.; Mortimer, M. D.; Knobler, C. B.; Hawthorne, M. F. *Inorg. Chem.* **1996**, *35*, 4355-4359.
- (29) Eriksson, L.; Winberg, K. J.; Claro, R. T.; Sjöberg, S. *J. Org. Chem.* **2003**, *68*, 3569-3573.
- (30) Zakharkin, L. I.; Guseva, V. V.; Ol'shevskaya, V. A. *Russ. J. Gen. Chem.* **2001**, *71*, 903-904.
- (31) (a) Beletskaya, I. P.; Bregadze, V. I.; Kabytaev, K. Z.; Zhigareva, G. G.; Petrovskii, P. V.; Glukhov, I. V.; Starikova, Z. A. *Organometallics* **2007**, *26*, 2340-2347. (b) Mukhin, S. N.; Kabytaev, K. Z.; Zhigareva, G. G.; Glukhov, I. V.; Starikova, Z. A.; Bregadze, V. I.; Beletskaya, I. P. *Organometallics* **2008**, *27*, 5937-5942.
- (32) Kabytaev, K. Z.; Mukhin, S. N.; Glukhov, I. V.; Starikova, Z. A.; Bregadze, V. I.; Beletskaya, I. P. *Organometallics* **2009**, *28*, 4758-4763.
- (33) Grafstein, D.; Bobinski, J.; Dvorak, J.; Paustian, J. E.; Smith, H. F.; Karlan, S.; Vogel, C.; Fein, M. M. *Inorg. Chem.* **1963**, *2*, 1125-1128.
- (34) (a) Wiesboeck, R. A.; Hawthorne, M. F. *J. Am. Chem. Soc.* **1964**, *86*, 1642-1643. (b) Hawthorne, M. F.; Young, D. C.; Garrett, P. M.; Owen, D. A.; Schwerin, S. G.; Tebbe, F. N.; Wegner, P. A. *J. Am. Chem. Soc.* **1968**, *90*, 862-868.
- (35) (a) Garrett, P. M.; Tebbe, F. N.; Hawthorne, M. F. *J. Am. Chem. Soc.* **1964**, *86*, 5016-5017. (b) Zakharkin, L. I.; Kalinin, V. N. *Izv. Akad. Nauk SSSR, Ser. Khim.* **1967**, 462-464.
- (36) (a) Zakharkin, L. I.; Kalinin, V. N. *Dokl. Akad. Nauk SSSR* **1965**, *163*, 110-112. (b) Zakharkin, L. I.; Kalinin, V. N. *Tetrahedron Lett.* **1965**, 407-409. (c)

- Zakharkin, L. I.; Kirillova, V. S. *Izv. Akad. Nauk SSSR, Ser. Khim.* **1975**, 2596-2598. (d) Aono, K.; Totani, T. *J. Chem. Soc., Dalton Trans.* **1981**, 1196-1203. (e) Haushalter, R. C.; Butler, W. M.; Rudolph, R. W. *J. Am. Chem. Soc.* **1981**, *103*, 2620-2627. (f) Zakharkin, L. I.; Ol'shevskaya, V. A.; Sulaimankulova, D. D.; Antonovich, V. A. *Izv. Akad. Nauk SSSR, Ser. Khim.* **1991**, 1145-1151. (g) Teixidor, F.; Viñas, C.; Abad, M. M.; Nuñez, R.; Kivekäs, R.; Sillanpää, R. *J. Organomet. Chem.* **1995**, *503*, 193-203. (h) Teixidor, F.; Viñas, C.; Benakki, R.; Kivekäs, R.; Sillanpää, R. *Inorg. Chem.* **1997**, *36*, 1719-1723. (i) Schaeck, J. J.; Kahl, S. B. *Inorg. Chem.* **1999**, *38*, 204-206. (j) Kazantsev, A. V.; Butyaikin, V. V.; Gaas, I. E.; Otrashchenkov, E. A.; Aksartov, M. M. *Russ. J. Org. Chem.* **2000**, *36*, 975-978. (k) Fox, M. A.; Goeta, A. E.; Hughes, A. K.; Johnson, A. L. *J. Chem. Soc., Dalton Trans.* **2002**, 2132-2141. (l) Wang, Y.; Liu, D.; Chan, H.-S.; Xie, Z. *Organometallics* **2008**, *27*, 2825-2832. (m) Liu, D.; Wang, Y.; Chan, H.-S.; Tang, Y.; Xie, Z. *Organometallics* **2008**, *27*, 5295-5302.
- (37) (a) Yoo, J.; Hwang, J.-W.; Do, Y. *Inorg. Chem.* **2001**, *40*, 568-570. (b) Ioppolo, J. A.; Clegg, J. K.; Rendina, L. M. *Dalton Trans.* **2007**, 1982-1985.
- (38) Batsanov, A. S.; Copley, R. C. B.; Davidson, M. G.; Fox, M. A.; Hibbert, T. G.; Howard, J. A. K.; Wade, K. *J. Cluster Sci.* **2006**, *17*, 119-137.
- (39) (a) Plesek, J.; Hermanek, S. *Chem. Ind.* **1973**, 381-382. (b) Busby, D. C.; Hawthorne, M. F. *Inorg. Chem.* **1982**, *21*, 4101-4103.
- (40) Davidson, M. G.; Fox, M. A.; Hibbert, T. G.; Howard, J. A. K.; Mackinnon, A.; Neretin, I. S.; Wade, K. *Chem. Commun.* **1999**, 1649-1650.
- (41) (a) Taoda, Y.; Sawabe, T.; Endo, Y.; Yamaguchi, K.; Fujii, S.; Kagechika, H. *Chem. Commun.* **2008**, 2049-2051. (b) Willans, C. E.; Kilner, C. A.; Fox, M.

A. *Chem.--Eur. J.* **2010**, *16*, 10644-10648.

- (42) Dunks, G. B.; Wiersema, R. J.; Hawthorne, M. F. *J. Am. Chem. Soc.* **1973**, *95*, 3174-3179.
- (43) (a) Zakharkin, L. I.; Podvisotskaya, L. S. *Zh. Obshch. Khim.* **1967**, *37*, 506-507. (b) Zakharkin, L. I.; Kalinin, V. N.; Podvisotskaya, L. S. *Izv. Akad. Nauk SSSR, Ser. Khim.* **1966**, 1495-1496. (c) Zakharkin, L. I.; Kalinin, V. N.; Kvasov, B. A.; Snyakin, A. P. *Zh. Obshch. Khim.* **1971**, *41*, 1726-1730. (d) Zakharkin, L. I.; Kalinin, V. N.; Podvisotskaya, L. S. *Izv. Akad. Nauk SSSR, Ser. Khim.* **1967**, 2310-2316.
- (44) (a) Zakharkin, L. I.; Kalinin, V. N. *Izv. Akad. Nauk SSSR, Ser. Khim.* **1969**, 194. (b) Stanko, V. I.; Babushkina, T. A.; Brattsev, V. A.; Klimova, T. P.; Alymov, A. M.; Vasil'ev, A. M.; Knyazev, S. P. *J. Organomet. Chem.* **1974**, *78*, 313-322. (c) Stanko, V. I.; Brattsev, V. A.; Gol'tyapin, Yu. V. *Dokl. Akad. Nauk SSSR* **1976**, *231*, 925-928.
- (45) (a) Zi, G.; Li, H.-W.; Xie, Z. *Chem. Commun.* **2001**, 1110-1111. (b) Zi, G.; Li, H.-W.; Xie, Z. *Organometallics* **2001**, *20*, 3836-3838. (c) Zi, G.; Li, H.-W.; Xie, Z. *Organometallics* **2002**, *21*, 5415-5427. (d) Deng, L.; Cheung, M.-S.; Chan, H.-S.; Xie, Z. *Organometallics* **2005**, *24*, 6244-6249.
- (46) Hawthorne, M. F.; Young, D. C.; Wegner, P. A. *J. Am. Chem. Soc.* **1965**, *87*, 1818-1819.
- (47) (a) Grimes, R. N. In *Comprehensive Organometallic Chemistry*; Wilkinson, G., Stone, F. G. A., Abel, E. W., Eds.; Pergamon: Oxford, 1982; Vol. 1, pp 459-542. (b) Grimes, R. N. In *Comprehensive Organometallic Chemistry II*; Abel, E. W., Stone, F. G. A., Wilkinson, G., Eds.; Elsevier: Oxford, 1995; Vol. 1, pp 373-430. (c) Hosmane, N. S.; Maguire, J. A. In *Comprehensive*

Organometallic Chemistry III; Crabtree, R. H., Mingos, D. M. P., Eds.; Elsevier: Oxford, 2007; Vol. 3, pp 175-264.

- (48) (a) Hawthorne, M. F. *Acc. Chem. Res.* **1968**, *1*, 281-288. (b) Todd, L. J. *Adv. Organomet. Chem.* **1970**, *8*, 87-115. (c) Hawthorne, M. F.; Dunks, G. B. *Science* **1972**, *178*, 462-471. (d) Hawthorne, M. F. *Pure Appl. Chem.* **1972**, *29*, 547-567. (e) Hawthorne, M. F. *Pure Appl. Chem.* **1973**, *33*, 475-488. (f) Grimes, R. N. *Pure Appl. Chem.* **1974**, *39*, 455-474. (g) Callahan, K. P.; Hawthorne, M. F. *Pure Appl. Chem.* **1974**, *39*, 475-495. (h) Hawthorne, M. F. *J. Organomet. Chem.* **1975**, *100*, 97-110. (i) Callahan, K. P.; Hawthorne, M. F. *Adv. Organomet. Chem.* **1976**, *14*, 145-186. (j) Grimes, R. N. *Acc. Chem. Res.* **1978**, *11*, 420-427. (k) O'Neill, M. E.; Wade, K. *Met. Interact. Boron Clusters* **1982**, 1-41. (l) Grimes, R. N. *Pure Appl. Chem.* **1982**, *54*, 43-58. (m) Grimes, R. N. *Acc. Chem. Res.* **1983**, *16*, 22-26. (n) Hosmane, N. S.; Maguire, J. A. *J. Cluster Sci.* **1993**, *4*, 297-349. (o) Saxena, A. K.; Hosmane, N. S. *Chem. Rev.* **1993**, *93*, 1081-1124. (p) Hosmane, N. S.; Wang, Y.; Oki, A. R.; Zhang, H.; Zhu, D.; McDonald, E. M.; Maguire, J. A. *Phosphorus, Sulfur Silicon Relat. Elem.* **1994**, *93-94*, 253-256. (q) Grimes, R. N. *Coord. Chem. Rev.* **1995**, *143*, 71-96. (r) Grimes, R. N. *Coord. Chem. Rev.* **2000**, *200-202*, 773-811. (s) Xie, Z. *Pure Appl. Chem.* **2001**, *73*, 361-365. (t) Xie, Z. *Coord. Chem. Rev.* **2002**, *231*, 23-46. (u) Hosmane, N. S. *Pure Appl. Chem.* **2003**, *75*, 1219-1229. (v) Hosmane, N. S.; Maguire, J. A. *Eur. J. Inorg. Chem.* **2003**, 3989-3999. (w) Hosmane, N. S.; Maguire, J. A. *Pure Appl. Chem.* **2006**, *78*, 1333-1340. (x) Corsini, M.; Fabrizi de Biani, F.; Zanello, P. *Coord. Chem. Rev.* **2006**, *250*, 1351-1372. (y) Deng, L.; Xie, Z. *Organometallics* **2007**, *26*, 1832-1845. (z) Deng, L.; Xie, Z. *Coord. Chem. Rev.* **2007**, *251*, 2452-2476.

- (49) Evans, W. J.; Hawthorne, M. F. *J. Am. Chem. Soc.* **1971**, *93*, 3063-3064.
- (50) (a) Dunks, G. B.; McKown, M. M.; Hawthorne, M. F. *J. Am. Chem. Soc.* **1971**, *93*, 2541-2543. (b) Churchill, M. R.; DeBoer, B. G. *J. Chem. Soc., Chem. Commun.* **1972**, 1326-1327.
- (51) (a) Xie, Z.; Wang, S.; Zhou, Z.-Y.; Mak, T. C. W. *Organometallics* **1998**, *17*, 1907-1909. (b) Xie, Z.; Wang, S.; Zhou, Z.-Y.; Mak, T. C. W. *Organometallics* **1999**, *18*, 1641-1652. (c) Xie, Z.; Wang, S.; Yang, Q.; Mak, T. C. W. *Organometallics* **1999**, *18*, 2420-2427. (d) Chui, K.; Yang, Q.; Mak, T. C. W.; Xie, Z. *Organometallics* **2000**, *19*, 1391-1401.
- (52) Wang, Y.; Wang, H.; Li, H.-W.; Xie, Z. *Organometallics* **2002**, *21*, 3311-3313.
- (53) Barker, G. K.; Garcia, M. P.; Green, M.; Stone, F. G. A.; Welch, A. J. *J. Chem. Soc., Chem. Commun.* **1983**, 137-139.
- (54) Donaghy, K. J.; Carroll, P. J.; Sneddon, L. G. *J. Organomet. Chem.* **1998**, *550*, 77-88.
- (55) Zi, G.; Li, H.-W.; Xie, Z. *Organometallics* **2002**, *21*, 3464-3470.
- (56) Kwong, W.-C.; Chan, H.-S.; Tang, Y.; Xie, Z. *Organometallics* **2004**, *23*, 3098-3100.
- (57) (a) McIntosh, R.; Ellis, D.; Gil-Lostes, J.; Dalby, K. J.; Rosair, G. M.; Welch, A. J. *Dalton Trans.* **2005**, 1842-1846. (b) Scott, G.; McAnaw, A.; McKay, D.; Boyd, A. S. F.; Ellis, D.; Rosair, G. M.; Macgregor, S. A.; Welch, A. J.; Laschi, F.; Rossi, F.; Zanello, P. *Dalton Trans.* **2010**, *39*, 5286-5300.
- (58) (a) Wong, K.-H.; Chan, H.-S.; Xie, Z. *Organometallics* **2003**, *22*, 1775-1778. (b) Abram, P. D.; McKay, D.; Ellis, D.; Macgregor, S. A.; Rosair, G. M.; Welch, A. J. *Dalton Trans.* **2010**, *39*, 2412-2422.

- (59) (a) Ellis, D.; Lopez, M. E.; McIntosh, R.; Rosair, G. M.; Welch, A. J.; Quenardelle, R. *Chem. Commun.* **2005**, 1348-1350. (b) Dalby, K. J.; Ellis, D.; Erhardt, S.; McIntosh, R. D.; Macgregor, S. A.; Rae, K.; Rosair, G. M.; Settels, V.; Welch, A. J.; Hodson, B. E.; McGrath, T. D.; Stone, F. G. A. *J. Am. Chem. Soc.* **2007**, *129*, 3302-3314. (c) Ellis, D.; McIntosh, R. D.; Esquirolea, S.; Viñas, C.; Rosair, G. M.; Teixidor, F.; Welch, A. J. *Dalton Trans.* **2008**, 1009-1017. (d) Abram, P. D.; Ellis, D.; Rosair, G. M.; Welch, A. *J. Chem. Commun.* **2009**, 5403-5405.
- (60) (a) Dustin, D. F.; Dunks, G. B.; Hawthorne, M. F. *J. Am. Chem. Soc.* **1973**, *95*, 1109-1115. (b) Burke, A.; McIntosh, R.; Ellis, D.; Rosair, G. M.; Welch, A. J. *Collect. Czech. Chem. Commun.* **2002**, *67*, 991-1006. (c) Zlatogorsky, S.; Ellis, D.; Rosair, G. M.; Welch, A. J. *Chem. Commun.* **2007**, 2178-2180.
- (61) Zlatogorsky, S.; Edie, M. J.; Ellis, D.; Erhardt, S.; Lopez, M. E.; Macgregor, S. A.; Rosair, G. M.; Welch, A. J. *Angew. Chem. Int. Ed.* **2007**, *46*, 6706-6709.
- (62) (a) Xie, Z.; Yan, C.; Yang, Q.; Mak, T. C. W. *Angew. Chem. Int. Ed.* **1999**, *38*, 1761-1763. (b) Xie, Z.; Chui, K.; Yang, Q.; Mak, T. C. W. *Organometallics* **1999**, *18*, 3947-3949. (c) Chui, K.; Yang, Q.; Mak, T. C. W.; Lam, W. H.; Lin, Z.; Xie, Z. *J. Am. Chem. Soc.* **2000**, *122*, 5758-5764. (d) Wang, S.; Li, H.-W.; Xie, Z. *Organometallics* **2001**, *20*, 3842-3844. (e) Wang, S.; Wang, Y.; Cheung, M.-S.; Chan, H.-S.; Xie, Z. *Tetrahedron* **2003**, *59*, 10373-10380. (f) Cheung, M.-S.; Chan, H.-S.; Xie, Z. *Organometallics* **2005**, *24*, 4468-4474.
- (63) Cheung, M.-S.; Chan, H.-S.; Bi, S.; Lin, Z.; Xie, Z. *Organometallics* **2005**, *24*, 4333-4336.

- (64) Evans, W. J.; Hawthorne, M. F. *J. Chem. Soc., Chem. Commun.* **1974**, 38-39.
- (65) Ellis, D.; Lopez, M. E.; McIntosh, R.; Rosair, G. M.; Welch, A. J. *Chem. Commun.* **2005**, 1917-1919.
- (66) (a) Brown, L. D.; Lipscomb, W. N. *Inorg. Chem.* **1977**, *16*, 2989-2996. (b) Bicerano, J.; Marynick, D. S.; Lipscomb, W. N. *Inorg. Chem.* **1978**, *17*, 2041-2042. (c) Bicerano, J.; Marynick, D. S.; Lipscomb, W. N. *Inorg. Chem.* **1978**, *17*, 3443-3453. (d) Schleyer, P. v. R.; Najafian, K.; Mebel, A. M. *Inorg. Chem.* **1998**, *37*, 6765-6772.
- (67) Boyd, A. S. F.; Burke, A.; Ellis, D.; Ferrer, D.; Giles, B. T.; Laguna, M. A.; McIntosh, R.; Macgregor, S. A.; Ormsby, D. L.; Rosair, G. M.; Schmidt, F.; Wilson, N. M. M.; Welch, A. J. *Pure Appl. Chem.* **2003**, *75*, 1325-1333.
- (68) Grimes, R. N. *Angew. Chem. Int. Ed.* **2003**, *42*, 1198-1200.
- (69) Burke, A.; Ellis, D.; Giles, B. T.; Hodson, B. E.; Macgregor, S. A.; Rosair, G. M.; Welch, A. J. *Angew. Chem. Int. Ed.* **2003**, *42*, 225-228.
- (70) (a) Salentine, C. G.; Hawthorne, M. F. *J. Am. Chem. Soc.* **1975**, *97*, 426-428. (b) Lo, F. Y.; Strouse, C. E.; Callahan, K. P.; Knobler, C. B.; Hawthorne, M. F. *J. Am. Chem. Soc.* **1975**, *97*, 428-429. (c) Salentine, C. G.; Hawthorne, M. F. *Inorg. Chem.* **1976**, *15*, 2872-2882.
- (71) (a) Khattar, R.; Manning, M. J.; Knobler, C. B.; Johnson, S. E.; Hawthorne, M. F. *Inorg. Chem.* **1992**, *31*, 268-273. (b) Xie, Z.; Liu, Z.; Yang, Q.; Mak, T. C. W. *Organometallics* **1999**, *18*, 3603-3609.
- (72) Matteson, D. S.; Davis, R. A. *Inorg. Chem.* **1974**, *13*, 859-862.
- (73) (a) Zakharkin, L. I. *Izv. Akad. Nauk SSSR, Ser. Khim.* **1965**, 1114-1116. (b) Paxson, T. E.; Kaloustian, M. K.; Tom, G. M.; Wiersema, R. J.; Hawthorne, M. F. *J. Am. Chem. Soc.* **1972**, *94*, 4882-4888.

- (74) Deng, L.; Chan, H.-S.; Xie, Z. *J. Am. Chem. Soc.* **2006**, *128*, 5219-5230.
- (75) Herzog, A.; Knobler, C. B.; Hawthorne, M. F. *J. Am. Chem. Soc.* **2001**, *123*, 12791-12797.
- (76) Xie, Z.; Manning, J.; Reed, R. W.; Mathur, R.; Boyd, P. D. W.; Benesi, A.; Reed, C. A. *J. Am. Chem. Soc.* **1996**, *118*, 2922-2928.
- (77) Fu, X.; Chan, H.-S.; Xie, Z. *J. Am. Chem. Soc.* **2007**, *129*, 8964-8965.
- (78) King, B. T.; Noll, B. C.; McKinley, A. J.; Michl, J. *J. Am. Chem. Soc.* **1996**, *118*, 10902-10903.
- (79) (a) Peymann, T.; Knobler, C. B.; Hawthorne, M. F. *Chem. Commun.* **1999**, 2039-2040. (b) Farha, O. K.; Julius, R. L.; Lee, M. W.; Huertas, R. E.; Knobler, C. B.; Hawthorne, M. F. *J. Am. Chem. Soc.* **2005**, *127*, 18243-18251.
- (80) Deng, L. *Synthesis, structural characterization and reactivity study of novel twelve-, thirteen, and fourteen-vertex carboranes and their derivatives*, The Chinese University of Hong Kong, 2006.
- (81) Deng, L.; Chan, H.-S.; Xie, Z. *Angew. Chem. Int. Ed.* **2005**, *44*, 2128-2131.
- (82) McIntosh, R. D.; Ellis, D.; Rosair, G. M.; Welch, A. J. *Angew. Chem. Int. Ed.* **2006**, *45*, 4313-4316.
- (83) Hota, N. K.; Matteson, D. S. *J. Am. Chem. Soc.* **1968**, *90*, 3570-3572.
- (84) Fox, M. A.; Whitesell, J. K. *Organic Chemistry, 3rd ed.*; Jones and Bartlett Publishers: Sudbury, Mass., 2004.
- (85) Hesse, M.; Meier, H.; Zeeh, B. *Spectroscopic Methods in Organic Chemistry*; G. Thieme: Stuttgart ; New York, 1995.
- (86) (a) King, R. B.; Rouvray, D. H. *J. Am. Chem. Soc.* **1977**, *99*, 7834-7840. (b) Cotton, F. A. *Chemical Applications of Group Theory, 3rd Ed.*; Wiley: New York, 1990.

- (87) Krüger, T.; Vorndran, K.; Linker, T. *Chem.--Eur. J.* **2009**, *15*, 12082-12091.
- (88) Clive, D. L. J.; Sunasee, R. *Org. Lett.* **2007**, *9*, 2677-2680.
- (89) Meijs, G. F.; Bunnett, J. F.; Beckwith, A. L. J. *J. Am. Chem. Soc.* **1986**, *108*, 4899-4904.
- (90) (a) Adcock, W.; Gupta, B. D.; Kitching, W. *J. Org. Chem.* **1976**, *41*, 1498-1504. (b) Bates, R. B.; Ogle, C. A. *J. Org. Chem.* **1982**, *47*, 3949-3952.
- (91) Jones, I. C.; Sharman, G. J.; Pidgeon, J. *Magn. Reson. Chem.* **2005**, *43*, 497-509.
- (92) Yus, M.; Herrera, R. P.; Guijarro, A. *Chem.--Eur. J.* **2002**, *8*, 2574-2584.
- (93) Mahesh, M.; Murphy, J. A.; Wessel, H. P. *J. Org. Chem.* **2005**, *70*, 4118-4123.
- (94) Nandi, P.; Dye, J. L.; Jackson, J. E. *J. Org. Chem.* **2009**, *74*, 5790-5792.
- (95) Papetti, S.; Heying, T. L. *Inorg. Chem.* **1963**, *2*, 1105-1107.
- (96) Yang, D.; Zhang, C. *J. Org. Chem.* **2001**, *66*, 4814-4818.
- (97) Viski, P.; Szeverényi, Z.; Simándi, L. I. *J. Org. Chem.* **1986**, *51*, 3213-3214.
- (98) (a) Burwell, R. L., Jr. *Chem. Rev.* **1954**, *54*, 615-685. (b) Grobelny, Z. *Eur. J. Org. Chem.* **2004**, 2973-2982.
- (99) Zakharkin, L. I.; Ol'shevskaya, V. A.; Guseva, V. V.; Shemyakin, N. F. *Russ. Chem. Bull.* **1998**, *47*, 475-477.
- (100) Schulz, A.; Thomas, J.; Villinger, A. *Chem. Commun.* **2010**, *46*, 3696-3698.
- (101) Smith, H. D.; Knowles, T. A.; Schroeder, H. *Inorg. Chem.* **1965**, *4*, 107-111.
- (102) Roy, C. D. *Aust. J. Chem.* **2006**, *59*, 657-659.
- (103) (a) Kalinin, V. N.; Kobel'kova, N. I.; Zakharkin, L. I. *Zh. Obshch. Khim.* **1977**, *47*, 963. (b) Kalinin, V. N.; Kobel'kova, N. I.; Astakhin, A. V.; Zakharkin, L. I. *Izv. Akad. Nauk SSSR, Ser. Khim.* **1977**, 2376-2378. (c)

- Kalinin, V. N.; Kobel'kova, N. I.; Astakhin, A. V.; Gusev, A. I.; Zakharkin, L. *I. J. Organomet. Chem.* **1978**, *149*, 9-21.
- (104) Körbe, S.; Schreiber, P. J.; Michl, J. *Chem. Rev.* **2006**, *106*, 5208-5249.
- (105) Gorenstein, D. G. *Phosphorus-31 NMR: Principles and Applications*; Academic Press: Orlando, Fla. ; London, 1984.
- (106) (a) Opitz, G.; Rieth, K.; Rimpler, G. *Tetrahedron Lett.* **1986**, *27*, 167-170. (b) Terrier, F.; Halle, J.-C.; Pouet, M.-J.; Simonnin, M.-P. *J. Org. Chem.* **1986**, *51*, 409-411. (c) Maresca, L.; Natile, G.; Fanizzi, F. P. *J. Chem. Soc., Dalton Trans.* **1992**, 1867-1868. (d) Chambers, R. D.; Korn, S. R.; Sandford, G. *Tetrahedron* **1992**, *48*, 7939-7950. (e) Ozeryanskii, V. A.; Pozharskii, A. F.; Vistorobskii, N. V. *Russ. J. Org. Chem.* **1997**, *33*, 251-256. (f) Romanova, E. Yu.; Pozharskii, A. F.; Borodkin, G. S. *Russ. Chem. Bull.* **2001**, *50*, 860-864. (g) Vinogradova, O. V.; Pozharskii, A. F.; Starikova, Z. A. *Russ. Chem. Bull.* **2003**, *52*, 208-217.
- (107) Finze, M. *Angew. Chem. Int. Ed.* **2007**, *46*, 8880-8882.
- (108) Laromaine, A.; Teixidor, F.; Viñas, C. *Angew. Chem. Int. Ed.* **2005**, *44*, 2220-2222.
- (109) Coulson, C. A.; Dingle, T. W. *Acta Crystallogr., Sect. B* **1968**, *24*, 153-155.
- (110) Paetzold, P. *Pure Appl. Chem.* **1991**, *63*, 345-350.
- (111) Power, P. P. *Chem. Rev.* **1999**, *99*, 3463-3503.
- (112) (a) Tolpin, E. I.; Lipscomb, W. N. *Inorg. Chem.* **1973**, *12*, 2257-2262. (b) Churchill, M. R.; DeBoer, B. G. *Inorg. Chem.* **1973**, *12*, 2674-2682. (c) Getman, T. D.; Knobler, C. B.; Hawthorne, M. F. *Inorg. Chem.* **1990**, *29*, 158-160.
- (113) (a) Nöth, H.; Weber, S.; Rasthofer, B.; Narula, Ch.; Konstantinov, A. *Pure*

- Appl. Chem.* **1983**, *55*, 1453-1461. (b) Kölle, P.; Nöth, H. *Chem. Rev.* **1985**, *85*, 399-418. (c) Piers, W. E.; Bourke, S. C.; Conroy, K. D. *Angew. Chem. Int. Ed.* **2005**, *44*, 5016-5036.
- (114) Zharov, I.; Havlas, Z.; Orendt, A. M.; Barich, D. H.; Grant, D. M.; Fete, M. G.; Michl, J. *J. Am. Chem. Soc.* **2006**, *128*, 6089-6100.
- (115) Thomas, S. E. *Organic Synthesis: The Roles of Boron and Silicon*; Oxford University Press: Oxford ; New York, 1991.
- (116) Ashby, M. T.; Sheshtawy, N. A. *Organometallics* **1994**, *13*, 236-243.
- (117) (a) Hernandez, D. M.; Huffman, J. C.; Todd, L. J. *Inorg. Chem.* **1987**, *26*, 213-215. (b) Quintana, W.; Ernest, R. L.; Carroll, P. J.; Sneddon, L. G. *Organometallics* **1988**, *7*, 166-172. (c) Quintana, W.; Sneddon, L. G. *Inorg. Chem.* **1990**, *29*, 3242-3245. (d) Whitaker, C. R.; Romerosa, A.; Teixidor, F.; Rius, J. *Acta Crystallogr., Sect. C* **1995**, *C51*, 188-190. (e) Jeffery, J. C.; Jelliss, P. A.; Karban, J.; Lebedev, V.; Stone, F. G. A. *J. Chem. Soc., Dalton Trans.* **1997**, 1219-1224. (f) Batsanov, A. S.; Fox, M. A.; Goeta, A. E.; Howard, J. A. K.; Hughes, A. K.; Malget, J. M. *J. Chem. Soc., Dalton Trans.* **2002**, 2624-2631. (g) Bould, J.; Laromaine, A.; Viñas, C.; Teixidor, F.; Barton, L.; Rath, N. P.; Winter, R. E. K.; Kivekäs, R.; Sillanpää, R. *Organometallics* **2004**, *23*, 3335-3342. (h) Franken, A.; Jelínek, T.; Taylor, R. G.; Ormsby, D. L.; Kilner, C. A.; Clegg, W.; Kennedy, J. D. *Dalton Trans.* **2006**, 5753-5769.
- (118) (a) Peymann, T.; Herzog, A.; Knobler, C. B.; Hawthorne, M. F. *Angew. Chem. Int. Ed.* **1999**, *38*, 1062-1064. (b) Cheung, M.-S.; Chan, H.-S.; Xie, Z. *Organometallics* **2004**, *23*, 517-526. (c) Stasko, D. J.; Perzynski, K. J.; Wasil, M. A. *Chem. Commun.* **2004**, 708-709.

- (119) (a) Ernest, R. L.; Quintana, W.; Rosen, R.; Carroll, P. J.; Sneddon, L. G. *Organometallics* **1987**, *6*, 80-88. (b) Franken, A.; Kilner, C. A.; Thornton-Pett, M.; Kennedy, J. D. *J. Organomet. Chem.* **2002**, *657*, 180-186.
- (120) (a) Maringgele, W.; Bromm, D.; Meller, A. *Tetrahedron* **1988**, *44*, 1053-1056. (b) Mansell, S. M.; Norman, N. C.; Russell, C. A. *Dalton Trans.* **2010**, *39*, 5084-5086.
- (121) Kühn, F. E.; Groarke, M.; Bencze, É.; Herdtweck, E.; Prazeres, A.; Santos, A. M.; Calhorda, M. J.; Romão, C. C.; Gonçalves, I. S.; Lopes, A. D.; Pillinger, M. *Chem.--Eur. J.* **2002**, *8*, 2370-2383.
- (122) Nishigaki, S.; Yoshioka, H.; Nakatsu, K. *Acta Crystallogr., Sect. B* **1978**, *B34*, 875-879.
- (123) (a) Weber, L. *Coord. Chem. Rev.* **2001**, *215*, 39-77. (b) Weber, L. *Coord. Chem. Rev.* **2008**, *252*, 1-31.
- (124) (a) Gaines, D. F.; Heppert, J. A.; Coons, D. E.; Jorgenson, M. W. *Inorg. Chem.* **1982**, *21*, 3662-3665. (b) Saulys, D. A.; Morrison, J. A. *Inorg. Chem.* **1990**, *29*, 4174-4179.
- (125) Nam, W.; Onak, T. *Inorg. Chem.* **1987**, *26*, 48-52.
- (126) (a) Krishnan, C. V.; Creutz, C.; Schwarz, H. A.; Sutin, N. *J. Am. Chem. Soc.* **1983**, *105*, 5617-5623. (b) Brewer, B.; Brooks, N. R.; Abdul-Halim, S.; Sykes, A. G. *J. Chem. Crystallogr.* **2003**, *33*, 651-662.
- (127) (a) Roth, M.; Meyer, F.; Paetzold, P. *Collect. Czech. Chem. Commun.* **1997**, *62*, 1299-1309. (b) Paetzold, P. *Eur. J. Inorg. Chem.* **1998**, 143-153.
- (128) Li, Y.; Sneddon, L. G. *J. Am. Chem. Soc.* **2008**, *130*, 11494-11502.
- (129) (a) Jelínek, T.; Plešek, J.; Heřmánek, S.; Štíbr, B. *Collect. Czech. Chem. Commun.* **1986**, *51*, 819-829. (b) Vyakaranam, K.; Körbe, S.; Divišová, H.;

- Michl, J. *J. Am. Chem. Soc.* **2004**, *126*, 15795-15801. (c) Vyakaranam, K.; Havlas, Z.; Michl, J. *J. Am. Chem. Soc.* **2007**, *129*, 4172-4174.
- (130) (a) Nakamura, H.; Aoyagi, K.; Yamamoto, Y. *J. Org. Chem.* **1997**, *62*, 780-781. (b) Nakamura, H.; Aoyagi, K.; Yamamoto, Y. *J. Organomet. Chem.* **1999**, *574*, 107-115.
- (131) (a) Zakharkin, L. I.; Chapovskii, Yu. A. *Tetrahedron Lett.* **1964**, 1147-1150. (b) Zakharkin, L. I.; L'Vov, A. I. *J. Organomet. Chem.* **1966**, *5*, 313-319. (c) Zakharkin, L. I.; Chapovskii, Yu. A.; Brattsev, V. A.; Stanko, V. I. *Zh. Obshch. Khim.* **1966**, *36*, 878-886.
- (132) (a) Janousek, Z.; Fusek, J.; Stibr, B. *J. Chem. Soc., Dalton Trans.* **1992**, 2649-2650. (b) Janoušek, Z.; Dostál, R.; Macháček, J.; Hnyk, D.; Štíbr, B. *Dalton Trans.* **2006**, 4664-4671.
- (133) Dornhaus, F.; Bolte, M.; Lerner, H.-W.; Wagner, M. *Eur. J. Inorg. Chem.* **2006**, 1777-1785.
- (134) (a) Brunel, J. M.; Faure, B.; Maffei, M. *Coord. Chem. Rev.* **1998**, *178-180*, 665-698. (b) Staubitz, A.; Robertson, A. P. M.; Sloan, M. E.; Manners, I. *Chem. Rev.* **2010**, *110*, 4023-4078.
- (135) Viñas, C.; Núñez, R.; Teixidor, F.; Sillanpää, R.; Kivekäs, R. *Organometallics* **1999**, *18*, 4712-4717.
- (136) Sheldrick, G. M. SADABS: Program for Empirical Absorption Correction of Area Detector Data. University of Göttingen: Germany, 1996.
- (137) Sheldrick, G. M. SHELXTL 5.10 for Windows NT: Structure Determination Software Programs. Bruker Analytical X-ray systems, Inc.: Madison, Wisconsin, USA, 1997.
- (138) Flack, H. D. *Acta Crystallogr., Sect. A* **1983**, *A39*, 876-881.

Appendix I. Publications Based on the Research Findings

1. Liang Deng, Jian Zhang, Hoi-Shan Chan, and Zuowei Xie. "Synthesis and Structure of 14- and 15-Vertex Ruthenacarboranes" *Angew. Chem. Int. Ed.* **2006**, *45*, 4309-4313.
2. Jian Zhang, Liang Deng, Hoi-Shan Chan, and Zuowei Xie. "Role of C,C'-Linkage in the Formation and Stabilization of Supercarboranes. Synthesis and Structure of Carbon-Atoms-Apart 13-Vertex Carborane and 14-Vertex Metalla-carborane" *J. Am. Chem. Soc.* **2007**, *129*, 18-19.
3. Jian Zhang, Hoi-Shan Chan, and Zuowei Xie. "Reaction of 13-Vertex Carboranes with Nucleophiles: Unprecedented Cage-Carbon Extrusion and Formation of Monocarba-*closo*-dodecaborate Anions" *Angew. Chem. Int. Ed.* **2008**, *47*, 9447-9449.
4. Jian Zhang, Fangrui Zheng, Hoi-Shan Chan, and Zuowei Xie. "Reaction of a 14-Vertex Carborane with Nucleophiles: Formation of *nido*-C₂B₁₂, *nido*-C₂B₁₁, and *closo*-CB₁₁ Carborane Anions" *Inorg. Chem.* **2009**, *48*, 9786-9791.
5. Jian Zhang and Zuowei Xie. "Recent Progress in the Chemistry of Supercarboranes" *Chem. Asian J.* **2010**, *5*, 1742-1757. FOCUS REVIEWS.

Appendix II. Crystal Data and Summary of Data Collection and Refinement

Compd. No.	4	5a	5b	6
formula	C ₆ H ₁₈ B ₁₀	C ₁₂ H ₂₁ B ₁₁	C ₁₂ H ₂₁ B ₁₁	C ₅ H ₁₇ B ₁₁
crystal size (mm)	0.50 x 0.40 x 0.30	0.50 x 0.40 x 0.30	0.40 x 0.30 x 0.20	0.50 x 0.40 x 0.30
fw	198.30	284.20	284.20	196.10
crystal system	Orthorhombic	Monoclinic	Monoclinic	Monoclinic
space group	<i>P</i> 2 ₁ 2 ₁ 2 ₁	<i>P</i> 2 ₁ / <i>n</i>	<i>P</i> 2 ₁ / <i>n</i>	<i>P</i> 2 ₁ / <i>c</i>
<i>a</i> , Å	8.8226(10)	10.614(2)	10.6435(3)	7.381(6)
<i>b</i> , Å	9.7699(11)	14.753(3)	14.7542(5)	13.807(12)
<i>c</i> , Å	14.1534(15)	10.845(2)	10.8336(3)	12.919(11)
α , deg	90	90	90	90
β , deg	90	99.102(5)	99.4030(10)	105.673(17)
γ , deg	90	90	90	90
<i>V</i> , Å ³	1220.0(2)	1676.9(6)	1678.41(9)	1267.5(18)
<i>Z</i>	4	4	4	4
<i>D</i> _{calcd} , Mg/m ³	1.080	1.126	1.125	1.028
radiation (λ), Å	Mo K α (0.71073)	Mo K α (0.71073)	Mo K α (0.71073)	Mo K α (0.71073)
2 θ range, deg	55.8	56.0	50.0	55.3
μ , mm ⁻¹	0.048	0.053	0.053	0.044
<i>F</i> (000)	416	592	592	408
no. of obsd reflns	2774	4038	2934	2944
no. of params refnd	145	208	208	145
goodness of fit	1.088	1.003	1.080	1.002
R1	0.0500	0.0498	0.0473	0.0807
wR2	0.0572	0.0718	0.0560	0.1145

Compd. No.	7	7'	11	[12a][Na ₄ (THF) ₁₂]
formula	C ₆ H ₁₉ B ₁₁	C ₇ H ₂₁ B ₁₁	C ₆ H ₂₀ B ₁₀ Si	C ₂₈ H ₆₃ B ₁₀ Na ₂ O ₆
crystal size (mm)	0.50 x 0.40 x 0.30	0.40 x 0.30 x 0.20	0.40 x 0.30 x 0.20	0.30 x 0.20 x 0.10
fw	210.12	224.15	228.41	649.86
crystal system	Orthorhombic	Orthorhombic	Monoclinic	Monoclinic
space group	<i>Pbca</i>	<i>Pnma</i>	<i>C2/c</i>	<i>P2₁/c</i>
<i>a</i> , Å	13.051(3)	14.3933(15)	12.077(6)	10.5794(11)
<i>b</i> , Å	12.607(3)	11.3659(12)	10.190(5)	16.3005(16)
<i>c</i> , Å	15.258(3)	8.3269(9)	12.910(6)	23.647(3)
α , deg	90	90	90	90
β , deg	90	90	115.676(9)	100.216(2)
γ , deg	90	90	90	90
<i>V</i> , Å ³	2510.4(9)	1362.2(3)	1431.9(12)	4013.3(7)
<i>Z</i>	8	4	4	4
<i>D</i> _{calcd} , Mg/m ³	1.112	1.093	1.060	1.076
radiation (λ), Å	Mo K α (0.71073)	Mo K α (0.71073)	Mo K α (0.71073)	Mo K α (0.71073)
2 θ range, deg	50.0	55.8	50.0	50.0
μ , mm ⁻¹	0.049	0.049	0.128	0.085
<i>F</i> (000)	880	472	480	1404
no. of obsd reflns	2197	1702	1259	7069
no. of params refnd	154	88	78	455
goodness of fit	1.148	1.014	1.166	1.127
R1	0.0646	0.0757	0.0821	0.0989
wR2	0.0930	0.1416	0.0870	0.1976

Compd. No.	[12b][Na ₂ (18-crown-6)]	[14][Na ₂ (THF) ₄]	16	17a
formula	C ₁₆ H ₃₇ B ₉ Na ₂ O ₇	C ₂₂ H ₅₄ B ₁₀ Na ₂ O ₅ Si ₂	C ₆ H ₂₁ B ₁₁ Si	C ₄ H ₁₇ B ₁₁
crystal size (mm)	0.40 x 0.30 x 0.20	0.50 x 0.50 x 0.40	0.50 x 0.40 x 0.30	0.40 x 0.30 x 0.30
fw	484.73	608.91	240.23	184.09
crystal system	Monoclinic	Monoclinic	Monoclinic	Monoclinic
space group	<i>C2/m</i>	<i>P2₁/n</i>	<i>P2₁/c</i>	<i>P2₁/m</i>
<i>a</i> , Å	11.085(3)	12.3686(13)	10.330(7)	7.0551(9)
<i>b</i> , Å	14.938(3)	12.1982(12)	10.249(7)	11.6875(14)
<i>c</i> , Å	16.007(4)	24.516(2)	14.120(8)	8.0262(10)
α , deg	90	90	90	90
β , deg	90.051(4)	90.255(2)	95.595(14)	115.576(2)
γ , deg	90	90	90	90
<i>V</i> , Å ³	2650.5(10)	3698.8(6)	1487.8(16)	596.96(13)
<i>Z</i>	4	4	4	2
<i>D</i> _{calcd.} , Mg/m ³	1.215	1.093	1.072	1.024
radiation (λ), Å	Mo K α (0.71073)	Mo K α (0.71073)	Mo K α (0.71073)	Mo K α (0.71073)
2 θ range, deg	56.0	50.0	50.2	50.0
μ , mm ⁻¹	0.110	0.148	0.125	0.043
<i>F</i> (000)	1024	1304	504	192
no. of obsd reflns	3307	6532	2599	1109
no. of params refnd	167	370	163	98
goodness of fit	1.100	1.027	1.029	1.071
R1	0.0727	0.0803	0.0510	0.0724
wR2	0.0883	0.1333	0.0893	0.0904

Compd. No.	19	20	21a	21b
formula	C ₁₆ H ₃₄ B ₁₀ RuSi	C ₇ H ₂₅ B ₁₁ Si	C ₁₇ H ₃₈ B ₁₀ RuSi	C ₁₇ H ₃₈ B ₁₀ RuSi
crystal size (mm)	0.50 x 0.20 x 0.20	0.50 x 0.40 x 0.20	0.40 x 0.30 x 0.10	0.50 x 0.40 x 0.30
fw	463.69	256.27	479.73	479.73
crystal system	Monoclinic	Monoclinic	Monoclinic	Monoclinic
space group	<i>P2₁/n</i>	<i>P2₁/c</i>	<i>P2₁/n</i>	<i>P2₁/n</i>
<i>a</i> , Å	9.1904(15)	7.0795(5)	8.9761(14)	8.8301(15)
<i>b</i> , Å	24.076(4)	11.6549(9)	15.806(2)	16.575(3)
<i>c</i> , Å	11.1276(18)	20.6859(15)	18.036(3)	17.179(3)
α , deg	90	90	90	90
β , deg	92.449(3)	96.0330(10)	96.903(4)	100.459(3)
γ , deg	90	90	90	90
<i>V</i> , Å ³	2459.9(7)	1697.4(2)	2540.4(7)	2472.6(7)
<i>Z</i>	4	4	4	4
<i>D</i> _{calcd} , Mg/m ³	1.252	1.003	1.254	1.289
radiation (λ), Å	Mo K α (0.71073)	Mo K α (0.71073)	Mo K α (0.71073)	Mo K α (0.71073)
2 θ range, deg	56.1	55.9	50.0	50.0
μ , mm ⁻¹	0.686	0.113	0.667	0.685
<i>F</i> (000)	952	544	992	992
no. of obsd reflns	5909	4071	4485	4359
no. of params refnd	253	172	271	266
goodness of fit	1.035	1.094	1.034	1.056
R1	0.0356	0.0573	0.0657	0.0525
wR2	0.0451	0.0914	0.0991	0.0577

Compd. No.	Me ₃ SBr	[23][Na ₂ (THF) ₄]	[26a][Na ₂ (THF) ₄]	[26b][Na ₂ (THF) ₄]
formula	C ₃ H ₉ BrS	C ₂₂ H ₅₃ B ₁₁ Na ₂ O ₄ Si	C ₂₀ H ₄₉ B ₁₁ Na ₂ O ₄	C ₂₀ H ₄₉ B ₁₁ Na ₂ O ₄
crystal size (mm)	0.40 x 0.30 x 0.10	0.50 x 0.30 x 0.30	0.50 x 0.40 x 0.30	0.50 x 0.40 x 0.30
fw	157.07	574.62	518.48	518.48
crystal system	Monoclinic	Orthorhombic	Tetragonal	Monoclinic
space group	<i>P2</i> ₁	<i>Pnma</i>	<i>Cmc2</i> ₁	<i>P2</i> ₁ / <i>n</i>
<i>a</i> , Å	5.7553(8)	11.4346(17)	16.7451(6)	16.201(2)
<i>b</i> , Å	7.4572(11)	19.023(3)	16.7451(6)	11.9984(17)
<i>c</i> , Å	7.2632(10)	15.856(2)	11.4298(6)	16.823(3)
α , deg	90	90	90	90
β , deg	92.484(2)	90	90	90.508(2)
γ , deg	90	90	90	90
<i>V</i> , Å ³	311.43(8)	3449.1(9)	3204.9(2)	3270.1(8)
<i>Z</i>	2	4	4	4
<i>D</i> _{calcd} , Mg/m ³	1.675	1.107	1.075	1.053
radiation (λ), Å	Mo K α (0.71073)	Mo K α (0.71073)	Mo K α (0.71073)	Mo K α (0.71073)
2 θ range, deg	55.7	56.0	50.0	50.5
μ , mm ⁻¹	6.789	0.120	0.087	0.085
<i>F</i> (000)	156	1232	1112	1112
no. of obsd reflns	1375	4264	2198	5916
no. of params refnd	46	215	175	424
goodness of fit	1.048	1.030	1.066	1.029
R1	0.0211	0.0754	0.0884	0.0911
wR2	0.0254	0.1597	0.1040	0.2033

Compd. No.	27a·C ₁₀ H ₈	28a	28b	29b
formula	C ₁₅ H ₂₆ B ₁₂	C ₆ H ₂₂ B ₁₂ Si	C ₆ H ₂₂ B ₁₂ Si	C ₆ H ₂₀ B ₁₂
crystal size (mm)	0.30 x 0.20 x 0.10	0.50 x 0.40 x 0.30	0.30 x 0.20 x 0.10	0.40 x 0.30 x 0.20
fw	336.08	252.05	252.05	221.94
crystal system	Monoclinic	Orthorhombic	Monoclinic	Monoclinic
space group	<i>P2₁/c</i>	<i>Pbca</i>	<i>P2₁/c</i>	<i>C2/c</i>
<i>a</i> , Å	7.836(4)	13.401(2)	7.1477(10)	12.270(5)
<i>b</i> , Å	16.662(8)	14.041(3)	14.2804(19)	9.712(5)
<i>c</i> , Å	15.795(8)	16.643(3)	15.2566(19)	12.111(5)
α , deg	90	90	90	90
β , deg	100.691(11)	90	95.450(3)	109.878(10)
γ , deg	90	90	90	90
<i>V</i> , Å ³	2026.6(18)	3131.6(10)	1550.2(4)	1357.3(10)
<i>Z</i>	4	8	4	4
<i>D</i> _{calcd} , Mg/m ³	1.102	1.069	1.080	1.086
radiation (λ), Å	Mo K α (0.71073)	Mo K α (0.71073)	Mo K α (0.71073)	Mo K α (0.71073)
2 θ range, deg	50.0	56.1	56.1	50.5
μ , mm ⁻¹	0.053	0.121	0.122	0.047
<i>F</i> (000)	704	1056	528	464
no. of obsd reflns	3571	3791	3751	1231
no. of params refnd	252	220	172	115
goodness of fit	1.031	1.002	0.969	1.041
R1	0.0774	0.0667	0.0690	0.0668
wR2	0.1171	0.1396	0.2187	0.0778

Compd. No.	30d	32a	33	35·CH ₂ Cl ₂
formula	C ₄ H ₁₈ B ₁₂	C ₁₆ H ₃₅ B ₁₁ RuSi	C ₁₄ H ₃₁ B ₁₁ Ru	C ₁₇ H ₃₈ B ₁₂ C ₁₂ RuSi
crystal size (mm)	0.50 x 0.30 x 0.20	0.50 x 0.40 x 0.30	0.30 x 0.20 x 0.10	0.50 x 0.40 x 0.30
fw	195.90	475.51	419.37	572.25
crystal system	Monoclinic	Monoclinic	Orthorhombic	Triclinic
space group	<i>C2/c</i>	<i>P2₁/n</i>	<i>P2₁2₁2₁</i>	<i>P-1</i>
<i>a</i> , Å	14.6928(8)	9.1795(13)	9.9962(13)	9.135(5)
<i>b</i> , Å	7.6394(4)	23.218(3)	12.7008(16)	11.802(6)
<i>c</i> , Å	12.0671(7)	12.0449(17)	16.033(2)	12.928(6)
α , deg	90	90	90	98.442(7)
β , deg	113.5700(10)	93.406(3)	90	95.820(8)
γ , deg	90	90	90	93.268(8)
<i>V</i> , Å ³	1241.46(12)	2562.5(6)	2035.5(4)	1367.9(12)
<i>Z</i>	4	4	4	2
<i>D</i> _{calcd} , Mg/m ³	1.048	1.233	1.368	1.389
radiation (λ), Å	Mo K α (0.71073)	Mo K α (0.71073)	Mo K α (0.71073)	Mo K α (0.71073)
2 θ range, deg	49.9	50.0	54.6	50.0
μ , mm ⁻¹	0.044	0.660	0.765	0.819
<i>F</i> (000)	408	976	856	584
no. of obsd reflns	1091	4519	3588	4783
no. of params refnd	97	266	239	298
goodness of fit	1.075	1.042	1.089	1.044
R1	0.0661	0.0281	0.0259	0.0357
wR2	0.0760	0.0372	0.0306	0.0391

Compd. No.	[36a][Me ₃ NH]	[36b][Me ₃ NH]	[36i']][PSH]	[37][Me ₃ NH]
formula	C ₉ H ₃₀ B ₁₁ NO	C ₉ H ₃₀ B ₁₁ NO	C ₂₀ H ₃₉ B ₁₁ N ₂ O	C ₈ H ₂₆ B ₁₁ N
crystal size (mm)	0.50 x 0.40 x 0.30	0.50 x 0.30 x 0.20	0.40 x 0.30 x 0.20	0.40 x 0.30 x 0.20
fw	287.25	287.25	442.44	255.21
crystal system	Monoclinic	Monoclinic	Monoclinic	Orthorhombic
space group	<i>P2₁/c</i>	<i>P2₁/n</i>	<i>P2₁/c</i>	<i>P2₁2₁2₁</i>
<i>a</i> , Å	7.924(3)	11.706(3)	15.5726(6)	7.8487(3)
<i>b</i> , Å	23.339(9)	12.298(3)	9.8303(4)	10.4150(3)
<i>c</i> , Å	9.662(4)	13.143(3)	18.0313(7)	20.1837(6)
α , deg	90	90	90	90
β , deg	97.494(7)	109.850(4)	104.0970(10)	90
γ , deg	90	90	90	90
<i>V</i> , Å ³	1771.5(13)	1779.6(6)	2677.16(18)	1649.90(9)
<i>Z</i>	4	4	4	4
<i>D</i> _{calcd} , Mg/m ³	1.077	1.072	1.098	1.027
radiation (λ), Å	Mo K α (0.71073)	Mo K α (0.71073)	Mo K α (0.71073)	Cu K α (1.54178)
2 θ range, deg	50.0	50.0	50.0	133.9
μ , mm ⁻¹	0.056	0.056	0.060	0.331
<i>F</i> (000)	616	616	944	544
no. of obsd reflns	3118	3127	4716	2592
no. of params refnd	203	199	307	182
goodness of fit	1.090	1.022	1.040	1.054
R1	0.0785	0.0681	0.0992	0.0991
wR2	0.1147	0.0955	0.1151	0.1139

Compd. No.	[37][PSH]	[38a][Me ₃ NH]	[38a][Me ₃ NH]	39
formula	C ₁₉ H ₃₅ B ₁₁ N ₂	C ₁₀ H ₃₂ B ₁₁ NO	C ₁₀ H ₃₂ B ₁₁ NO	C ₉ H ₂₈ B ₁₁ N
crystal size (mm)	0.50 x 0.40 x 0.20	0.40 x 0.30 x 0.20	0.40 x 0.40 x 0.30	0.50 x 0.40 x 0.30
fw	410.40	301.28	301.28	269.23
crystal system	Monoclinic	Orthorhombic	Monoclinic	Monoclinic
space group	<i>P2₁/c</i>	<i>Pna2₁</i>	<i>P2₁/c</i>	<i>P2₁/n</i>
<i>a</i> , Å	15.035(4)	19.3435(12)	7.9842(2)	7.6806(3)
<i>b</i> , Å	9.147(2)	11.8867(7)	23.0960(5)	11.2799(5)
<i>c</i> , Å	19.884(5)	8.0716(5)	10.5943(2)	19.8375(9)
α , deg	90	90	90	90
β , deg	109.851(5)	90	101.79	99.6080(10)
γ , deg	90	90	90	90
<i>V</i> , Å ³	2572.2(10)	1855.9(2)	1912.40(7)	1694.54(13)
<i>Z</i>	4	4	4	4
<i>D</i> _{calcd} , Mg/m ³	1.060	1.078	1.046	1.055
radiation (λ), Å	Mo K α (0.71073)	Mo K α (0.71073)	Mo K α (0.71073)	Mo K α (0.71073)
2 θ range, deg	50.5	50.0	50.0	55.9
μ , mm ⁻¹	0.055	0.056	0.054	0.050
<i>F</i> (000)	872	648	648	576
no. of obsd reflns	4639	3188	3359	4015
no. of params refnd	299	208	208	190
goodness of fit	1.578	1.046	1.023	1.021
R1	0.1574	0.0372	0.0740	0.0544
wR2	0.1837	0.0472	0.0898	0.0930

Compd. No.	40a	[40i'] [PPN]	41·CH ₂ Cl ₂	[43] [Me ₄ N]
formula	C ₉ H ₂₈ B ₁₁ N	C ₄₅ H ₅₇ B ₁₁ N ₂ P ₂	C ₂₄ H ₃₄ B ₁₁ Cl ₂ P	C ₉ H ₃₀ B ₁₁ N
crystal size (mm)	0.40 x 0.30 x 0.20	0.50 x 0.40 x 0.30	0.50 x 0.40 x 0.30	0.40 x 0.40 x 0.20
fw	269.23	806.78	543.29	271.25
crystal system	Monoclinic	Orthorhombic	Orthorhombic	Monoclinic
space group	<i>Cc</i>	<i>Pnma</i>	<i>P2₁2₁2₁</i>	<i>P2₁/c</i>
<i>a</i> , Å	12.2118(12)	18.9260(9)	10.6285(5)	8.3503(7)
<i>b</i> , Å	9.7445(10)	27.3459(12)	12.9424(6)	16.1189(14)
<i>c</i> , Å	14.4119(15)	18.0299(8)	21.7636(10)	13.5540(12)
α , deg	90	90	90	90
β , deg	93.958(2)	90	90	91.960(2)
γ , deg	90	90	90	90
<i>V</i> , Å ³	1710.9(3)	9331.3(7)	2993.8(2)	1823.3(3)
<i>Z</i>	4	8	4	4
<i>D</i> _{calcd} , Mg/m ³	1.045	1.149	1.205	0.988
radiation (λ), Å	Mo K α (0.71073)	Mo K α (0.71073)	Mo K α (0.71073)	Mo K α (0.71073)
2 θ range, deg	56.8	50.0	50.0	50.0
μ , mm ⁻¹	0.050	0.127	0.285	0.047
<i>F</i> (000)	576	3408	1128	584
no. of obsd reflns	3474	8390	5234	3195
no. of params refnd	190	607	343	233
goodness of fit	1.109	1.082	1.053	1.016
R1	0.0652	0.0751	0.0489	0.0944
wR2	0.0718	0.1098	0.0561	0.1910

Compd. No.	[43][Na ₂ (18-crown-6)(THF) ₂]	[44][PPN]	[45][PPN]	46a
formula	C ₂₅ H ₅₈ B ₁₁ NaO ₈	C ₄₁ H ₄₆ B ₁₁ NP ₂	C ₄₂ H ₄₈ B ₁₁ NP ₂	C ₁₁ H ₃₂ B ₁₁ N
crystal size (mm)	0.40 x 0.30 x 0.20	0.50 x 0.40 x 0.30	0.40 x 0.30 x 0.30	0.50 x 0.40 x 0.30
fw	628.61	733.64	747.66	297.29
crystal system	Triclinic	Orthorhombic	Monoclinic	Monoclinic
space group	<i>P</i> -1	<i>Pbcm</i>	<i>P2</i> ₁ / <i>c</i>	<i>P2</i> ₁ / <i>m</i>
<i>a</i> , Å	10.645(4)	9.154(2)	12.7941(9)	8.2436(8)
<i>b</i> , Å	11.441(4)	18.404(4)	17.3171(12)	11.4715(12)
<i>c</i> , Å	16.211(6)	25.013(6)	18.3531(13)	10.3203(10)
α , deg	70.551(7)	90	90	90
β , deg	77.140(7)	90	97.124(2)	109.448(2)
γ , deg	88.427(8)	90	90	90
<i>V</i> , Å ³	1812.7(11)	4213.7(16)	4034.9(5)	920.27(16)
<i>Z</i>	2	4	4	2
<i>D</i> _{calcd} , Mg/m ³	1.152	1.156	1.231	1.073
radiation (λ), Å	Mo K α (0.71073)	Mo K α (0.71073)	Mo K α (0.71073)	Mo K α (0.71073)
2 θ range, deg	50.0	50.0	50.0	50.0
μ , mm ⁻¹	0.085	0.134	0.141	0.052
<i>F</i> (000)	676	1536	1568	320
no. of obsd reflns	5954	3795	7099	1703
no. of params refnd	406	279	505	148
goodness of fit	1.878	1.068	1.017	1.085
R1	0.1592	0.0599	0.0499	0.0811
wR2	0.2019	0.0893	0.0794	0.1013

Compd. No.	46b	47b	[48][PSH]	[48'] [PSH]
formula	C ₁₁ H ₃₂ B ₁₁ N	C ₁₉ H ₃₅ B ₁₁ N ₂	C ₂₁ H ₄₃ B ₁₁ N ₂ O ₂	C ₂₃ H ₄₇ B ₁₁ N ₂ O ₂
crystal size (mm)	0.50 x 0.40 x 0.30	0.40 x 0.30 x 0.20	0.50 x 0.30 x 0.20	0.40 x 0.40 x 0.30
fw	297.29	410.40	474.48	518.54
crystal system	Orthorhombic	Monoclinic	Triclinic	Triclinic
space group	<i>Pbca</i>	<i>P2₁/c</i>	<i>P</i> -1	<i>P</i> -1
<i>a</i> , Å	11.3889(7)	7.0376(5)	8.4249(4)	10.4048(5)
<i>b</i> , Å	14.4573(9)	13.2110(7)	10.9067(6)	12.2367(6)
<i>c</i> , Å	22.1940(15)	26.0158(17)	15.1728(8)	13.6975(7)
α , deg	90	90	85.3560(10)	76.9250(10)
β , deg	90	96.547(4)	86.9400(10)	70.0840(10)
γ , deg	90	90	83.3410(10)	74.0880(10)
<i>V</i> , Å ³	3654.3(4)	2403.0(3)	1378.88(12)	1559.73(13)
<i>Z</i>	8	4	2	2
<i>D</i> _{calcd} , Mg/m ³	1.081	1.134	1.143	1.104
radiation (λ), Å	Mo K α (0.71073)	Cu K α (1.54178)	Mo K α (0.71073)	Mo K α (0.71073)
2 θ range, deg	50.0	83.5	50.5	50.5
μ , mm ⁻¹	0.052	0.422	0.065	0.065
<i>F</i> (000)	1280	872	508	556
no. of obsd reflns	3222	1578	4967	5640
no. of params refnd	208	293	337	360
goodness of fit	1.052	1.088	1.092	0.990
R1	0.0639	0.0863	0.0523	0.0628
wR2	0.1105	0.1127	0.0626	0.1004

Compd. No.	[49][Et ₃ NH]	[49][PSH]	[50][PSH]	[51][PSH]
formula	C ₁₃ H ₃₈ B ₁₁ NO	C ₂₁ H ₄₁ B ₁₁ N ₂ O	C ₂₂ H ₄₅ B ₁₁ N ₂ O ₂	C ₁₉ H ₃₈ B ₁₀ N ₂ O
crystal size (mm)	0.50 x 0.40 x 0.20	0.50 x 0.40 x 0.30	0.40 x 0.30 x 0.20	0.40 x 0.30 x 0.20
fw	343.35	456.47	488.51	418.61
crystal system	Triclinic	Triclinic	Triclinic	Monoclinic
space group	<i>P</i> -1	<i>P</i> -1	<i>P</i> -1	<i>P</i> 2 ₁ / <i>c</i>
<i>a</i> , Å	8.345(3)	8.3906(15)	9.4687(7)	11.666(2)
<i>b</i> , Å	8.931(3)	10.904(2)	9.6287(8)	10.466(2)
<i>c</i> , Å	30.583(11)	15.541(3)	17.0590(13)	20.948(4)
α , deg	82.019(9)	99.131(3)	102.413(2)	90
β , deg	87.889(6)	94.715(3)	97.696(2)	90.327(4)
γ , deg	76.408(7)	102.261(3)	97.792(2)	90
<i>V</i> , Å ³	2194.1(13)	1361.8(4)	1483.4(2)	2557.8(8)
<i>Z</i>	4	2	2	4
<i>D</i> _{calcd} , Mg/m ³	1.039	1.113	1.094	1.087
radiation (λ), Å	Mo K α (0.71073)	Mo K α (0.71073)	Mo K α (0.71073)	Mo K α (0.71073)
2 θ range, deg	50.0	50.0	55.4	50.5
μ , mm ⁻¹	0.054	0.060	0.062	0.059
<i>F</i> (000)	744	488	524	896
no. of obsd reflns	7672	4751	6800	4625
no. of params refnd	477	320	347	301
goodness of fit	1.216	1.063	1.124	1.008
R1	0.2481	0.0762	0.1146	0.0642
wR2	0.3250	0.1147	0.2579	0.1382

Compd. No.	[52][PSH]	53a	54	55
formula	C ₂₀ H ₄₀ B ₁₀ N ₂ O	C ₁₀ H ₂₂ B ₁₁ N	C ₁₅ H ₂₇ B ₁₁ N ₂	C ₁₇ H ₃₁ B ₁₁ N ₂
crystal size (mm)	0.50 x 0.40 x 0.30	0.50 x 0.40 x 0.30	0.40 x 0.30 x 0.20	0.50 x 0.40 x 0.30
fw	432.64	275.20	354.30	382.35
crystal system	Monoclinic	Orthrohombic	Orthrohombic	Monoclinic
space group	<i>P2₁/c</i>	<i>Pbca</i>	<i>P2₁2₁2₁</i>	<i>P2₁/n</i>
<i>a</i> , Å	13.5073(5)	12.6628(9)	9.2420(15)	10.3177(8)
<i>b</i> , Å	12.4931(5)	14.1099(10)	12.376(2)	14.8096(13)
<i>c</i> , Å	15.3521(6)	18.2836(13)	18.093(3)	15.0601(13)
α , deg	90	90	90	90
β , deg	90.3520(10)	90	90	90.522(2)
γ , deg	90	90	90	90
<i>V</i> , Å ³	2590.59(17)	3266.7(4)	2069.5(6)	2301.1(3)
<i>Z</i>	4	8	4	4
<i>D</i> _{calcd} , Mg/m ³	1.109	1.119	1.137	1.104
radiation (λ), Å	Mo K α (0.71073)	Mo K α (0.71073)	Mo K α (0.71073)	Mo K α (0.71073)
2 θ range, deg	50.5	50.5	50.5	50.5
μ , mm ⁻¹	0.061	0.054	0.058	0.057
<i>F</i> (000)	928	1152	744	808
no. of obsd reflins	4680	2960	3724	4159
no. of params refnd	310	199	262	279
goodness of fit	1.041	1.083	0.971	1.062
R1	0.0562	0.0557	0.0581	0.1120
wR2	0.0753	0.0702	0.1639	0.1673

Compd. No.	56	57a·CH ₂ Cl ₂	59	60
formula	C ₉₂ H ₁₇₂ B ₄₄ N ₈	C ₁₂ H ₂₆ B ₁₁ Cl ₂ N	C ₁₅ H ₂₃ B ₁₁ N ₂	C ₁₆ H ₂₅ B ₁₁ N ₂
crystal size (mm)	0.50 x 0.40 x 0.30	0.50 x 0.40 x 0.30	0.40 x 0.30 x 0.20	0.40 x 0.30 x 0.20
fw	1866.02	374.15	350.26	364.29
crystal system	Triclinic	Monoclinic	Orthorhombic	Tetragonal
space group	<i>P</i> -1	<i>Cc</i>	<i>Pna</i> 2 ₁	<i>P</i> -42 ₁ <i>c</i>
<i>a</i> , Å	12.5579(11)	16.7150(10)	24.3055(18)	16.853(3)
<i>b</i> , Å	15.0847(10)	16.0143(9)	16.5785(11)	16.853(3)
<i>c</i> , Å	16.2226(10)	8.6111(5)	14.2903(10)	14.176(3)
α , deg	93.524(7)	90	90	90
β , deg	108.248(2)	115.9900(10)	90	90
γ , deg	91.081(2)	90	90	90
<i>V</i> , Å ³	2910.7(4)	2071.9(2)	5758.3(7)	4026.2(14)
<i>Z</i>	1	4	12	8
<i>D</i> _{calcd} , Mg/m ³	1.065	1.199	1.212	1.202
radiation (λ), Å	Mo K α (0.71073)	Mo K α (0.71073)	Mo K α (0.71073)	Mo K α (0.71073)
2 θ range, deg	50.5	50.5	50.5	50.5
μ , mm ⁻¹	0.055	0.309	0.062	0.062
<i>F</i> (000)	1000	776	2184	1520
no. of obsd reflns	10410	3335	10305	3653
no. of params refnd	657	235	757	262
goodness of fit	1.066	1.079	1.038	1.064
R1	0.0738	0.0542	0.0816	0.0539
wR2	0.1536	0.0719	0.1480	0.0853

Compd. No.	61	62	[65][PSH]	[67][PPN]·THF
formula	$C_{17}H_{25}B_{11}N_2$	$C_{18}H_{27}B_{11}N_2$	$C_{20}H_{39}B_{11}N_2$	$C_{53}H_{64}B_{11}NOP_2S$
crystal size (mm)	0.50 x 0.40 x 0.30	0.50 x 0.40 x 0.30	0.40 x 0.30 x 0.20	0.50 x 0.40 x 0.20
fw	376.30	390.33	426.44	943.96
crystal system	Monoclinic	Monoclinic	Triclinic	Triclinic
space group	$P2_1/c$	$P2_1/c$	$P-1$	$P-1$
a , Å	12.7697(8)	13.1718(9)	11.4918(13)	11.125(8)
b , Å	22.4968(14)	28.9671(19)	14.8547(17)	14.248(11)
c , Å	15.3478(9)	11.9075(8)	16.1670(18)	17.751(14)
α , deg	90	90	78.932(2)	98.412(17)
β , deg	107.7010(10)	107.7820(10)	88.899(3)	104.365(14)
γ , deg	90	90	74.307(3)	98.182(15)
V , Å ³	4200.3(4)	4326.2(5)	2606.0(5)	2649(3)
Z	8	8	4	2
D_{calcd} , Mg/m ³	1.190	1.199	1.087	1.183
radiation (λ), Å	Mo K α (0.71073)	Mo K α (0.71073)	Mo K α (0.71073)	Mo K α (0.71073)
2θ range, deg	50.5	50.5	50.5	50.5
μ , mm ⁻¹	0.062	0.062	0.056	0.161
$F(000)$	1568	1632	912	996
no. of obsd reflns	7602	7820	9240	9561
no. of params refnd	541	559	615	622
goodness of fit	1.109	1.008	1.020	1.017
R1	0.1046	0.0644	0.0710	0.0528
wR2	0.1412	0.1037	0.1317	0.0719

Compd. No.	68	[69][PPN]	[70][PPN]	[71a][Me ₃ NH]
formula	C ₁₀ H ₃₀ B ₁₁ N	C ₄₄ H ₅₅ B ₁₁ N ₂ P ₂	C ₄₆ H ₅₉ B ₁₁ N ₂ P ₂	C ₈ H ₃₀ B ₁₁ NO
crystal size (mm)	0.50 x 0.40 x 0.30	0.50 x 0.40 x 0.30	0.50 x 0.40 x 0.20	0.40 x 0.30 x 0.20
fw	283.26	792.75	820.80	275.24
crystal system	Monoclinic	Monoclinic	Monoclinic	Monoclinic
space group	<i>P2₁/c</i>	<i>P2₁/c</i>	<i>P2₁/c</i>	<i>P2₁/n</i>
<i>a</i> , Å	7.4647(12)	13.3528(12)	16.747(3)	7.966(3)
<i>b</i> , Å	14.673(2)	9.1868(9)	10.655(2)	11.576(4)
<i>c</i> , Å	16.269(3)	37.516(4)	26.720(5)	19.451(7)
α , deg	90	90	90	90
β , deg	94.198(3)	100.747(2)	99.830(3)	94.581(6)
γ , deg	90	90	90	90
<i>V</i> , Å ³	1777.1(5)	4521.3(8)	4698.0(15)	1788.0(10)
<i>Z</i>	4	4	4	4
<i>D</i> _{calcd} , Mg/m ³	1.059	1.165	1.160	1.022
radiation (λ), Å	Mo K α (0.71073)	Mo K α (0.71073)	Mo K α (0.71073)	Mo K α (0.71073)
2 θ range, deg	56.0	56.1	50.5	56.3
μ , mm ⁻¹	0.051	0.130	0.128	0.053
<i>F</i> (000)	608	1672	1736	592
no. of obsd reflns	4253	10877	8499	4332
no. of params refnd	207	532	550	194
goodness of fit	1.011	1.238	0.989	0.973
R1	0.0592	0.0892	0.0676	0.0755
wR2	0.0775	0.1029	0.2157	0.1922

Compd. No.	[72][Me ₃ NH]	[74][PPN]	[77][Na ₂ (18-crown-6)(H ₂ O)]	[78][PPN]
formula	C ₇ H ₂₆ B ₁₁ N	C ₃₉ H ₄₄ B ₉ NP ₂	C ₃₂ H ₈₈ B ₂₂ Na ₂ O ₁₄	C ₄₂ H ₅₃ B ₁₁ N ₂ P ₂
crystal size (mm)	0.40 x 0.30 x 0.20	0.50 x 0.40 x 0.30	0.50 x 0.40 x 0.30	0.40 x 0.30 x 0.20
fw	243.20	685.98	980.82	766.71
crystal system	Triclinic	Monoclinic	Orthorhombic	Orthorhombic
space group	<i>P</i> -1	<i>P</i> 2 ₁ / <i>n</i>	<i>Pna</i> 2 ₁	<i>Pbca</i>
<i>a</i> , Å	7.9653(5)	27.878(11)	28.160(5)	18.346(9)
<i>b</i> , Å	9.3459(6)	10.317(4)	12.389(2)	18.637(9)
<i>c</i> , Å	11.4112(7)	27.994(10)	16.082(3)	26.087(12)
α , deg	89.0240(10)	90	90	90
β , deg	73.9460(10)	104.993(7)	90	90
γ , deg	79.0100(10)	90	90	90
<i>V</i> , Å ³	800.81(9)	7778(5)	5610.6(17)	8920(7)
<i>Z</i>	2	8	4	8
<i>D</i> _{calcd} , Mg/m ³	1.009	1.172	1.161	1.142
radiation (λ), Å	Mo K α (0.71073)	Mo K α (0.71073)	Mo K α (0.71073)	Mo K α (0.71073)
2 θ range, deg	50.0	50.5	50.0	50.0
μ , mm ⁻¹	0.047	0.141	0.089	0.130
<i>F</i> (000)	260	2880	2096	3232
no. of obsd reflns	2716	14093	9366	7845
no. of params refnd	176	919	631	518
goodness of fit	1.129	2.555	1.038	1.128
R1	0.0571	0.2000	0.0800	0.0682
wR2	0.1093	0.2245	0.1141	0.1137

Compd. No.	[79][PPN]	[80][Me ₃ NH]	[81][(Me ₃ NH) ₂ Cl]
formula	C ₁₆ H ₂₈ B ₁₁ P	C ₉ H ₃₁ B ₁₂ NO	C ₃₃ H ₁₁₄ B ₃₃ Cl ₃ N ₆
crystal size (mm)	0.40 x 0.30 x 0.20	0.40 x 0.30 x 0.20	0.40 x 0.30 x 0.20
fw	370.26	299.07	1058.38
crystal system	Orthorhombic	Monoclinic	Orthorhombic
space group	<i>P2₁2₁2₁</i>	<i>P2₁/n</i>	<i>Pnma</i>
<i>a</i> , Å	10.1525(7)	22.267(5)	11.8388(15)
<i>b</i> , Å	14.5833(9)	7.9141(16)	34.882(4)
<i>c</i> , Å	14.5977(8)	22.267(5)	16.429(2)
α , deg	90	90	90
β , deg	90	93.3	90
γ , deg	90	90	90
<i>V</i> , Å ³	2161.3(2)	3917.4(14)	6784.6(15)
<i>Z</i>	4	8	4
<i>D</i> _{calcd} , Mg/m ³	1.138	1.014	1.036
radiation (λ), Å	Mo K α (0.71073)	Mo K α (0.71073)	Mo K α (0.71073)
2 θ range, deg	50.5	50.0	50.0
μ , mm ⁻¹	0.127	0.052	0.166
<i>F</i> (000)	776	1280	2280
no. of obsd reflns	3914	6875	6070
no. of params refnd	253	419	371
goodness of fit	1.030	1.078	1.035
R1	0.0464	0.1930	0.1056
wR2	0.0651	0.2530	0.1626